

7 DYNAMIC DERIVATIVES

Dynamic derivatives are associated with those aerodynamic forces and moments caused by the angular velocities and linear accelerations of the vehicle motion. A detailed discussion of wing, body, and wing-body dynamic derivatives is given in the introduction to each of the subject sections. In most cases the methods presented are based on theories that necessarily assume attached-flow conditions. They are thus limited to low angles of attack except for high-aspect-ratio wings below stall at subsonic speeds.

In general, dynamic derivatives for attached-flow conditions are smaller and of less importance than those for separated-flow conditions. For separated-flow conditions the derivatives become functions of the amplitude and frequency of oscillation. Such conditions exist on low-aspect-ratio wings and bodies at all speeds and at all angles of attack except for a narrow range around zero.

Because of the limited amount of data at high angles of attack and the complexity of deriving adequate generalized methods, particularly for the frequency and amplitude variations, no methods are presented that cover separated-flow conditions. Rather, a literature summary is presented in table 7-A and a bibliography on pages 7-1 through -10.

REFERENCES

1. Anon.: A General Investigation of Hypersonic Stability and Control Under Trimmed Flight Conditions. Flight Sci. Lab. R-63-011-104, 1964. (U)
2. Bauer, R. C.: An Investigation of the Influence of Several Shape Parameters on the Dynamic Stability of Ballistic Re-entry Configurations. Phase I. Effect of Afterbody Configuration at Mach Numbers 0.5 Through 1.5. AEDC-TN-59-78, 1959. (U)
3. Beam, B. H.: The Effects of Oscillation Amplitude and Frequency on the Experimental Damping in Pitch of a Triangular Wing Having an Aspect Ratio of 4. NACA RM A52G07, 1952. (U)
4. Beam, B. H., Reed, V. D., and Lopez, A. E.: Wind-Tunnel Measurements at Subsonic Speeds of the Static and Dynamic-Rotary Stability Derivatives of a Triangular-Wing Airplane Model Having a Triangular Vertical Tail. NACA RM A55A28, 1955. (U)
5. Bennett, C. V., and Johnson, J. L.: Experimental Determination of the Damping in Roll and Aileron Rolling Effectiveness of Three Wings Having 2°, 42°, and 62° Sweepback. NACA TN 1278, 1947. (U)
6. Bielat, R. P., and Wiley, H. G.: Dynamic Longitudinal and Directional Stability Derivatives for a 45° Sweptback-Wing Airplane Model at Transonic Speeds. NASA TM X-39, 1959. (U)
7. Bird, J. D., Jaquet, B. M., and Cowan, J. W.: Effect of Fuselage and Tail Surfaces on Low-Speed Yawing Characteristics of a Swept-Wing Model as Determined in Curved-Flow Test Section of Langley Stability Tunnel. NACA RM L8G13, 1948. (U)
8. Bird, J. D., Jaquet, B. M., and Cowan, J. W.: Effect of Fuselage and Tail Surfaces on Low-Speed Yawing Characteristics of a Swept-Wing Model as Determined in Curved-Flow Test Section of Langley Stability Tunnel. NACA TN 2483, 1951. (U)
9. Bird, J. D., Lichtenstein, J. H., and Jaquet, B. M.: Investigation of the Influence of Fuselage and Tail Surfaces on Low-Speed Static Stability and Rolling Characteristics of a Swept-Wing Model. NACA TN 2741, 1952. (U)
10. Bird, J. D.: Some Theoretical Low-Speed Span Loading Characteristics of Swept Wings in Roll and Sideslip. NACA TN 1839, 1949. (U)
11. Bird, J. D.: Some Theoretical Low-Speed Span Loading Characteristics of Swept Wings in Roll and Sideslip. NACA TR 969, 1950. (U)

12. Bird, J. D., and Jaquet, B. M.: A Study of the Use of Experimental Stability Derivatives in the Calculation of the Lateral Disturbed Motions of a Swept-Wing Airplane and Comparison with Flight Results. NACA TN 2013, 1950. (U)
13. Bird, J. D., Lichtenstein, J. H., and Jaquet, B. M.: Investigation of the Influence of Fuselage and Tail Surfaces on Low-Speed Static Stability and Rolling Characteristics of a Swept-Wing Model. NACA RM L7H15, 1947. (U)
14. Bland, W. M., Jr.: Effect of Fuselage Interference on the Damping in Roll of Delta Wings of Aspect Ratio 4 in the Mach Number Range Between 0.6 and 1.6 as Determined with Rocket-Propelled Vehicles. NACA RM L52E13, 1952. (U)
15. Bland, W. M., Jr., and Dietz, A. E.: Some Effects of Fuselage Interference, Wing Interference, and Sweepback on the Damping in Roll of Untapered Wings as Determined by Techniques Employing Rocket-Propelled Vehicles. NACA RM L51D25, 1951. (U)
16. Bland, W. M., Jr., and Sandahl, C. A.: A Technique Utilizing Rocket-Propelled Test Vehicles for the Measurement of the Damping in Roll of Sting-Mounted Models and Some Initial Results for Delta and Up-swept Tapered Wings. NACA RM L50D24, 1950. (U)
17. Bond R., and Packard, B. B.: Unsteady Aerodynamic Forces on a Slender Body of Revolution in Supersonic Flow. NASA TN D-859, 1961. (U)
18. Bradley, W. G.: Measurement of the Lateral Stability Derivatives of a Morane-Saulnier M.S. 760 'Paris' Aircraft G-APRU. CoA Report Aero. 185, 1965. (U)
19. Brewer, J. D., and Fisher, L. R.: Effect of Taper Ratio on the Low-Speed Rolling Stability Derivatives of Swept and Unswept Wings of Aspect Ratio 2.61. NACA TN 2555, 1951. (U)
20. Brown, C. E., and Heinke, H. S., Jr.: Preliminary Wind-Tunnel Tests of Triangular and Rectangular Wings in Steady Roll at Mach Numbers of 1.62 and 1.92. NACA RM L8L30, 1949. (U)
21. Brown, C. E., and Adams, M. C.: Damping in Pitch and Roll of Triangular Wings at Supersonic Speeds. NACA TR 892, 1948. (U)
22. Buell, D. A., Reed, V. D., and Lopez, A. E.: The Static and Dynamic-Rotary Stability Derivatives at Subsonic Speeds of an Airplane Model with an Unswept Wing and a High Horizontal Tail. NACA RM A56I04, 1956. (U)
23. Campbell, J. P., and Woodling, C. H.: Calculated Effects of the Lateral Acceleration Derivatives on the Dynamic Lateral Stability of a Delta-Wing Airplane. NACA RM L54K26, 1955. (U)
24. Campbell, J. P., and Mathews, W. O.: Experimental Determination of the Yawing Moment Due to Yawing Contributed by the Wing, Fuselage, and Vertical Tail of a Midwing Airplane Model. NACA L-387, 1943. (U)
25. Campbell, J. P., Johnson, J. L., Jr., and Heviss, D. E.: Low-Speed Study of the Effect of Frequency on the Stability Derivatives of Wings Oscillating in Yaw with Particular Reference to High Angle-of-Attack Conditions. NACA RM L55H05, 1955. (U)
26. Campbell, J. P., and Goodman, A.: A Semiempirical Method for Estimating the Rolling Moment Due to Yawing of Airplanes. NACA TN 1984, 1949. (U)
27. Chapman, R., Jr., and Morrow, J. D.: Longitudinal Stability and Drag Characteristics at Mach Numbers from 0.70 to 1.37 of Rocket-Propelled Models Having a Modified Triangular Wing. NACA RM L52A31, 1952. (U)
28. Clay, J. T.: Nose Bluntness, Cone Angle, and Mach Number Effects on the Stability Derivatives of Slender Cones. ARL 67-0185, 1967. (U)
29. Cole, I. J., and Margolis, K.: Lift and Pitching Moment at Supersonic Speeds Due to Constant Vertical Acceleration for Thin Sweptback Tapered Wings with Streamwise Tips. Supersonic Leading and Trailing Edges. NACA TN 3196, 1954. (U)
30. Conlin, L. T., and Orlik-Rückemann, K. J.: Comparison of Some Experimental and Theoretical Data on Damping-in-Roll of a Delta-Wing Body Configuration at Supersonic Speeds. NRC LR-266, 1959. (U)
31. Cox, A. P., and Butler, S. F. J.: Low-Speed Wind-Tunnel Measurements of Damping in Yaw (η_y) on an A.R.9 Jet-Flap Model. ARC CP 869, 1967. (U)
32. Curtiss, H. C., Jr.: Some Basic Considerations Regarding the Longitudinal Dynamics of Aircraft and Helicopters. Princeton Univ. Report 562, 1961. (U)

33. D'Aiutolo, C. T.: Low-Amplitude Damping-in-Pitch Characteristics of Tailless Delta-Wing Body Combinations at Mach Numbers from 0.80 to 1.35 as Obtained with Rocket-Powered Models. NACA RM L54D29, 1954. (U)
34. D'Aiutolo, C. T., and Parker, R. N.: Preliminary Investigation of the Low-Amplitude Damping in Pitch of Tailless Delta- and Swept-Wing Configurations at Mach Numbers from 0.7 to 1.35. NACA RM L52G09, 1952. (U)
35. D'Aiutolo, C. T., and Mason, H. P.: Preliminary Results of the Flight Investigation Between Mach Numbers of 0.80 and 1.36 of a Rocket-Powered Model of a Supersonic Airplane Configuration Having a Tapered Wing with Circular-Arc Section and 40° Sweepback. NACA RM L50H29a, 1950. (U)
36. Delaney, B. R., and Thompson, W. E.: Dynamic Stability Characteristics in Pitch and in Yaw for a Model of a Variable-Sweep Supersonic Transport Configuration at Mach Numbers of 2.40, 2.98, and 3.60. NASA TM X-761, 1963. (U)
37. Dietz, A. E., and Edmondson, J. L.: The Damping in Roll of Rocket-Powered Test Vehicles Having Rectangular Wings with a NACA 65-006 and Symmetrical Double-Wedge Airfoil Sections of Aspect Ratio 4.5. NACA RM L50B10, 1950. (U)
38. Dorrance, W. H.: Nonsteady Supersonic Flow About Pointed Bodies of Revolution. Jour. of Aero. Sci., Vol. 18, No. 8, 1951. (U)
39. Dubose, H. C.: Static and Dynamic Stability of Blunt Bodies. AGARD Rept. 347, 1961. (U)
40. Edmondson, J. L., and Sanders, E. C., Jr.: A Free-Flight Technique for Measuring Damping in Roll by Use of Rocket-Powered Models and Some Initial Results for Rectangular Wings. NACA RM L91O1, 1949. (U)
41. Emerson, H. F., and Robison, R. C.: Experimental Wind-Tunnel Investigation of the Transonic Damping-in-Pitch Characteristics of Two Wing-Body Combinations. NASA Memo 11-30-58A, 1958. (U)
42. Ericsson, L. E., and Reding, J. P.: Aerodynamic Effects of Bulbous Bases. NASA CR-1339, 1969. (U)
43. Ericsson, L. E.: Effect of Boundary Layer Transition on Vehicle Dynamics. AIAA Paper 69-106, 1969. (U)
44. Feigenbaum, D., and Goodman, A.: Preliminary Investigation at Low Speeds of Swept Wings in Rolling Flow. NACA RM L7E09, 1947. (U)
45. Fink, M. R., and Carroll, J. B.: Hypersonic Static and Dynamic Stability of Wing-Fuselage Configurations. UAL C910188-17, 1965. (U)
46. Fisher, L. R.: Approximate Corrections for the Effects of Compressibility on the Subsonic Stability Derivatives of Swept Wings. NACA TN 1854, 1949. (U)
47. Fisher, L. R., and Fletcher, H. S.: Effect of Lag of Sidewash on the Vertical-Tail Contribution to Oscillatory Damping in Yaw of Airplane Models. NACA TN 3356, 1955. (U)
48. Fisher, L. R.: Equations and Charts for Determining the Hypersonic Stability Derivatives of Combinations of Cone Frustums Computed by Newtonian Impact Theory. NASA TN D-149, 1959. (U)
49. Fisher, L. R.: Experimental Determination of the Effects of Frequency and Amplitude on the Lateral Stability Derivatives for a Delta, a Swept, and an Unswept Wing Oscillating in Yaw. NACA RM A56L19, 1956. (U)
50. Fisher, L. R.: Experimental Determination of the Effects of Frequency and Amplitude on the Lateral Stability Derivatives for a Delta, a Swept, and an Unswept Wing Oscillating in Yaw. NACA TR 1357, 1958. (U)
51. Fisher, L. R.: Experimental Determination of the Effects of Frequency and Amplitude of Oscillation on the Roll-Stability Derivatives for a 60° Delta-Wing Airplane Model. NASA TN D-232, 1960. (U)
52. Fisher, L. R., and Michael, W. H., Jr.: An Investigation of the Effect of Vertical-Fin Location and Area on Low-Speed Lateral Stability Derivatives of a Semitailless Airplane Model. NACA RM L51A10, 1951. (U)
53. Fisher, L. R., Lichtenstein, J. H., and Williams, K. D.: A Preliminary Investigation of the Effects of Frequency and Amplitude on an Unswept-Wing Model Oscillating in Roll. NACA TN 3554, 1956. (U)
54. Fletcher, H. S.: Low-Speed Experimental Determination of the Effects of Leading-Edge Radius and Profile Thickness on Static and Oscillatory Lateral Stability Derivatives for a Delta Wing with 60° of Leading-Edge Sweep. NACA TN 4341, 1958. (U)

55. Gillis, C. L., Peck, R. F., and Vitale, A. J.: Preliminary Results from a Free-Flight Investigation at Transonic and Supersonic Speeds of the Longitudinal Stability and Control Characteristics of an Airplane Configuration with a Thin Straight Wing of Aspect Ratio 3. NACA RM L9K25a, 1950. (U)
56. Gillis, C. L., and Chapman, R., Jr.: Summary of Pitch-Damping Derivatives of Complete Airplane and Missile Configurations as Measured in Flight at Transonic and Supersonic Speeds. NACA RM L52K20, 1953. (U)
57. Gillis, C. L., and Vitale, A. J.: Wing-on and Wing-off Longitudinal Characteristics of an Airplane Configuration Having a Thin Unswept Tapered Wing of Aspect Ratio 3, as Obtained from Rocket-Propelled Models at Mach Numbers from 0.8 to 1.4. NACA RM L50K16, 1951. (U)
58. Gilmore, A. W., et al.: Investigation of Dynamic Stability Derivatives of Vehicles Flying at Hypersonic Velocity. ASD-TDR-62-460, 1963. (U)
59. Goodman, A., and Thomas, D. F., Jr.: Effects of Wing Position and Fuselage Size on the Low-Speed Static and Rolling Stability Characteristics of a Delta-Wing Model. NACA TN 3063, 1954. (U)
60. Goodman, A., and Adair, G. H.: Estimation of the Damping in Roll of Wings Through the Normal Flight Range of Lift Coefficient. NACA TN 1924, 1949. (U)
61. Goodman, A., and Fisher, L. R.: Investigation at Low Speeds of the Effect of Aspect Ratio and Sweep on Rolling Stability Derivatives of Untapered Wings. NACA TN 1835, 1949. (U)
62. Goodman, A., and Fisher, L. R.: Investigation at Low Speeds of the Effect of Aspect Ratio and Sweep on Rolling Stability Derivatives of Untapered Wings. NACA TR 968, 1950. (U)
63. Goodman, A., and Brewer, J. D.: Investigation at Low Speeds of the Effect of Aspect Ratio and Sweep on Static and Yawing Stability Derivatives of Untapered Wings. NACA TN 1669, 1948. (U)
64. Goodman, A., and Feigenbaum, D.: Preliminary Investigation at Low Speeds of Swept Wings in Yawing Flow. NACA RM L7I09, 1948. (U)
65. Greenwood, G. H.: Free-Flight Measurements of the Dynamic Longitudinal-Stability Characteristics of a Wind Tunnel Interference Model ($M = 0.92$ to 1.35). ARC CP 648, 1963. (U)
66. Guyett, P. R., and Curran, J. D.: Aerodynamic Derivative Measurements on a Rectangular Wing of Aspect Ratio 3.3. ARC R&M 3171, 1961. (U)
67. Harmon, S. M.: Stability Derivatives at Supersonic Speeds of Thin Rectangular Wings with Diagonals Ahead of Tip Mach Lines. NACA TR 925, 1949. (U)
68. Harmon, S. M.: Stability Derivatives of Thin Rectangular Wings at Supersonic Speeds. NACA TN 1706, 1948. (U)
69. Harmon, S. M., and Jeffreys, I.: Theoretical Lift and Damping in Roll of Thin Wings with Arbitrary Sweep and Taper at Supersonic Speeds — Supersonic Leading and Trailing Edges. NACA TN 2114, 1950. (U)
70. Henderson, A., Jr.: Pitching-Moment Derivatives C_{Mq} and C_{Ma} at Supersonic Speeds for a Slender-Delta-Wing and Slender-Body Combination and Approximate Solutions for Broad-Delta-Wing and Slender-Body Combinations. NACA TN 2553, 1951. (U)
71. Hewes, D. E.: Low-Speed Measurement of Static Stability and Damping Derivatives of a 60° Delta-Wing Model for Angles of Attack of 0° to 90° . NACA RM L54G22a, 1954. (U)
72. Hoerner, S.: Forces and Moments on a Yawed Airfoil. NACA TM 906, 1939. (U)
73. Holleman, E. C.: Longitudinal Frequency-Response and Stability Characteristics of the Douglas D-558-II Airplane as Determined from Transient Response to a Mach Number of 0.96. NACA RM L52E02, 1952. (U)
74. Holt, C. F., and Kron, G. J.: Delta Wing Stability in the Pitch Plane. AIAA Student Jour., Feb. 1965. (U)
75. Hopko, R. N.: A Flight Investigation of the Damping in Roll and Rolling Effectiveness Including Aeroelastic Effects of Rocket-Propelled Missile Models Having Cruciform, Triangular, Interdigitated Wings and Tails. NACA RM L51D16, 1951. (U)
76. Howe, R. M.: An Investigation of the Relative Effect of Stability Derivatives on the Dynamic Characteristics of the F-100A. WADC TN 57-297, 1957. (U)

77. Hui, W. H.: Stability Derivatives of Sharp Wedges in Viscous Hypersonic Flow Including the Effects of Thickness and Wave Reflection. Univ. of Southampton, AASU Rept. 278, 1967. (U)
78. Hunt, G. K.: Free-Flight Model Measurements of the Dynamic Stability of a Supersonic Strike Aircraft (TSR2). ARC CP 918, 1967. (U)
79. Hunton, L. W., and Dew, J. K.: Measurements of the Damping in Roll of Large-Scale Swept-Forward and Swept-Back Wings in Rolling Flow. NACA RM A7D11, 1947. (U)
80. Ishii, T., and Yanagizawa, M.: Measurements of the Aerodynamic Derivatives of an Oscillating Biconvex-Flat Airfoil in Supersonic Flow at Mach Number 2 to 3. National Aerospace Lab. of Japan, TR-57T, 1963. (U)
81. Jaffe, P., and Pristin, R. H.: Effect of Boundary Layer Transition on Dynamic Stability Over Large Amplitudes of Oscillation. AIAA Paper 64-427, 1964. (U)
82. Jaquet, B. M., and Brewer, J. D.: Effects of Various Outboard and Central Fins on Low-Speed Static-Stability and Rolling Characteristics of a Triangular-Wing Model. NACA RM L9E18, 1949. (U)
83. Jaquet, B. M., and Fletcher, H. S.: Experimental Steady-State Yawing Derivatives of a 60° Delta-Wing Model as Affected by Changes in Vertical Position of the Wing and in Ratio of Fuselage Diameter to Wing Span. NACA TN 3843, 1956. (U)
84. Jaquet, B. M., and Brewer, J. D.: Low-Speed Static-Stability and Rolling Characteristics of Low-Aspect-Ratio Wings of Triangular and Modified Triangular Plan Forms. NACA RM L8L29, 1949. (U)
85. Johnson, J. L., Jr.: Low-Speed Measurements of Rolling and Yawing Stability Derivatives of a 60° Delta-Wing Model. NACA RM L54G27, 1954. (U)
86. Johnson, J. L., Jr.: Low-Speed Measurements of Static Stability, Damping in Yaw, and Damping in Roll of a Delta, a Swept, and an Unswept Wing for Angles of Attack from 0° to 90°. NACA RM L56B01, 1956. (U)
87. Jones, A. L., and Alksne, A.: The Damping Due to Roll of Triangular, Trapezoidal, and Related Plan Forms in Supersonic Flow. NACA TN 1548, 1948. (U)
88. Kemp, W. B., Jr., and Becht, R. E.: Damping-in-Pitch Characteristics at High Subsonic and Transonic Speeds of Four 35° Sweptback Wings. NACA L53G29a, 1953. (U)
89. Kennet, H., Ashley, H., and Stapleford, R. L.: Forces and Moments on Oscillating Slender Wing-Body Combinations at Supersonic Speed. Part II — Applications and Comparison with Experiment. OSR TN 58-114, MIT Fluid Dynamics Research Group Rept. 57-5, 1957. (U)
90. Kennet, H., and Ashley, H.: Review of Unsteady Aerodynamic Studies in the Fluid Dynamics Research Group, 1955-1958. OSR TN 59-6, MIT Fluid Dynamics Research Group Rept. 58-6, 1958. (U)
91. Kilgore, R. A., and Hillje, E. R.: Some Transonic Dynamic Longitudinal and Directional Stability Parameters of a Canard Airplane Model Designed for Supersonic Flight. NASA TM X-533, 1961. (U)
92. Kind, R. J., and Orlík-Rückemann, K.: Stability Derivatives of Sharp Cones in Viscous Hypersonic Flow. NRC LR-427, 1965. (U)
93. Kuhn, R. E., and Myers, B. C., II: Effects of Mach Number and Sweep on the Damping-in-Roll Characteristics of Wings of Aspect Ratio 4. NACA RM L9E10, 1949. (U)
94. Kuhn, R. E.: Notes on Damping in Roll and Load Distributions in Roll at High Angles of Attack and High Subsonic Speed. NACA RM L53G13a, 1953. (U)
95. Kuhn, R. E., and Wiggins, J. W.: Wind-Tunnel Investigation to Determine the Aerodynamic Characteristics in Steady Roll of a Model at High Subsonic Speeds. NACA RM L52K24, 1953. (U)
96. Lampkin, B. A., and Tunnell, P. J.: Static and Dynamic Rotary Stability Derivatives of an Airplane Model with an Unswept Wing and a High Horizontal Tail at Mach Numbers of 2.5, 3.0, and 3.5. NACA RM A58F17, 1958. (U)
97. Landahl, M. T.: The Flow Around Oscillating Low Aspect Ratio Wings at Transonic Speeds. Royal Institute of Technology, KTH Aero TN 40, 1954. (U)
98. Landahl, M. T.: Forces and Moments on Oscillating Slender Wing-Body Combinations of Sonic Speed. OSR TN 56-109, MIT Fluid Dynamics Research Group Rept. 56-1, 1956. (U)

99. Lehrian, D. E.: Calculation of Stability Derivatives for Oscillating Wings. ARC R&M 2922, 1956. (U)
100. Letko, W., and Brewer, J. D.: Effect of Airfoil Profile of Symmetrical Sections on the Low-Speed Rolling Derivatives of 45° Sweptback-Wing Models of Aspect Ratio 2.61 NACA LBL31a, 1949. (U)
101. Letko, W., and Jaquet, B. M.: Effect of Airfoil Profile of Symmetrical Sections on the Low-Speed Static-Stability and Yawing Derivatives of 45° Sweptback Wing Models of Aspect Ratio 2.61. NACA RM L8H10, 1948. (U)
102. Letko, W., and Fletcher, H. S.: Effects of Frequency and Amplitude on the Yawing Derivatives of Triangular, Swept, and Unswept Wings and of a Triangular-Wing-Fuselage Combination With and Without a Triangular Tail Performing Sinusoidal Yawing Oscillations. NACA TN 4390, 1958. (U)
103. Letko, W., and Wolhart, W. D.: Effect of Sweepback on the Low-Speed Static and Rolling Stability Derivatives of Thin Tapered Wings of Aspect Ratio 4. NACA RM L9F14, 1949. (U)
104. Letko, W., and Cowan, J. W.: Effect of Taper Ratio on Low-Speed Static and Yawing Stability Derivatives of 45° Sweptback Wings with Aspect Ratio of 2.61. NACA TN 1671, 1948. (U)
105. Letko, W., and Riley, D. R.: Effect of an Unswept Wing on the Contributions of Unswept-Tail Configurations to the Low-Speed Static- and Rolling-Stability Derivatives of a Midwing Airplane Model. NACA TN 2175, 1960. (U)
106. Letko, W.: Effect of Vertical-Tail Area and Length on the Yawing Stability Characteristics of a Model Having a 45° Sweptback Wing. NACA TN 2358, 1951. (U)
107. Letko, W.: Experimental Determination at Subsonic Speeds of the Oscillatory and Static Lateral Stability Derivatives of a Series of Delta Wings with Leading-Edge Sweep from 30° to 86.5°. NACA RM L57A30, 1957. (U)
108. Lichtenstein, J. H., and Williams, J. L.: Effect of Frequency of Sideslipping Motion on the Lateral Stability Derivatives of a Typical Delta-Wing Airplane. NACA RM L57F07, 1957. (U)
109. Lichtenstein, J. H.: Effect of High-Lift Devices on the Low-Speed Static Lateral and Yawing Stability Characteristics of an Untapered 45° Sweptback Wing. NACA TN 2689, 1952. (U)
110. Lockwood, V. E.: Damping-in-Roll Characteristics of a 42.7° Sweptback Wing as Determined from a Wind-Tunnel Investigation of a Twisted Semispan Wing. NACA L9F15, 1949. (U)
111. Lockwood, V. E.: Effects of Sweep on the Damping-in-Roll Characteristics of Three Sweptback Wings Having an Aspect Ratio of 4 at Transonic Speeds. NACA RM L50J19, 1950. (U)
112. Lomax, H., and Heaslet, M. A.: Damping-in-Roll Calculations for Slender Swept-Back Wings and Slender Wing-Body Combinations. NACA TN 1950, 1949. (U)
113. Lopez, A. E., Buell, D. A., and Tinling, B. E.: The Static and Dynamic Rotary Stability Derivatives at Subsonic Speeds of an Airplane Model Having Wing and Tail Surfaces Swept Back 45°. NASA Memo 5-16-59A, 1959. (U)
114. MacLachlan, R., and Letko, W.: Correlation of Two Experimental Methods of Determining the Rolling Characteristics of Unswept Wings. NACA TN 1309, 1947. (U)
115. MacLachlan, R., and Fisher, L. R.: Wind-Tunnel Investigation at Low Speeds of the Pitching Derivatives of Untapered Swept Wings. NACA RM L8G19, 1948. (U)
116. Maggin, B., and Bennett, C. V.: Low-Speed Stability and Damping-in-Roll Characteristics of Some Highly Swept Wings. NACA TN 1286, 1947. (U)
117. Malvestuto, F. S., Jr., and Hoover, D. M.: Lift and Pitching Derivatives of Thin Sweptback Tapered Wings with Streamwise Tips and Subsonic Leading Edges at Supersonic Speeds. NACA TM 2254, 1951. (U)
118. Malvestuto, F. S., Jr., and Hoover, D. M.: Supersonic Lift and Pitching Moment of Thin Sweptback Tapered Wings Produced by Constant Vertical Acceleration - Subsonic Leading Edges and Supersonic Trailing Edges. NACA TN 2315, 1951. (U)
119. Malvestuto, F. S., Jr., Margolis, K., and Ribner, H. S.: Theoretical Lift and Damping in Roll at Supersonic Speeds of Thin Sweptback Tapered Wings with Streamwise Tips, Subsonic Leading Edges, and Supersonic Trailing Edges. NACA TR 970, 1950. (U)

120. Malvestuto, F. S., Jr., Margolis, K., and Ribner, H. S.: Theoretical Lift and Damping in Roll of Thin Sweptback Wings of Arbitrary Taper and Sweep at Supersonic Speeds — Subsonic Leading Edges and Supersonic Trailing Edges. NACA TN 1860, 1950. (U)
121. Malvestuto, F. S., Jr., and Margolis, K.: Theoretical Stability Derivatives of Thin Sweptback Wings Tapered to a Point with Sweptforward Trailing Edges for a Limited Range of Supersonic Speeds. NACA TR 971, 1950. (U)
122. Mangler, K. W.: A Method of Calculating the Short-Period Longitudinal Stability Derivatives of a Wing in Linearized Unsteady Compressible Flow. ARC R&M 2924, 1957. (U)
123. Mantle, P. J.: On the Rolling Motion of Low-Aspect-Ratio Delta Wings. Jour. of Aero. Sci., May 1961. (U)
124. Mantle, P. J.: Some Free Flight Results of the Lift Curve Slope and Rolling Derivatives of Low Aspect Ratio Delta Wings. Canadian Arm. Res. and Devel. Est. TM AB-67, 1960. (U)
125. Margolis, K., and Babbitt, P. J.: Theoretical Calculations of the Stability Derivatives at Supersonic Speeds for a High-Speed Airplane Configuration. NACA RM L53G17, 1953. (U)
126. Martin, J. C., Margolis, K., and Jeffreys, I.: Calculation of Lift and Pitching Moments Due to Angle of Attack and Steady Pitching Velocity at Supersonic Speeds for Thin Sweptback Tapered Wings with Streamwise Tips and Supersonic Leading and Trailing Edges. NACA TN 2699, 1952. (U)
127. Martina, A. P.: Method for Calculating the Rolling and Yawing Moments Due to Rolling for Unswept Wings With or Without Flaps or Ailerons by Use of Nonlinear Section Lift Data. NACA TN 2937, 1953. (U)
128. McDearmon, R. W., and Heinke, H. S., Jr.: Investigations of the Damping in Roll of Swept and Tapered Wings at Supersonic Speeds. NACA RM L53A13, 1953. (U)
129. Miles, J. W.: Quasi-Stationary Airfoil Theory in Compressible Flow. Jour. of Aero. Sci., Vol. 16, No. 8, August 1949. (U)
130. Mitcham, G. L., Crabbill, N. L., and Stevens, J. E.: Flight Determination of the Drag and Longitudinal Stability and Control Characteristics of a Rocket-Powered Model of a 60° Delta-Wing Airplane from Mach Numbers of 0.75 to 1.70. NACA L51104, 1951. (U)
131. Mitcham, G. L., and Blanchard, W. S., Jr.: Summary of the Aerodynamic Characteristics and Flying Qualities Obtained from Flights of Rocket-Propelled Models of an Airplane Configuration Incorporating a Sweptback Inversely Tapered Wing at Transonic and Low Supersonic Speeds. NACA RM L50G18a, 1950. (U)
132. Myers, B. C., II, and Kuhn, R. E.: High-Subsonic Damping-in-Roll Characteristics of a Wing with the Quarter-Chord Line Swept Back 35° and with Aspect Ratio 3 and Taper Ratio 0.6. NACA RM L9C23, 1949. (U)
133. Nethaway, J. E., and Clark, J.: Flight Tests to Investigate the Dynamic Lateral-Stability Characteristics of a 45-deg. Delta, Cropped to Give Three Aspect Ratios. ARC R&M 3243, 1962. (U)
134. Ohman, L. H.: A Surface Flow Solution and Stability Derivatives for Bodies of Revolution in Complex Supersonic Flow. Part I — Theory and Some Representative Results. NRL LR-418, 1964. (U)
135. Ohman, L. H.: A Surface Flow Solution and Stability Derivatives for Bodies of Revolution in Complex Supersonic Flow. Part II — Results for Two Families of Bodies of Revolution for $1.1 \leq M \leq 5$. NRL LR-419, 1964. (U)
136. Orlik-Rückemann, K. J.: Stability Derivatives of Sharp Wedges in Viscous Hypersonic Flow. NRC LR-431, 1965. (U)
137. Orlik-Rückemann, K. J., and Laberge, J. G.: Static and Dynamic Longitudinal Stability Characteristics of a Series of Delta and Sweptback Wings at Supersonic Speeds. NRC LR-396, 1966. (U)
138. Parks, J. H.: Longitudinal Aerodynamic Characteristics of a Model Airplane Configuration Equipped with a Scaled X-1 Airplane Wing. NACA RM L51L10a, 1952. (U)
139. Parks, J. H., and Kohlet, A. B.: Longitudinal Stability, Trim, and Drag Characteristics of a Rocket-Propelled Model of an Airplane Configuration Having a 45° Sweptback Wing and an Unswept Horizontal Tail. NACA RM L52F05, 1952. (U)
140. Pearson, H. A., and Jones, R. T.: Theoretical Stability and Control Characteristics of Wings with Various Amounts of Taper and Twist. NACA TR 635, 1938. (U)
141. Peck, R. F., and Mitchell, J. L.: Rocket-Model Investigation of Longitudinal Stability and Drag Characteristics of an Airplane Configuration Having a 60° Delta Wing and High Unswept Horizontal Tail. NACA RM L52K04a, 1953. (U)

142. Piland, R. O.: Summary of the Theoretical Lift, Damping-in-Roll, and Center-of-Pressure Characteristics of Various Wing Plan Forms at Supersonic Speeds. NACA TN 1977, 1949. (U)
143. Pinsker, W. J. G.: A Semiempirical Method for Estimating the Rotary Rolling Moment Derivatives of Swept and Slender Wings. ARC CP 524, 1960. (U)
144. Platzer, M. F., and Sherer, A. D.: Dynamic Stability Analysis of Bodies of Revolution in Supersonic Flow. AIAA Paper 67-607, 1967. (U)
145. Platzer, M. F., and Hoffman, G. H.: Quasi-Slender Body Theory for Slowly Oscillating Bodies of Revolution in Supersonic Flow. NASA TN D-3440, 1966. (U)
146. Polhamus, E. C.: A Simple Method of Estimating the Subsonic Lift and Damping in Roll of Sweptback Wings. NACA TN 1862, 1949. (U)
147. Queijo, M. J. and Jaquet, B. M.: Calculated Effects of Geometric Dihedral on the Low-Speed Rolling Derivatives of Swept Wings. NACA TN 1732, 1948. (U)
148. Queijo, M. J., and Jaquet, B. M.: Investigation of Effects of Geometric Dihedral on Low-Speed Static Stability and Yawing Characteristics of an Untapered 45° Sweptback-Wing Model of Aspect Ratio 2.61. NACA TN 1668, 1948. (U)
149. Queijo, M. J., et al.: Preliminary Measurements of the Aerodynamic Yawing Derivatives of a Triangular, a Swept, and an Unswept Wing Performing Pure Yawing Oscillations, with a Description of the Instrument Employed. NACA RM L55L14, 1956. (U)
150. Queijo, M. J., and Wells, E. G.: Wind-Tunnel Investigation of the Low-Speed Static and Rotary Stability Derivatives of a 0.13-Scale Model of the Douglas D-558-II Airplane in the Landing Configuration. NACA RM L52G07, 1952. (U)
151. Quinn, B.: The Hypersonic Roll Damping Derivative of a Blunt Cone. ARL 68-0137, 1968. (U)
152. Ribner, H.: The Stability Derivatives of Low-Aspect-Ratio Triangular Wings at Subsonic and Supersonic Speeds. NACA TN 1423, 1947. (U)
153. Ribner, H. S., and Malvestuto, F. S., Jr.: Stability Derivatives of Triangular Wings at Supersonic Speeds. NACA TR 908, 1948. (U)
154. Rightley, E. C.: Dynamic Stability Derivatives for a 10° Blunt Cone at Mach Numbers from 0.5 to 21. Sandia Corp. Report SC-R-65-907, 1965. (U)
155. Ross, A. J.: The Lateral Oscillation of Slender Aircraft. ARC CP 845, 1966. (U)
156. Sadoff, M., Ankenbruck, H. O., and O'Hare, W.: Stability and Control Measurements Obtained During USAF-NACA Cooperative Flight-Test Program on the X-4 Airplane (USAF NO. 46-677). NACA RM A51H09, 1951. (U)
157. Sanders, E. C., Jr., and Edmondson, J. L.: Damping in Roll of Rocket-Powered Test Vehicles Having Swept, Tapered Wings of Low Aspect Ratio. NACA RM L51G06, 1951. (U)
158. Sanders, E. C., Jr.: Damping in Roll of Straight and 45° Swept Wings of Various Taper Ratios Determined at High Subsonic, Transonic, and Supersonic Speeds with Rocket-Powered Models. NACA RM L51H14, 1951. (U)
159. Scruton, C., Woodgate, L., and Alexander, A. J.: Measurement of the Aerodynamic Derivatives for Swept Wings of Low Aspect Ratio Describing Pitching and Plunging Oscillations in Incompressible Flow. ARC R&M 2925, 1957. (U)
160. Scruton, C., et al.: Measurement of Pitching-Moment Derivatives for Aerofoils Oscillating in Two-Dimensional Supersonic Flow. ARC R&M 3234, 1962. (U)
161. Smith, C. B., and Beane, B. J.: Damping in Pitch of Bodies of Revolution at Supersonic Speeds. IAS Preprint 311, 1951. (U)
162. Statler, I.C., Tufts, O.B., and Hirtreiter, W. J.: The Development and Evaluation of the CAL/Air Force Dynamic Wind-Tunnel Testing System, Part I—Description and Dynamic Tests of an F-80 Model. AFFDL-TR-66-153 Part I, 1967. (U)
163. Statler, I. C.: The Development and Evaluation of the CAL/Air Force Dynamic Wind-Tunnel Testing System, Part II—Dynamic Tests of an F-104 Model. AFFDL-TR-66-153 Part II, 1967. (U)

164. Statler, I.C.: Dynamic Stability at High Speeds from Unsteady Flow Theory. Jour of Aero Sci, Vol. 17, No. 4, 1950. (U)
165. Stone, D. G., and Sandahl, C. A.: A Comparison of Two Techniques Utilizing Rocket-Propelled Vehicles for the Determination of the Damping-in-Roll Derivative. NACA L51A16, 1951. (U)
166. Swanson, R. S., and Priddy, E. L.: Lifting-Surface-Theory Values of the Damping in Roll and of the Parameter Used in Estimating Aileron Stick Forces. NACA L-53, 1946. (U)
167. Thomas, H. H. B. M., and Ross, A. J.: The Calculation of the Rotary Lateral Stability Derivatives of a Jet-Flapped Wing. ARC R&M 3277, 1962. (U)
168. Thompson, J. S., Fail, R. A., and Inglesby, J. V.: Low Speed Wind Tunnel Measurements of the Oscillatory Lateral Stability Derivatives for a Model of a Slender Aircraft (HP 115) Including the Effects of Frequency Parameter. RAE TR 69018, 1969. (U)
169. Tobak, M.: Damping in Pitch of Low-Aspect-Ratio Wings at Subsonic and Supersonic Speeds. NACA RM A52L04a, 1953. (U)
170. Tobak, M., and Lessing, H. C.: Estimation of Rotary Stability Derivatives at Subsonic and Transonic Speeds. AGARD Report 343, 1961. (U)
171. Tobak, M., Reese, D. E. Jr., and Beam, B. H.: Experimental Damping in Pitch of 45° Triangular Wings. NACA RM A50J26, 1950. (U)
172. Tobak, M., and Wehrend, W. R.: Stability Derivatives of Cones at Supersonic Speeds. NACA TN 3788, 1956. (U)
173. Toll, T. A., and Queijo, M. J.: Approximate Relations and Charts for Low-Speed Stability Derivatives of Swept Wings. NACA TN 1581, 1948. (U)
174. Tosti, L. P.: Low-Speed Static Stability and Damping-in-Roll Characteristics of Some Swept and Unswept Low-Aspect-Ratio Wings. NACA TN 1488, 1947. (U)
175. Triplett, W. C., and Van Dyke, R. D., Jr.: Preliminary Flight Investigation of the Dynamic Longitudinal-Stability Characteristics of a 35° Swept-Wing Airplane. NACA RM A50J09a, 1950. (U)
176. Tucker, W. A., and Piland, R. O.: Estimating of the Damping in Roll of Supersonic-Leading-Edge Wing-Body Combinations. NACA TN 2151, 1950. (U)
177. Turner, K. J., Ross, A. J., and Earley, G.: The Dynamic Stability Derivatives of a Slender Wing, a Comparison of Theory with Free-Flight Model Tests at Near-Zero Lift, $M = 8.0$ to 2.4 . ARC CP 995, 1968. (U)
178. Turner, K. J., and Hunt, G. K.: Free-Flight Measurements for the Transonic Roll-Damping Characteristics of Three Related Wings of Aspect Ratio 2.83. ARC R&M 3274, 1962. (U)
179. Turner, K. J.: Measurements of Dynamic Stability from Three Simplified Free-Flight Models of a Supersonic Research Aircraft (Bristol T.188) Over the Mach Number Range 1.2-2.6. ARC CP 816, 1965. (U)
180. Vitale, A. J., McFall, J. C., Jr., and Morrow, J. D.: Longitudinal Stability and Drag Characteristics at Mach Numbers from 0.75 to 1.5 of an Airplane Configuration Having a 30° Swept Wing of Aspect Ratio 2.24 as Obtained from Rocket-Propelled Models. NACA L51K06, 1952. (U)
181. Walchner, O., and Clay, J. T.: Hypersonic Stability Derivatives of Blunted Slender Cones. AIAA Journal, Vol 8, No. 4, April 1966. (U)
182. Walker, H. J., and Ballantyne, M. B.: Pressure Distribution and Damping in Steady Roll at Supersonic Mach Numbers of Flat Swept-Back Wings with Subsonic Edges. NACA TN 2047, 1960. (U)
183. Wehrend, W. R., Jr.: A Wind-Tunnel Investigation of the Effect of Changes in Base Contour on the Damping in Pitch of a Blunted Cone NASA TN D-2062, 1963. (U)
184. Wehrend, W. R., Jr.: Wind-Tunnel Investigation of the Static and Dynamic Stability Characteristics of a 10° Semivortex Angle Blunted Cone. NASA TN D-1202, 1962. (U)
185. Wiggins, J. W.: Wind-Tunnel Investigation of Effect of Sweep on Rolling Derivatives at Angles of Attack up to 13° and at High Subsonic Mach Numbers, Including a Semiempirical Method of Estimating the Rolling Derivatives. NACA TN 4185, 1968. (U)

186. Wiggins, J. W.: Wind-Tunnel Investigation at High Subsonic Speeds to Determine the Rolling Derivatives of Two Wing-Fuselage Combinations Having Triangular Wings, Including a Semiempirical Method of Estimating the Rolling Derivatives. NACA RM L53L18e, 1953. (U)
187. Williams, J. L.: Measured and Estimated Lateral Static and Rotary Derivatives of a 1/12-Scale Model of a High-Speed Fighter Airplane with Unswept Wings. NACA RM L53K09, 1954. (U)
188. Woithart, W. D.: Influence of Wing and Fuselage on the Vertical-Tail Contribution to the Low-Speed Rolling Derivatives of Midwing Airplane Models with 45° Swept Back Surfaces. NACA TN 2587, 1951. (U)
189. Wood, R. M., and Murphy, C. H.: Aerodynamic Derivatives for Both Steady and Nonsteady Motion of Slender Bodies. Jour. of Aero. Sci., Vol. 22, No. 12, 1955. (U)
190. Woodgate, L., and Pugh, P. G.: Measurements of the Pitching-Moment Derivatives on a Sharp-Edged Delta Wing in Incompressible Flow. ARC R&M 3379, 1963. (U)
191. Wright, B. R., and Brower, M. L.: Aerodynamic Damping and Oscillatory Stability in Pitch for a Model of a Typical Subsonic Jet-Transport Airplane. NASA TN D-3159, 1966. (U)
192. Zartarian, G., and Ashley, H.: Forces and Moments on Oscillating Slender Wing-Body Combinations at Supersonic Speed, Part I - Basic Theory. OSR TN 57-386, MIT Fluid Dynamics Research Group Rpt. 57-2, 1957. (U)

TABLE 7-A

DYNAMIC DERIVATIVES

Ref.	Derivative	A	$\Delta(\lambda)$ (deg)	λ	M	Freq.	Ampl.	Config.
2	$C_m_q + C_{m\dot{\alpha}}$	-	-	-	.5 → 1.5	X	X	S
3	$C_m_q + C_{m\dot{\alpha}}$	4	45 LE	0	.10 → .95	X	X	WB
4	$C_m_q + C_{m\dot{\alpha}}, C_{l_p}, C_{n_p}$ $C_{l_r} - C_{l_p}, C_{n_r} - C_{n_p}$	2.2	60 LE	.03	.25 → .95	X	X	WB
5	C_l_p	10 5.9 2.5	2 c/4 42 62 ↓	.5	Low speed	-	-	W
6	$C_m_q + C_{m\dot{\alpha}}$ $C_{n_r} - C_{n_p} \cos \alpha$	4	45 c/4	.2	.70 → 1.15	X	X	WBHV, BHV, WBH, WBV
7	C_Y_r, C_{n_r}, C_{l_r}	2.63	45 c/4	1.0	.13	-	-	W, WB
8	C_Y_r, C_{n_r}, C_{l_r}	2.61	45 c/4	1.0	.13	-	-	W, WB
9	$C_{l_p}, C_{n_p}, C_{Y_p}$	2.61	45 c/4	1.0	.17	-	-	W, WB
10	C_{n_r} (theor.)	1.5, 3.5, 6	0, 30, 45, 60 c/4	0, .5, 1.5	Low speed	-	-	W
11	C_{l_p} (theor.)	1.5, 3.5, 6, 10	0, 30, 45, 60 c/4	0, .5, 1.0	Low speed	-	-	W
12	$C_{n_p}, C_{l_p}, C_{Y_p}$ $C_{n_r}, C_{l_r}, C_{Y_r}$	4.51	35 c/4	1.84	.17 .13	-	-	WB

TABLE 7-A (CONTD)

Ref.	Derivative	A	$\Delta(\lambda)$ (deg)	λ	M	Freq.	Ampl.	Config.
13	$C_{X_p}, C_{Y_p}, C_{n_p}$	2.83	45 LE	1.0	.17	-	-	W, WB
14	C_{ℓ_p}	4	45 LE	0	.8 → 1.8	-	-	W, WB
15	C_{ℓ_p}	3.7	0, 45 LE	1.0	.8 → 1.7	-	-	W, WB
16	C_{ℓ_p}	4.0	45 LE 0 c/2	0 .5	.8 → 1.7	-	-	W, WB
17	$C_{m_q} + C_{m_\alpha}$	-	-	-	1.1 → 2.4	X	-	B
19	$C_{Y_p}, C_{n_p}, C_{\ell_p}$	2.61	0 c/4 45 c/4	.5, 1.0 .5, .25, 1.0	.17	-	-	W
20	βC_{ℓ_p}	1.47 → 4.0	0 → 45 LE (12 configurations)	1.0, 0	1.62, 1.92	-	-	WB
21	C_{L_q}, C_{m_q} C_{ℓ_p} (theor.)	$4 \cot \Delta_{LE}$	$\tan^{-1} \frac{4}{A} LE$	0	Supersonic	-	-	W
22	$C_{m_q} + C_{m_\alpha}, C_{\ell_p}, C_{n_p},$ $C_{\ell_r} - C_{\ell_\beta}, C_{n_r} - C_{n_\beta}$	2.44	27 LE	.38	.25 → .94	X	X	WBHV, WBV, B, WB, BV, BHV
23	$C_{n_p}, C_{\ell_p}, C_{n_r}, C_{\ell_r},$ $C_{n_\beta}, C_{\ell_\beta}$ (theor.)	2.2	60 LE	0	-	X	-	WBV
24	C_{n_r}	6 6.7	0 LE	1.0 .40	Low speed	-	-	W WB
25	$C_{n_r} - C_{n_\beta}$ $C_{\ell_r} - C_{\ell_\beta}$	2.31 2.61 3.0	60 LE 45 c/4 0 c/2	0 .26 .50	Low speed	X	X	W
26	C_{ℓ_r}	1.34 2.61 5.16 2.61 4 2.31	{ 0 LE 45 60 45 45 52.2 c/4 }	1.0 .50, .25 .8 0	Low speed	-	-	W, WB
27	$C_{m_q} + C_{m_\alpha}$	2.83	50.86 c/4	0	.70 → 1.37	-	-	WB
28	$C_{m_q} + C_{m_\alpha}$	-	-	-	14.2	-	-	B
29	$C_{L_\alpha}, C_{m_\alpha}$ (theor.)	$\beta A = 3 \rightarrow 20$ $\beta A = 2 \rightarrow 20$	$\beta \cot \Delta_{LE} = 1 \rightarrow \infty$ $\beta \cot \Delta_{LE} = 1 \rightarrow \infty$	0, .25, .5, .75 1.0	Supersonic	-	-	W
30	C_{ℓ_p}	2	63.4 LE	0	1.35 → 2.03	X	X	WBV
31	C_{n_β}	9.20	6 c/4	.48	Low speed	X	X	W, WB, WBV, WBHV

TABLE 7-A (CONT'D)

Ref.	Derivative	A	$\Delta(\lambda)$ (deg)	λ	M	Freq.	Ampl.	Config.
33	$C_{m_q} + C_{m_{\dot{\alpha}}}$	2	63.43 LE	0	.80 → 1.35	—	—	WB
		3	53.07 LE					
34	$C_{m_q} + C_{m_{\dot{\alpha}}}$.4	45 LE	0	.7 → 1.35	—	—	WB
		3	37.5 ↓	.6				
		3.6	39. ↓	.4				
35	$C_{m_q} + C_{m_{\dot{\alpha}}}$	4	40 c/4	.5	.80 → 1.36	—	—	WB
36	$C_{m_q} + C_{m_{\dot{\alpha}}} - k^2 C_{m_q'}$ $C_{\beta_p} \cos \alpha + k^2 C_{\beta_r'}$ $C_{n_r} - C_{n_{\beta}} \cos \alpha,$ $C_{n_{\beta}} \cos \alpha + k^2 C_{n_r'}$	1.66	70/75 LE	—	2.4, 2.98, 3.6	X	X	WBHV, WBV, WBH
37	C_{β_p}	4.5	0 LE	1.0	.85 → 1.45	—	—	WB
38	$C_{L_{\dot{\alpha}}}, C_{m_{\dot{\alpha}}}, C_{L_q}, C_{m_q}$ (theor.)	—	—	—	Supersonic	X	X	B
39	$C_{m_q} + C_{m_{\dot{\alpha}}}$	—	—	—	.7 → 5.0	X	X	B
40	C_{β_p}	3.71	0 LE	1.0	.85 → 1.40	—	—	WB
41	$C_{m_q} + C_{m_{\dot{\alpha}}}$	2	63.4 LE	0	.6 → 1.18	X	X	WB
		3	—	.4065				
42	$C_{m_q}, C_{m_q} + C_{m_{\dot{\alpha}}'}$ $C_{m_{\dot{\alpha}}} - \bar{\omega}^2 C_{m_q'}$	—	—	—	.25 → 5	X	X	B
43	$C_{m_q} + C_{m_{\dot{\alpha}}}$	—	—	—	5, 6, 7, 8	—	—	B
44	$C_{Y_p}, C_{n_p}, C_{\beta_p}$	2.61	-45 LE	1.0	.17	—	—	W
		5.16	0 ↓					
		2.61	45 ↓					
		1.34	60 ↓					
45	$C_{m_q} + C_{m_{\dot{\alpha}}}, C_{m_q}$.4 (exposed)	0 LE	1	4.8, 8.08, 10,	X	—	B, WB
		.8 ↓	79 ↓	0	17			
		1.6 ↓	70 ↓	0				
46	$C_{L_q}, C_{m_q}, C_{\beta_r},$ $C_{\beta_p}, C_{n_p}, C_{Y_p}$ C_{β_p} (theor.)	4	30 c/4	—	0 → 1.0	—	—	W
		4	50 ↓	—	0 → 1.0			
		2, 6 ↓	0 ↓	1.0 ↓	0 → .9			
		4 ↓	30 ↓					
		4 ↓	45 ↓					
47	C_{n_r}	4	45, 0 c/4	.6	Low speed	—	—	WB

TABLE 7-A (CONTD)

Ref.	Derivative	A	$\Delta(\lambda)$ (deg)	λ	M	Freq.	Ampl.	Config.
48	C_{L_q}, C_{m_q} (theor.)	-	-	-	Hypersonic	-	-	B
49	C_{q_r}, C_{n_r} , $C_{n_r} - C_{n_\beta}, C_{q_r} - C_{q_\beta}$	2.31 4	60 LE 0, 45 c/4	0 .6	.13	X	X	W
50	C_{n_r}, C_{q_r}	2.31 4	60 LE 0, 45 c/4	0 .6	.13	X	X	W
51	C_{n_p}, C_{q_p}	2.31	60 LE	0	.13	X	X	W, WB
52	$C_{Y_p}, C_{n_p}, C_{q_p}$	3.60	41.57 LE	.455	.13, .16	-	-	W, WB
53	$C_{Y_p}, C_{n_p}, C_{q_p}$	6	2 c/4	.5	.13	X	X	WB
54	$C_{n_r} - C_{n_\beta}, C_{q_r} - C_{q_\beta}$	2.31	60 LE	0	.13	X	X	W
55	$C_{m_q} + C_{m_\alpha}$	3	16 c/4	.4	.9 → 1.36	-	-	WB
56	$C_{m_q} + C_{m_\alpha}$	1.87 → 6.02	1.9 → 60 c/4 (18 configurations)	0 → 1.63	.6 → 1.7	-	-	WB
57	$C_{m_q} + C_{m_\alpha}$	3	16 c/4	.4	.8 → 1.4	-	-	WB
58	C_{N_q} (theor.), C_{m_q} , $C_{m_q} + C_{m_\alpha}$	1.456	70 LE	0	8.08	-	X	B, W
59	$C_{Y_p}, C_{n_p}, C_{q_p}$	2.31	60 LE	0	.17	-	-	W, WB
60	C_{q_p}	1.34 → 5.9	0 → 60 c/4 (22 configurations)	0 → 1.0	0 → 1.3	-	-	W
61	$C_{q_p}, C_{n_p}, C_{Y_p}$	1.34 ↓ 2.61 ↓ 5.16 ↓	0 LE 45 60 0 45 60 0 45 60	1.0	.13, .17	-	-	W
62	$C_{q_p}, C_{n_p}, C_{Y_p}$	1.34 ↓ 2.81 ↓ 5.16 ↓	0 LE 45 60 0 45 60 0 45 60	1.0	.17	-	-	W

TABLE 7-A (CONT'D)

Ref.	Derivative	A	$\Delta(\lambda)$ (deg)	λ	M	Freq.	Ampl.	Config.
63	$C_{\delta_r}, C_{Y_r}, C_{n_r}$	1.34 ↓ 2.61 ↓ 5.16 ↓	0 LE 45 60 0 45 60 0 45 60	1.0	.13	-	-	W
64	$C_{n_r}, C_{Y_r}, C_{\delta_r}$	2.61 5.16 2.61 1.34	-45 LE 0 45 60	1.0	.13	-	-	W
66	$C_{m_q} + C_{m\dot{\alpha}}$ (theor.)	2.83	45 c/2	.333	.92 → 1.35	X	-	WB
66	$C_{L_q}, C_{m_q}, C_{\delta_q}, C_{L\dot{\alpha}}, C_{m\dot{\alpha}}$ $C_{\delta_p}, C_{m_p}, C_{\delta_p}$, $C_{L_p} + .263 C_{L\dot{\alpha}}$, and other combinations	3.35	0	1.0	0 → .125	X	X	W
67	$C_{L_q}, C_{m_q}, C_{\delta_p}, C_{Y_p}$, $C_{n_p}, C_{\delta_r}, C_{Y_r}, C_{n_r}$, (theor.)	$\beta A = 1 \rightarrow 20$	0 LE	1.0	Supersonic	-	-	W
68	C_{δ_p} or C_{X_r}, C_{Y_p} or C_{Y_r} , C_{n_p} or C_{n_r} (theor.)	$\beta A = 0 \rightarrow 20$	-	-	Supersonic	-	-	W
69	C_{δ_p} (theor.)	2.4 2.4 $0 \rightarrow 10$ 2.4 $\beta A = 3, 4, 5, 6,$ $8, 10, 12, 16, 20$	53 LE 0 → 60 53 53 $\beta \cos \Lambda = 1 \rightarrow \infty$.5 .5 .5 0 → 1.0 0, .25, .5, .75, 1.0	1.2 → 2.6 2 2 2	-	-	W
70	$C_{m_q} + C_{m\dot{\alpha}}$ (theor.)	1.07 2.31 4 6.93	75 LE 60 45 30	0	1 → 5 1 → 3 1 → 1.8 1 → 1.5	-	-	WB
71	$C_{\delta_p} + C_{\delta_p} \sin \theta$, $C_{n_r} - C_{n_p} \cos \theta$	2.2	60 LE	0	Low speed	-	-	WB
72	C_{δ_r}, C_{n_r} (theor.)	6, 1.25	0 LE	1.0	-	-	-	W
73	$C_{m_q} + C_{m\dot{\alpha}}$	3.57	35 .3c	.565	.6 → .96	-	-	WB
74	C_{L_q}, C_{m_q} (theor.)	2	60 LE	0	.13	-	-	W
75	C_{δ_p}	2.3	45, 60 LE	0	.8 → 1.8	-	-	WB

TABLE 7-A (CONT'D)

Ref.	Derivative	A	$\Delta(\)$ (deg)	λ	M	Freq.	Ampl.	Config.
76	$C_{L_d}, C_{m_d}, C_{L_{\dot{\alpha}}}, C_{m_{\dot{\alpha}}}$ $C_{Y_p}, C_{\ell_p}, C_{n_p}$ $C_{Y_r}, C_{\ell_r}, C_{n_r}$ (theor.)	-	-	-	.6, 1.2	-	-	WBHV
77	C_{m_q} (theor.)	-	78 \rightarrow 88 LE	0	10, 17	-	-	W
78	$C_{m_q} + C_{m_{\dot{\alpha}}}, C_{\ell_p}, C_{n_r}$	1.96	-	0	.74 \rightarrow 1.4	X	X	WBHV
79	C_{ℓ_p}	3.12 4.69 4.62 4.84 3.64	-45 c/4 -30 0 30 45	.38 .40 .55 .44 .42	Low speed, high speed	-	-	W
81	$C_{m_q} + C_{m_{\dot{\alpha}}}$	-	-	-	2.01, 3.02, 4.56	X	-	B
82	$C_{Y_p}, C_{n_p}, C_{\ell_p}$	2.31	60 LE	0	.13	-	-	W, WB
83	$C_{Y_r}, C_{n_r}, C_{\ell_r}$	2.31	60 LE	0	.13	-	-	WB
84	$C_{Y_p}, C_{n_p}, C_{\ell_p}$	2.31 1.07 4 3 2 1	60 LE 75 45 0	0 0 .15 .36 .58	.13	-	-	W
85	$C_{\ell_p}, C_{n_p}, C_{n_r}$	2.2	60 LE	0	Low speed	-	-	WB
86	C_{ℓ_p}, C_{n_r}	2.31 2.61 3.0	60 LE 45 c/4 0 c/2	0 .25 .50	Low speed	X	-	W
87	βC_{ℓ_p} (theor.)	-	0 LE	1.0, 0	Supersonic	-	-	W
88	$C_{m_q} + C_{m_{\dot{\alpha}}}$	3	35 c/4	.6	High subsonic, transonic	-	-	W
89	$C_{m_q} + C_{m_{\dot{\alpha}}}$ $C_{m_q} + C_{m_{\dot{\alpha}}} \text{ (theor.)}$	2.309	60 LE	0	Supersonic	-	-	WB
90	$C_{m_q} + C_{m_{\dot{\alpha}}}$ $C_{m_q} + C_{m_{\dot{\alpha}}} \text{ (theor.)}$	2.0	63.4 LE	0	Transonic	X	X	WB
91	$C_{m_q} + C_{m_{\dot{\alpha}}}$ $C_{n_r} - C_{n_r} \cos \alpha$.904	62 LE	.418	.8, .9, 1.0, 1.2	X	X	WB + Canard
92	C_{L_q}, C_{m_q} (theor.)	-	-	-	8.8, 17	-	-	B

TABLE 7-A (CONT'D)

Ref.	Derivative	A	$\Delta(\lambda)$ (deg)	λ	M	Freq.	Ampl.	Config.
93	C_{ℓ_p}	4	3.6, 32.6, 46 c/4	.6	.4 → .91	—	—	W
94	C_{ℓ_p}	4 2.31	3.6, 32.6, 45 c/4 60 LE	.6 0	.2 → .91	—	—	WB
95	$C_{n_p}, C_{Y_p}, C_{\ell_p}$	4	45 c/4	.6	.4 → .95	—	—	WB
96	$C_{m_q} + C_{m_{\dot{\alpha}}}$ $C_{n_r} - C_{n_{\dot{\beta}}} \cos \alpha_r$ $C_{\ell_r} - C_{\ell_{\dot{\beta}}} \cos \alpha_r$ $C_{\ell_p} + C_{\ell_{\dot{p}}} \sin \alpha_r$ $C_{n_p} + C_{n_{\dot{p}}} \sin \alpha_r$	2.44	27 LE	.38	2.5, 3.0, 3.6	X	X	WB, WBHV
97	$C_{L_{\dot{\alpha}}}, C_{m_{\dot{\alpha}}}, C_{L_q}, C_{m_q}$ $C_{m_q} + C_{m_{\dot{\alpha}}} (\text{theor.})$	1.0 1.5 2.0 2.5 3.0 3.5 4.0	75.9 LE 69.5 63.4 58. 53.1 48.8 45	0	Transonic	X	X	W
98	$C_{L_{\dot{\alpha}}}, C_{m_{\dot{\alpha}}}, C_{L_q}, C_{m_q}$ $C_{m_q} + C_{m_{\dot{\alpha}}} (\text{theor.})$	1.5 2.0 2.5	69.5 LE 63.4 58.	0	Transonic	X	X	B, W, WB
99	$C_{L_q}, C_{m_q}, C_{L_{\dot{\alpha}}}, C_{m_{\dot{\alpha}}}$ (theor.)	1.2 2.0 3.0 1.32	68.2 LE	.143 .389	Subsonic Subsonic .4 → .9 Subsonic	X X X X	X X X X	W
100	$C_{Y_p}, C_{n_p}, C_{\ell_p}$	2.61	45 LE	1.0	.17	—	—	W
101	$C_{Y_r}, C_{n_r}, C_{\ell_r}$	2.61	45 LE	1.0	.13	—	—	W
102	C_{ℓ_r}, C_{n_r}	2.31 4	60 LE 45.0 c/4	0 .6	Low speed	X	X	W, WB
103	$C_{Y_p}, C_{n_p}, C_{\ell_p}$	4	46.7 c/4	.6	.13	—	—	W
104	$C_{Y_r}, C_{n_r}, C_{\ell_r}$	2.61	45 c/4	1.0, .50, .25	.13	—	—	W
105	$C_{Y_p}, C_{n_p}, C_{\ell_p}$	4	0 c/4	.6	.17	—	—	W, WB
106	$C_{Y_r}, C_{n_r}, C_{\ell_r}$	4	45 c/4	.6	.13	—	—	W, WB
107	$C_{\ell_r} - C_{\ell_{\dot{\beta}}}$ $C_{n_r} - C_{n_{\dot{\beta}}}$.53 1.07 2.31	82.5 LE 75 60	0	.13	X	X	W

TABLE 7-A (CONT'D)

Ref.	Derivative	A	$\Delta(\lambda)$ (deg)	λ	M	Freq.	Ampl.	Config.
108	$C_{Y_r}, C_{n_r}, C_{\alpha_r}, C_{Y_p},$ $C_{n_p}, C_{\alpha_p}, C_{n_r} - C_{n_p},$ $C_{\alpha_r} - C_{\alpha_p}$	2.51	60 LE	0	.13	X	X	WB
109	$C_{\alpha_r}, C_{n_r}, C_{Y_r}$	2.61	45 LE	1.0	.13	-	-	W
110	C_{α_p}	4	42.7 LE	.5	.6 → 1.15, 1.9	-	-	W
111	C_{α_p}	4	0 c/4 35 45 ↓	.6	.8, .7, .8, 85, .9, .95, 1.0, 1.05, 1.10, 1.15	-	-	WB
112	C_{α_p} (theor.)	Low	45 LE	0, ~1.0	Low	-	-	W, WB
113	$C_{\alpha_p}, C_{n_p}, C_{\alpha_r}, C_{n_r},$ $C_{m_q} + C_{m_{\alpha}}, C_{n_r} - C_{n_p},$ $C_{\alpha_r} - C_{\alpha_p}$	3.66	45 c/4	.3	.23 → .94	X	X	B, WB, WBH, BH, WBHV, BHV, BV
114	C_{α_p}	6.38 6.	0 LE 18.4 ↓	1.0 .333	Subsonic	-	-	W
115	C_{m_q}, C_{L_q}	1.34 2.61 5.18 2.61	0 LE 45 60 -45 ↓	1.0	.13	-	-	W
116	C_{α_p}	2 3 5.9	42 LE -36, 42 LE -36, 42 LE	.793 .707 .50	Low speed	-	-	W
117	C_{L_q}, C_{m_q} C_{L_q} (theor.)	$\beta A = 2 \rightarrow 10$ 2.4 $\beta \rightarrow 9$ 2.4 2.4	- 53 LE 53 45 → 66 53 ↓	.25, .50, .75 .5 .5 .5 0 → .75	Supersonic Supersonic	-	-	W
118	$C_{L_{\alpha}}, C_{m_{\alpha}}$ (theor.)	$\beta A = 2 \rightarrow 10$	$\beta \cot \Delta_{LE} = 0 \rightarrow 1$.25, .50, .75	Supersonic	-	-	W
119	C_{α_p} (theor.)	2.4 1.65 → 5.4 2.4	53 LE 53 45 → 66 ↓	.5 .5 .5	1.2 → 1.6 1.5 1.414	-	-	W
120	C_{α_p} (theor.)	2.4 2.4 1.8, 5.4 2.4 $\beta A = 2, 3, 4, 5,$ 8, 8, 10	53 LE 45 → 60 53 53 ↓ $\beta \cot \Delta = 0 \rightarrow 1.0$.5 .5 .5 0, .7 0, .25, .50	1.2 → 1.6 1.5 1.5 1.414	-	-	W

TABLE 7-A (CONTD)

Ref.	Derivative	A	$\Delta(\lambda)$ (deg)	λ	M	Freq.	Ampl.	Config.
121	$C_{L\dot{\alpha}}, C_{m\dot{\alpha}}, C_{Lq}, C_{mq}$ $C_{\dot{p}}, C_{n\dot{p}}, C_Y, C_{\dot{p}}$ C_{n_r}, C_Y (theor.)	$\frac{\beta A}{4} < 1$	$\beta \cot \Delta_{LE} < 1$ $\beta \cot \Delta_{LE} >$ $\frac{4 \cot \Delta_{LE}}{1 - \frac{A}{A}}$	0	Supersonic	--	-	W
122	$C_{L\dot{\alpha}}, C_{m\dot{\alpha}}, C_{Lq}, C_{mq}$ $C_{mq} + C_{m\dot{\alpha}}$ (theor.)	$4 \cot \Delta_{LE}$	$\tan^{-1} \frac{4}{A} \Delta_{LE}$	0	Subsonic, transonic, supersonic	X	X	W
123	$C_{\dot{p}} / (AR)^3$.5, 1, 2	-	0	$1.2 \rightarrow 2.5$	-	-	W
124	$C_{\dot{p}} / (AR)^3$.5, 1, 2	-	0	-	-	-	W
125	$C_{mq} + C_{m\dot{\alpha}}$ (theor.)	3.20	55 LE	0	$1.414 \rightarrow 3.0$	-	-	WBH
126	C_{Lq}, C_{mq} (theor.)	$\beta A = 3 \rightarrow 20$ $\beta A = 2 \rightarrow 20$	$\beta \cot \Delta_{LE} = 1 \rightarrow \infty$	0, .25, .5, .75 1.0	Supersonic	-	-	W
127	$C_{\dot{p}}, C_{n\dot{p}}$ (theor.)	4 9.021	- -	.8 .4	-	-	-	W
128	$C_{\dot{p}}$	$1.82 \rightarrow 3.4$	$21.2 \rightarrow 70$ LE (28 configurations)	0, .25	1.62, 1.83, 2.41	-	-	W
129	C_{mq} (theor.)	-	-	-	Supersonic	X	X	W
130	$C_{mq} + C_{mD\dot{\alpha}}$	2.31	60 LE	0	$.76 \rightarrow 1.70$	-	-	WB
131	$C_{mq} + C_{mD\dot{\alpha}}$	3.07	40 c/2	1.826	.55 \rightarrow 1.2	-	-	WB
132	$C_{\dot{p}}$	3	36 c/4	.8	.4 \rightarrow .91	-	-	WB
133	$C_{\dot{p}}, C_{n\dot{p}}, C_{\dot{p}}$ (theor.) C_{n_r}	3.8 3.0 2.3	45 LE	.026 .147 .274	.2 \rightarrow 9	X	-	WBHV
134	$C_{Nq}, C_{N\dot{\alpha}}, C_{mq}, C_{m\dot{\alpha}}$ $C_{mq} + C_{m\dot{\alpha}}$ (theor.)	-	-	-	$1.1 \rightarrow 5$	-	-	B
135	$C_{Nq}, C_{N\dot{\alpha}}, C_{mq}, C_{m\dot{\alpha}}$ (theor.)	-	-	-	$1.1 \rightarrow 5$	-	-	B
136	$C_{mq} + C_{m\dot{\alpha}}$ (theor.)	-	87, 84, 81 LE	0	9, 17	-	-	W
137	$C_{m\dot{\theta}}, C_{L\dot{\theta}}$	3. 2. 1.25 3. 2. 1.25	49.1 LE 60 70.1 49.1 60 70.1	.072 .238	$1.22 \rightarrow 2,$ $5 \rightarrow 1.14$	X	X	W

TABLE 7-A (CONT'D)

Ref.	Derivative	A	$\Delta(\lambda)$ (deg)	λ	M	Freq.	Ampl.	Config.
138	$C_{m_q} + C_{m_{\dot{\alpha}}}$	6.02	0, 4c	.5	.6 → 1.17	X	—	WB
139	$C_{m_q} + C_{m_{\dot{\alpha}}}$	4	45 c/4	.6	.63 → 1.16	—	—	WB
140	$C_{n_r}, C_{\ell_r}, C_{n_p}, C_{\ell_p}$ (theor.)	6, 10, 16	0 c/4	1, 50, .25	—	—	—	W
141	$C_{m_q} + C_{m_{\dot{\alpha}}}$	2.31	60 LE	0	.9 → 1.37	—	—	WB
142	C_{ℓ_p} (theor.)	2 → 8	0 → 69.4 LE (44 configurations)	0 → 1.0	Supersonic	—	—	W
143	C_{ℓ_p}	.75, 1.0	—	0	Low speed	—	—	W
144	$C_{N_{\dot{\alpha}}} + C_{N_q}$ (theor.), $C_{m_q} + C_{m_{\dot{\alpha}}}$	—	—	—	.7 → 8.2, 1.1 → 2.4	—	—	B
145	$C_{m_q} + C_{m_{\dot{\alpha}}}$ $C_{N_{\dot{\alpha}}} + C_{N_q}$ (theor.)	—	—	—	1.2 → 3.0	—	—	B
146	C_{ℓ_p} (theor.)	1.0 → 5	0 → 60 c/4	0 → 1.0	—	—	—	W
147	$C_{Y_p}, C_{n_p}, C_{\ell_p}$	2.61	45 LE	1.0	Low speed	—	—	W
148	$C_{\ell_r}, C_{n_r}, C_{Y_r}$	2.61	45 LE	1.0	.13	—	—	W
149	$C_{n_r}, C_{\ell_r}, C_{Y_r}$	2.31 4.0	60 LE 0, 45 c/4	0 .6	Low speed	—	—	W
150	$C_{Y_p}, C_{n_p}, C_{\ell_p}, C_{Y_r},$ C_{n_r}, C_{ℓ_r}	3.57	35 c/3	.566	.13, .17	—	—	WB
151	C_{ℓ_p} (theor.)	—	—	—	14	—	—	B
152	$C_{L_{\dot{\alpha}}}, C_{m_q}, C_{\ell_p}, C_{\ell_r},$ $C_{n_p}, C_{n_r}, C_{Y_p}, C_{Y_r}$ (theor.)	<.5	—	0	Subsonic Supersonic	—	—	W
153	$C_{L_{\dot{\alpha}}}, C_{m_{\dot{\alpha}}}, C_{\ell_r}, C_{Y_r}$ C_{n_p}, C_{Y_p} (theor.)	$\frac{\beta A}{4} < 1$	$\beta \cot \Delta_{LE} < 1$	0	Supersonic	—	—	W
154	$C_{m_q} + C_{m_{\dot{\alpha}}}$	Varies	Varies	Varies	.5 → 21	X	X	B
155	C_{ℓ_r}, C_{n_r} (theor.) C_{n_p}, C_{ℓ_p}	1	—	0	Low speed	—	—	W + fin

TABLE 7-A (CONT'D)

Ref.	Derivative	A	Δ_1 (deg)	λ	M	Freq.	Ampl.	Config.
156	$C_{m_q} + C_{m\dot{\alpha}}$	3.6	41.57 LE	.456	.4 → .88	—	—	WB
157	C_{ℓ_p}	4 3.5 2.9 4 3.5 6	42.7 LE 36.5 23.1 374, 46.7, 60.9 63 46.2	.5 .56 .41 .8 .26 .6	.7 → 1.4	—	—	WB
158	C_{ℓ_p}	3.71	0, 45 c/4	1, .5, .3, 0	.8 → 1.45	—	—	WB
159	C_{L_q}, C_{m_q}	1.2 1.6 1.32	68.2 LE	.143 0 .389	Subsonic	X	—	W
160	$C_{m\dot{\beta}}$	4.4	0	1	1.37 → 2.43	X	—	W
161	C_{m_q} (theor.)	—	—	—	Supersonic	—	—	B
162	$C_{L_\alpha}, C_{m_\alpha}, C_{L_q}, C_{m_q}$	—	—	—	.5 → .8	X	—	WBHV
163	$C_{L_q}, C_{m_q}, C_{L_q}, C_{m_q}$	2.46	—	—	.70 → 1.10	X	—	WBHV
164	$C_{L_\alpha}, C_{m_\alpha}, C_{L_q}, C_{m_q}$ (theor.)	—	—	—	.30, .50, .70, .75	X	X	WBH
165	C_{ℓ_p}	3.7	—	1.0	.6 → 1.4	—	—	WB
166	C_{ℓ_p} (theor.)	6	—	1, .5, .25	—	—	—	W
167	$C_{\ell_p}, C_{\ell_r}, C_{n_p}, C_{n_r}$ (theor.)	4, 6, 8	—	—	—	—	—	W
168	$C_{n_r} - C_{n\dot{\beta}} \cos \alpha,$ $C_{Y_r} - C_{Y\dot{\beta}} \cos \alpha,$ $C_{\ell_r} - C_{\ell\dot{\beta}} \cos \alpha,$ $C_{n_p} + C_{n\dot{\beta}} \sin \alpha,$ $C_{Y_p} + C_{Y\dot{\beta}} \sin \alpha,$ $C_{\ell_p} + C_{\ell\dot{\beta}} \sin \alpha$.92	74 LE	0	.094 → .267	X	—	WBV
169	$C_{m_q} + C_{m\dot{\alpha}}$	2 3 4 3 3	63.4 LE 53 45 45 19.1	0 .403 .407	1.2 → 1.9	—	—	WB

TABLE 7-A (CONT'D)

Ref.	Derivative	A	$\Delta(\lambda)$ (deg)	λ	M	Freq.	Ampl.	Config.
170	$C_{L\dot{\alpha}}, C_{m\dot{\alpha}}, C_{L\alpha}, C_{m\alpha}$ $C_{m_q} + C_{m\dot{\alpha}}$ (theor.)	$0 < \beta A < 4$	$\tan^{-1} \frac{4}{A} LE$	0	$0 \rightarrow 1.0$	-	-	W
171	$C_{m_q} + C_{m\dot{\alpha}}$	4	45 LE	0	$1.15 \rightarrow 1.70$	-	-	W, WB
172	$C_{L\dot{\alpha}}, C_{m\dot{\alpha}}, C_{L\alpha}, C_{m\alpha}$ (theor.)	-	-	-	Supersonic, hypersonic	-	-	B
173	$C_{\rho_p}, C_{n_p}, C_{Y_p}$ $C_{\rho_r}, C_{n_r}, C_{Y_r}$ C_{L_q}, C_{m_q}	2.81 5.16 2.81 1.34	-45 LE 0 45 60	1.0	Low speed	-	-	W
174	C_{ρ_p}	$.5 \rightarrow 10$	$0 \rightarrow 80.4 c/4$ (17 configurations)	$0 \rightarrow 1.0$	Low speed	-	-	W
175	$C_{m_q} + C_{m\dot{\alpha}}$	4.79	$35.23 c/4$.51	$.5 \rightarrow 1.04$	-	-	WB
176	C_{ρ_p} (theor.)	-	0	1.0 0	-	-	-	WB
177	$C_{m_2} + C_{m\dot{\alpha}}, C_{\rho_p},$ $C_{n_r} - C_{n\dot{p}}$.886	73.3 LE	0	$1.06 \rightarrow 1.8$	x	-	W + fin
178	C_{ρ_p}	2.83	27.95, 53.55 LE 49.97	.33 .066	.7 \rightarrow 1.4	-	-	WBV
179	C_{ρ_p}, C_{n_r}	3.1	0/38/66 LE	(.13)	$1.2 \rightarrow 2.6$	x	-	WBHV
180	$C_{m_q} + C_{m\dot{\alpha}}$	2.24	$60 c/4$.333	$.75 \rightarrow 1.50$	-	-	WB
181	C_{m_q} (theor.)	-	-	-	-	-	-	B
182	C_{ρ_p}	3.5	63 LE	.25	$1.2 \rightarrow 1.7$	--	-	W
183	$C_{m_q} + C_{m\dot{\alpha}}$	-	-	-	$.26 \rightarrow 2.20$	-	x	B
184	$C_{m_q} + C_{m\dot{\alpha}}$	-	-	-	$.86 \rightarrow 2.20$	x	x	B
185	$C_{Y_p}, C_{n_p}, C_{\rho_p}$	4	$3.6, 32.6, 45, 60 c/4$.6	$.5 \sim .95$	-	-	WB
186	$C_{\rho_p}, C_{n_p}, C_{Y_p}$	4 3.31	45 LE 60	0	$.5 \rightarrow .95$	-	-	WB
187	$C_{Y_p}, C_{n_p}, C_{\rho_p}$ $C_{Y_r}, C_{n_r}, C_{\rho_r}$	5.80	0 LE	.473	.13, .17	-	-	WB

TABLE 7-A (CONTD)

Ref.	Derivative	A	$\Delta(\lambda)$ (deg)	λ	M	Freq.	Ampl.	Config.
188	$C_{Y_p}, C_{n_p}, C_{\rho_p}$	4	45 c/4	.6	.17	-	-	W
189	$C_{L_\alpha}, C_{m_\alpha}, C_{L_q}, C_{m_q}$ (theor.)	-	-	-	Supersonic	-	-	B
190	C_{m_q}	1.484	-	0	.09, .18	X	X	W
191	$C_{m_q} + C_{m_\alpha'}$ $C_{m_\alpha'} - k^2 C_{m_q}$	7.035	41.5/37.5 LE	(.33)	.20 → .94	X	X	WB
192	$C_{L_\alpha}, C_{m_\alpha}, C_{L_q}, C_{m_q}$ $C_{m_q} + C_{m_\alpha}$ (theor.)	1.5 2.0 2.5	69.5 LE 63.4 58 ↓	0	Supersonic	-	-	B, W, WB

7.1 WING DYNAMIC DERIVATIVES

The methods presented in this section are to be used for the estimation of pitching, acceleration, rolling, and yawing dynamic derivatives of isolated lifting surfaces. The methods and charts applicable to this section are based on lifting-surface theory for subsonic speeds and on linearized theory for supersonic speeds. The charts are thus limited to conditions for which the flow is essentially attached over the surface of the wing, i.e., the linear lift-curve range. This means that at subsonic speeds the methods are valid for high-aspect-ratio wings up to stall angles of attack but are limited for low-aspect-ratio wings to low angles of attack.

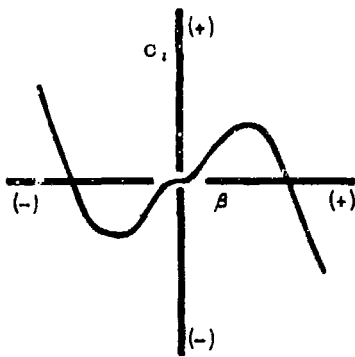
For wings operating under conditions of partially separated flow, such as low-aspect-ratio wings at moderate to high angles of attack, experimental data, e.g., references 1 and 2, show that substantial nonlinearities exist in the dynamic derivatives. In addition, tests made by wind-tunnel oscillating-mode techniques show that the dynamic derivatives are functions of both the amplitude and frequency of oscillation. In general, dynamic derivatives for separated-flow conditions are larger and therefore more significant than for attached-flow conditions. Because of the complexity of the separated-flow case, no quantitative information on these effects is presented in the Datcom. Instead, a qualitative discussion of the characteristics of dynamic derivatives under partially separated-flow conditions is given.

Flow separation on wings at angles of attack below stall is discussed in Sections 4.1.3.3 and 4.1.3.4. The dominant feature of flow over low-aspect-ratio or swept wings, i.e., wings for which flow separation below stall is important, is the leading-edge vortex. The strength of the leading-edge vortex is determined by wing planform and airfoil leading-edge geometry.

In general, large leading-edge sweep angles and sharp airfoil sections are conducive to high vortex strengths. The strength of the leading-edge vortex, in turn, determines the nature and magnitude of the nonlinear static force, moment, and dynamic-derivative characteristics. The effects of geometry on the dynamic derivatives of a triangular wing at low speed are presented in reference 3.

Partially separated flow over a wing causes the dynamic derivatives to be frequency-dependent. The reason is that a change in wing attitude changes the boundary-layer conditions, which, in turn, alter the flow-separation pattern. The time required for the flow to adjust to a change in attitude is appreciable, and the dynamic derivatives become functions of the rate change of attitude (or frequency). The flow about wings with essentially attached flow is less dependent upon the boundary layer and therefore adjusts more rapidly to attitude changes. Hence the dynamic derivatives for these conditions are not frequency-dependent over the practical frequency range.

For wings that exhibit nonlinearities in their static forces and moments (partially separated flow exists), the dynamic derivatives also depend upon the amplitude of the attitude changes. For instance, sketch (a) (reference 2) shows the rolling moment in sideslip for a triangular wing at high angles of attack. It is clear that the rotary derivative C_{l_r} depends upon the amplitude of oscillation about the Z-axis.



SKETCH (a)

REFERENCES

1. Campbell, J. P., Johnson, J. L., Jr., and Hewes, D. E.: Low-Speed Study of the Effect of Frequency on the Stability Derivatives of Wings Oscillating in Yaw with Particular Reference to High Angle-of-Attack Conditions. NACA RM L55H05, 1955. (U)
2. Johnson, J. L., Jr.: Low-Speed Measurements of Static Stability, Damping in Yaw, and Damping in Roll of a Delta, a Swept, and an Unswept Wing for Angles of Attack from 0° to 90°. NACA RM L56B01, 1956. (U)
3. Fletcher, H. S.: Low-Speed Experimental Determination of the Effects of Leading-Edge Radius and Profile Thickness on Static and Oscillatory Lateral Stability Derivatives for a Delta Wing with 60° of Leading-Edge Sweep. NACA TN 4341, 1958. (U)

7.1.1 WING PITCHING DERIVATIVES

7.1.1.1 WING PITCHING DERIVATIVE C_{Lq}

The wing pitching derivative C_{Lq} is generally small compared to other terms in the equations of motion and is frequently neglected. However, methods are presented for determining C_{Lq} of the wing in subsonic and supersonic speed ranges. The supersonic value of C_{Lq} is used in estimating supersonic values of $C_m q$ in Section 7.1.1.2.

If the wing pitching derivative C_{Lq} is to be used in method 1 of Section 7.3.1.1 to obtain $(C_{Lq})_{WB}$, the exposed wing planform area should be used for all calculations in the Datcom methods. Using the exposed planform area will yield C_{Lq} based on the product of exposed wing area and exposed wing MAC, rather than the product of total wing area and wing MAC as indicated.

DATCOM METHODS

A. SUBSONIC

The equation for estimating the subsonic pitching derivative C_{Lq} (derived in reference 1), based on the product of wing area and wing MAC $S_w \bar{c}_w$, is given by

$$C_{Lq} = \left(\frac{1}{2} + 2 \frac{\bar{x}}{\bar{c}} \right) C_{L\alpha} \quad 7.1.1.1-a$$

where $\frac{\bar{x}}{\bar{c}}$ can be expressed as

$$\frac{\bar{x}}{\bar{c}} = \frac{x_{a.c.}}{\bar{c}} - \frac{x_{c.g.}}{\bar{c}} \quad 7.1.1.1-b$$

and

\bar{x} is the distance between the center of gravity and the aerodynamic center, positive for aerodynamic center behind center of gravity.

$\frac{x_{a.c.}}{\bar{c}} = \left(\frac{x_{a.c.}}{c_r} \right)_{4.1.4.2} \left(\frac{c_r}{\bar{c}} \right)$, the longitudinal distance from the wing leading-edge vertex to the aerodynamic center measured in mean aerodynamic chords, positive aft.

$\frac{x_{c.g.}}{\bar{c}}$ is the longitudinal distance from the wing leading-edge vertex to the center of gravity measured in mean aerodynamic chords, positive aft.

$C_{L\alpha}$ is the wing lift-curve slope (Section 4.1.3.2) at the Mach number under consideration, based on the total wing area.

Sample Problem

Given:

$$A = 4.0$$

$$\lambda = 0.68$$

$$\Lambda_{LE} = 46.3^\circ$$

$$\frac{c_r}{\bar{c}} = 1.18$$

$$\frac{x_{c.g.}}{c_r} = 1.04 \text{ (from planform geometry with c.g. at } \bar{c}/4) \quad M = 0.20$$

$$C_{L\alpha} = 3.20 \text{ per rad} \quad (\text{Section 4.1.3.2})$$

Compute:

Calculate $\frac{x_{a.c.}}{c_r}$ using the method of Section 4.1.4.2

$$\tan \Lambda_{LE} = 1.046$$

$$A \tan \Lambda_{LE} = 4.18$$

$$\beta = 0.98$$

$$\beta/\tan \Lambda_{LE} = 0.937$$

$$\frac{x_{a.c.}}{c_r} = 1.05 \quad (\text{figures 4.1.4.2-26d, -26e, -26f})$$

Calculate the distance between the center of gravity and the aerodynamic center

$$\frac{\bar{x}}{\bar{c}} = \frac{x_{a.c.}}{\bar{c}} - \frac{x_{c.g.}}{\bar{c}} \quad (\text{equation 7.1.1.1-b})$$

$$= \left(\frac{x_{a.c.}}{c_r} - \frac{x_{c.g.}}{c_r} \right) \frac{c_r}{\bar{c}}$$

$$= (1.05 - 1.04) 1.18$$

$$= 0.0118$$

Solution:

Calculate the wing pitching derivative

$$C_{L_q} = \left(\frac{1}{2} + 2 \frac{\bar{x}}{\bar{c}} \right) C_{L_\alpha} \quad (\text{equation 7.1.1.1-a})$$

$$= \left[\frac{1}{2} + 2(0.0118) \right] 3.20$$

$$= (0.52) (3.20)$$

$$= 1.66 \text{ per rad (based on } S_w \bar{c}_w)$$

B. TRANSONIC

There are few data and no theory available on the derivative C_{L_q} in the transonic region. For the purpose of the Datcom, it is suggested that equation 7.1.1.1-a be applied in the transonic region.

C. SUPERSONIC

The supersonic value of C_{L_q} , based on the product of wing area and wing MAC $S_w \bar{c}_w$, is given by

$$C_{L_q} = C_{L_q}' + 2 \left(\frac{\bar{x}}{\bar{c}} \right) C_{N_\alpha} \quad (\text{per radian}) \quad 7.1.1.1-c$$

where

$$\frac{\bar{x}}{\bar{c}} = \frac{x_{a.c.}}{\bar{c}} - \frac{x_{c.g.}}{\bar{c}} \quad 7.1.1.1-b$$

and

C_{L_q}' is referred to body axis with the origin at the wing aerodynamic center and is obtained as indicated below, based on the product of total wing area and wing MAC $S_w \bar{c}_w$.

C_{N_α} is the wing normal-force-curve slope (Section 4.1.3.2) at the Mach number under consideration, based on the total wing area (per radian).

Methods of estimating C_{Lq}'

1. Wings with subsonic leading edges ($\beta \cot \Lambda_{LE} < 1.0$)

For wings with subsonic leading edges, C_{Lq}' is obtained by the method of reference 3 for $\lambda = 0$ and by the method of reference 4 for $\lambda = 0.25$ to 1.0. The following methods are not valid if the Mach line from the trailing-edge vertex intersects the leading edge or if the wing-tip Mach lines intersect on the wings or intersect the opposite wing tips.

a. Zero-taper-ratio wings ($\lambda = 0$)

C_{Lq}' is derived in reference 3 as

$$C_{Lq}' = \frac{\pi}{2} A [3G(\beta C) F_3(N) - 2E''(\beta C) F_4(N)] + 2 \frac{(d - x_{a.c.})}{\bar{c}} C_{N\alpha} \text{ (per radian)}$$

7.1.1.1-d

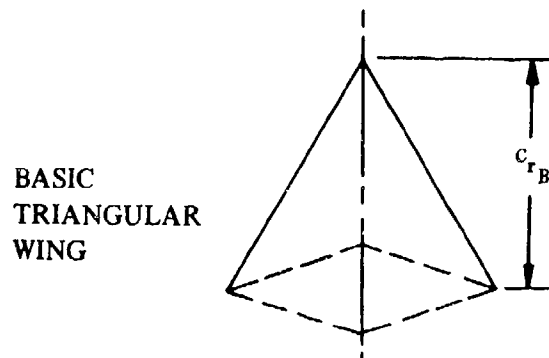
where

$E''(\beta C)$ and $G(\beta C)$ are obtained from figure 7.1.1.1-8.

$F_3(N)$ and $F_4(N)$ are obtained from figure 7.1.1.1-9.

d is two-thirds the basic triangular wing root chord $(d = \frac{2}{3} c_{rB})$. (See sketch (a).)

A is the aspect ratio of the wing.



SKETCH (a)

b. Wings with $\lambda = 0.25$ to 1.0

C_{L_q}' is derived in reference 4 as

$$C_{L_q}' = C_{L_q}'' - 2 \left(\frac{x_{a.c.}}{\bar{c}} \right) C_{N_\alpha} \quad (\text{per radian}) \quad 7.1.1.1-e$$

where

C_{L_q}'' is referred to body axis with the origin at the wing leading-edge vertex and is obtained from figures 7.1.1.1-10a, 7.1.1.1-10b, and 7.1.1.1-10c, for $\lambda = 0.25, 0.50$, and 0.75 , respectively, and from the equations of reference 4 for $\lambda > 0.75$.

2. Wings with supersonic leading edges ($\beta \cot \Lambda_{LE} > 1.0$)

For wings with supersonic leading edges, C_{L_q}' is obtained from figures 7.1.1.1-11a through 7.1.1.1-11k. This method, derived in reference 5, is valid for the range of Mach numbers for which the Mach lines from the leading-edge vertex intersect the trailing edge. An additional limitation is that the foremost Mach line from either wing tip may not intersect the remote half of the wing.

Sample Problem

Given:

$$A = 3.46 \quad \Lambda_{LE} = 60^\circ \quad \frac{c_r}{\bar{c}} = 1.50 \quad M = 1.50 \quad \lambda = 0$$

$$b = 16 \text{ ft} \quad \text{c.g. at } \frac{\bar{c}}{4} \quad c_r = 9.25 \text{ ft} \quad \bar{c} = 6.17 \text{ ft}$$

Compute:

$$\beta = \sqrt{M^2 - 1} = 1.12$$

$$\beta \cot \Lambda_{LE} = 0.647 \text{ (subsonic leading edge)}$$

$$N = 1 - \frac{4 \cot \Lambda_{LE}}{A} = 0.333$$

$$\begin{aligned} E''(\beta C) &= 0.770 \\ G(\beta C) &= 0.570 \end{aligned} \quad \text{(figure 7.1.1.1-8)}$$

$$\begin{aligned} F_3(N) &= 0.913 \\ F_4(N) &= 1.12 \end{aligned} \quad \text{(figure 7.1.1.1-9)}$$

Obtain C_{N_α} from Section 4.1.3.2

$$\beta / \tan \Lambda_{LE} = 0.647$$

$$A \tan \Lambda_{LE} = 6.0$$

$$\tan \Lambda_{LE} C_{N_\alpha} = 5.40 \text{ per rad} \quad (\text{figure 4.1.3.2-56a})$$

$$C_{N_\alpha} = 3.12 \text{ per rad}$$

Obtain $\frac{x_{a.c.}}{\bar{c}}$ from Section 4.1.4.2

$$\frac{x_{a.c.}}{c_r} = 0.90 \quad (\text{figure 4.1.4.2-26a})$$

$$\frac{x_{a.c.}}{\bar{c}} = \left(\frac{x_{a.c.}}{c_r} \right) \left(\frac{c_r}{\bar{c}} \right) = 1.35$$

$$x_{a.c.} = 1.35 \bar{c} = (1.35)(6.17) = 8.33$$

Calculate $\frac{\bar{x}}{\bar{c}}$

$$\frac{x_{c.g.}}{c_r} = 0.67 \quad (\text{from planform geometry with c.g. at } \bar{c}/4)$$

$$\frac{\bar{x}}{\bar{c}} = \left(\frac{x_{a.c.}}{\bar{c}} - \frac{x_{c.g.}}{\bar{c}} \right) \quad (\text{equation 7.1.1.1-b})$$

$$= \left(\frac{x_{a.c.}}{c_r} - \frac{x_{c.g.}}{c_r} \right) \frac{c_r}{\bar{c}}$$

$$= (0.90 - 0.67) 1.50 = 0.345$$

Calculate d from the characteristics of the basic triangular wing (see sketch (a))

$$A_B = \frac{b^2}{\frac{1}{2} b c_{r_b}} = \frac{4}{\tan \Lambda_{LE}} = \frac{4}{1.732} = 2.31$$

$$c_{r_b} = \frac{2b}{A_B} = \frac{2(16)}{2.31} = 13.85 \text{ ft}$$

$$d = \frac{2}{3} c_{r_b} = \frac{2}{3} (13.85) = 9.233 \text{ ft}$$

Solution for C_{L_q}'

$$C_{L_q}' = \frac{\pi A}{2} [3G(\beta C) F_3(N) - 2E''(\beta C) F_4(N)] + 2 \frac{(d - x_{a.c.})}{\bar{c}} C_{N_\alpha} \quad (\text{equation 7.1.1.1-d})$$

$$= \frac{\pi}{2} (3.46) [3(0.57)(0.913) - 2(0.77)(1.12)] + 2 \frac{(9.233 - 8.33)}{6.17} \quad (3.12)$$

$$= -0.891 + 0.913$$

$$= 0.022 \text{ per rad (based on } S_w \bar{c}_w)$$

Solution for C_{L_q}

$$C_{L_q} = C_{L_q}' + 2 \left(\frac{\bar{x}}{\bar{c}} \right) C_{N_\alpha} \quad (\text{equation 7.1.1.1-c})$$

$$= 0.022 + 2(0.345) 3.12$$

$$= 2.175 \text{ per rad (based on } S_w \bar{c}_w)$$

REFERENCES

1. Toll, T., and Queijo, M.: Approximate Relations and Charts for Low-Speed Stability Derivatives of Swept Wings. NACA TN 1581, 1948. (U)
2. MacLachlan, R., and Fisher, L. R.: Wind-Tunnel Investigation at Low Speeds of the Pitching Derivatives of Untapered Swept Wings. NACA RM L8G19, 1948. (U)
3. Malvestuto, F. S., Jr., and Margolis, K.: Theoretical Stability Derivatives of Thin Sweptback Wings Tapered to a Point with Sweptback or Sweptforward Trailing Edges for a Limited Range of Supersonic Speeds. NACA TR 971, 1950. (U)
4. Malvestuto, F. S., Jr., and Hoover, D. M.: Lift and Pitching Derivatives of Thin Sweptback Tapered Wings with Streamwise Tips and Subsonic Leading Edges at Supersonic Speeds. NACA TN 2294, 1951. (U)
5. Martin, J. C., Margolis, K., and Jeffreys, I.: Calculation of Lift and Pitching Moments Due to Angle of Attack and Steady Pitching Velocity at Supersonic Speeds for Thin Sweptback Tapered Wings with Streamwise Tips and Supersonic Leading and Trailing Edges. NACA TN 2699, 1952. (U)

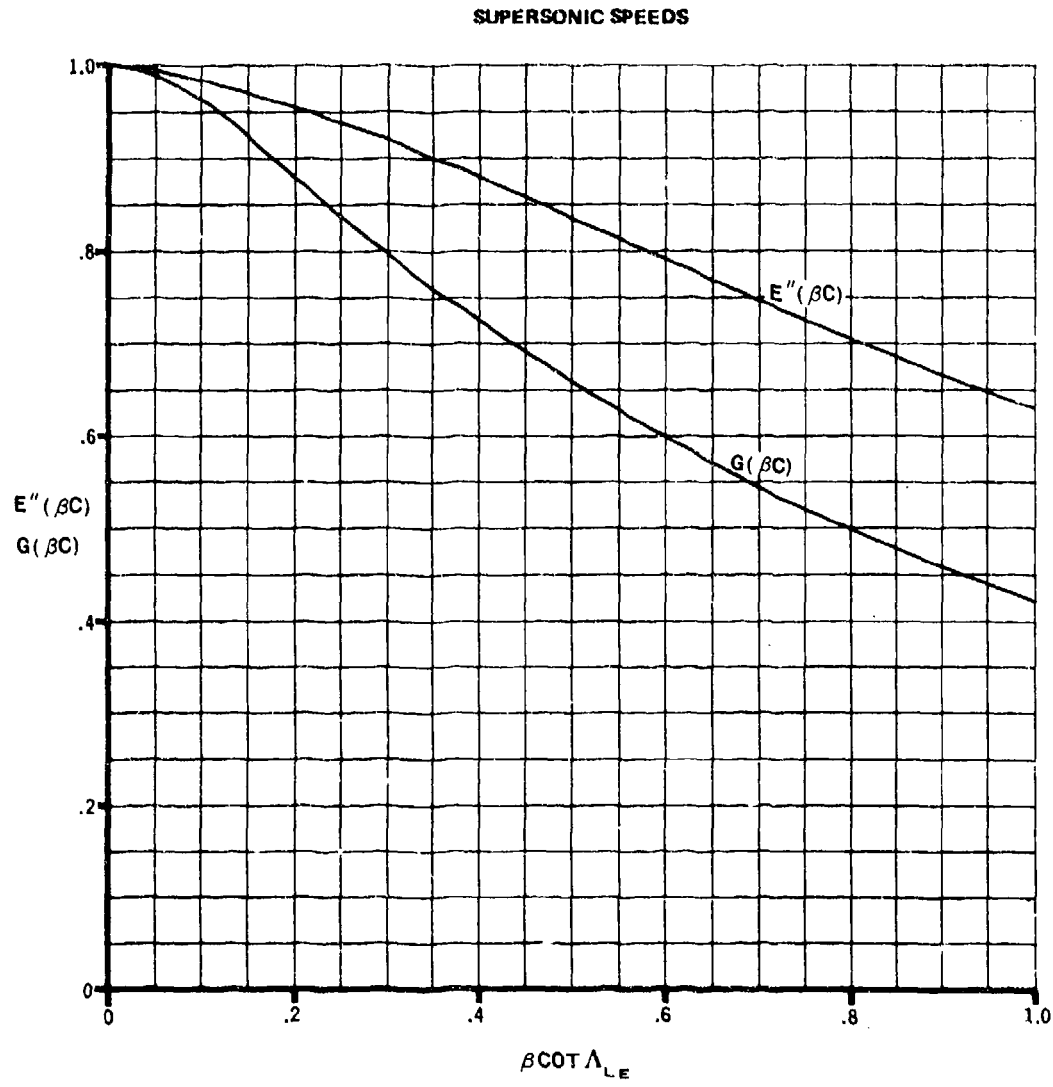


FIGURE 7.1.1.1-8 ELLIPTIC INTEGRAL FACTORS OF THE STABILITY DERIVATIVE

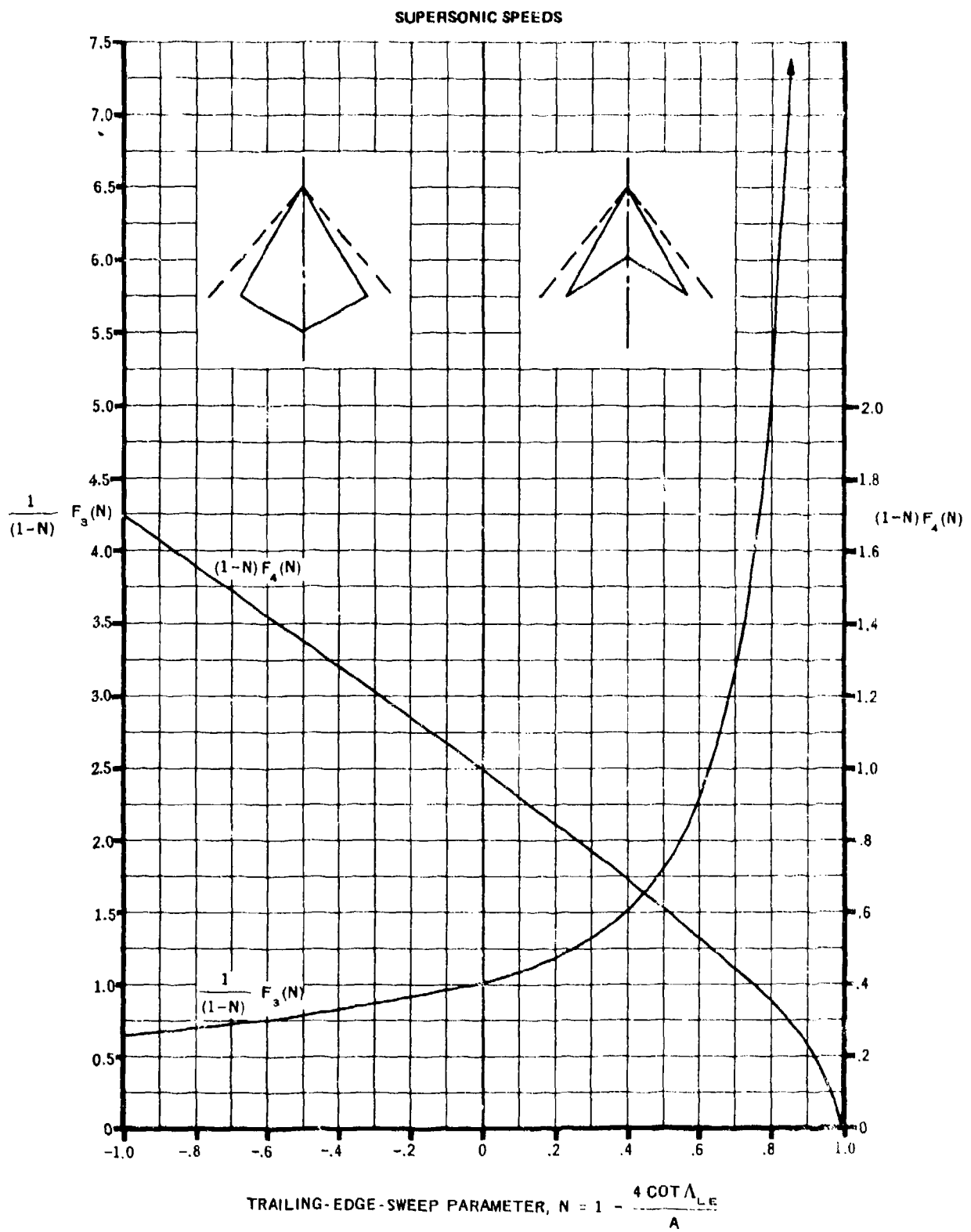


FIGURE 7.1.1.1-9 F(N) FACTORS OF THE STABILITY DERIVATIVE

SUBSONIC LEADING EDGE

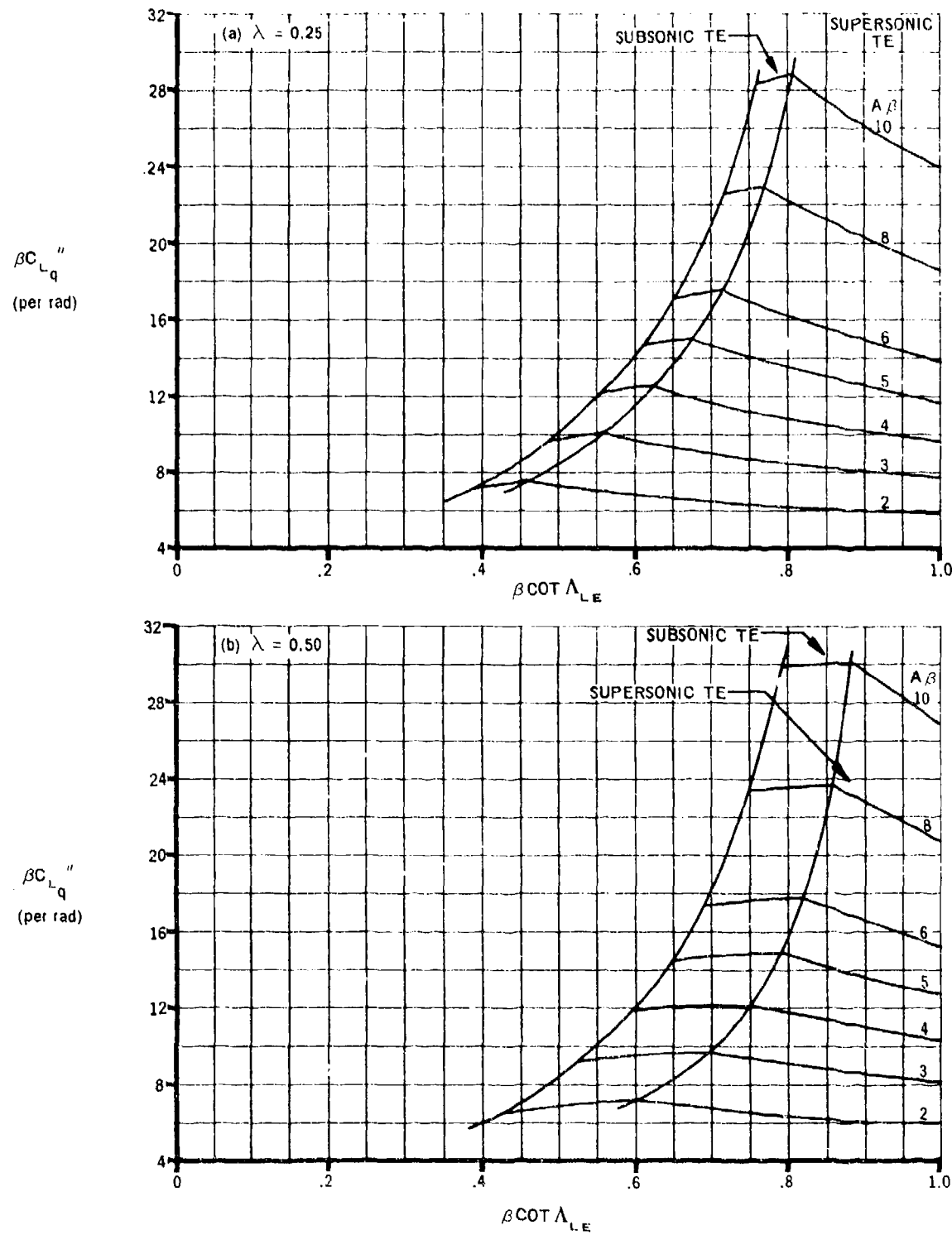


FIGURE 7.1.1.1-10 VARIATION OF $\beta C_{L_q}''$ WITH $\beta \cot \Lambda_{LE}$

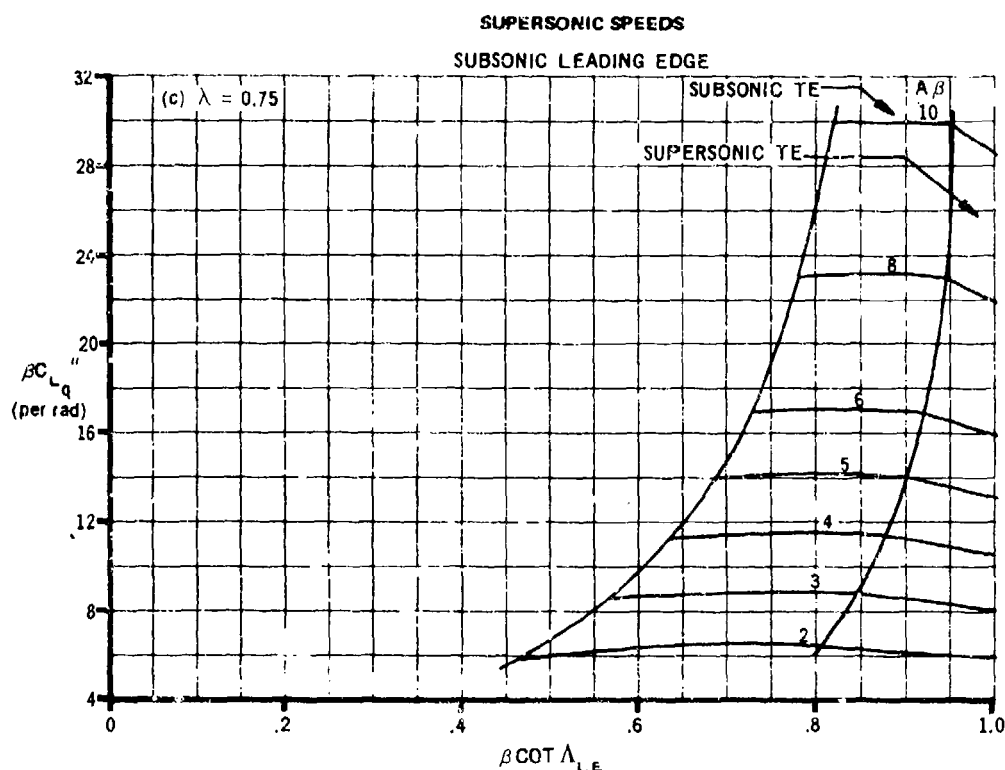


FIGURE 7.1.1.1-10(CONTD)

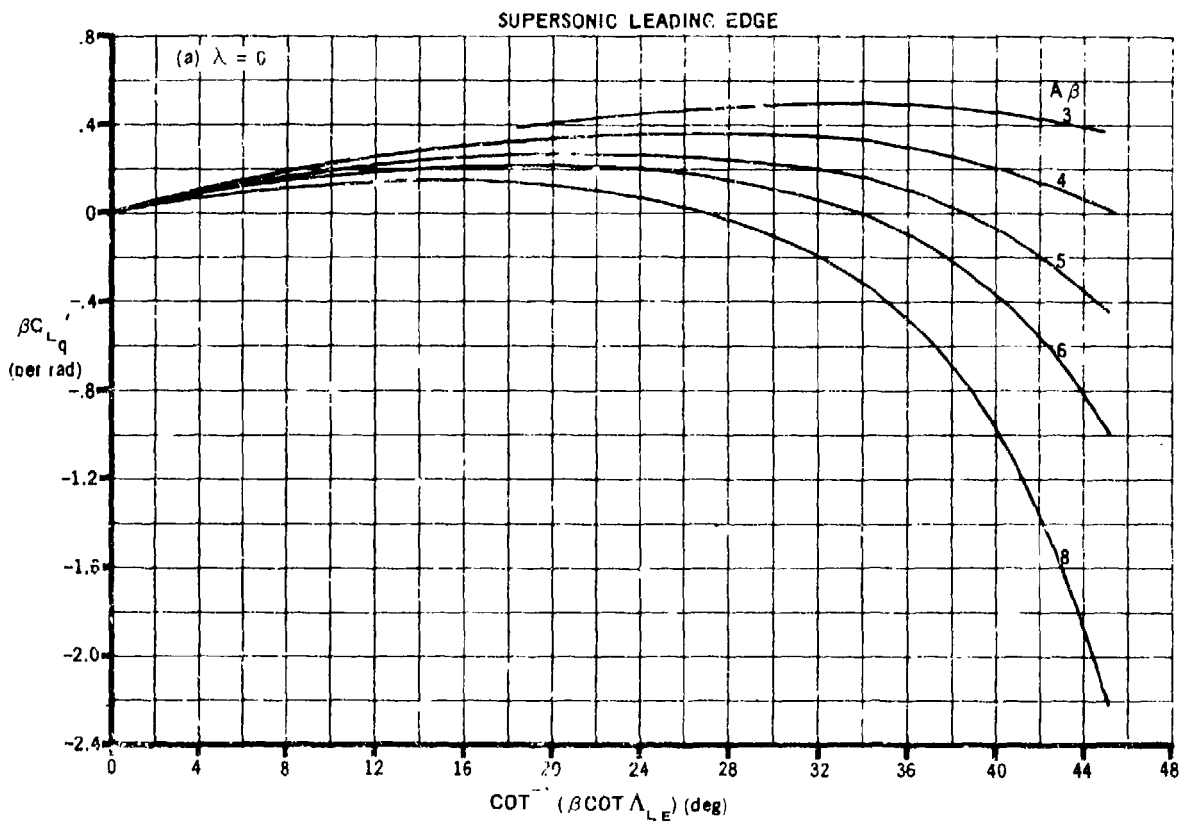


FIGURE 7.1.1.1-11 VARIATION OF $\beta C L_q'''$ WITH $\cot^{-1}(\beta \cot \Lambda_{LE})$

SUPersonic SPEEDS

SUPersonic LEADING EDGE

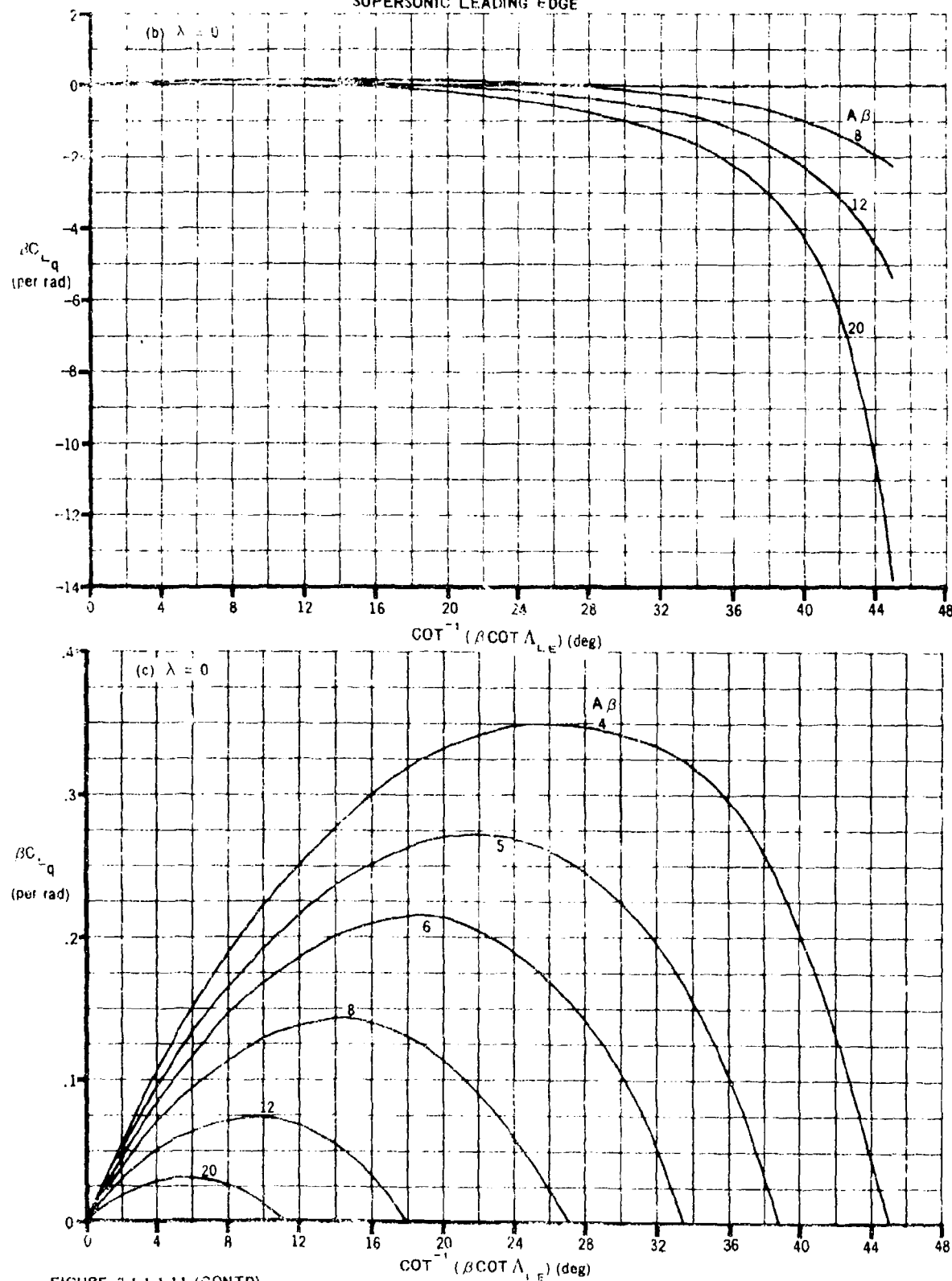


FIGURE 7.1.1.1-11 (CONT'D)

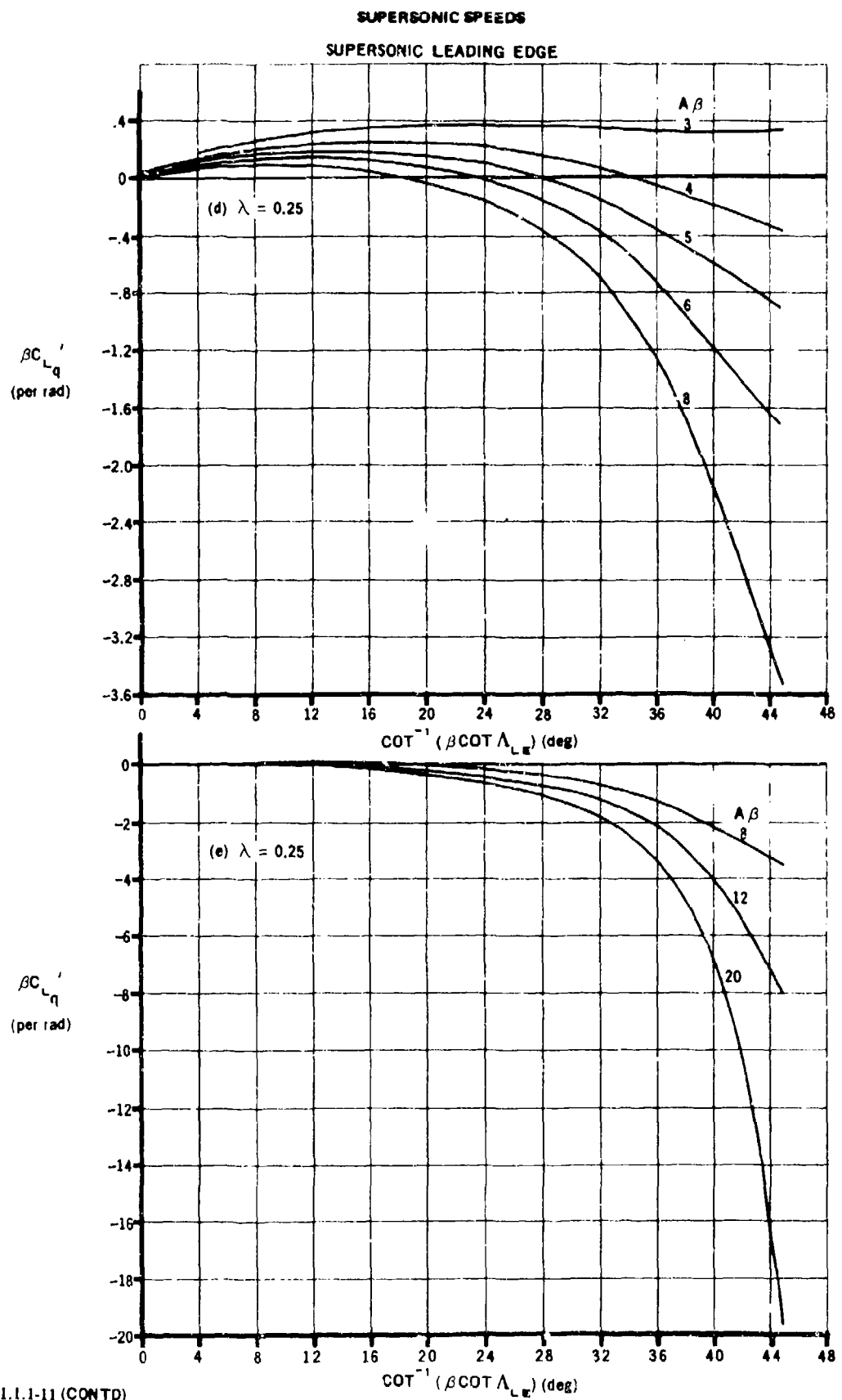


FIGURE 7.1.1.1-11 (CONT'D)

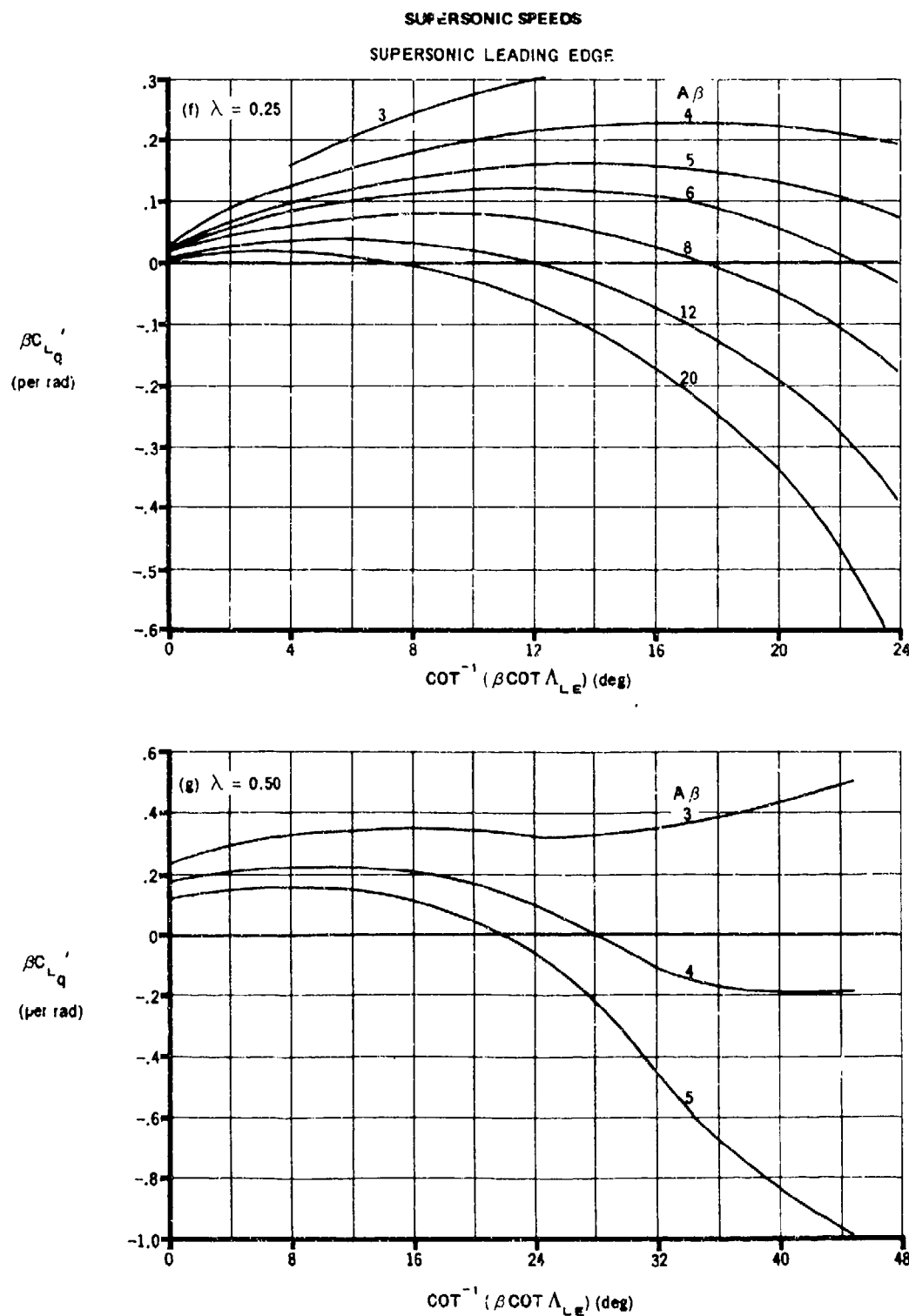


FIGURE 7.1.1.1-11 (CONT'D)

SUPersonic SPEEDS
SUPersonic LEADING EDGE

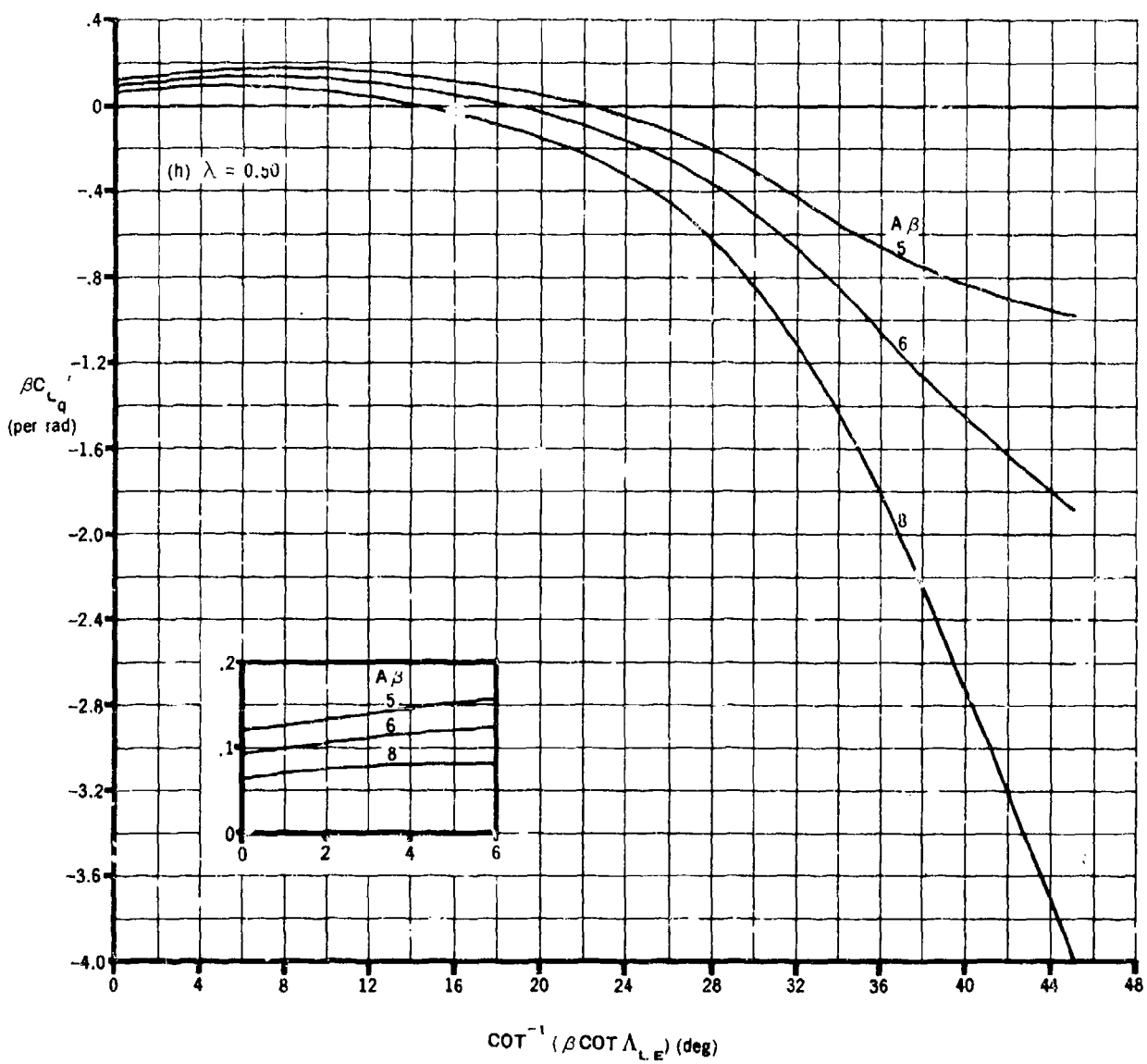


FIGURE 7.1.1.1-11 (CONT'D)

SUPersonic SPEEDS
SUPersonic LEADING EDGE

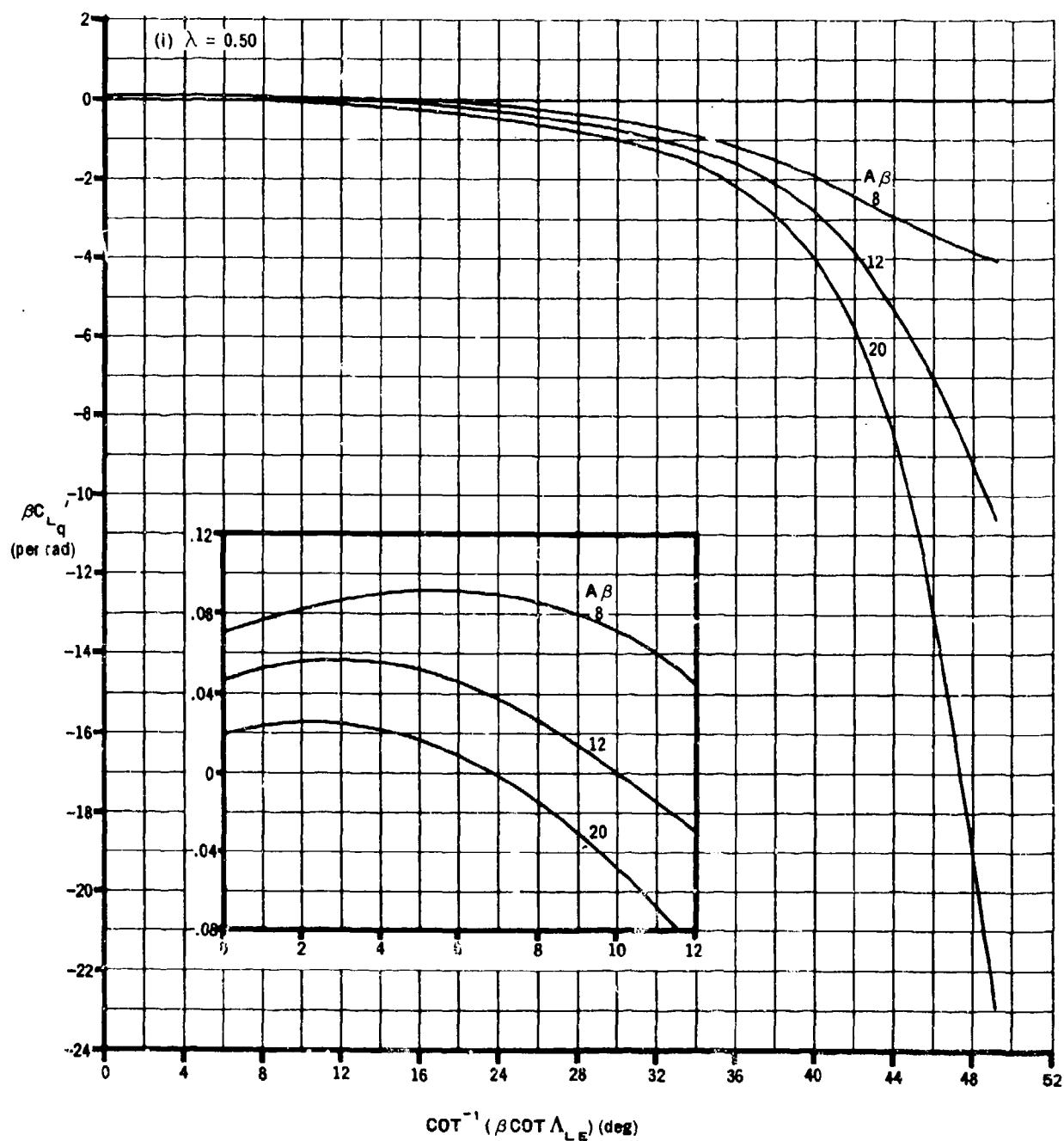


FIGURE 7.1.1.1-11 (CONT'D)

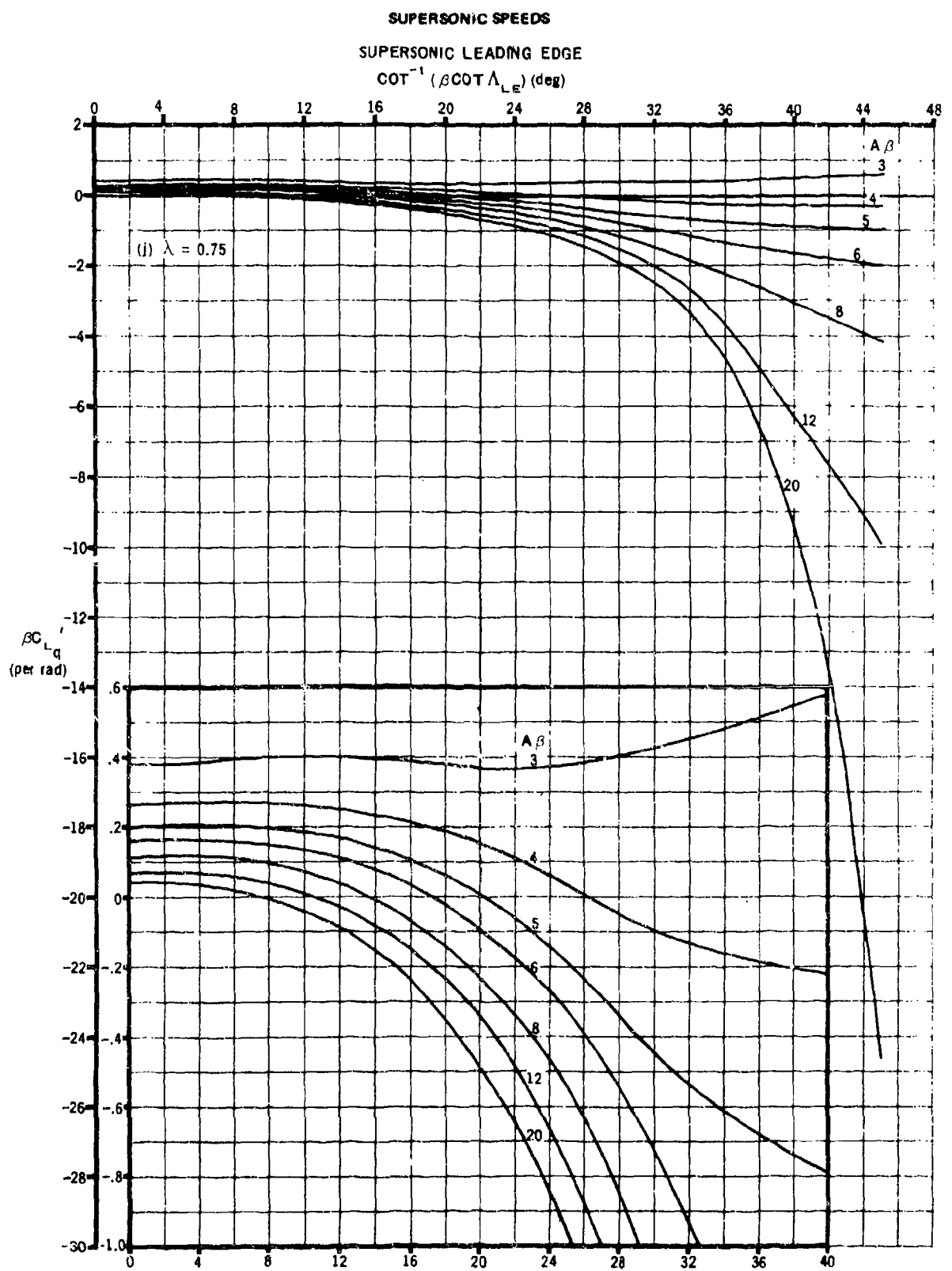


FIGURE 7.1.1.1-11 (CONTD)

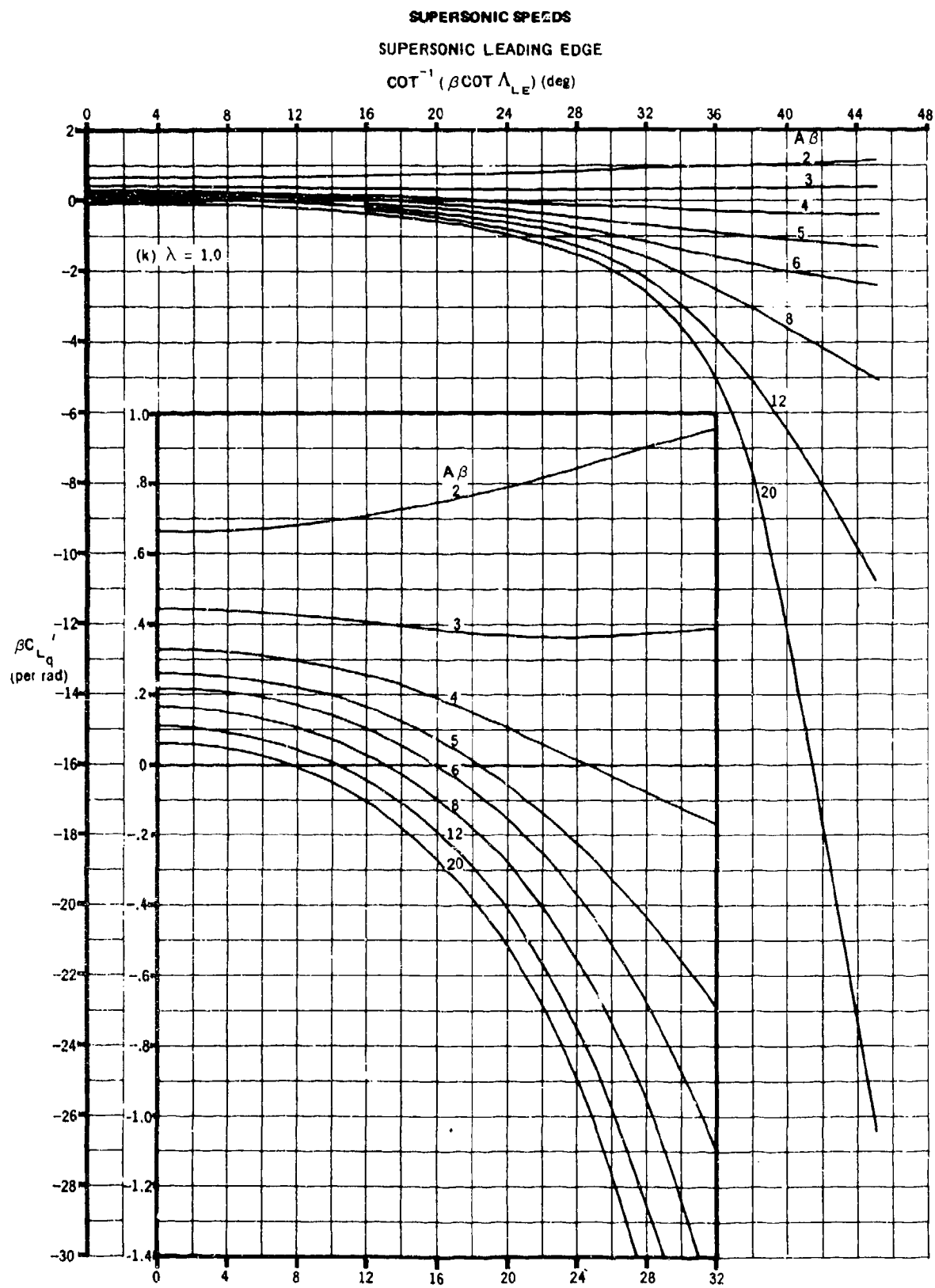


FIGURE 7.1.1-11 (CONT'D)

7.1.1.2 WING PITCHING DERIVATIVE C_{m_q}

When a wing rotates in pitch about a given center of gravity at an angular velocity θ in a free-stream velocity V_∞ , changes in local angle of attack are produced that are proportional to w/V (w is the local vertical disturbance velocity). For wings having sweepback, an additional increment in angle of attack is produced that is a function of spanwise wing station. These local changes in angle of attack produce an effective angle-of-attack increment for the complete wing that results in a pitching-moment increment. This pitching-moment increment is expressed as the wing contribution to the derivative C_{m_q} .

If the wing pitching derivative C_{m_q} is to be used in method 1 of Section 7.3.1.2 to obtain $(C_{m_q})_{WB}$, the exposed wing planform area should be used for all calculations in the Datcom methods. Using the exposed planform area will yield C_{m_q} based on the product of exposed wing area and the square of exposed wing MAC, rather than the product of total wing area and the square of wing MAC as indicated.

DATCOM METHOD

A. SUBSONIC

The low-speed value ($M \approx 0.2$) of C_{m_q} , based on the product of total wing area and the square of wing MAC $S_w \bar{c}_w^2$, is given by

$$(C_{m_q})_{M \approx 0.2} = -0.7 c_{\ell_\alpha} \cos \Lambda_{c/4} \left\{ \frac{A \left[\frac{1}{2} \frac{\bar{x}}{\bar{c}} + 2 \left(\frac{\bar{x}}{\bar{c}} \right)^2 \right]}{A + 2 \cos \Lambda_{c/4}} + \frac{1}{24} \left(\frac{A^3 \tan^2 \Lambda_{c/4}}{A + 6 \cos \Lambda_{c/4}} \right) + \frac{1}{8} \right\} \quad (\text{per radian}) \quad 7.1.1.2-a$$

where

$\frac{\bar{x}}{\bar{c}}$ is defined in Section 7.1 .1.

c_{ℓ_α} is the wing section lift curve slope from Section 4.1.1. (per radian).

This equation is a modified form of that derived in reference 1. The equation was modified in reference 2 by the empirical factor 0.7. It is strictly applicable to aspect ratios between 1 and 6. For aspect ratios of about 10 or 12 the empirical factor should be approximately 0.9, but there are no experimental data available to show how this empirical factor should vary for intermediate aspect ratios. It is suggested that a smooth fairing be used.

For higher subsonic speeds the derivative C_{m_q} , based on the product of wing area and the square of wing MAC $S_w \bar{c}_w^2$, is obtained by applying an approximate compressibility correction derived in reference 3:

$$\left(C_{m_q}\right)_{M>0.2} = \begin{bmatrix} \frac{A^3 \tan^2 \Lambda_{c/4}}{AB + 6 \cos \Lambda_{c/4}} + \frac{3}{B} \\ \frac{A^3 \tan^2 \Lambda_{c/4}}{A + 6 \cos \Lambda_{c/4}} + 3 \end{bmatrix} \left(C_{m_q}\right)_{M \approx 0.2} \text{ (per radian)} \quad 7.1.1.2-b$$

where

$$\left(C_{m_q}\right)_{M \approx 0.2} \text{ is obtained from equation 7.1.1.2-a.}$$

$$B = \sqrt{1 - M^2 \cos^2 \Lambda_{c/4}}$$

Sample Problem

Given: Same wing as in sample problem of paragraph A, Section 7.1.1.1.

$$A = 4.0 \quad \lambda = 0.68 \quad \Lambda_{c/4} = 45^\circ \quad \frac{c_r}{c} = 1.18$$

Additional Characteristics:

Airfoil: 64-006 Smooth airfoil surface $M = 0.2, 0.6$

$$\frac{\bar{x}}{c} = 0.0118 \text{ (sample problem, paragraph A, Section 7.1.1.1)}$$

Compute:

$$c_{\ell_\alpha} = 0.109 \text{ per deg (table 4.1.1-B)}$$

$$\cos \Lambda_{c/4} = 0.707; \tan \Lambda_{c/4} = 1.0$$

$$\text{At } M = 0.6, B = \sqrt{1 - M^2 \cos^2 \Lambda_{c/4}} = \sqrt{1 - (0.36)(0.50)} = 0.905$$

Solution ($M = 0.2$):

$$\left(C_{m_q}\right)_{M \approx 0.2} = -0.7 c_{\ell_\alpha} \cos \Lambda_{c/4} \left\{ \frac{A \left[\frac{1}{2} \frac{\bar{x}}{c} + 2 \left(\frac{\bar{x}}{c} \right)^2 \right]}{A + 2 \cos \Lambda_{c/4}} + \frac{1}{24} \left(\frac{A^3 \tan^2 \Lambda_{c/4}}{A + 6 \cos \Lambda_{c/4}} \right) + \frac{1}{8} \right\} \quad (\text{equation 7.1.1.2-a})$$

$$\begin{aligned}
&= (-0.7)(0.109)(57.3)(0.707) \left\{ \frac{4 \left[\frac{1}{2}(0.0118) + 2(0.0118)^2 \right]}{4 + 2(0.707)} \right. \\
&\quad \left. + \frac{1}{24} \left[\frac{(4)^3(1)}{4 + 6(0.707)} \right] + \frac{1}{8} \right\} \\
&= -3.090 \left[\frac{0.0247}{5.414} + \frac{1}{24} \left(\frac{64}{8.242} \right) + \frac{1}{8} \right] \\
&= -3.090(0.00456 + 0.3235 + 0.125) \\
&= -1.400 \text{ per rad (based on } S_w \bar{c}_w^2)
\end{aligned}$$

Solution ($M = 0.6$):

$$\begin{aligned}
(C_m q)_{M > 0.2} &= \left[\frac{\frac{A^3 \tan^2 \Lambda_{c/4}}{AB + 6 \cos \Lambda_{c/4}} + \frac{3}{B}}{\frac{A^3 \tan^2 \Lambda_{c/4}}{A + 6 \cos \Lambda_{c/4}} + 3} \right] (C_m q)_{M \approx 0.2} \quad (\text{equation 7.1.1.2-b}) \\
&= \left[\frac{\frac{(4)^3(1)}{4(0.905) + 6(0.707)} + \frac{3}{0.905}}{\frac{(4)^3(1)}{4 + 6(0.707)} + 3} \right] (-1.40) \\
&= \left[\frac{\frac{64}{7.862} + 3.31}{\frac{64}{8.242} + 3} \right] (-1.40) \\
&= \left(\frac{8.14 + 3.31}{7.77 + 3} \right) (-1.40) \\
&= -1.49 \text{ per rad (based on } S_w \bar{c}_w^2)
\end{aligned}$$

B. TRANSONIC

At transonic speeds the derivative C_{m_q} , based on the product of wing area and the square of wing MAC $S_w \bar{c}_w^2$, is estimated by

$$C_{m_q} = \frac{\left(C_{L_\alpha}\right)_M - \left(C_{L_\alpha}\right)_{M_{cr}}}{\left(C_{L_\alpha}\right)_{M=1.2} - \left(C_{L_\alpha}\right)_{M_{cr}}} \left[\left(C_{m_q}\right)_{M=1.2} - \left(C_{m_q}\right)_{M_{cr}} \right] + \left(C_{m_q}\right)_{M_{cr}} \quad (\text{per radian})$$

7.1.1.2-c

where

C_{L_α} is the wing lift-curve slope (Section 4.1.3.2) at the Mach number under consideration, based on the total wing area (per radian).

$\left(C_{m_q}\right)_{M=1.2}$ is obtained from the supersonic method of paragraph C of this section, based on the product of wing area and the square of wing MAC $S_w \bar{c}_w^2$ (per radian).

$\left(C_{m_q}\right)_{M_{cr}}$ is obtained from equation 7.1.1.2-b at the critical Mach number, based on the product of wing area and the square of wing MAC $S_w \bar{c}_w^2$ (per radian).

For this purpose the critical Mach number M_{cr} is taken equal to the force-break Mach number M_{fb} defined in paragraph B of Section 4.1.3.2.

C. SUPERSONIC

The supersonic value of C_{m_q} , referred to body axis and for any center-of-gravity location and based on the product of wing area and the square of wing MAC $S_w \bar{c}_w^2$, is given by

$$C_{m_q} = C_{m_q}' - \left(\frac{\bar{x}}{\bar{c}}\right) C_{L_q} \quad (\text{per radian}) \quad 7.1.1.2-d$$

where

C_{L_q}' is obtained from Section 7.1.1.1, based on the product of wing area and wing MAC (per radian).

$\frac{\bar{x}}{\bar{c}}$ is defined in Section 7.1.1.1.

C_{m_q}' is referred to body axis with the origin at the wing aerodynamic center, based on the product of wing area and the square of wing MAC $S_w \bar{c}_w^2$, and obtained as indicated below.

7.1.1.2-4

Methods for estimating C_{m_q}'

1. Wings with subsonic leading edges ($\beta \cot \Lambda_{LE} < 1.0$)

For wings with subsonic leading edges, C_{m_q}' is obtained by the method of reference 4 for $\lambda = 0$ and by the method of reference 5 for $\lambda = 0.25$ to 1.0. The following methods are not valid if the Mach line from the trailing-edge vertex intersects the leading edge or if the wing-tip Mach lines intersect on the wings or intersect the opposite wing tips.

a. Zero-taper-ratio wings ($\lambda = 0$)

C_{m_q}' is derived in reference 4 as

$$C_{m_q}' = -\frac{3}{16} \pi A \left\{ G(\beta C) F_7(N) + \frac{16}{3} E''(\beta C) \left[\frac{F_5(N)}{F_{11}(N)} \right] \right\}$$

$$= \left(\frac{d - x_{a.c.}}{\bar{c}} \right) C_{L_q}'' + 2 \left(\frac{d - x_{a.c.}}{\bar{c}} \right)^2 C_{N_\alpha} \quad (\text{per radian}) \quad 7.1.1.2-e$$

where

$G(\beta C)$ and $E''(\beta C)$ are obtained from figure 7.1.1.1-8.

$F_5(N)$, $F_7(N)$, and $F_{11}(N)$ are obtained from figure 7.1.1.2-8.

$\frac{x_{a.c.}}{\bar{c}}$ is defined in paragraph A of Section 7.1.1.1.

C_{N_α} is the wing normal-force-curve slope (Section 4.1.3.2) at the Mach number under consideration, based on the total wing area (per radian).

d is defined in paragraph C of Section 7.1.1.1.

C_{L_q}'' is obtained from paragraph C of Section 7.1.1.1, based on the product of wing area and wing MAC (per radian).

b. Wings with $\lambda = 0.25$ to 1.0

C_{m_q}' is derived in reference 5 as

$$C_{m_q}' = C_{m_q}''' + \left(\frac{x_{a.c.}}{\bar{c}} \right) C_{L_q}''' \quad (\text{per radian}) \quad 7.1.1.2-f$$

where

C_{m_q}'' is referred to body axis with the origin at the wing leading-edge vertex and is obtained from figures 7.1.1.2-9a, 7.1.1.2-9b, and 7.1.1.2-9c, for $\lambda = 0.25, 0.50$, and 0.75 , respectively, and from the equations of reference 5 for $\lambda > 0.75$ (per radian).

C_{L_q}'' is obtained from paragraph C of Section 7.1.1.1, based on the product of wing area and wing MAC (per radian).

$\frac{x_{a.c.}}{\bar{c}}$ is defined in paragraph A of Section 7.1.1.1.

2. Wings with supersonic leading edges ($\beta \cot \Lambda_{LE} > 1.0$)

For wings with supersonic leading edges, C_{m_q}' is obtained from figures 7.1.1.2-10a through 7.1.1.2-10k. This method is derived in reference 6 and is valid for the range of Mach numbers for which the Mach lines from the leading-edge vertex intersect the trailing edge. An additional limitation is that the foremost Mach line from either wing tip may not intersect the remote half of the wing.

Sample Problem

Given: Same wing as in sample problem of paragraph C, Section 7.1.1.1.

$$A = 3.46 \quad \lambda = 0 \quad \Lambda_{LE} = 60^\circ \quad \frac{c_r}{\bar{c}} = 1.50 \quad b = 16 \text{ ft}$$

$$\text{c.g. at } \frac{\bar{c}}{4} \quad M = 1.50 \quad \bar{c} = 6.17 \text{ ft} \quad c_z = 9.25 \text{ ft}$$

From sample problem of paragraph C, Section 7.1.1.1:

$$\beta \cot \Lambda_{LE} = 0.647 \text{ (subsonic leading edge)}$$

$$N = 0.333 \quad E''(\beta C) = 0.770 \quad G(\beta C) = 5.70 \quad C_{N_\alpha} = 3.12 \text{ per rad}$$

$$C_{L_q}' = 0.022 \text{ per rad} \quad C_{L_q} = 2.175 \text{ per rad} \quad \frac{d - x_{a.c.}}{\bar{c}} = 0.146 \quad \frac{\bar{x}}{\bar{c}} = 0.345$$

Compute:

$$\left. \begin{array}{l} F_5(N) = 0.133 \\ F_7(N) = -0.200 \\ F_{11}(N) = 0.660 \end{array} \right\} \text{(figure 7.1.1.2-8)}$$

Solution:

$$\begin{aligned}
 C_{m_q}' &= -\frac{3}{16} \pi A \left\{ G(\beta C) F_7(N) + \frac{16}{3} E''(\beta C) \left[\frac{F_5(N)}{F_{11}(N)} \right] \right\} \\
 &\quad - \left(\frac{d - x_{a.c.}}{\bar{c}} \right) C_{L_q} + 2 \left(\frac{d - x_{a.c.}}{\bar{c}} \right)^2 C_{N_\alpha} \quad (\text{equation 7.1.1.2-e}) \\
 &= -\frac{3}{16} \pi (3.46) \left[(0.570)(-0.200) + \frac{16}{3} (0.770) \frac{0.133}{0.660} \right] \\
 &\quad - (0.146)(0.022) + 2(0.146)^2 (3.12) \\
 &= -2.038(-0.1140 + 0.8276) - 0.0032 + 0.1330 \\
 &= -1.325 \text{ per rad} \\
 C_{m_q} &= C_{m_q}' - \left(\frac{\bar{x}}{\bar{c}} \right) C_{L_q} \quad (\text{equation 7.1.1.2-d}) \\
 &= -1.325 - (0.345)(2.175) \\
 &= -2.075 \text{ per rad (based on } S_w \bar{c}_w^2)
 \end{aligned}$$

REFERENCES

1. Toll, T., and Queijo, M.: Approximate Relations and Charts for Low-Speed Stability Derivatives of Swept Wings. NACA TN 1581, 1948. (U)
2. MacLachlan, R., and Fisher, L. R.: Wind-Tunnel Investigation at Low Speeds of the Pitching Derivatives of Untapered Swept Wings. NACA RM L8G19, 1948. (U)
3. Fisher, L. R.: Approximate Corrections for the Effects of Compressibility on the Subsonic Stability Derivatives of Swept Wings. NACA TN 1854, 1949. (U)
4. Malvestuto, F. S., Jr., and Margolis, K.: Theoretical Stability Derivatives of Thin Sweptback Wings Tapered to a Point with Sweptback or Sweptforward Trailing Edges for a Limited Range of Supersonic Speeds. NACA TR 971, 1950. (U)
5. Malvestuto, F. S., Jr., and Hoover, D. M.: Lift and Pitching Derivatives of Thin Sweptback Tapered Wings with Streamwise Tips and Subsonic Leading Edges at Supersonic Speeds. NACA TN 2294, 1951. (U)
6. Martin, J., Margolis, K., and Jeffreys, I.: Calculation of Lift and Pitching Moments Due to Angle of Attack and Steady Pitching Velocity at Supersonic Speeds for Thin Sweptback Tapered Wings with Streamwise Tips and Supersonic Leading and Trailing Edges. NACA TN 2699, 1952. (U)

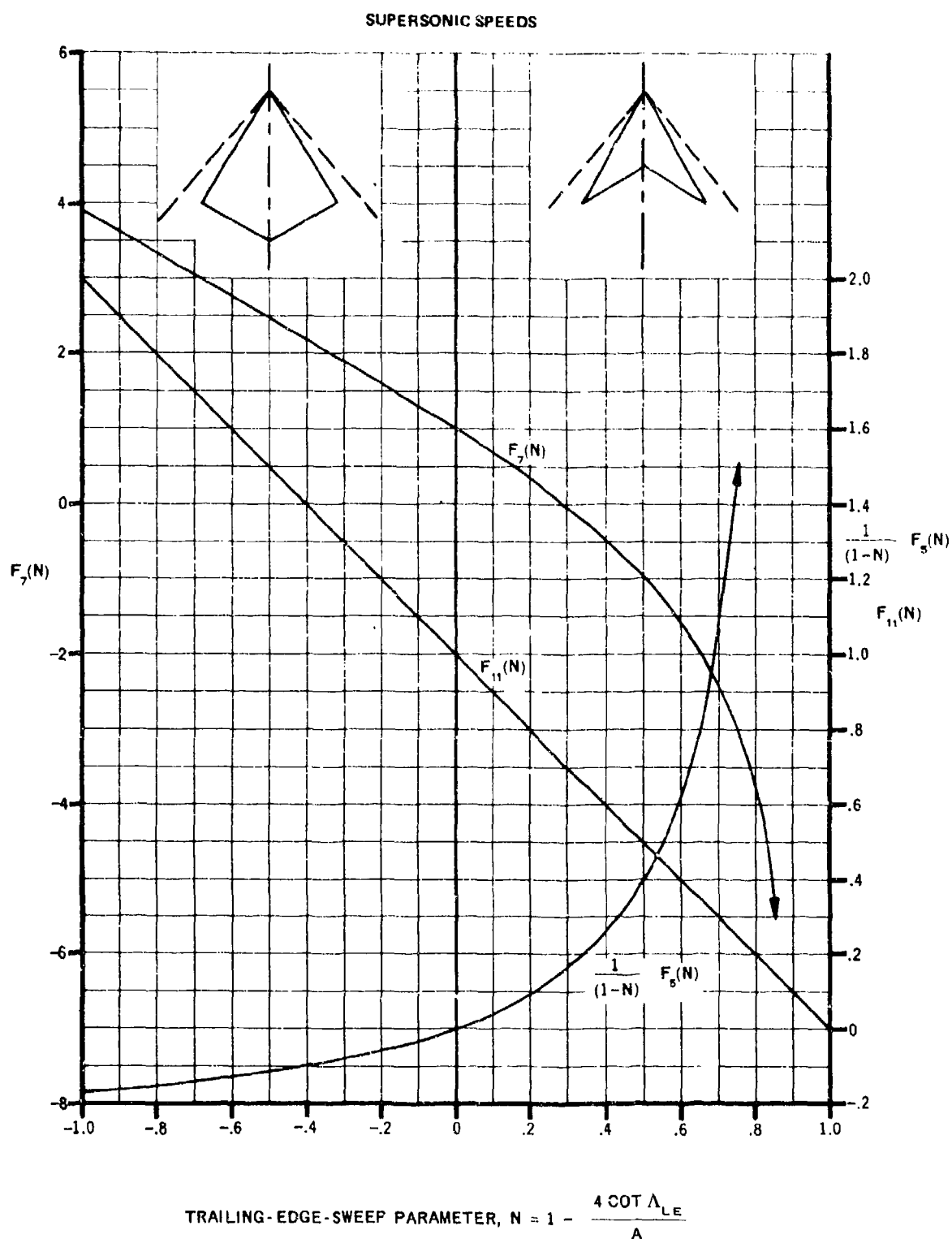


FIGURE 7.1.1.2-8 $F(N)$ FACTORS OF THE STABILITY DERIVATIVE

7.1.1.2-8

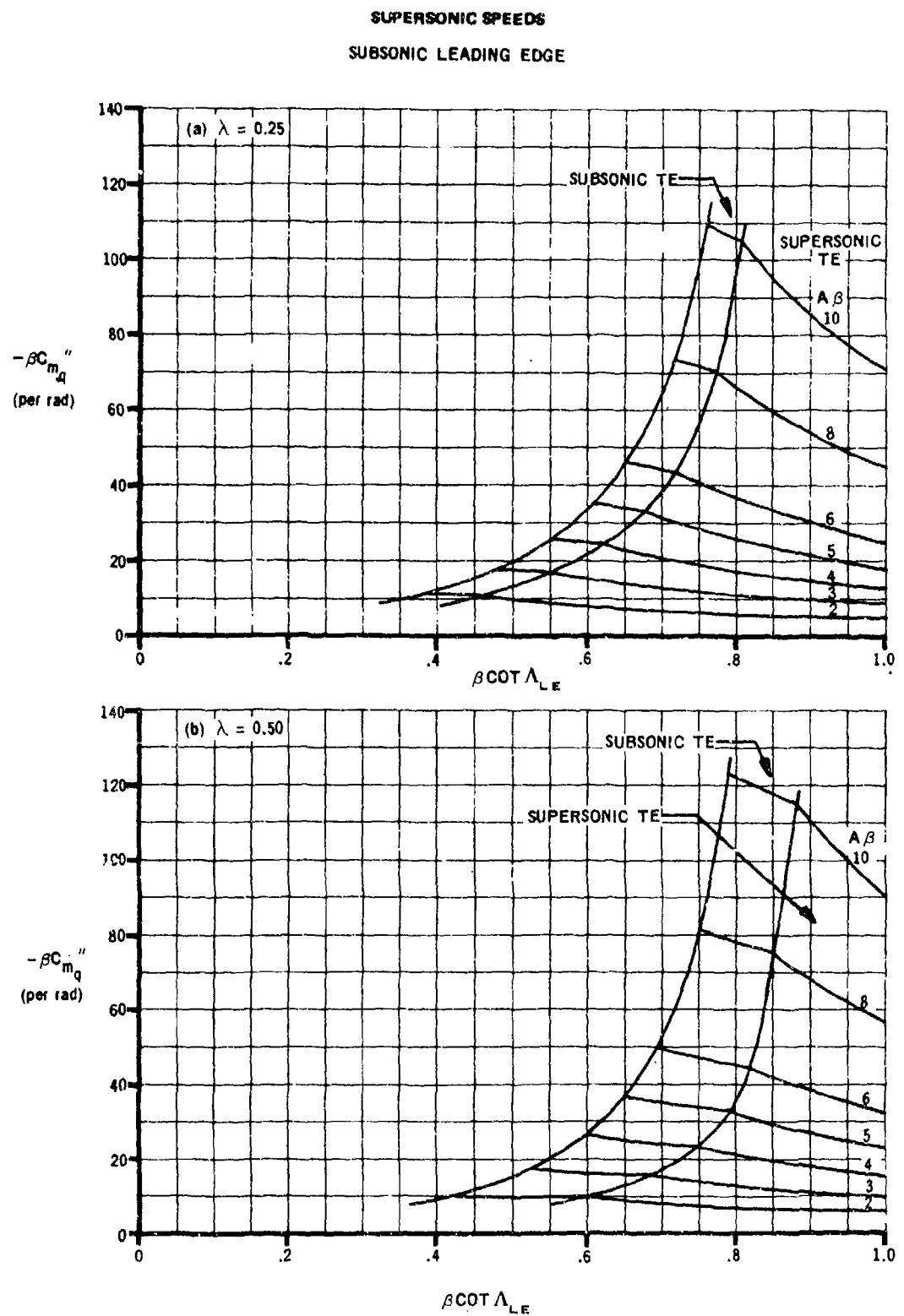


FIGURE 7.1.1.2-9 VARIATION OF $\beta C_{m_q}''$ WITH $\beta \cot A_{LE}$

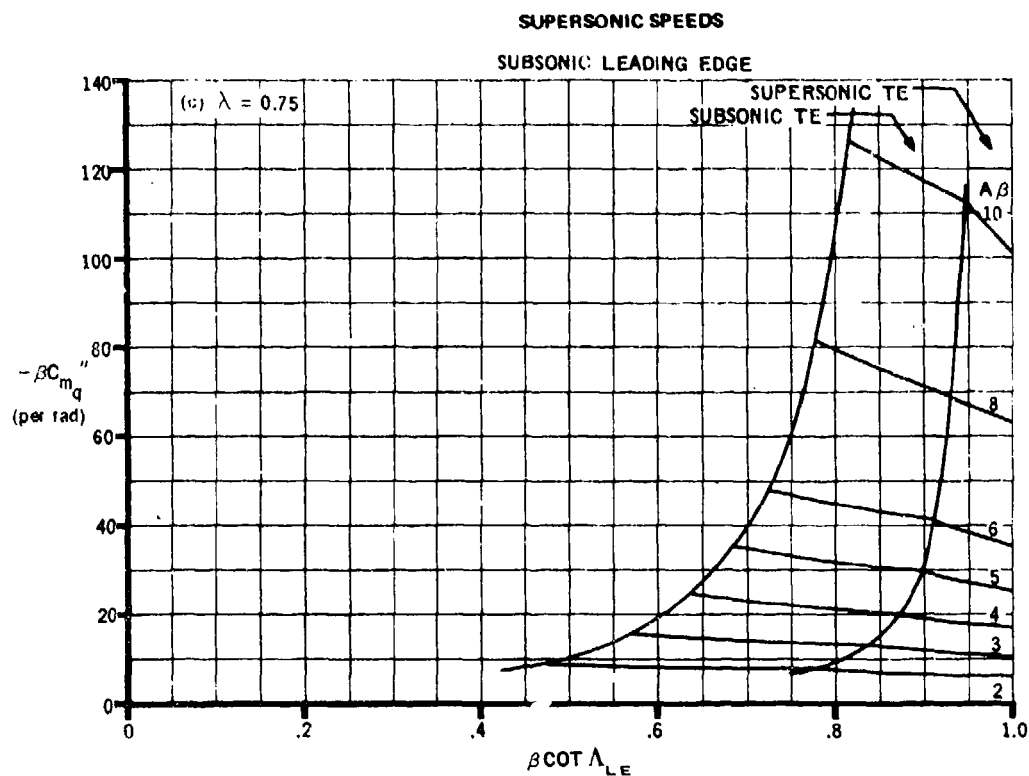


FIGURE 7.1.1.2-9 (CONTD)

SUPersonic LEADING EDGE

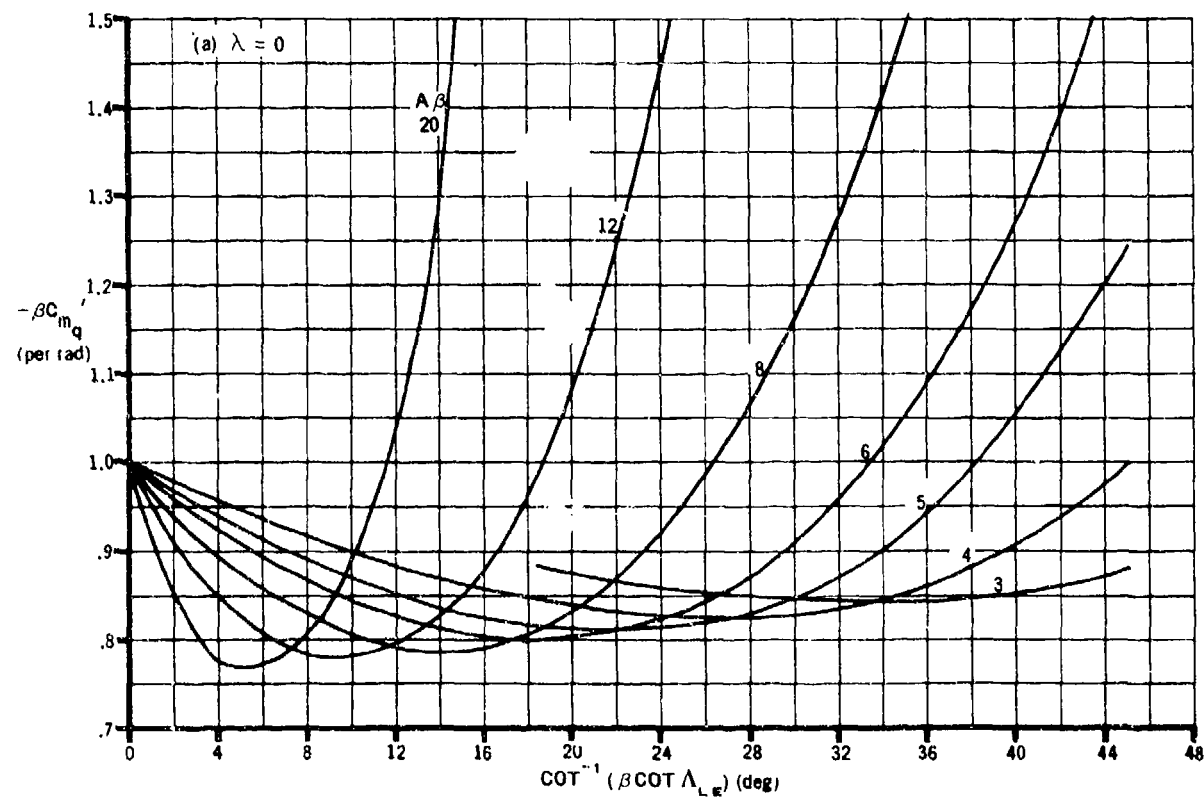


FIGURE 7.1.1.2-10 VARIATION OF $\beta C_{m_q}'$ WITH $\cot^{-1}(\beta \cot \lambda_{LE})$

7.1.1.2-10

SUPersonic SPEEDS
SUPersonic LEADING EDGE

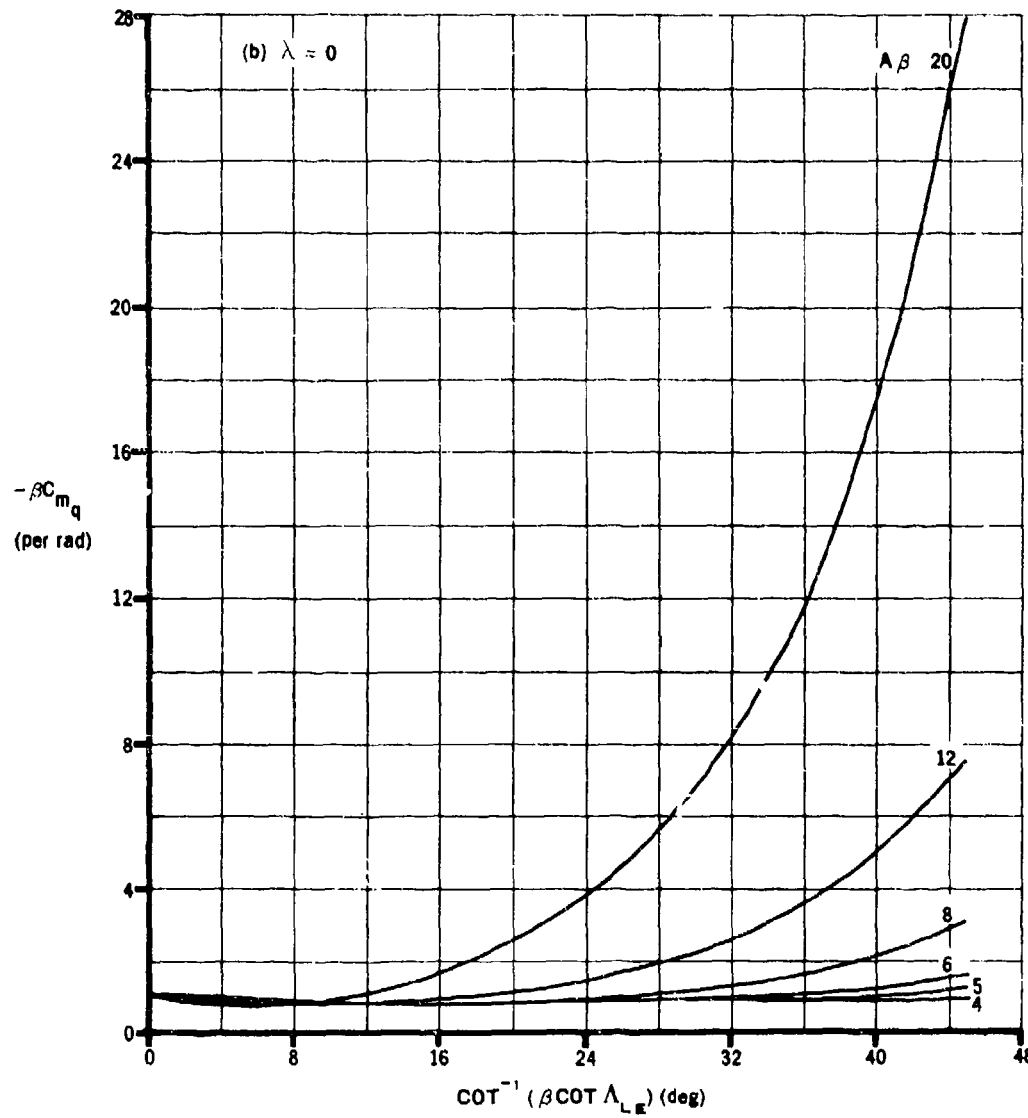


FIGURE 7.1.1.2-10 (CONT'D)

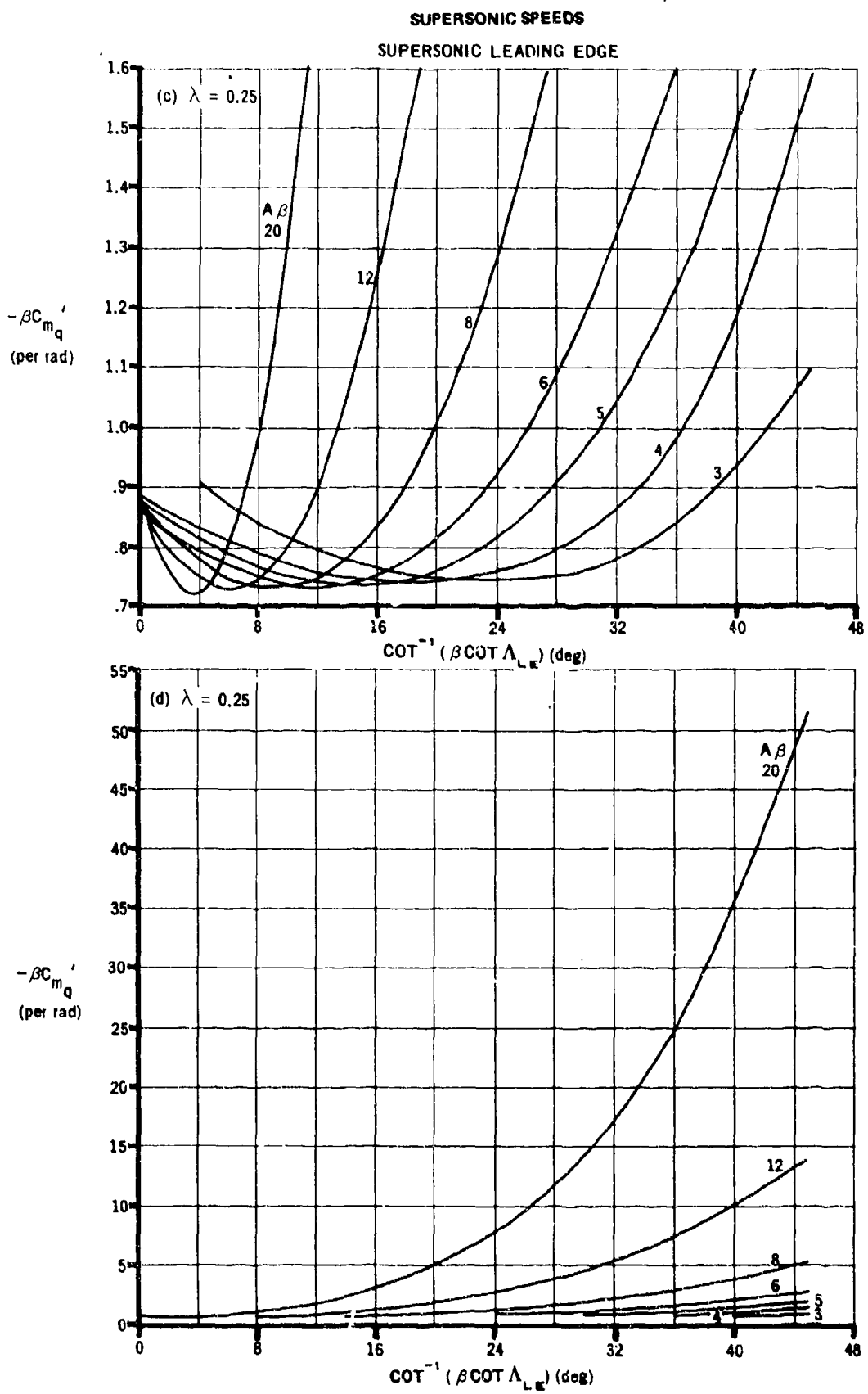


FIGURE 7.1.1.2-10 (CONT'D)

7.1.1.2-12

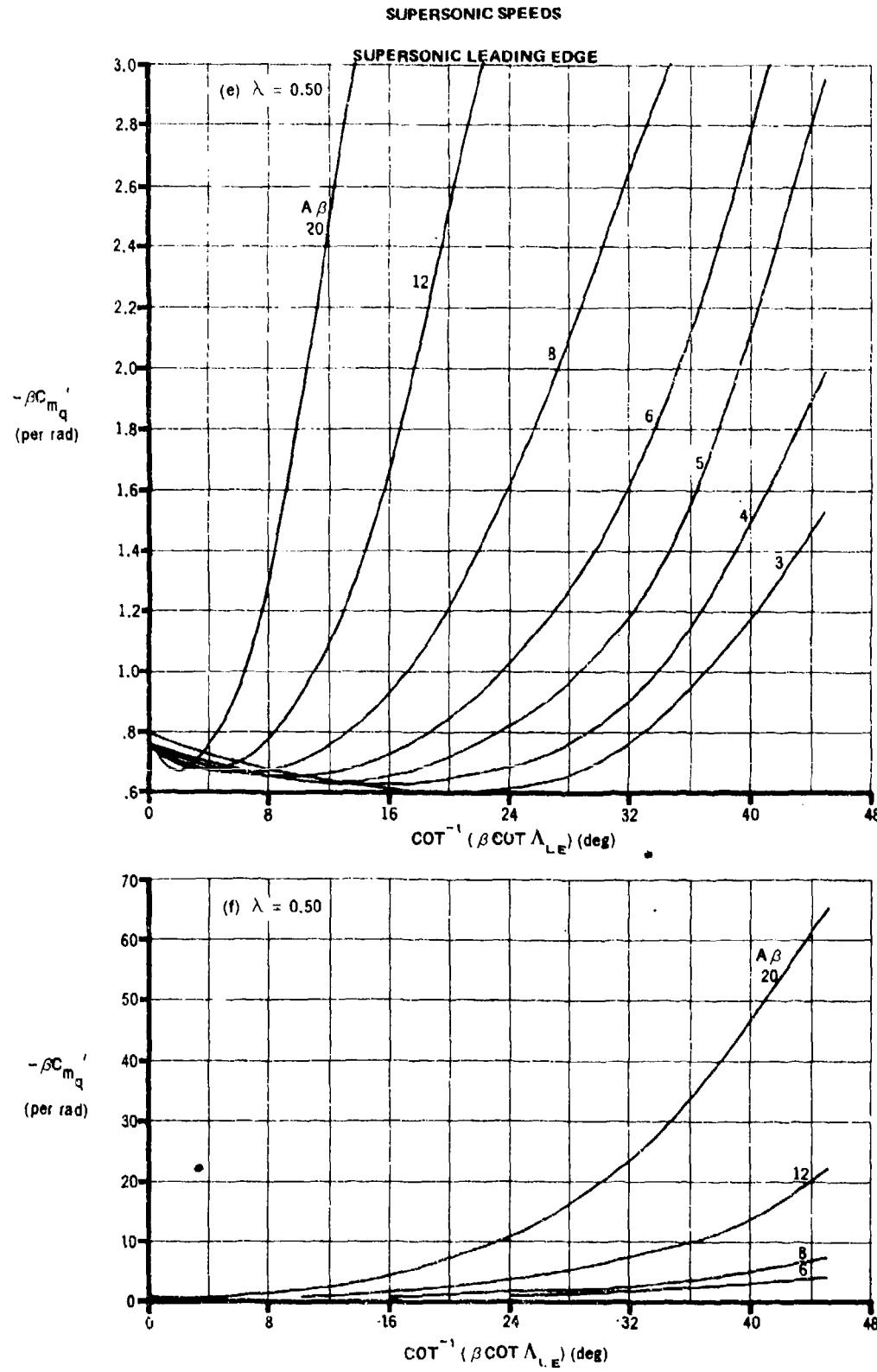


FIGURE 7.1.1.2-10 (CONTD)

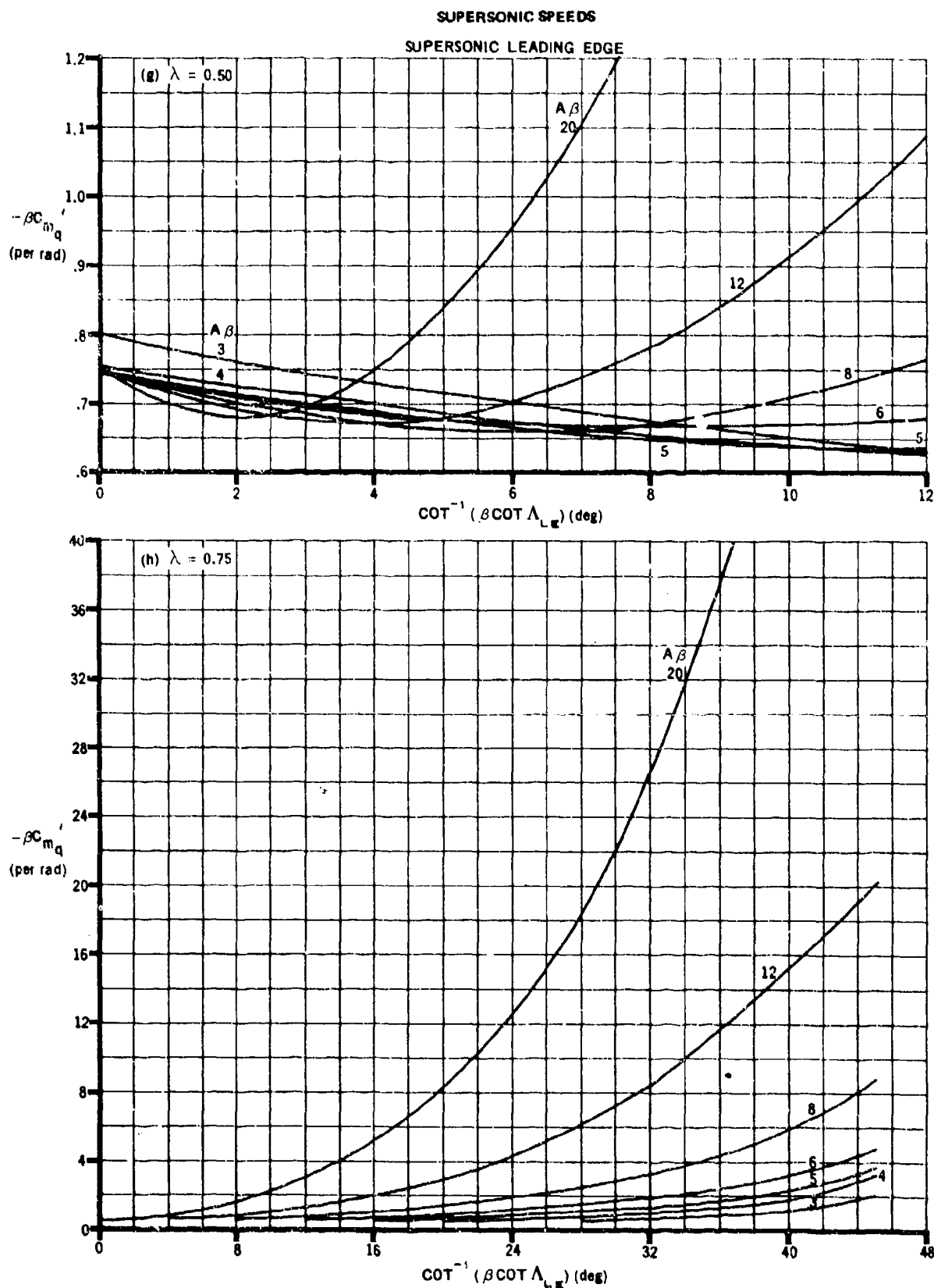


FIGURE 7.1.1.2-10 (CONTD)

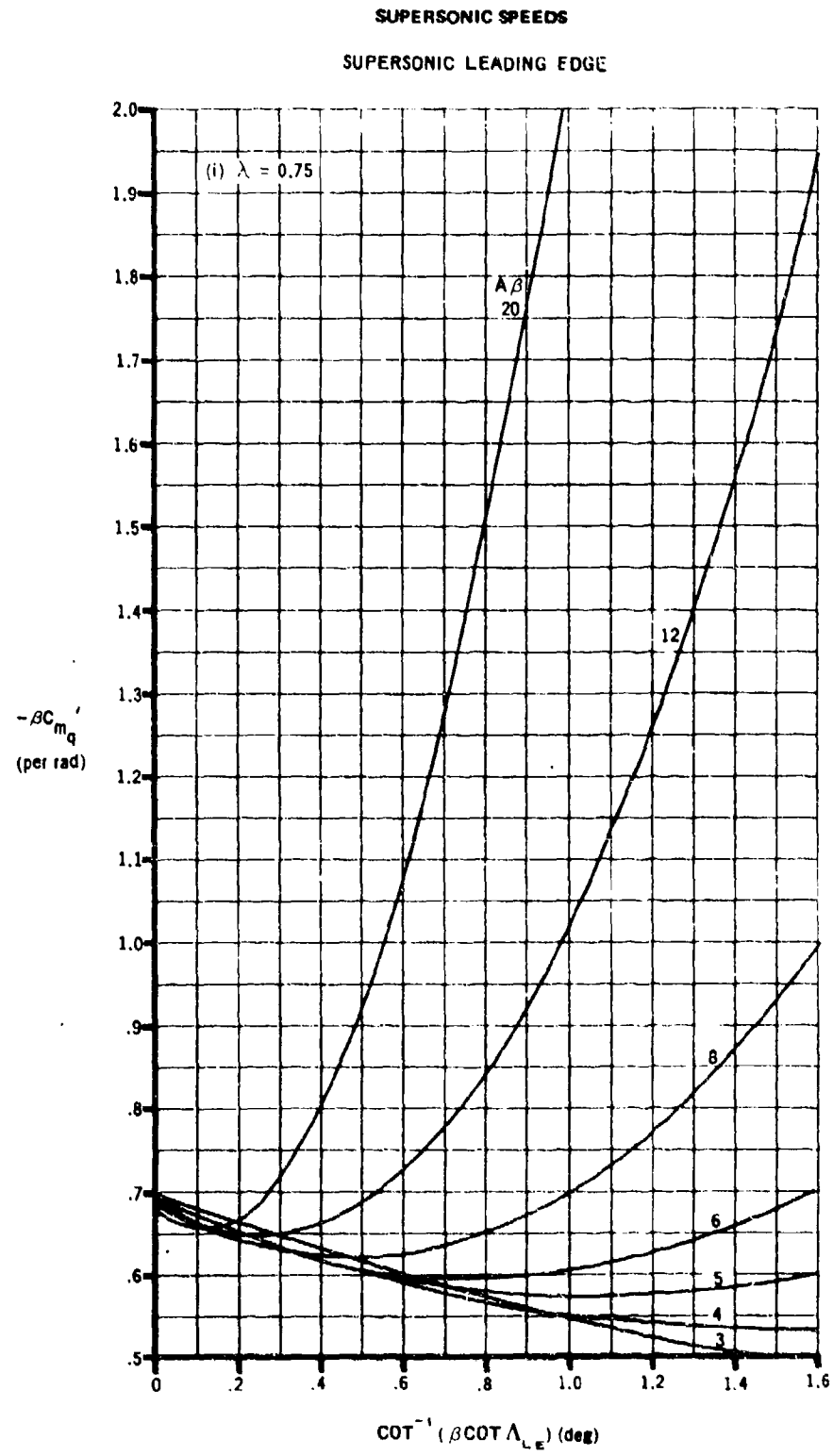


FIGURE 7.1.1.2-10 (CONT'D)

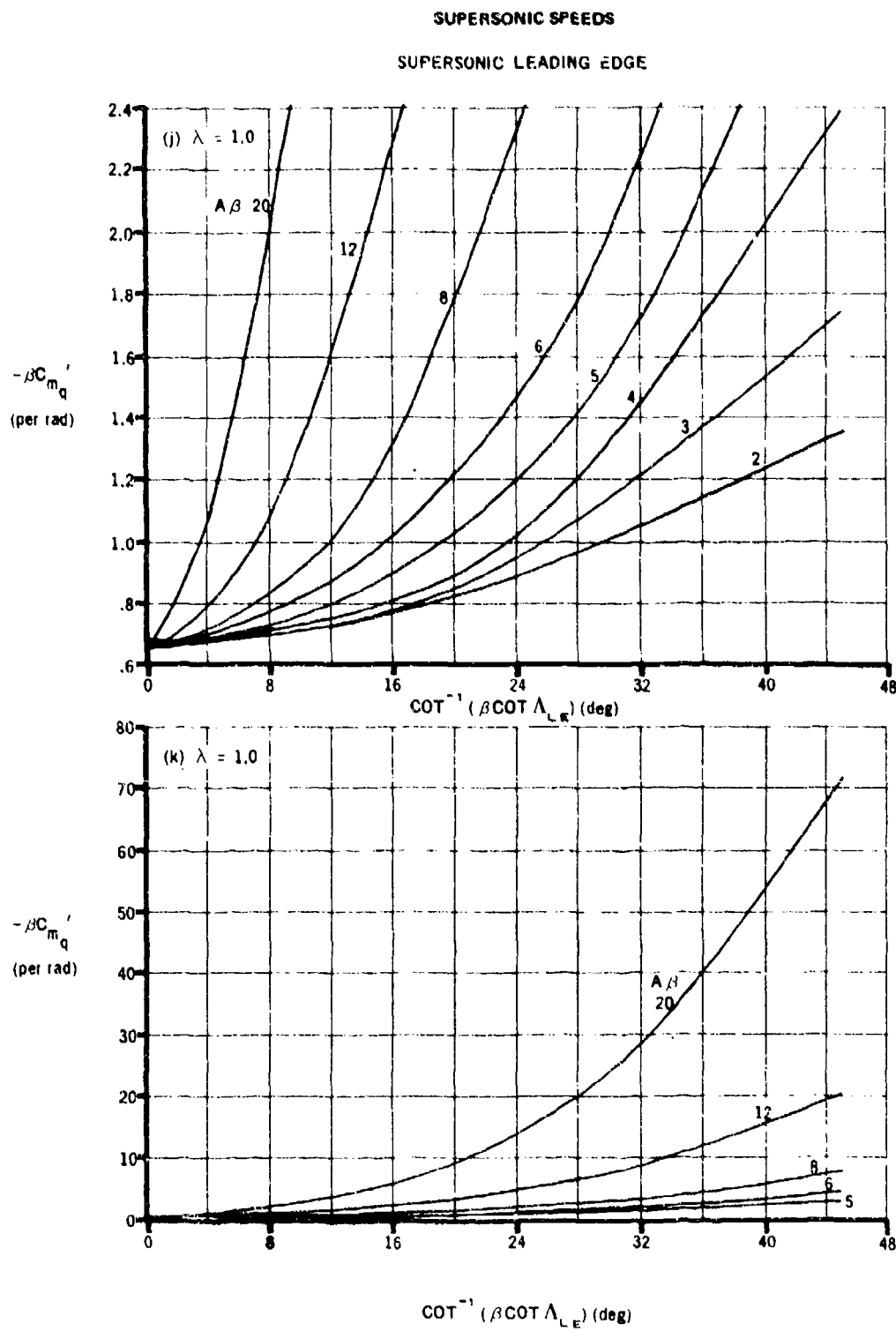


FIGURE 7.1.1.2-10 (CONTD)

7.1.1.3 WING PITCHING DERIVATIVE C_{D_q}

This section presents a method for estimating the wing contribution to the pitching derivative C_{D_q} at subsonic speeds. This derivative is the change in drag coefficient due to a change in pitching velocity at a constant angle of attack and is defined as

$$C_{D_q} = \frac{\partial C_D}{\partial \left(\frac{qc}{2V} \right)}, \text{ where } C_D \text{ is based on } S_w.$$

In general, this derivative is small and has a negligible effect on longitudinal stability; hence, it is usually neglected.

A. SUBSONIC

The method presented herein uses the Weissinger method of Reference 1 to calculate the section lift due to angle of attack, twist, and pitch rate. The lift is then rotated through the local downwash angle due to each of these effects to produce a chordwise component of force.

DATCOM METHOD

Design charts for predicting the wing contribution to C_{D_q} are available only at Mach numbers of 0.2 and 0.8. The wing pitching derivative C_{D_q} is given by

$$C_{D_q} = C_{D_{q_0}}(-\theta) + \frac{\partial C_{D_q}}{\partial \alpha_F} \alpha_F + \frac{\partial C_{D_q}}{\partial \left(\frac{qc}{2V} \right)} \left(\frac{qc}{2V} \right) \quad 7.1.1.3-a$$

where

$C_{D_{q_0}}$ is the contribution due to zero-angle-of-attack loading obtained from Figures 7.1.1.3-3a through -3f as a function of wing aspect ratio, taper ratio, and sweep.

θ is the wing twist in degrees between the root and tip sections, negative for washout (see Figure 5.1.2.1-30b).

$\frac{\partial C_{D_q}}{\partial \alpha_F}$ is the contribution due to angle of attack obtained from Figures 7.1.1.3- 7a through - 7f as a function of wing aspect ratio, taper ratio, and sweep.

α_F is the fuselage angle of attack in degrees.

$\frac{\partial C_{D_q}}{\partial \left(\frac{qc}{2V} \right)}$ is the contribution due to the rate of change of pitch obtained from Figures 7.1.1.3-12a through -12f as a function of wing aspect ratio, taper ratio, and sweep.

q is the pitch rate in degrees per second.

\bar{c} is the wing mean aerodynamic chord.

V is the free-stream velocity.

Sample Problem

Given: The following wing-body configuration

Wing Characteristics:

$$\begin{array}{lll} A = 7 & \lambda = 0.25 & \Lambda_{LE} = 35^\circ \\ \bar{c} = 25.0 \text{ ft} & S_W = 3500 \text{ ft}^2 & \theta = -5.0^\circ \end{array}$$

Additional Characteristics:

$$\begin{array}{lll} M = 0.8 & \alpha_F = 1^\circ & q = 5 \text{ deg/sec} \\ V = 796 \text{ ft/sec} \quad (h = 30,000 \text{ ft}) & & \end{array}$$

Compute:

$$C_{D_{q_0}} = 0.00036 \text{ per deg}^2 \text{ (interpolated using Figures 7.1.1.3-3d, -3e, and -3f)}$$

$$\frac{\partial C_{D_q}}{\partial \alpha_F} = 0.000876 \text{ per deg}^2 \text{ (interpolated using Figures 7.1.1.3- 7d, - 7e, and - 7f)}$$

$$\frac{\partial C_{D_q}}{\partial \left(\frac{q\bar{c}}{2V} \right)} = 0.00061 \text{ per deg}^2 \text{ (interpolated using Figures 7.1.1.3-12d, -12e, and -12f)}$$

$$\frac{q\bar{c}}{2V} = \frac{(5)(25)}{2(796)} = 0.0785 \text{ deg}$$

Solution:

$$C_{D_q} = C_{D_{q_0}} (+\theta) + \frac{\partial C_{D_q}}{\partial \alpha_F} \alpha_F + \frac{\partial C_{D_q}}{\partial \left(\frac{q\bar{c}}{2V} \right)} \left(\frac{q\bar{c}}{2V} \right) \quad (\text{Equation 7.1.1.3-a})$$

$$= (0.00036)(+5.0) + (0.000876)(1.0) + (0.00061)(0.0785)$$

$$= 0.00272 \text{ per deg}$$

B. TRANSONIC

No method is presented.

C. SUPERSONIC

No method is presented.

REFERENCE

1. De Young, J., and Harper, C. W.: Theoretical Symmetric Span Loading at Subsonic Speeds for Wings Having Arbitrary Planform. NACA TR 921, 1948. (U)

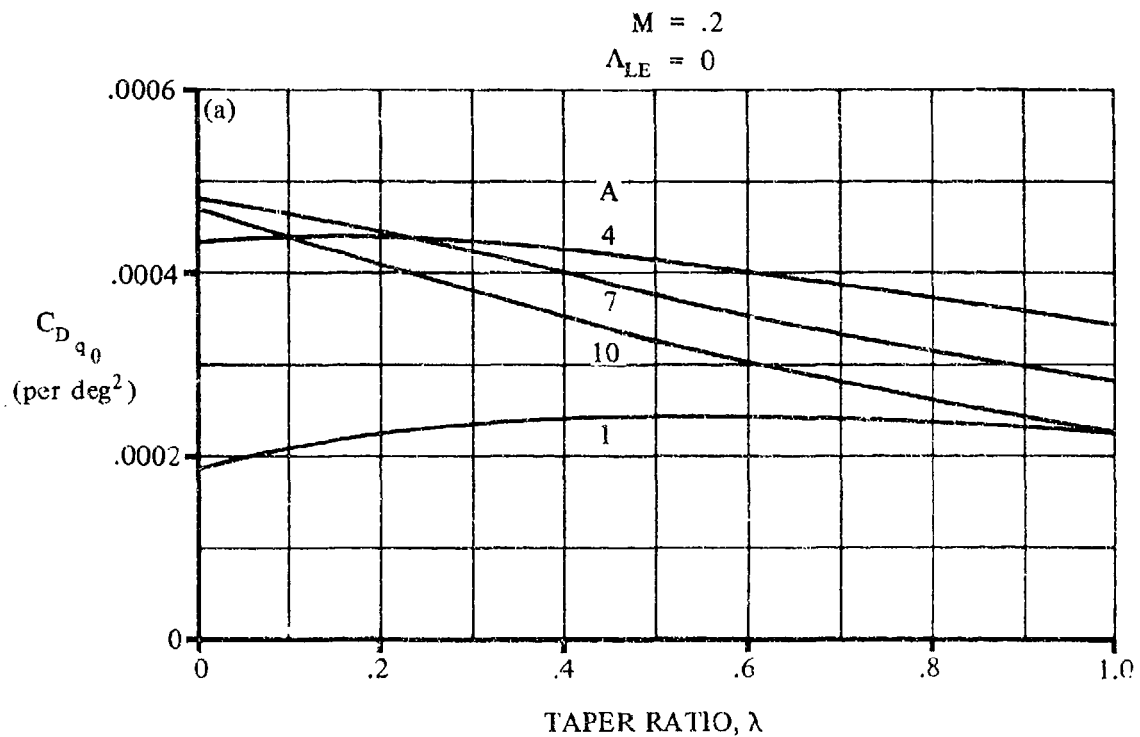


FIGURE 7.1.1.3-3 THE ZERO-ANGLE-OF-ATTACK LOADING CONTRIBUTION TO THE WING PITCHING DERIVATIVE C_{Dq_0}

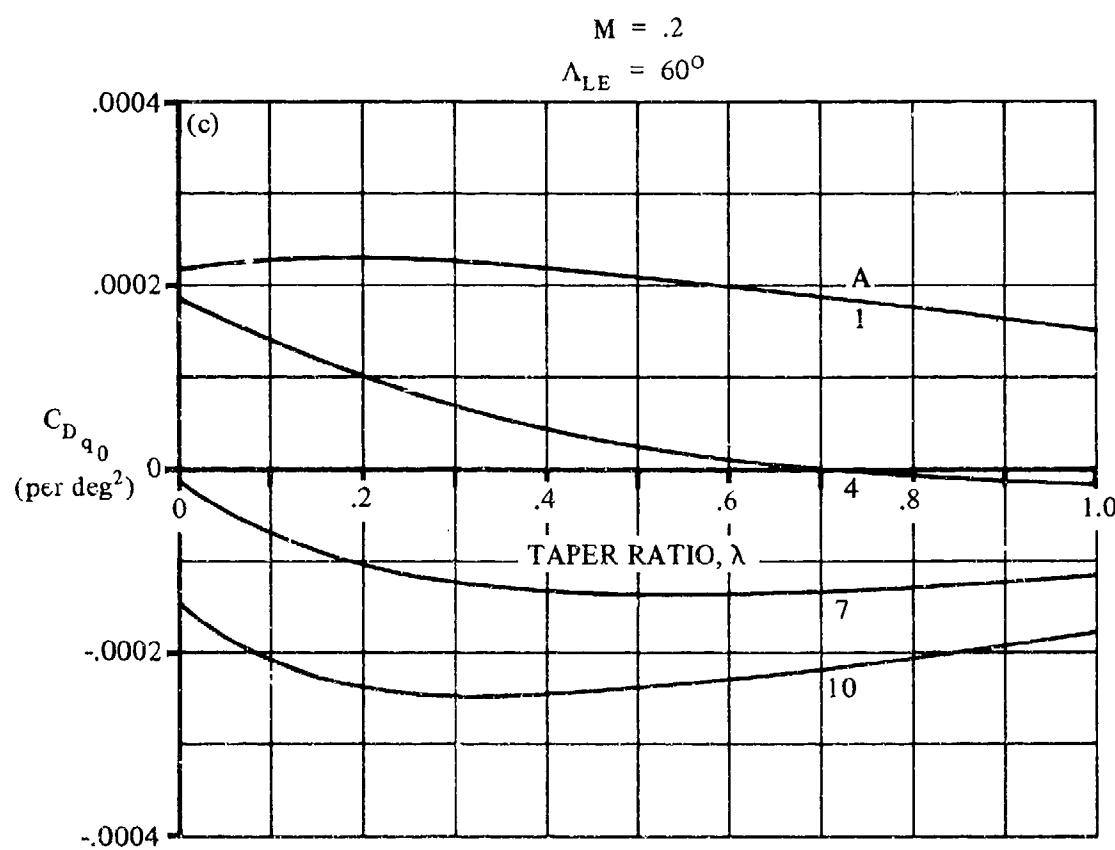
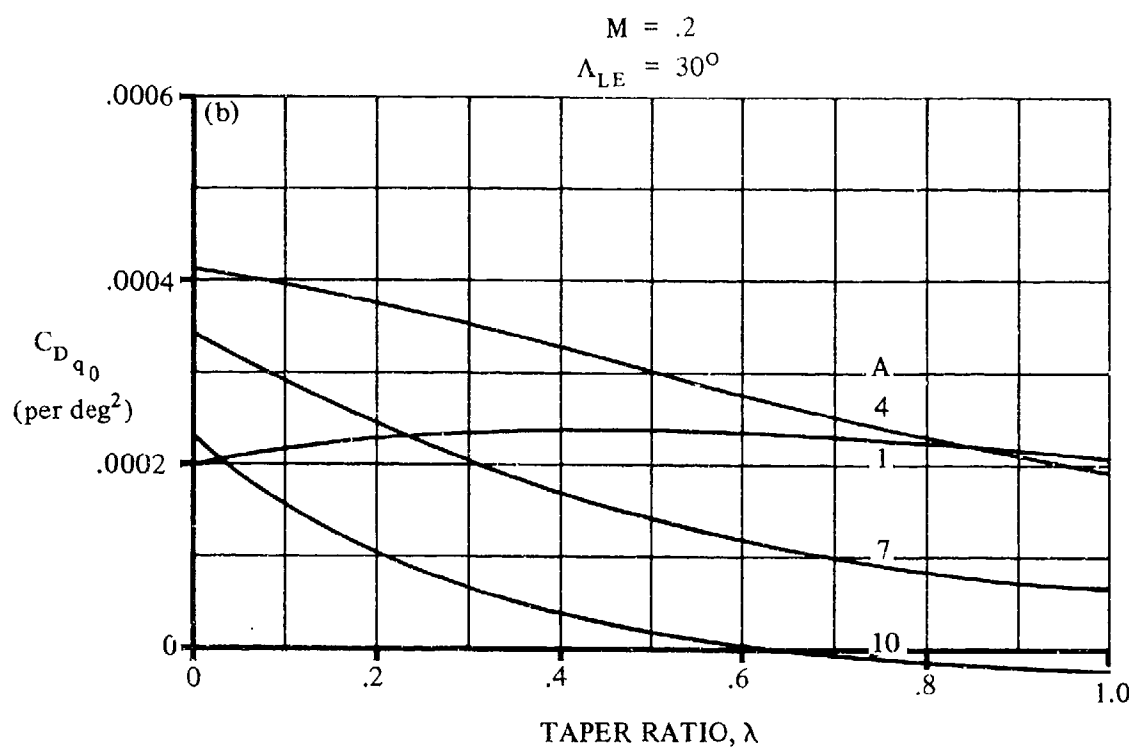


FIGURE 7.1.1.3-3 (CONT'D)

7.1.1.3-4

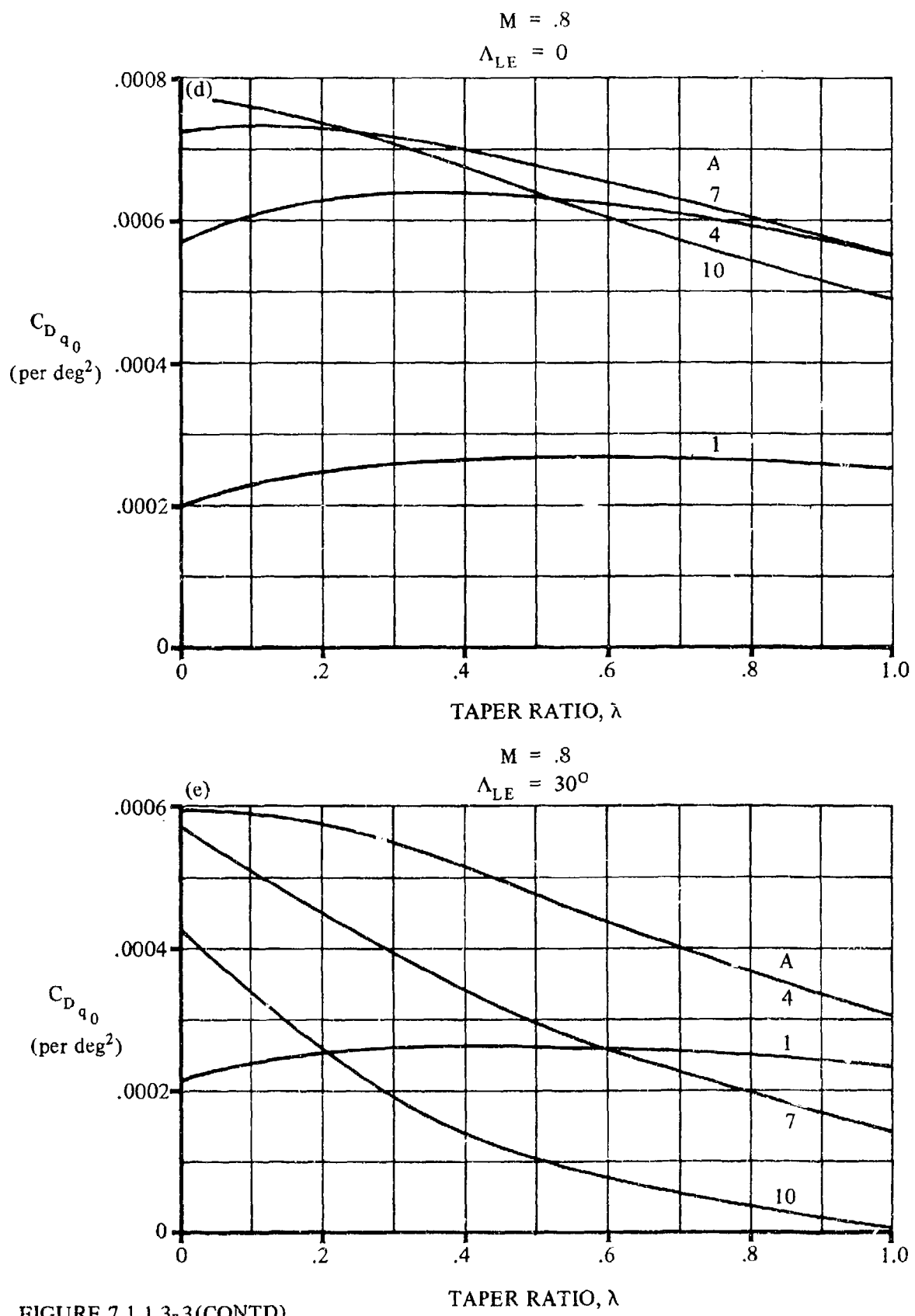


FIGURE 7.1.1.3-3(CONTD)

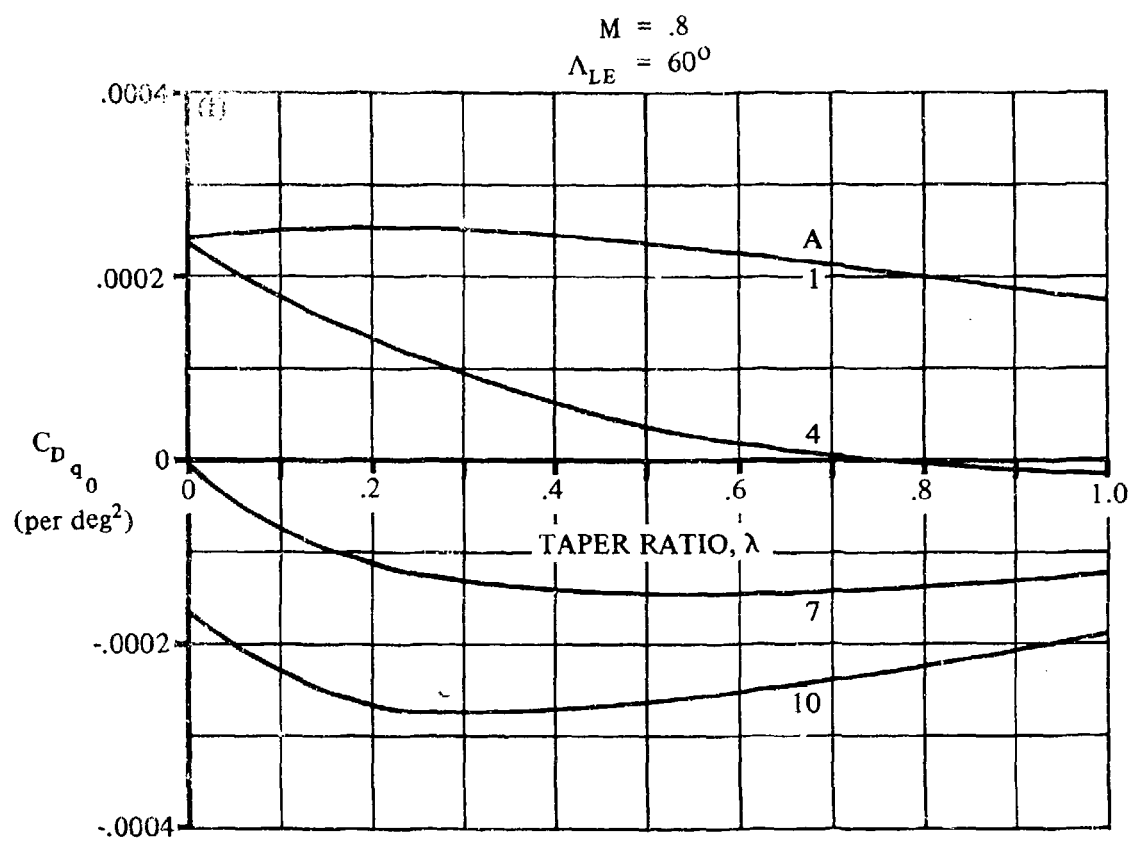


FIGURE 7.1.1.3-3 (CONTD)

7.1.1.3-6

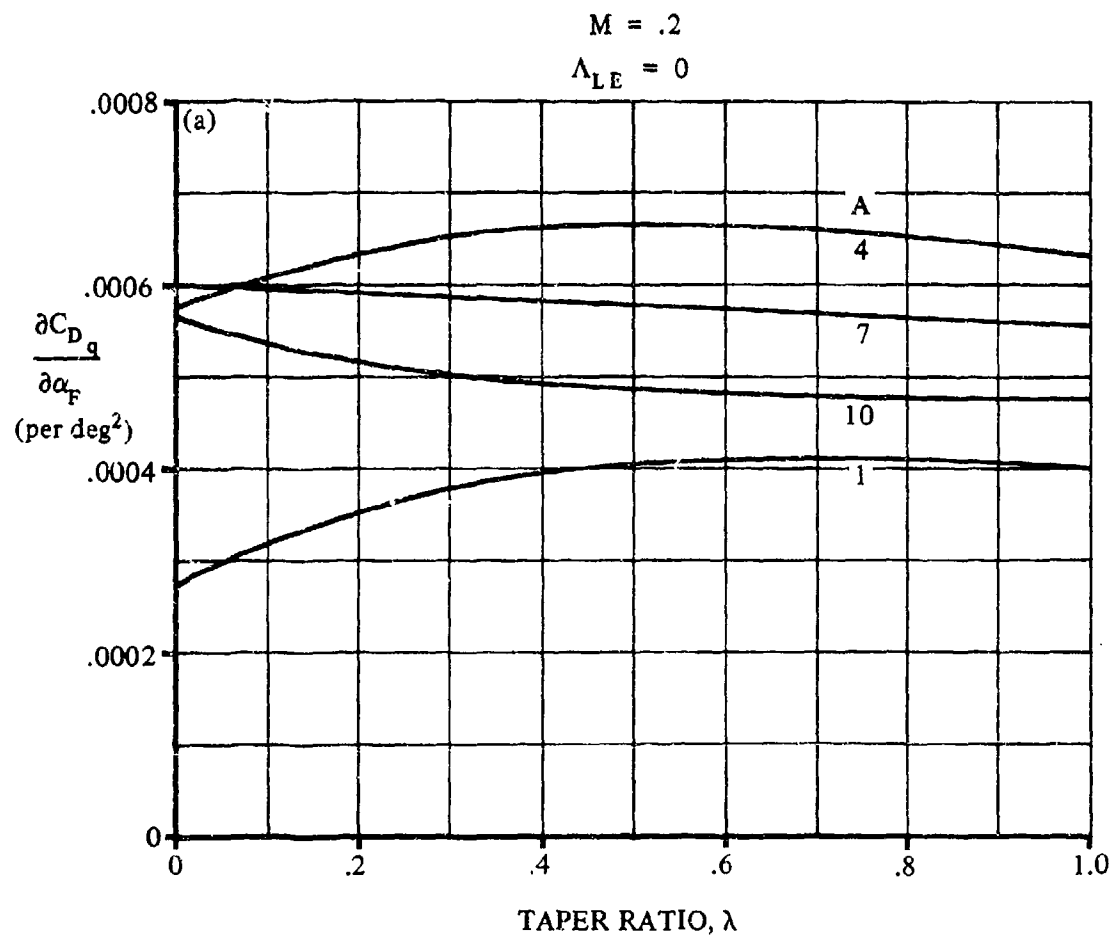


FIGURE 7.1.1.3- 7 THE ANGLE-OF-ATTACK CONTRIBUTION TO THE WING PITCHING DERIVATIVE C_{Dq}

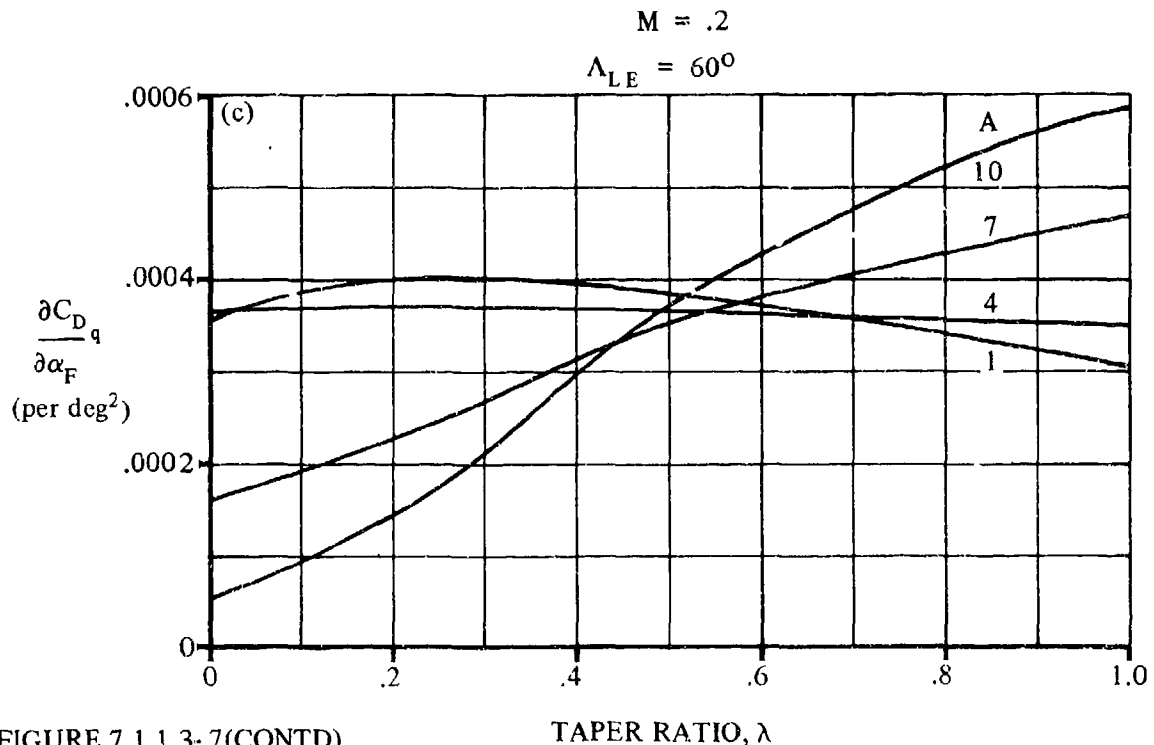
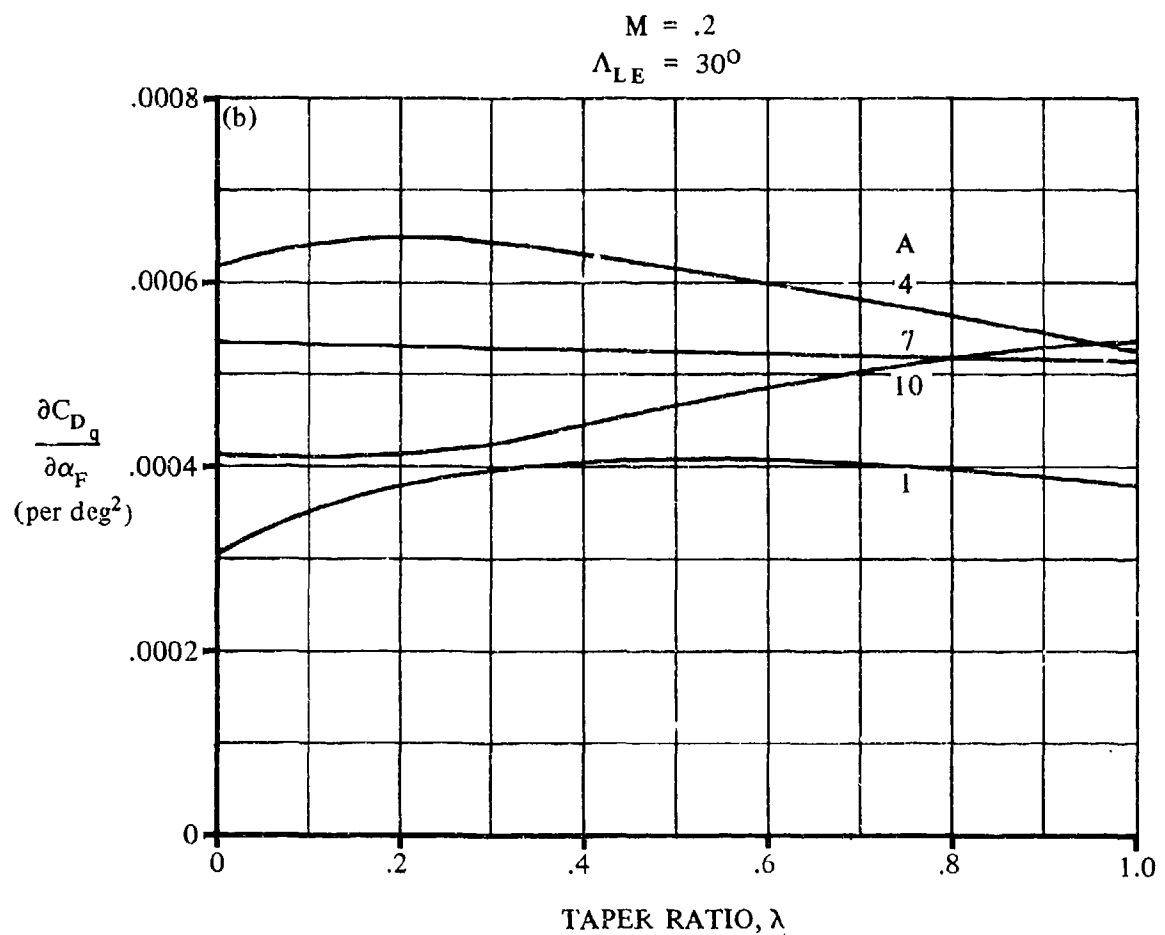


FIGURE 7.1.1.3-7(CONTD)

7.1.1.3-8

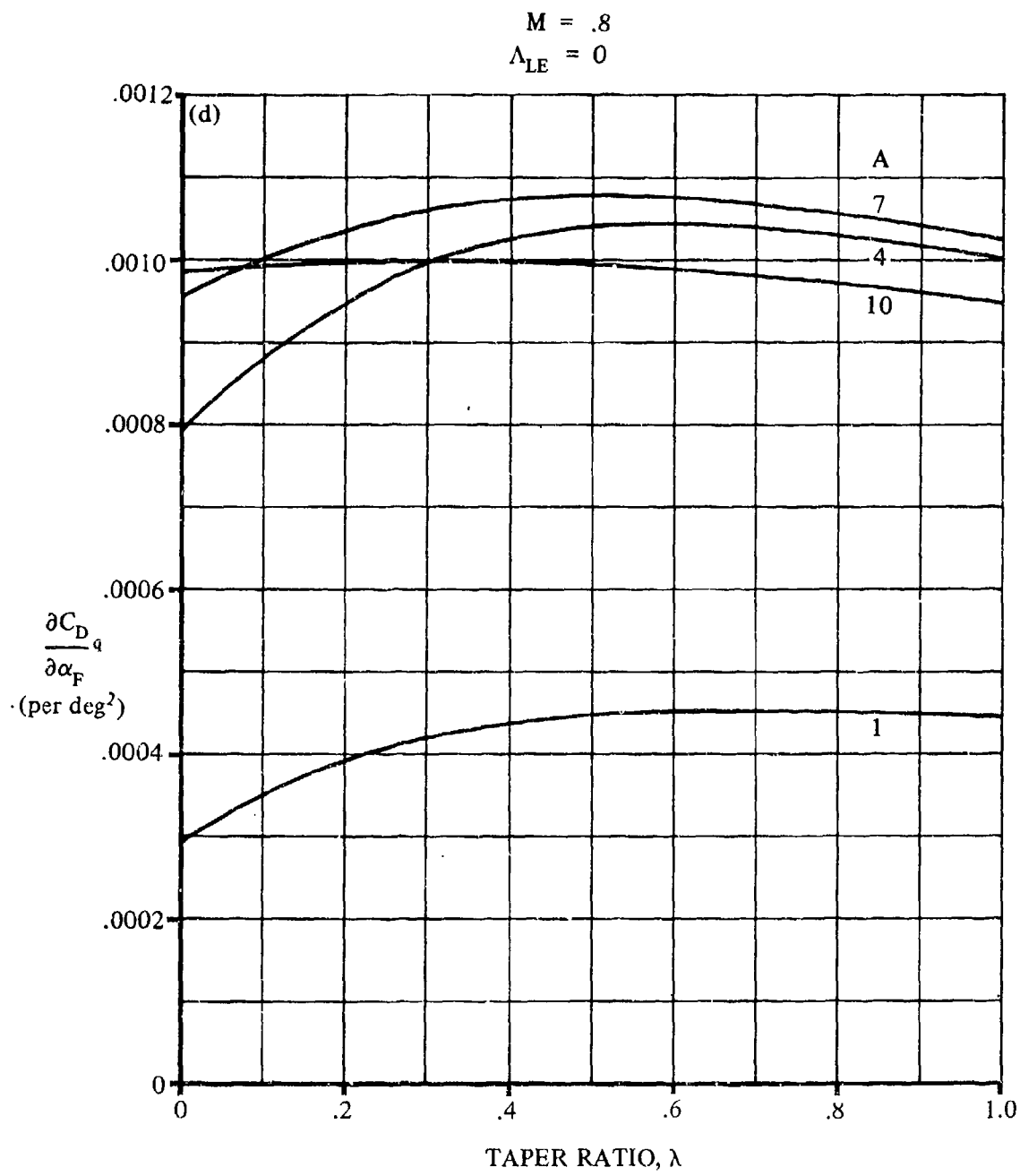


FIGURE 7.1.1.3- 7(CONTD)

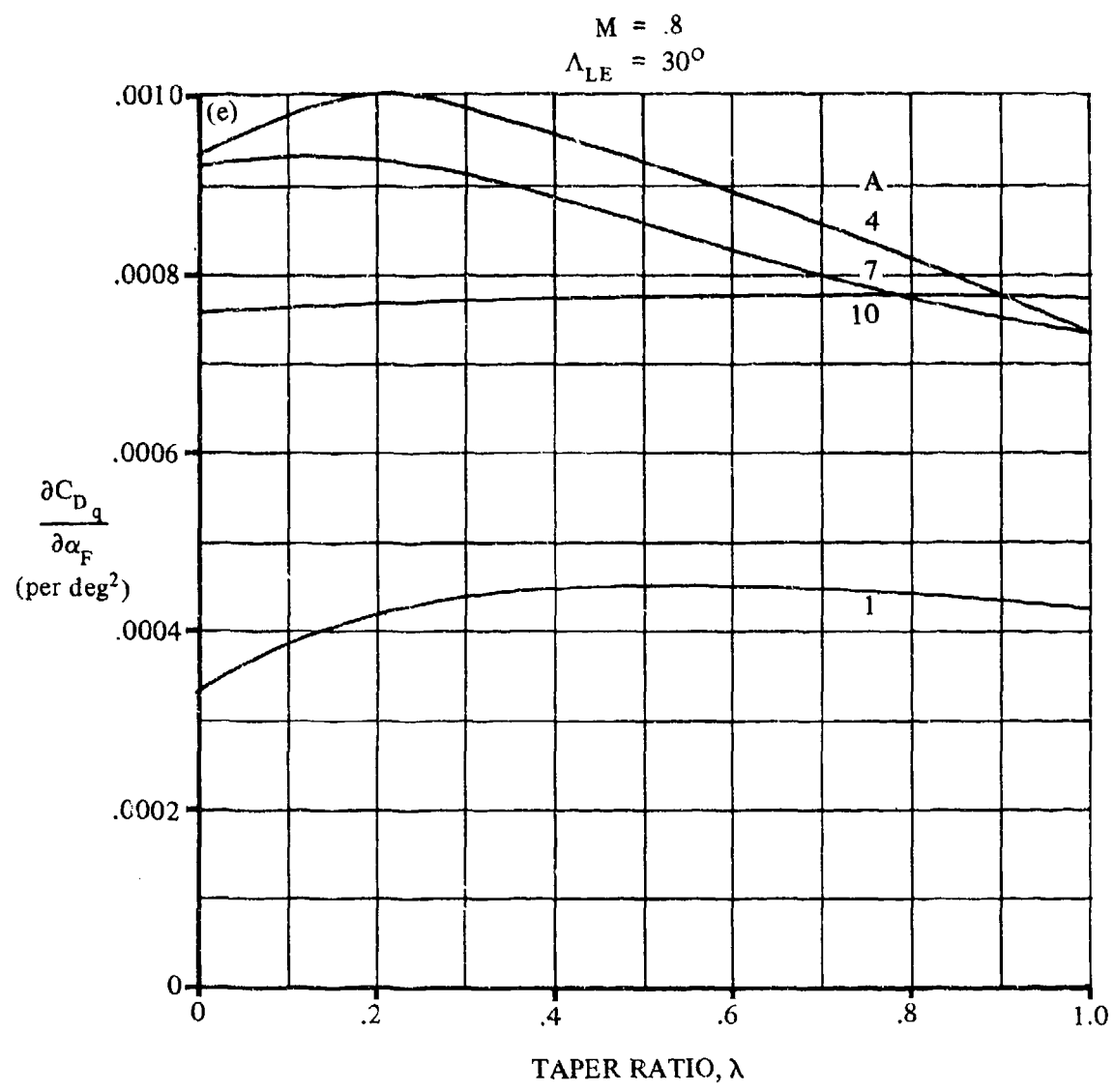


FIGURE 7.1.1.3- 7(CONTD)

7.1.1.3-10

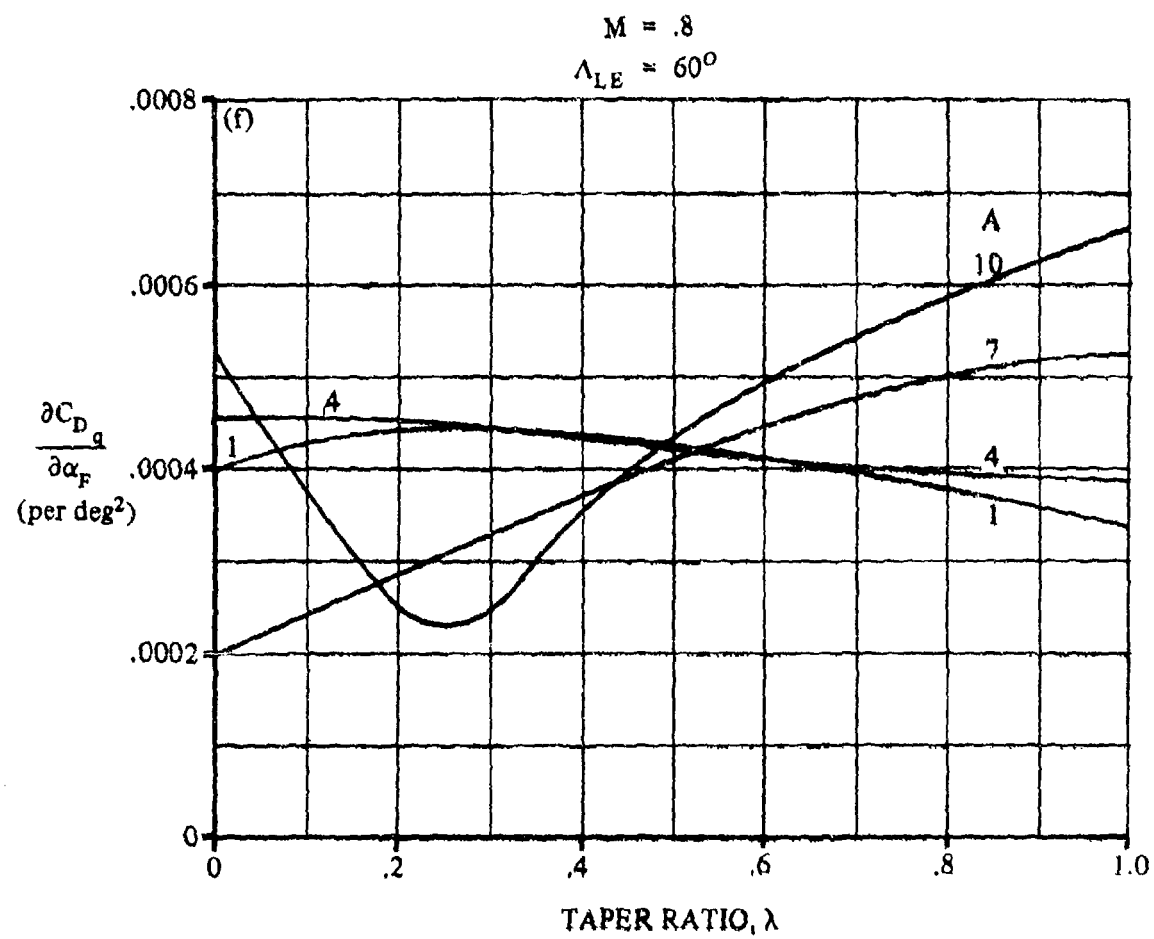


FIGURE 7.1.1.3-7(CONTD)

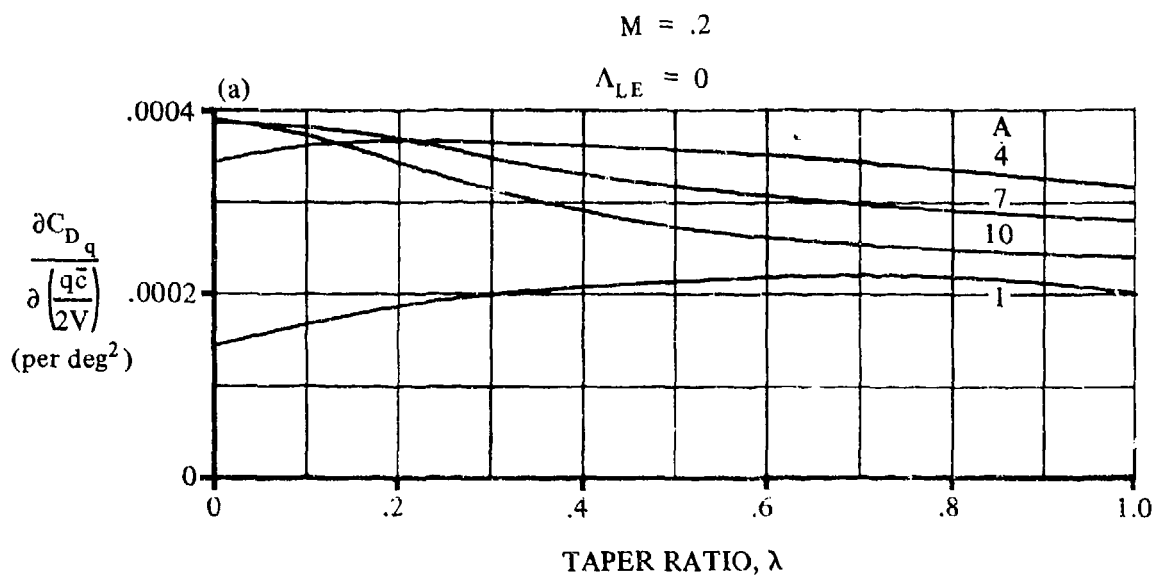


FIGURE 7.1.1.3-12 THE PITCH-RATE CONTRIBUTION TO THE WING PITCHING DERIVATIVE C_{D_q}

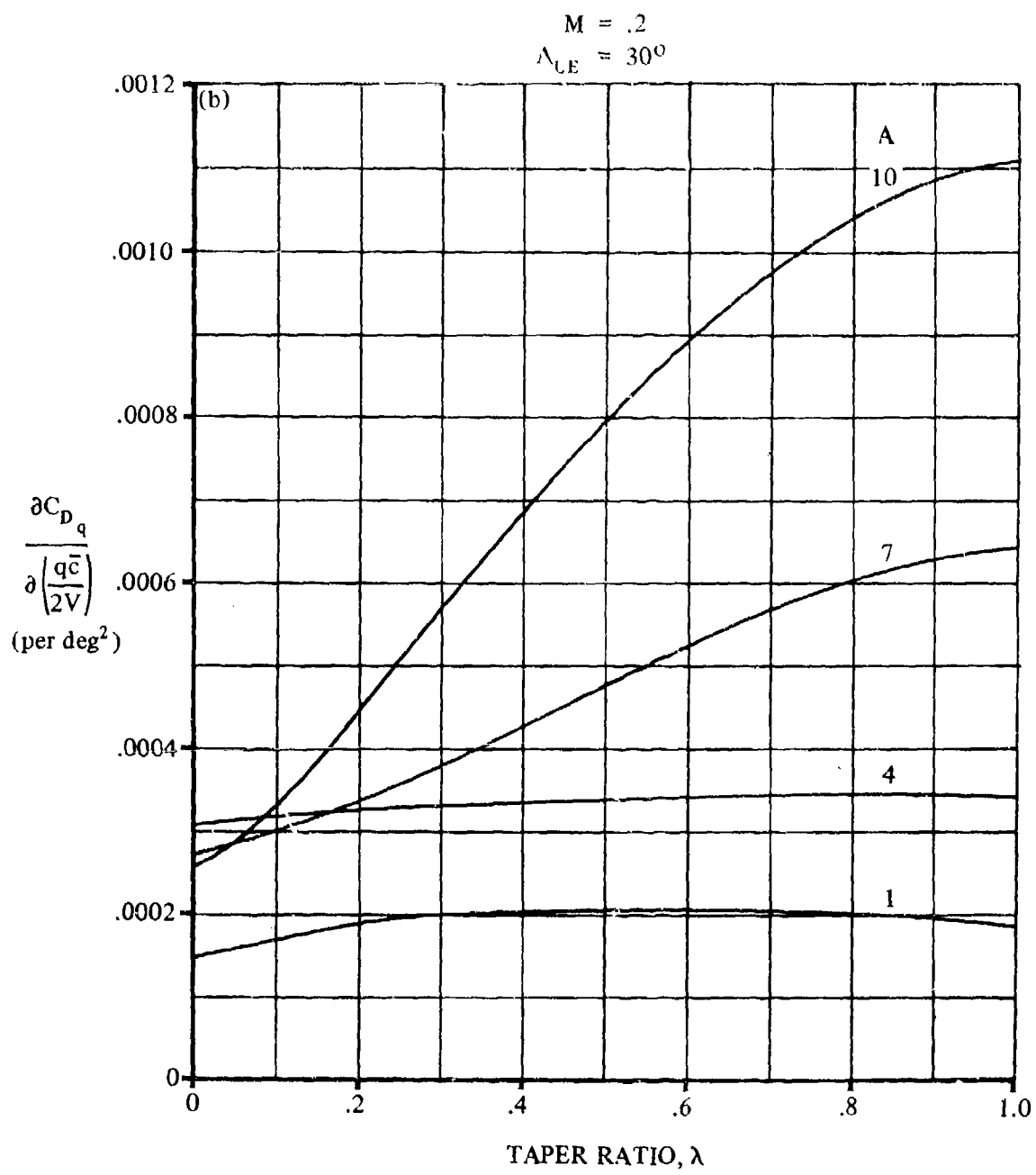


FIGURE 7.1.1.3-12 (CONTD)

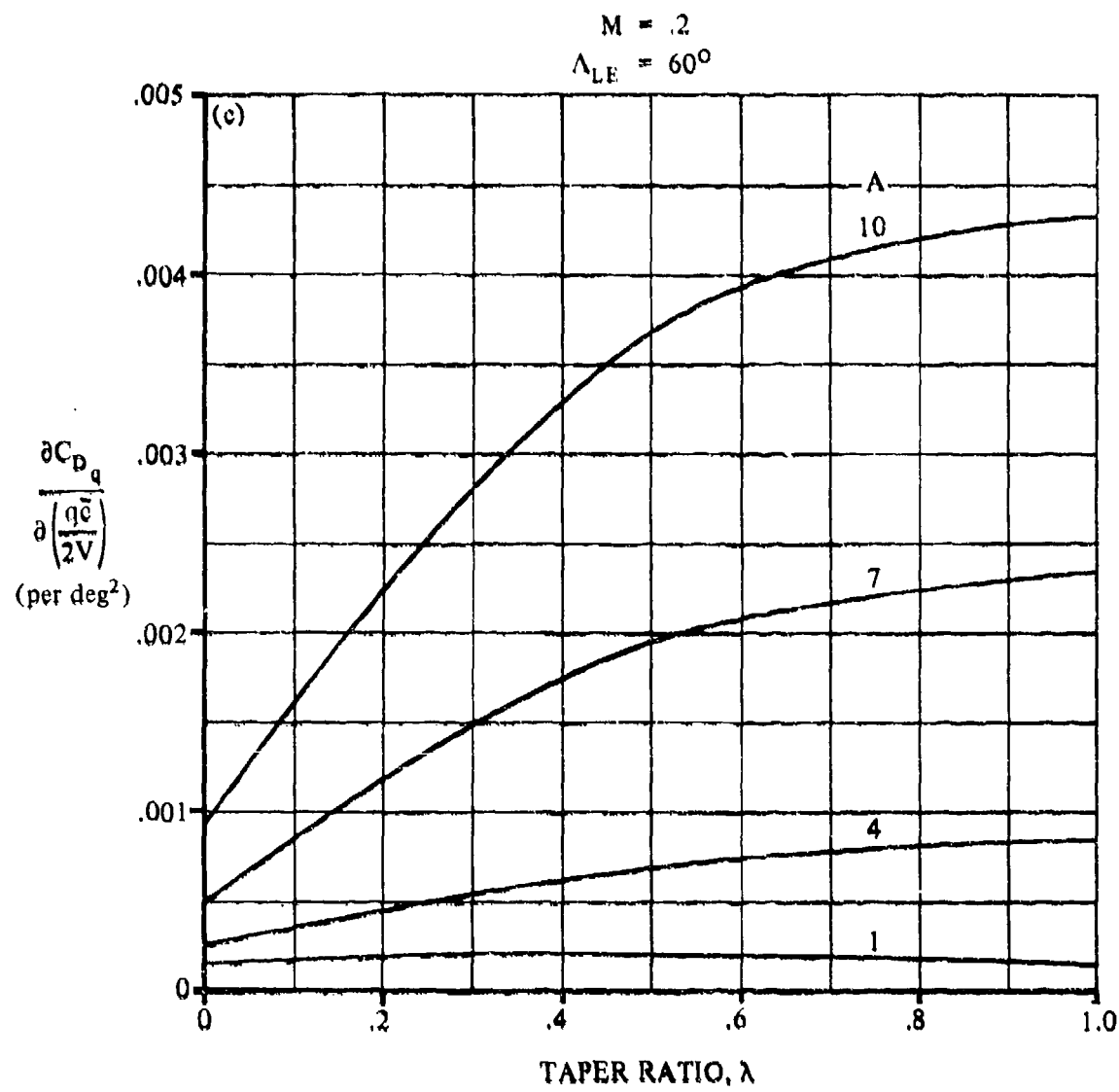


FIGURE 7.1.1.3-12 (CONT'D)

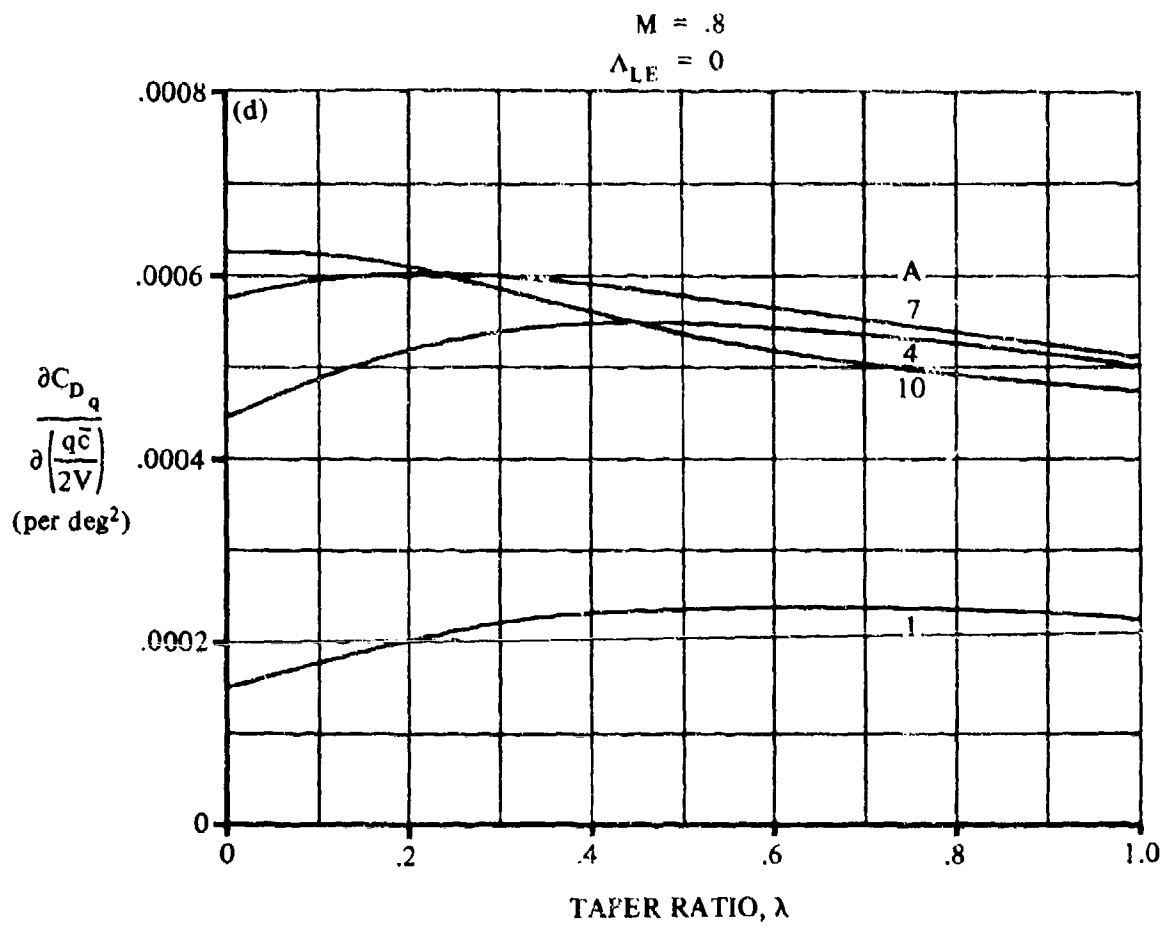


FIGURE 7.1.1.3-12 (CONTD)

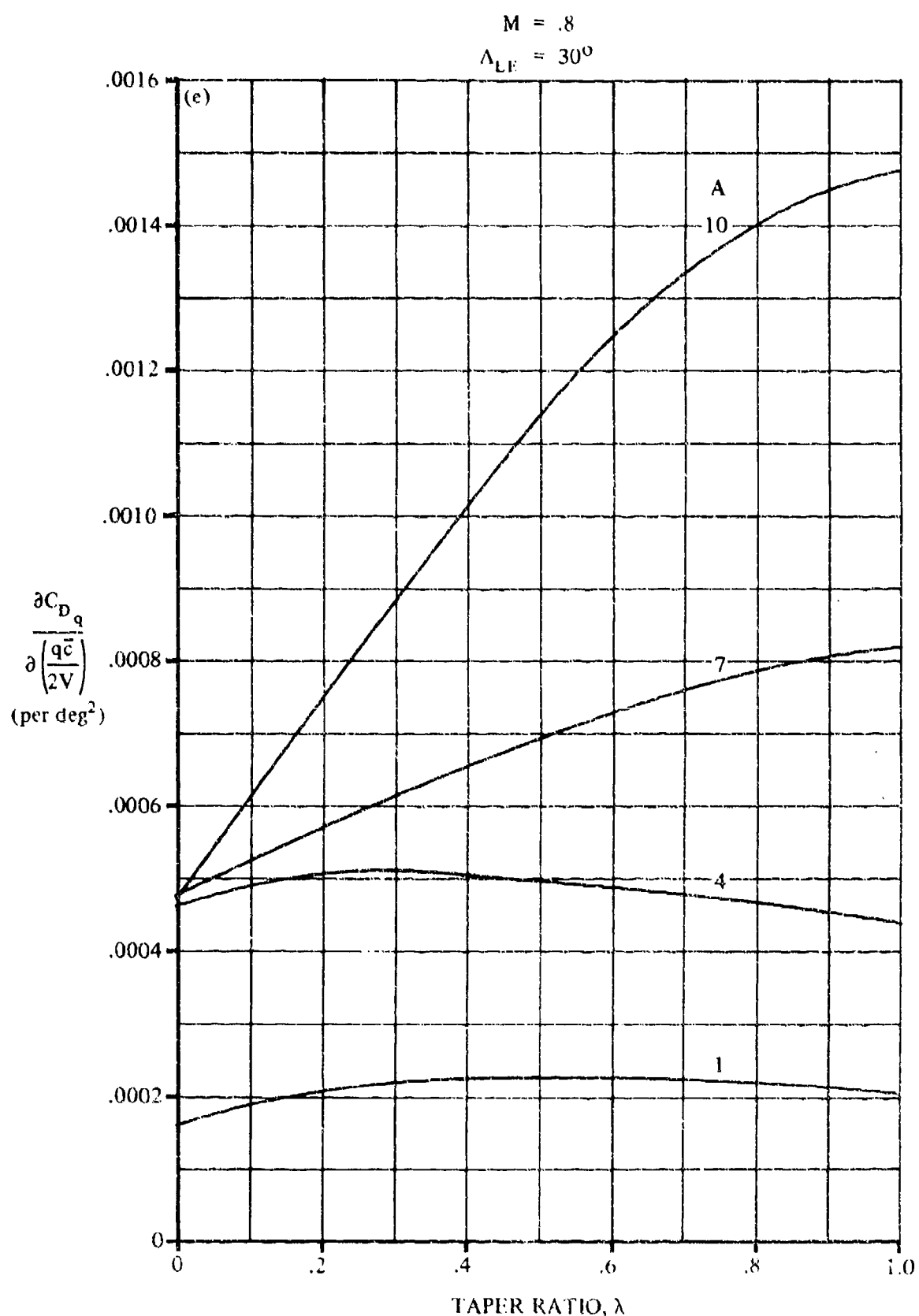


FIGURE 7.1.1.3-12 (CONTD)

7.1.1.3-16

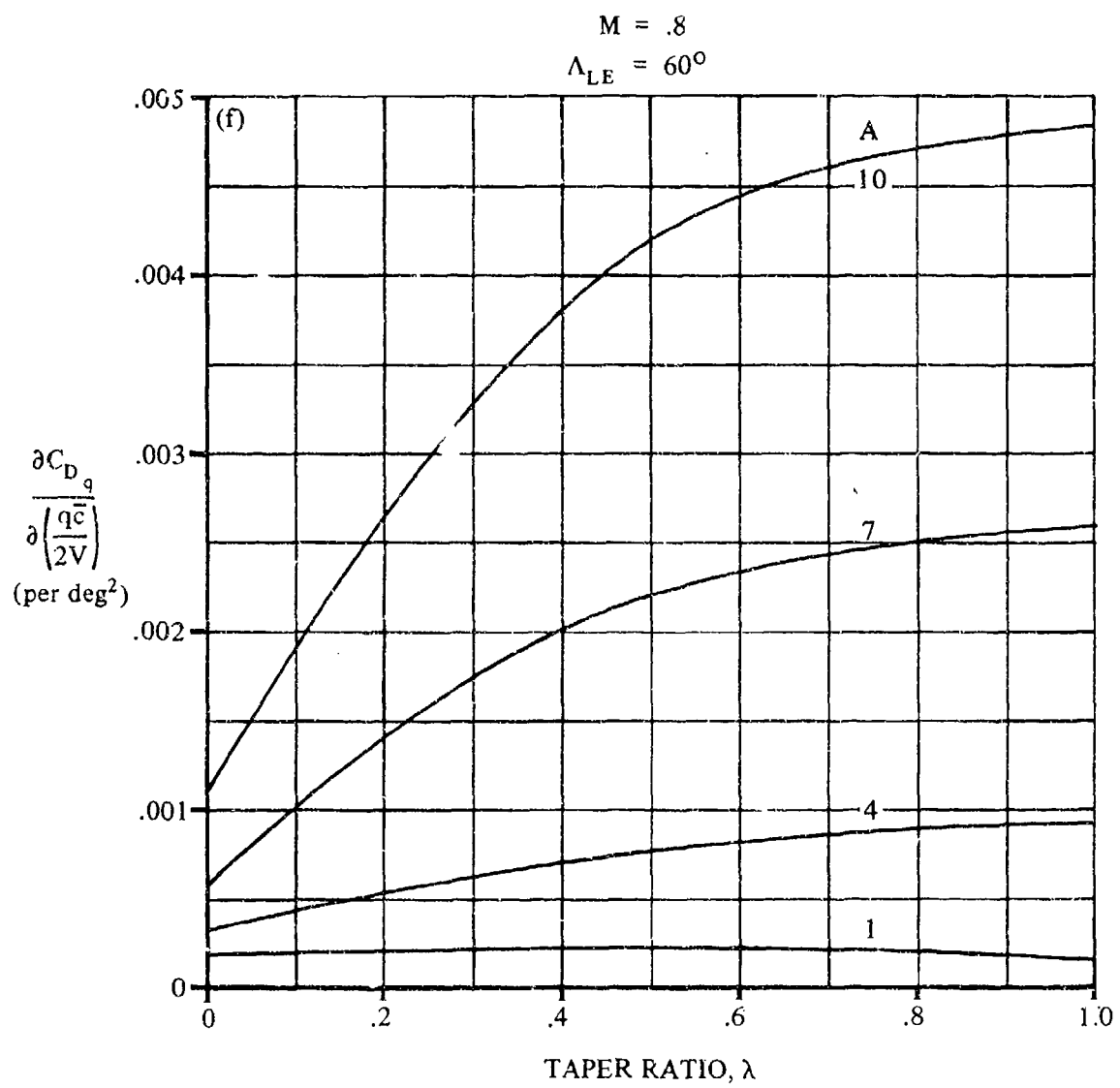


FIGURE 7.1.1.3-12 (CONT'D)

7.1.2 WING ROLLING DERIVATIVES

7.1.2.1 WING ROLLING DERIVATIVE C_{Y_p}

This section presents methods for estimating the wing contribution to the rolling derivative C_{Y_p} at subsonic and supersonic speeds. This derivative is the change in side-force coefficient with change in wing-tip helix angle and is expressed as

$$C_{Y_p} = \frac{\partial C_Y}{\partial \left(\frac{pb}{2V_\infty} \right)}$$

A. SUBSONIC

The wing rolling derivative C_{Y_p} results from the angle-of-attack distribution and the tip-suction effects of rolling wings.

The angle-of-attack distribution caused by rolling produces incremental changes in aerodynamic forces. For wings having sweep and/or dihedral, these incremental changes have components in the lateral direction, causing a side force. The contribution to C_{Y_p} due to the angle-of-attack distribution caused by rolling is derived in reference 1, based on simple sweep theory. This result is limited to swept, untapered wings at low lift coefficients. The effect of taper ratio has been derived based on the experimental results presented in reference 2. The effect of dihedral is taken from reference 3. Although the expression for the dihedral effect has been derived specifically for untapered wings, it should be reasonably reliable for wings of any taper ratio over the range of wing dihedral angles of practical interest.

The side force due to rolling of unswept wings is not accounted for by the theory of reference 1. This value is presumed to be caused by tip suction and is given by the empirical expression developed in reference 4. Experimental results show that the tip-suction effect is independent of sweep and varies inversely as the aspect ratio.

The method of reference 5 is applied to extrapolate the potential-flow values to high lift coefficients by using experimental values of the lift and drag at high lift coefficients. If experimental lift and drag data for the particular planform of interest are not available at the chosen Mach number, no attempt should be made to estimate the variation of C_{Y_p} with lift coefficient. The negligible importance of this derivative does not warrant the effort involved in estimating the wing lift and drag variation. Furthermore, no known general method for estimating the variation of drag coefficient will give results reliable enough to use in determining the correction factor for extrapolating the potential-flow values to higher lift coefficients.

DATCOM METHOD

The variation of the wing rolling derivative C_{Y_p} with lift coefficient, based on the product of the wing area and wing span, is given by

$$C_{Y_p} = K \left[\left(\frac{C_{Y_p}}{C_L} \right)_{\substack{C_L=0 \\ M}} C_L \right] + (\Delta C_{Y_p})_\Gamma \quad (\text{per radian}) \quad 7.1.2.1-a$$

where

$$\left(\frac{C_{Y_p}}{C_L} \right)_{\substack{C_L=0 \\ M}}$$

is the slope of the side force due to rolling at zero lift given by

$$\left(\frac{C_{Y_p}}{C_L} \right)_{\substack{C_L=0 \\ M}} = \frac{A + 4 \cos \Lambda_{c/4}}{AB + 4 \cos \Lambda_{c/4}} \quad \frac{AB + \cos \Lambda_{c/4}}{A + \cos \Lambda_{c/4}} \left(\frac{C_{Y_p}}{C_L} \right)_{\substack{C_L=0 \\ M=0}} \quad 7.1.2.1-b$$

where $B = \sqrt{1 - M^2 \cos^2 \Lambda_{c/4}}$ and

$$\left(\frac{C_{Y_p}}{C_L} \right)_{\substack{C_L=0 \\ M=0}}$$

is the slope of the low-speed side force due to rolling at zero lift, obtained from figure 7.1.2.1-9 as a function of aspect ratio, sweep of the quarter-chord, and taper ratio. This chart has been derived by using the results of references 1, 2, and 4. Equation 7.1.2.1-b modifies the low-speed value by means of the Prandtl-Glauert rule to yield approximate corrections for the first-order three-dimensional effects of compressible flow up to the critical Mach number.

C_L is the wing lift coefficient.

$(\Delta C_{Y_p})_\Gamma$ is the increment in C_{Y_p} due to dihedral given by

$$(\Delta C_{Y_p})_\Gamma = \left[3 \sin \Gamma \left(1 - 2 \frac{z}{b/2} \sin \Gamma \right) \right] \left(C_{I_p} \right)_{\substack{\Gamma=0 \\ C_L=0}} \quad (\text{per radian}) \quad 7.1.2.1-c$$

where

Γ is the geometric dihedral angle in degrees, positive for the wing tip above the plane of the root chord.

z is the vertical distance between the c.g. and the wing root quarter-chord point, positive for the c.g. above the wing root chord. (This parameter is independent of angle of attack.)

b is the wing span.

$(C_{I_p})_{\substack{r=0 \\ C_L=0}}$ is the roll-damping derivative of the wing without dihedral and at zero lift. This value is obtained from paragraph A of Section 7.1.2.2 and is given by (see equation 7.1.2.2-a)*

$$(C_{I_p})_{\substack{r=0 \\ C_L=0}} = \left(\frac{\beta C_{I_p}}{\kappa} \right)_{C_L=0} \frac{\kappa}{\beta} \quad (\text{per radian})$$

K is a dimensionless correction factor used to extrapolate the potential-flow values to high lift coefficients. At zero lift this factor is taken as 1.0. At lift coefficients other than zero this factor accounts for the variation of profile drag with lift coefficient and is given by

$$K = \frac{\frac{\partial}{\partial \alpha} (C_L \tan \alpha) - \frac{\partial}{\partial \alpha} (C_D - C_{D_0})}{\frac{\partial}{\partial \alpha} (C_L \tan \alpha) - \frac{\partial}{\partial \alpha} \left(\frac{C_L^2}{\pi A} \right)} \quad 7.1.2.1-d$$

Test values of lift and drag at the chosen Mach number for the particular planform of interest must be used in evaluating equation 7.1.2.1-d. The terms of equation 7.1.2.1-d are evaluated by taking the slopes of $C_L \tan \alpha$, $C_D - C_{D_0}$, and $C_L^2/(\pi A)$, plotted versus angle of attack.

If reliable values of the static-force coefficients are available, the method should provide results within ± 20 percent accuracy throughout the lift-coefficient range to the stall.

Sample Problem:

Given: The wing designated 32.6-4-0.6-006 of references 5 and 8.

Wing Characteristics:

$$A = 4.0 \quad \lambda = 0.60 \quad \Lambda_{c/4} = 32.6^\circ \quad \Gamma = 0$$

$$S = 2.25 \text{ sq ft}$$

Additional Characteristics:

$$M = 0.7$$

The following test values from reference 8 at $M = 0.7$

$$C_{D_0} = 0.01$$

*The effect of profile drag on the roll damping at zero lift is neglected.

C_L	.05	.1	.2	.3	.4	.5	.6	.7
α	.75	1.50	2.95	4.30	5.60	7.20	8.80	11.20
C_D	.011	.0115	.015	.021	.033	.0535	.078	.145

Compute:

Determine C_{Y_p}/C_L at zero lift

$$\left(\frac{C_{Y_p}}{C_L} \right)_{\substack{C_L=0 \\ M=0}} = 0.42 \text{ per rad} \quad (\text{figure 7.1.2.1-9})$$

$$B = \sqrt{1 - M^2 \cos^2 \Lambda_{c/4}} = \sqrt{1 - (0.7)^2 (\cos 32.6^\circ)^2} = 0.808$$

$$\frac{A + 4 \cos \Lambda_{c/4}}{AB + 4 \cos \Lambda_{c/4}} = \frac{4.0 + 4 \cos 32.6^\circ}{(4.0)(0.808) + 4 \cos 32.6^\circ} = 1.116$$

$$\frac{AB + \cos \Lambda_{c/4}}{A + \cos \Lambda_{c/4}} = \frac{(4.0)(0.808) + \cos 32.6^\circ}{4.0 + \cos 32.6^\circ} = 0.8414$$

$$\frac{A + 4 \cos \Lambda_{c/4}}{AB + 4 \cos \Lambda_{c/4}} \cdot \frac{AB + \cos \Lambda_{c/4}}{A + \cos \Lambda_{c/4}} = (1.116)(0.8414) = 0.939$$

$$\left(\frac{C_{Y_p}}{C_L} \right)_{\substack{C_L=0 \\ M=0}} = \frac{A + 4 \cos \Lambda_{c/4}}{AB + 4 \cos \Lambda_{c/4}} \cdot \frac{AB + \cos \Lambda_{c/4}}{A + \cos \Lambda_{c/4}} \left(\frac{C_{Y_p}}{C_L} \right)_{\substack{C_L=0 \\ M=0}} \quad (\text{equation 7.1.2.1-b})$$

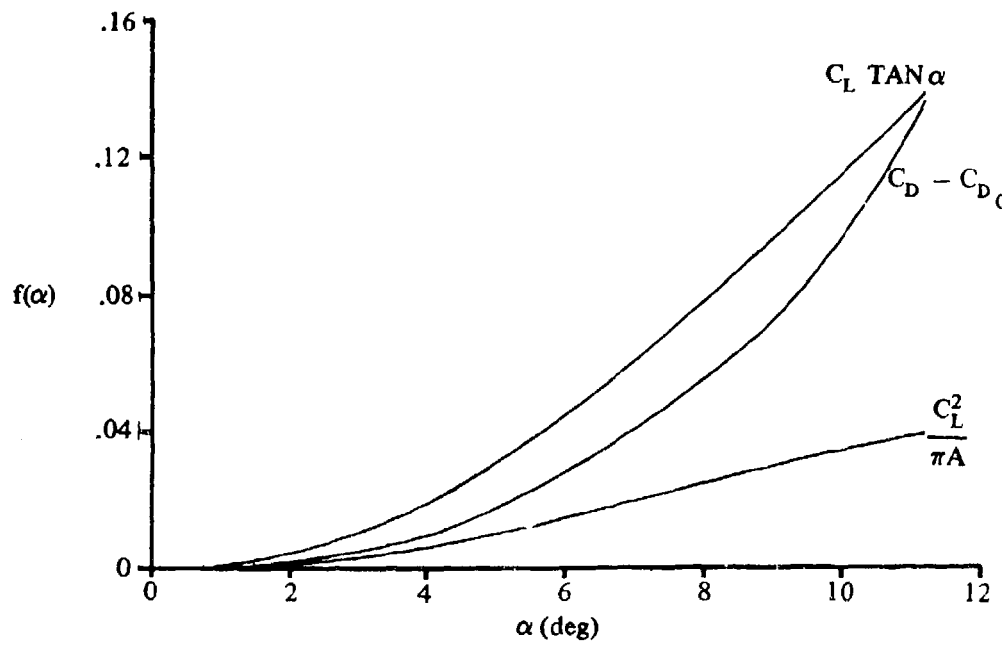
$$= (0.939)(0.42) = 0.394$$

Determine the K factor

$$K = \frac{\frac{\partial}{\partial \alpha} (C_L \tan \alpha) - \frac{\partial}{\partial \alpha} (C_D - C_{D_0})}{\frac{\partial}{\partial \alpha} (C_L \tan \alpha) - \frac{\partial}{\partial \alpha} \left(\frac{C_L^2}{\pi A} \right)} \quad (\text{equation 7.1.2.1-d})$$

① C_L	② α Test (deg)	③ $\tan \alpha$ $\tan ②$	④ $C_L \tan \alpha$ ① ③	⑤ C_D Test	⑥ $C_D - C_{D_0}$ ⑤ -- 0.01	⑦ $C_L^2 / (\pi A)$ ① ² / (4π)
.05	.75	.01309	.0007	.011	.001	.0002
.10	1.5	.02619	.0026	.0115	.0015	.0008
.20	2.95	.06153	.0103	.015	.005	.0032
.30	4.30	.07519	.0226	.021	.011	.0072
.40	5.60	.09805	.0392	.033	.023	.0127
.50	7.20	.1263	.0632	.0535	.0435	.0199
.60	8.80	.1548	.0929	.078	.068	.0287
.70	11.20	.1980	.1386	.145	.135	.0390

Plot $C_L \tan \alpha$, $C_D - C_{D_0}$, and $C_L^2 / (\pi A)$ versus angle of attack (see sketch (a)).



SKETCH (a)

① C_L	② $\frac{\partial}{\partial \alpha} (C_L \tan \alpha)$	③ $\frac{\partial}{\partial \alpha} (C_D - C_{D_0})$	④ $\frac{\partial}{\partial \alpha} \left(\frac{C_L^2}{\pi A} \right)$	⑤ $K = \frac{(② - ③)}{(② - ④)}$ (eq. 7.1.2.1-d)
0	-	-	-	1.000
.05	.0018	.00095	.0002	.531
.10	.0040	.0012	.00115	.982
.20	.0066	.0030	.0022	.818
.30	.0105	.0066	.00325	.538
.40	.0136	.0116	.0044	.228
.50	.0168	.0152	.0049	.136
.60	.0184	.0195	.0052	-.083
.70	.01865	.0279	.0031	-.595

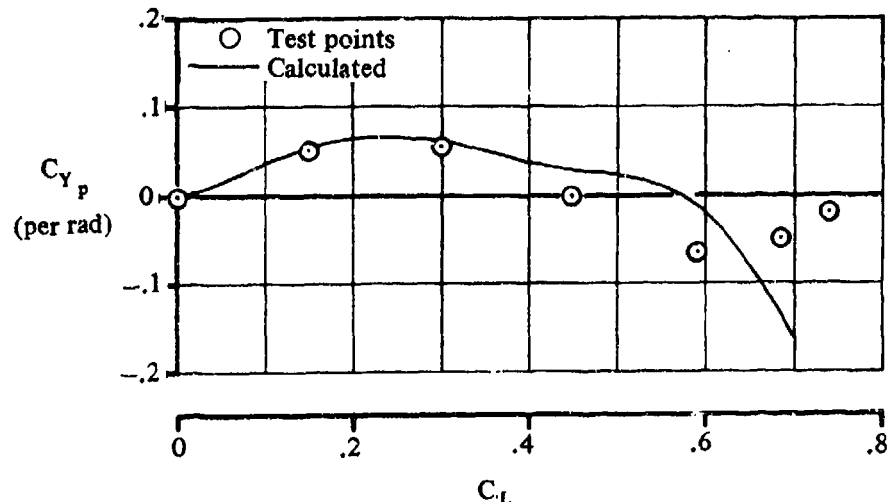
Solution:

$$C_{Y_p} = K \left[\left(\frac{C_{Y_p}}{C_L} \right)_{\substack{C_L=0 \\ M}} C_L + (\Delta C_{Y_p})_r \right] \quad (\text{equation 7.1.2.1-a})$$

$$= K [(0.394) C_L] + 0 = 0.394 K C_L$$

C_L	K	C_{Y_p} (based on $S_W b_W$) (per rad) (eq. 7.1.2.1-a)
0	1.000	0
.05	.531	.0105
.10	.982	.0387
.20	.818	.0645
.30	.538	.0636
.40	.228	.0359
.50	.136	.0266
.60	-.083	-.0196
.70	-.595	-.1641

The calculated results are compared with test values from reference 5 in sketch (b).



SKETCH (b)

B. TRANSONIC

No generalized method is available in the literature for estimating transonic values of the rolling derivative C_{Y_p} . Furthermore, no known experimental results are available for this derivative at transonic speeds.

C. SUPERSONIC

At supersonic speeds a design chart based on theoretical calculations is presented for estimating the rolling derivative C_{Y_p} at low values of the lift coefficient. The design chart is based on the results of reference 6 for wings with subsonic leading edges and supersonic trailing edges, and the results of reference 7 for wings with supersonic leading edges and either subsonic or supersonic trailing edges. The results of both references 6 and 7 are based on linearized-supersonic-flow theory and are therefore restricted to thin, swept-back, tapered wings with streamwise tips. The lateral force due to rolling is taken as that arising entirely from suction forces on the wing edges. For wings with supersonic leading edges no suction forces are induced along the leading edges, and the determination of C_{Y_p} involves only the unbalanced suction forces along the wing tips. Therefore, for zero-taper wings with supersonic leading edges the theory gives $C_{Y_p} = 0$.

No experimental data are available for this derivative at supersonic speeds. Therefore, the validity of linearized-supersonic-flow theory for estimating C_{Y_p} cannot be determined.

DATCOM METHOD

The wing contribution to the rolling derivative C_{Y_p} at supersonic speeds and at low values of the lift coefficient is obtained from figure 7.1.2.1-10 as a function of the wing aspect ratio, taper ratio, leading-edge sweep, and Mach number.

Sample Problem

Given: Tapered, swept-back wing.

$$A = 3.22 \quad \lambda = 0.25 \quad \Lambda_{LE} = 55.2^\circ$$

$$M = 2.41; \beta = 2.19$$

Compute:

$$\beta A = (2.19)(3.22) = 7.07$$

Solution:

$$\frac{C_Y p}{\alpha} = 0.50 \text{ per rad}^2 \text{ (based on } S_w b_w \text{) (figure 7.1.2.1-10)}$$

REFERENCES

1. Toll, T. A., and Queijo, M. J.: Approximate Relations and Charts for Low-Speed Stability and Control Derivatives of Swept Wings. NACA TN 1581, 1948. (U)
2. Brewer, J. D., and Fisher, L. R.: Effect of Taper Ratio on the Low-Speed Rolling Stability Derivatives of Swept and Unswept Wings of Aspect Ratio 2.61. NACA TN 2555, 1951. (U)
3. Queijo, M. J., and Jaquet, B. M.: Calculated Effects of Geometric Dihedral on the Low-Speed Rolling Derivatives of Swept Wings. NACA TN 1732, 1948. (U)
4. Goodman, A., and Fisher, L. R.: Investigation at Low Speeds of the Effect of Aspect Ratio and Sweep on Rolling Stability Derivatives of Untapered Wings. NACA TR 968, 1950. (U)
5. Wiggins, J. W.: Wind-Tunnel Investigation of Effect of Sweep on Rolling Derivatives at Angles of Attack Up to 13° and at High Subsonic Mach Numbers, Including a Semiempirical Method of Estimating the Rolling Derivatives. NACA TN 4185, 1958. (U)
6. Margolis, K.: Theoretical Calculations of the Lateral Force and Yawing Moment Due to Rolling at Supersonic Speeds for Sweptback Tapered Wings With Streamwise Tips. Subsonic Leading Edges. NACA TN 2122, 1950. (U)
7. Harmon, S. M., and Martin, J. C.: Theoretical Calculations of the Lateral Force and Yawing Moment Due to Rolling at Supersonic Speeds for Sweptback Tapered Wings With Streamwise Tips. Supersonic Leading Edges. NACA TN 2156, 1950. (U)
8. Wiggins, J. W., and Kuhn, R. E.: Wind-Tunnel Investigation of the Aerodynamic Characteristics in Pitch of Wing-Fuselage Combinations at High Subsonic Speeds. Sweep Series. NACA RM L52D18, 1952. (U)

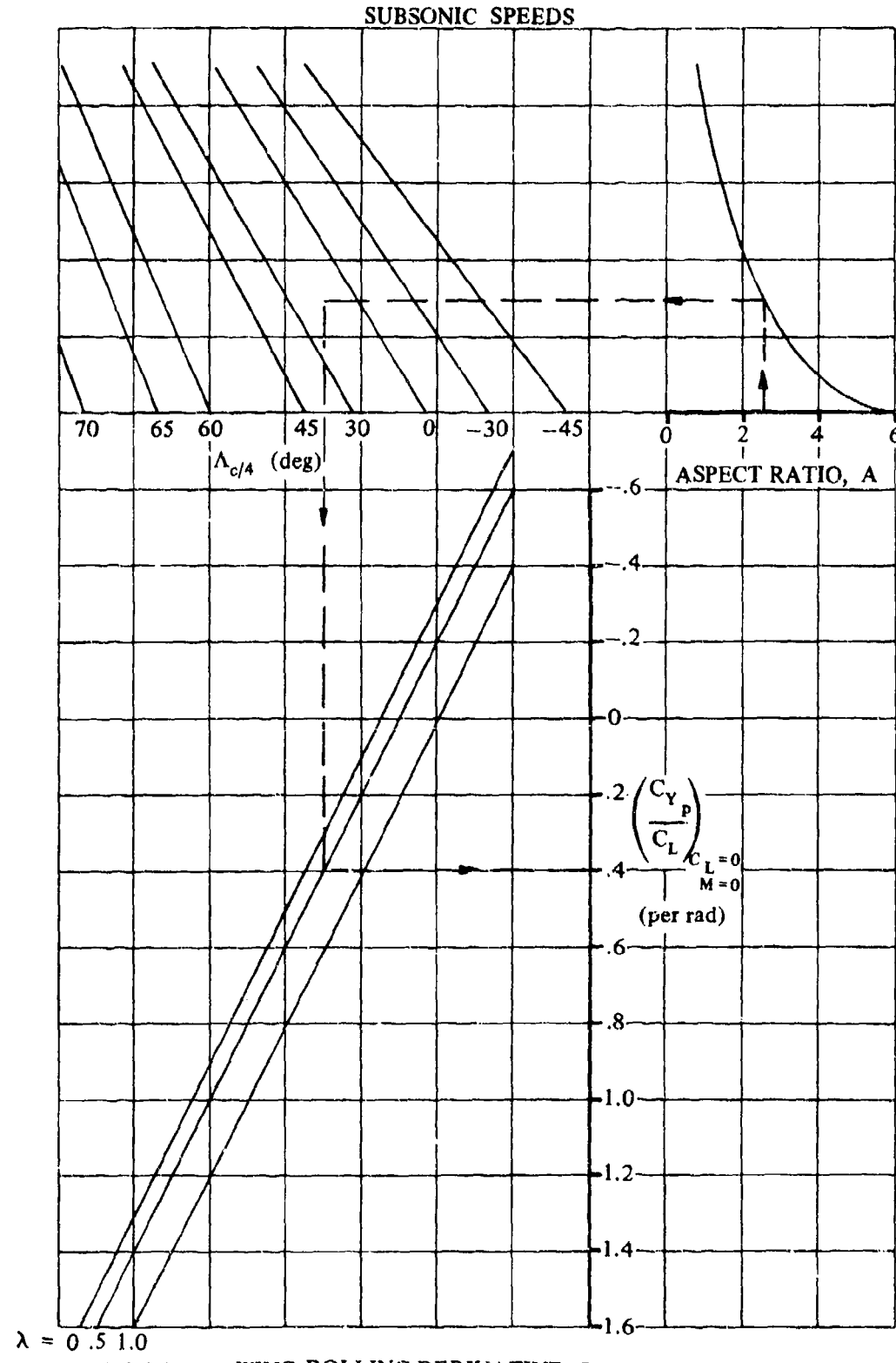
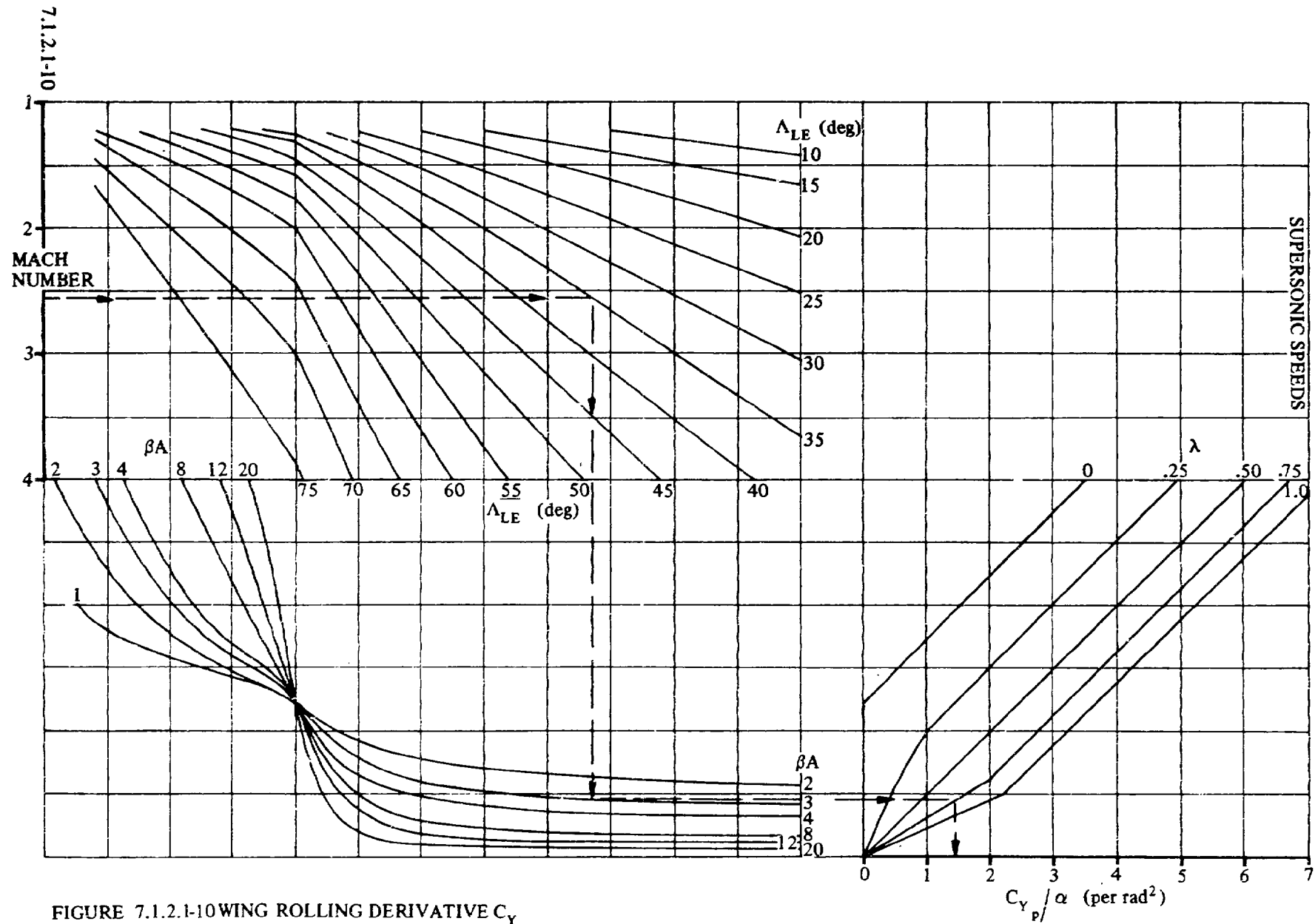


FIGURE 7.1.2.1-9 WING ROLLING DERIVATIVE, C_Y



7.1.2.2 WING ROLLING DERIVATIVE C_{l_p}

This section presents methods for estimating the wing contribution to the rolling derivative C_{l_p} at subsonic and supersonic speeds. This derivative is the change in rolling-moment coefficient with change in wing-tip helix angle and is expressed as

$$C_{l_p} = \frac{\partial C_l}{\partial \left(\frac{pb}{2V_\infty} \right)}$$

A. SUBSONIC

The wing rolling derivative C_{l_p} at subsonic speeds is a function of the wing lift-curve slope, the wing drag, and geometric dihedral. The effects of dihedral become significant when the displacement of the rolling axis from the wing root chord is moderate or large.

For unswept wings of moderately high aspect ratio the lift-curve slope undergoes only small changes throughout the lift-coefficient range, and the drag contribution is relatively unimportant. Therefore, potential flow values of C_{l_p} at zero lift are generally satisfactory at all lift coefficients below the stall for these planforms.

Several methods are available for estimating the potential flow value of C_{l_p} . Reference 1 presents design charts for C_{l_p} at zero lift of unswept wings based on lifting-line theory. An effective edge-velocity correction is applied to the lifting-line theory results of reference 1 in reference 2. Finally the results of reference 2 are modified for the effects of sweep in reference 3. A similar method that accounts for the effects of sweep on the edge-velocity correction is presented in reference 4. Reference 5 presents a more rigorous method of estimating C_{l_p} for wings of arbitrary planform at zero lift, based on the simplified lifting-surface theory of Weissinger for determining the additional span loading due to rolling. The Datcom method for estimating C_{l_p} at zero lift is taken from reference 6. It is essentially that of reference 5 corrected for compressibility effects and extended to a wider range of planform parameters.

For wings of moderate to high aspect ratios and with moderate sweep, the value of C_{l_p} in the nonlinear-lift range is estimated to a first approximation by assuming that variations in the lift-curve slope will affect C_{l_p} in the same proportion as C_{L_a} .

On low-aspect-ratio and/or highly swept wings, the flow separates and forms a stable leading-edge vortex that is responsible for the generation of considerable additional lift on the outer portions of the wing. The drag associated with these high lift coefficients causes significant changes in C_{l_p} . The increment in C_{l_p} due to drag is derived in reference 7, based on the strip-theory procedure of reference 3. Since the effects of drag due to lift and of profile drag on the roll-damping derivative are not of equal importance, they are considered separately in determining the increment due to drag.

The correction for geometric dihedral is considered in detail in reference 8. Although the expression for the dihedral effect has been derived specifically for untapered wings, it should be reasonably reliable for wings of any taper ratio over the range of wing dihedral angles of practical interest.

The Datcom method accounts for the variations in wing lift-curve slope, drag due to lift, and profile

drag, as well as the effect of dihedral. The method requires knowledge of the variation of lift and drag over the angle-of-attack range to the stall for the particular configuration at the appropriate Mach number. Therefore, this method is quite readily applied if experimental lift and drag data are available.

DATCOM METHOD

The value of the wing rolling derivative C_{l_p} at a given lift coefficient at subsonic speeds, based on the product of the wing area and the square of the wing span $S_w b_w^2$, is given by

$$C_{l_p} = \left(\frac{\beta C_{l_p}}{\kappa} \right)_{C_L=0} \left(\frac{\kappa}{\beta} \right) \frac{(C_{L_\alpha})_{C_L}}{(C_{L_\alpha})_{C_L=0}} \frac{(C_{l_p})_\Gamma}{(C_{l_p})_{\Gamma=0}} + (\Delta C_{l_p})_{\text{dih}} \quad (\text{per radian}) \quad 7.1.2.2-a$$

where

$\left(\frac{\beta C_{l_p}}{\kappa} \right)_{C_L=0}$ is the roll-damping parameter at zero lift, obtained from figure 7.1.2.2-20 as a function of Λ_β and $\beta A/\kappa$.

The parameter κ is the ratio of the two-dimensional lift-curve slope at the appropriate Mach number to $2\pi/\beta$; i.e., $(C_{L_\alpha})_M/(2\pi/\beta)$. The two-dimensional lift-curve slope is obtained from Section 4.1.1.2. For wings with airfoil sections varying in a reasonably linear manner with span, the average value of the lift-curve slopes of the root and tip sections is adequate.

The parameter Λ_β is the compressible sweep parameter given as

$$\Lambda_\beta = \tan^{-1} \left(\frac{\tan \Lambda_c/4}{\beta} \right), \text{ where } \beta = \sqrt{1 - M^2}.$$

$(C_{L_\alpha})_{C_L=0}$ is the wing lift-curve slope at zero lift, obtained from test data or estimated by using the straight-tapered wing method of paragraph A of Section 4.1.3.2 at the appropriate Mach number.

$(C_{L_\alpha})_{C_L}$ is the wing lift-curve slope at any lift coefficient below the stall, obtained from test data or estimated by using the straight-tapered wing method of paragraph A of Section 4.1.3.3 at the appropriate Mach number.

$\frac{(C_{l_p})_\Gamma}{(C_{l_p})_{\Gamma=0}}$ is the dihedral-effect parameter given by

$$\frac{(C_{l_p})_\Gamma}{(C_{l_p})_{\Gamma=0}} = \left[1 - 2 \frac{z}{b/2} \sin \Gamma + 3 \left(\frac{z}{b/2} \right)^2 \sin^2 \Gamma \right] \quad 7.1.2.2-b$$

where

- Γ is the geometric dihedral angle, positive for the wing tip above the plane of the root chord.
- z is the vertical distance between the c.g. and the wing root chord, positive for the c.g. above the root chord.
- b is the wing span.

$(\Delta C_{I_p})_{drag}$ is the increment in the roll-damping derivative due to drag, given by

$$(\Delta C_{I_p})_{drag} = \frac{(C_{I_p})_{C_{D_L}}}{C_L^2} C_L^2 - \frac{1}{8} C_{D_0} \quad (\text{per radian}) \quad 7.1.2.2-e$$

where

$$\frac{(C_{I_p})_{C_{D_L}}}{C_L^2}$$

is the drag-due-to-lift roll-damping parameter obtained from figure 7.1.2.2-24 as a function of A and $\Lambda_{c/4}$.

C_L is the wing lift coefficient below the stall.

C_{D_0} is the profile or total zero-lift drag coefficient. If experimental data are not available, C_{D_0} may be estimated by the method of paragraph A of Section 4.1.5.1 at the appropriate Mach number.

This method includes the effects of compressibility and may be applied up to the critical Mach number. (The drag-due-to-lift term does not include a Mach number correction; however, it is small except at high C_L where the Mach number is generally low.)

The most important factor considered in this method is the variation of the wing lift-curve slope. If reliable values of this parameter are available over the lift-coefficient range, the method will in most cases give satisfactory results over that C_L range for configurations with aspect ratios of approximately 2 or greater.

For wings of low aspect ratio and/or high sweep the accuracy of the method rapidly deteriorates with increasing C_L , even when experimental values of lift and drag are used. The error results from the fact that the high values of $(C_{I_p})_{C_{D_L}}$ obtained from figure 7.1.2.2-24 for these configurations are not

realized in practice. Therefore, as C_L increases the calculated values of the roll-damping derivative become progressively smaller than those given by experiment.

A comparison of the roll-damping derivative calculated by using this method with test results is presented as table 7.1.2.2-A. Experimental values of lift and drag have been used in evaluating the roll-damping derivative of all the configurations listed in the table. Several additional references containing test results of the damping-in-roll characteristics of straight-tapered wings are listed in table 7-A.

Sample Problem

Given: Model 8 of reference 17.

Wing Characteristics:

$$A = 3.0 \quad \lambda = 0.15 \quad \Lambda_{c/4} = 36.9^\circ \quad \Gamma = 0$$

Airfoil Characteristics:

$$\text{NACA 0012 airfoil} \quad \frac{Y_{90}}{2} = 1.448 \quad \frac{Y_{99}}{2} = 0.260$$

Additional Characteristics:

$$M = 0.13; \quad \beta = 0.992 \quad R_f = 1.254 \times 10^6 \quad C_{D_0} = 0.036 \text{ (test value)}$$

The following test values from reference 17:

C_L	0	.1	.2	.3	.4	.5	.6	.7	.8
$C_{L\alpha}$.0525	.0525	.0525	.053	.053	.054	.054	.050	.030

Compute:

Determine the roll-damping parameter at zero lift $\left(\frac{\beta C_l}{\kappa} \right) c_L = 0$

$$\tan \frac{1}{2} \phi'_{TE} = \frac{\frac{Y_{90}}{2} - \frac{Y_{99}}{2}}{9} = \frac{1.448 - 0.26}{9} = 0.132$$

$$\frac{(c_{l\alpha})}{(c_{l\alpha})_{\text{theory}}} = 0.768 \quad (\text{figure 4.1.1.2-8a, extrapolated by plotting vs } \log_{10} R_f)$$

$$(c_{l\alpha})_{\text{theory}} = 6.88 \quad (\text{figure 4.1.1.2-8b})$$

$$(c_{l\alpha})_M = \frac{1.05}{\beta} \frac{(c_{l\alpha})}{(c_{l\alpha})_{\text{theory}}} (c_{l\alpha})_{\text{theory}} \quad (\text{equation 4.1.1.2-a})$$

$$= \frac{1.05}{0.992} (0.768) (6.88) = 5.59 \text{ per rad}$$

$$\kappa = \frac{(c_{l\alpha})_M}{2\pi/\beta} = \frac{5.59}{2\pi/0.992} = 0.883$$

$$\frac{\beta A}{\kappa} = \frac{(0.992)(3.0)}{0.883} = 3.37$$

$$\Lambda_\beta = \tan^{-1} \left(\frac{\tan \Lambda_{c/4}}{\beta} \right) = \tan^{-1} \left(\frac{0.7508}{0.992} \right) = \tan^{-1} 0.7569 = 37.12^\circ$$

$$\left(\frac{\beta C_{I_p}}{\kappa} \right)_{C_L=0} = -0.251 \text{ per rad (figure 7.1.2.2-20, interpolated)}$$

Determine the dihedral-effect parameter

$$\frac{(C_{I_p})_r}{(C_{I_p})_{r=0}} = 1.0 \text{ (equation 7.1.2.2-b at } \Gamma = 0)$$

Determine the increment in roll damping due to drag $(\Delta C_{I_p})_{\text{drag}}$

$$\frac{(C_{I_p})_{C_{D_L}}}{C_L^2} = -0.034 \text{ (figure 7.1.2.2-24)}$$

$$(\Delta C_{I_p})_{\text{drag}} = \frac{(C_{I_p})_{C_{D_L}}}{C_L^2} C_L^2 - \frac{1}{8} C_{D_0} \text{ (equation 7.1.2.2-c)}$$

$$= (-0.034)C_L^2 - \frac{1}{8} 0.036 \text{ per rad}$$

① C_L	② C_L^2	③ $\frac{1}{8} C_{D_0}$	④ ΔC_{I_p} $-0.034 \text{ (2) } - \text{ (3)}$
0	0	0.0045	-0.0045
0.1	0.01		-0.0048
0.2	0.04		-0.0059
0.3	0.09		-0.0076
0.4	0.16		-0.0099
0.5	0.25		-0.0130
0.6	0.36		-0.0167
0.7	0.49		-0.0212
0.8	0.64		-0.0263

Solution:

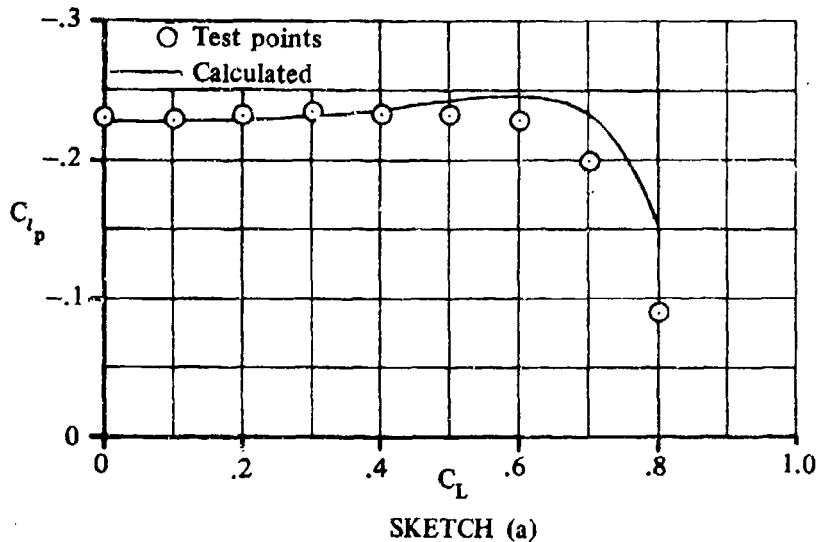
$$C_{I_p} = \left(\frac{\beta C_{I_p}}{\kappa} \right)_{C_L=0} \left(\frac{\kappa}{\beta} \right) \frac{(C_{L\alpha})_{C_L}}{(C_{L\alpha})_{C_L=0}} \frac{(C_{I_p})_r}{(C_{I_p})_{r=0}} + (\Delta C_{I_p})_{drag} \quad (\text{equation 7.1.2.2-a})$$

$$= (-0.251) \frac{0.883}{0.992} \frac{(C_{L\alpha})_{C_L}}{(C_{L\alpha})_{C_L=0}} (1.0) + (\Delta C_{I_p})_{drag}$$

$$= -0.223 \frac{(C_{L\alpha})_{C_L}}{(C_{L\alpha})_{C_L=0}} + (\Delta C_{I_p})_{drag}$$

C_L	$(C_{L\alpha})_{C_L}$ (test results)	$\frac{(C_{L\alpha})_{C_L}}{(C_{L\alpha})_{C_L=0}}$ ② / 0.0625	$(\Delta C_{I_p})_{drag}$ (per rad) (eq. 7.1.2.2-c)	C_{I_p} (based on $S_W b_W^2$) (per rad) -0.223 ③ + ④
0	0.0625	1.00	-0.0045	-0.2275
0.1	↓	↓	-0.0048	-0.2278
0.2	↓	↓	-0.0059	-0.2289
0.3	0.053	1.01	-0.0076	-0.2328
0.4	↓	↓	-0.0099	-0.2361
0.5	0.054	1.03	-0.0130	-0.2427
0.6	↓	↓	-0.0167	-0.2464
0.7	0.050	0.952	-0.0212	-0.2336
0.8	0.030	0.571	-0.0263	-0.1536

The calculated results are compared with test values in sketch (a) and in table 7.1.2.2-A.



SKETCH (a)

B. TRANSONIC

There are no reliable methods for estimating the derivative C_{l_p} in the transonic region. Although this derivative might be expected to vary with Mach number in the same manner as the lift-curve slope, this trend is not exhibited by experimental data. A considerable quantity of test data is available, however, and reference should be made to table 7-A.

C. SUPERSONIC

At supersonic speeds design charts based on theoretical calculations are presented for estimating the rolling derivative C_{l_p} of wings of vanishing thickness.

The design charts are those of reference 9 and are based on the results presented in the following references:

Reference 10 — in the region of supersonic leading and trailing edges

Reference 11 — in the region of subsonic leading edges and supersonic trailing edges

Reference 12 — for values of $\beta A < 2$

The results presented in references 10 and 11 are based on linearized supersonic-flow theory while those of reference 12 are based on slender-wing theory. The slender-wing-theory value of C_{l_p} for $\beta^A = 0$ was used to establish a straight-line relationship between slender-wing theory and the low limit of the linearized supersonic-flow theory. Thin airfoils have been assumed in these theories. Thickness effects are not important except for conditions where the Mach lines lie on or near the wing leading edge. Under these conditions the wing-leading-edge shock position is displaced forward from its theoretical position by the finite thickness effects of the leading edge. This displacement results in substantial losses in normal-force-curve slope and consequently, in roll damping.

The empirical chart presented in Section 4.1.3.2 for determining the leading-edge-thickness effect on the normal-force-curve slope of straight-tapered wings has been adopted in this section to determine the leading-edge-thickness effect on the roll damping. This chart is presented as figure 7.1.2.2-27 in the form

of a ratio of the actual roll-damping derivative to the theoretical roll-damping derivative. For straight-tapered wings with sharp leading edges, the airfoil nose semiwedge angle (measured normal to the wing leading edge) determines the shock position relative to the wing. Experimental data indicate that the parameter corresponding to the nose semiwedge angle is $\Delta y_{\perp} = \Delta y / \cos \Lambda_{LE}$, where Δy is the difference between the upper-surface ordinates at the 6-percent- and 0.15-percent-chord stations. The parameter Δy is presented for several airfoil shapes in figure 2.2.1-8. For double-wedge and biconvex airfoils there is a linear relationship between Δy_{\perp} and the leading-edge semiwedge angle, given by

$$\Delta y_{\perp} = 5.85 \tan \delta_{\perp}$$

Either Δy_{\perp} or δ_{\perp} may be used to calculate the thickness effects.

The Datcom method is applicable to straight-tapered wings of arbitrary taper ratio with wing tips parallel to the free stream and with subsonic or supersonic leading edges and supersonic trailing edges. A further restriction is that the foremost Mach line from the tip may not intersect the remote half-wing.

Wings with inverse taper ($\lambda > 1$) have not been considered. Wings with swept-forward leading edges are included through the use of the reversibility theorem (references 13 and 14). The reversibility theorem states that the roll-damping derivative C_{l_p} of the wing in forward flight equals the roll-damping derivative of the same wing in reverse flight.

DATCOM METHOD

The wing contribution to the roll-damping derivative C_{l_p} at supersonic speeds, based on the product of wing area and the square of the wing span $S_w b_w^2$, is given by

$$C_{l_p} = \left[\frac{(C_{l_p})_{\text{theory}}}{A} \right] A \frac{C_{l_p}}{(C_{l_p})_{\text{theory}}} \quad (\text{per radian}) \quad 7.1.2.2-d$$

where

A is the wing aspect ratio.

$\frac{(C_{l_p})_{\text{theory}}}{A}$ is the theoretical roll-damping parameter obtained from figures 7.1.2.2-25a through 7.1.2.2-25e.

$\frac{C_{l_p}}{(C_{l_p})_{\text{theory}}}$ is the empirical thickness correction factor obtained from figure 7.1.2.2-27.

The sonic trailing-edge boundaries on figures 7.1.2.2-25a through 7.1.2.2-25e represent an upper limit for the true theoretical values of the derivatives. Values below the sonic trailing-edge boundary are for wings with subsonic trailing edges and are in violation of one of the basic assumptions of the theory. For configurations with subsonic trailing edges ($\beta \cot \Lambda_{TE} < 1$) the design charts will overestimate the roll-damping derivative.

It should be noted that the "kinks" in the curves of figures 7.1.2.2-25a through 7.1.2.2-25e correspond to the conditions of sonic leading or trailing edges. Experimental evidence shows that these "kinks" do not occur in practice.

Comparisons of the supersonic roll-damping derivative in the linear-lift range calculated by this method with test results are presented in tables 7.1.2.2-B and 7.1.2.2-C. The configurations listed in table 7.1.2.2-B have supersonic leading edges, while those of table 7.1.2.2-C have either sonic or subsonic leading edges. The roll damping is predicted quite accurately by the Datcom method when the wing leading edges are supersonic. However, when the wing leading edges are sonic or subsonic, the calculated roll damping is in almost all cases considerably greater than that given by experiment. Application of the thickness correction factor presented as figure 7.1.2.2-27 improves the agreement between the calculated and experimental values of roll damping in almost all cases presented in table 7.1.2.2-C, since this factor represents a reduction in roll damping. For wings with subsonic leading edges the theoretical results presented in figures 7.1.2.2-25a through 7.1.2.2-25e show the poorest agreement with experiment at the lower values of $\beta \cot \Lambda_{LE}$ for a given value of βA .

Sample Problem

Given: Wing 14 of reference 23.

$$\Lambda_{LE} = 60^\circ \quad \Lambda_{c/4} = 53.4^\circ \quad A = 3.12 \quad \lambda = 0.25$$

Airfoil: Constant 3/16-in. thickness with symmetrical 5° bevel on all edges in a direction parallel to the root chord.

$$\delta_1 = 10^\circ$$

$$M = 2.41; \beta = 2.19$$

Compute:

$$\beta A = (2.19)(3.12) = 6.83$$

$$A \tan \Lambda_{c/2} = (3.12)(\tan 53.4^\circ) = 4.20$$

$$\frac{(C_{I_p})_{theory}}{A} = -0.0716 \text{ per rad} \quad (\text{figure 7.1.2.2-25b})$$

$$\beta \cot \Lambda_{LE} = 2.19 (\cot 60^\circ) = 1.265 \quad (\text{supersonic leading edge})$$

$$\frac{\tan \Lambda_{LE}}{\beta} = \frac{\tan 60^\circ}{2.19} = 0.791$$

$$\frac{C_{I_p}}{(C_{I_p})_{theory}} = 0.865 \quad (\text{figure 7.1.2.2-27})$$

Solution:

$$C_{I_p} = \left[\frac{(C_{I_p})_{\text{theory}}}{A} \right] A - \frac{C_{I_p}}{(C_{I_p})_{\text{theory}}} \quad (\text{equation 7.1.2.2-d})$$
$$= (-0.0716) (3.12) (0.865)$$
$$= -0.193 \text{ per rad} \quad (\text{based on } S_w b_w^2)$$

This compares with a test result of -0.188 per radian from reference 23.

REFERENCES

1. Pearson, H. A., and Jones, R. T.: Theoretical Stability and Control Characteristics of Wings With Various Amounts of Taper and Twist. NACA TR 636, 1938. (U)
2. Swanson, R. S., and Priddy, E. L.: Lifting-Surface-Theory Values of the Damping in Roll and of the Parameter Used in Estimating Aileron Stick Forces. NACA WR L-53, 1945. (U)
3. Toll, T. A., and Queijo, M. J.: Approximate Relations and Charts for Low-Speed Stability Derivatives of Swept Wings. NACA TN 1581, 1948. (U)
4. Polhamus, E. C.: A Simple Method of Estimating the Subsonic Lift and Damping in Roll of Sweptback Wings. NACA TN 1862, 1949. (U)
5. Bird, J. D.: Some Theoretical Low-Speed Span-Loading Characteristics of Swept Wings in Roll and Sideslip. NACA TR 969, 1950. (U)
6. De Young, J.: Theoretical Antisymmetric Span Loading for Wings of Arbitrary Plan Form at Subsonic Speeds. NACA TR 1056, 1951. (U)
7. Goodman, A., and Adair, G. H.: Estimation of the Damping in Roll of Wings Through the Normal Flight Range of Lift Coefficient. NACA TN 1924, 1949. (U)
8. Queijo, M. J., and Jaquet, B. M.: Calculated Effects of Geometric Dihedral on the Low-Speed Rolling Derivatives of Swept Wings. NACA TN 1732, 1948. (U)
9. Anon: Royal Aeronautical Society Data Sheets — Aerodynamics, Vol. III (Aircraft S.06.03.01), 1957. (U)
10. Harmon, S. M., and Jeffreys, I.: Theoretical Lift and Damping in Roll of Thin Wings With Arbitrary Sweep and Taper at Supersonic Speeds. Supersonic Leading and Trailing Edges. NACA TN 2114, 1950. (U)
11. Malvestuto, F. S., Jr., Margolis, K., and Ribner, H. S.: Theoretical Lift and Damping in Roll at Supersonic Speeds of Thin Sweptback Wings of Arbitrary Taper and Sweep at Supersonic Speeds. Subsonic Leading Edges and Supersonic Trailing Edges. NACA TR 970, 1950. (U)
12. Mangler, K. W.: Calculations of the Pressure Distribution Over a Wing at Sonic Speeds. ARC R&M 2888, 1955. (U)
13. Harmon, S. M.: Theoretical Relations Between the Stability Derivatives of a Wing in Direct and in Reverse Supersonic Flow. NACA TN 1943, 1949. (U)
14. Brown, C. E.: The Reversibility Theorem for Thin Airfoils in Subsonic and Supersonic Flow. NACA TN 1944, 1949. (U)
15. Letko, W., and Wolhart, W. D.: Effect of Sweepback on the Low-Speed Static and Rolling Stability Derivatives of Thin Tapered Wings of Aspect Ratio 4. NACA RM L9F14, 1949. (U)
16. Jaquet, B. M., and Brewer, J. D.: Effects of Various Outboard and Central Fins on Low-Speed Static-Stability and Rolling Characteristics of a Triangular-Wing Model. NACA RM L8E18, 1948. (U)

17. Jaquet, B. M., and Brewer, J. D.: Low-Speed Static-Stability and Rolling Characteristics of Low-Aspect-Ratio Wings of Triangular and Modified Triangular Plan Forms. NACA RM L8L29, 1949. (U)
18. Bird, J. D., Lichtenstein, J. H., and Jaquet, B. M.: Investigation of the Influence of Fuselage and Tail Surfaces on Low-Speed Static Stability and Rolling Characteristics of a Swept-Wing Model. NACA TN 2741, 1952. (U)
19. Fisher, L. R., and Michael, W. H., Jr.: An Investigation of the Effect of Vertical-Fin Location and Area on Low-Speed Lateral Stability Derivatives of a Semitailless Airplane Model. NACA RM L51A10, 1951. (U)
20. Goodman, A., and Thomas, D. F., Jr.: Effect of Wing Position and Fuselage Size on the Low-Speed Static and Rolling Stability Characteristics of a Delta-Wing Model. NACA TR 1224, 1955. (U)
21. Letko, W. and Riley, D. R.: Effect of an Unswept Wing on the Contribution of Unswept-Tail Configurations to the Low-Speed Static and Rolling-Stability Derivatives of a Midwing Airplane Model. NACA TN 2175, 1950. (U)
22. Wiggins, J. W., and Kuhn, R. E.: Wind-Tunnel Investigation of the Aerodynamic Characteristics in Pitch of Wing-Fuselage Combinations at High Subsonic Speeds — Sweep Series. NACA RM L52D18, 1952. (U)
23. McDearmon, R. W., and Heinke, H. S., Jr.: Investigations of the Damping in Roll of Swept and Tapered Wings at Supersonic Speeds. NACA RM L53A13, 1963. (U)
24. Bland, W. M., Jr., and Sandahl, C. A.: A Technique Utilizing Rocket-Propelled Test Vehicles for the Measurement of the Damping in Roll of Sting-Mounted Models and Some Initial Results for Delta and Unswept Tapered Wings. NACA RM L50D24, 1950. (U)
25. Bland, W. M., Jr., and Dietz, A. E.: Some Effects of Fuselage Interference, Wing Interference, and Sweepback on the Damping in Roll of Untapered Wings as Determined by Techniques Employing Rocket-Propelled Vehicles. NACA RM L51D25, 1951. (U)

TABLE 7.1.2.2-A
SUBSONIC WING ROLLING DERIVATIVE C_{I_p}
DATA SUMMARY

Ref.	A	λ	$\Delta c/4$ (deg)	Airfoil Section	Γ (deg)	M	R_f $\times 10^{-6}$	C_L	$C_{L\alpha}$ (per deg) (test)	C_{D0} (test)	C_{I_p} Calc. (per rad)	C_{I_p} Test (per rad)	% Percent Error
15	4.0	0.60	3.6	65A006	0	0.13	0.72	0	0.065	0.033	-0.322	-0.345	6.7
								0.1	0.072		-0.356	-0.346	-2.9
								0.2	0.072		-0.357	-0.347	-2.9
								0.3	0.072		-0.357	-0.348	-2.6
								0.4	0.067		-0.334	-0.355	5.9
								0.5	0.067		-0.334	-0.370	9.7
								0.6	0.063		-0.316	-0.370	14.6
								0.7	0.047		-0.240	-0.275	12.7
								0	0.062	0.033	-0.308	-0.330	6.7
								0.1	0.062		-0.308	-0.330	6.7
								0.2	0.062		-0.309	-0.336	8.0
								0.3	0.066		-0.329	-0.360	8.6
								0.4	0.066		-0.330	-0.387	14.7
								0.5	0.066		-0.332	-0.370	10.3
								0.6	0.061		-0.309	-0.295	-4.7
								0.7	0.046		-0.234	-0.195	-20.0
								0.8	0.027		-0.145	-0.085	-70.6

TABLE 7.1.2.2-A (CONTD)

Ref.	A	λ	$\Delta c/4$ (deg)	Airfoil Section	Γ (deg)	M	$R_f \times 10^{-6}$	C_L	$C_{L\alpha}$ (per deg) (test)	C_{D_0} (test)	C_{I_p} Calc. (per rad)	C_{I_p} Test (per rad)	e Percent Error
15	4.0	0.60	46.7	65A006	0	0.13	0.72	0	0.062	0.033	-0.287	-0.300	4.3
								0.1	0.062		-0.288	-0.305	5.6
								0.2	0.062		-0.288	-0.335	14.0
								0.3	0.066		-0.309	-0.378	18.3
								0.4	0.066		-0.312	-0.392	20.4
								0.5	0.066		-0.315	-0.382	17.5
								0.6	0.059		-0.285	-0.350	18.6
								0.7	0.046		-0.230	-0.297	22.6
								0.8	0.036		-0.193	-0.256	24.6
16	2.31	0	52.2	65(06)-006.5	0	0.13	1.624	0	0.045	0.020	-0.172	-0.165	-4.2
								0.1			-0.173	-0.175	1.1
								0.2			-0.176	-0.180	2.2
								0.3			-0.180	-0.180	0
								0.4			-0.106	-0.182	-2.2
								0.5			-0.195	-0.182	-7.1
								0.6			-0.205	-0.180	-13.9
								0.7			-0.218	-0.179	-21.8
								0.8			-0.233	-0.172	-36.5
17	3.0	0.15	36.9	0012	0	0.13	1.254	0	0.0525	0.036	-0.228	-0.230	0.9
								0.1	0.0525		-0.228	-0.230	0.9
								0.2	0.0525		-0.229	-0.232	1.3
								0.3	0.053		-0.233	-0.235	0.9
								0.4	0.053		-0.235	-0.232	-1.3
								0.5	0.054		-0.243	-0.232	-4.7
								0.6	0.054		-0.246	-0.228	-7.9
								0.7	0.050		-0.234	-0.198	-10.1
								0.8	0.030		-0.154	-0.090	-71.1
2.31	0	52.2			1.624	0	0.11	0.033	-0.168	-0.150	-12.0		
								0.1			-0.169	-0.150	-12.7
								0.2			-0.172	-0.150	-14.0
								0.3			-0.176	-0.149	-18.1
								0.4			-0.183	-0.143	-28.0
								0.5			-0.191	-0.138	-38.4
								0.6	0.0435		-0.212	-0.128	-65.6
								0.7	0.0435		-0.225	-0.120	-87.5
								0.8	0.046		-0.245	-0.127	-92.9

TABLE 7.1.2.2-A (CONTD)

Ref.	A	λ	$\Delta c/4$ (deg)	Airfoil Section	Γ (deg)	M	$R_L \times 10^{-6}$	C_L	$C_{L\alpha}$ (per deg) (test)	$C_D 0$ (test)	C_{I_p} Calc. (per rad)	C_{I_p} Test (per rad)	% Percent Error
	4.0	0	38.0				1.232	0	0.066	0.037	-0.239	-0.227	-5.3
								0.1			-0.239	-0.230	-3.9
								0.2			-0.240	-0.230	-4.3
								0.3			-0.241	-0.236	-2.6
								0.4			-0.243	-0.228	-6.6
								0.5			-0.245	-0.200	-22.5
								0.6	0.0645		-0.242	-0.180	-51.2
								0.7	0.047		-0.214	-0.117	-82.9
								0.8	0.037		-0.178	-	-
	2.0	0.38	38.0				1.335	0	0.036	0.041	-0.183	-0.228	19.7
								0.1	0.041		-0.208	-0.221	5.9
								0.2	0.044		-0.224	-0.231	3.0
								0.3			-0.226	-0.232	2.6
								0.4			-0.229	-0.222	-3.2
								0.5			-0.233	-0.228	-2.2
								0.6			-0.238	-0.242	1.7
								0.7	0.043		-0.239	-0.250	4.4
								0.8	0.063		-0.295	-0.240	-22.9
18	2.61	1.00	46.0	0012(LE)	0	0.17	1.40	0	0.0452	0.023	-0.218	-0.230	5.2
								0.1			-0.218	-0.232	6.0
								0.2			-0.219	-0.235	6.8
								0.3			-0.223	-0.240	7.1
								0.4			-0.227	-0.242	6.2
								0.5	0.048		-0.245	-0.256	4.3
								0.6	0.060		-0.260	-0.275	5.5
								0.7	0.065		-0.339	-0.318	-6.6
								0.8	0.0745		-0.393	-0.385	-2.1
19	3.00	0.465	38.16	0010-64	0	0.16	1.138	0	0.0515	0.018	-0.271	-0.266	-1.9
								0.1	0.055		-0.290	-0.261	-11.1
								0.2			-0.290	-0.279	-3.9
								0.3			-0.292	-0.290	-0.7
								0.4	0.056		-0.300	-0.299	-0.3
								0.5	0.054		-0.292	-0.292	0
								0.6	0.046		-0.254	-0.248	-2.4
								0.7	0.036		-0.200	-0.150	-33.3
								0.8	0.017		-0.110	-0.126	12.0

TABLE 7.1.2.2-A (CONT'D)

Ref.	A	λ	$\Delta_{\mu/4}$ (deg)	Airfoil Section	Γ (deg)	M	R_L $\times 10^{-6}$	C_L	$C_{L\alpha}$ (per deg) (test)	C_{D0} (test)	C_{I_p} Calc. (per rad)	C_{I_p} Test (per rad)	e Percent Error
20	2.31	0	52.4	65A003	0	0.17	2.06	0	0.042	0.015	-0.170	-0.160	-6.3
								0.1			-0.171	-0.155	-10.3
								0.2			-0.175	-0.158	-10.8
								0.3	0.0455		-0.193	-0.165	-17.0
								0.4	0.047		-0.205	-0.165	-24.2
								0.5	0.048		-0.218	-0.162	-34.6
								0.6	0.048		-0.228	-0.155	-47.1
								0.7	0.047		-0.236	-0.150	-57.3
								0.8	0.047		-0.250	-0.157	-59.2
21	4.0	0.6	0	65A008	0	0.166	0.88	0	0.061	0.027	-0.317	-0.330	3.9
								0.1			-0.317	-0.340	6.8
								0.2			-0.318	-0.370	14.1
								0.3			-0.318	-0.392	18.9
								0.4			-0.320	-0.384	16.7
								0.5			-0.321	-0.355	9.6
								0.6			-0.321	-0.336	4.5
Average Error = $\frac{\sum e }{n} = 11.5\%$													

TABLE 7.1.2.2-B
 SUPERSONIC WING ROLLING DERIVATIVE C_{I_p}
 SUPERSONIC LEADING EDGES
 DATA SUMMARY

Ref.	A	λ	Λ_{LE} (deg)	M	$\beta \cot \Lambda_{LE}$	Airfoil Section	δ_L (deg)	$\frac{(C_{I_p})_{theory}}{A}$ (per rad)	$\frac{(C_{I_p})}{(C_{I_p})_{theory}}$	C_{I_p} Calc. (per rad)	C_{I_p} Test (per rad)	ϵ Percent Error
23	3.07	0	60.0	2.41	1.27	Beveled Flat Plate	10.0	-0.0636	0.865	-0.142	-0.139	2.2
	1.90	0.25	60.0	2.41	1.27		10.0	-0.0982	0.865	-0.161	-0.163	-1.2
	1.91	0.25	55.0	1.93	1.16		8.75	-0.1126	0.860	-0.185	-0.195	-5.1
	↓	↓	↓	2.41	1.54		↓	-0.0980	0.913	-0.171	-0.188	-9.0
	2.37	0.25	55.0	1.93	1.16		8.75	-0.1016	0.860	-0.207	-0.210	-1.4
	↓	↓	↓	2.41	1.54		↓	-0.0834	0.913	-0.181	-0.200	-9.5
	3.12	0.25	60.0	2.41	1.27		10.0	-0.0716	0.865	-0.193	-0.188	2.7
	3.22	0.25	55.2	1.93	1.16		8.75	-0.0853	0.850	-0.234	-0.225	4.0
	↓	↓	↓	2.41	1.53		↓	-0.0669	0.915	-0.197	-0.211	-6.6
	3.12	0.25	45.0	1.62	1.27		7.08	-0.1010	0.895	-0.282	-0.272	3.3
	↓	↓	↓	1.93	1.65		↓	-0.0839	0.945	-0.248	-0.253	-2.0
	↓	↓	↓	2.41	2.20		↓	-0.0642	1.000	-0.200	-0.190	5.3
	1.83	0	55.0	1.93	1.16		8.75	-0.0972	0.860	-0.163	-0.160	-4.4
	↓	↓	↓	2.41	1.54		↓	-0.0758	0.913	-0.127	-0.138	-8.0
	1.82	0	50.0	1.62	1.07		7.8	-0.1070	0.863	-0.166	-0.185	-10.3
	↓	↓	↓	1.93	1.39		↓	-0.0960	0.902	-0.168	-0.176	-10.2
	2.34	0	54.9	1.93	1.16		8.7	-0.0815	0.860	-0.164	-0.170	-3.5
	↓	↓	↓	2.41	1.55		↓	-0.0625	0.913	-0.133	-0.155	-14.2
	2.31	0	45.0	1.62	1.27		7.08	-0.0982	0.895	-0.203	-0.210	-3.3
	↓	↓	↓	1.93	1.65		↓	-0.0790	0.945	-0.172	-0.187	-8.0
	2.34	0	40.4	1.62	1.50		7.08	-0.0610	1.000	-0.141	-0.140	0.7
	↓	↓	↓	1.93	1.94		↓	-0.0775	0.995	-0.180	-0.170	5.9
	↓	↓	↓	2.41	2.59		↓	-0.0599	1.000	-0.140	-0.166	-9.7

TABLE 7.1.2.2-B (CONTD)

Ref.	A	λ	Δ_{LE} (deg)	M	$\beta \cot \Delta_{LE}$	Airfoil Section	ΔY_L	$\frac{(C_{I_p})}{A}$ theory	$\frac{C_{I_p}}{(C_{I_p})_{\text{theory}}}$	C_{I_p} Calc. (per rad)	C_{I_p} Test (per rad)	Percent Error
23	3.07	0	46.0	1.62	1.27	Beveled Flat Plate	7.08	-0.0795	0.895	-0.218	-0.214	1.9
				1.93	1.65			-0.0627	0.945	-0.181	-0.200	-9.5
				2.41	2.20			-0.0483	1.000	-0.148	-0.144	2.8
	3.02	0	33.4	1.62	1.93		6.08	-0.0778	1.000	-0.235	-0.225	4.4
				1.93	2.50			-0.0613	1.000	-0.185	-0.178	3.9
				2.41	3.34			-0.0480	1.000	-0.145	-0.134	8.2
	1.88	0.25	33.5	1.62	1.93		6.0	-0.1292	1.000	-0.243	-0.257	-6.4
				1.93	2.50			-0.1163	1.000	-0.219	-0.210	4.3
				2.41	3.31			-0.0960	1.000	-0.180	-0.167	7.8
	2.33	0.25	46.0	1.62	1.27		7.08	-0.1163	0.895	-0.243	-0.240	1.3
				1.93	1.65			-0.1032	0.945	-0.227	-0.235	-3.4
				2.41	2.00			-0.0823	1.000	-0.192	-0.186	3.2
	2.41	0.25	27.3	1.62	2.46		5.64	-0.1172	1.000	-0.282	-0.275	2.5
				1.93	3.20			-0.0990	1.000	-0.239	-0.225	6.2
				2.41	4.25			-0.0780	1.000	-0.168	-0.178	5.6
	2.37	0.25	27.4	1.62	2.46		5.65	-0.1185	1.000	-0.281	-0.267	5.2
				1.93	3.19			-0.0998	1.000	-0.237	-0.218	8.7
				2.41	4.25			-0.0790	1.000	-0.187	-0.173	8.1
	3.22	0.25	21.2	1.62	3.28		5.36	-0.0965	1.000	-0.311	-0.317	-1.9
				1.93	4.25			-0.0775	1.000	-0.250	-0.220	13.6
				2.41	5.66			-0.0605	1.000	-0.195	-0.175	11.4
	2.32	0	60.0	2.41	1.27		10.0	-0.0651	0.865	-0.131	-0.138	-5.1
				1.93	1.16		8.75	-0.0858	0.860	-0.207	-0.167	24.0
				2.41	1.54			-0.0651	0.913	-0.167	-0.160	4.4
	2.81	0	55.0	1.93	1.07		7.8	-0.0778	0.855	-0.226	-0.205	10.2
				1.93	1.39			-0.0595	0.905	-0.183	-0.205	-10.7
				2.41	1.84			-0.0453	0.965	-0.149	-0.156	-4.5

TABLE 7.1.2.2-B (CONTD)

Ref.	A	λ	Λ_{LE} (deg)	M	$\beta \cot \Lambda_{LE}$	Airfoil Section	Δy_1	$\frac{(c_{I_p})_{theory}}{A}$	$\frac{c_{I_p}}{(c_{I_p})_{theory}}$	c_{I_p} Calc. (per rad)	c_{I_p} Test (per rad)	ϵ Percent Error
24	4.00	0	45.0	1.485	1.097	Symmetrical dbl. wedge t/c = 0.04	3.24	-0.075	0.934	-0.280	-0.280	0
	4.00	0	45.0	1.485	1.097	Symmetrical dbl. wedge t/c = 0.09	7.3	-0.075	0.867	-0.260	-0.230	13.0
	4.00	0.50	9.5	1.70	8.21	Symmetrical dbl. wedge t/c = 0.046	2.67	-0.084	1.000	-0.336	-0.350	- 4.0
	↓	↓	↓	↓	↓		↓	-0.100	1.000	-0.400	-0.405	- 1.2
	↓	↓	↓	↓	↓		↓	-0.106	1.000	-0.424	-0.440	- 3.6
25	3.70	1.00	0	1.60	∞	65A009	16.6	-0.101	1.000	-0.374	-0.342	9.4
	↓	↓	↓	↓	↓		↓	-0.1075	1.000	-0.398	-0.360	10.6
	↓	↓	↓	↓	↓		↓	-0.1140	1.000	-0.423	-0.376	12.5
	↓	↓	↓	↓	↓		↓	-0.1235	1.000	-0.457	-0.390	17.2
	3.70	1.00	45.0	1.80	1.25	65A009	16.6	-0.101	0.812	-0.303	-0.310	- 2.3
	↓	↓	↓	↓	↓		↓	-0.105	0.792	-0.308	-0.307	0.3
$\text{Average Error} = \frac{\sum \epsilon }{n} = 6.2\%$												

TABLE 7.1.2.2-C
SUPERSONIC WING ROLLING DERIVATIVE C_{l_p}

SUBSONIC OR SONIC LEADING EDGE

DATA SUMMARY

Ref.	A	λ	Δ_{LE} (deg)	M	$\beta \cot \Delta_{LE}$	Airfoil Section	Δv_1	$\frac{(C_{l_p})}{(C_l)_p}$ theory	$\frac{C_{l_p}}{(C_l)_p}$ theory	C_{l_p} Calc. (per rad)	C_{l_p} Test (per rad)	e Percent Error
								A (per rad)				
2.3	1.82	0	70.0	1.62	0.465	Beveled Flat Plate	1.52	-0.0810	1.000	-0.147	-0.120	22.5
								-0.0795	0.922	-0.134	-0.114	17.5
								-0.0769	0.820	-0.115	-0.090	27.8
2.34	0	69.9	1.12	1.62	0.465		1.52	-0.0707	1.000	-0.165	-0.092	79.3
								-0.0698	0.920	-0.150	-0.098	53.1
								-0.0669	0.818	-0.128	-0.080	60.0
2.33	0	65.0	1.62	0.595			1.22	-0.0797	0.914	-0.175	-0.140	25.0
								-0.0770	0.850	-0.152	-0.116	31.0
								-0.0683	0.800	-0.127	-0.118	7.6
3.06	0	65.0	1.62	0.595			1.22	-0.0686	0.940	-0.197	-0.143	37.8
								-0.0662	0.850	-0.173	-0.116	49.1
								-0.0587	0.800	-0.144	-0.109	32.1
3.07	0	60.0	1.62	0.735			1.03	-0.0752	0.880	-0.203	-0.174	16.7
								-0.0705	0.820	-0.177	-0.158	12.0
								-0.0622	0.850	-0.173	-0.116	49.1
1.87	0.25	70.0	1.62	0.465			1.52	-0.0937	1.000	-0.176	-0.098	78.6
								-0.0943	0.922	-0.162	-0.116	39.7
								-0.0916	0.820	-0.140	-0.086	0.8
1.84	0.25	64.7	1.62	0.604			1.21	-0.1058	0.938	-0.183	-0.187	-2.1
								-0.1046	0.845	-0.162	-0.135	20.0
								-0.0988	0.807	-0.147	-0.113	30.1
1.90	0.25	60.0	1.62	0.735			1.03	-0.1115	0.880	-0.187	-0.219	-14.6
								-0.1097	0.820	-0.171	-0.176	-2.0
								-0.1175	0.840	-0.188	-0.222	-15.3
2.37	0.25	70.0	1.62	0.465			1.52	-0.0805	1.000	-0.191	-0.142	34.5
								-0.0833	0.922	-0.182	-0.118	54.2
								-0.0822	0.820	-0.160	-0.098	66.7

TABLE 7.1.2.2-C (CONTD)

Ref.	A	λ	Λ_{LE} (deg)	M	$\beta \cot \Lambda_{LE}$	Airfoil Section	ΔV_L	$\frac{(C_{I_p})}{(C_{I_p})_{theory}}$	$\frac{C_{I_p}}{(C_{I_p})_{theory}}$	C_{I_p} Calc. (per rad)	C_{I_p} Test (per rad)	Percent Error
								A (per rad)	$(C_{I_p})_{theory}$	C_{I_p} Calc. (per rad)	C_{I_p} Test (per rad)	Percent Error
23	2.34	0.25	65.0	1.62	0.595	Beveled Flat Plate	1.22	-0.0955	0.940	-0.210	-0.183	14.8
					1.93			-0.0934	0.850	-0.186	-0.127	48.5
					2.41			-0.0870	0.800	-0.163	-0.127	28.3
	2.37	0.25	55.0	1.62	0.892		0.90	-0.1092	0.840	-0.218	-0.221	-1.4
	3.06	0.25	65.1	1.62	0.592		1.22	-0.0825	0.950	-0.239	-0.155	54.2
					1.93			-0.0818	0.860	-0.213	-0.132	61.4
					2.41			-0.0757	0.800	-0.185	-0.120	54.2
	3.12	0.25	80.0	1.62	0.735		1.03	-0.0805	0.800	-0.248	-0.230	7.8
					1.93			-0.0870	0.820	-0.222	-0.205	8.3
	3.22	0.25	85.2	1.62	0.895		0.90	-0.0848	0.840	-0.256	-0.228	12.3
	1.83	0	55.0	1.62	0.890		0.90	-0.1040	0.840	-0.180	-0.156	2.6
	2.34	0	64.0	1.62	0.895		0.905	-0.0957	0.835	-0.187	-0.187	0
	2.32	0	60.0	1.62	0.735		1.03	-0.0890	0.880	-0.181	-0.158	14.6
					1.93			-0.0868	0.820	-0.163	-0.155	5.2
	2.81	0	55.0	1.62	0.890		0.90	-0.0890	0.840	-0.210	-0.172	22.1
24	4.00	0	45.0	1.414	1.000	Symmetrical dbl. wedge t/c = 0.04	0.332	-0.085	0.910	-0.309	-0.280	10.4
	4.00	0	45.0	1.414	1.000	Symmetrical dbl. wedge t/c = 0.09	0.75	-0.085	0.848	-0.288	-0.230	25.2
25	3.70	1.00	45.0	1.414	1.000	65A009	1.74	-0.106	0.770	-0.302	-0.265	14.0
					1.30			-0.1055	0.800	-0.312	-0.311	0.3
Average Error = $\frac{\sum e }{n} = 28.4\%$												

SUBSONIC SPEEDS

(a) $\lambda = 0$

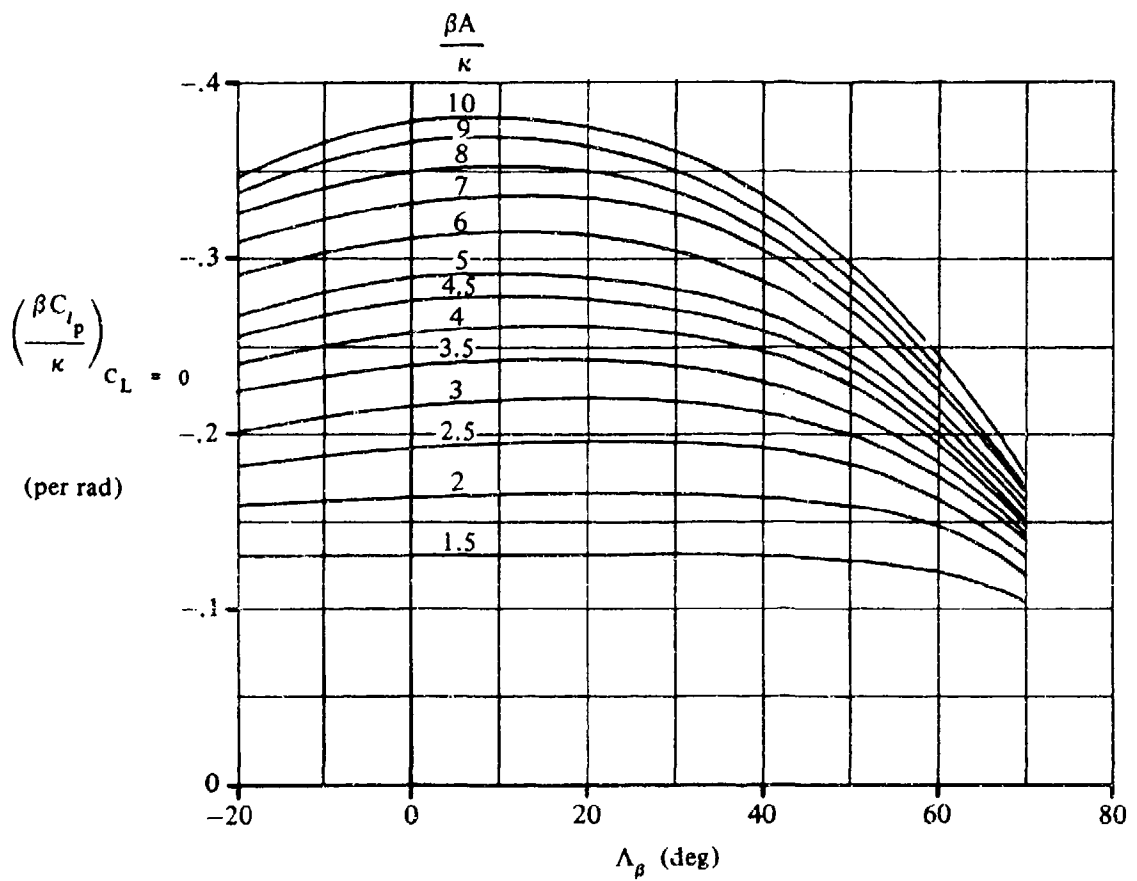


FIGURE 7.1.2.2-20 ROLL-DAMPING PARAMETER AT ZERO LIFT

SUBSONIC SPEEDS

(b) $\lambda = 0.25$

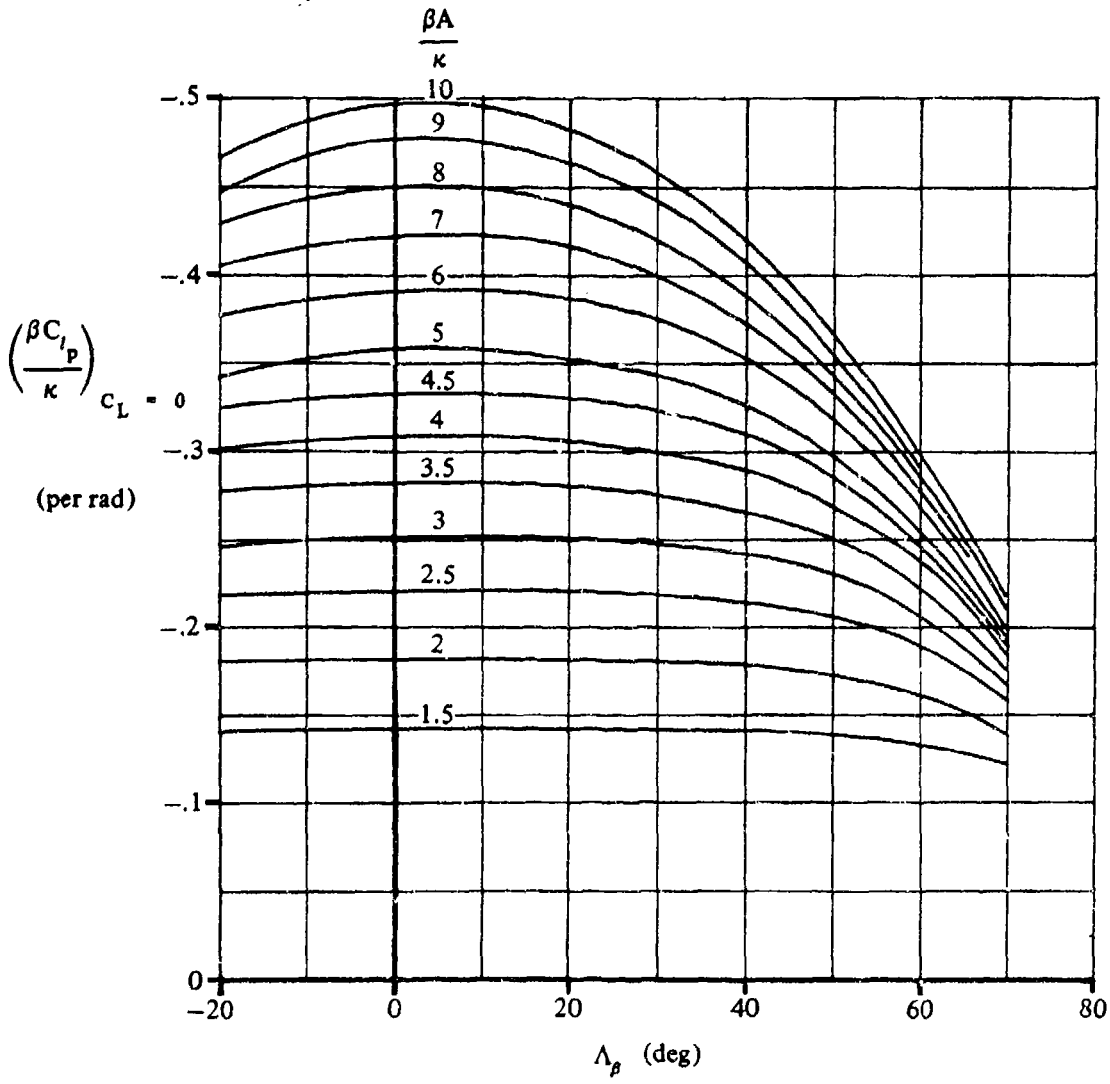


FIGURE 7.1.2.2-20 (CONTD)

SUBSONIC SPEEDS

(c) $\lambda = 0.50$

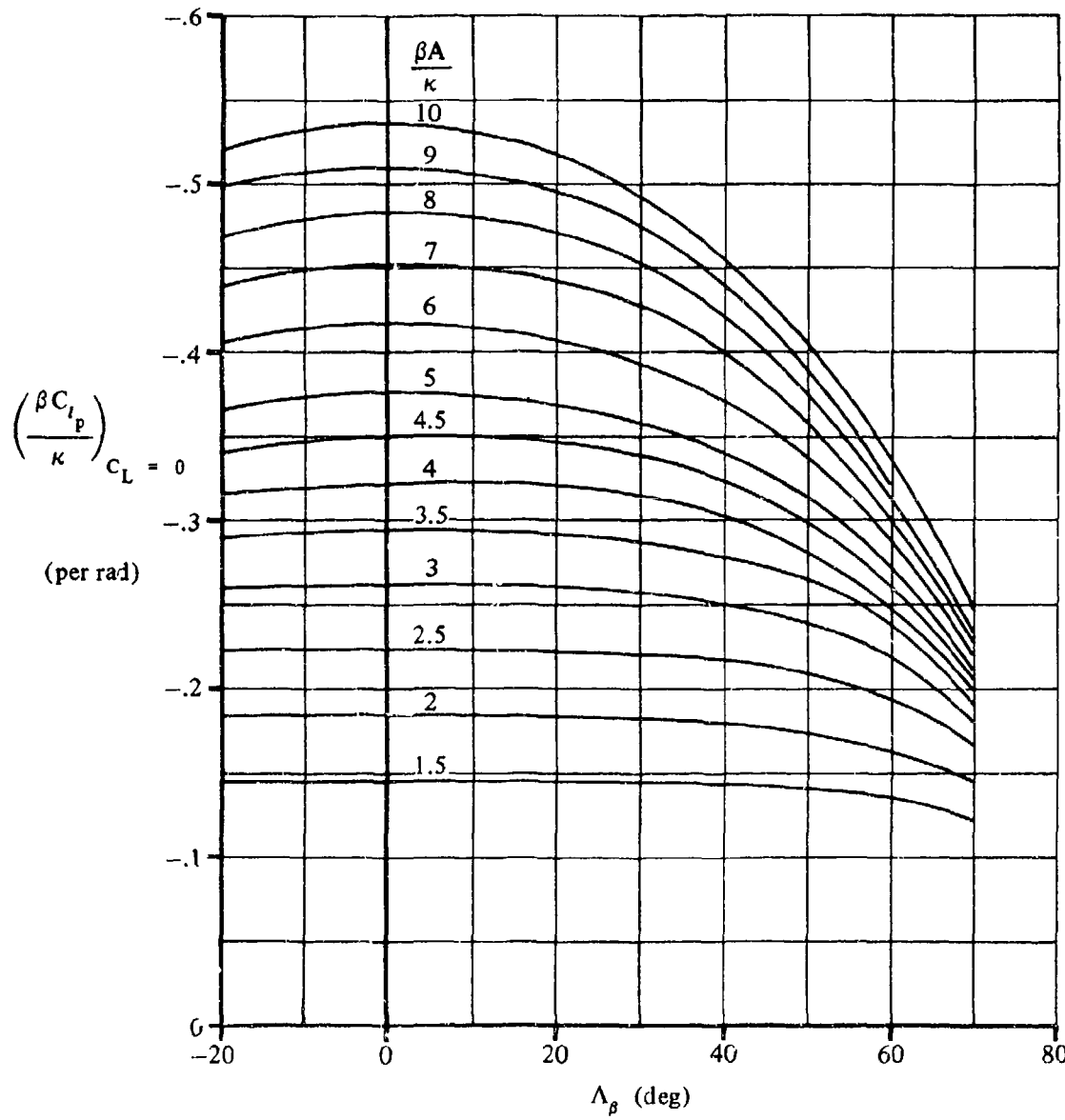


FIGURE 7.1.2.2-20 (CONTD)

SUBSONIC SPEEDS

(d) $\lambda = 1.0$

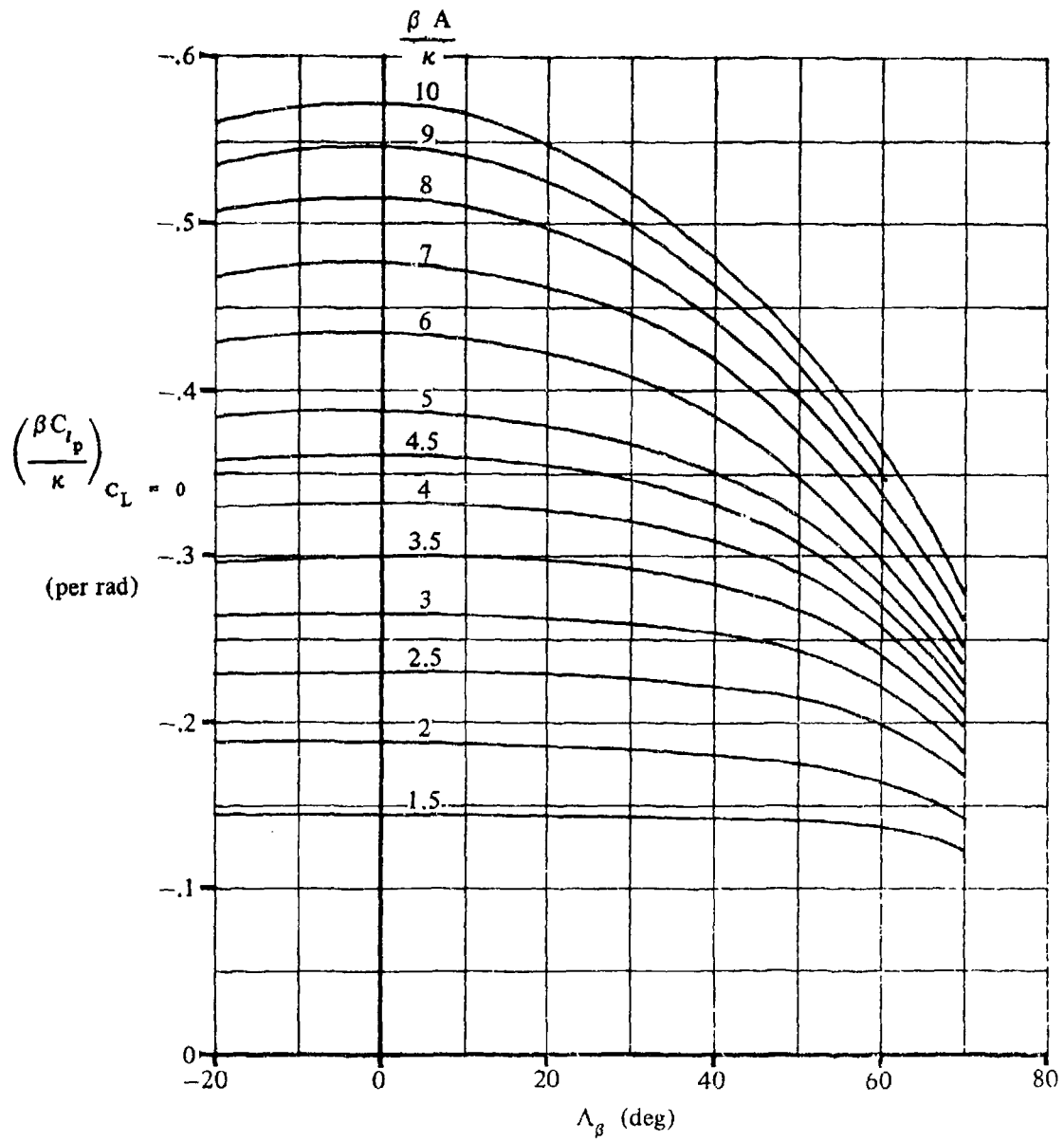


FIGURE 7.1.2.2-20 (CONTD)

SUBSONIC SPEEDS

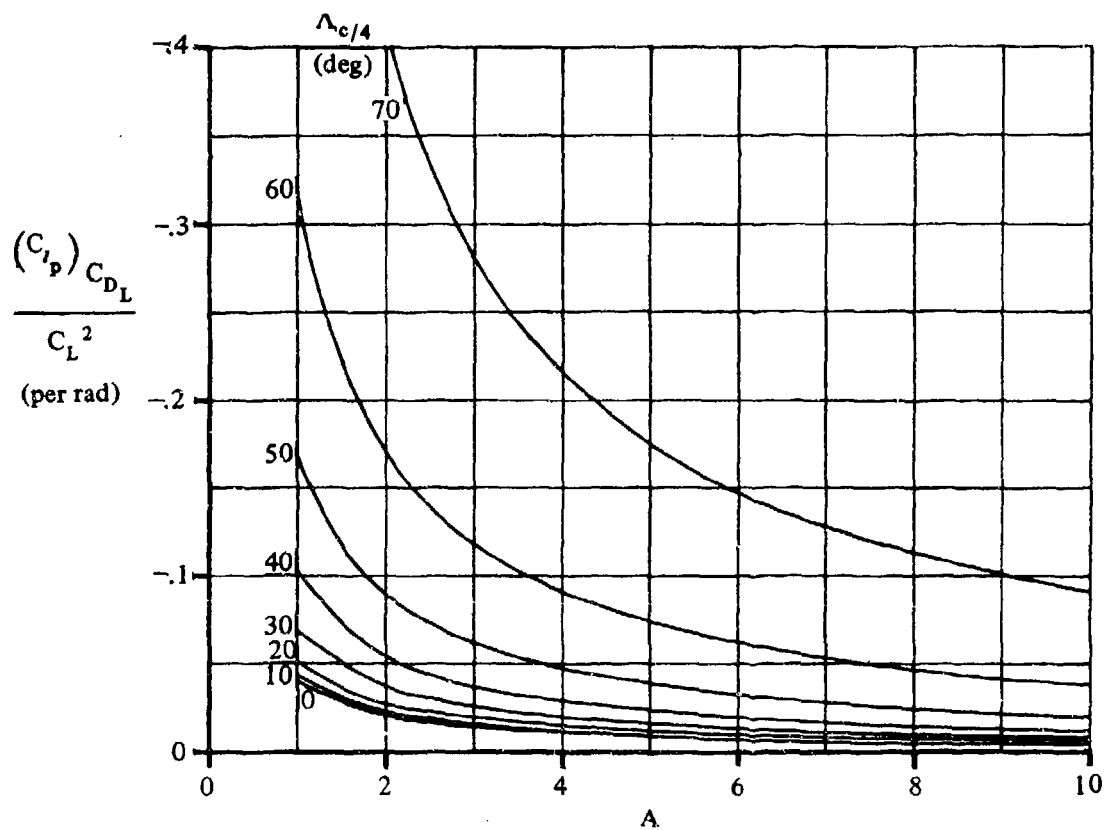


FIGURE 7.1.2.2-24 DRAG-DUE-TO-LIFT ROLL-DAMPING PARAMETER

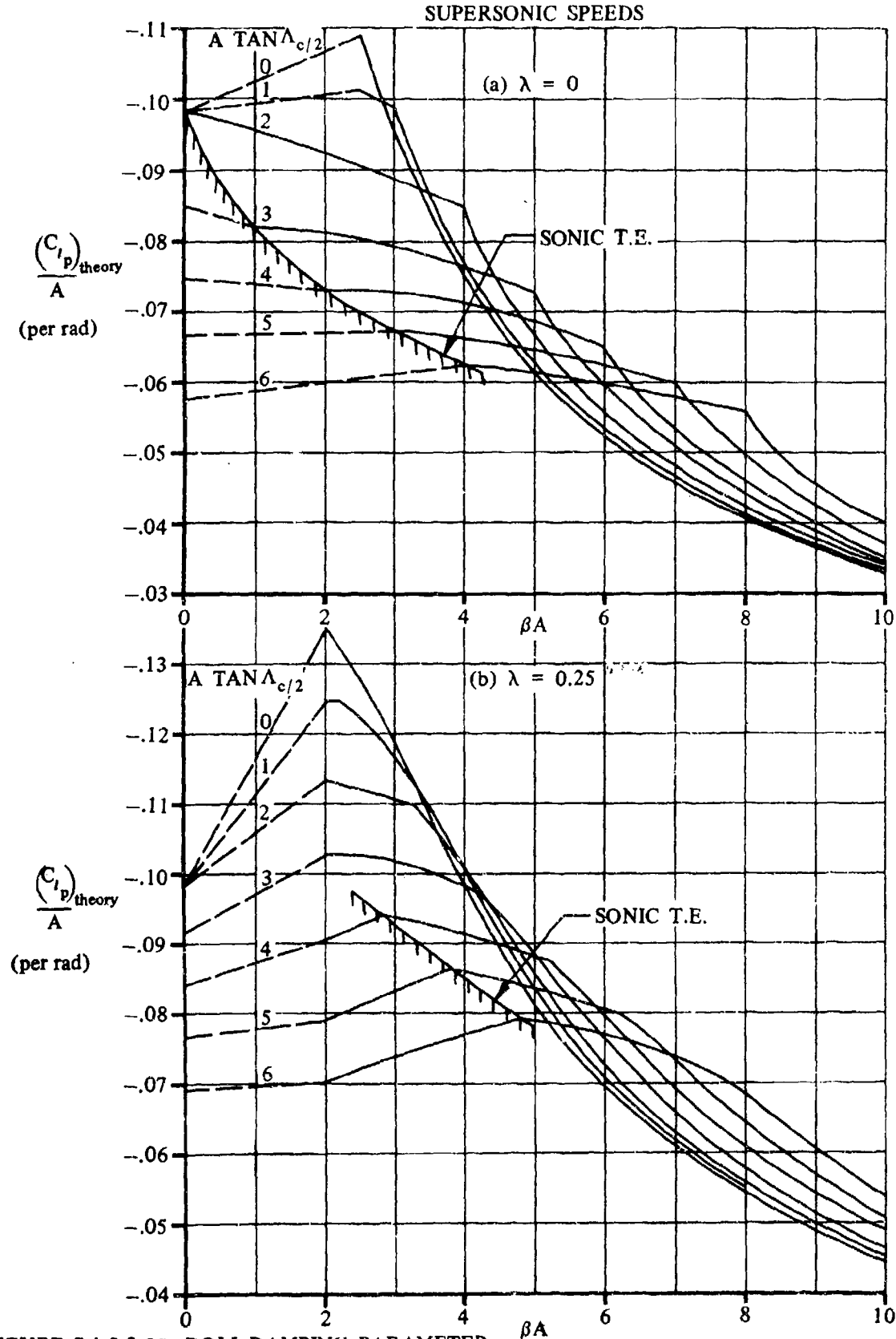


FIGURE 7.1.2.2-25 ROLL-DAMPING PARAMETER

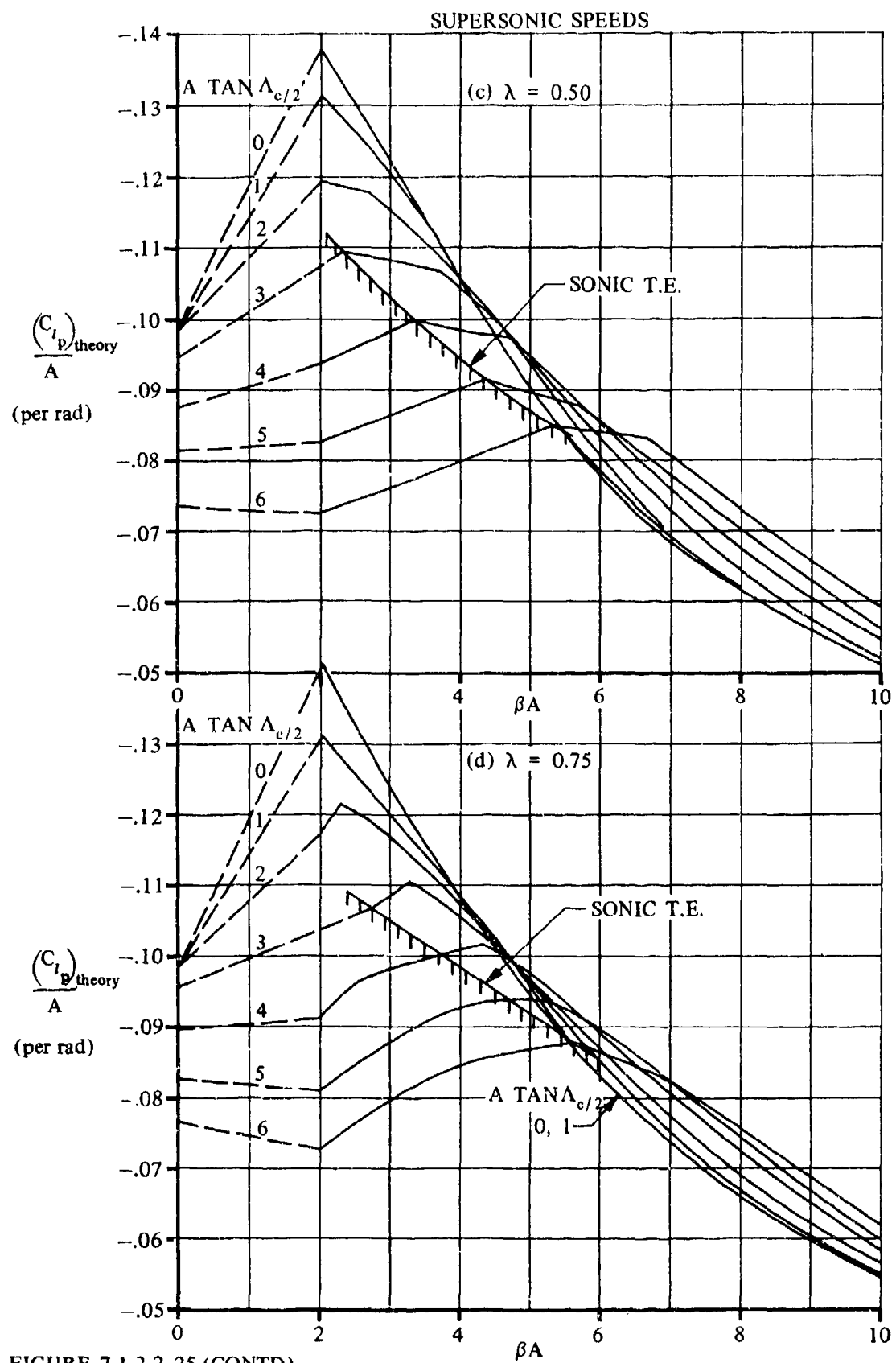


FIGURE 7.1.2.2-25 (CONTD)

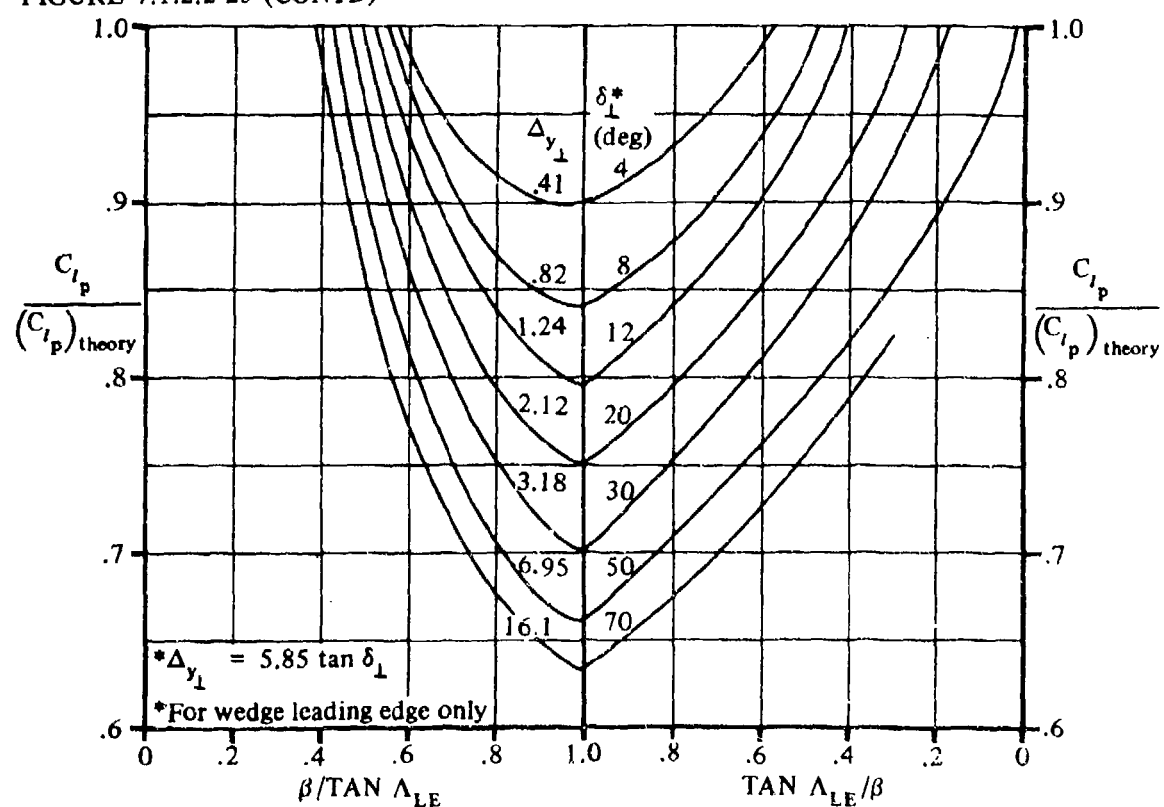
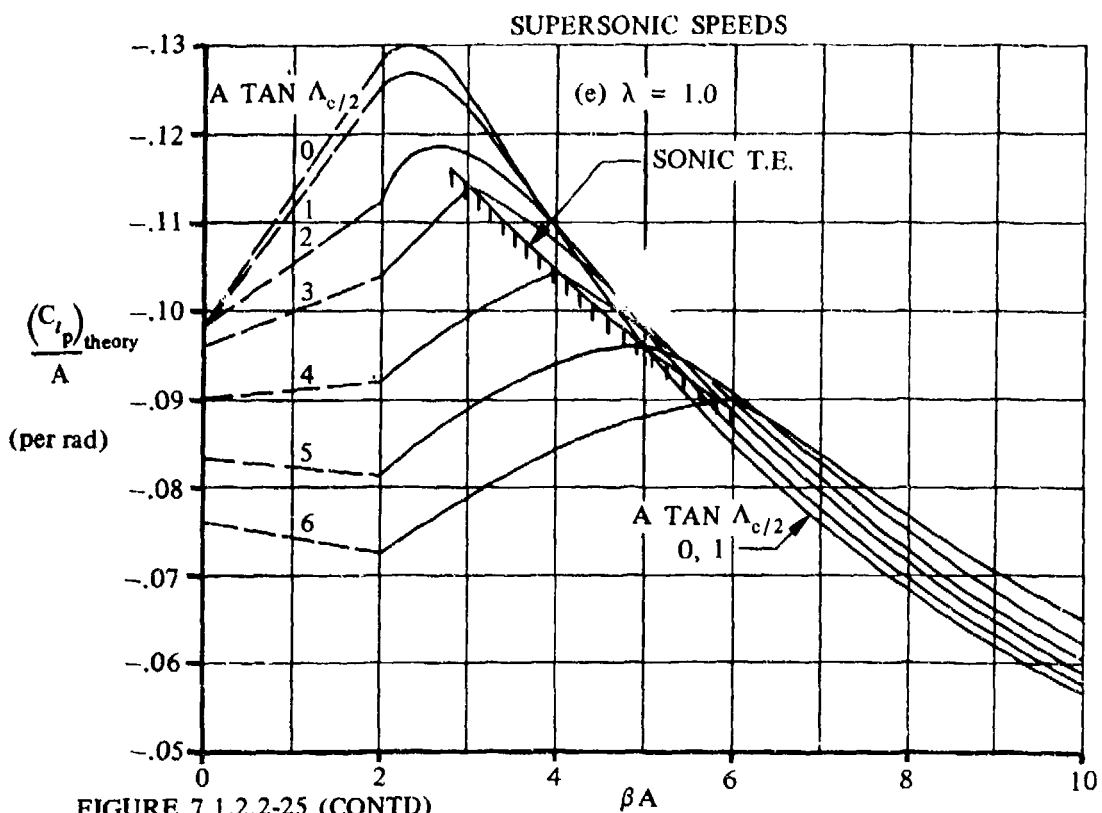


FIGURE 7.1.2.2-27 DAMPING-IN-ROLL CORRECTION FACTOR FOR SONIC-LEADING-EDGE REGION

7.1.2.3 WING ROLLING DERIVATIVE C_{n_p}

This section presents methods for estimating the wing contribution to the rolling derivative C_{n_p} at subsonic and supersonic speeds. This derivative is the change in yawing-moment coefficient with change in wing-tip helix angle and is expressed as

$$C_{n_p} = \frac{\partial C_n}{\partial \left(\frac{pb}{2V_\infty} \right)}$$

A SUBSONIC

The wing rolling derivative C_{n_p} results because the unsymmetrical lift distribution causes a difference in drag between the wing panels when the wing is rolling.

The method for estimating the wing rolling derivative C_{n_p} is derived from an analysis of references 1 through 5. The method is applicable over the lift-coefficient range up to the stall, providing reliable values of lift and drag are available over this range.

The value of C_{n_p} near zero-lift coefficient is the potential-flow value based on simple-sweep theory from reference 1. The effects of linear wing twist and symmetric flap deflection are taken from references 1 and 3. Geometric dihedral also causes an increment in yawing moment that is associated with the increment in lateral force. The empirical results of reference 4 show that this increment is independent of lift coefficient over the low to moderate lift-coefficient range and increases at the higher values of lift coefficient. However, over the range of wing dihedral angles of practical interest the increment in C_{n_p} due to dihedral is very small and may be neglected.

At moderate or high lift coefficients, a comparatively large change in C_{n_p}/C_L occurs, especially for swept wings, due to the rise in drag associated with the increase in lift. In references 2 and 5, methods are presented for evaluating C_{n_p} over the lift-coefficient range up to the stall by using a correction factor to account for the variation of profile drag with lift coefficient. Results obtained by using the methods of both references 2 and 5 for estimating C_{n_p} over the lift-coefficient range have been analyzed and the method of reference 5 selected for the Datcom.

Theoretically, the tip-suction contribution to the lateral force also contributes to the yawing moment. Since this contribution is inversely proportional to aspect ratio, the increment in C_{n_p} due to tip suction becomes quite significant for highly swept and/or low-aspect-ratio planforms. A comparison has been made of C_{n_p} calculated with and without the tip-suction effect of reference 5 with test results. In all cases better agreement was obtained when the tip-suction effects were neglected. The analysis indicates a loss in tip suction particularly at the higher lift coefficients. Therefore, the effect of tip suction has been omitted from the Datcom.

If experimental lift and drag data for the particular planform of interest are not available at the chosen Mach number, no attempt should be made to estimate the variation of C_{n_p} with lift coefficient. No known general method for estimating the variation of drag coefficient will give results reliable enough to use in determining the correction factor for extrapolating the potential-flow values to higher lift coefficients.

DATCOM METHOD

The variation of the wing rolling derivative C_{n_p} with lift coefficient at subsonic speeds, based on the product of the wing area and the square of the wing span $S_W b_W^2$, is given by

$$C_{n_p} = -C_{I_p} \tan \alpha - K \left[-C_{I_p} \tan \alpha - \left(\frac{C_{n_p}}{C_L} \right)_{\substack{C_L=0 \\ M}} C_L \right] + \left(\frac{\Delta C_{n_p}}{\theta} \right) \theta \\ + \left[\frac{\Delta C_{n_p}}{\left(\frac{\partial \alpha}{\partial \delta} \right)_f \delta_f} \right] \left(\frac{\partial \alpha}{\partial \delta} \right)_f \delta_f \quad (\text{per radian}) \quad 7.1.2.3-a$$

where

C_{I_p} is the roll-damping derivative at the appropriate Mach number estimated by using the method of paragraph A of Section 7.1.2.2.

α is the angle of attack in degrees.

C_L is the lift coefficient.

$\left(\frac{C_{n_p}}{C_L} \right)_{\substack{C_L=0 \\ M}}$ is the slope of the yawing moment due to rolling at zero lift given by

$$\left(\frac{C_{n_p}}{C_L} \right)_{\substack{C_L=0 \\ M}} = \left(\frac{A + 4 \cos \Lambda_{c/4}}{AB + 4 \cos \Lambda_{c/4}} \right) \left[\frac{AB + \frac{1}{2} (AB + \cos \Lambda_{c/4}) \tan^2 \Lambda_{c/4}}{A + \frac{1}{2} (A + \cos \Lambda_{c/4}) \tan^2 \Lambda_{c/4}} \right] \left(\frac{C_{n_p}}{C_L} \right)_{\substack{C_L=0 \\ M=0}}$$

7.1.2.3-b

where $B = \sqrt{1 - M^2 \cos^2 \Lambda_{c/4}}$ and

$\left(\frac{C_{n_p}}{C_L} \right)_{\substack{C_L=0 \\ M=0}}$ is the slope of the low-speed yawing moment due to rolling at zero lift given by

$$\left(\frac{C_{n_p}}{C_L} \right)_{\substack{C_L=0 \\ M=0}} = -\frac{1}{6} \frac{A + 6(A + \cos \Lambda_{c/4}) \left(\frac{\bar{x}}{c} \frac{\tan \Lambda_{c/4}}{A} + \frac{\tan^2 \Lambda_{c/4}}{12} \right)}{A + 4 \cos \Lambda_{c/4}} \quad (\text{per radian}) \quad 7.1.2.3-c$$

7.1.2.3-2

where \bar{x} is the distance from the center of gravity to the aerodynamic center, positive when the a.c. is aft of the c.g. and c is the wing mean aerodynamic chord. Equation 7.1.2.3-b modifies the low-speed value of equation 7.1.2.3-c by means of the Prandtl-Glauert rule to yield approximate corrections for the first-order three-dimensional effects of compressible flow up to the critical Mach number.

$$\frac{\Delta C_{n_p}}{\theta}$$

is the effect of linear wing twist obtained from figure 7.1.2.3-12.

θ

is the wing twist between the root and tip stations in degrees, negative for washout (see figure 7.1.2.3-12).

$$\frac{\Delta C_{n_p}}{\left(\frac{\partial \alpha}{\partial \delta}\right)_r \delta_f}$$

is the effect of symmetric flap deflection obtained from figure 7.1.2.3-13.

δ_f

is the streamwise flap deflection in degrees.

$$\left(\frac{\partial \alpha}{\partial \delta}\right)_r$$

is the two-dimensional lift-effectiveness parameter α_s obtained from Section 6.1.1.1.

K

is a dimensionless correction factor used to extrapolate the potential-flow values to high lift coefficients. This is the same correction factor used in Section 7.1.2.1 to account for the variation of profile drag with lift coefficient. At zero lift this factor is taken as 1.0. At lift coefficients other than zero this factor accounts for the variation of profile drag with lift coefficient and is given by

$$K = \frac{\frac{\partial}{\partial \alpha} (C_L \tan \alpha) - \frac{\partial}{\partial \alpha} (C_D - C_{D_0})}{\frac{\partial}{\partial \alpha} (C_L \tan \alpha) - \frac{\partial}{\partial \alpha} \left(\frac{C_L^2}{\pi A} \right)}$$

7.1.2.3-d

Test values of lift and drag at the chosen Mach number for the particular planform of interest must be used in evaluating equation 7.1.2.3-d. The terms of this equation are evaluated by taking the slopes of $C_L \tan \alpha$, $(C_D - C_{D_0})$, and $C_L^2 / (\pi A)$, plotted versus angle of attack.

If reliable values of the static-force coefficients are available, the method should provide results within ± 20 percent accuracy throughout the lift-coefficient range to the stall.

7.1.2.3-3

Sample Problem

Given: The wing designated 45-4.0-0.6-006 of references 5 and 8.

Wing Characteristics:

$$A = 4.0 \quad \lambda = 0.6 \quad \Lambda_{c/4} = 45^\circ \quad \theta = 0$$

$$S = 2.25 \text{ sq ft} \quad b = 3.0 \text{ ft}$$

NACA 65A006 Airfoil $\bar{x} = 0$ [origin of moments (c.g.) located at $x_{a.c.}$]

Additional Characteristics:

$$M = 0.70; \beta = 0.714 \quad R_f = 3.1 \times 10^6$$

The following values of α and C_D are test results from reference 8. The variation of C_{I_p} with C_L has been calculated using the method of paragraph A of Section 7.1.2.2.

C_L	0	.1	.2	.3	.4	.5	.6	.7	.75
α	0	1.70	3.30	4.90	6.55	8.00	9.60	11.80	13.20
C_D	.011	.012	.016	.024	.040	.063	.094	.138	.170
C_{I_p}	-.314	-.314	-.313	-.312	-.326	-.325	-.280	-.181	-.156

Compute:

Determine the slope of the yawing moment due to rolling at zero lift $\left(\frac{C_{n_p}}{C_L} \right)_{\substack{C_L=0 \\ M=0}}$

$$\left(\frac{C_{n_p}}{C_L} \right)_{\substack{C_L=0 \\ M=0}} = -\frac{1}{6} \frac{A + 6(A + \cos \Lambda_{c/4}) \left(\frac{\bar{x}}{c} \frac{\tan \Lambda_{c/4}}{A} + \frac{\tan^2 \Lambda_{c/4}}{12} \right)}{A + 4 \cos \Lambda_{c/4}} \quad (\text{equation 7.1.2.3-c})$$

$$= -\frac{1}{6} \frac{4.0 + 6(4.0 + \cos 45^\circ) \left(0 + \frac{\tan^2 45^\circ}{12} \right)}{4.0 + 4 \cos 45^\circ}$$

$$= -\frac{1}{6} \frac{4.0 + 6(4.7071) \left(0 + \frac{1}{12} \right)}{4.0 + 2.828} = -0.155 \text{ per rad}$$

$$B = \sqrt{1 - M^2 \cos^2 \Lambda_{c/4}} = \sqrt{1 - (0.7)^2 (0.7071)^2} = 0.87$$

$$\frac{A + 4 \cos \Lambda_{c/4}}{AB + 4 \cos \Lambda_{c/4}} = \frac{4.0 + (4.0)(0.7071)}{(4.0)(0.87) + (4.0)(0.7071)} = \frac{6.828}{6.308} = 1.082$$

$$\frac{\frac{AB + \frac{1}{2}(AB + \cos \Lambda_{c/4}) \tan^2 \Lambda_{c/4}}{A + \frac{1}{2}(A + \cos \Lambda_{c/4}) \tan^2 \Lambda_{c/4}}}{\frac{(4.0)(0.87) + \frac{1}{2}[(4.0)(0.87) + 0.7071](1)}{4.0 + \frac{1}{2}[4.0 + 0.7071](1)}} = \frac{5.574}{6.354} = 0.877$$

$$\left(\frac{C_{n_p}}{C_L}\right)_{\substack{C_L=0 \\ M}} = \left(\frac{A + 4 \cos \Lambda_{c/4}}{AB + 4 \cos \Lambda_{c/4}}\right) \left[\frac{AB + \frac{1}{2}(AB + \cos \Lambda_{c/4}) \tan^2 \Lambda_{c/4}}{A + \frac{1}{2}(A + \cos \Lambda_{c/4}) \tan^2 \Lambda_{c/4}} \right] \left(\frac{C_{n_p}}{C_L}\right)_{\substack{C_L=0 \\ M=0}}$$

(equation 7.1.2.3-b)

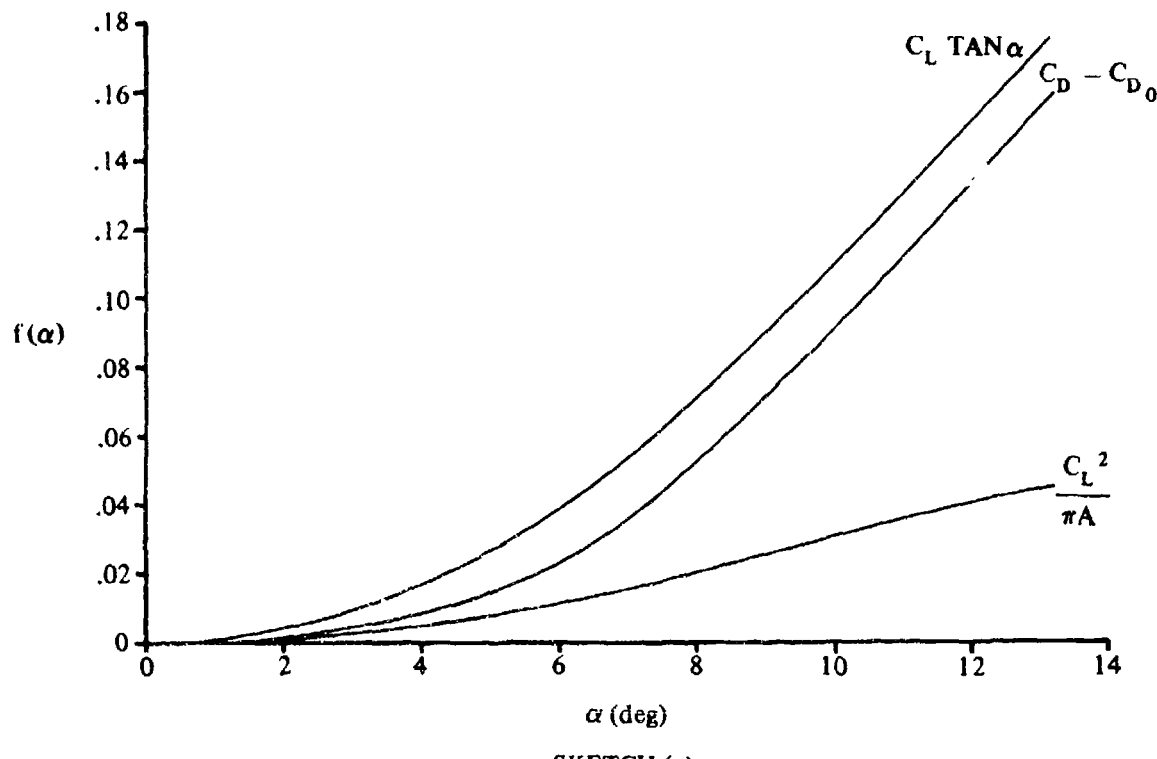
$$= (1.082)(0.877)(-0.155) = -0.147 \text{ per rad}$$

Determine the K factor

$$K = \frac{\frac{\partial}{\partial \alpha} (C_L \tan \alpha) - \frac{\partial}{\partial \alpha} (C_D - C_{D_0})}{\frac{\partial}{\partial \alpha} (C_L \tan \alpha) - \frac{\partial}{\partial \alpha} \left(\frac{C_L^2}{\pi A} \right)} \quad (\text{equation 7.1.2.3-d})$$

① C_L	② α Test (deg)	③ $\tan \alpha$	④ $C_L \tan \alpha$ ① ③	⑤ C_D Test	⑥ $C_D - C_{D_0}$ ⑤ - 0.011	⑦ $C_L^2 / (\pi A)$ ① ² / (4π)
0	0	0	0	.011	0	0
.1	1.70	.02968	.00297	.012	.001	.00080
.2	3.30	.05766	.01153	.016	.005	.00318
.3	4.90	.08573	.02572	.024	.013	.00716
.4	6.55	.1148	.04592	.040	.029	.01273
.5	8.00	.1406	.07027	.063	.052	.01990
.6	9.60	.1691	.1015	.094	.083	.02860
.7	11.80	.2089	.1462	.138	.127	.03600
.76	13.20	.2346	.1769	.170	.159	.04476

Plot $C_L \tan \alpha$, $C_D - C_{D_0}$, and $\frac{C_L^2}{\pi A}$ versus angle of attack (see sketch (a)).



SKETCH (a)

(1)	(2)	(3)	(4)	(5)
C_L	$\frac{\partial}{\partial \alpha} (C_L \tan \alpha)$	$\frac{\partial}{\partial \alpha} (C_D - C_{D_0})$	$\frac{\partial}{\partial \alpha} \left(\frac{C_L^2}{\pi A} \right)$	$\frac{(2) - (3)}{(2) - (4)}$ (eq. 7.1.2.3-d)
0	-	-	-	1.00
.1	.0033	.0014	.0010	.826
.2	.00755	.0036	.0019	.699
.3	.01065	.0069	.0030	.483
.4	.01440	.0128	.0040	.154
.5	.01720	.0173	.00515	-.008
.6	.0195	.0195	.0051	0
.7	.0212	.0215	.0041	-.018
.75	.0216	.0220	.0039	-.023

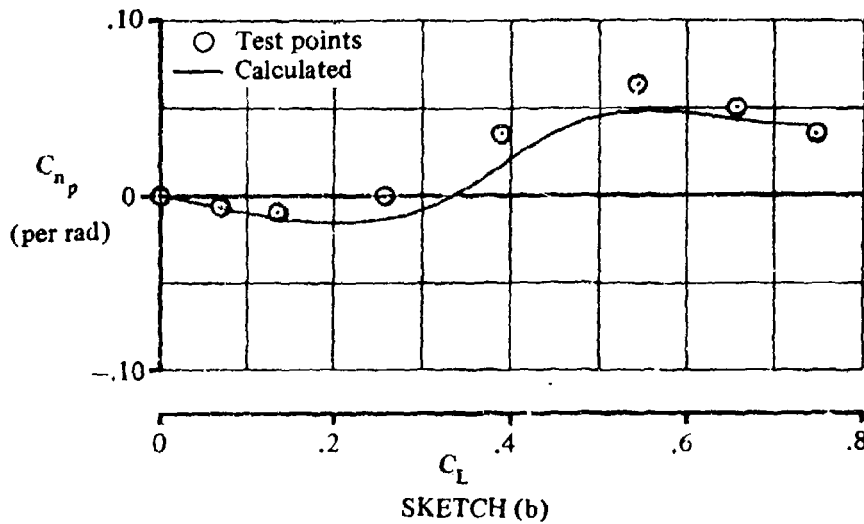
Solution:

$$C_{n_p} = -C_{I_p} \tan \alpha - K \left[-C_{I_p} \tan \alpha - \left(\frac{C_{n_p}}{C_L} \right) C_L \right] \quad (\text{equation 7.1.2.3-a})$$

$$= -C_{I_p} \tan \alpha - K [-C_{I_p} \tan \alpha - (-0.147) C_L] = -C_{I_p} \tan \alpha (1 - K) - 0.147 C_L K$$

1	2	3	4	5	6	7	8
C_L	C_{I_p} Sec. 7.1.2.2 (per rad)	$C_{I_p} \tan \alpha$ $\textcircled{2} \tan \alpha$	K	$1 - K$ $1 - \textcircled{4}$	$-C_{I_p} \tan \alpha (1 - K)$ $- \textcircled{3} \textcircled{5}$	$0.147 K C_L$ $0.147 \textcircled{4} \textcircled{1}$	C_{n_p} based on $S_W b_W^2$ eq. 7.1.2.3-a (per rad) $\textcircled{6} - \textcircled{7}$
0	-0.314	0	1.00	0	0	0	0
.1	-0.314	-0.0093	.826	.174	.00162	.0121	-0.0105
.2	-0.313	-0.0180	.699	.301	.00542	.0206	-0.0152
.3	-0.312	-0.0267	.483	.517	.0138	.0213	-0.0075
.4	-0.326	-0.0374	.154	.846	.0317	.0091	.0226
.5	-0.325	-0.0457	-0.008	1.008	.0460	0	.0460
.6	-0.280	-0.0474	0	1.00	.0474	0	.0474
.7	-0.181	-0.0378	-0.018	1.018	.0385	-0.0019	.0404
.75	-0.156	-0.0366	-0.023	1.023	.0374	-0.0025	.0399

The calculated results are compared with test values from reference 5 in sketch (b).



B. TRANSONIC

No generalized method is available in the literature for estimating transonic values of the rolling derivative C_{n_p} . Furthermore, no known experimental results are available for this derivative at transonic speeds.

C. SUPERSONIC

At supersonic speeds design charts based on theoretical calculations are presented for estimating the rolling derivative C_{n_p} at low values of the lift coefficient.

The design charts are based on the results of reference 6 for wings with subsonic leading edges and supersonic trailing edges, and on the results of reference 7 for wings with supersonic leading edges and either subsonic or supersonic trailing edges. The results of both references 6 and 7 are based on linearized-supersonic-flow theory and are therefore restricted to thin, swept-back, tapered wings with streamwise tips. The yawing moment due to rolling is taken as that arising entirely from suction forces on the wing edges. For wings with supersonic leading edges no suction forces are induced along the leading edges; consequently, the determination of C_{n_p} involves only the unbalanced suction forces along the wing tips. Therefore, no design chart is presented for zero-taper wings with supersonic leading edges, since the theory gives $C_{n_p} = 0$.

The design charts for wings with subsonic leading edges give values of C_{n_p} that are referred to body axes with the origin located at the wing apex. The design charts for wings with supersonic leading edges give values of C_{n_p} that are referred to body axes with the origin located at the projection of the leading edge of the tip on the wing root chord. The Datcom method presents transformation formulas for conversion from body axes to stability axes with the origin located at an arbitrary distance from the leading edge.

No experimental data are available for this derivative at supersonic speeds. Therefore, the validity of linearized-supersonic-flow theory for estimating C_{n_p} cannot be determined.

DATCOM METHOD

Subsonic Leading Edges ($\beta \cot \Lambda_{LE} < 1$)

For wings with subsonic leading edges the contribution to the rolling derivative C_{n_p} at supersonic speeds, and at low values of the lift coefficient is given by

$$\frac{C_{n_p}}{\alpha} = \left(\frac{C_{n_p}}{\alpha} \right)_{\text{body axis}} + \frac{2 x_{c.g.}}{A(1+\lambda)} \left(\frac{C_Y}{\alpha} \right) - (C_{l_p} - C_{n_r}) \quad (\text{per radian}^2) \quad 7.1.2.3-e$$

where

$$\frac{C_{n_p}}{\alpha}$$

is the supersonic yawing moment due to rolling referred to stability axes with the origin at the center of gravity.

$$\left(\frac{C_{n_p}}{\alpha}\right)_{\text{body axis}}$$

is the supersonic yawing moment due to rolling referred to body axes with the origin at the wing apex, given by

$$\left(\frac{C_{n_p}}{\alpha}\right)_{\text{body axis}} = \left(\frac{C_{n_p}}{\alpha}\right)_1 + \left(\frac{C_{n_p}}{\alpha}\right)_2 + \left(\frac{C_{n_p}}{\alpha}\right)_3 \text{ (per radian}^2\text{)} \quad 7.1.2.3-f$$

where

$\left(\frac{C_{n_p}}{\alpha}\right)_1$ is obtained from figure 7.1.2.3-14a through 7.1.2.3-14d as a function of βA , $\beta \cot \Lambda_{LE}$, and taper ratio. For $\lambda = 0$, $(C_{n_p}/\alpha)_1 = 0$.

$\left(\frac{C_{n_p}}{\alpha}\right)_2$ and $\left(\frac{C_{n_p}}{\alpha}\right)_3$ are obtained from figure 7.1.2.3-16 as a function of $\beta \cot \Lambda_{LE}$.

$x_{c.g.}$

is the distance from the wing apex to the center of gravity in root chords, positive when the c.g. is aft of the wing apex.

$\frac{C_{Y_p}}{\alpha}$

is the supersonic side force due to rolling obtained by using the method of paragraph C of Section 7.1.2.1.

C_{I_p}

is the supersonic roll-damping derivative obtained by using the method of paragraph C of Section 7.1.2.2.

C_{n_r}

is the supersonic yaw-damping derivative. It is negligible except for very low-aspect-ratio wings. References are noted in paragraph C of Section 7.1.3.3 that outline approximate methods that may be used to determine this derivative.

α

is the angle of attack in radians.

Supersonic Leading Edges ($\beta \cot \Lambda_{LE} > 1$)

For wings with supersonic leading edges the contribution to the rolling derivative C_{n_p} at supersonic speeds and at low values of the lift coefficient is given by

$$\frac{C_{n_p}}{\alpha} = \left(\frac{C_{n_p}}{\alpha}\right)_{\text{body axis}} + \left[\frac{2 x_{c.g.}}{A(1 + \lambda)} - \frac{1}{2} \tan \Lambda_{LE} \right] \frac{C_{Y_p}}{\alpha} - C_{I_p} \text{ (per radian}^2\text{)}$$

7.1.2.3-g

7.1.2.3-9

where

$$\frac{C_{n_p}}{\alpha}$$

is the supersonic yawing moment due to rolling referred to stability axes with the origin at the center of gravity.

$$\left(\frac{C_{n_p}}{\alpha} \right)_{\text{body axis}}$$

is the supersonic yawing moment due to rolling referred to body axes with the origin at the projection of the leading edge of the tip on the wing root chord. It is obtained from figures 7.1.2.3-17a through 7.1.2.3-17d as a function of βA , $\beta \cot \Lambda_{LE}$, and taper ratio. No design chart is presented for zero-taper wings since $(C_{n_p}/\alpha)_{\text{body axis}} = 0$ for these planforms. For wings with taper ratios less than

0.25 ($\lambda < 0.25$) values of $(C_{n_p}/\alpha)_{\text{body axis}}$ should be obtained by extrapolating values from figures 7.1.2.3-17a through 7.1.2.3-17d.

The remaining terms in equation 7.1.2.3-g are defined under the subsonic-leading-edge case.

Sample Problem

Given: Tapered, swept-back wing

$$A = 3.22 \quad \lambda = 0.25 \quad \Lambda_{LE} = 55.20 \quad \Lambda_{c/2} = 46.80$$

$$M = 2.41; \beta = 2.19 \quad x_{c.g.} = 0.742$$

Compute:

$$\beta \cot \Lambda_{LE} = (2.19) (\cot 55.20) = 1.522 \quad (\text{supersonic leading edge})$$

$$\beta A = (2.19) (3.22) = 7.07$$

$$\frac{C_Y}{\alpha} = 0.50 \text{ per rad}^2 \quad (\text{figure 7.1.2.1-10})$$

$$\left(\frac{C_{n_p}}{\alpha} \right)_{\text{body axis}} = -0.0114 \text{ per rad}^2 \quad (\text{figure 7.1.2.3-17a})$$

$$A \tan \Lambda_{c/2} = (3.22) (\tan 46.80) = 3.433$$

$$\frac{C_I}{A} = -0.066 \text{ per rad} \quad (\text{figure 7.1.2.2-25b})$$

$$C_{l_p} = (-0.066) (3.22) = -0.213 \text{ per rad}$$

Solution:

$$\begin{aligned} \frac{C_{n_p}}{\alpha} &= \left(\frac{C_{n_p}}{\alpha} \right)_{\substack{\text{body} \\ \text{axis}}} + \left[\frac{2 x_{c.g.}}{A(1+\lambda)} - \frac{1}{2} \tan \Lambda_{LE} \right] \frac{C_{Y_p}}{\alpha} - C_{l_p} \quad (\text{equation 7.1.2.3-g}) \\ &= -0.0114 + \left[\frac{2 (0.742)}{3.22 (1+0.25)} - \frac{1}{2} \tan 55.2^\circ \right] 0.50 - (-0.213) \\ &= -0.0114 + [0.3687 - 0.7194] 0.50 + 0.213 \\ &= 0.026 \text{ per rad}^2 \quad (\text{referred to stability axes with origin at } x_{c.g.} \text{ and based on } S_W b_W^2) \end{aligned}$$

REFERENCES

1. Toll, T. A., and Queijo, M. J.: Approximate Relations and Charts for Low-Speed Stability and Control Derivatives of Swept Wings. NACA TN 1581, 1948. (U)
2. Goodman, A., and Fisher, L. R.: Investigation at Low Speeds of the Effect of Aspect Ratio and Sweep on Rolling Stability Derivatives of Untapered Wings. NACA TR 968, 1950. (U)
3. Pinsker, W.: The Aerodynamic Coefficients of Free Lateral Motion. DVL UM 1144/1 and 1144/2, 1943. (U)
4. Queijo, M. J., and Jaquet, B. M.: Calculated Effects of Geometric Dihedral on the Low-Speed Rolling Derivatives of Swept Wings. NACA TN 1732, 1948. (U)
5. Wiggins, J. W.: Wind-Tunnel Investigation of Effect of Sweep on Rolling Derivatives at High Angles of Attack up to 13° and at High Subsonic Mach Numbers, Including a Semiempirical Method of Estimating the Rolling Derivatives. NACA TN 4185, 1958. (U)
6. Margolis, K.: Theoretical Calculations of the Lateral Force and Yawing Moment Due to Rolling at Supersonic Speeds for Sweptback Tapered Wings With Streamwise Tips. Subsonic Leading Edges. NACA TN 2122, 1950. (U)
7. Harmon, S. M., and Martin, J. C.: Theoretical Calculations of the Lateral Force and Yawing Moment Due to Rolling at Supersonic Speeds for Sweptback Tapered Wings With Streamwise Tips. Supersonic Leading Edges. NACA TN 2156, 1950. (U)
8. Kuhn, R. E., and Wiggins, J. W.: Wind-Tunnel Investigation of the Aerodynamic Characteristics in Pitch of Wing-Fuselage Combinations at High Subsonic Speeds. Aspect Ratio Series. NACA RM L52A29, 1952. (U)

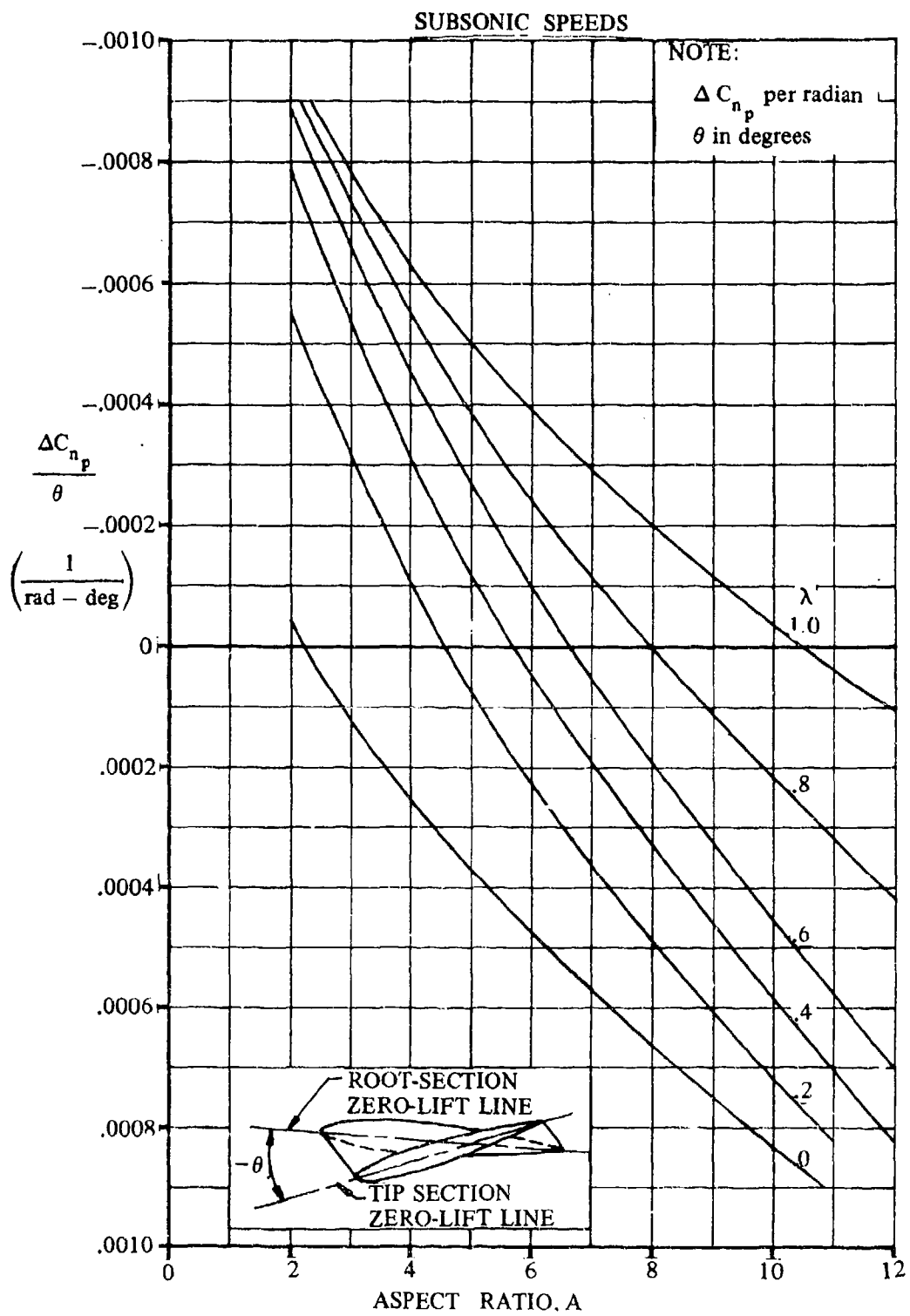


FIGURE 7.1.2.3-12 EFFECT OF WING TWIST ON WING ROLLING DERIVATIVE C_{n_p}

7.1.2.3-12

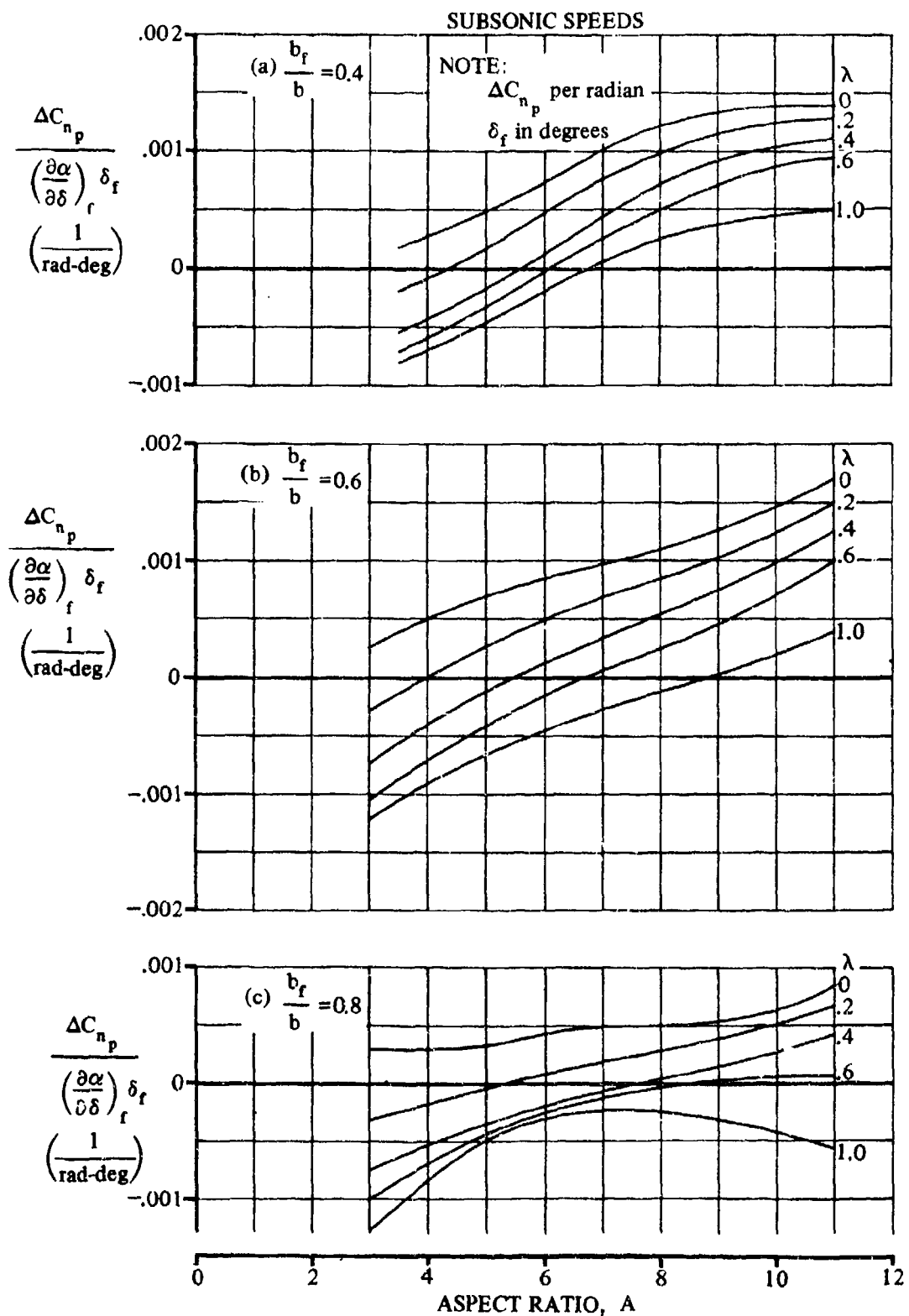


FIGURE 7.1.2.3-13 EFFECT OF FLAP DEFLECTION ON WING ROLLING DERIVATIVE, C_{n_p}

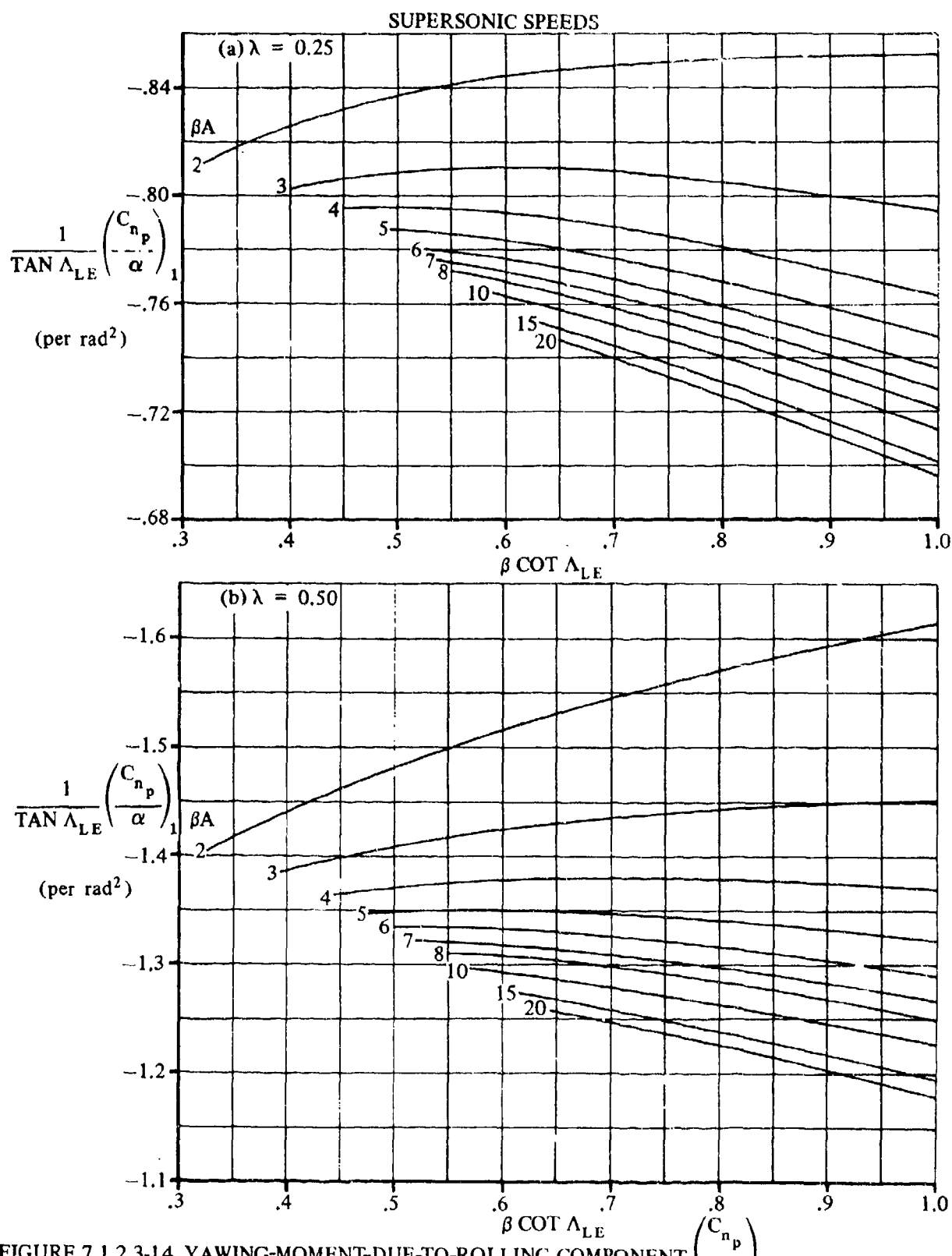


FIGURE 7.1.2.3-14 YAWING-MOMENT-DUE-TO-ROLLING COMPONENT $\left(\frac{C_{n_p}}{\alpha} \right)_1$ -
SUBSONIC LEADING EDGE

7.1.2.3-14

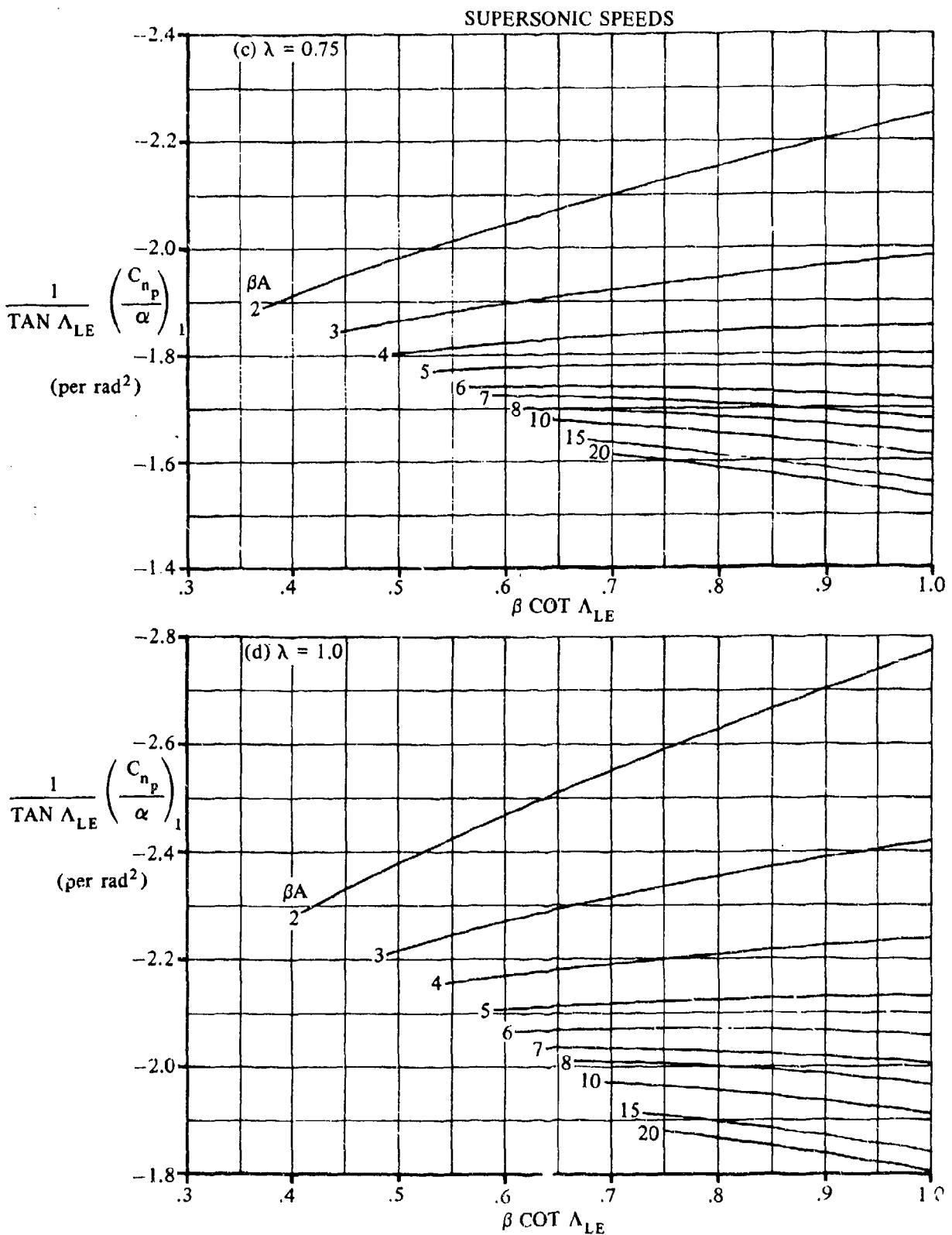


FIGURE 7.1.2.3-14 (CONTD)

SUPersonic SPEEDS

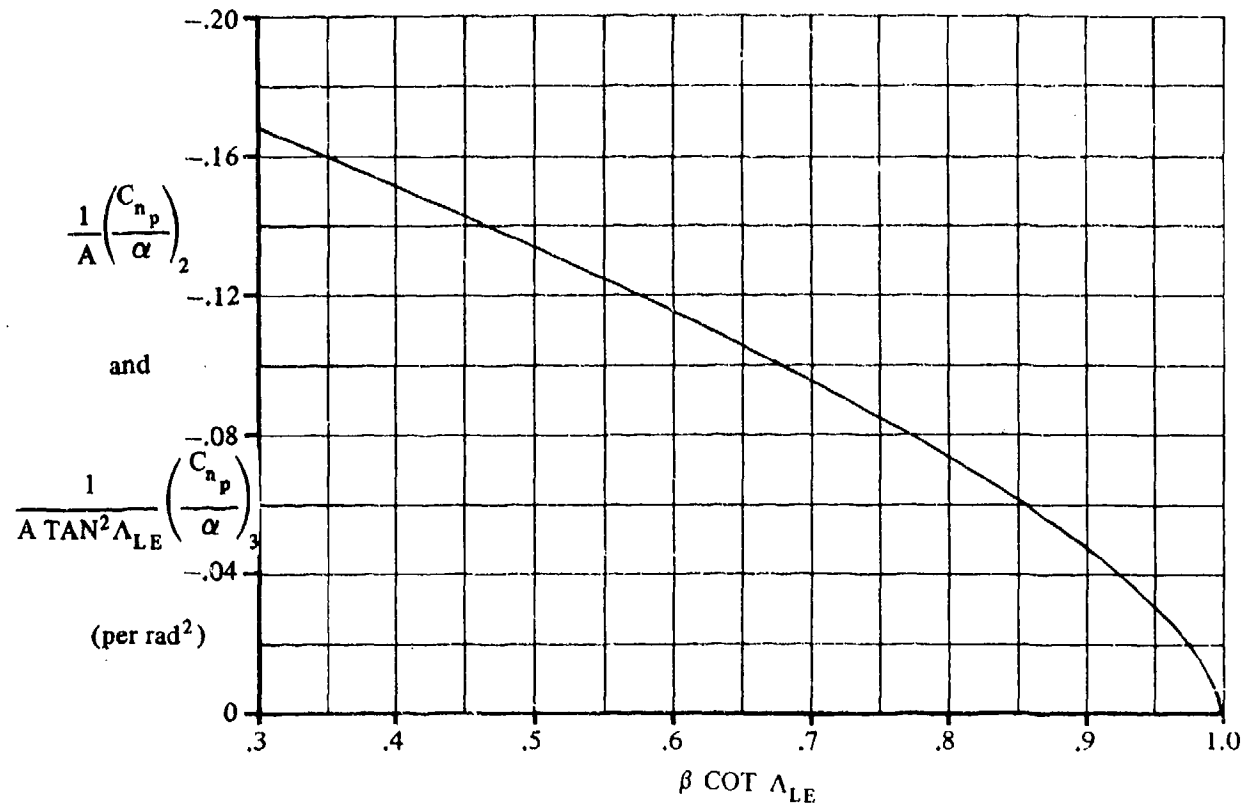


FIGURE 7.1.2.3-16 YAWING-MOMENT-DUE-TO-ROLLING COMPONENTS $\left(\frac{C_{n_p}}{\alpha} \right)_2$ AND $\left(\frac{C_{n_p}}{\alpha} \right)_3$
SUBSONIC LEADING EDGES

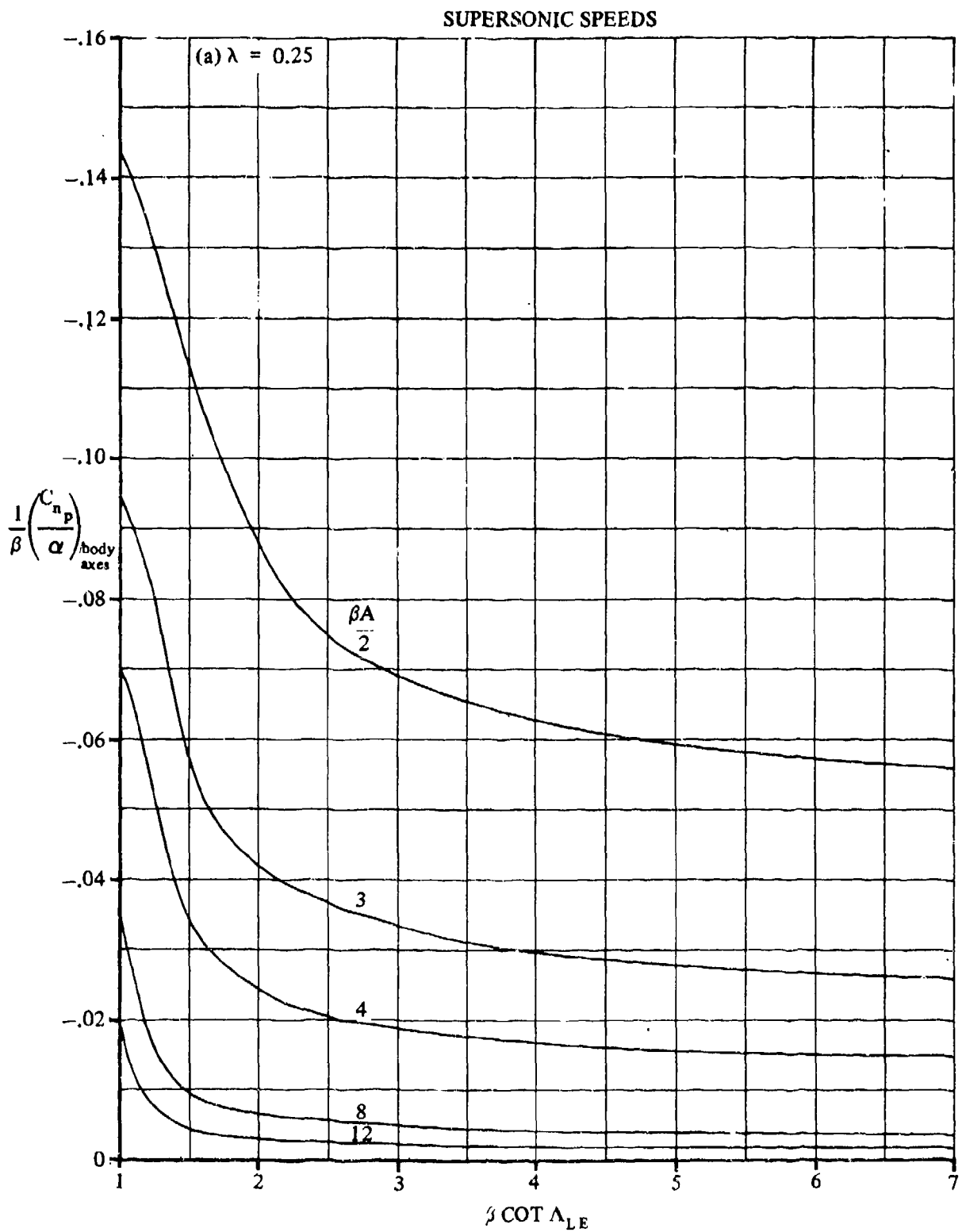


FIGURE 7.1.2.3-17 YAWING MOMENT DUE TO ROLLING – SUPersonic LEADING EDGES – BODY AXES

SUPersonic SPEEDS

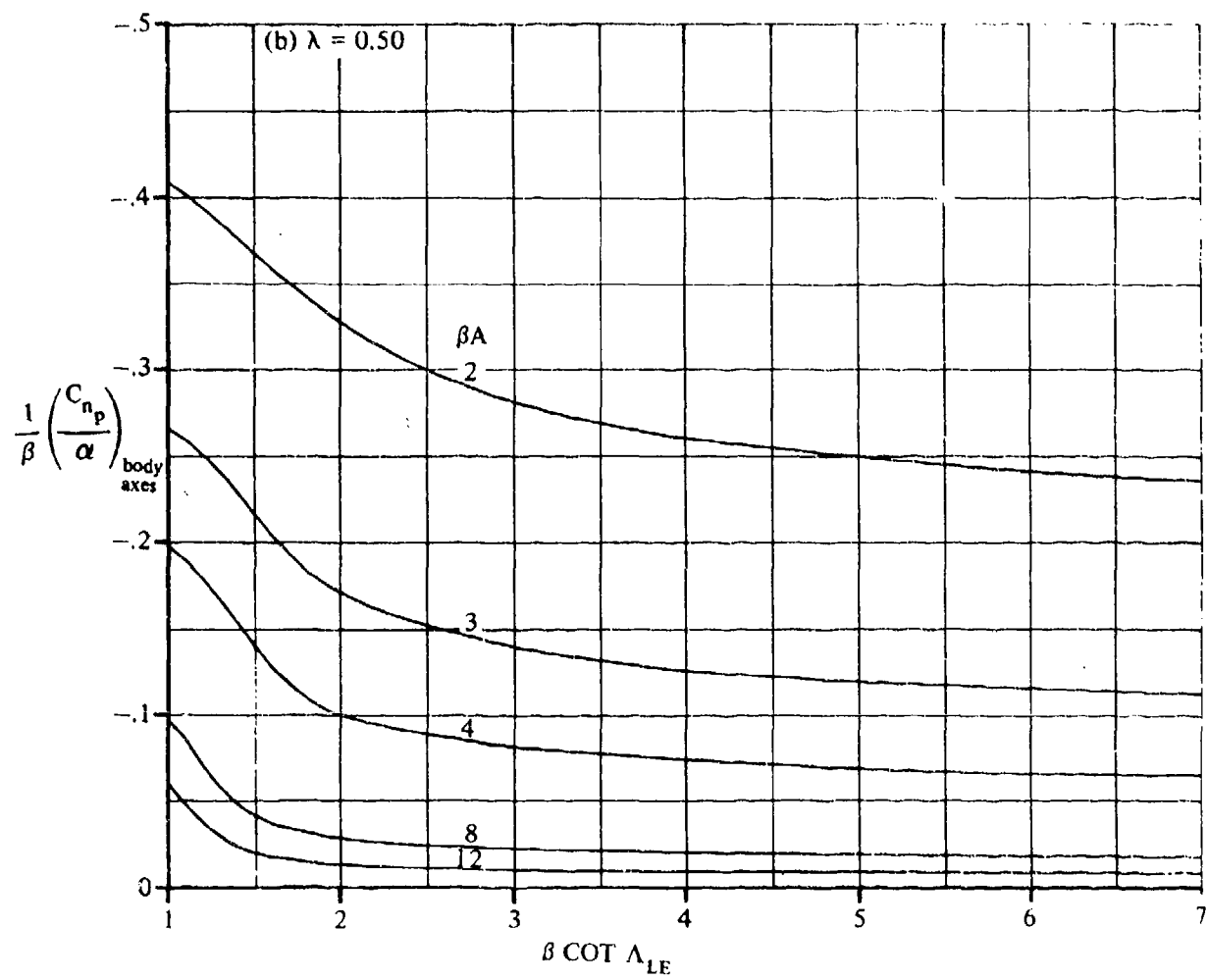


FIGURE 7.1.2.3-17 (CONTD)

SUPersonic SPEEDS

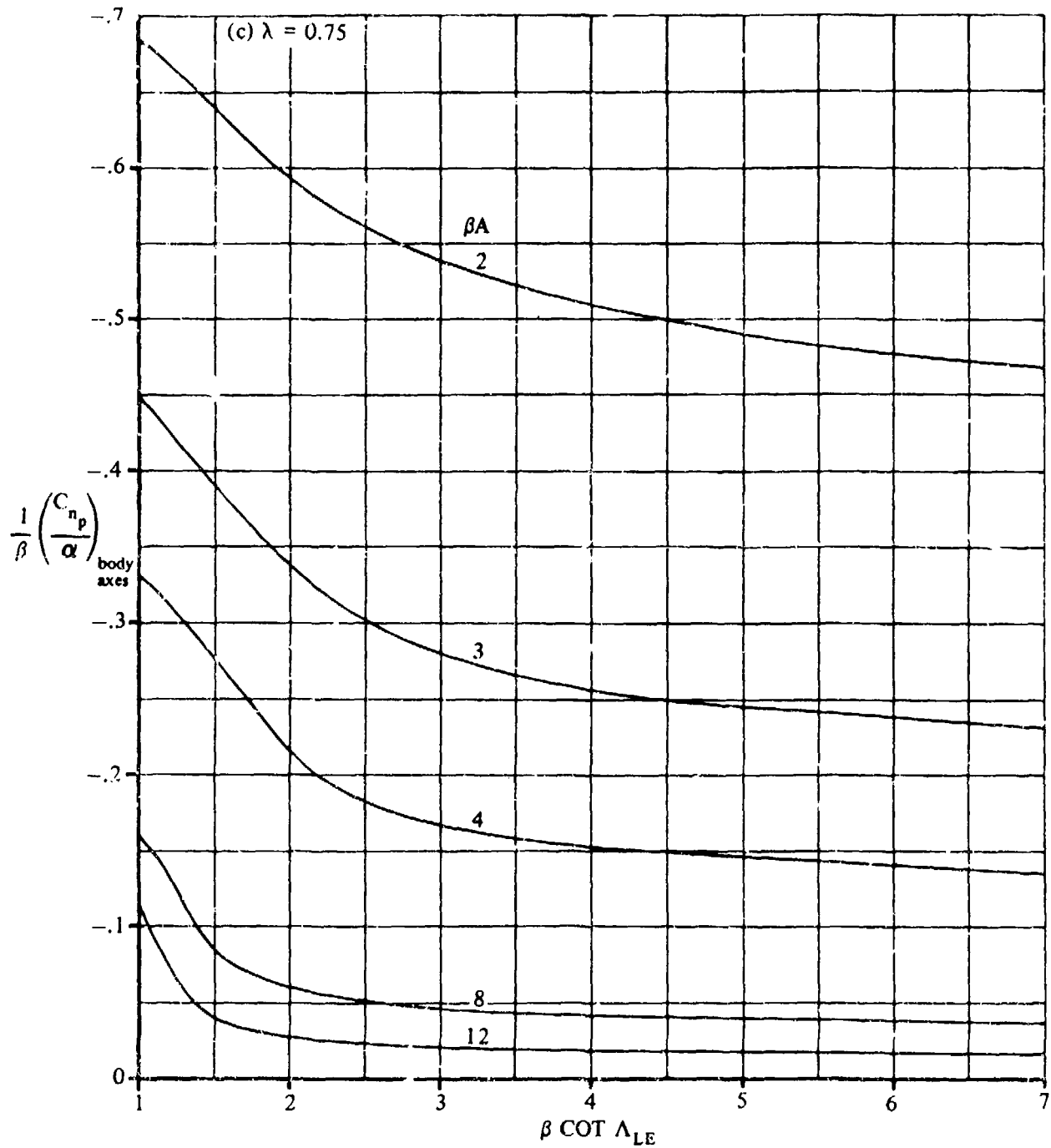


FIGURE 7.1.2.3-17 (CONTD)

SUPersonic SPEEDS

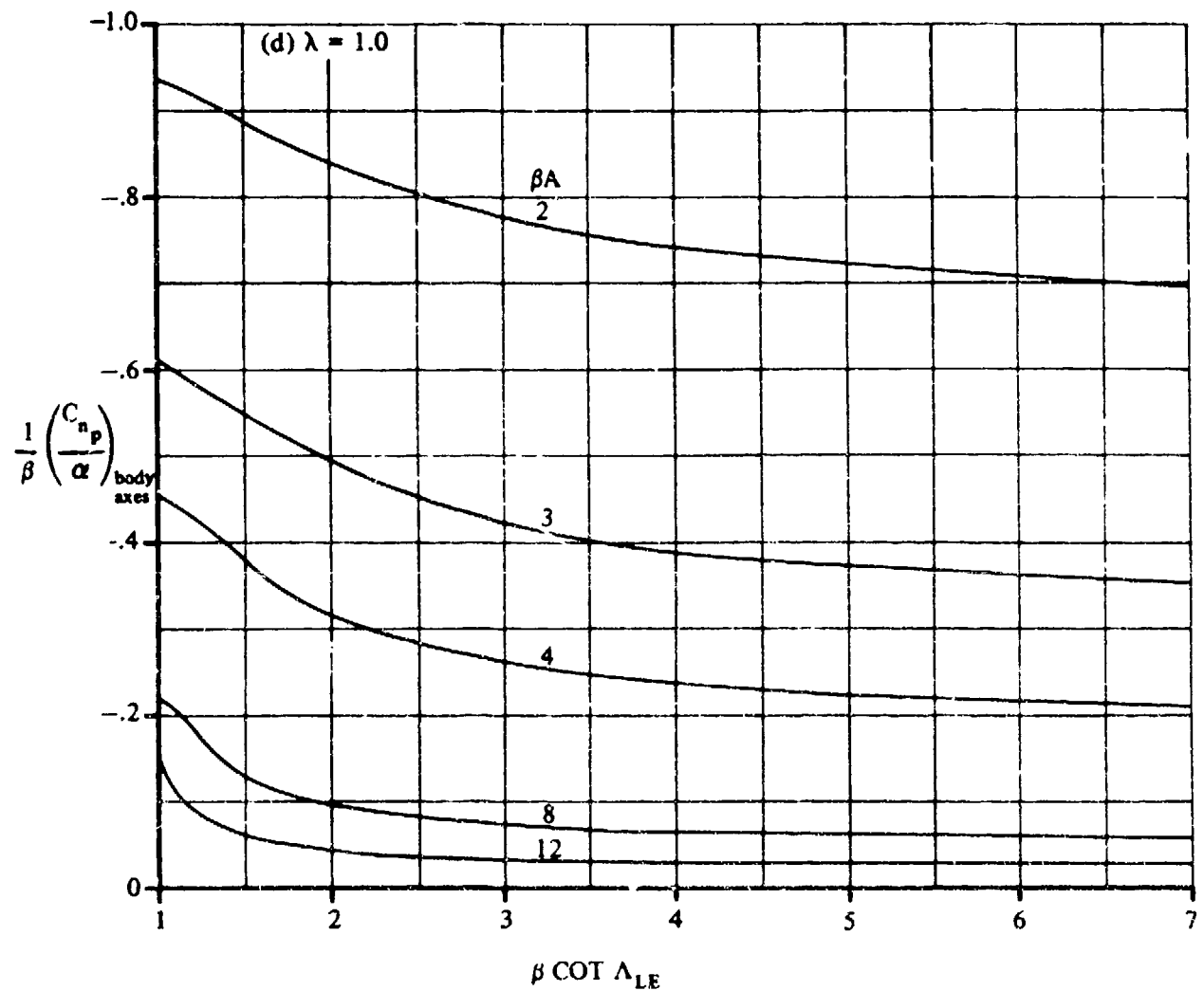


FIGURE 7.1.2.8-17 (CONTD)

7.1.3 WING YAWING DERIVATIVES

7.1.3.1 WING YAWING DERIVATIVE C_{Y_r}

This section recommends methods for estimating the wing contribution to the yawing derivative C_{Y_r} at subsonic and supersonic speeds. However, at subsonic, transonic, and supersonic speeds no generalized methods are available for estimating the wing contribution to C_{Y_r} . This derivative is the change in side-force coefficient with variation in yawing velocity and is expressed as

$$C_{Y_r} = \frac{\partial C_Y}{\partial \left(\frac{rb}{2V_\infty} \right)}$$

A. SUBSONIC

The wing contribution to C_{Y_r} is best evaluated from available experimental data (see table 7-A and references 1, 2, 3, and 4), since no generalized method is available in the literature. However, a method is available in reference 1 for wings with a taper ratio of one and moderate sweep at low subsonic speeds. The range and accuracy of this method are limited and generally inadequate for making reliable estimates of the wing contribution.

Since the wing contribution to C_{Y_r} is usually quite small in comparison to the vertical-tail contribution, it is sometimes neglected.

B. TRANSONIC

No generalized method is available in the literature for estimating transonic values of the wing contribution to the yawing derivative C_{Y_r} . Furthermore, there is a scarcity of experimental data for this derivative at transonic speeds.

C. SUPERSONIC

No generalized method is available in the literature for estimating supersonic values of the wing contribution to the yawing derivative C_{Y_r} . A few theoretical methods are available for specific configurations (see table 7-A). Although the use of experimental data for a similar configuration is preferable to theoretical methods, experimental data are so scarce that the use of the limited theoretical methods becomes the only alternative for most configurations.

REFERENCES

1. Toll, T. A., and Queijo, M. J.: Approximate Relations and Charts for Low-Speed Stability Derivatives of Swept Wings. NACA TN 1581, 1948. (U)

2. Queijo, M. J., and Jaquet, B. M.: Investigation of Effects of Geometric Dihedral on Low-Speed Static Stability and Yawing Characteristics of an Untapered 45° Sweepback-Wing Model of Aspect Ratio 2.61. NACA TN 1668, 1948. (U)
3. Goodman, A., and Brewer, J. D.: Investigation at Low Speeds of the Effect of Aspect Ratio and Sweep on Static and Yawing Stability Derivatives of Untapered Wings. NACA TN 1689, 1948. (U)
4. Letko, W., and Cowan, J. W.: Effect of Taper Ratio on Low-Speed Static and Yawing Stability Derivatives of 45° Sweepback Wings with Aspect Ratio of 2.61. NACA TN 1671, 1948. (U)

7.1.3.2 WING YAWING DERIVATIVE C_{l_r}

This section presents a method for estimating the wing contribution to the yawing derivative C_{l_r} at subsonic speeds. No generalized methods are available for estimating C_{l_r} at transonic and supersonic speeds; however, theoretical methods for determining this derivative at supersonic speeds for special classes of wing planforms are discussed. This derivative is the change in rolling-moment coefficient with change in the yawing-velocity parameter and is expressed as

$$C_{l_r} = \frac{\partial C_l}{\partial \left(\frac{rb}{2V_\infty} \right)}$$

A. SUBSONIC

The wing yawing derivative C_{l_r} results from the lift differential between the wing panels when the vehicle is yawed about its vertical axis.

Over the range of lift coefficients for which C_{l_r} is linear with C_L , the derivative C_{l_r} for wings without geometric dihedral, twist, or flaps is based on the lifting-line theory of reference 1 for aspect ratios greater than three and on the experimental data of references 2 and 3 for aspect ratios less than three. The increment in C_{l_r} due to geometric dihedral is taken from reference 4. The effects of symmetric flap deflection and wing twist are taken from reference 1.

In addition to the increments in C_{l_r} due to dihedral, twist, and flaps, an additional increment in C_{l_r} arises due to C_{Y_r} if the center of gravity does not lie at the same height as the quarter-chord point of the wing MAC. This contribution is obtained from the expression

$$(\Delta C_{l_r})_{\text{side force}} = -C_{Y_r} \frac{z}{b}$$

where z is the vertical distance between the center of gravity and the quarter-chord point of the wing MAC, positive for the c.g. above $\bar{c}/4$. The side force due to yawing C_{Y_r} is small except at high angles of attack. Therefore, this increment in C_{l_r} is omitted from the Datcom method.

The fore and aft movement of the center of gravity also affects C_{l_r} , but this effect is neglected because of the questionable accuracy of the basic effect of wing sweep.

The method of reference 5 is applied to extrapolate the potential-flow value of C_{l_r} to higher lift coefficients. The method is semiempirical in that it requires test values to determine the correction factors to be applied to the theory. Analysis of experimental data shows that the discrepancies between theoretical and experimental values of C_{l_r} for wings are similar to the discrepancies between theoretical and experimental values of the static derivative C_{l_0} . Based on this analysis, a correction factor is applied in reference 5, which is the incremental value of C_{l_r} obtained by subtracting the experimental value from the theoretical value.

Experimental data indicate that for unswept wings C_{l_r} is nearly proportional to the lift coefficient until maximum lift occurs. For sweptback wings, a linear variation is obtained over only a limited lift range, which is reduced as sweep increases. At high lift coefficients C_{l_r} decreases, and for sweptback wings may become negative near maximum lift.

If reliable values of the rolling moment due to sideslip C_{β} are available, the method should provide results within ± 20 -percent accuracy over the lift-coefficient range for which C_{l_r} is approximately linear with C_L .

DATCOM METHOD

The variation of the wing yawing derivative C_{l_r} with lift coefficient, based on the product of the wing area and the square of the wing span $S_w b_w^2$, is given by

$$C_{l_r} = C_L \left(\frac{C_{l_r}}{C_L} \right)_{\substack{C_L=0 \\ M}} + (\Delta C_{l_r})_{C_L} + \left(\frac{\Delta C_{l_r}}{\Gamma} \right) \Gamma + \left(\frac{\Delta C_{l_r}}{\theta} \right) \theta + \left[\frac{\Delta C_{l_r}}{\left(\frac{\partial \alpha}{\partial \delta} \right)_f \delta_f} \right] \left(\frac{\partial \alpha}{\partial \delta} \right)_f \delta_f \quad (per \ radian) \quad 7.1.3.2-a$$

where

$$\left(\frac{C_{l_r}}{C_L} \right)_{\substack{C_L=0 \\ M}} \quad \text{is the slope of the rolling moment due to yawing at zero lift given by}$$

$$\left(\frac{C_{l_r}}{C_L} \right)_{\substack{C_L=0 \\ M}} = \frac{1 + \frac{A(1 - B^2)}{2B(AB + 2 \cos \Lambda_{c/4})} + \frac{AB + 2 \cos \Lambda_{c/4}}{AB + 4 \cos \Lambda_{c/4}} \frac{\tan^2 \Lambda_{c/4}}{8}}{1 + \frac{A + 2 \cos \Lambda_{c/4}}{A + 4 \cos \Lambda_{c/4}} \frac{\tan^2 \Lambda_{c/4}}{8}} \left(\frac{C_{l_r}}{C_L} \right)_{\substack{C_L=0 \\ M=0}} \quad 7.1.3.2-b$$

where $B = \sqrt{1 - M^2 \cos^2 \Lambda_{c/4}}$ and

$$\left(\frac{C_{l_r}}{C_L} \right)_{\substack{C_L=0 \\ M=0}} \quad \text{is the slope of the low-speed rolling moment due to yawing at zero lift, obtained from figure 7.1.3.2-10 as a function of aspect ratio, sweep of the quarter-chord, and taper ratio. This chart has been derived by using the results of references 1, 2, and 3. Equation 7.1.3.2-b modifies the low-speed value by means of the Prandtl-Glauert rule to yield approximate corrections for the first-order three-dimensional effects of compressible flow up to the critical Mach number.}$$

C_L is the wing lift coefficient.

$(\Delta C_{I_r})_{C_L}$ is a semiempirical correction factor used to extrapolate the potential-flow values of C_{I_r} to higher lift coefficients. This parameter is given by

$$(\Delta C_{I_r})_{C_L} = C_L \left(\frac{C_{I_\beta}}{C_L} \right) - (C_{I_\beta})_{\text{test}} \quad (\text{per radian}) \quad 7.1.3.2-c$$

where

$\frac{C_{I_\beta}}{C_L}$ is the theoretical value of the slope of the rolling moment due to sideslip at zero lift obtained by using the method of paragraph A of Section 5.1.2.1, neglecting the effects of twist and dihedral. In applying this method the compressibility correction to the sweep contribution should be considered.

$(C_{I_\beta})_{\text{test}}$ is the experimental value of the rolling moment due to sideslip at the appropriate Mach number.

$\frac{\Delta C_{I_r}}{\Gamma}$ is the increment in C_{I_r} due to dihedral, given by

$$\frac{\Delta C_{I_r}}{\Gamma} = \frac{1}{12} \frac{\pi A \sin \Lambda_{c/4}}{A + 4 \cos \Lambda_{c/4}} \quad (\text{per radian}^2) \quad 7.1.3.2-d$$

Γ is the geometric dihedral angle in radians, positive for the wing tip above the plane of the root chord.

$\frac{\Delta C_{I_r}}{\theta}$ is the increment in C_{I_r} due to wing twist obtained from figure 7.1.3.2-11.

θ is the wing twist between the root and tip sections in degrees, negative for washout (see figure 7.1.3.2-11).

$\frac{\Delta C_{I_r}}{\left(\frac{\partial \alpha}{\partial \delta} \right)_f \delta_f}$ is the effect of symmetric flap deflection obtained from figure 7.1.3.2-12.

δ_f is the streamwise flap deflection in degrees.

$\left(\frac{\partial \alpha}{\partial \delta}\right)_f$ is the two-dimensional lift-effectiveness parameter α_δ obtained from Section 6.1.1.1.

The expression given for the effect of dihedral (equation 7.1.3.2-d) is based on an extension of the simple-sweep theory of reference 6. It has been shown by comparison with test data that the increment in C_{l_r} due to dihedral is underestimated by equation 7.1.3.2-d. However, it has not been possible to improve upon the simple-sweep-theory result because of a lack of experimental data.

Furthermore, not enough data are available to examine the validity of the lifting-line-theory results presented for the increments in C_{l_r} due to either twist or flap deflection.

A comparison of the slope of the rolling moment due to yawing at zero lift, obtained by using figure 7.1.3.2-10, with test results is presented as table 7.1.3.2-A.

The sample problem illustrates the application of the method over the lift-coefficient range to the stall.

Sample Problem

Given: The sweptback, untapered wing of reference 4.

Wing Characteristics:

$$A = 2.61 \quad \lambda = 1.0 \quad \Lambda_{c/4} = 45^\circ \quad \Lambda_{c/2} = 45^\circ \quad \Gamma = 10^\circ \quad \theta = 0$$

Additional Characteristics:

Low speed; $M \approx 0$

The following test values from reference 4:

C_L	0	.1	.2	.3	.4	.5	.6	.7	.8	.9	1.0	1.1
C_{l_r} (per rad)	-0.0458	-0.1031	-0.140	-0.176	-0.206	-0.235	-0.260	-0.274	-0.260	-0.211	-0.102	0.0287

Compute:

$$\left(\frac{C_{l_r}}{C_L} \right)_{\substack{C_L=0 \\ M=0}} = 0.419 \text{ per rad (figure 7.1.3.2-10)}$$

Determine the theoretical value of C_{I_β}/C_L (Section 5.1.2.1)

$$\left(\frac{C_{I_\beta}}{C_L} \right)_{\Lambda_{c/2}} = -0.0038 \text{ per deg} \quad (\text{figure 5.1.2.1-27})$$

$$\left(\frac{C_{I_\beta}}{C_L} \right)_A = -0.0044 \text{ per deg} \quad (\text{figure 5.1.2.1-28b})$$

$$K_{M_A} = 1.0 \quad (\text{figure 5.1.2.1-28a for } M \approx 0)$$

$$C_{I_\beta} = C_L \left[\left(\frac{C_{I_\beta}}{C_L} \right)_{\Lambda_{c/2}} K_{M_A} + \left(\frac{C_{I_\beta}}{C_L} \right)_A \right] + \Gamma \left(\frac{C_{I_\beta}}{\Gamma} K_{M_\Gamma} \right) + \theta \tan \Lambda_{c/4} \frac{\Delta C_{I_\beta}}{\theta \tan \Lambda_{c/4}}$$

(equation 5.1.2.1-a)

Neglecting the effects of twist and dihedral

$$\begin{aligned} \frac{C_{I_\beta}}{C_L} &= \left[\left(\frac{C_{I_\beta}}{C_L} \right)_{\Lambda_{c/2}} K_{M_A} + \left(\frac{C_{I_\beta}}{C_L} \right)_A \right] \\ &= (-0.0038)(1.0) + (-0.0044) \\ &= -0.0082 \text{ per deg} \\ &= -0.470 \text{ per rad} \end{aligned}$$

$$(\Delta C_{I_r})_{C_L} = C_L \left(\frac{C_{I_\beta}}{C_L} \right) - (C_{I_\beta})_{\text{test}} \quad (\text{equation 7.1.3.2-c})$$

$$= C_L (-0.470) - (C_{I_\beta})_{\text{test}} \quad (\text{see calculation table})$$

$$\frac{\Delta C_{l_r}}{\Gamma} = \frac{1}{12} \frac{\pi A \sin \Lambda_c/4}{A + 4 \cos \Lambda_c/4} \quad (\text{equation 7.1.3.2-d})$$

$$= \frac{1}{12} \frac{\pi(2.61) (\sin 45^\circ)}{2.61 + 4 \cos 45^\circ} = \frac{1}{12} \frac{\pi(2.61) (0.7071)}{2.61 + 4(0.7071)}$$

$$= 0.0884 \text{ per rad}^2$$

Solution:

$$C_{l_r} = C_L \left(\frac{C_{l_r}}{C_L} \right)_{\substack{C_L=0 \\ M=0}} + (\Delta C_{l_r})_{C_L} + \left(\frac{\Delta C_{l_r}}{\Gamma} \right) \Gamma \quad (\text{equation 7.1.3.2-a})$$

$$= C_L (0.419) + [C_L (-0.470) - C_{l_\beta \text{ test}}] + (0.0884) \frac{10}{57.3}$$

$$= 0.419 C_L + [-0.470 C_L - C_{l_\beta \text{ test}}] + 0.0154$$

①

②

③

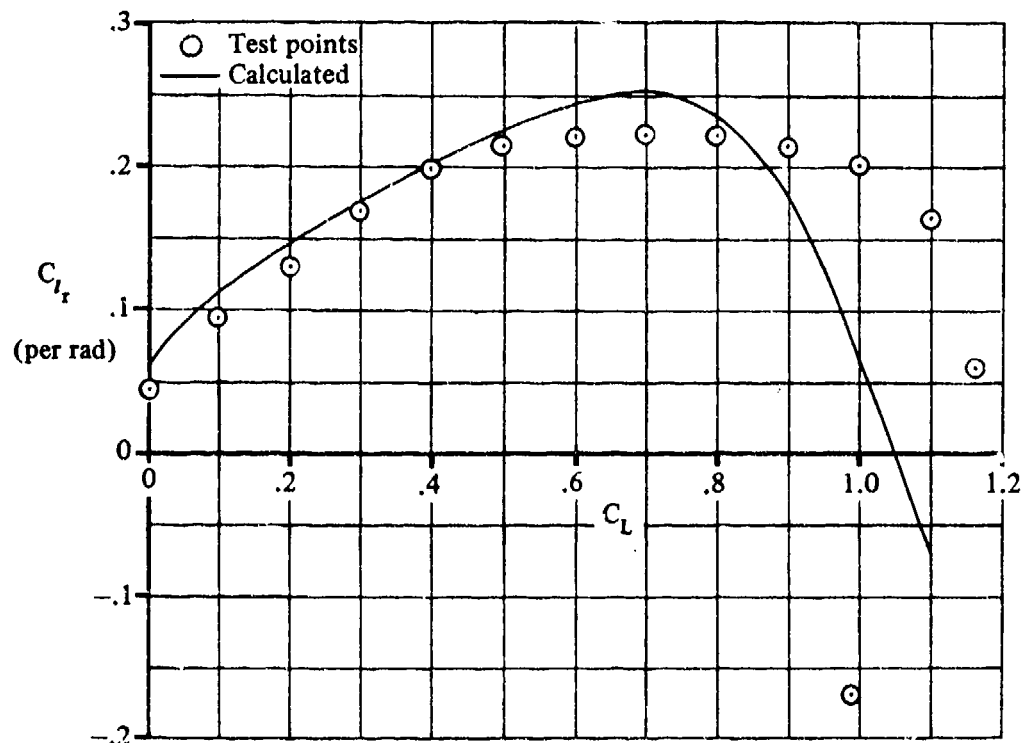
④

⑤

⑥

C_L	$C_{l_\beta \text{ (test)}}$ (per rad)	$\left(\frac{C_{l_r}}{C_L} \right)_{\substack{C_L=0 \\ M=0}}$ 0.419 ①	$\left(\frac{C_{l_\beta}}{C_L} \right) C_L$ -0.470 ①	$(\Delta C_{l_r})_{C_L}$ (eq. 7.1.3.2-c) ④ - ② (per rad)	C_{l_r} (based on $S_W b_W^2$) (eq. 7.1.3.2-a) ③ + ⑤ + 0.0154 (per rad)
0	-0.0458	0	0	.0458	.0612
.1	-0.1031	.0419	-0.0470	0.0561	0.1134
.2	-0.1400	.0838	-0.0940	0.0460	0.1452
.3	-0.1760	.1257	-0.1410	0.0360	0.1761
.4	-0.2060	.1676	-0.1880	0.0180	0.2010
.5	-0.2350	.2095	-0.2350	0	0.2249
.6	-0.2600	.2514	-0.2820	-0.0220	0.2448
.7	-0.2740	.2933	-0.3290	-0.0650	0.2537
.8	-0.2600	.3352	-0.3760	-0.1160	0.2346
.9	-0.2110	.3771	-0.4230	-0.2120	0.1805
1.0	-0.1020	.4190	-0.4700	-0.3680	0.0664
1.1	0287	.4609	-0.5170	-0.5457	-0.0694

The calculated results are compared with test values from reference 4 in sketch (a).



SKETCH (a)

B. TRANSONIC

In the transonic speed régime no theoretical methods are available for estimating the wing yawing derivative C_{I_r} . Furthermore, no known experimental results are available for this derivative at transonic speeds.

C. SUPERSONIC

No general method is available for evaluating the wing contribution to the yawing derivative C_{I_r} at supersonic speeds. However, methods are presented in references 7, 8, and 9 for evaluating C_{I_r} for special classes of wing planforms. The results presented in these references are based on supersonic linear theory. The methods are restricted to estimating C_{I_r} over a limited range of Mach numbers for zero-thickness wings with no dihedral. Furthermore, the methods are considered tentative, since the spanwise variation of Mach number in the case of yawing has been neglected.

REFERENCES

1. Pinsker, W.: The Aerodynamic Coefficients of Free Lateral Motion. DVL UM 1144/1 and UM 1144/2, 1943. (U)
2. Goodman, A., and Brewer, J. D.: Investigation at Low Speeds of the Effect of Aspect Ratio and Sweep on Static and Yawing Stability Derivatives of Untapered Wings. NACA TN 1669, 1948. (U)
3. Letko, W., and Cowan, J. W.: Effect of Taper Ratio on Low-Speed Static and Yawing Stability Derivatives of 45° Sweptback Wings With Aspect Ratio of 2.61. NACA TN 1671, 1948. (U)
4. Queijo, M. J., and Jaquet, B. M.: Investigation of Effects of Geometric Dihedral on Low-Speed Static Stability and Yawing Characteristics of an Untapered 45° Sweptback-Wing Model of Aspect Ratio 2.61. NACA TN 1668, 1948. (U)
5. Campbell, J. P., and Goodman, A.: A Semiempirical Method for Estimating the Rolling Moment Due to Yawing of Airplanes. NACA TN 1984, 1949. (U)
6. Toll, T. A., and Queijo, M. J.: Approximate Relations and Charts for Low-Speed Stability Derivatives of Swept Wings. NACA TN 1581, 1948. (U)
7. Ribner, H. S., and Malvestuto, F. S., Jr.: Stability Derivatives of Triangular Wings at Supersonic Speeds. NACA TR 908, 1948. (U)
8. Harmon, S. M.: Stability Derivatives at Supersonic Speeds of Thin Rectangular Wings With Diagonals Ahead of Tip Mach Lines. NACA TR 925, 1949. (U)
9. Malvestuto, F. S., Jr., and Margolis, K.: Theoretical Stability Derivatives of Thin Sweptback Wings Tapered to a Point With Sweptback or Sweptforward Trailing Edges for a Limited Range of Supersonic Speeds. NACA TR 971, 1950. (U)
10. Lichtenstein, J. H.: Effect of High-Lift Devices on the Low-Speed Static Lateral and Yawing Stability Characteristics of an Untapered 45° Sweptback Wing. NACA TN 2689, 1952. (U)
11. Letko, W.: Effect of Vertical-Tail Area and Length on the Yawing Stability Characteristics of a Model Having a 45° Sweptback Wing. NACA TN 2358, 1951. (U)
12. Williams, J. L.: Measured and Estimated Lateral Static and Rotary Derivatives of a 1/12-Scale Model of a High-Speed Fighter Airplane with Unswept Wings. NACA RM L53K09, 1954. (U)
13. Goodman, A., and Feigenbaum, D.: Preliminary Investigation at Low Speeds of Swept Wings in Yawing Flow. NACA RM L7109, 1948. (U)
14. Letko, W., and Jaquet, B. M.: Effect of Airfoil Profile of Symmetrical Sections on the Low-Speed Static-Stability and Yawing Derivatives of 45° Sweptback Wing Models of Aspect Ratio 2.61. NACA RM L8H10, 1948. (U)
15. Bird, J. D., Jaquet, B. M., and Cowan, J. W.: Effect of Fuselage and Tail Surfaces on Low-Speed Yawing Characteristics of a Swept-Wing Model as Determined in Curved-Flow Test Section of Langley Stability Tunnel. NACA TN 2483, 1951. (U)
16. Jaquet, B. M., and Fletcher, H. S.: Experimental Steady-State Yawing Derivatives of a 60° Delta-Wing Model as Affected by Changes in Vertical Position of the Wing and in Ratio of Fuselage Diameter to Wing Span. NACA TN 3843, 1956. (U)

TABLE 7.1.3.2-A
SUBSONIC WING ROLLING MOMENT DUE TO YAWING
DATA SUMMARY

Ref.	A	λ	$\Delta_c/4$ (deg)	C_l/C_L Calc. (per rad)	C_l/C_L Test (per rad)	ϵ Percent Error
10	2.61	1.0	45.0	0.419	0.415	1.0
11	4.00	0.80	45.0	0.413	0.396	4.3
12	5.90	0.473	-3.6	0.240	0.225	6.7
13	1.34	1.0	60.0	0.445	0.470	-5.3
	↓	5.16	1.0	0	0.280	18.2
2	1.34	1.0	0	0.195	0.161	21.1
	↑		45.0	0.363	0.350	0.9
	2.61		0	0.230	0.260	-11.5
	↑		60.0	0.526	0.558	-5.9
	5.16		45.0	0.475	0.480	-1.0
	↓		60.0	0.596	0.550	8.4
6	2.61	0.50	45.0	0.365	0.300	21.7
	↑	0.25	45.0	0.302	0.315	-4.1
	2.31	0	52.2	0.295	0.285	3.5

$$\text{Average Error} = \frac{\sum |\epsilon|}{n} = 8.1\%$$

SUBSONIC SPEEDS

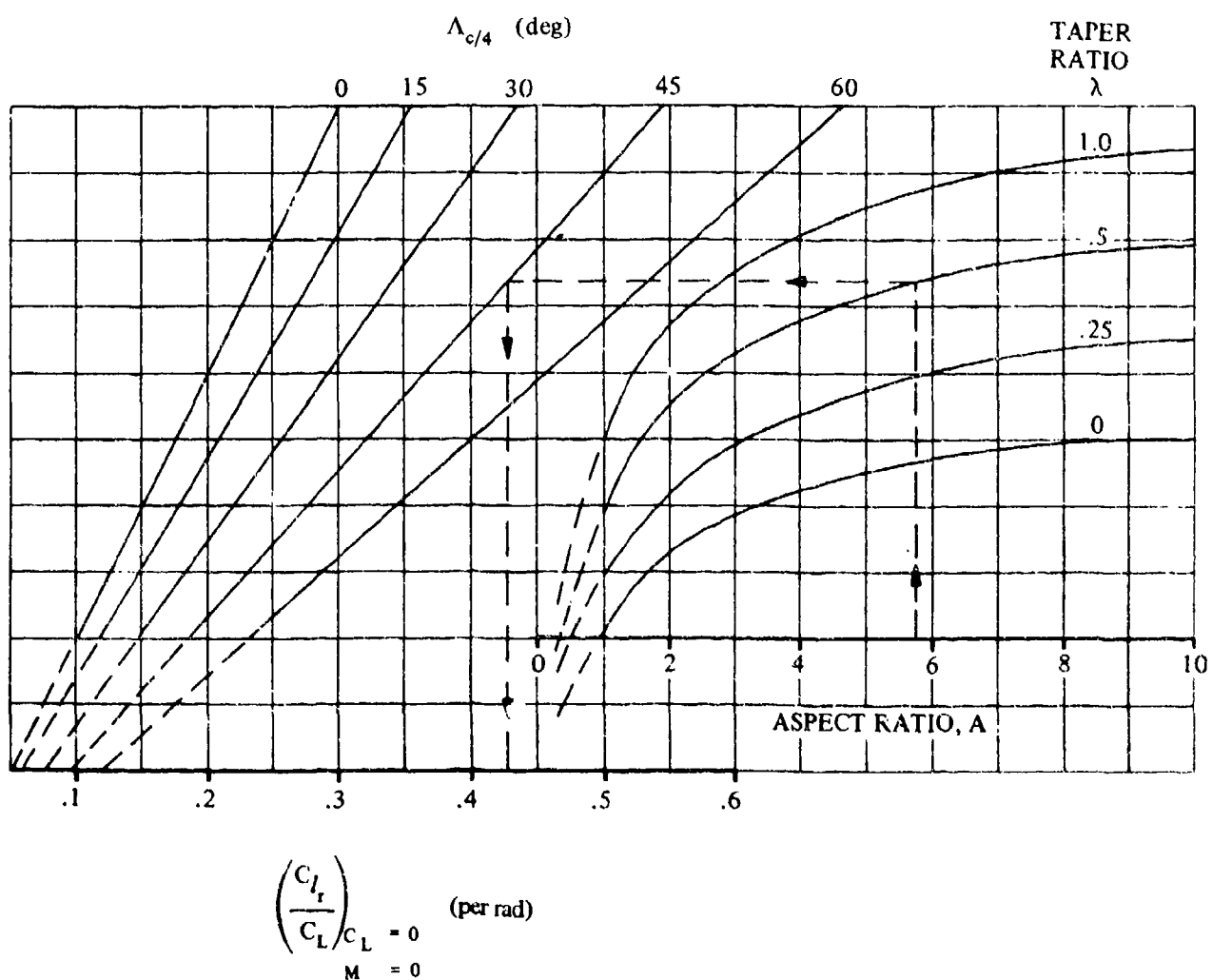


FIGURE 7.1.3.2-10 WING YAWING DERIVATIVE C_{l_r}

SUBSONIC SPEEDS

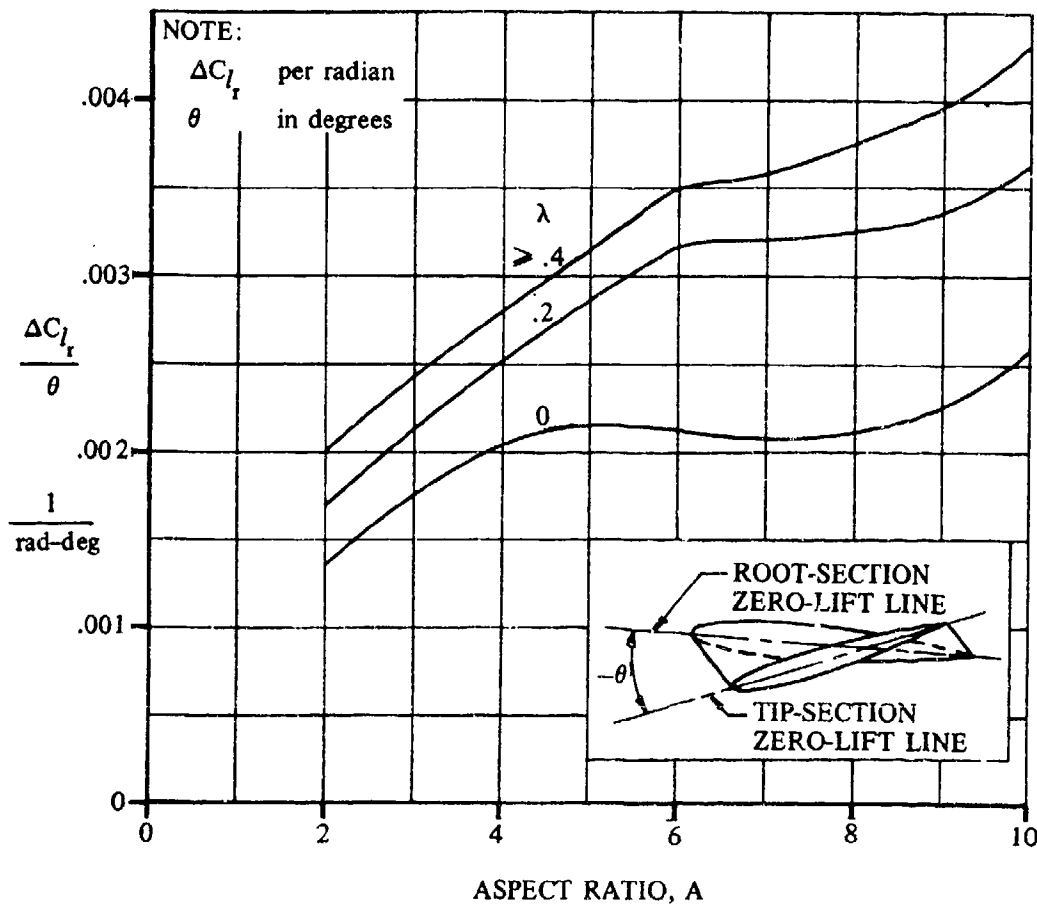
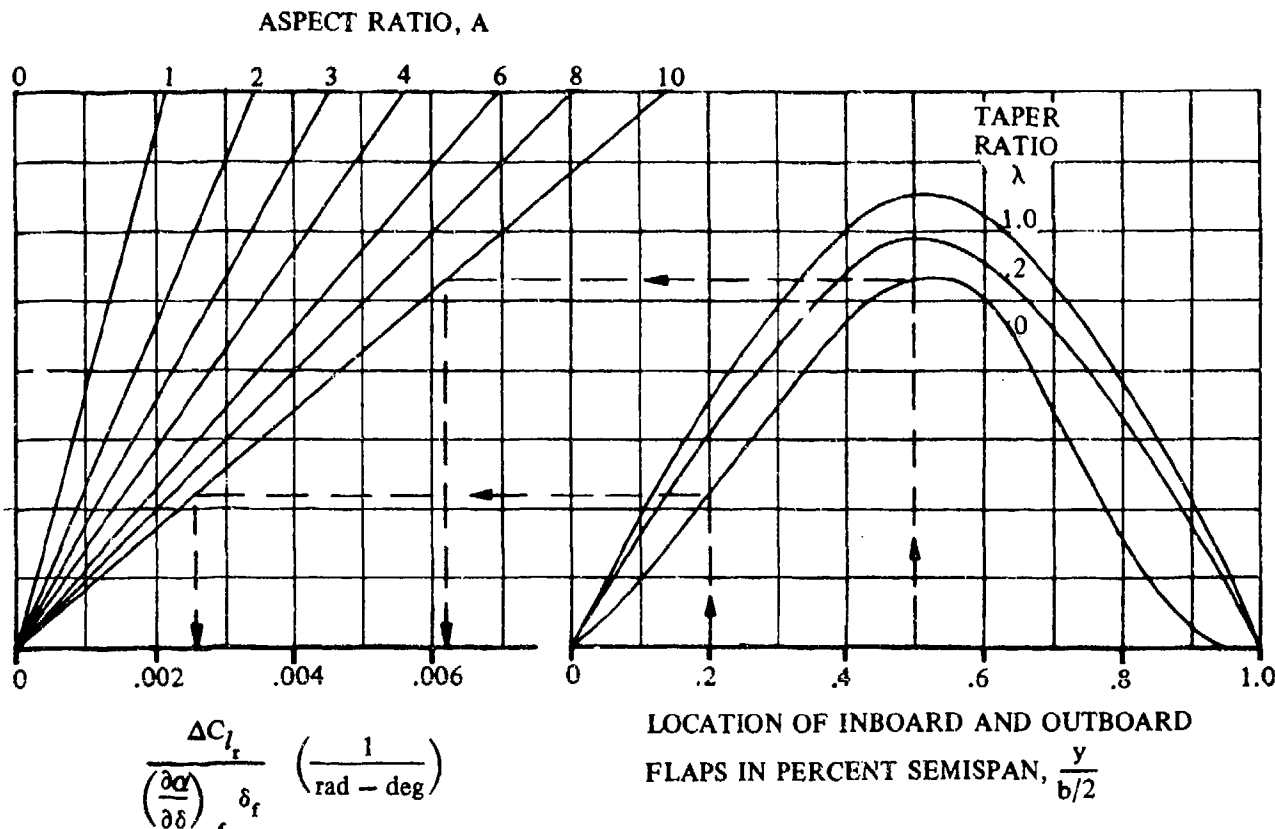


FIGURE 7.1.3.2-11 EFFECT OF WING TWIST ON WING YAWING DERIVATIVE C_{l_r}

SUBSONIC SPEEDS



NOTE:

ΔC_{L_f} per radian

δ_f in degrees

NOTE:
$$\frac{\Delta C_{L_f}}{\left(\frac{\partial \alpha}{\partial \delta}\right)_f \delta_f} = \left[\frac{\Delta C_{L_f}}{\left(\frac{\partial \alpha}{\partial \delta}\right)_f \delta_f} \right]_{\text{outboard}} - \left[\frac{\Delta C_{L_f}}{\left(\frac{\partial \alpha}{\partial \delta}\right)_f \delta_f} \right]_{\text{inboard}}$$

FIGURE 7.1.3.2-12 EFFECT OF FLAPS ON C_{L_f}

7.1.3.3 WING YAWING DERIVATIVE C_{n_r}

This section presents a method for estimating the wing contribution to the yawing derivative C_{n_r} at subsonic speeds. No generalized methods are available for estimating C_{n_r} at transonic and supersonic speeds; however, theoretical methods for determining this derivative at supersonic speeds for special classes of wing planforms are discussed. This derivative is the change in yawing-moment coefficient with change in the yawing-velocity parameter. It is commonly referred to as the yaw damping and is expressed as

$$C_{n_r} = \frac{\partial C_n}{\partial \left(\frac{rb}{2V_\infty} \right)}$$

A. SUBSONIC

The wing yawing derivative C_{n_r} is due to the antisymmetrical lift and drag distributions over the wing resulting from the yawing velocity.

The wing contribution to the yaw damping in the range of lift coefficients for which C_{n_r} varies linearly with C_L is composed of two major contributions; namely, that resulting from the drag due to lift and that resulting from the profile drag. The contribution resulting from the drag due to lift is given to a first approximation by the simple-sweep-theory result of reference 1. It is a negative quantity except for highly swept wings in which case it can become positive.

The increment in C_{n_r} due to profile drag is also taken from reference 1. Although the spanwise distribution of profile drag is required for an accurate determination of the effect of profile drag on C_{n_r} , the profile drag has been assumed constant over the wing surface in the analysis reported in reference 1. This approximation greatly simplifies the analysis, since it allows the profile-drag effect to be expressed as a function of only the wing geometry.

Flaps and wing twist will also induce increments in C_{n_r} , primarily as a result of their influencing the lift distribution across the span. However, the technique of the superposition of lift distribution proportional to angle of attack, which was used to determine the effects of either flaps and/or twist on the rotary derivatives C_{n_p} and C_{l_r} , cannot be applied in this case. The contribution of the drag-due-to-lift component to C_{n_r} increases as the square of the angle of attack. Therefore, a breakdown of the lift distribution proportional to angle of attack is not possible. No methods are available in the literature for estimating the effects of flaps or wing twist on the wing contribution to C_{n_r} . Furthermore, not enough test data are available to allow derivation of an empirical method.

The wing side force due to yawing C_Y will also produce a yawing moment when the center of gravity does not lie at the same longitudinal station as the quarter-chord of the wing MAC. However, the side force due to yawing is small except at high angles of attack; consequently, this increment in C_{n_r} is omitted from the Datcom.

Experimental data indicate that for unswept wings the yaw damping is nearly proportional to the lift coefficient until maximum lift occurs. On the other hand, for sweptback wings linear variations of C_{n_r} are obtained over only a limited lift coefficient range, which is reduced as sweep and/or aspect ratio increase. Experimental data also show that, in general, the yaw damping of a sweptback wing

changes sign and becomes positive at some moderate lift coefficient. The lift coefficient at which this change in sign occurs is reduced as wing sweep and/or aspect ratio increase.

Results obtained by using the Datcom method agree reasonably well with test data over the range of lift coefficients for which C_{n_r} varies linearly with C_L .

Since the wing contribution to the total C_{n_r} of the airplane is small, no method has been developed to account for the effects of compressibility. For the purpose of the Datcom the effects of compressibility are accounted for by evaluating the wing profile-drag coefficient at the desired Mach number.

Experimental data show that the effect of wing dihedral on the yaw damping is negligible.

Because of the insignificance of the wing contribution to the total yaw damping and the approximate nature of the Datcom method, the method is applicable to wings with twist and/or symmetric flap deflection as well as to plain wings.

DATCOM METHOD

The variation of the wing yawing derivative C_{n_r} with lift coefficient at subsonic speeds, based on the product of the wing area and the square of the wing span $S_W b_W^2$, is given by

$$C_{n_r} = \left(\frac{C_{n_r}}{C_L^2} \right) C_L^2 + \left(\frac{C_{n_r}}{C_{D_0}} \right) C_{D_0} \quad (\text{per radian}) \quad 7.1.3.3-a$$

where

C_L is the wing lift coefficient.

$\frac{C_{n_r}}{C_L^2}$ is the low-speed drag-due-to-lift yaw-damp. parameter obtained from figure 7.1.3.3-6 as a function of wing aspect ratio, taper ratio, sweepback, and c.g. position.

$\frac{C_{n_r}}{C_{D_0}}$ is the low-speed profile-drag yaw-damping parameter obtained from figure 7.1.3.3-7 as a function of the wing aspect ratio, sweep-back, and c.g. position.

C_{D_0} is the wing profile drag coefficient evaluated at the appropriate Mach number. For this application C_{D_0} is assumed to be the profile drag associated with the theoretical ideal drag due to lift and is given by

$$C_{D_0} = C_D - \frac{C_L^2}{\pi A}$$

where C_D is the total drag coefficient at a given lift coefficient, obtained from experimental data.

Sample Problem

Given: The delta-wing model of references 5 and 6.

Wing Characteristics:

$$A = 2.31 \quad \lambda = 0 \quad \Lambda_{c/4} = 52.4^\circ \quad \theta = 0$$

$$\bar{x}/\bar{c} = 0 \text{ (c.g. at } \bar{c}/4)$$

Additional Characteristics:

$$M = 0.13$$

The following test values from reference 6.

C_L	0	.1	.2	.3	.4	.5	.6	.7	.8
C_D	.017	.020	.029	.047	.074	.105	.141	.184	.235

Compute:

$$\frac{C_{n_r}}{C_L^2} = 0.0080 \text{ per rad} \quad (\text{figure 7.1.3.3-6})$$

$$\frac{C_{n_r}}{C_{D_0}} = -0.68 \text{ per rad} \quad (\text{figure 7.1.3.3-7})$$

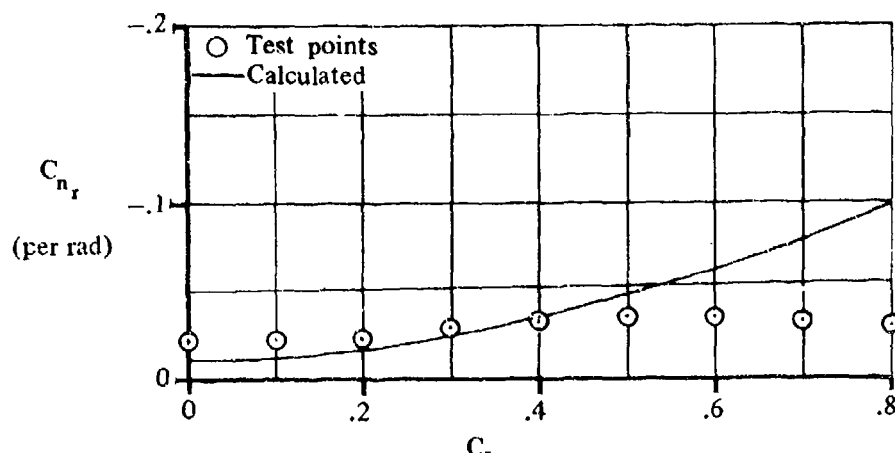
Solution:

$$C_{n_r} = \left(\frac{C_{n_r}}{C_L^2} \right) C_L^2 + \left(\frac{C_{n_r}}{C_{D_0}} \right) C_{D_0} \quad (\text{equation 7.1.3.3-a})$$

$$= +0.008 C_L^2 + (-0.68) C_{D_0}$$

①	②	③	④	⑤	⑥	⑦	⑧
C_L	C_L^2 ① ²	$\left(\frac{C_{n_r}}{C_L}\right) C_L^2$ (0.008) ②	C_D (test)	$\frac{C_L^2}{\pi A}$ ② / (π 2.31)	C_{D_0} $C_D - C_L^2 / (\pi A)$ ④ - ⑤	$\left(\frac{C_{n_r}}{C_{D_0}}\right) C_{D_0}$ (-0.68) ⑥	C_{n_r} (based on $S_W b_W^2$) (eq. 7.1.3.3-a) ③ + ⑦ (per rad)
0	0	0	.017	0	.0170	-.0116	-.0116
.1	.01	.00008	.020	.00138	.0186	-.0127	-.0126
.2	.04	.0003	.029	.00551	.0236	-.0160	-.0157
.3	.09	.0007	.047	.01240	.0346	-.0236	-.0228
.4	.16	.0013	.074	.0220	.0520	-.0354	-.0331
.5	.25	.0020	.106	.0344	.0706	-.0480	-.0460
.6	.36	.0029	.141	.0496	.0914	-.0621	-.0592
.7	.49	.0039	.184	.0675	.1165	-.0792	-.0753
.8	.64	.0051	.236	.0882	.1468	-.0998	-.0947

The calculated results are compared with test values from reference 5 in sketch (d).



SKETCH (a)

B. TRANSONIC

In the transonic speed regime no theoretical methods are available for estimating the wing yawing derivative C_{n_r} . Furthermore, no known experimental results are available for this derivative at transonic speeds.

C. SUPERSONIC

No general method is available for evaluating the wing contribution to the yawing derivative C_{n_r} at supersonic speeds. However, methods are presented in references 2, 3, and 4 for evaluating C_{n_r} for special classes of wing planforms. The results presented in these references are based on supersonic linear theory. The methods are restricted to estimating C_{n_r} over a limited range of Mach numbers for zero-thickness wings with no dihedral. Furthermore, the methods are considered tentative, since the spanwise variation of Mach number in the case of yawing has been neglected.

REFERENCES

1. Toll, T. A., and Quelje, M. J.: Approximate Relations and Charts for Low-Speed Stability Derivatives of Swept Wings. NACA TN 1581, 1948. (U)
2. Ribner, H. S., and Malvestuto, F. S., Jr.: Stability Derivatives of Triangular Wings at Supersonic Speeds. NACA TR 908, 1948. (U)
3. Harmon, S. M.: Stability Derivatives at Supersonic Speeds of Thin Rectangular Wings With Diagonals Ahead of Tip Mach Lines. NACA TR 925, 1949. (U)
4. Malvestuto, F. S., Jr., and Margolis, K.: Theoretical Stability Derivatives of Thin Sweptback Wings Tapered to a Point With Sweptback and Sweepforward Trailing Edges for a Limited Range of Supersonic Speeds. NACA TR 971, 1950. (U)
5. Jaquet, B. M., and Fletcher, H. S.: Experimental Steady-State Yawing Derivatives of a 60° Delta-Wing Model as Affected by Changes in Vertical Position of the Wing and in Ratio of Fuselage Diameter to Wing Span. NACA TN 3843, 1956. (U)
6. Goodman, A., and Thomas, D. F., Jr.: Effects of Wing Position and Fuselage Size on the Low-Speed Static and Rolling Stability Characteristics of a Delta-Wing Model. NACA TR 1224, 1955. (U)
7. Williams, J. L.: Measured and Estimated Lateral Static and Rotary Derivatives of a 1/12-Scale Model of a High-Speed Fighter Airplane With Unswept Wings. NACA RM L53C09, 1954. (U)
8. Goodman, A., and Brewer, J. D.: Investigation at Low Speed of the Effect of Aspect Ratio and Sweep on Static and Yawing Stability Derivatives of Untapered Wings. NACA TN 1839, 1948. (U)
9. Bird, J. D., Jaquet, B. M., and Cowen, J. W.: Effect of Fuselage and Tail Surfaces on Low-Speed Yawing Characteristics of a Swept-Wing Model as Determined in Curved-Flow Test Section of Langley Stability Tunnel. NACA TN 2483, 1951. (U)
10. Letko, W., and Jaquet, B. M.: Effect of Airfoil Profile of Symmetrical Sections on the Low-Speed Static-Stability and Yawing Derivatives of 45° Sweepback Wing Models of Aspect Ratio 2.61. NACA RM L8H10, 1948. (U)
11. Letko, W.: Effect of Vertical-Tail Area and Length on the Yawing Stability Characteristics of a Model Having a 45° Sweepback Wing. NACA TN 2358, 1951. (U)

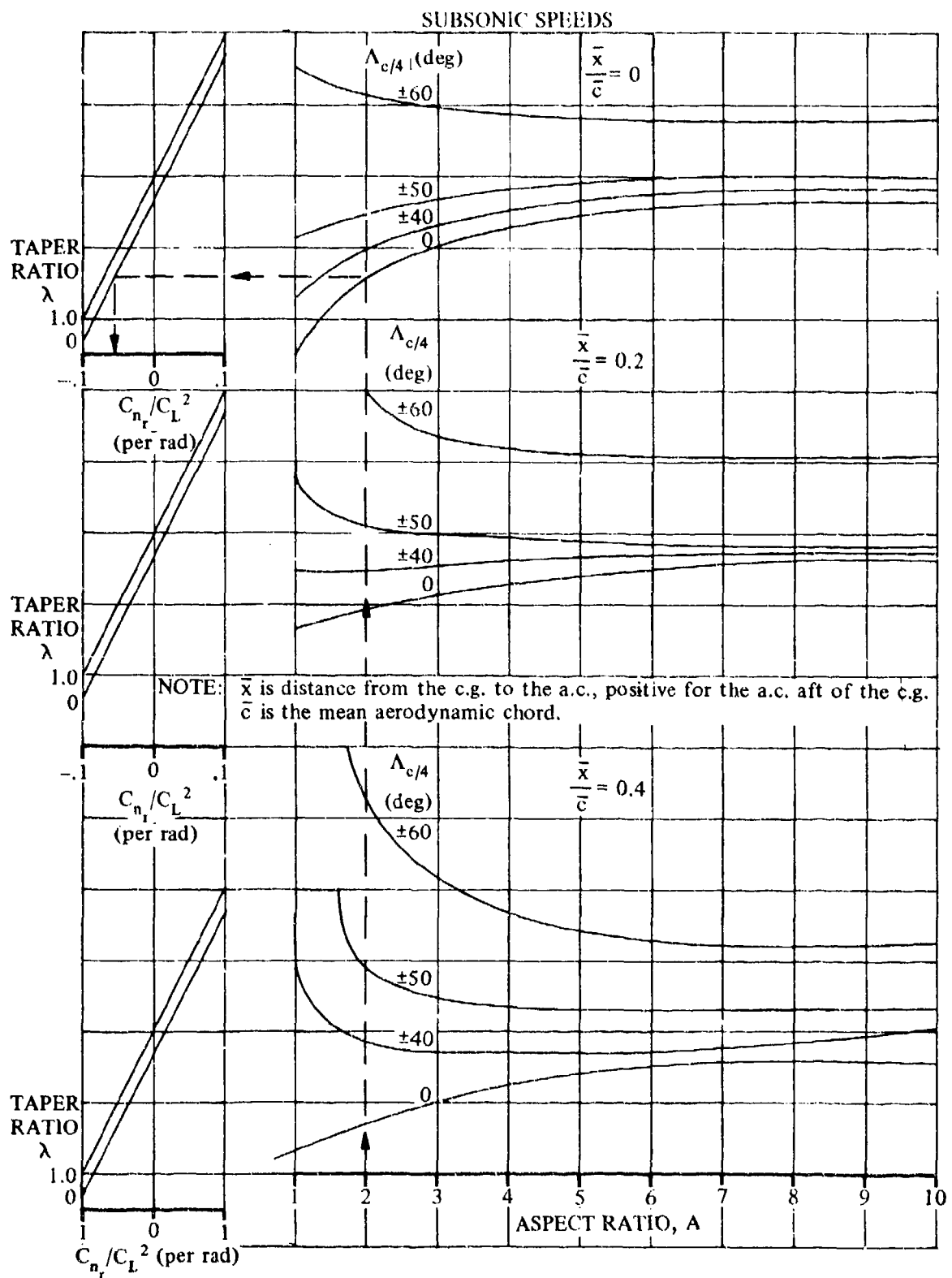
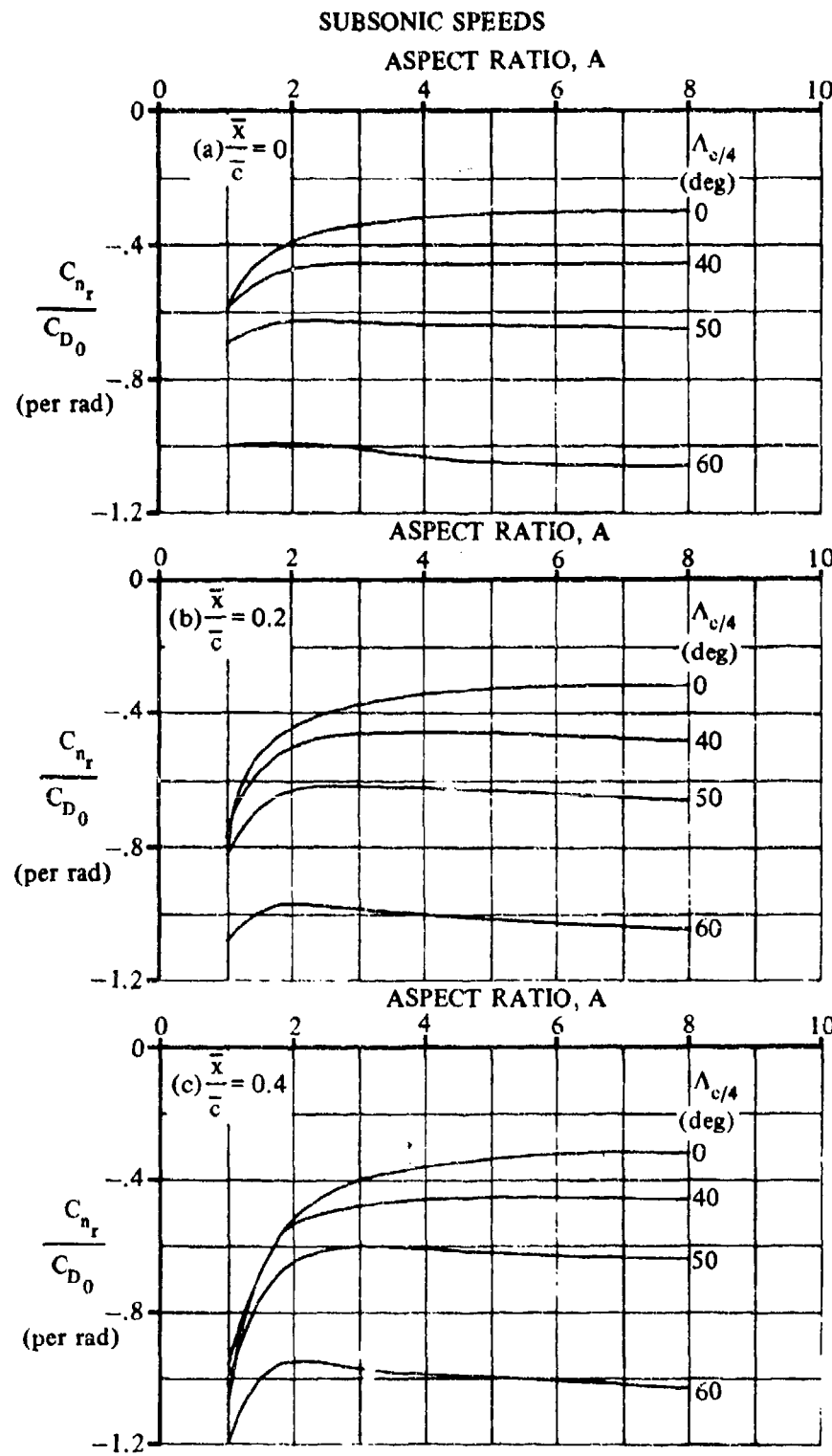


FIGURE 7.1.3.3-6 LOW-SPEED DRAG-DUE-TO-LIFT YAW-DAMPING PARAMETER

7.1.3.3-6



NOTE: \bar{x} is the distance from the c.g. to the a.c., positive for the a.c. aft of the c.g.
 \bar{c} is the wing mean aerodynamic chord.

FIGURE 7.1.3.3-7 LOW-SPEED PROFILE-DRAG YAW-DAMPING PARAMETER

7.1.4 WING ACCELERATION DERIVATIVES

7.1.4.1 WING ACCELERATION DERIVATIVE $C_{L\dot{\alpha}}$

Methods are presented for estimating the wing contribution to the derivative $C_{L\dot{\alpha}}$ at low angles of attack for a triangular planform in the subsonic and low transonic speed ranges and for planforms with the leading edge swept back and the trailing edge swept back or swept forward in the supersonic speed range. In addition, the supersonic results are directly applicable to wings with swept-forward leading edges, in view of the reversibility theorem (see reference 5). This derivative is used in estimating $C_{m\dot{\alpha}}$ in Section 7.1.4.2.

If the wing acceleration derivative $C_{L\dot{\alpha}}$ is to be used in method 1 of Section 7.3.4.1 to obtain $(C_{L\dot{\alpha}})_{WB}$, the exposed wing planform area should be used for all calculations in the Datcom methods. Using the exposed planform area will yield $C_{L\dot{\alpha}}$ based on the product of the exposed wing area and the exposed wing MAC, rather than the product of wing area and wing MAC as indicated.

DATCOM METHODS

A. SUBSONIC

An equation for estimating the subsonic acceleration derivative $C_{L\dot{\alpha}}$ of a triangular wing (derived in reference 1), based on the product of wing area and wing MAC $S_w \bar{c}_w$, is given by

$$C_{L\dot{\alpha}} = 1.5 \left(\frac{x_{a.c.}}{c_r} \right) C_{L\alpha} + 3 C_L(g) \quad (\text{per radian}) \quad 7.1.4.1-a$$

where

$C_{L\alpha}$ is the wing lift-curve slope (Section 4.1.3.2) at the Mach number under consideration, based on the total wing area (per radian).

$\frac{x_{a.c.}}{c_r}$ is obtained from Section 4.1.4.2.

$C_L(g)$ is the lift-coefficient correction term obtained from figure 7.1.4.1-6 (per radian).

Because of the restrictions placed on the lift-coefficient correction term, this method is valid only for $0 < \beta A < 4$.

Explicit expressions for estimating $C_{L\dot{\alpha}}$ of other wing planforms in the subsonic region are not available at this time.

Sample Problem

Given:

$$A = 4.0 \quad \lambda = 0 \quad \Lambda_{LE} = 45^\circ \quad C_{L\alpha} = 4.0 \text{ per rad (Section 4.1.3.2)}$$

$$M = 0.6$$

Compute:

$$\beta = \sqrt{1 - M^2} = 0.80$$

$$\tan \Lambda_{LE} = 1.0$$

$$\beta / \tan \Lambda_{LE} = 0.80$$

$$\beta A = 3.20$$

$$A \tan \Lambda_{LE} = 4.0$$

$$\frac{x_{a.c.}}{c_r} = 0.570 \text{ (figure 4.1.4.2-26a)}$$

$$\frac{-\beta^2 C_L(g)}{\pi A/2} = 0.1245 \text{ per rad (figure 7.1.4.1-6)}$$

$$C_L(g) = -1.22 \text{ per rad}$$

Solution:

$$C_{L\dot{\alpha}} = 1.5 \left(\frac{x_{a.c.}}{c_r} \right) C_{L\alpha} + 3 C_L(g) \quad (\text{equation 7.1.4.1-a})$$

$$= (1.5)(0.570)(4.0) + (3)(-1.22)$$

$$= -0.240 \text{ per rad (based on } S_w \bar{c}_w)$$

B. TRANSONIC

The value of $C_{L\dot{\alpha}}$ of a triangular wing from the critical Mach number to $M = 1.0$ is given by the method of paragraph A, provided $0 < \beta A < 4$.

There is no general theory available in the literature that gives the transonic values of $C_{L\dot{\alpha}}$, either for additional wing-geometry parameters or for Mach numbers greater than 1.0. Furthermore, there is a scarcity of test data in the transonic region for any wing planform.

C. SUPERSONIC

The supersonic value of $C_{L\dot{\alpha}}$, based on the product of wing area and wing MAC $S_w \bar{c}_w$, is derived in references 2 and 3 for wings with subsonic leading edges and in reference 4 for wings with supersonic leading edges.

1. Wings with subsonic leading edges ($\beta \cot \Lambda_{LE} < 1.0$)

For wings with subsonic leading edges, $C_{L\dot{\alpha}}$ is obtained by the method of reference 2 for $\lambda = 0$ and by the method of reference 3 for $\lambda = 0.25$ to 1.0. The following methods are not valid if the Mach line from the vertex of the trailing edge intersects the leading edge or if the wing-tip Mach lines intersect on the wings or intersect the opposite wing tips.

a. Zero-taper-ratio wings ($\lambda = 0$)

$C_{L\dot{\alpha}}$ is derived in reference 2 as

$$C_{L\dot{\alpha}} = - \frac{\pi A M^2}{2\beta^2} \left[-3G(\beta C) F_3(N) + 2E''(\beta C) F_2(N) + \frac{1}{M^2} E''(\beta C) F_1(N) \right] \quad (\text{per radian}) \quad 7.1.4.1-b$$

where

$E''(\beta C)$ and $G(\beta C)$ are obtained from figure 7.1.1.1-8.

$F_1(N)$, $F_2(N)$, and $F_3(N)$ are obtained from figure 7.1.4.1-7.

b. Wings with $\lambda = 0.25$ to 1.0

$C_{L\dot{\alpha}}$ is derived in reference 3 as

$$C_{L\dot{\alpha}} = \frac{M^2}{\beta^2} (C_{L\dot{\alpha}})_1 - \frac{1}{\beta^2} (C_{L\dot{\alpha}})_2 \quad (\text{per radian}) \quad 7.1.4.1-c$$

where

$(C_{L\dot{\alpha}})_1$ and $(C_{L\dot{\alpha}})_2$ are obtained from figures 7.1.4.1-8a through 7.1.4.1-8f for $\lambda = 0.25, 0.50$, and 0.75 and from the equations of reference 3 for $\lambda > 0.75$.

2. Wings with supersonic leading edges ($\beta \cot \Lambda_{LE} > 1.0$)

For wings with supersonic leading edges, $C_{L\dot{\alpha}}$ (derived in reference 4) is given by equation 7.1.4.1-c with $(C_{L\dot{\alpha}})_1$ and $(C_{L\dot{\alpha}})_2$ obtained from figures 7.1.4.1-11a through 7.1.4.1-11o.

Figures 7.1.4.1-11a through 7.1.4.1-11o are valid for the range of Mach numbers for which the Mach lines from the leading-edge vertex intersect the trailing edge. An additional limitation is that the foremost Mach line from either wing tip may not intersect the remote half-wing.

Sample Problem

1. Wing with subsonic leading edge

Given:

$$A = 5.80 \quad \lambda = 0 \quad \Lambda_{LE} = 60^\circ \quad M = 1.50$$

Compute:

$$\beta = \sqrt{M^2 - 1} = 1.12$$

$$\cot \Lambda_{LE} = 0.5774$$

$$\beta \cot \Lambda_{LE} = 0.647$$

$$N = 1 - \frac{4 \cot \Lambda_{LE}}{A} = 0.602$$

$$\left. \begin{array}{l} E''(\beta C) = 0.770 \\ G(\beta C) = 0.570 \end{array} \right\} \text{(figure 7.1.1.1-8)}$$

$$\left. \begin{array}{l} F_1(N) = 0.520 \\ F_2(N) = 1.090 \\ F_3(N) = 0.907 \end{array} \right\} \text{(figure 7.1.4.1-7)}$$

Solution:

$$C_{L\dot{\alpha}} = - \frac{\pi A M^2}{2\beta^2} \left[-3G(\beta C) F_3(N) + 2E''(\beta C) F_2(N) + \frac{1}{M^2} E''(\beta C) F_1(N) \right] \quad (\text{equation 7.1.4.1-b})$$

$$= - \frac{\pi(5.80)(2.25)}{2(1.25)} \left[-3(0.570)(0.907) + 2(0.770)(1.090) + \frac{1}{2.25} (0.770)(0.520) \right]$$

$$= -5.22 \pi (-1.551 + 1.679 + 0.178)$$

$$= -5.02 \text{ per rad (based on } S_w \bar{c}_w)$$

2. Wing with supersonic leading edge

Given:

$$A = 4.0$$

$$\lambda = 0.25$$

$$\Lambda_{LE} = 45^\circ$$

$$M = 2.0$$

Compute:

$$\beta = \sqrt{M^2 - 1} = 1.732$$

$$\beta A = 6.928$$

$$\cot \Lambda_{LE} = 1.00$$

$$\beta \cot \Lambda_{LE} = 1.732$$

$$\cot^{-1} (\beta \cot \Lambda_{LE}) = 30^\circ$$

$$\beta (C_{L\dot{\alpha}})_1 = -0.390 \text{ per rad (figure 7.1.4.1-11d)}$$

$$(C_{L\dot{\alpha}})_1 = -0.225 \text{ per rad}$$

$$\beta (C_{L\dot{\alpha}})_2 = 4.200 \text{ per rad (figure 7.1.4.1-11f)}$$

$$(C_{L\dot{\alpha}})_2 = 2.425 \text{ per rad}$$

Solution:

$$C_{L\dot{\alpha}} = \frac{M^2}{\beta^2} (C_{L\dot{\alpha}})_1 - \frac{1}{\beta^2} (C_{L\dot{\alpha}})_2 \text{ (equation 7.1.4.1-c)}$$

$$= \frac{4}{3} (-0.225) + \frac{1}{3} (2.425)$$

$$= -1.108 \text{ per rad (based on } S_w \bar{c}_w)$$

REFERENCES

1. Tobak, M., and Lessing, H. C.: Estimation of Rotary Stability Derivatives at Subsonic and Transonic Speeds. Agard Report No. 343, Apr 1961. (U)
2. Malvestuto, F. S., Jr., and Margolis, K.: Theoretical Stability Derivatives of Thin Sweptback Wings Tapered to a Point with Sweptback or Sweptforward Trailing Edges for a Limited Range of Supersonic Speeds. NACA TR 971, 1950. (U)
3. Malvestuto, F. S., Jr., and Hoover, D. M.: Supersonic Lift and Pitching Moment of Thin Sweptback Tapered Wings Produced by Constant Vertical Acceleration. Subsonic Leading Edges and Supersonic Trailing Edges. NACA TN 2315, Mar 1951. (U)
4. Cole, I. J., and Margolis, K.: Lift and Pitching Moment at Supersonic Speeds due to Constant Vertical Acceleration for Thin Sweptback Tapered Wings with Streamwise Tips. Supersonic Leading and Trailing Edges. NACA TN 3196, Jul 1954. (U)
5. Harmon, S. M.: Theoretical Relations Between the Stability Derivatives of a Wing in Direct and Reverse Supersonic Flow. NACA TN 1943, 1949. (U)

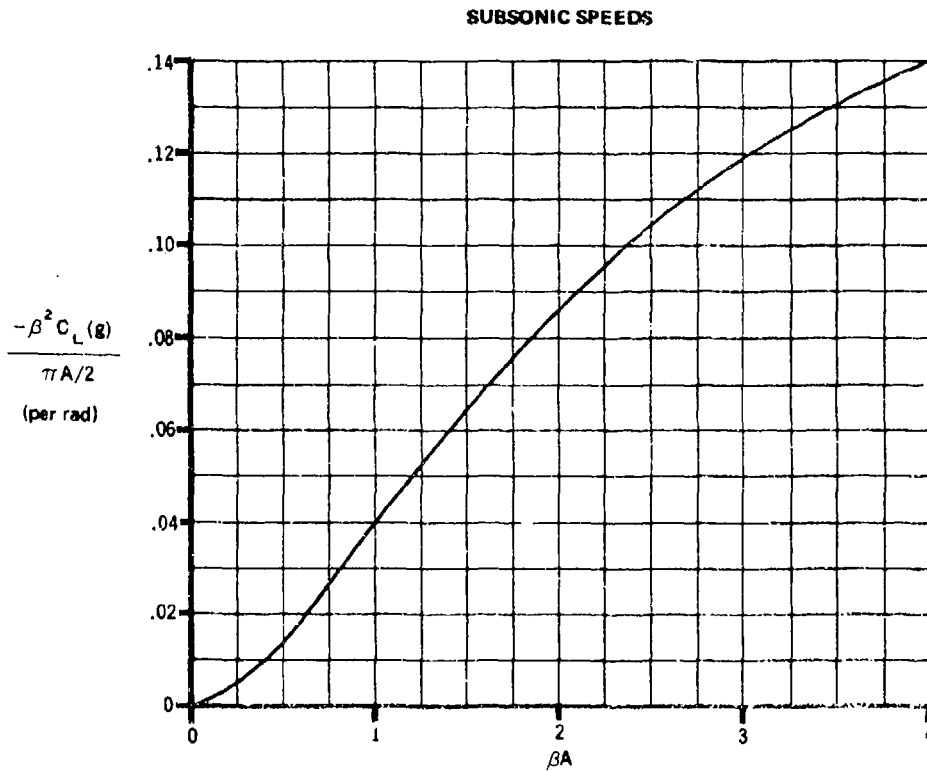


FIGURE 7.1.4.1-6 VARIATION OF LIFT-COEFFICIENT CORRECTION TERM WITH βA .
TRIANGULAR WING. $0 < \beta A \leq 4$.

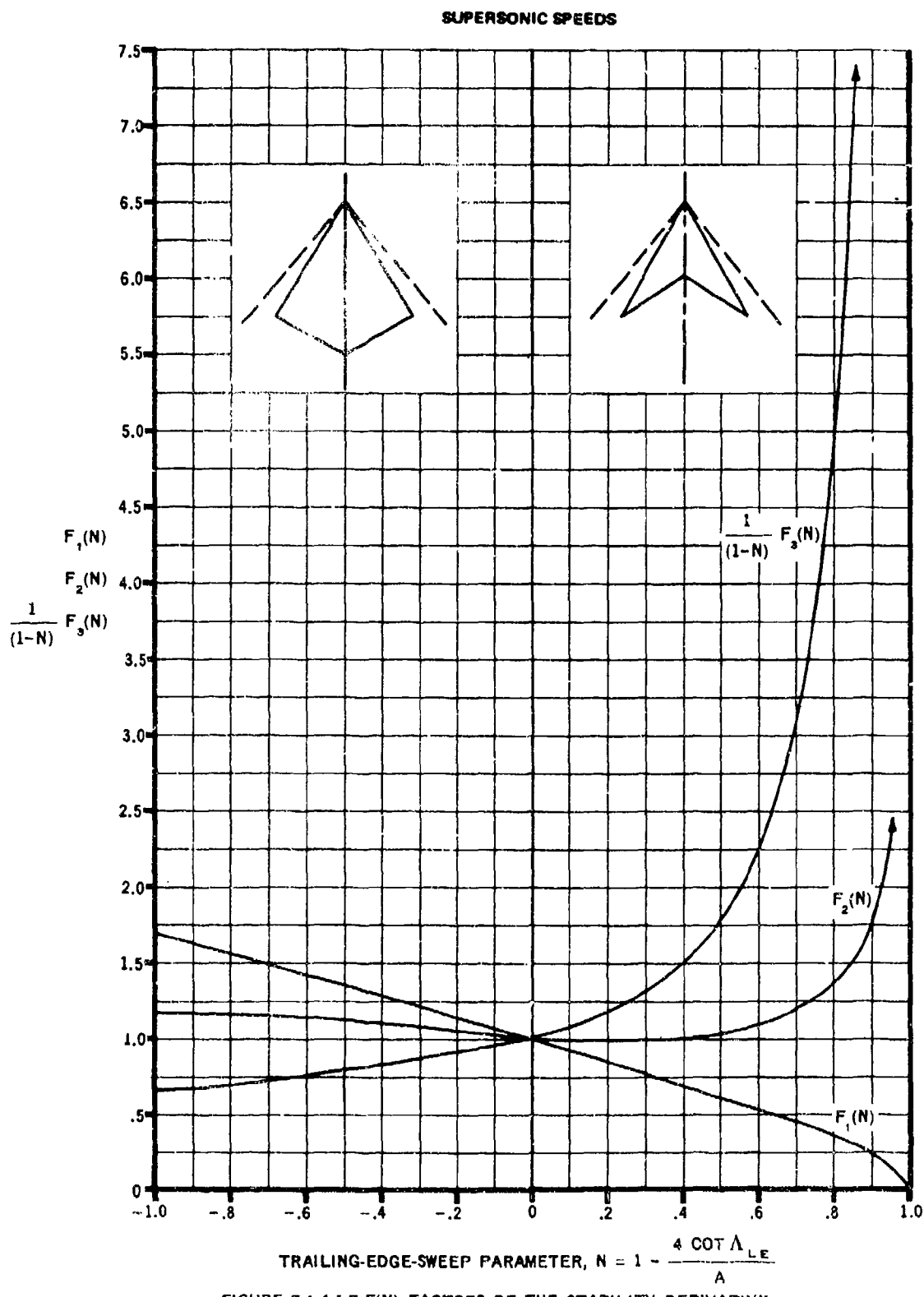


FIGURE 7.1.4.1-7 $F(N)$ FACTORS OF THE STABILITY DERIVATIVE

SUPersonic SPEEDS
SUBSONIC LEADING EDGE

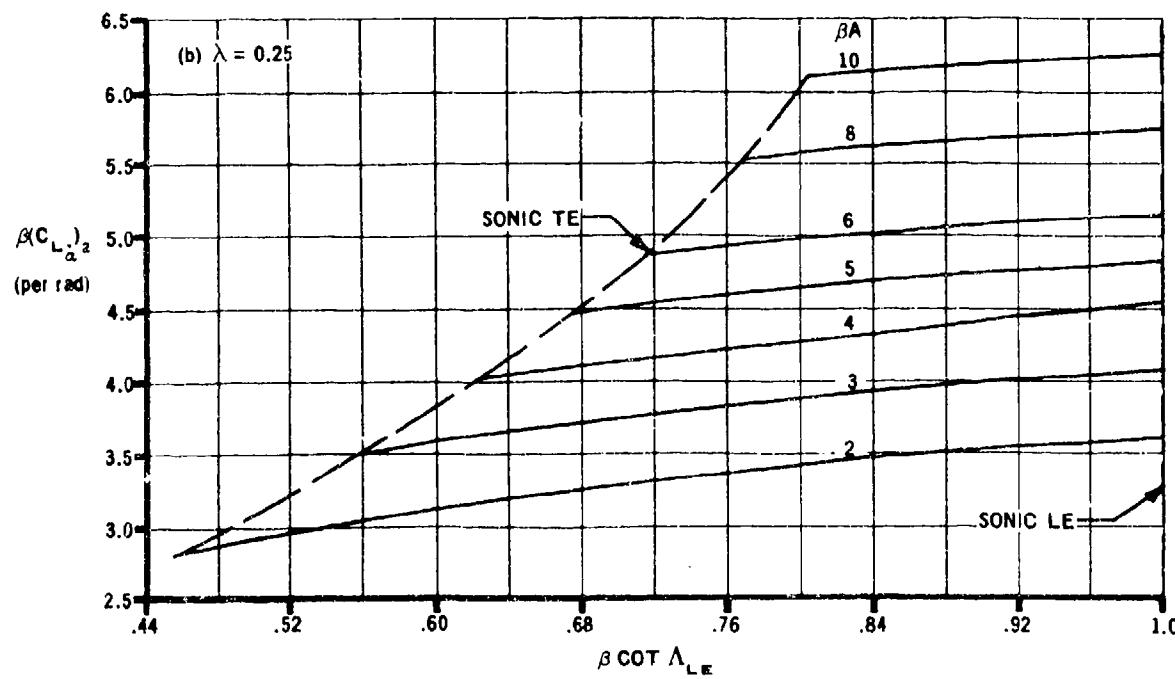
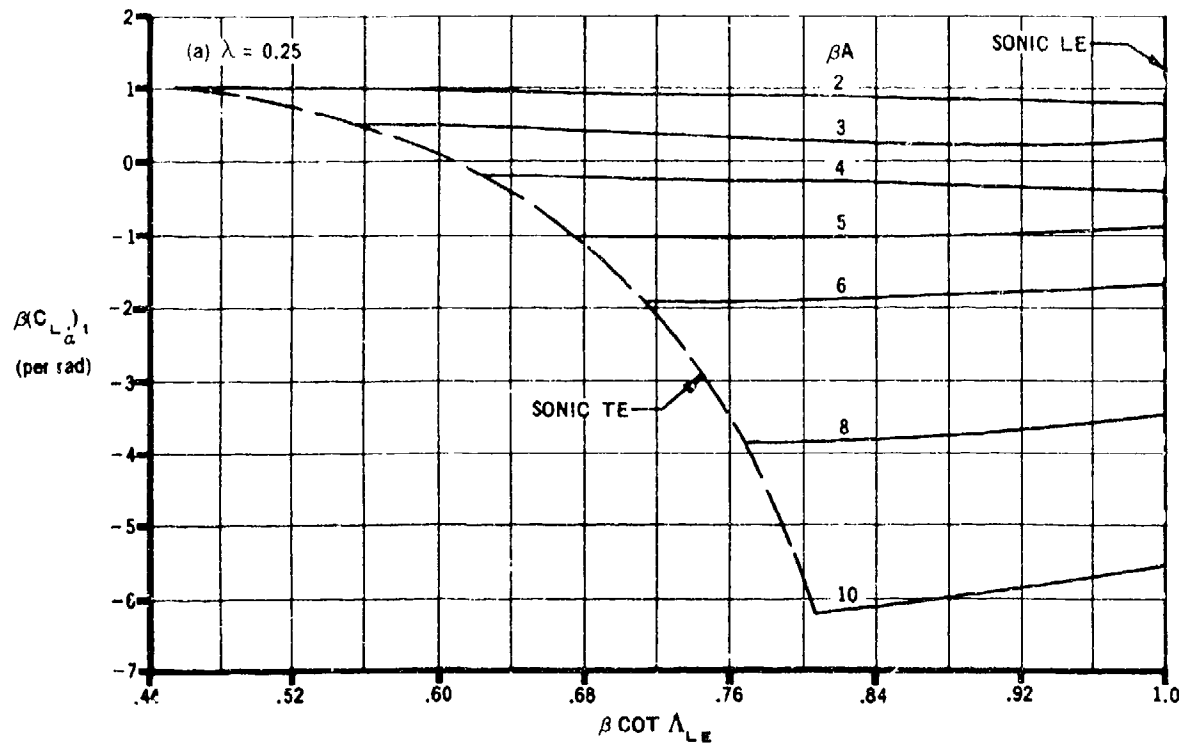


FIGURE 7.1.4.1-8 VARIATION OF $\beta(C_L_\alpha)_1$ AND $\beta(C_L_\alpha)_2$ WITH $\beta \cot \Lambda_{LE}$

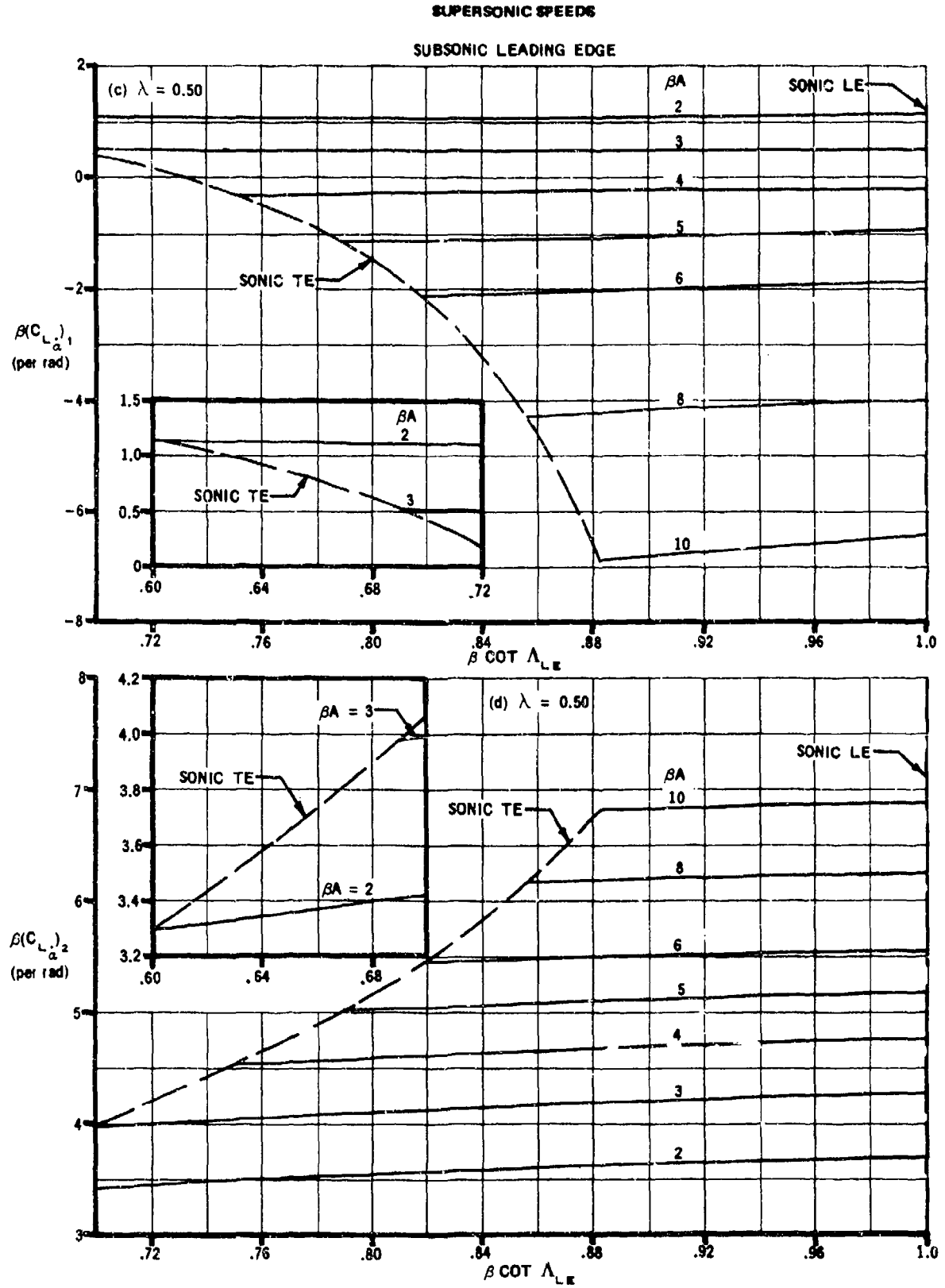


FIGURE 7.1.4.1-8 (CONTD)

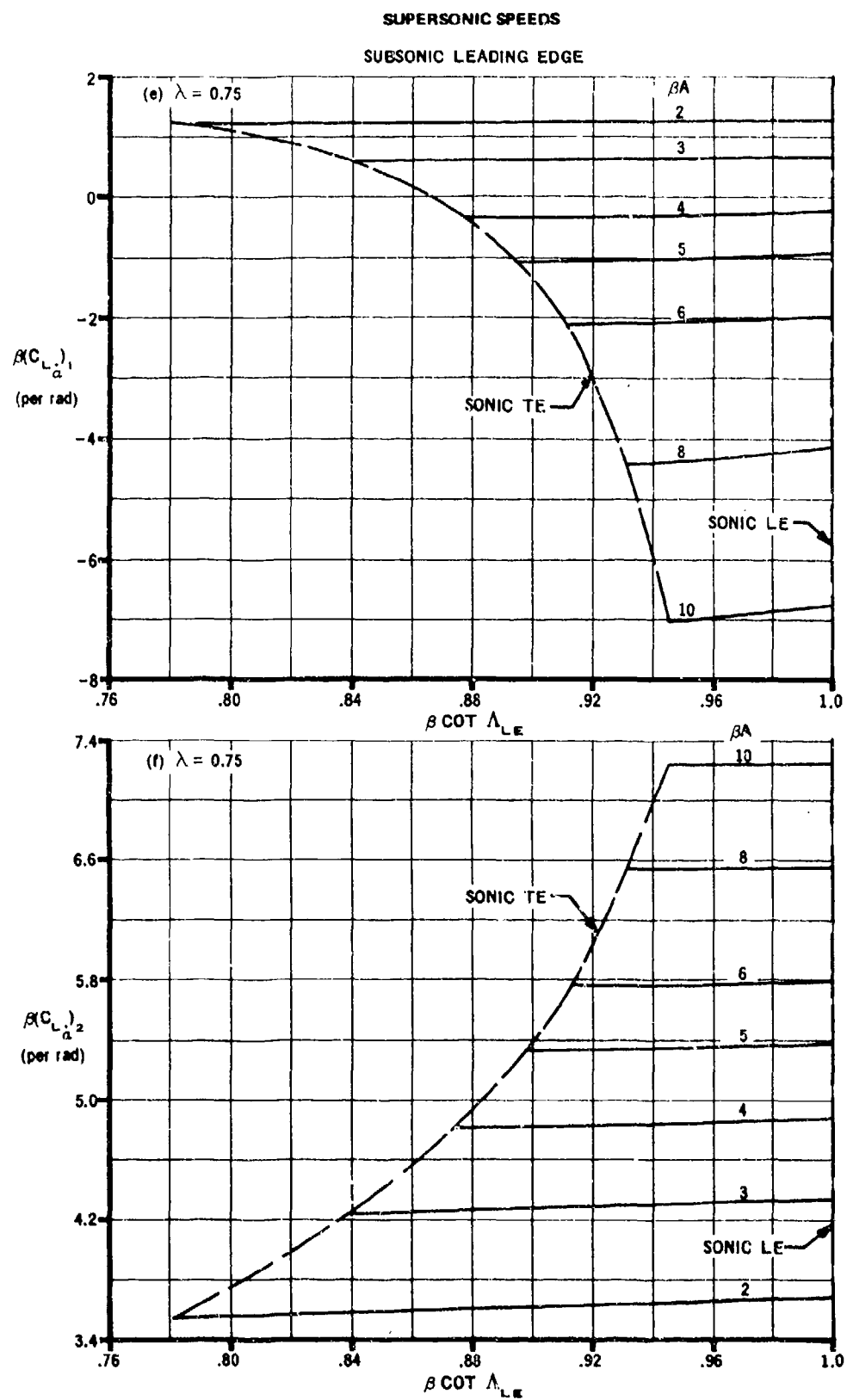


FIGURE 7.1.4.1-8 (CONT'D)

7.1.4.1-10

SUPersonic SPEEDS

SUPersonic LEADING EDGE

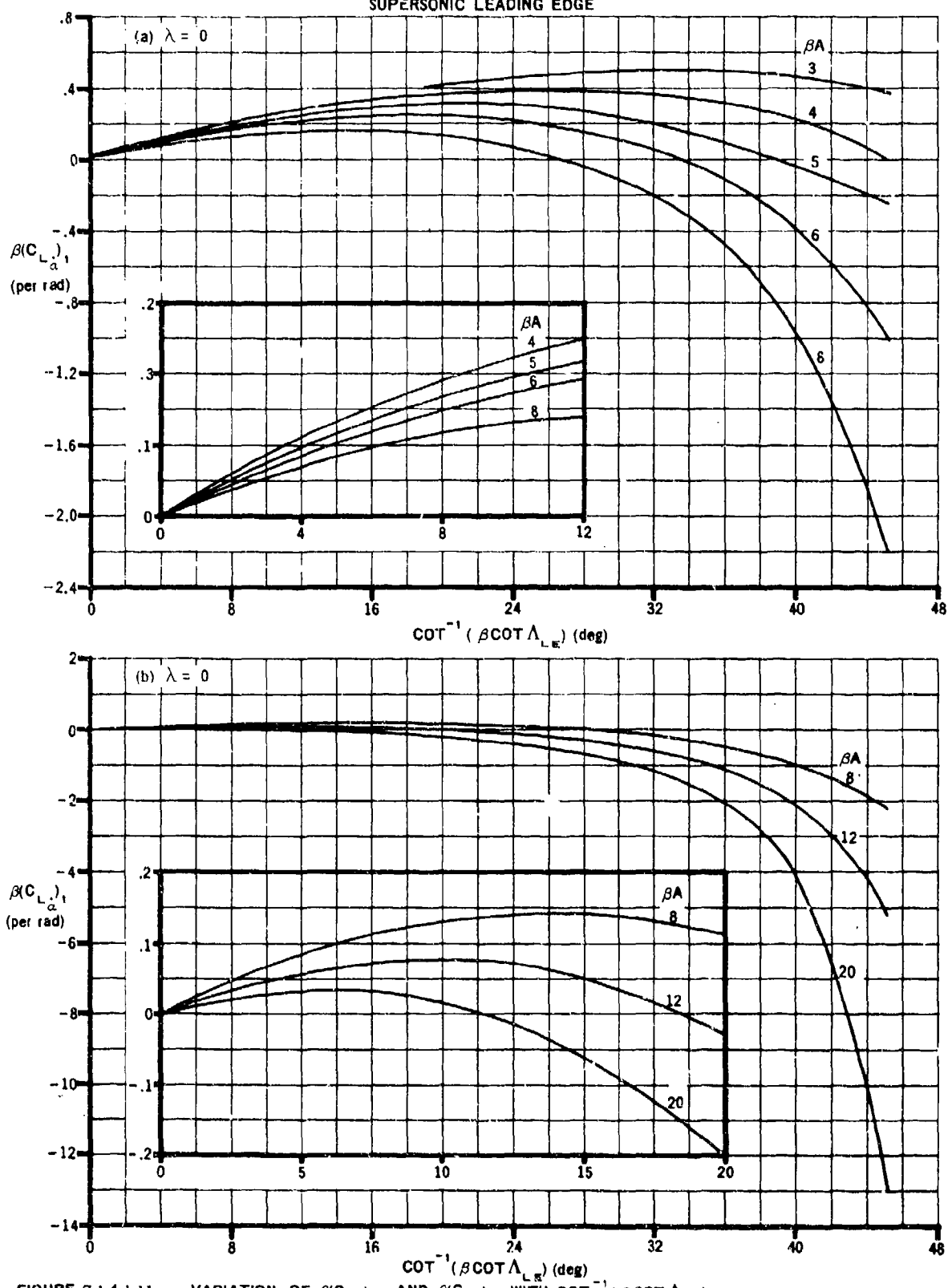


FIGURE 7.1.4.1-11 VARIATION OF $\beta(C_{L_x})_1$ AND $\beta(C_{L_x})_2$ WITH $\text{COT}^{-1}(\beta \text{COT} \Lambda_{LE})$

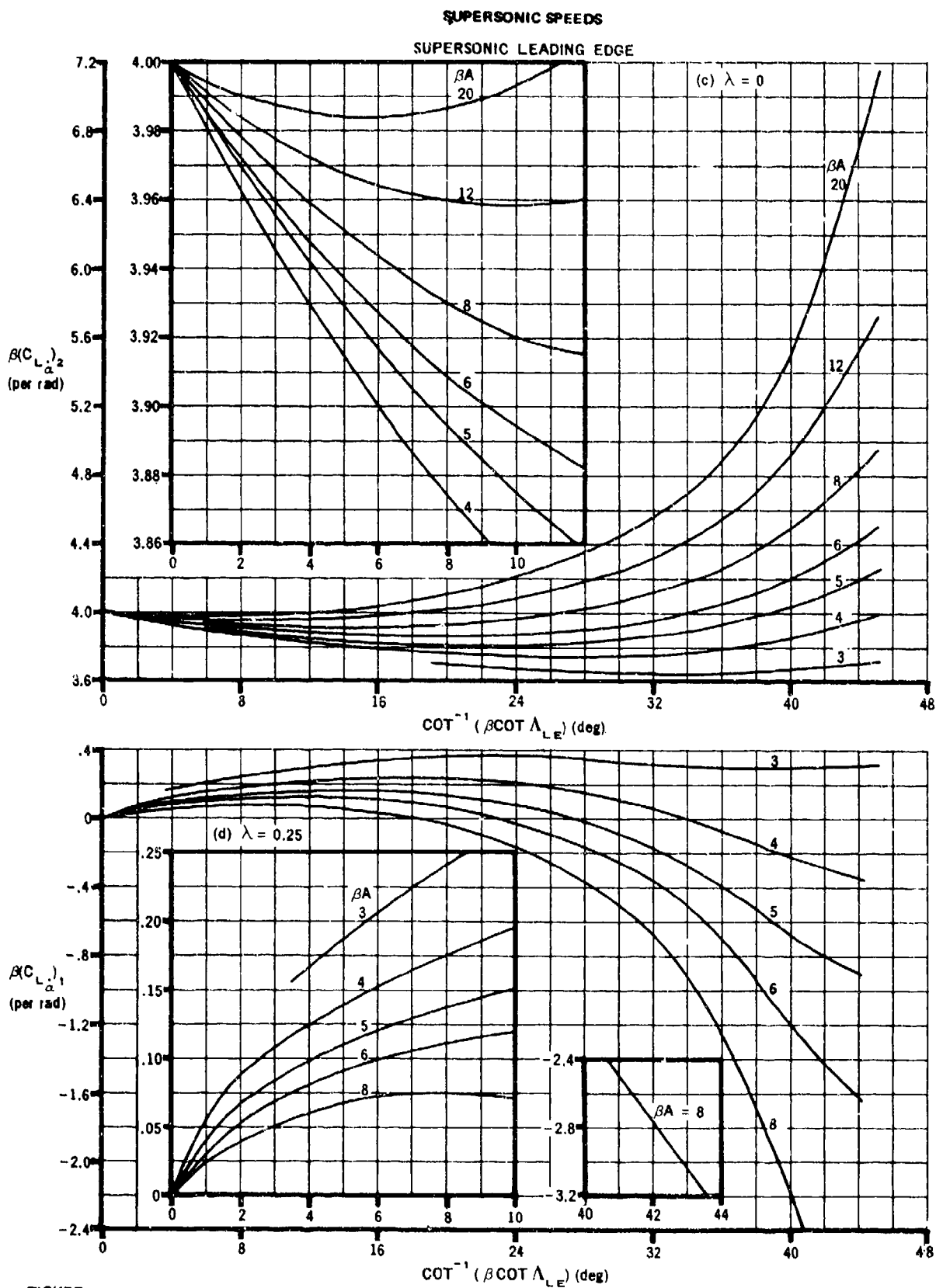


FIGURE 7.1.4.1-11 (CONTD)

7.1.4.1-12

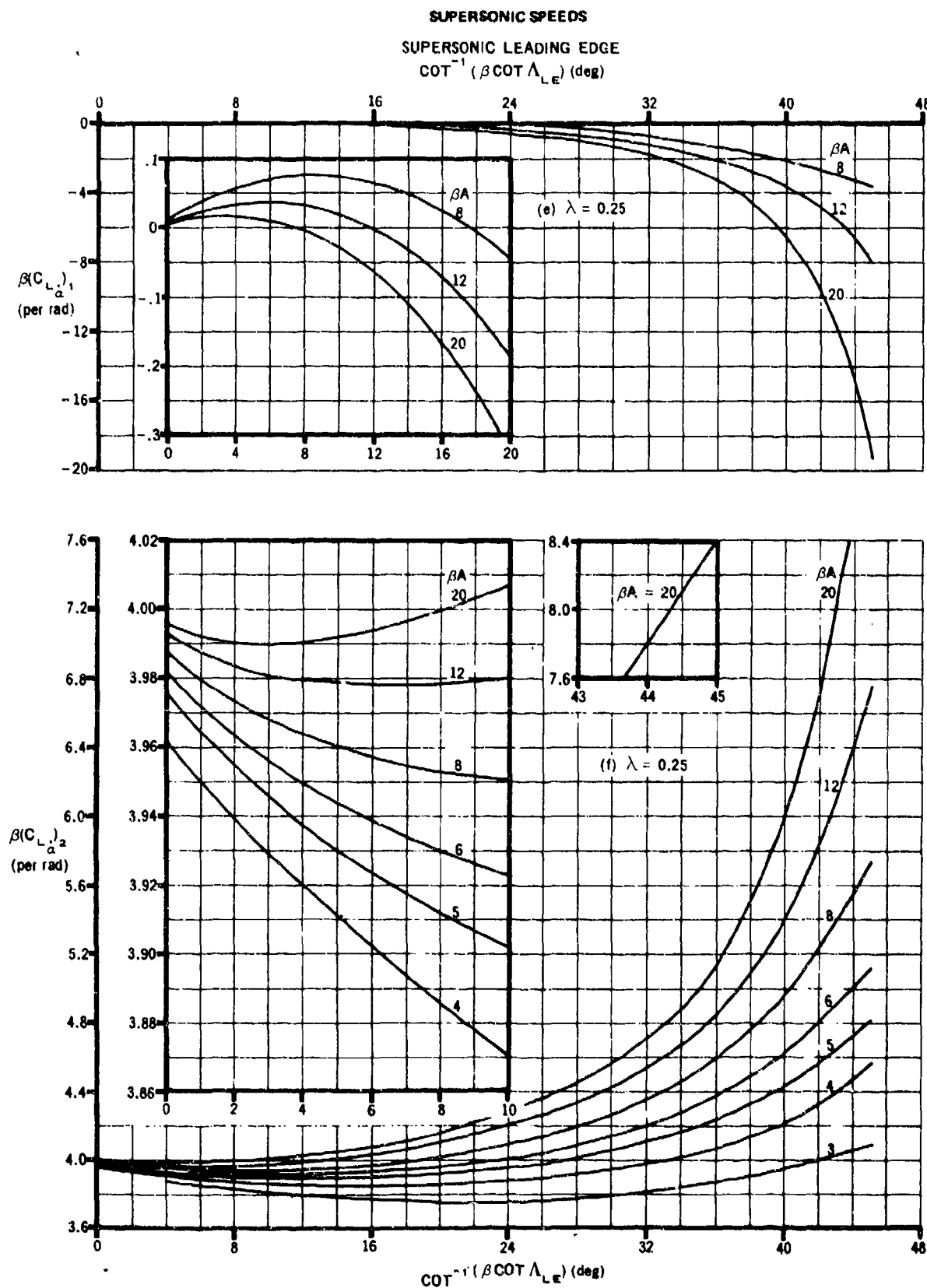


FIGURE 7.1.4.1-11 (CONTD)

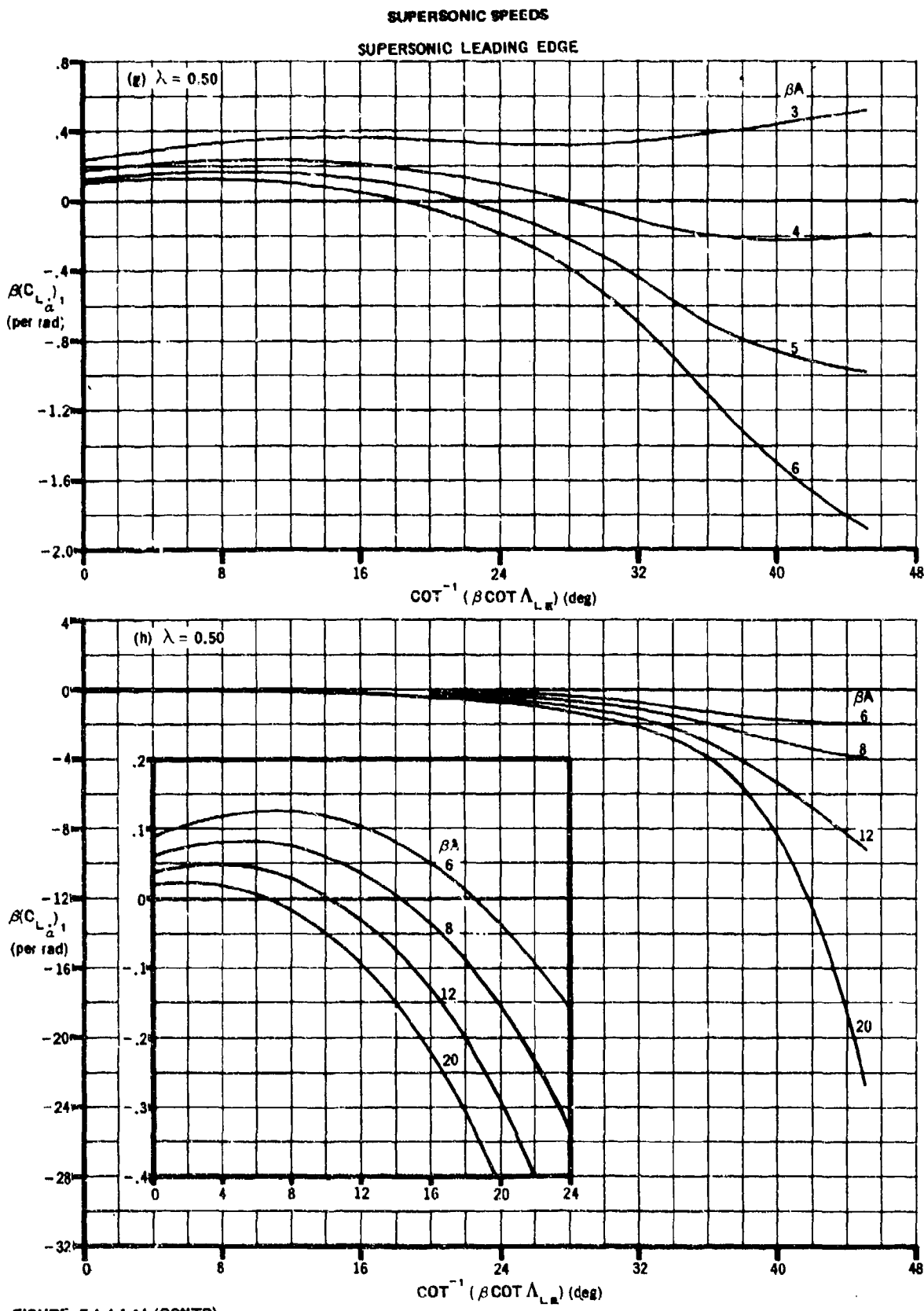


FIGURE 7.1.4.1-11 (CONT'D)

SUPersonic SPEEDS

SUPersonic LEADING EDGE

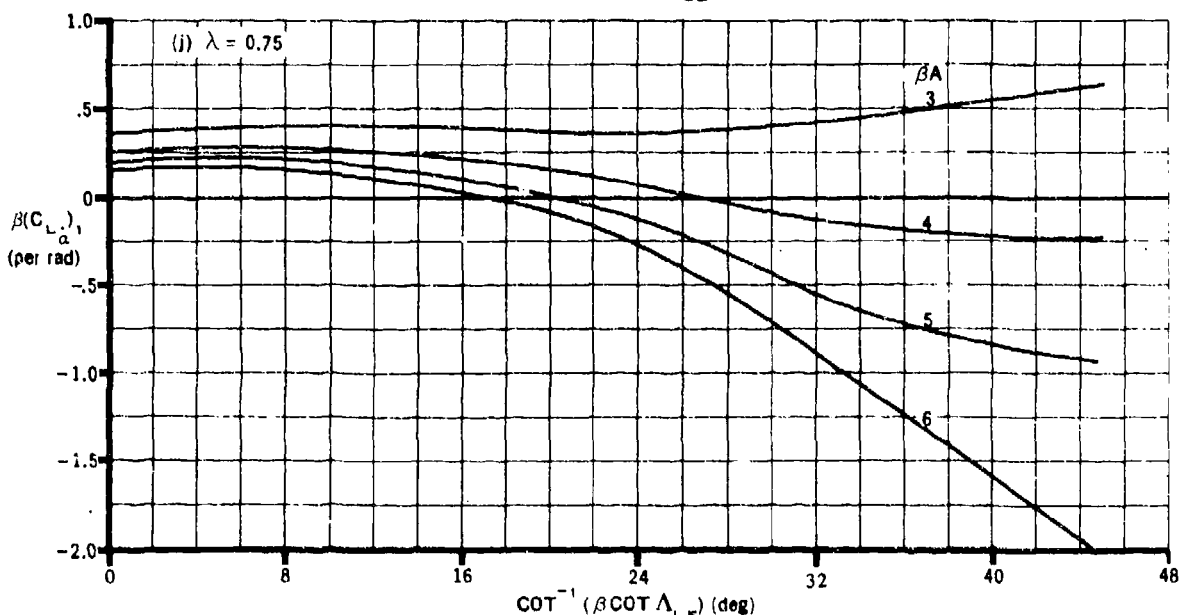
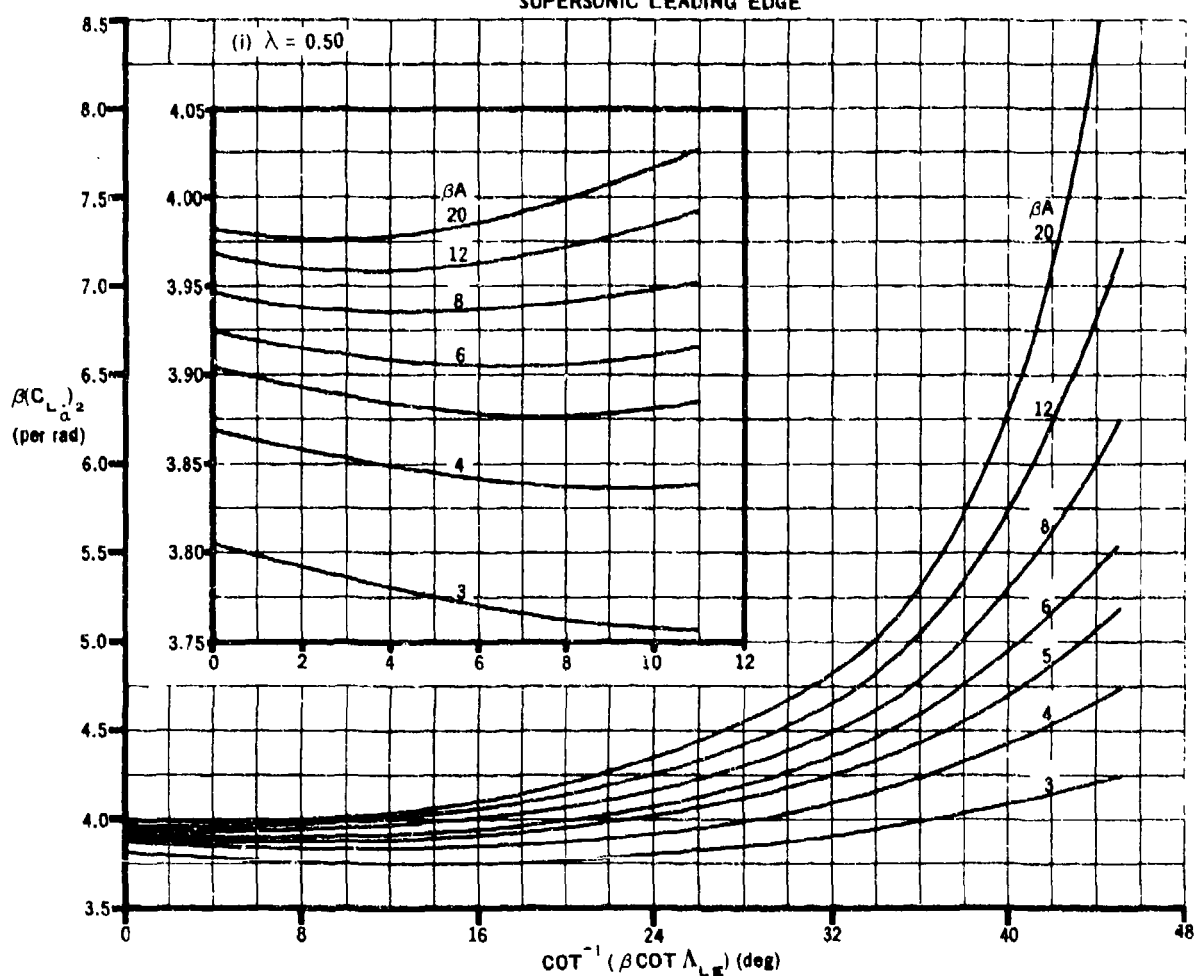


FIGURE 7.1.4.1-11 (CONT'D)

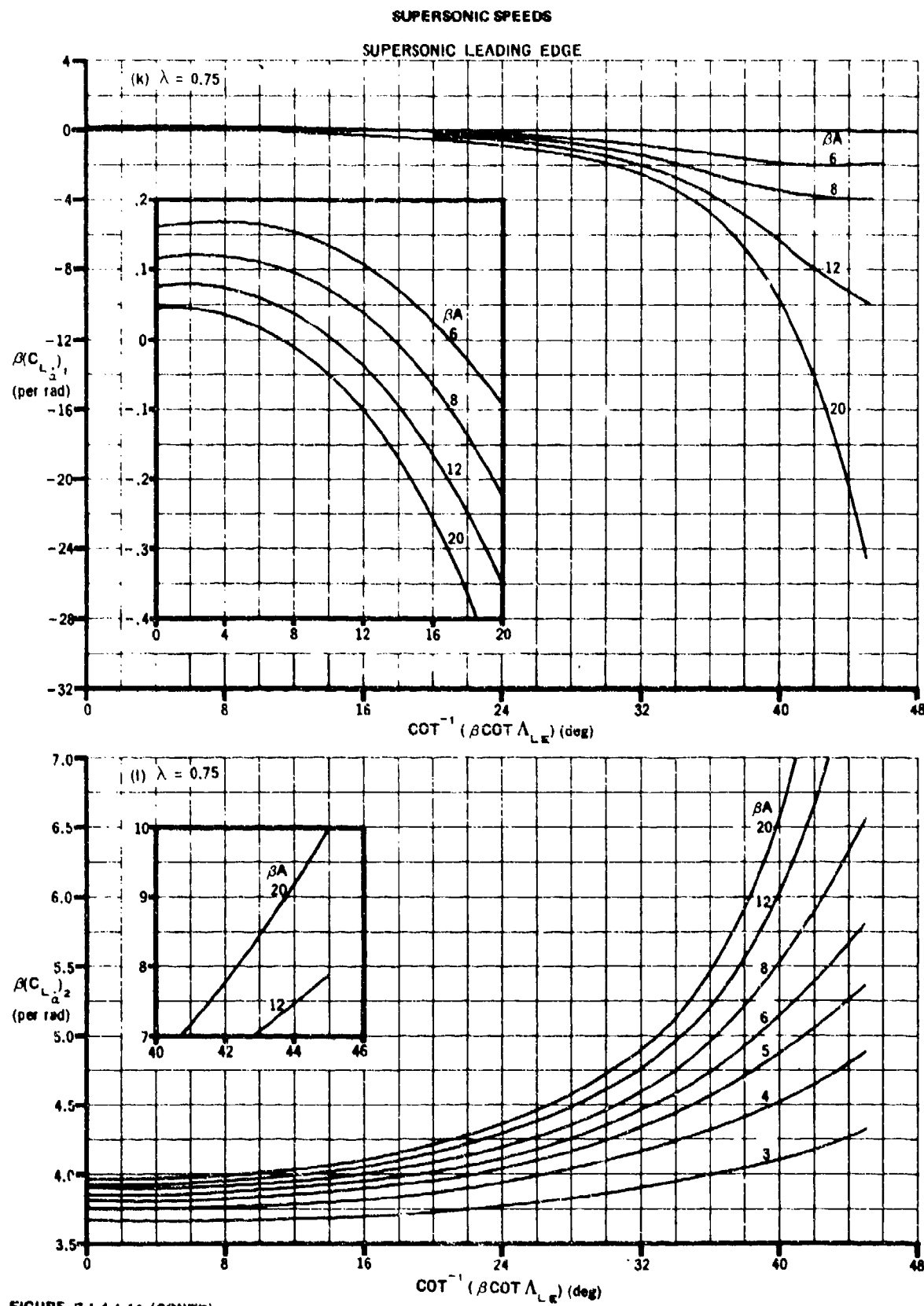


FIGURE 7.1.4.1-11 (CONT'D)

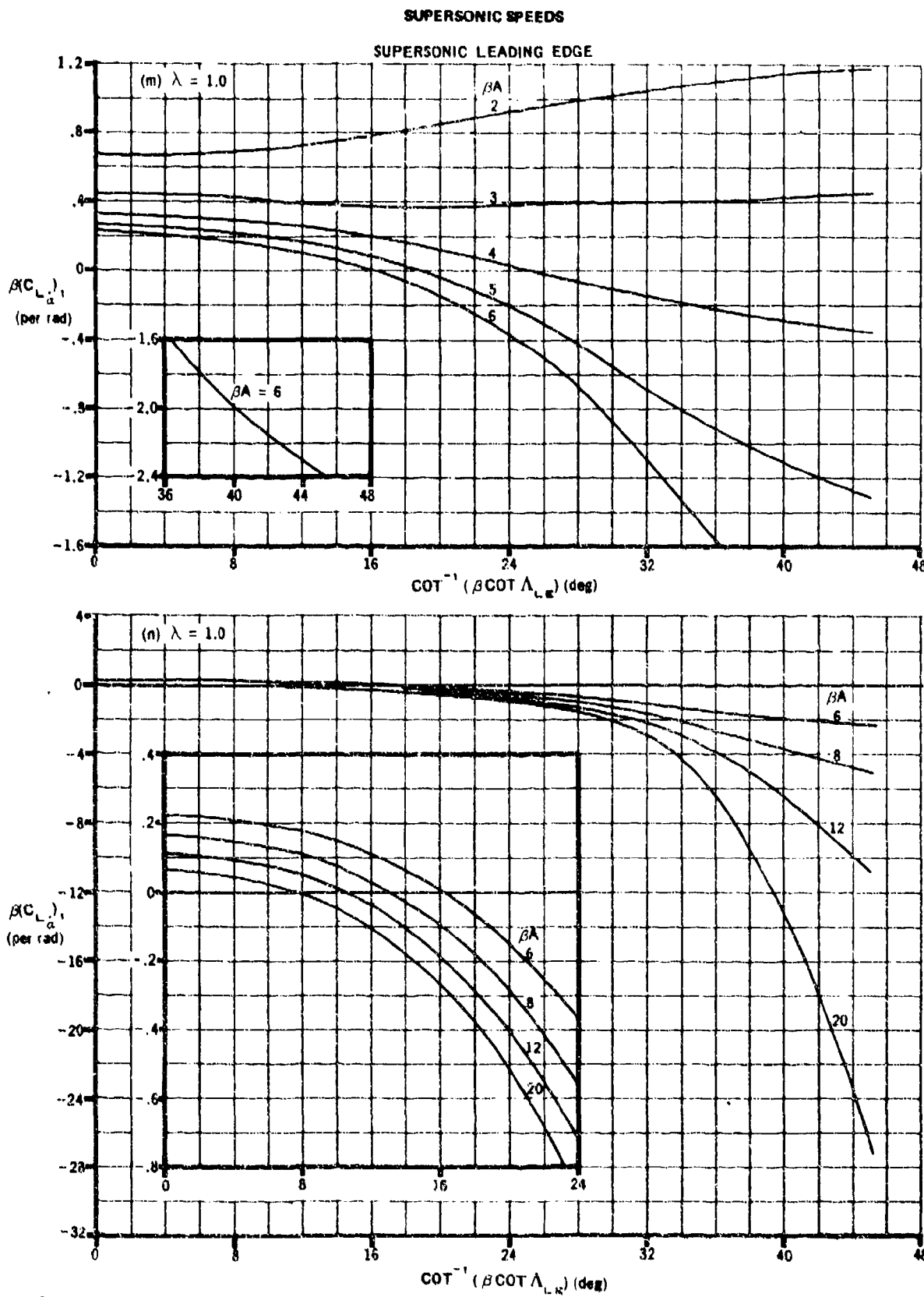


FIGURE 7.1.4.1-11 (CONT'D)

SUPersonic SPEEDS
SUPersonic LEADING EDGE

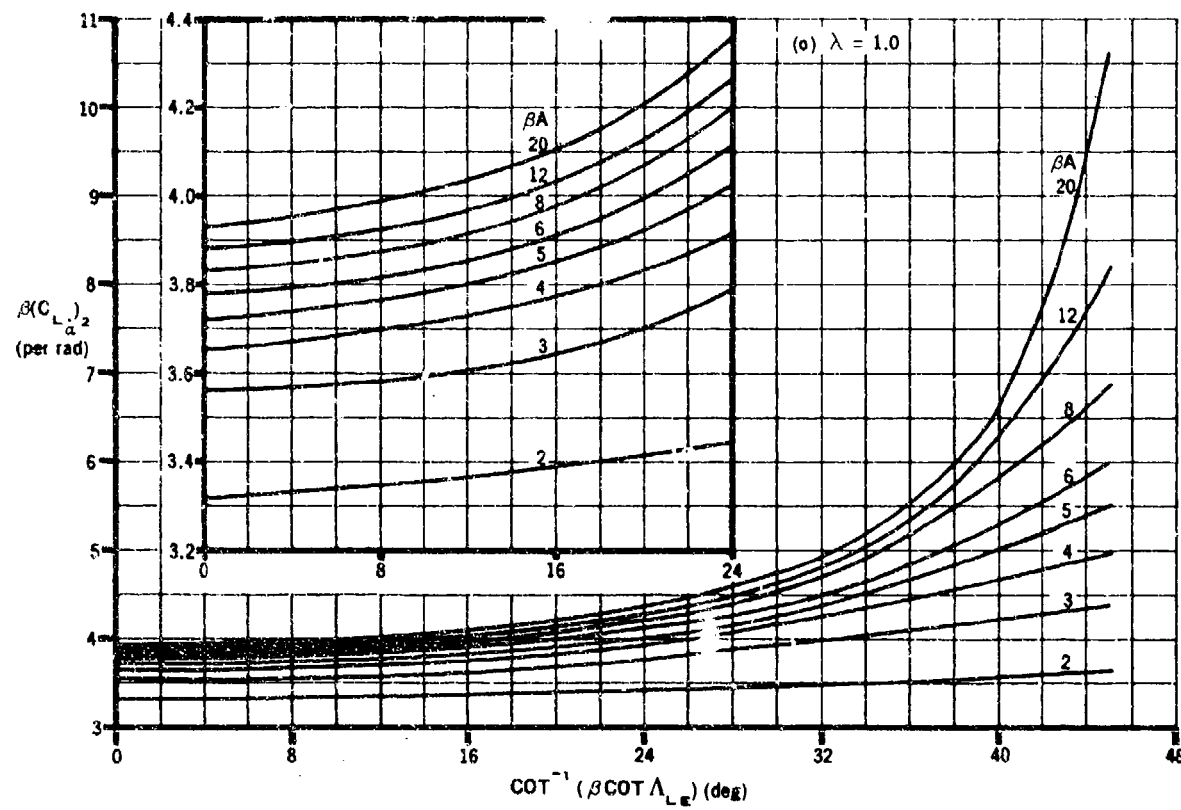


FIGURE 7.1.4.1-11 (CONTD)

7.1.4.2 WING ACCELERATION DERIVATIVE $C_{m\dot{\alpha}}$

Methods are presented for estimating the wing contribution to the derivative $C_{m\dot{\alpha}}$ for a triangular planform in the subsonic and low transonic speed ranges and for planforms with the leading edge swept back and the trailing edge swept back or swept forward in the supersonic speed range.

If the wing acceleration derivative $C_{m\dot{\alpha}}$ is to be used in method 1 of Section 7.3.4.2 to obtain $(C_{m\dot{\alpha}})_{WB}$, the exposed wing planform area should be used for all calculations in the Datcom methods. Using the exposed planform area will yield $C_{m\dot{\alpha}}$ based on the product of the exposed wing area and the square of the exposed wing MAC, rather than the product of the wing area and the square of the wing MAC as indicated.

DATCOM METHODS

A. SUBSONIC

The subsonic value of $C_{m\dot{\alpha}}$, based on the product of wing area and the square of wing MAC $S_w \bar{c}_w^2$, referred to body axis and for any center-of-gravity location is given by

$$C_{m\dot{\alpha}} = C_{m\dot{\alpha}}'' + \left(\frac{x_{c.g.}}{\bar{c}} \right) C_{L\dot{\alpha}} \quad (\text{per radian}) \quad 7.1.4.2-a$$

where

$C_{m\dot{\alpha}}''$ is referred to body axis with the origin at the wing leading-edge vertex and is obtained as indicated below (per radian).

$\frac{x_{c.g.}}{\bar{c}}$ is the longitudinal distance from the wing leading-edge vertex to the center of gravity, measured in mean aerodynamic chords, positive aft.

$C_{L\dot{\alpha}}$ is obtained from Section 7.1.4.1, based on the product of wing area and wing MAC (per radian).

A method of estimating the subsonic acceleration derivative $C_{m\dot{\alpha}}''$ of a triangular wing is derived in reference 1 as

$$C_{m\dot{\alpha}}'' = - \frac{81}{32} \left(\frac{x_{a.c.}}{c_t} \right)^2 C_{L\dot{\alpha}} + \frac{9}{2} C_{m_0}(g) \quad (\text{per radian}) \quad 7.1.4.2-b$$

where

$C_{L\alpha}$ is the wing lift-curve slope (Section 4.1.3.2) at the Mach number under consideration, based on the total wing area (per radian).

$\frac{x_{a.c.}}{c_r}$ is obtained from Section 4.1.4.2.

$C_{m_0}(g)$ is the pitching-moment-coefficient correction term obtained from figure 7.1.4.2-8 (per radian).

Because of restrictions placed on the pitching-moment-coefficient correction term, equation 7.1.4.2-b is valid only for $0 < \beta A < 4$.

Explicit expressions for estimating $C_{m\dot{\alpha}}$ of other wing planforms in the subsonic region are not available. An approximation may be made by subtracting the value of C_{m_q} (Section 7.1.1.2) from the appropriate test value of total pitch damping ($C_{m_q} + C_{m\dot{\alpha}}$) taken from table 7-A. Tests indicate that the relative importance of body damping of a conventional configuration in subsonic flow is small; therefore the use of wing-body test data of total pitch damping in this region is acceptable for an approximation, provided the test data are for a conventional design.

Sample Problem

Given: Same wing as in sample problem of paragraph A, Section 7.1.4.1

$$A = 4.0 \quad \lambda = 0 \quad \Lambda_{LE} = 45^\circ \quad C_{L\alpha} = 4.0 \text{ per rad} \quad (\text{Section 4.1.3.2})$$

$$\frac{x_{c.g.}}{\bar{c}} = 0.75 \quad (\text{from planform geometry with c.g. at } \bar{c}/4) \quad M = 0.6$$

From sample problem of paragraph A, Section 7.1.4.1

$$\frac{x_{a.c.}}{c_r} = 0.570 \quad \beta = 0.8 \quad \beta A = 3.20 \quad C_{L\dot{\alpha}} = -0.240 \text{ per rad}$$

Compute:

$$\frac{\beta^2 C_{m_0}(g)}{\pi A/2} = 0.071 \text{ per rad} \quad (\text{figure 7.1.4.2-8})$$

$$C_{m_0}(g) = 0.697 \text{ per rad}$$

Solution:

$$\begin{aligned}
 C_{m\dot{\alpha}}'' &= -\frac{81}{32} \left(\frac{x_{a.c.}}{c_r} \right)^2 C_{L\dot{\alpha}} + \frac{9}{2} C_{m_0}(g) \quad (\text{equation 7.1.4.2-b}) \\
 &= -\frac{81}{32} (0.570)^2 (4.0) + \frac{9}{2} (0.697) \\
 &= -0.153 \text{ per rad}
 \end{aligned}$$

$$\begin{aligned}
 C_{m\dot{\alpha}} &= C_{m\dot{\alpha}}'' + \left(\frac{x_{c.g.}}{c} \right) C_{L\dot{\alpha}} \quad (\text{equation 7.1.4.2-a}) \\
 &= -0.153 + (0.75)(-0.240) \\
 &= -0.333 \text{ per rad (based on } S_w \bar{c}_w^2)
 \end{aligned}$$

B. TRANSONIC

The variation of $C_{m\dot{\alpha}}$ of a triangular wing from the critical Mach number to $M = 1.0$ is given by the method of paragraph A, provided $0 < \beta A < 4$.

There is no generalized theory available in the literature that gives the transonic values of $C_{m\dot{\alpha}}$, either for additional wing-geometry parameters or for Mach numbers greater than 1.0. An approximation may be made by subtracting the value of C_{m_q} (Section 7.1.1.2) from the appropriate test value of total pitch damping ($C_{m_q} + C_{m\dot{\alpha}}$) taken from table 7-A. Although the importance of body damping in this region is unknown because of a lack of experimental data, wing-body test data of total pitch damping will probably have to be utilized if an approximation of $C_{m\dot{\alpha}}$ is to be made, simply because of the lack of sufficient wing-alone test data. This method of analysis gives only a rough approximation and is limited to conventional designs where test data are available.

C. SUPERSONIC

The supersonic value of $C_{m\dot{\alpha}}$, based on the product of wing area and the square of wing MAC $S_w \bar{c}_w^2$, referred to body axis and for any center-of-gravity location, is given by equation 7.1.4.2-a, i.e.,

$$C_{m\dot{\alpha}} = C_{m\dot{\alpha}}'' + \left(\frac{x_{c.g.}}{c} \right) C_{L\dot{\alpha}} \quad (\text{per radian})$$

where the parameters are defined in paragraph A and the supersonic value of $C_{m\dot{\alpha}}''$ is obtained as indicated below.

Methods for estimating $C_{m\dot{\alpha}}''$

1. Wings with subsonic leading edges ($\beta \cot \Lambda_{LE} < 1.0$)

For wings with subsonic leading edges, $C_{m\dot{\alpha}}''$ is obtained by the method of reference 2 for $\lambda = 0$ and by the method of reference 3 for $\lambda = 0.25$ to 1.0. The following methods are not valid if the Mach line from the vertex of the trailing edge intersects the leading edge or if the wing-tip Mach lines intersect on the wings or intersect the opposite wing tips.

a. Zero-taper-ratio wings ($\lambda = 0$)

$C_{m\dot{\alpha}}''$ is derived in reference 2 as

$$C_{m\dot{\alpha}}'' = - \frac{3\pi AM^2}{16\beta^2} \left[G(\beta C) F_7(N) + \frac{16}{3} E''(\beta C) \frac{F_5(N)}{F_{11}(N)} \right] \\ + \frac{16AM^2}{9\beta^2} [E''(\beta C) F_8(N)] + \frac{\pi A}{16\beta^2} [E''(\beta C) F_6(N)] - \left(\frac{d}{c} \right) C_{L\dot{\alpha}}$$

(per radian) 7.1.4.2-c

where

$E''(\beta C)$ and $G(\beta C)$ are obtained from figure 7.1.1.1-8.

$F_5(N)$, $F_7(N)$, and $F_{11}(N)$ are obtained from figure 7.1.1.2-8.

$F_6(N)$ and $F_8(N)$ are obtained from figure 7.1.4.2-9.

d is two-thirds the basic triangular wing root chord, $d = \frac{2}{3} c_{r_B}$ (see sketch (a), Section 7.1.1.1).

$C_{L\dot{\alpha}}$ is obtained from paragraph C of Section 7.1.4.1, based on the product of wing area and wing MAC.

b. Wings with $\lambda = 0.25$ to 1.0

$C_{m\dot{\alpha}}''$ is derived in reference 3 as

$$C_{m\dot{\alpha}}'' = \frac{M^2}{\beta^2} (C_{m\dot{\alpha}})_1 - \frac{1}{\beta^2} (C_{m\dot{\alpha}})_2 \quad (\text{per radian}) \quad 7.1.4.2-d$$

where

$(C_m \dot{\alpha})_1$ and $(C_m \dot{\alpha})_2$ are obtained from figures 7.1.4.2-10a through 7.1.4.2-10f for $\lambda = 0.25, 0.50$, and 0.75 and from the equations of reference 3 for $\lambda > 0.75$.

2. Wings with supersonic leading edges ($\beta \cot \Lambda_{LE} > 1.0$)

For wings with supersonic leading edges $C_m \ddot{\alpha}$ is derived in reference 4 as

$$C_m \ddot{\alpha} = \frac{M^2}{\beta^2} (C_m \dot{\alpha})_1 + \left(\frac{M^2}{\beta^2} + 1 \right) (C_m \dot{\alpha})_2 \text{ (per radian)} \quad 7.1.4.2-e$$

where

$(C_m \dot{\alpha})_1$ and $(C_m \dot{\alpha})_2$ are obtained from figures 7.1.4.2-13a through 7.1.4.2-13p.

Figures 7.1.4.2-13a through 7.1.4.2-13p are valid for the range of Mach numbers for which the Mach lines from the leading-edge vertex intersect the trailing edge. An additional limitation is that the foremost Mach line from either wing tip may not intersect the remote half-wing.

Sample Problems

1. Wing with subsonic leading edge

Given: Same wing as in sample problem 1 of paragraph C, Section 7.1.4.1.

$$A = 5.80 \quad \lambda = 0 \quad \Lambda_{LE} = 60^\circ \quad \text{c.g. at } \frac{\bar{c}}{4} \quad b = 16 \text{ ft} \quad M = 1.50$$

$$\frac{x_{\text{c.g.}}}{\bar{c}} = 1.50 \text{ (from planform geometry with c.g. at } \bar{c}/4)$$

From sample problem 1 of paragraph C, Section 7.1.4.1:

$$\beta = 1.12$$

$$\beta \cot \Lambda_{LE} = 0.647$$

$$N = 0.602$$

$$E''(\beta C) = 0.770$$

$$G(\beta C) = 0.570$$

$$C_{L\dot{\alpha}} = -5.02 \text{ per rad}$$

Compute:

$$\left. \begin{array}{l} F_5(N) = 0.251 \\ F_7(N) = -1.620 \\ F_{11}(N) = 0.395 \end{array} \right\} \text{(figure 7.1.1.2-8)}$$

$$\left. \begin{array}{l} F_6(N) = -2.600 \\ F_8(N) = 0.880 \end{array} \right\} \text{(figure 7.1.4.2-9)}$$

Obtain d from the characteristics of the basic triangular wing (see sketch (a), Section 7.1.1.1).

$$A_B = \frac{4}{\tan \Lambda_{LE}} = 2.31$$

$$c_{rB} = \frac{2b}{A_B} = 13.85 \text{ ft}$$

$$d = \frac{2}{3} c_{rB} = 9.233 \text{ ft}$$

$$c_r = \frac{2b}{A} = 5.517 \text{ ft}$$

$$\bar{c} = 3.678 \text{ ft}$$

Solution:

$$\begin{aligned} C_m'' &= -\frac{3\pi AM^2}{16\beta^2} \left[G(\beta C) F_7(N) + \frac{16}{3} E''(\beta C) \frac{F_5(N)}{F_{11}(N)} \right] \\ &\quad + \frac{16AM^2}{9\beta^2} [E''(\beta C) F_8(N)] + \frac{\pi A}{16\beta^2} [E''(\beta C) F_6(N)] - \left(\frac{d}{\bar{c}} \right) C_L \dot{\alpha} \\ &= -\frac{3\pi(5.80)(2.25)}{16(1.25)} \left[(0.570)(-1.620) + \frac{16}{3} (0.770) \frac{(0.251)}{(0.395)} \right] \\ &\quad + \frac{16(5.80)(2.25)}{9(1.25)} [(0.770)(0.880)] + \frac{\pi(5.80)}{16(1.25)} [(0.770)(-2.600)] \\ &\quad - \frac{(9.233)}{(3.678)} (-5.02) \end{aligned} \quad (\text{equation 7.1.4.2-c})$$

$$\begin{aligned}
 &= -6.15(-0.9234 + 2.610) + 12.576 - 1.824 + 12.602 \\
 &= 12.98 \text{ per rad}
 \end{aligned}$$

$$\begin{aligned}
 C_{m\dot{\alpha}}'' &= C_{m\dot{\alpha}}'' + \frac{x_{c.g.}}{\bar{c}} C_{L\dot{\alpha}} \quad (\text{equation 7.1.4.2-a}) \\
 &= 12.98 + (1.5)(-5.02) \\
 &= 5.45 \text{ per rad (based on } S_w \bar{c}_w^2)
 \end{aligned}$$

2. Wing with supersonic leading edge

Given: Same wing as in sample problem 2 of paragraph C, Section 7.1.4.1.

$$A = 4.0 \quad \lambda = 0.25 \quad \Lambda_{LE} = 45^\circ \quad \text{c.g. at } \frac{\bar{c}}{4} \quad M = 2.0$$

$$\frac{x_{c.g.}}{\bar{c}} = 0.964 \text{ (from planform geometry with c.g. at } \bar{c}/4)$$

From sample problem 2 of paragraph C, Section 7.1.4.1:

$$\beta = 1.732 \quad \beta A = 6.928 \quad \beta \cot \Lambda_{LE} = 1.732$$

$$\cot^{-1}(\beta \cot \Lambda_{LE}) = 30^\circ \quad C_{L\dot{\alpha}} = -1.108 \text{ per rad}$$

Compute:

$$\beta (C_{m\dot{\alpha}})_1 = 11.80 \text{ per rad (figure 7.1.4.2-13d)}$$

$$(C_{m\dot{\alpha}})_1 = 6.813 \text{ per rad}$$

$$\beta (C_{m\dot{\alpha}})_2 = -5.530 \text{ per rad (figure 7.1.4.2-13f)}$$

$$(C_{m\dot{\alpha}})_2 = -3.193 \text{ per rad}$$

Solution:

$$C_{m\dot{\alpha}}'' = \frac{M^2}{\beta^2} (C_{m\dot{\alpha}})_1 + \left(\frac{M^2}{\beta^2} + 1 \right) (C_{m\dot{\alpha}})_2 \quad (\text{equation 7.1.4.2-e})$$

$$\begin{aligned}
 &= \frac{4}{3} (6.813) + \left(\frac{4}{3} + 1 \right) (-3.193) \\
 &= 9.08 - 7.45 \\
 &= 1.63 \text{ per rad}
 \end{aligned}$$

$$\begin{aligned}
 C_{m\dot{\alpha}} &= C_{m\dot{\alpha}}'' + \frac{x_{c.g.}}{\bar{c}} C_{L\dot{\alpha}} \quad (\text{equation 7.1.4.2-a}) \\
 &= 1.63 + (0.964) (-1.108) \\
 &= 0.562 \text{ per rad (based on } S_w \bar{c}_w^2 \text{)}
 \end{aligned}$$

REFERENCES

1. Tobak, M., and Lessing, H. C.: Estimation of Rotary Stability Derivatives at Subsonic and Transonic Speeds. AGARD Report 343, 1961. (U)
2. Malvestuto, F. S., Jr., and Margolis, K.: Theoretical Stability Derivatives of Thin Sweptback Wings Tapered to a Point with Sweptback or Sweptforward Trailing Edges for a Limited Range of Supersonic Speeds. NACA TR 971, 1950. (U)
3. Malvestuto, F. S., Jr., and Hoover, D. M.: Supersonic Lift and Pitching Moment of Thin Sweptback Tapered Wings Produced by Constant Vertical Acceleration. Subsonic Leading Edges and Supersonic Trailing Edges. NACA TN 2315, 1951. (U)
4. Cole, I. J., and Margolis, K.: Lift and Pitching Moment at Supersonic Speeds due to Constant Vertical Acceleration for Thin Sweptback Tapered Wings with Streamwise Tips. Supersonic Leading and Trailing Edges. NACA TN 3196, 1954. (U)

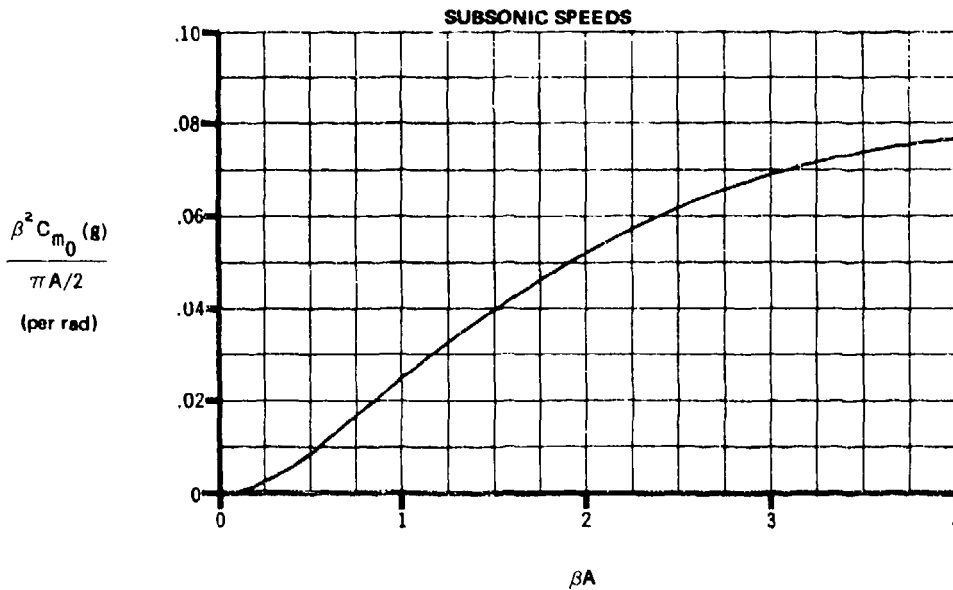


FIGURE 7.1.4.2-8 VARIATION OF PITCHING-MOMENT COEFFICIENT CORRECTION TERM WITH βA .
TRIANGULAR WING $0 < \beta A \leq 4$.

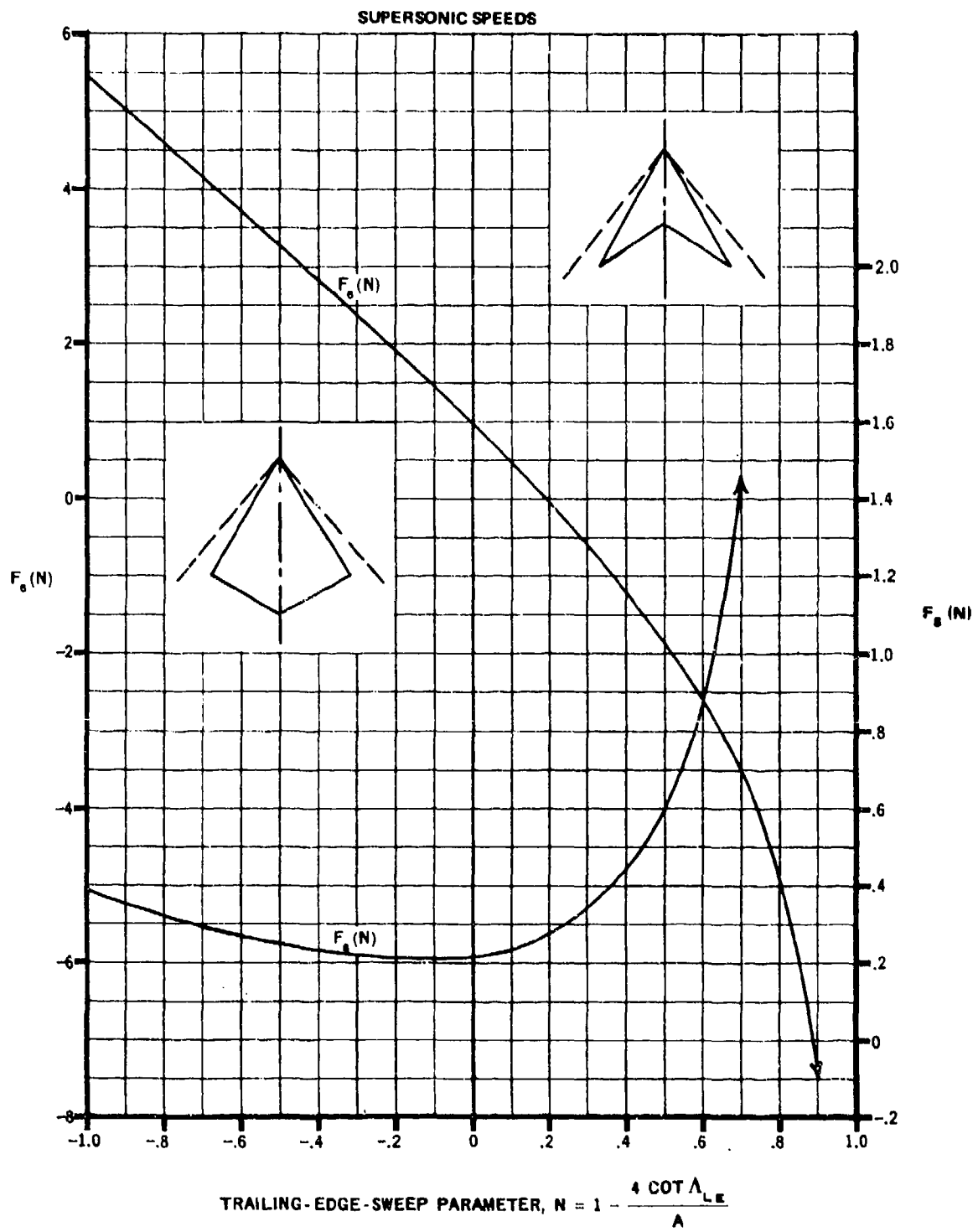


FIGURE 7.1.4.2-9 $F(N)$ FACTORS OF THE STABILITY DERIVATIVE

SUPersonic SPEEDS

SUBSONIC LEADING EDGE

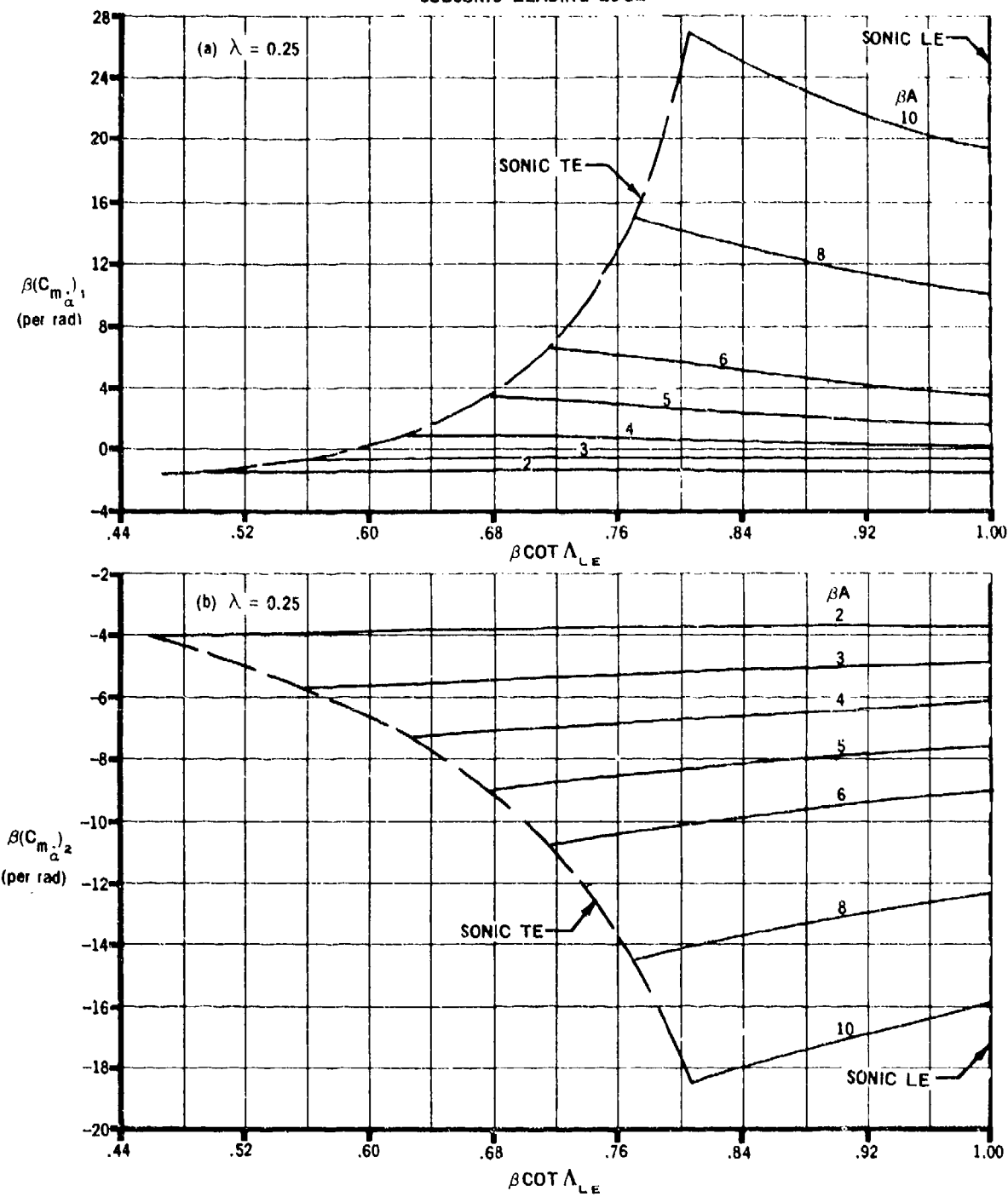


FIGURE 7.1.4.2-10 VARIATION OF $\beta(C_m)_1$ AND $\beta(C_m)_2$ WITH $\beta \cot \Lambda_{LE}$

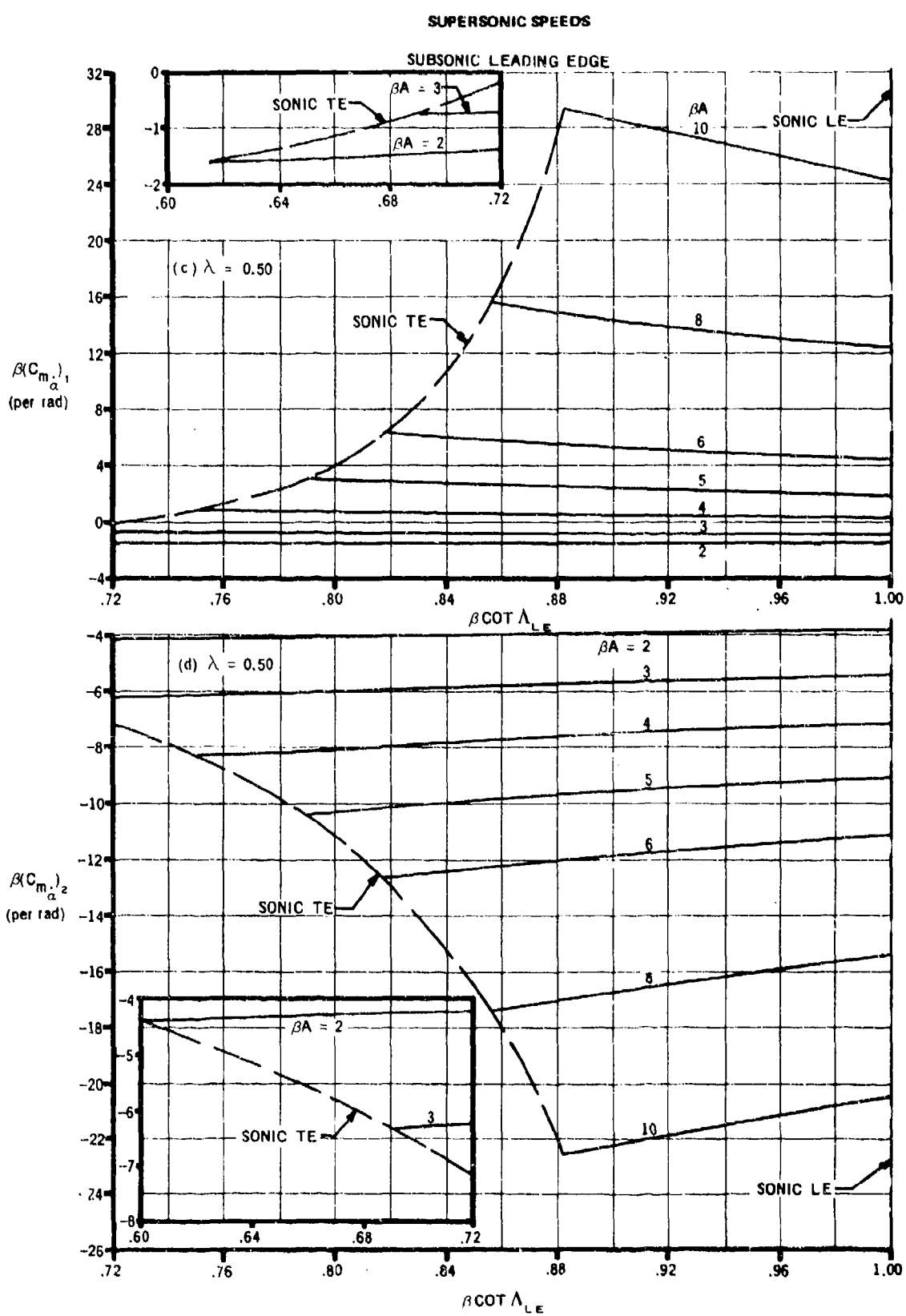


FIGURE 7.1.4.2-10 (CONT'D)

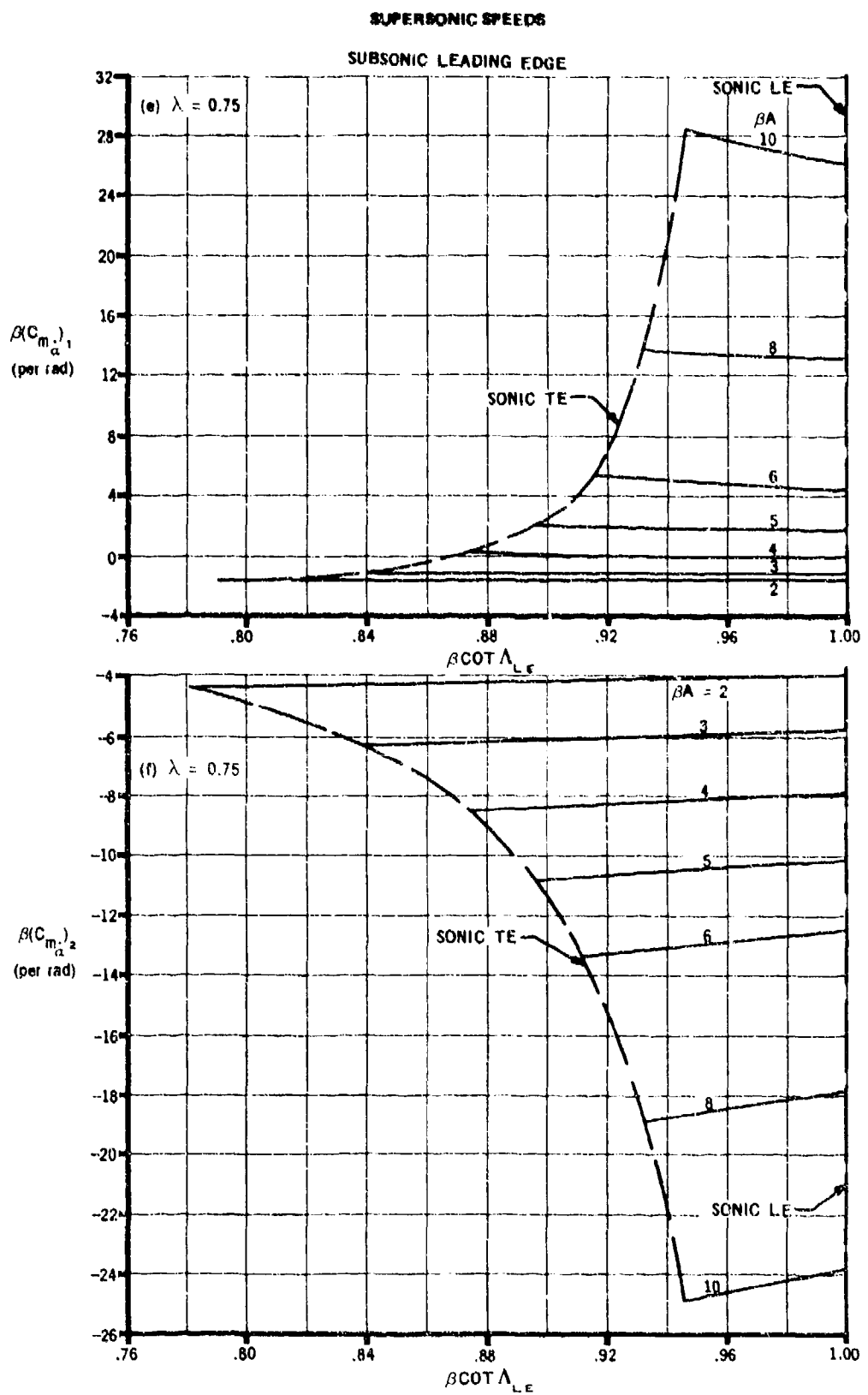


FIGURE 7.1.4.2-10 (CONTD)

7.1.4.2-12

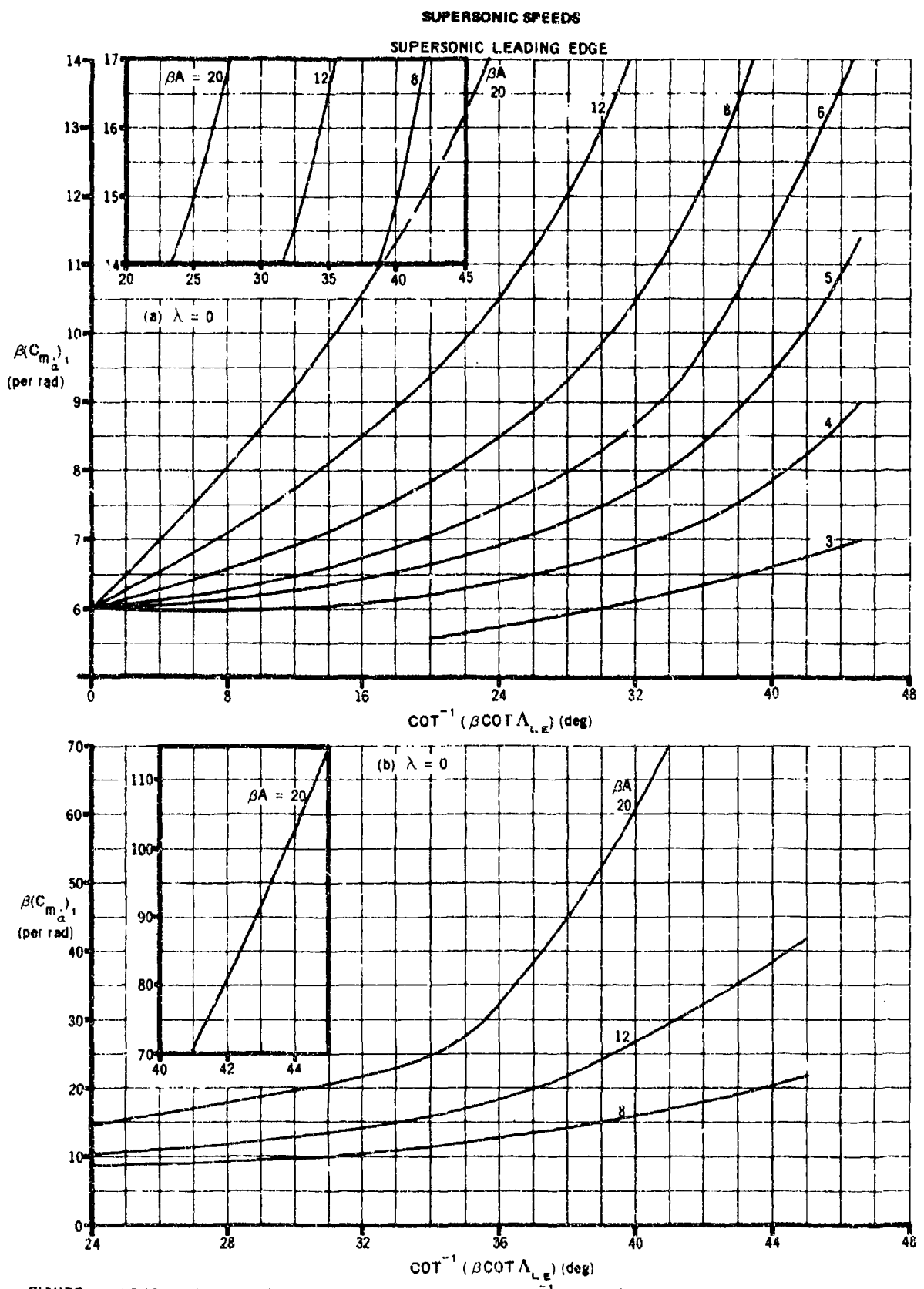


FIGURE 7.1.4.2-13 VARIATION OF $\beta(C_{m\alpha})_1$ AND $\beta(C_{m\alpha})_2$ WITH $\cot^{-1}(\beta \cot \Lambda_{LE})$

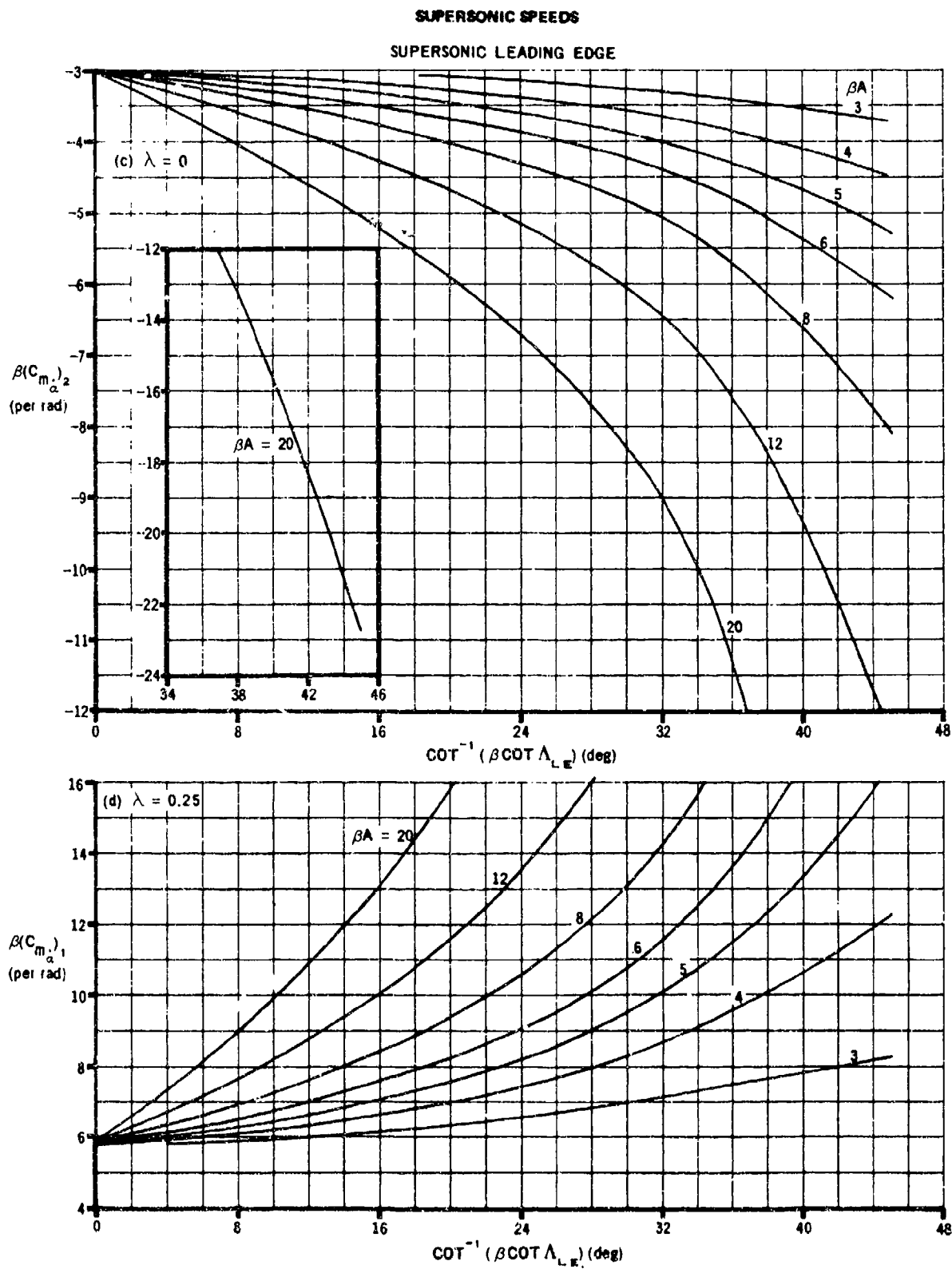


FIGURE 7.1.4.2-13 (CONT'D)

SUPersonic SPEEDS

SUPersonic LEADING EDGE

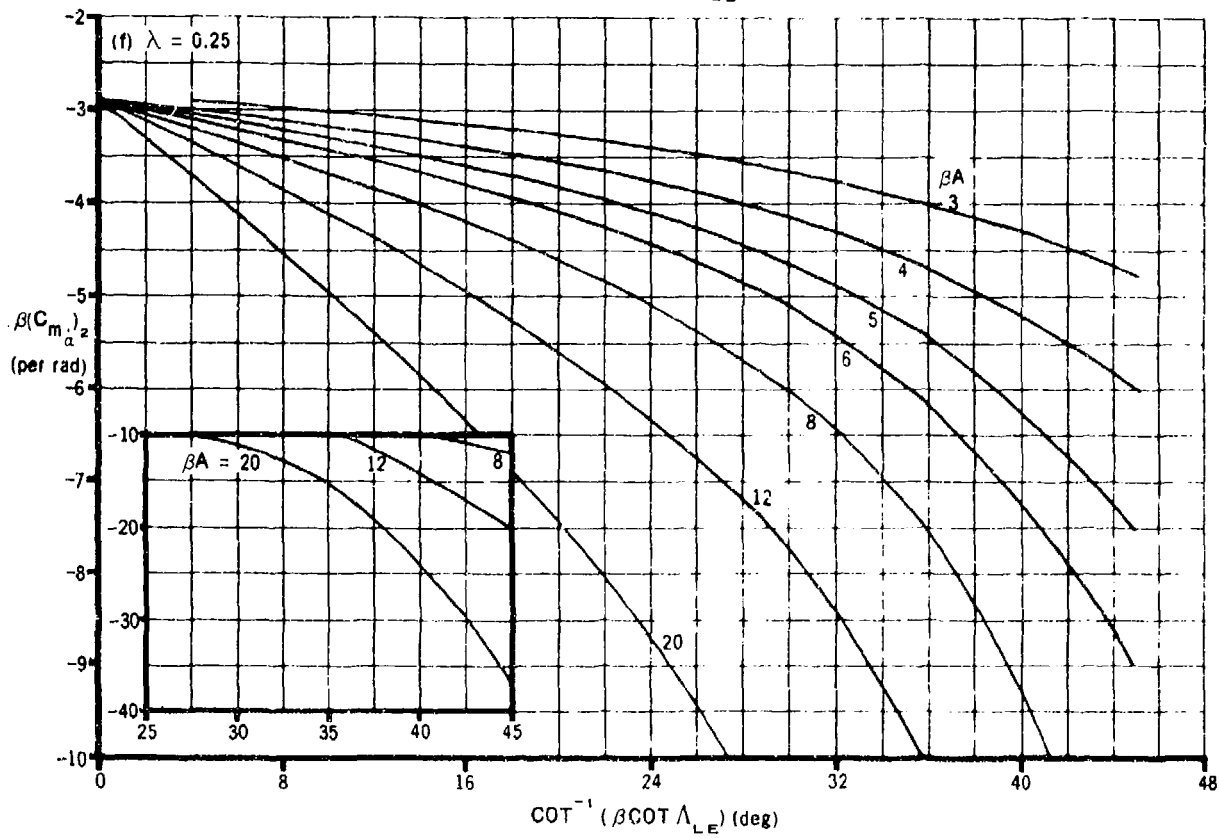
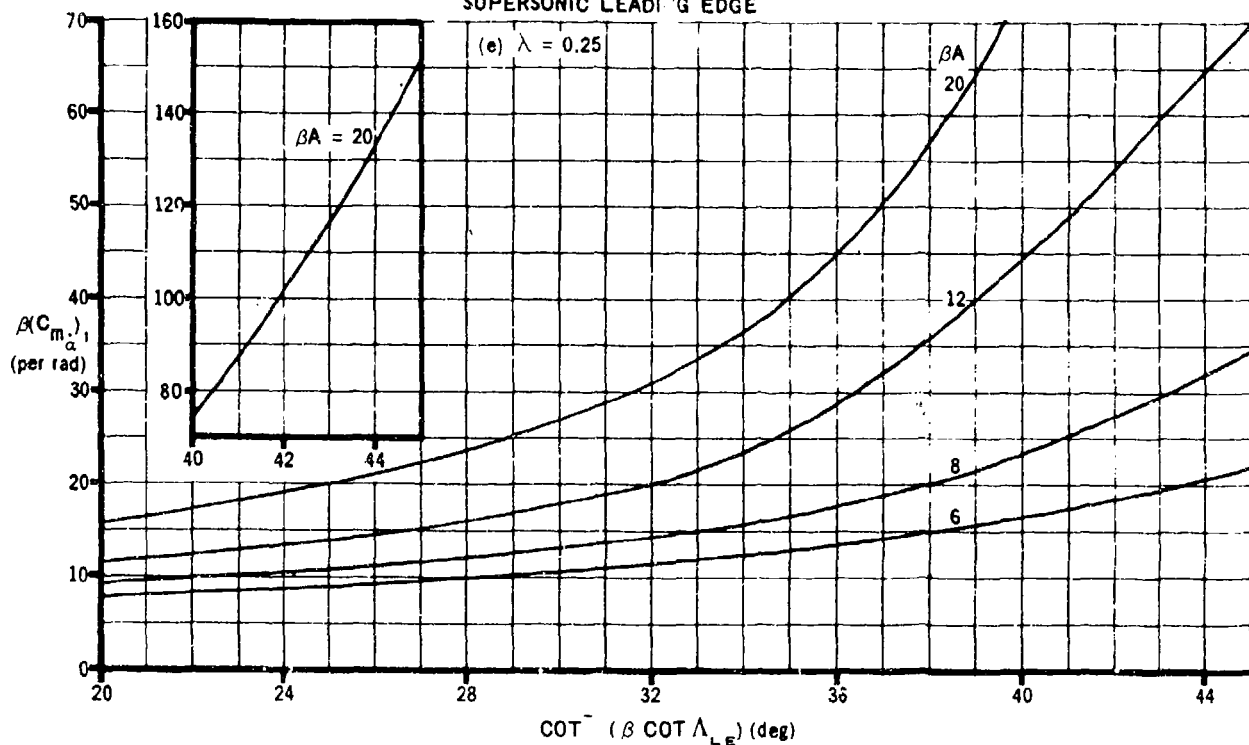


FIGURE 7.1.4.2-13 (CONTD)

SUPersonic SPEEDS

SUPersonic LEADING EDGE

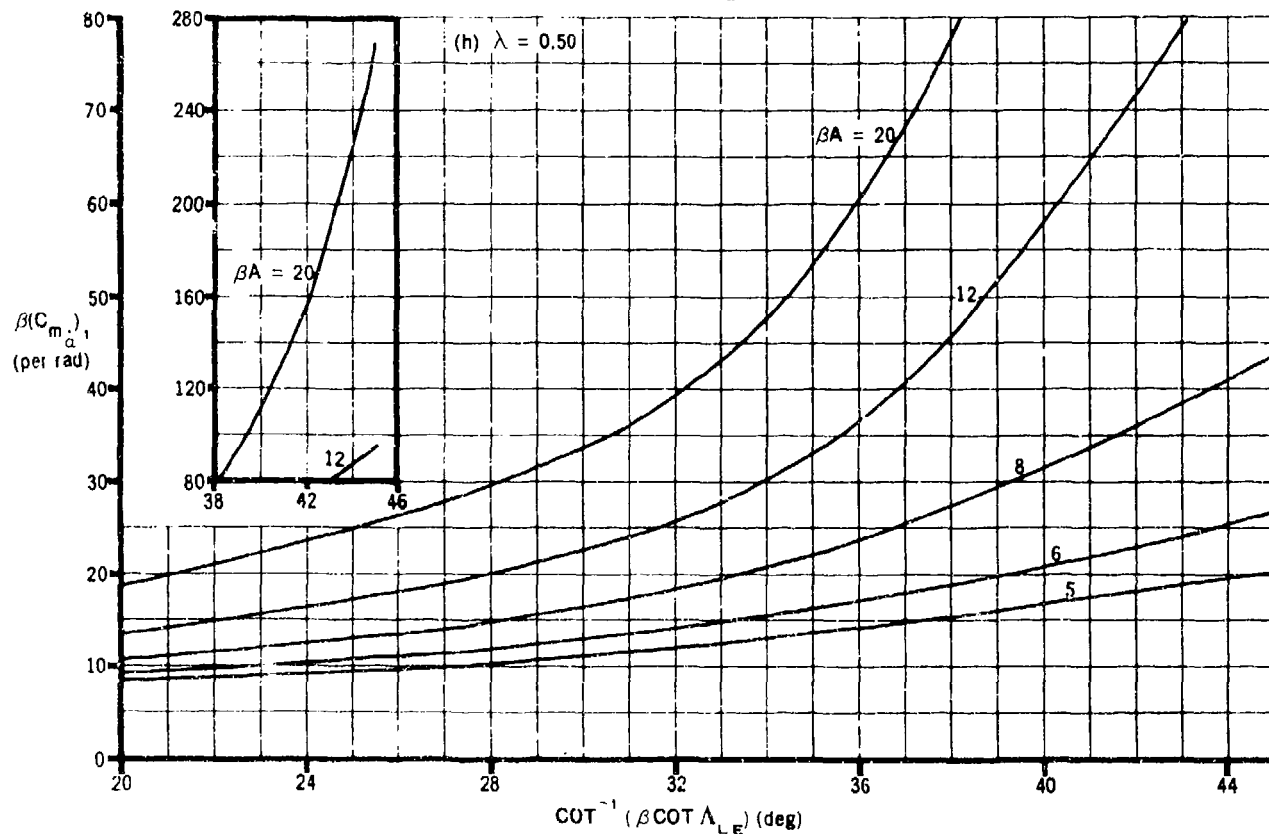
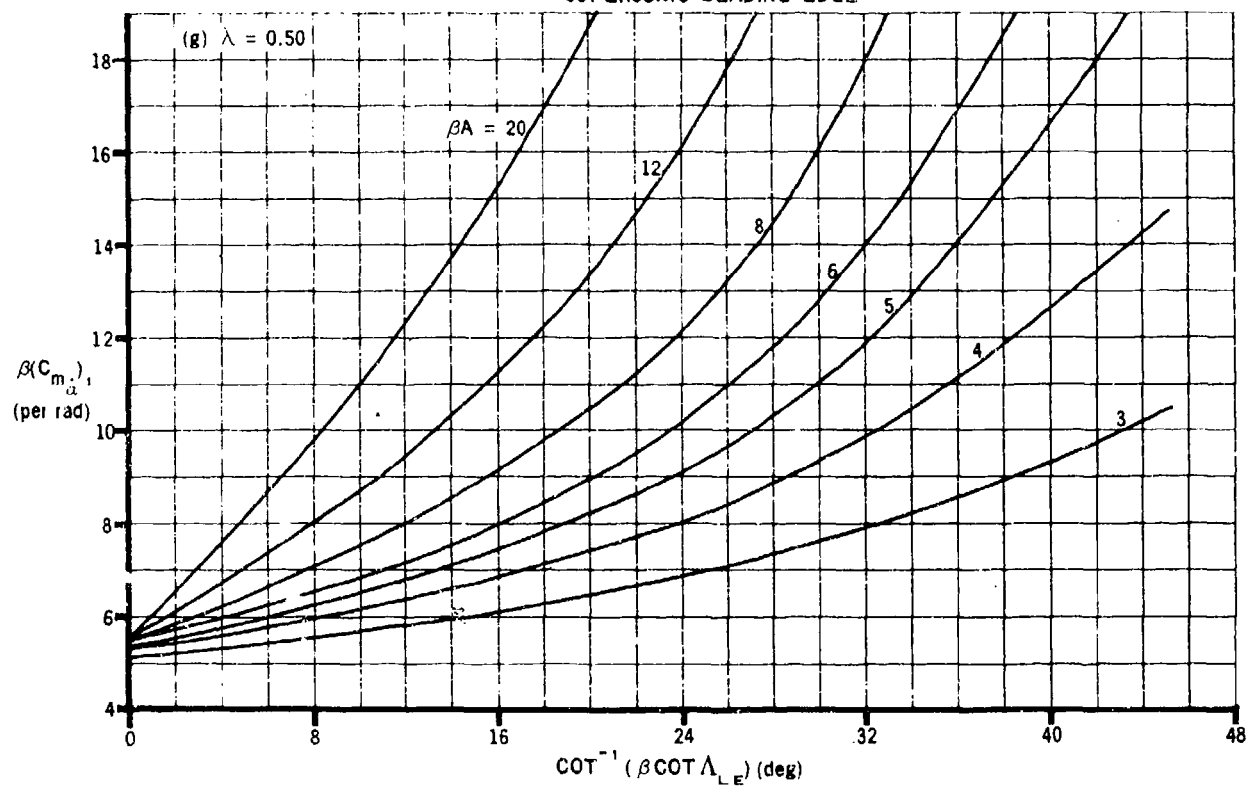


FIGURE 7.1.4.2-13 (CONTD)

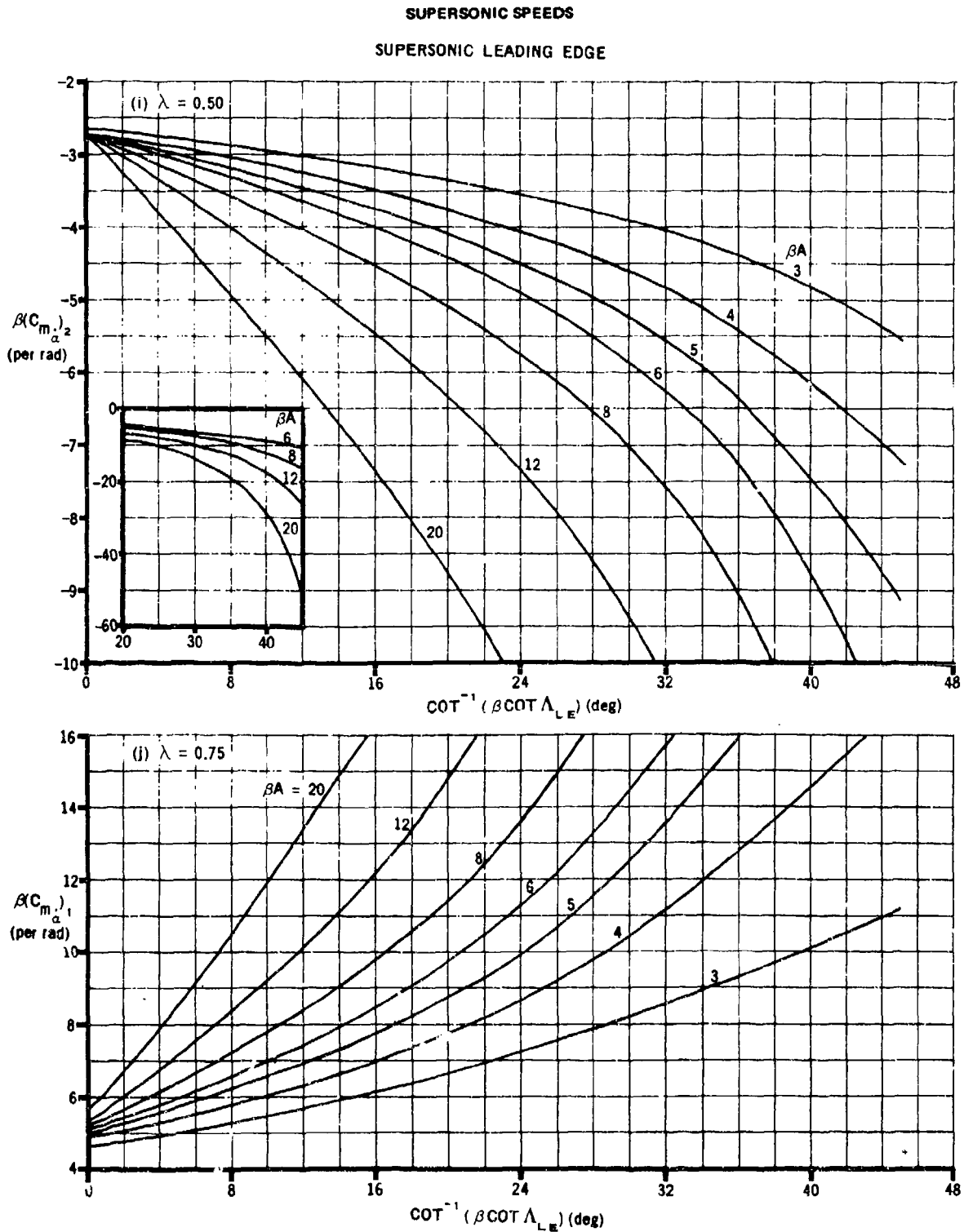


FIGURE 7.1.4.2-13 (CONTD)

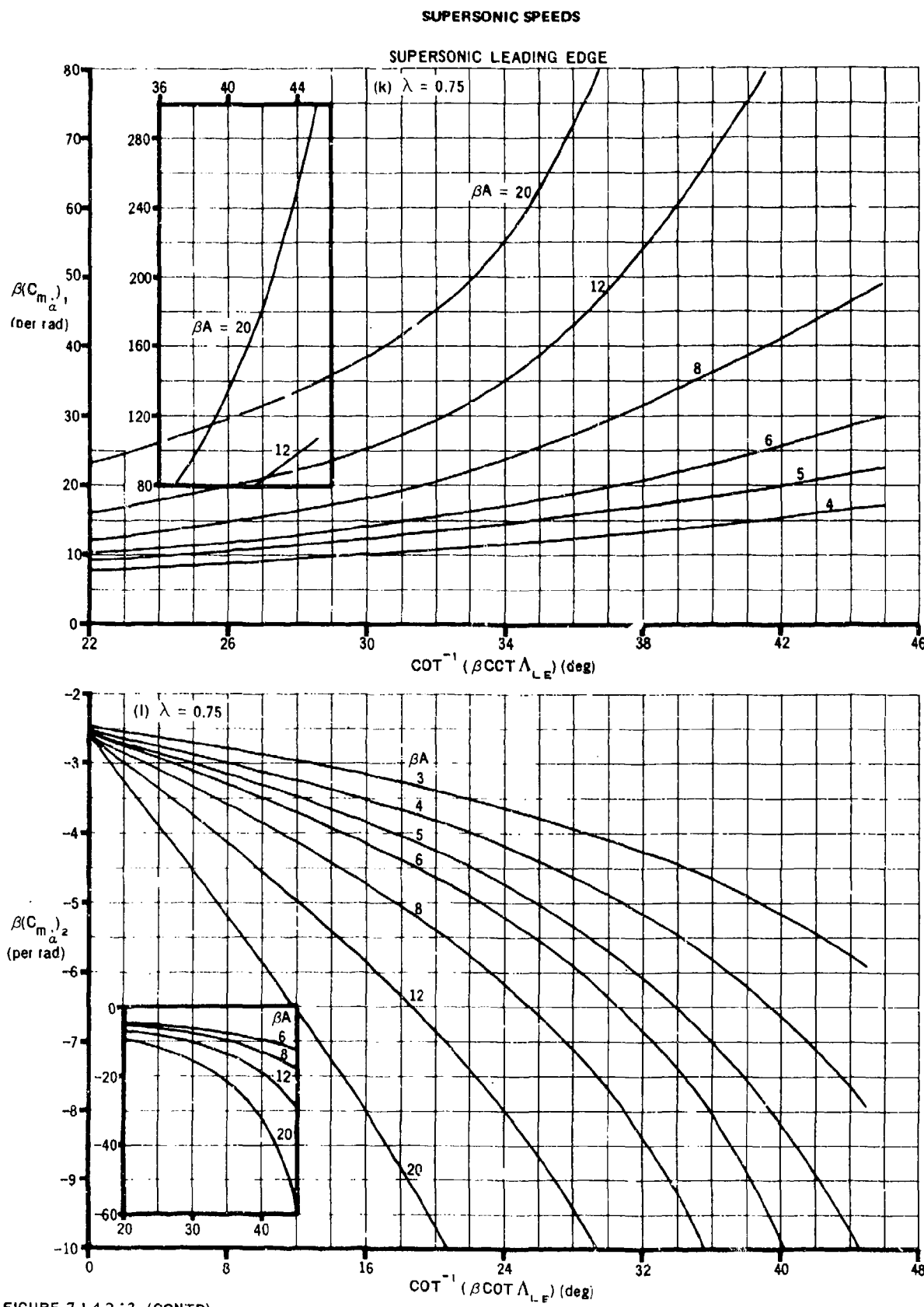


FIGURE 7.1.4.2-13 (CONT'D)

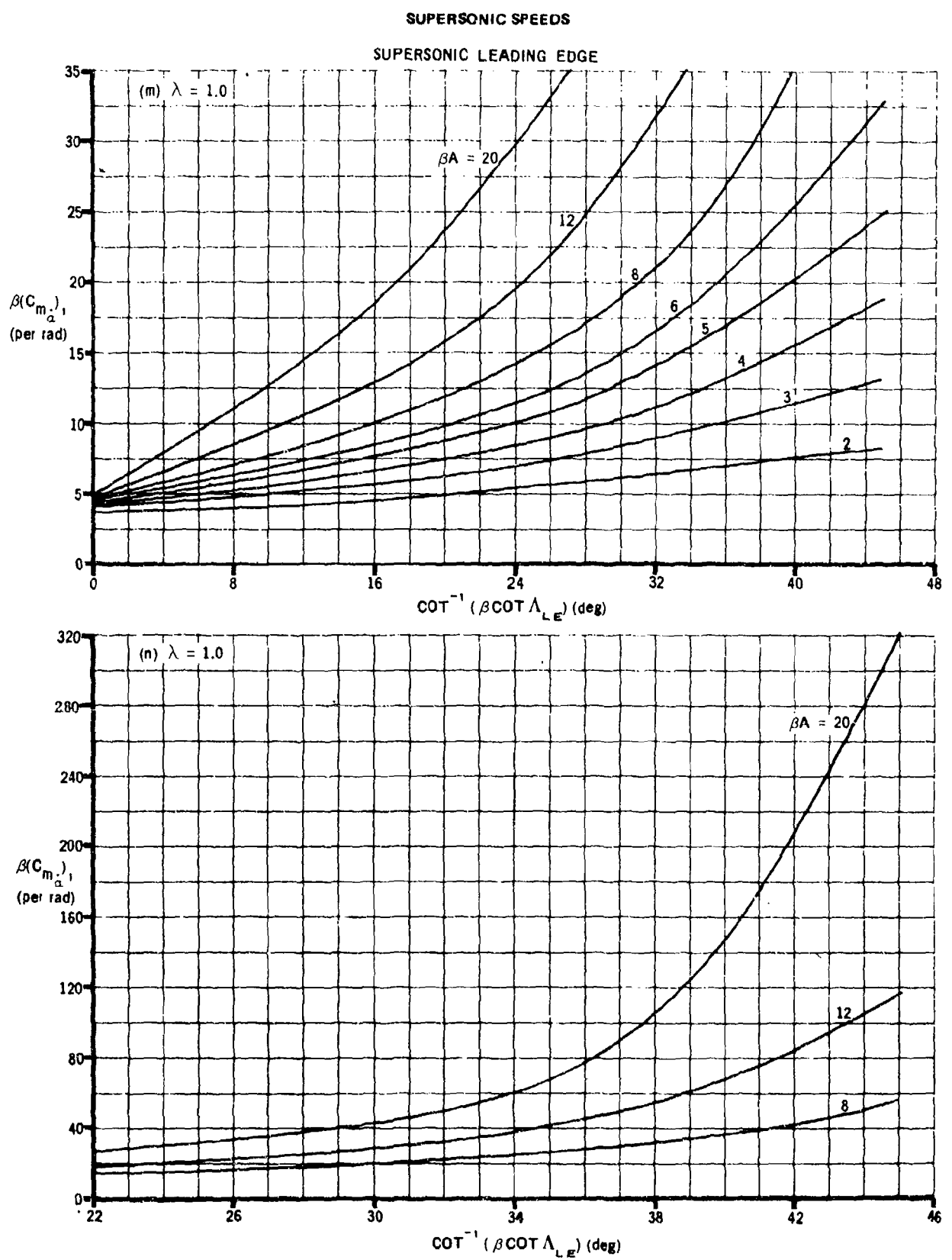


FIGURE 7.1.4.2-13 (CONT'D)

SUPersonic SPEEDS

SUPersonic LEADING EDGE

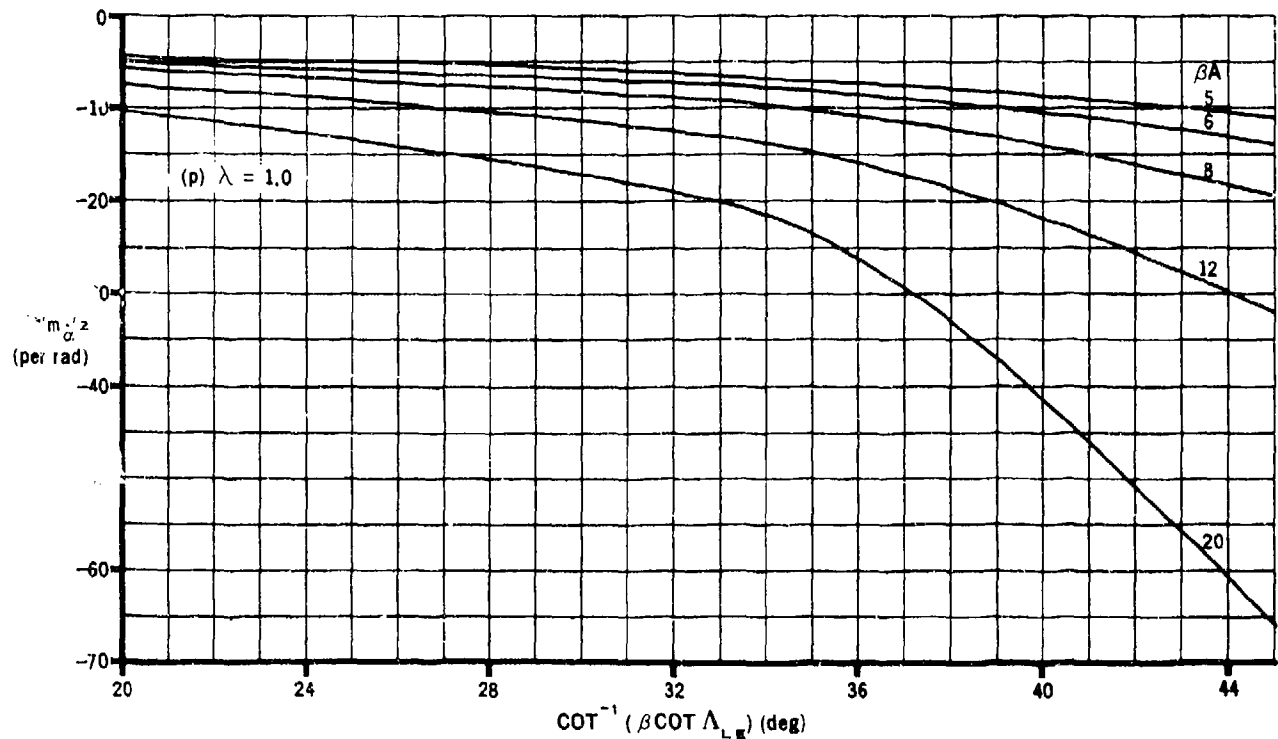
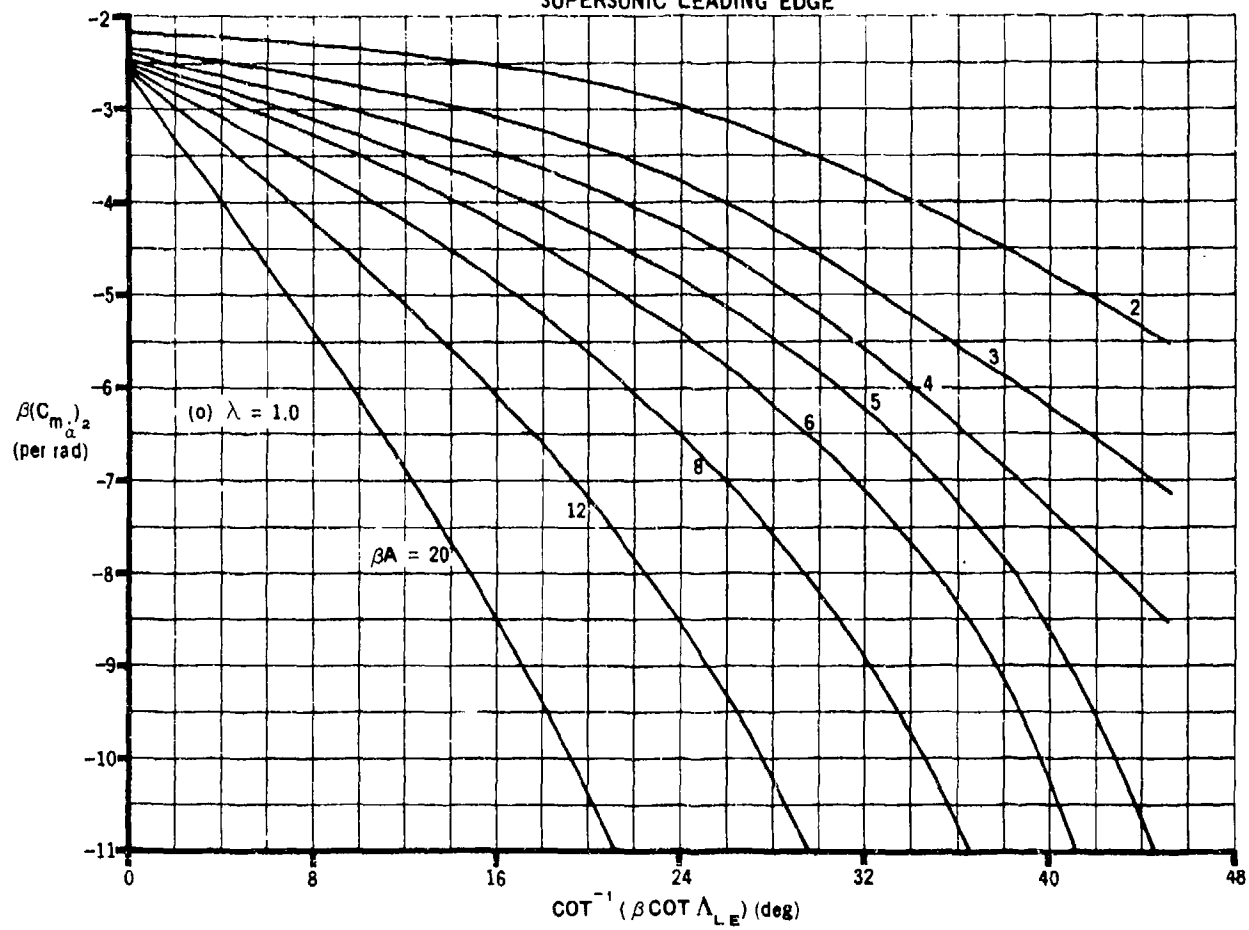


FIGURE 7.1.4.2-13 (CONT'D)

7.1.4.3 WING DERIVATIVE $C_{D\dot{\alpha}}$

This section presents a method for estimating the wing contribution to the derivative $C_{D\dot{\alpha}}$ at subsonic speeds. This derivative is the change in drag coefficient due to a change in $\dot{\alpha}$ at a constant pitch rate and is defined as

$$C_{D\dot{\alpha}} = \frac{\partial C_D}{\partial \left(\frac{\dot{\alpha}c}{2V} \right)}, \text{ where } C_D \text{ is based on } S_W.$$

In general, this derivative is small and has a negligible effect on longitudinal stability; hence, it is usually neglected.

A. SUBSONIC

DATCOM METHOD

From the two-dimensional unsteady-flow theory of Garrick (Reference 1), the perturbation section drag coefficient of an oscillating surface can be approximated by

$$c_d = \frac{\pi}{2} c \frac{1}{V} [1 + 2C(k)] \alpha \dot{\alpha} \quad 7.1.4.3-a$$

where

c_d is the drag coefficient per unit span.

c is the wing chord.

V is the free-stream velocity

$C(k)$ is Theodorsen's function, defined as

$$C(k) = F(k) + iG(k) \quad 7.1.4.3-b$$

where

$F(k), G(k)$ are Theodorsen's functions obtained from Table 7.1.4.3-A as a function of the reduced frequency k , where k is defined as

$$k = \frac{\omega c}{2V} \quad 7.1.4.3-c$$

where c and V are as defined above, and ω is the angular velocity (rad/sec)

Only one part of the complex equation is needed. It is arbitrary whether to use the real or imaginary part. If the wing oscillation can be defined as

$$\alpha = \alpha_1 e^{i\omega t} = \alpha_1 \cos \omega t + i\alpha_1 \sin \omega t$$

7.1.4.3-d

where

α is the complex form of the angle of attack of oscillation

α_1 is the amplitude of the oscillation (radians)

t is the time

then by substitution and expansion the imaginary part of Equation 7.1.4.3-a can be shown to be equal to the following:

$$c_d = \frac{\pi c}{2 V} \alpha_1^2 \omega \left\{ (1 + 2F)(\cos^2 \omega t - \sin^2 \omega t) - 4G \sin \omega t \cos \omega t \right\}^* \quad 7.1.4.3-e$$

7.1.4.3-e

where all the terms are defined above and where the oscillation is given by $\alpha = \alpha_1 \sin \omega t$.

The three-dimensional drag may be obtained by

$$C_D = 2 \int_0^{b/2} \frac{c_d c}{S_W} dy \quad 7.1.4.3-f$$

7.1.4.3-f

where

c_d is the two-dimensional drag from Equation 7.1.4.3-e.

c is the local wing chord.

S_W is the wing reference area.

If the derivative $C_{D\dot{\alpha}}$ is desired, variations in C_D may be calculated for different values of $\dot{\alpha}$. For α as defined by Equation 7.1.4.3-d, the imaginary part of $\dot{\alpha}$ (to be used in conjunction with Equation 7.1.4.3-e) may be expressed as

$$\dot{\alpha} = \alpha_1 \omega \cos \omega t$$

7.1.4.3-g

where the terms are defined above.

*The expression in brackets could also be written as $[(1 + 2F) \cos 2\omega t - 2G \sin 2\omega t]$, which would indicate that c_d varies at twice the angular velocity.

Then $C_{D\dot{\alpha}}$ may be approximated by

$$C_{D\dot{\alpha}} = \frac{\partial C_D}{\partial \left(\frac{\dot{\alpha}c}{2V} \right)} = \frac{(C_D)_{t_2} - (C_D)_{t_1}}{[(\dot{\alpha})_{t_2} - (\dot{\alpha})_{t_1}] \frac{c}{2V}} \quad 7.1.4.3-h$$

where

C_D is the three-dimensional drag coefficient obtained by application of Equation 7.1.4.3-f

$\dot{\alpha}$ is the rate of change of angle of attack obtained by application of Equation 7.1.4.3-g

and the subscript t_n refers to a specified time such that $t_2 - t_1$ is the time interval over which C_D and $\dot{\alpha}$ are evaluated.

Sample Problem

Given: The following wing-body combination

Wing Characteristics:

$$A = 4 \quad \Lambda = 0 \quad \lambda = 1.0 \quad S_W = 64.0 \text{ ft}^2 \quad c = 4.0 \text{ ft}$$

Additional Characteristics:

$$V = 200 \text{ ft/sec} \quad \omega = 2\pi \text{ rad/sec}$$

$$\alpha = \alpha_1 (\cos \omega t + i \sin \omega t) \quad \alpha_1 = 1^\circ$$

Compute c_d at $t = 1 \text{ sec}$:

Find the reduced frequency k

$$k = \frac{\omega c}{2V} \quad (\text{Equation 7.1.4.3-c})$$

$$= \frac{(2\pi)(4.0)}{2(200)}$$

$$= 0.0628 \text{ rad}$$

$$\begin{aligned} F &= 0.8875 \\ G &= -0.1451 \end{aligned} \quad \text{Table 7.1.4.3-A (linear interpolation)}$$

$$c_d = \frac{\pi}{2} \frac{c}{V} \alpha_1^2 \omega \left\{ (1 + 2F)(\cos^2 \omega t - \sin^2 \omega t) - 4G \sin \omega t \cos \omega t \right\} \quad (\text{Equation 7.1.4.3-e})$$

$$\begin{aligned}
&= \frac{\pi}{2} \left(\frac{4.0}{200} \right) \left(\frac{1}{57.3} \right)^2 2\pi \left\{ [1 + 2(0.8876)](1.0 - 0) - 4(-0.1451)(0)(1) \right\} \\
&= \frac{\pi}{2} \left(\frac{4.0}{200} \right) \left(\frac{1}{57.3} \right)^2 2\pi \left\{ [1 + 2(0.8876)] 1.0 \right\} \\
&= 0.000167
\end{aligned}$$

$$\dot{\alpha} = \alpha_1 \omega \cos \omega t \quad (\text{Equation 7.1.4.3-g})$$

$$\begin{aligned}
&= \frac{1}{57.3} (2\pi)(1) \\
&= 0.110
\end{aligned}$$

$$C_D = 2 \int_0^{b/2} \frac{c_d c}{S_w} dy \quad (\text{Equation 7.1.4.3-f})$$

$$= 2 \frac{c_d c}{S_w} \frac{b}{2} = 2 \frac{c_d c}{bc} \frac{b}{2} = c_d \quad (\text{Rect wing } S_w = bc)$$

$$C_D = 0.000167$$

Compute c_d for $t = 1.1$ sec:

$$\begin{aligned}
c_d &= \frac{\pi}{2} \frac{c}{V} \alpha_1^2 \omega \left\{ (1 + 2F)(\cos^2 \omega t - \sin^2 \omega t) - 4G \sin \omega t \cos \omega t \right\} \quad (\text{Equation 7.1.4.3-e}) \\
&= \frac{\pi}{2} \left(\frac{4.0}{200} \right) \left(\frac{1}{57.3} \right)^2 2\pi \left\{ [1 + 2(0.8876)] [(0.8090)^2 - (0.5878)^2] \right. \\
&\quad \left. - 4(-0.1451)(0.8090)(0.5878) \right\} \\
&= 0.0000681
\end{aligned}$$

$$\dot{\alpha} = \alpha_1 \omega \cos \omega t \quad (\text{Equation 7.1.4.3-g})$$

$$\begin{aligned}
&= \frac{1}{57.3} 2\pi(0.809) \\
&= 0.0887
\end{aligned}$$

$$C_D = 2 \int_0^{b/2} \frac{c_d c}{S_w} dy \quad (\text{Equation 7.1.4.3-f})$$

$$= 2 \frac{c_d c}{S_w} \frac{b}{2} = .2 \frac{c_d c}{bc} \frac{b}{2} = c_d \quad (\text{Rect Wing } S_w = bc)$$

$$C_D = 0.0000681$$

Solution:

$$C_{D_{\dot{\alpha}}} = \frac{\partial C_D}{\partial \left(\frac{\dot{\alpha} \bar{c}}{2V} \right)} = \frac{(C_D)_{t_2} - (C_D)_{t_1}}{[(\dot{\alpha})_{t_2} - (\dot{\alpha})_{t_1}] \frac{\bar{c}}{2V}} \quad (\text{Equation 7.1.4.3-h})$$

$$= \frac{(0.0000681 - 0.000167)}{(0.0887 - 0.110) \frac{4.0}{2(200)}}$$

$$= 0.464 \text{ per rad}$$

$$= 0.0081 \text{ per deg}$$

B. TRANSONIC

No method is presented.

C. SUPERSONIC

No method is presented.

REFERENCE

1. Garrick, I. E.: Propulsion of a Flapping and Oscillating Airfoil. NACA TR 567, 1936. (U)

TABLE 7.1.4.3-A
THEODORSEN'S FUNCTIONS

k	F	-G
∞	0.5000	0
10.00	0.5006	0.0206
6.00	0.5017	0.0206
4.00	0.5037	0.0305
3.00	0.5063	0.0400
2.00	0.5129	0.0577
1.50	0.5210	0.0736
1.20	0.5300	0.0877
1.00	0.5394	0.1003
0.80	0.5541	0.1165
0.66	0.5699	0.1308
0.60	0.5788	0.1378
0.56	0.5856	0.1428
0.50	0.5979	0.1507
0.44	0.6130	0.1592
0.40	0.6250	0.1650
0.34	0.6469	0.1738
0.30	0.6650	0.1793
0.24	0.6989	0.1862
0.20	0.7276	0.1886
0.16	0.7628	0.1876
0.12	0.8063	0.1801
0.10	0.8320	0.1723
0.08	0.8604	0.1604
0.06	0.8920	0.1426
0.05	0.9090	0.1305
0.04	0.9267	0.1160
0.025	0.9545	0.0872
0.01	0.9824	0.0482
0	1.000	0

7.2 BODY DYNAMIC DERIVATIVES

The methods presented in this section are for estimating pitching and acceleration dynamic derivatives of isolated bodies. The methods and charts of the subsonic, transonic, and supersonic speed ranges are based on a combination of slender-body theory and the theories used in predicting the body-lift-curve slope and pitching-moment-curve slope in Sections 4.2.1.1 and 4.2.2.1, respectively. Newtonian impact theory is used in the hypersonic speed range. The methods are restricted to angles of attack near zero and should yield values suitable for first approximations to dynamic stability.

No test data are available on body dynamic derivatives. Therefore, all theoretical methods must be considered tentative until compared with experimental results. A brief discussion of available theoretical methods is presented.

The starting point of almost all theories is the well-known linearized potential equation. Various methods based on linear theory have been developed for obtaining the flow field about bodies in supersonic flow. The problem of determining the dynamic stability derivatives for bodies has been treated principally within the assumptions of slender-body theory. The application of Munk's slender-body theory to the calculation of the aerodynamic coefficients describing steady motion has been made by a number of authors (see references 1 through 4). In reference 5, slender-body values of the aerodynamic coefficients associated with nonsteady angle of attack have been obtained as a by-product of a linear analysis of the potential equation for nonsteady supersonic flow. However, approximations made in the analysis effectively limit its application to bodies of vanishingly small thickness. The problem of determining the dynamic derivatives for a smooth slender body of arbitrary cross section performing slow maneuvers is treated within the assumptions of slender-body theory by Sacks in reference 6. This approach is novel in slender-body theory in that the squared terms in the pressure relation for slender configurations are retained and all motions of the configuration are treated simultaneously. However, the derivatives are obtained in terms of the mapping functions of the cross sections and are too complex for inclusion in the Datcom.

A method is developed for estimating aerodynamic loads on slender, symmetrical configurations performing small lateral oscillations of limited reduced frequency in sonic and supersonic flow in references 7 and 8, respectively. This method is an extension of an iterative technique originally proposed by Adams and Sears in reference 9, and is a combination of first-order and second-order cross-flow solutions. The results consist of slender-body-theory terms plus higher-order effects of fineness ratio. For sonic flow about a body of revolution, reference 7 shows that by retaining only the first-order terms in reduced frequency the pitching derivatives are given by simple slender-body theory; whereas the acceleration derivatives are influenced by the second-order terms and contain logarithms of the reduced frequency. Under certain limitations on the rapidity of the oscillations, all derivatives in supersonic flow prove to be independent of changes in reduced frequency; consequently the method can be applied to slow time-dependent motions. At present this method is limited to slender bodies of revolution, and in most cases requires a considerable amount of mathematical manipulation to obtain a solution. This method can be applied to bodies of more general cross section; however, the practicality of such an analysis would depend on the possibility of solving the integrals that appear.

In reference 10 an attempt has been made to overcome the slender-body limitation by adapting hybrid theory to the calculation of the body dynamic derivatives. (This method, derived by Van Dyke in reference 11, has proved successful in calculations for the static aerodynamic derivatives.) This method is used to predict the dynamic derivatives of a cone, and the results are consistent with those obtained by impact theory at the higher Mach numbers. In order to extend this method to bodies of more general shape, it is necessary to satisfy the boundary conditions corresponding to the specified body. Unfortunately, the analytical expressions required to do so have been found only for the cone.

The application of simple slender-body theory appears to be the only method of solution warranted at the present time, in view of the large effects of viscosity on the forces acting over slender bodies, the mathematical complexity involved in solution of the linearized equations for general planforms, and the lack of test data.

Since extensive use is made of slender-body-theory results throughout this section, the term "slender" is clarified.* Tsien, in reference 2, pointed out that slender-body theory applies to the flow about inclined, pointed projectiles at supersonic speeds. Subsequently, Jones, in reference 12, indicated that his slender-wing theory (slender-body theory extended to wings) applies to both subsonic and supersonic speeds, at least for pointed planforms. Actually, the meaning of the term "slender" is somewhat different in the various speed regimes. For supersonic Mach numbers "slender" implies that the body lies well within the Mach cone from the body apex. This leads directly to the limitation to pointed bodies. It also leads to the conclusion that relatively blunt bodies may qualify as "slender" at low supersonic speeds; while for hypersonic speeds the method must fail for practical shapes. At subsonic speeds the term "slender" becomes less restrictive as the Mach number increases from 0 to 1, until at sonic speed all bodies become slender. Thus, slender-body theory is seen to apply to at least some body shapes throughout the speed range from low subsonic to hypersonic.

REFERENCES

1. Munk, M. M.: The Aerodynamic Forces on Airship Hulls. NACA TR 184, 1924. (U)
2. Tsien, H. S.: Supersonic Flow Over an Inclined Body of Revolution. Jour. Aero. Sci., Vol. 5, No. 12, October 1938. (U)
3. Laitone, E. V.: Linearized Subsonic and Supersonic Flow About Inclined Slender Bodies of Revolution. Jour. Aero. Sci., Vol. 14, No. 11, November 1947. (U)
4. Tobak, M., Resse, D. E., Jr., and Bean, B. H.: Experimental Damping in Pitch of 45° Triangular Wings. NACA RM A50J26, 1950. (U)
5. Dorrance, W. H.: Nonsteady Supersonic Flow About Pointed Bodies of Revolution. Jour. Aero. Sci., Vol. 18, No. 8, August 1951. (U)
6. Sacks, A. H.: Aerodynamic Forces, Moments, and Stability Derivatives for Slender Bodies of General Cross Section. NACA TN 3283, 1954. (U)
7. Landahl, M. T.: Forces and Moments on Oscillating Slender Wing-Body Combinations at Sonic Speed. MIT Fluid Dynamics Research Group Report No. 56-1, 1956. (U)
8. Zartarian, G., and Ashley, H.: Forces and Moments on Oscillating Slender Wing-Body Combinations at Supersonic Speed. Part I - Basic Theory. MIT Fluid Dynamics Research Group Report No. 57-2, 1957. (U)

*This discussion is essentially quoted from reference 9

9. Adams, M. C., and Sears, W. R.: Slender-Body Theory - Review and Extension. Jour. Aero. Sci., Vol. 20, No. 2, February 1963. (U)
10. Tobak, M., and Wehrend, W. R.: Stability Derivatives of Cones at Supersonic Speeds. NACA TN 3788, 1966. (U)
11. Van Dyke, M. D.: First- and Second-Order Theory of Supersonic Flow Past Bodies of Revolution. Jour. Aero. Sci., Vol. 18, No. 3, March 1951. (U)
12. Jones, R. T.: Properties of Low Aspect Ratio Wings at Speeds Below and Above the Speed of Sound. NACA TR 835, 1946. (U)

7.2.1 BODY PITCHING DERIVATIVES

7.2.1.1 BODY PITCHING DERIVATIVE C_{Lq}

The pitching derivative C_{Lq} is a measure of the lift produced by rotational motion of the airframe about a spanwise axis. This derivative is generally small compared to other terms in the equations of motion and is frequently neglected. However, methods are presented for determining the body contribution to C_{Lq} in the subsonic, transonic, supersonic, and hypersonic speed ranges. The value of C_{Nq} in the hypersonic speed range is used to obtain the value of C_{mq} in the hypersonic speed range in Section 7.2.1.2.

In the subsonic, transonic, and supersonic speed ranges the Datcom methods are based on the relatively simple results derived from slender-body theory and the assumption that a relationship of corresponding slender-body derivatives may be employed with reasonable accuracy to the case of steady pitching in a manner similar to that of reference 1. This approach to the calculation of body dynamic derivatives has been applied with reasonable success by Walker and Wolowicz in reference 2. It was shown in reference 1 that, although slender-body theory alone does not accurately predict the characteristics of nonslender configurations, the ratio of corresponding slender-body derivatives may be employed with reasonable accuracy in predicting the static forces on nonslender configurations. The body contribution to C_{Lq} is thus given as the product of the lift-curve slope $C_{L\alpha}$ and the ratio of slender-body derivatives, i.e.,

$$C_{Lq} = C_{L\alpha} \left(\frac{C_{Lq}}{C_{L\alpha}} \right)_{\text{slender-body theory}}$$

Slender-body theory states that body force characteristics are independent of Mach number. The effect of Mach number is taken into account by the static force coefficient. Therefore, the limitations of these methods are determined by the limitations of the methods employed in determining the static derivative $C_{L\alpha}$ in the various speed regimes. Experimental data should be used for the body lift-curve slope when available.

A. SUBSONIC

There is no explicit method available in the literature for obtaining the body dynamic derivatives for general planforms.

The method presented is based on the application of the results of slender-body theory in the manner previously discussed.

DATCOM METHOD

The body contribution to C_{Lq} , based on body base area and body length and referred to the center of rotation, is given by

$$C_{L_q} = 2 C_{L_\alpha} \left(1 - \frac{x_m}{\ell_B} \right) \quad (\text{per radian}) \quad 7.2.1.1-a$$

where

C_{L_α} is the body lift-curve slope from paragraph A of Section 4.2.1.1 multiplied by $(V_B^{2/3}/S_b)$ (per radian).

x_m is the longitudinal distance from the body vertex to the center of rotation, positive aft.

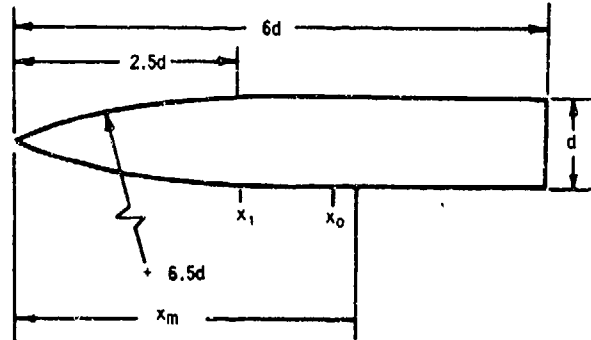
ℓ_B is the length of the body.

V_B is the total body volume from Section 2.3.

S_b is the body base area.

Sample Problem

Given:



$$d = 1.0 \text{ ft}$$

$$\ell_B = 6.0 \text{ ft}$$

$$\text{Fineness Ratio} = 6.0$$

$$x_m = 3.8 \text{ ft}$$

$$C_{L_\alpha} = 0.548 \text{ per rad (based on } V_B^{2/3} \text{)} \text{ (Section 4.2.1.1)}$$

$$V_B^{2/3} = 2.47 \text{ sq ft (Section 2.3)}$$

$$S_b = 0.785 \text{ sq ft}$$

Compute:

$$C_{L_q} = (0.548) \cdot \frac{(V_B)^{2/3}}{S_b} = (0.548) \left(\frac{2.47}{0.785} \right) = 1.724 \text{ per rad (based on } S_b \text{)}$$

$$\left(1 - \frac{x_m}{l_B}\right) = \left(1 - \frac{3.8}{6}\right) = 0.367$$

Solution:

$$\begin{aligned} C_{L_q} &= 2 C_{L_\alpha} \left(1 - \frac{x_m}{l_B}\right) \quad (\text{equation 7.2.1.1-a}) \\ &= 2(1.724)(0.367) \\ &= 1.265 \text{ per rad (based on } S_b l_B) \end{aligned}$$

B. TRANSONIC

The linearization of the transonic flow problem has been accomplished by Landahl, in reference 3, by introducing a small amount of unsteadiness into the motion. This theoretical method is briefly discussed in Section 7.2. By neglecting the second-order effects of reduced frequency the pitching derivatives of a slender body of revolution are those given by slender-body theory. Since slender-body theory does not predict a dependence on configuration parameters, this method cannot be expected to give reasonable approximations for the pitching derivatives of nonslender configurations. Therefore, the method of paragraph A is applied throughout the transonic speed range.

C. SUPERSONIC

Several of the theoretical methods that have been developed for estimating the body pitching derivative C_{N_q} in the supersonic speed range are briefly discussed in Section 7.2. The available theoretical methods are limited to simple slender-body theory, theories treated within the assumptions of slender-body theory, and hybrid theory. The method presented here is based on simple slender-body theory. Theories treated within the assumption of slender-body theory are mathematically complex and restricted to specific body shapes; therefore, no general quantitative results are presented.

The supersonic C_{N_q} for cones can be estimated by the hybrid theory solutions presented in reference 4.

DATCOM METHOD

The method presented here for determining the body contribution to C_{N_q} , based on the cone-cylinder or ogive-cylinder maximum frontal area and body length and referred to the center of rotation, is the same as that of paragraph A and is given by equation 7.2.1.1-a, i.e.,

$$C_{N_q} = 2 C_{N_\alpha} \left(1 - \frac{x_m}{l_B}\right) \text{ (per radian)}$$

where $C_{N\alpha}$ is the body normal-force-curve slope from paragraph C of Section 4.2.1.1, evaluated at the appropriate Mach number and based on the cone-cylinder or ogive-cylinder maximum frontal area (per radian).

D. HYPERSONIC

Simple Newtonian theory is used in this section to estimate the contribution of cone frustum bodies, with or without spherical noses, to the derivative C_{Nq} . Newtonian theory is discussed in paragraph D, Section 4.2.1.1.

DATCOM METHOD

Charts taken from reference 5, based on simple Newtonian theory, are presented for determining C_{Nq} of spherical segments and cone frustums at small angles of attack.

The coefficients of these charts are referred to the body base area and base diameter and to a moment center at the forward face of the segment. By proper use of the data presented, the total C_{Nq} may be determined for bodies composed of multiple cone frustums with or without spherically blunted noses.

The Newtonian value of the derivative C_{Nq} for a complex body is obtained as follows:

- Step 1. Compute C_{Nq}' for each body segment about its front face using figures 7.2.1.1-9a and 7.2.1.1-9b.
- Step 2. Transfer the individual derivatives C_{Nq}' to a common reference axis by applying the following transfer equation to each body segment

$$C_{Nq} = C_{Nq}' - 2\left(\frac{n}{d}\right)C_{N\alpha} \quad 7.2.1.1-b$$

where

$C_{N\alpha}$ is the normal-force-curve slope for each segment based on individual base areas from paragraph D, Section 4.2.1.1.

C_{Nq}' is the pitching derivative for each segment based on individual base areas and base diameters and referred to a moment center at the forward face of the segment, from figures 7.2.1.1-9a and 7.2.1.1-9b.

n is the distance from the face of a given frustum to the desired moment reference axis of the configuration, positive aft.

d is the base diameter of a given frustum.

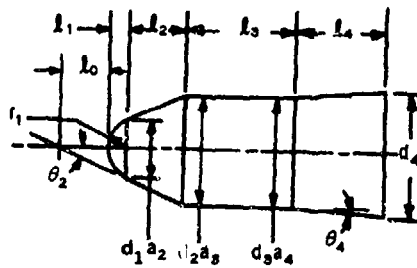
- Step 3. The transferred derivatives of the individual body segments are converted to a common reference area and diameter and added. The total derivative is given by

$$C_{N_q} = \sum_{n=1}^m (C_{N_q})_n \left(\frac{d_n}{d_b} \right)^3$$

7.2.1.1-c

Sample Problem

Given: Same multiple-segment body as sample problem of paragraph D of Sections 4.2.1.1 and 4.2.2.1.



$$l_0 = 0.55 \text{ ft (distance from moment reference center to body nose)}$$

Spherical segment

$$r_1 = 0.18 \text{ ft}$$

$$r_1 = 0.36 \text{ ft}$$

$$d_1 = 0.62 \text{ ft}$$

Forward cone frustum

$$a_2 = 0.62 \text{ ft}$$

$$d_2 = 1.20 \text{ ft}$$

$$l_2 = 0.72 \text{ ft}$$

$$\theta_2 = 22.5^\circ$$

Cylinder

$$a_3 = 1.20 \text{ ft}$$

$$d_3 = 1.20 \text{ ft}$$

$$l_3 = 1.20 \text{ ft}$$

$$\theta_3 = 0$$

Rear cone frustum

$$a_4 = 1.20 \text{ ft}$$

$$d_4 = 1.368 \text{ ft}$$

$$l_4 = 0.96 \text{ ft}$$

$$\theta_4 = 5^\circ$$

7.2.1.1-5

Compute:

Spherical segment

$$2\ell_1/d_s = \ell_1/r_1 = 0.50$$

$$C_{Nq_1}^{\prime} = 0.865 \text{ per rad (figure 7.2.1.1-9b)}$$

$$n_1 = -\ell_0 = -0.55 \text{ ft}$$

$$d_1 = a_2 = 0.62 \text{ ft}$$

$$C_{N\alpha_1} = 0.75 \text{ per rad (figure 4.2.1.1-23)}$$

$$\begin{aligned} C_{Nq_1} &= C_{Nq_1}^{\prime} - 2\left(\frac{n_1}{d_1}\right)C_{N\alpha_1} \quad (\text{equation 7.2.1.1-b}) \\ &= 0.865 - 2\left(\frac{-0.55}{0.62}\right)0.75 \\ &= 2.195 \text{ per rad } \left(\text{based on } \frac{\pi d_1^3}{4}\right) \end{aligned}$$

Forward cone frustum

$$a_2/d_2 = \lambda_2 = 0.517$$

$$C_{Nq_2}^{\prime} = 1.22 \text{ per rad (figure 7.2.1.1-9a)}$$

$$n_2 = -(\ell_0 + \ell_1) = -0.73$$

$$C_{N\alpha_2} = 1.250 \text{ per rad (figure 4.2.1.1-26)}$$

$$\begin{aligned} C_{Nq_2} &= C_{Nq_2}^{\prime} - 2\left(\frac{n_2}{d_2}\right)C_{N\alpha_2} \quad (\text{equation 7.2.1.1-b}) \\ &= 1.22 - 2\left(\frac{-0.73}{1.20}\right)1.250 \end{aligned}$$

$$= 2.74 \text{ per rad} \left(\text{based on } \frac{\pi d_2^3}{4} \right)$$

Cylinder

$$a_3/d_3 = \lambda_3 = 1.0$$

$$C_{N_{q_3}'} = 0 \text{ (figure 7.2.1.1-9a)}$$

$$n_3 = -(\ell_0 + \ell_1 + \ell_2) = -1.45$$

$$C_{N_{\alpha_3}} = 0 \text{ (figure 4.2.1.1-26)}$$

$$C_{N_{q_3}} = C_{N_{q_3}'} - 2 \left(\frac{n_3}{d_2} \right) C_{N_{\alpha_3}} \quad (\text{equation 7.2.1.1-b})$$

$$= 0$$

Rear cone frustum

$$a_4/d_4 = \lambda_4 = 0.877$$

$$C_{N_{q_4}'} = 0.36 \text{ per rad (figure 7.2.1.1-9a)}$$

$$n_4 = -(\ell_0 + \ell_1 + \ell_2 + \ell_3) = -2.65$$

$$C_{N_{\alpha_4}} = 0.450 \text{ per rad (figure 4.2.1.1-26)}$$

$$C_{N_{q_4}} = C_{N_{q_4}'} - 2 \left(\frac{n_4}{d_4} \right) C_{N_{\alpha_4}} \quad (\text{equation 7.2.1.1-b})$$

$$= 0.36 - 2 \left(\frac{-2.65}{1.368} \right) 0.45$$

$$= 2.10 \text{ per rad} \left(\text{based on } \frac{\pi d_4^3}{4} \right)$$

Solution:

Converting the derivative for each segment to a common reference area and diameter, the base area and diameter of the rear cone frustum, and adding

$$C_{N_q} = \sum_{n=1}^m (C_{N_q})_n \left(\frac{d_n}{d_b} \right)^3 \quad (\text{equation 7.2.1.1-c})$$

$$C_{N_q} = C_{N_q_1} \left(\frac{d_1}{d_4} \right)^3 + C_{N_q_2} \left(\frac{d_2}{d_4} \right)^3 + C_{N_q_3} \left(\frac{d_3}{d_4} \right)^3 + C_{N_q_4}$$

$$= 2.195 \left(\frac{0.62}{1.368} \right)^3 + 2.74 \left(\frac{1.20}{1.368} \right)^3 + 0 + (2.10)$$

$$= 0.2043 + 1.8494 + 2.10$$

$$= 4.154 \text{ per rad} \quad \left(\text{based on } \frac{\pi d_4^3}{4} \right)$$

REFERENCES

1. Pitts, W. C., Nielsen, J. N., and Kaattari, G. E.: Lift and Center of Pressure of Wing-Body-Tail Combinations at Subsonic, Transonic, and Supersonic Speeds. NACA TR 1307, 1959. (U)
2. Walker, H. J., and Welowicz, C. H.: Theoretical Stability Derivatives for the X-15 Research Airplane at Supersonic and Hypersonic Speeds Including a Comparison with Wind-Tunnel Results. NASA TM X-287, 1960. (U)
3. Landahl, M. T.: Forces and Moments on Oscillating Slender Wing-Body Combinations at Sonic Speed. MIT Fluid Dynamics Research Group Report No. 56-1, 1956. (U)
4. Tobek, M., and Wehrend, W. R.: Stability Derivatives of Cones at Supersonic Speeds. NACA TN 3788, 1956. (U)
5. Fisher, L. R.: Equations and Charts for Computing the Hypersonic Stability Derivatives of Cone Frustums Computed by Newtonian Impact Theory. NASA TN D-149, 1959. (U)

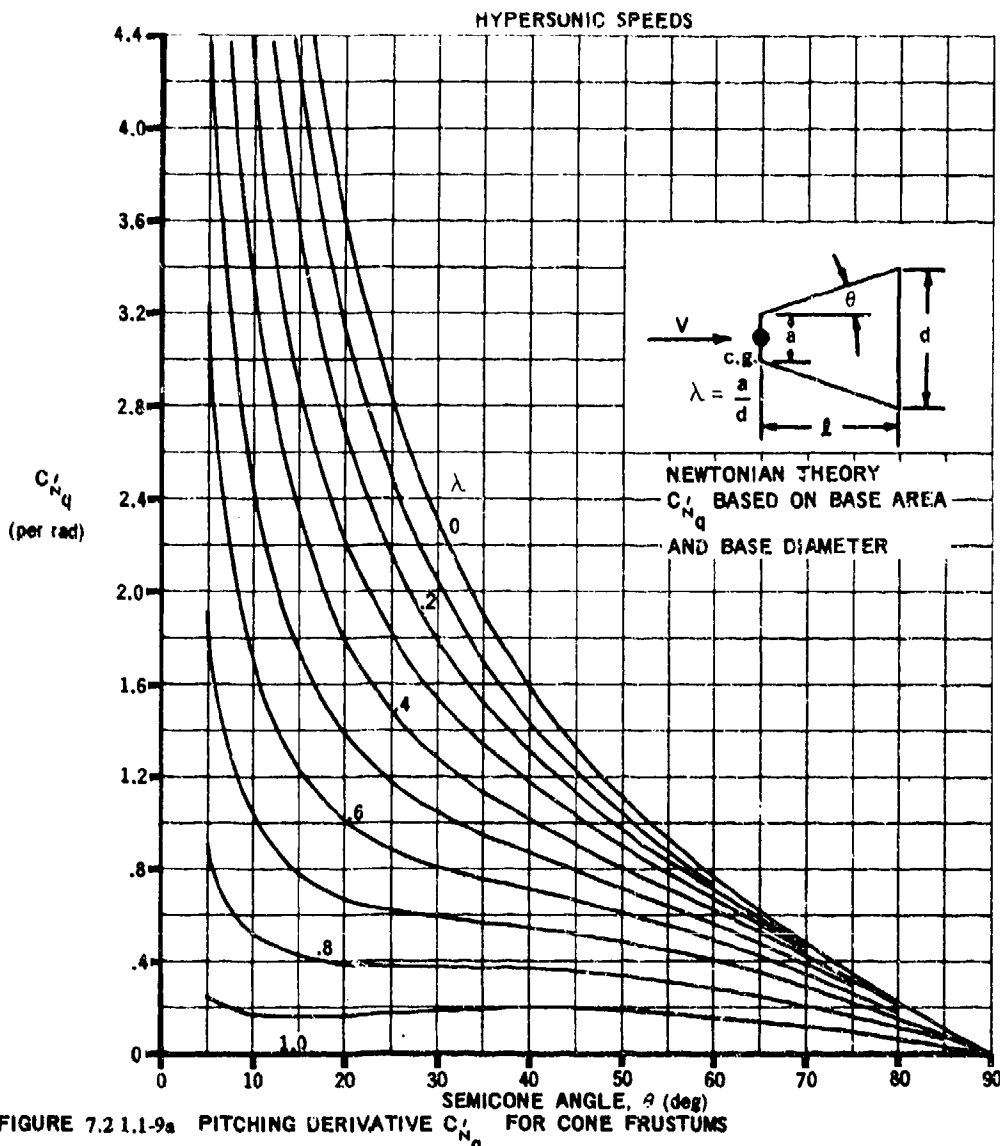


FIGURE 7.2.1.1-9a PITCHING DERIVATIVE C'_Nq FOR CONE FRUSTUMS

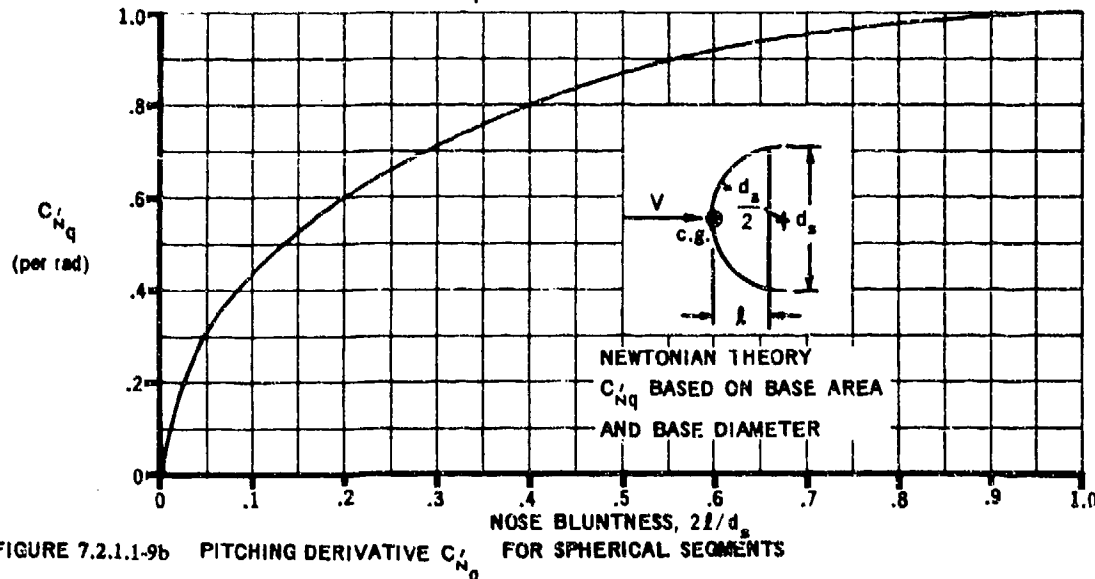


FIGURE 7.2.1.1-9b PITCHING DERIVATIVE C'_Nq FOR SPHERICAL SEGMENTS

7.2.1.2 BODY PITCHING DERIVATIVE C_{m_q}

The derivative C_{m_q} is a measure of the pitching moment produced by rotational motion of the airframe about a spanwise axis and is commonly referred to as the pitch-damping derivative. Methods are presented for determining the body contribution to this derivative in the subsonic, transonic, supersonic, and hypersonic speed ranges.

In the subsonic, transonic, and supersonic speed ranges the Datcom methods are based on the same assumption that was made in regard to the body contribution to the derivative C_{L_q} , and the general discussion of Section 7.2.1.1 is directly applicable here.

The body contribution to C_{m_q} is expressed as

$$C_{m_q} = C_{m_\alpha} \left(\frac{C_{m_q}}{C_{m_\alpha}} \right)_{\text{slender-body theory}}$$

The limitations of these methods are determined by the limitations of the methods employed in determining the static derivative C_{m_α} in the various speed regimes. Experimental data should be used for the body pitching-moment-curve slope when available.

A. SUBSONIC

The comments of paragraph A of Section 7.2.1.1 are directly applicable here.

DATCOM METHOD

The body contribution to C_{m_q} , based on body base area and the square of body length and referred to the center of rotation, is given by

$$C_{m_q} = 2 C_{m_\alpha} \left[\frac{\left(1 - \frac{x_m}{l_B}\right)^2 - \frac{V_B}{S_b l_B} \left(\frac{x_c}{l_B} - \frac{x_m}{l_B}\right)}{\left(1 - \frac{x_m}{l_B}\right) - \frac{V_B}{S_b l_B}} \right] \quad 7.2.1.2-a$$

where

C_{m_α} is the body pitching-moment-curve slope from paragraph A of Section 4.2.2.1, multiplied by $V_B/(S_b l_B)$.

V_B is the total body volume from Section 2.3.

S_b is the body base area.

x_c is the longitudinal distance from the vertex to the centroid of the volume and is given by

$$x_c = \frac{\int_0^{l_B} S(x) x \, dx}{V_B} \quad 7.2.1.2-b$$

where

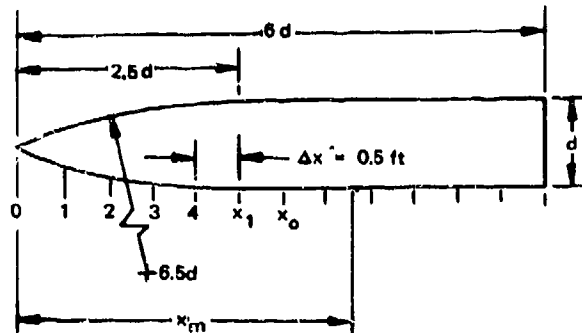
$S(x)$ is the body cross-sectional area at any station. It is not feasible to present generalized design charts of x_c , but the equation can be integrated for any arbitrary body of revolution.

l_B is the length of the body.

x_m is the longitudinal distance from the body vertex to the center of rotation, positive aft.

Sample Problem

Given: Same ogive-cylinder configuration as sample problem of paragraph A of Section 7.2.1.1.



$$d = 1.0 \text{ ft}$$

$$L_B = 6.0 \text{ ft}$$

Fineness Ratio = 6.0

$$x_m = 3.8 \text{ ft}$$

$$x_1 = 2.5 \text{ ft}$$

$$x_0 = 3.6 \text{ ft}$$

$$(k_2 - k_1) = 0.863$$

$$S_s = 0.785 \text{ sq ft}$$

$$V_p = 3.88 \text{ cu ft}$$

(Section 4.2.1.1)

Compute:

Determine $C_{m\alpha}$

Station	d	S_x	$\Delta S_x \approx \frac{dS_x}{dx} \Delta x$	$(x_m - x)^*$	$\frac{dS_x}{dx} (x_m - x) \Delta x$
1	0.4	0.126	0.126	3.467	0.4368
2	0.68	0.363	0.237	3.028	0.7176
3	0.89	0.622	0.259	2.539	0.8576
4	0.98	0.754	0.132	2.046	0.2701
x_1	1.0	0.785	0.031	1.549	0.0480
x_o	1.0	0.785	0	0.75	0

$$\sum_{x=0}^{x_o} \frac{dS_x}{dx} (x_m - x) \Delta x = 2.1301$$

$$C_{m\alpha} = \frac{2(k_2 - k_1)}{V_B} \sum_{x=0}^{x_o} \frac{dS_x}{dx} (x_m - x) \Delta x \quad (\text{equation 4.2.2.1-a})$$

$$= \frac{(2)(0.863)(2.1301)}{3.88}$$

$$= 0.948 \text{ per rad (based on } V_B)$$

$$C_{m\alpha} = (0.948) \left(\frac{V_B}{S_b l_B} \right)$$

$$= (0.948) \left(\frac{3.88}{4.71} \right)$$

$$= 0.781 \text{ per rad (based on } S_b l_B)$$

*x is taken to be at the center of volume of each body segment.

Determine x_c

Station	d	S(x)	x^*	$S(x) \times \Delta x$
1	0.4	0.126	0.333	0.0210
2	0.68	0.363	0.772	0.1400
3	0.89	0.622	1.261	0.3920
4	0.98	0.754	1.754	0.6615
5	1.00	0.785	2.251	0.8836
6	1.00	0.785	2.75	1.0795
7	1.00	0.785	3.25	1.2755
8	1.00	0.785	3.75	1.4720
9	1.00	0.785	4.25	1.6680
10	1.00	0.785	4.75	1.8645
11	1.00	0.785	5.25	2.0606
12	1.00	0.785	5.75	2.2570

$$\sum_{x=0}^{l_B} S(x)x \Delta x = 13.775$$

$$x_c = \frac{\int_0^{l_B} S(x) x dx}{V_B} \quad (\text{equation 7.2.1.2-b})$$

$$= \frac{13.775}{3.88} = 3.55 \text{ ft}$$

$$\frac{V_B}{S_b l_B} = \frac{(3.88)}{(0.785)(6.0)} = 0.824$$

$$\left(1 - \frac{x_m}{l_B}\right) = 1 - \frac{3.8}{6.0} = 0.367$$

Solution:

$$C_{m_q} = 2 C_{m_\alpha} \left[\frac{\left(1 - \frac{x_m}{l_B}\right)^2 - \frac{V_B}{S_b l_B} \left(\frac{x_c}{l_B} - \frac{x_m}{l_B}\right)}{\left(1 - \frac{x_m}{l_B}\right) - \frac{V_B}{S_b l_B}} \right] \quad (\text{equation 7.2.1.2-a})$$

*x is taken to be at the center of volume of each body segment.

$$\begin{aligned}
 &= (2)(0.781) \left[\frac{(0.367)^2 - (0.824)\left(\frac{3.55}{6.0} - \frac{3.8}{6.0}\right)}{0.367 - 0.824} \right] \\
 &= 1.562 \left[\frac{0.135 - (0.824)(-0.0417)}{-0.457} \right] \\
 &= 1.562 \left[\frac{0.1693}{-0.457} \right] \\
 &\approx -0.579 \text{ per rad (based on } S_b l_B^2)
 \end{aligned}$$

B. TRANSONIC

The comments of paragraph B of Section 7.2.1.1 are directly applicable here. The method of paragraph A is applicable throughout the transonic speed range.

C. SUPERSONIC

The theoretical methods applicable for the estimation of the body contribution to the derivative C_{m_q} parallel those of the body contribution to the derivative C_{L_q} .

Therefore, the general comments of paragraph C of Section 7.2.1.1 are also applicable here.

The supersonic C_{m_q} for cones can be estimated from the hybrid theory solutions presented in reference 1.

DATCOM METHOD

The method presented here for the body contribution to C_{m_q} , based on body base area and the square of body length and referred to the center of rotation, is the same as that of paragraph A and is given by equation 7.2.1.2-a, i.e.,

$$C_{m_q} = 2 C_{m_\alpha} \left[\frac{\left(1 - \frac{x_m}{l_B}\right)^2 - \frac{V_B}{S_b l_B} \left(\frac{x_c}{l_B} - \frac{x_m}{l_B}\right)}{\left(1 - \frac{x_m}{l_B}\right) - \frac{V_B}{S_b l_B}} \right]$$

where C_{m_α} is the body pitching-moment-curve slope from paragraph C of Section 4.2.2.1 evaluated at the appropriate Mach number.

D. HYPERSONIC

Simple Newtonian theory is used in this section to estimate the derivative C_{m_q} of cone frustum bodies with or without spherical noses. Newtonian theory is discussed in paragraph D, Section 4.2.1.1.

DATCOM METHOD

Charts based on simple Newtonian theory (reference 2) are presented for determining C_{m_q} of spherical segments and cone frustums at small angles of attack. The coefficients of these charts are referred to the base area and the square of the base diameter and to a moment center at the forward face of the segment. By proper use of the data presented, the total C_{m_q} may be determined for bodies composed of multiple cone frustums with or without spherically blunted noses.

The Newtonian value of the stability derivative C_{m_q} for a complex body is obtained as follows:

- Step 1. Compute C_{m_q}' for each body segment about its own front face using figures 7.2.1.2-12 and 7.2.1.2-13b if the body has a spherically blunted nose, and figures 7.2.1.2-12 and 7.2.1.2-13a if the body nose is a cone frustum.
- Step 2. Transfer the individual derivatives C_{m_q}' to a common moment center by applying the following axis transfer equation to each body segment:

$$C_{m_q} = C_{m_q}' - 2 \frac{n}{d} C_{m_\alpha}' + \frac{n}{d} C_{N_q}' - 2 \left(\frac{n}{d} \right)^2 C_{N_\alpha} \quad 7.2.1.2-c$$

where

C_{N_α} is the normal-force-curve slope for each segment based on individual base areas from Section 4.2.1.1.

C_{N_q}' is the pitching derivative for each segment based on individual base areas and base diameters and referred to a moment center at the forward face of the segment. This derivative is obtained from paragraph D of Section 7.2.1.1.

C_{m_α}' is the pitching-moment-curve slope for each segment based on individual base areas and base diameters and referred to a moment center at the forward face of the segment. This derivative is obtained from paragraph D of Section 4.2.2.1.

C_{m_q}' is the pitching derivative for each body segment based on individual base areas and the square of base diameters and referred to a moment center at

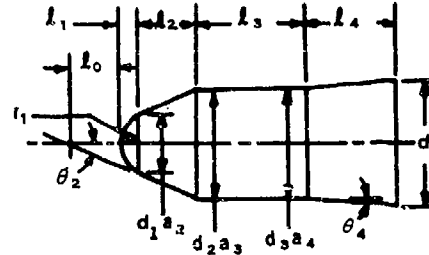
the forward face of the segment. If a complex body consists of combinations of cone frustums, the derivative for the first frustum must be obtained from figure 7.2.1.2-13a, which accounts for the front face being exposed to the air stream. If the body has a spherically blunted nose, the derivative of the nose is obtained from figure 7.2.1.2-13b. For subsequent frustums the derivatives are obtained from figure 7.2.1.2-12.

Step 3. The transferred derivatives of the individual body segments are added after being converted to a common reference area and squared diameter. The total derivative of the individual body segments is given by

$$C_{m_q} = \sum_{n=1}^m (C_{m_q})_n \left(\frac{d_n}{d_b} \right)^4 \quad 7.2.1.2-d$$

Sample Problem

Given: Same multiple-segment body as sample problems of paragraph D of Sections 4.2.1.1, 4.2.2.1, and 7.2.1.1.



$$\ell_0 = 0.55 \text{ ft (distance from moment reference center to body nose)}$$

Spherical segment

$$\ell_1 = 0.18 \text{ ft}$$

$$r_1 = 0.36 \text{ ft}$$

$$d_1 = 0.62 \text{ ft}$$

Forward cone frustum

$$a_2 = 0.62 \text{ ft}$$

$$d_2 = 1.20 \text{ ft}$$

$$\ell_2 = 0.72 \text{ ft}$$

$$\theta_2 = 22.5^\circ$$

Cylinder

$$a_3 = 1.20 \text{ ft}$$

$$d_3 = 1.20 \text{ ft}$$

$$\ell_3 = 1.20 \text{ ft}$$

$$\theta_3 = 0$$

Rear cone frustum

$$a_4 = 1.20 \text{ ft}$$

$$d_4 = 1.368 \text{ ft}$$

$$\ell_4 = 0.96 \text{ ft}$$

$$\theta_4 = 5^\circ$$

Compute:

Spherical segment

$$2\ell_1/d_s = \ell_1/r_1 = 0.50$$

$$C_{m_{q_1}}' = -0.50 \text{ per rad} \quad (\text{figure 7.2.1.2-13b})$$

$$n_1 = -\ell_0 = -0.55 \text{ ft}$$

$$d_1 = a_2 = 0.62 \text{ ft}$$

$$C_{N_{\alpha_1}} = 0.75 \text{ per rad} \quad (\text{figure 4.2.1.1-23})$$

$$C_{m_{\alpha_1}}' = -0.430 \text{ per rad} \quad (\text{figure 4.2.2.1-20b})$$

$$C_{N_{q_1}}' = 0.865 \text{ per rad} \quad (\text{figure 7.2.1.1-9b})$$

$$C_{m_{q_1}} = C_{m_{q_1}}' - 2 \frac{n_1}{d_1} C_{m_{\alpha_1}}' + \frac{n_1}{d_1} C_{N_{q_1}}' - 2 \left(\frac{n_1}{d_1} \right)^2 C_{N_{\alpha_1}} \quad (\text{equation 7.2.1.2-c})$$

$$= -0.50 - (-1.774)(-0.43) + (-0.887)(0.865) - (1.574)(0.75)$$

$$= -0.50 - 0.763 - 0.767 - 1.180$$

$$= -3.210 \text{ per rad} \left(\text{based on } \frac{\pi d_1^4}{4} \right)$$

Forward cone frustum

$$a_2/d_2 = \lambda_2 = 0.517$$

$$C_{m_{q_2}'} = -0.68 \text{ per rad} \quad (\text{figure 7.2.1.2-12})$$

$$n_2 = -(l_0 + l_1) = -0.73$$

$$C_{N_{\alpha_2}} = 1.250 \text{ per rad} \quad (\text{figure 4.2.1.1-26})$$

$$C_{m_{\alpha_2}'} = -0.590 \text{ per rad} \quad (\text{figure 4.2.2.1-20a})$$

$$C_{N_{q_2}'} = 1.22 \text{ per rad} \quad (\text{figure 7.2.1.1-9a})$$

$$C_{m_{q_2}} = C_{m_{q_2}'} - 2 \frac{n_2}{d_2} C_{m_{\alpha_2}'} + \frac{n_2}{d_2} C_{N_{q_2}'} - 2 \left(\frac{n_2}{d_2} \right)^2 C_{N_{\alpha_2}} \quad (\text{equation 7.2.1.2-c})$$

$$= -0.68 - (-1.217)(-0.590) + (-0.608)(1.22) - (0.74)(1.25)$$

$$= -0.68 - 0.718 - 0.742 - 0.925$$

$$= -3.065 \text{ per rad} \left(\text{based on } \frac{\pi d_2^4}{4} \right)$$

Cylinder

$$a_3/d_3 = \lambda_3 = 1.0$$

$$C_{m_{q_3}'} = 0 \quad (\text{figure 7.2.1.2-12})$$

$$n_3 = -(l_0 + l_1 + l_2) = -1.45$$

$$C_{N_{\alpha_3}} = 0 \quad (\text{figure 4.2.1.1-26})$$

$$C_{m_{\alpha_3}'} = 0 \quad (\text{figure 4.2.2.1-20a})$$

$$C_{N_{q_3}'} = 0 \quad (\text{figure 7.2.1.1-9a})$$

$$C_{m_{q_3}} = 0$$

Rear cone frustum

$$a_4/d_4 = \lambda_4 = 0.877$$

$$C_{m_{q_4}'} = -0.250 \text{ per rad (figure 7.2.1.2-12)}$$

$$n_4 = -(l_0 + l_1 + l_2 + l_3) = -2.65$$

$$C_{N_{\alpha_4}} = 0.450 \text{ per rad (figure 4.2.1.1-26)}$$

$$C_{m_{\alpha_4}'} = -0.19 \text{ per rad (figure 4.2.2.1-20a)}$$

$$C_{N_{q_4}'} = 0.36 \text{ per rad (figure 7.2.1.1-9a)}$$

$$C_{m_{q_4}} = C_{m_{q_4}'} - 2 \frac{n_4}{d_4} C_{m_{\alpha_4}'} + \frac{n_4}{d_4} C_{N_{q_4}'} - 2 \left(\frac{n_4}{d_4} \right)^2 C_{N_{\alpha_4}} \quad (\text{equation 7.2.1.2-c})$$

$$= -0.25 - (-3.87)(-0.19) + (-1.94)(0.36) - (7.53)(0.45)$$

$$= -0.25 - 0.735 - 0.698 - 3.388$$

$$= -5.072 \text{ per rad (based on } \frac{\pi d_4^4}{4} \text{)}$$

Solution:

Converting the derivative for each segment to a common reference area and square of the diameter, the base area and diameter of the rear cone frustum, and adding gives

$$C_{m_q} = C_{m_{q_1}} \left(\frac{d_1}{d_4} \right)^4 + C_{m_{q_2}} \left(\frac{d_2}{d_4} \right)^4 + C_{m_{q_3}} \left(\frac{d_3}{d_4} \right)^4 + C_{m_{q_4}} \quad (\text{equation 7.2.1.2-d})$$

$$= -3.210 \left(\frac{0.62}{1.368} \right)^4 - 3.065 \left(\frac{1.20}{1.368} \right)^4 + 0 + (-5.072)$$

$$= -0.1354 - 1.8148 - 5.072$$

$$= -7.022 \text{ per rad (based on } \frac{\pi d_4^4}{4} \text{)}$$

REFERENCES

1. Tobek, M., and Wehrend, W. R.: Stability Derivatives of Cones at Supersonic Speeds. NACA TN 3788, 1956. (U)
2. Fisher, L. R.: Equations and Charts for Determining the Hypersonic Stability Derivatives of Cone Frustums Computed by Newtonian Impact Theory. NASA TN D-149, 1959. (U)

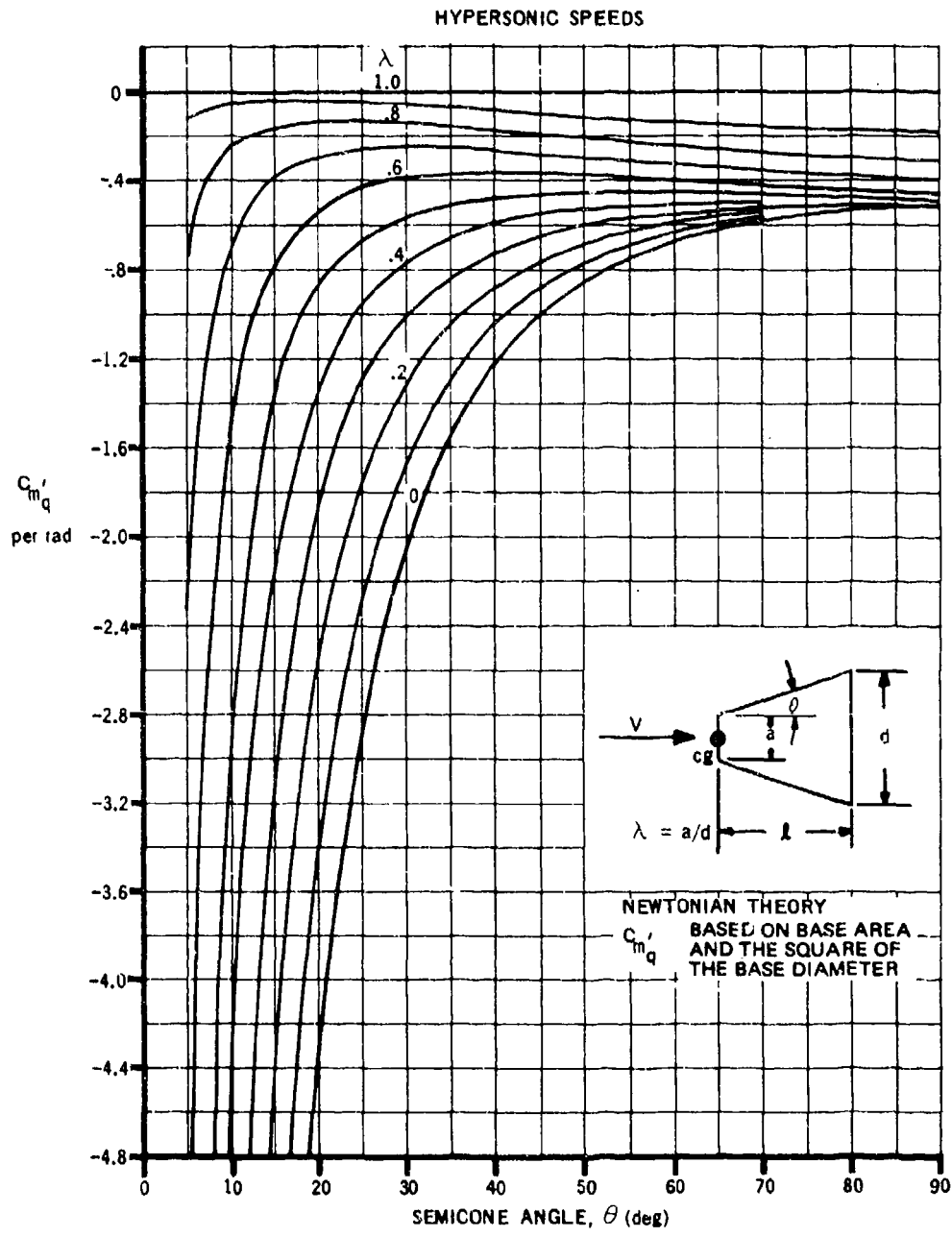


FIGURE 7.2.1.2-12 PITCHING DERIVATIVE C_{m_q}' DUE TO INCLINED SIDES OF CONE FRUSTUMS

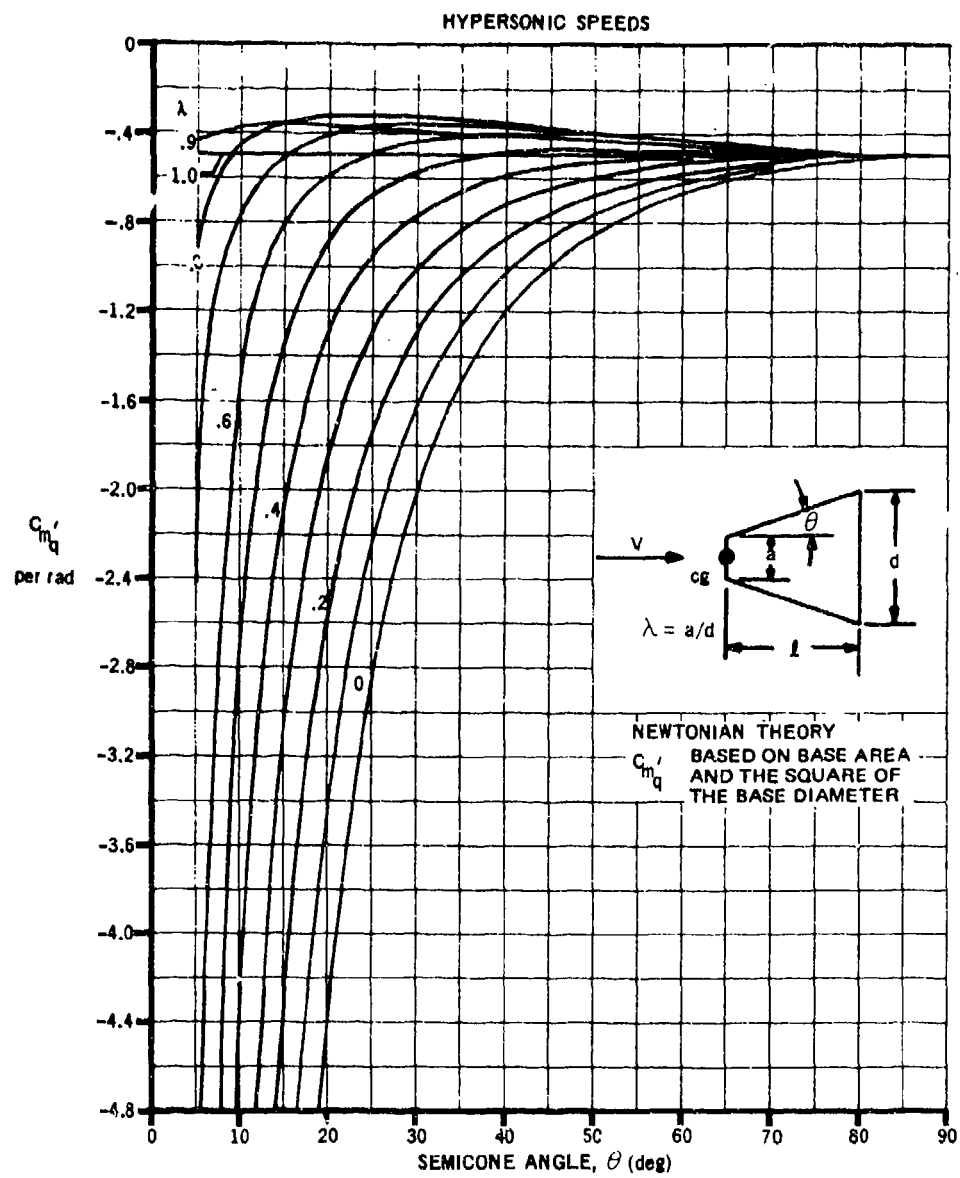


FIGURE 7.2.1.2-13a PITCHING DERIVATIVE C_{m_q}' FOR CONE FRUSTUMS

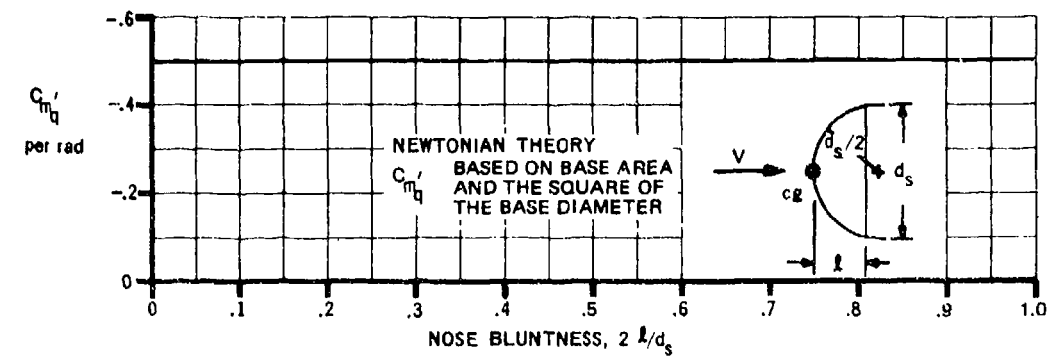


FIGURE 7.2.1.2-13b PITCHING DERIVATIVE C_{m_q}' FOR SPHERICAL SEGMENTS

7.2.2 BODY ACCELERATION DERIVATIVES

7.2.2.1 BODY ACCELERATION DERIVATIVE $C_{L\dot{\alpha}}$

Methods are presented for determining the body contribution to the derivative $C_{L\dot{\alpha}}$ in the subsonic, transonic, and supersonic speed ranges.

Datcom methods are based on the relatively simple results derived from slender-body theory in a manner similar to that used to predict the body pitching derivatives. It is assumed that a relationship of corresponding slender-body derivatives may be applied with reasonable accuracy to the case of vertical acceleration in a manner similar to that of reference 1. This approach to the calculation of body dynamic derivatives has been applied with reasonable success by Walker and Wolowicz in reference 2. It was shown in reference 1 that, although slender-body theory alone does not accurately predict the characteristics of nonslender bodies, the ratio of corresponding slender-body derivatives may be used with reasonable accuracy to predict the static forces on nonslender configurations. The body contribution to $C_{L\dot{\alpha}}$ is then given as the product of the lift-curve slope $C_{L\alpha}$ and the ratio of slender-body derivatives, i.e.,

$$C_{L\dot{\alpha}} = C_{L\alpha} \left(\frac{C_{L\dot{\alpha}}}{C_{L\alpha}} \right)_{\text{slender-body theory}}$$

Since slender-body theory states that body force characteristics are independent of Mach number, the limitations of these methods are determined by the limitations of the methods used in determining the derivative $C_{L\alpha}$ in the various speed regimes. Experimental data should be used for the body lift-curve slope when available.

A. SUBSONIC

There is no explicit method available in the literature for the estimation of body acceleration derivatives in the subsonic speed range. The method presented below is based on the application of slender-body theory in the manner previously discussed.

DATCOM METHOD

The body contribution to $C_{L\dot{\alpha}}$, based on body base area and body length, is given by

$$C_{L\dot{\alpha}} = 2 C_{L\alpha} \left(\frac{V_B}{S_b l_B} \right) \quad (\text{per radian})$$

7.2.2.1-a

7.2.2.1-1

where

$C_{L\alpha}$ is the body lift-curve slope from paragraph A of Section 4.2.1.1 multiplied by $(V_B^{2/3}/S_b)$, based on S_b (per radian).

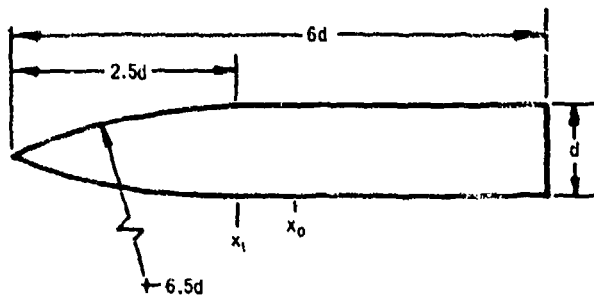
V_B is the total body volume from Section 2.3.

S_b is the body base area.

ℓ_B is the length of the body.

Sample Problem

Given: Same ogive-cylinder configuration as sample problem of paragraph A of Section 7.2.1.1.



$$d = 1 \text{ ft} \quad \ell_B = 6.0 \text{ ft} \quad \text{Fineness Ratio} = 6.0$$

$$V_B = 3.88 \text{ cu ft (Section 2.3)} \quad S_b = 0.785 \text{ sq ft}$$

$$C_{L\alpha} = 1.724 \text{ per rad (based on } S_b, \text{ Section 7.2.1.1)}$$

Compute:

$$\frac{V_B}{S_b \ell_B} = \frac{(3.88)}{(0.785)(6.0)} = 0.824$$

Solution:

$$C_{L\alpha} = 2 C_{L\alpha} \left(\frac{V_B}{S_b \ell_B} \right) \quad (\text{equation 7.2.2.1-a})$$

$$= 2(1.724)(0.824)$$

$$= 2.84 \text{ per rad (based on } S_b \ell_B)$$

B. TRANSONIC

The only available method for determining the body dynamic stability derivatives at transonic speeds is that of Landahl in reference 3. However, Landahl's results for the acceleration derivatives are frequency-dependent and no quantitative information is presented. Since slender-body theory states that body force characteristics are independent of Mach number, the method of paragraph A is applicable throughout the transonic speed range.

C. SUPERSONIC

Several of the theoretical methods available for estimating the body acceleration derivatives in the supersonic speed range are briefly discussed in Section 7.2. These include simple slender-body theory, theories treated within the assumptions of slender-body theory, and hybrid theory. The method presented here is based on the results of simple slender-body theory. Theories treated within the assumptions of slender-body theory are mathematically complex and restricted to specific planforms; therefore, no general quantitative information of their results is presented.

The supersonic $C_{N\dot{\alpha}}$ of cones may be obtained from the hybrid theory solution of reference 4.

DATCOM METHOD

The method presented here for determining the body contribution to $C_{N\dot{\alpha}}$, based on body base area and body length, is the same as that of paragraph A and is given by equation 7.2.2.1-a, i.e.,

$$C_{N\dot{\alpha}} = 2 C_{N\alpha} \left(\frac{V_B}{S_b l_B} \right)$$

where $C_{N\alpha}$ is the body normal-force-curve slope from paragraph C of Section 4.2.1.1, evaluated at the appropriate Mach number. The other parameters are defined in paragraph A of this section.

D HYPERSONIC

The body contribution to the derivative $C_{N\dot{\alpha}}$ in the hypersonic speed range is shown in reference 5 to be zero when determined by the Newtonian impact theory.

REFERENCES

1. Pitts, W. C., Nielsen, J. N., and Kaettner, G. E.: Lift and Center of Pressure of Wing-Body-Tail Combinations at Subsonic, Transonic, and Supersonic Speeds. NACA TN 1307, 1957. (U)
2. Walker, H. J., and Wolowicz, C. H.: Theoretical Stability Derivatives for the X-15 Research Airplane at Supersonic and Hypersonic Speeds Including a Comparison with Wind-Tunnel Results. NASA TM X-287, 1960. (U)
3. Landahl, M. T.: Forces and Moments on Oscillating Slender Wing-Body Combinations at Sonic Speed. MIT Fluid Dynamics Research Group Report No. 56-1, 1956. (U)

4. Tobak, M., and Wehrend, W. R.: Stability Derivatives of a Cone at Supersonic Speeds. NACA TN 3788, 1956. (U)
5. Fisher, L. R.: Equations and Charts for Determining the Hypersonic Stability Derivatives of Cone Frustums Computed by Newtonian Impact Theory. NASA TN D-149, 1959. (U)

7.2.2.2 BODY ACCELERATION DERIVATIVE $C_{m\dot{\alpha}}$

Methods are presented for determining the body contribution to the acceleration derivative $C_{m\dot{\alpha}}$ in the subsonic, transonic, and supersonic speed ranges.

Datcom methods are based on the same assumptions that were made in regard to the estimation of the body contribution to the derivative $C_{L\dot{\alpha}}$, and the general discussion of Section 7.2.2.1 is directly applicable here. The body contribution to $C_{m\dot{\alpha}}$ is expressed as

$$C_{m\dot{\alpha}} = C_{m\alpha} \left(\frac{C_{m\dot{\alpha}}}{C_{m\alpha}} \right)_{\text{slender-body theory}}$$

The limitations of these methods are determined by the limitations of the methods used in estimating the static derivative $C_{m\alpha}$ in the various speed regimes. Experimental data should be used for the body pitching-moment-curve slope when available.

A. SUBSONIC

The comments of Paragraph A of Section 7.2.2.1 are directly applicable here.

DATCOM METHOD

The body contribution to $C_{m\dot{\alpha}}$, based on body base area and the square of the body length and referred to an arbitrary moment center, is given by

$$C_{m\dot{\alpha}} = 2 C_{m\alpha} \left[\frac{\frac{V_B}{S_B l_B} \left(\frac{x_c}{l_B} - \frac{x_m}{l_B} \right)}{\left(1 - \frac{x_m}{l_B} \right) - \frac{V_B}{S_B l_B}} \right] \quad 7.2.2.2-a$$

where

$C_{m\alpha}$ is the body pitching-moment-curve slope from Paragraph A of Section 4.2.2.1, multiplied by $V_B/(S_B l_B)$.

x_c is the longitudinal distance from the vertex to the centroid of the volume and is given by Equation 7.2.1.2-b, i.e.,

$$x_c = \frac{\int_0^{l_B} S(x) x dx}{V_B}$$

x_m is the longitudinal distance from the body vertex to the center of rotation, positive aft.

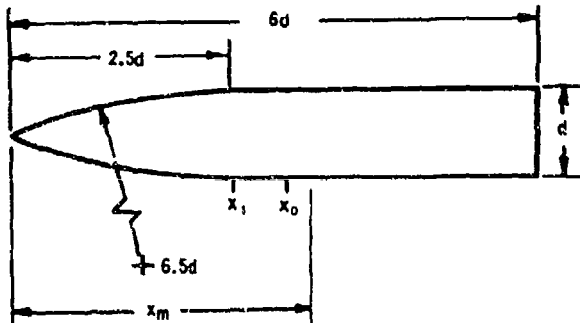
ℓ_B is the length of the body.

V_B is the total body volume from Section 2.3.

S_b is the body base area.

Sample Problem

Given: Same ogive-cylinder configuration as sample problems of Paragraph A of Sections 7.2.1.2 and 7.2.2.1.



$$d = 1 \text{ ft}$$

$$\ell_B = 6.0 \text{ ft}$$

$$\text{Fineness Ratio} = 6.0$$

$$x_m = 3.8 \text{ ft}$$

$$\frac{V_B}{S_b \ell_B} = 0.824 \text{ (Section 7.2.2.1)}$$

$$\left. \begin{array}{l} C_{m\alpha} = 0.781 \text{ per rad} \\ x_c = 3.55 \text{ ft} \end{array} \right\} \text{ (Section 7.2.1.2)}$$

Solution:

$$\left(1 - \frac{x_m}{\ell_B}\right) = \left(1 - \frac{3.8}{6.0}\right) = 0.367$$

$$\begin{aligned}
 C_{m\dot{\alpha}} &= 2 C_{m\alpha} \frac{\left[\frac{V_B}{S_b l_B} \left(\frac{x_c}{l_B} - \frac{x_m}{l_B} \right) \right]}{\left[\left(1 - \frac{x_m}{l_B} \right) - \frac{V_B}{S_b l_B} \right]} \quad (\text{Equation 7.2.2.2-a}) \\
 &= 2(0.781) \frac{\left[0.824 \left(\frac{3.55}{6.0} - \frac{3.8}{6.0} \right) \right]}{0.367 - 0.824} \\
 &= 1.562 \left(\frac{-0.0343}{-0.457} \right) \\
 &= 0.117 \text{ per rad (based on } S_b l_B^2)
 \end{aligned}$$

B. TRANSONIC

The comments of Paragraph B of Section 7.2.2.1 are directly applicable here. The method of Paragraph A is applicable throughout the transonic speed range.

C. SUPERSONIC

The theoretical methods applicable for the estimation of the body contribution to the derivative $C_{m\dot{\alpha}}$ parallel those of the body contribution to the derivative $C_{L\dot{\alpha}}$. Therefore, the general comments of Paragraph C of Section 7.2.2.1 are also applicable here.

The supersonic $C_{m\dot{\alpha}}$ for a cone can be estimated by the hybrid theory solutions presented in Reference 1.

DATCOM METHOD

The method presented here for the body contribution to $C_{m\dot{\alpha}}$, based on body base area and the square of the body length and referred to an arbitrary moment center, is the same as that of Paragraph A and is given by Equation 7.2.2.2-a, i.e.,

$$C_{m\dot{\alpha}} = 2 C_{m\alpha} \frac{\left[\frac{V_B}{S_b l_B} \left(\frac{x_c}{l_B} - \frac{x_m}{l_B} \right) \right]}{\left[\left(1 - \frac{x_m}{l_B} \right) - \frac{V_B}{S_b l_B} \right]}$$

where $C_{m\alpha}$ is the body pitching-moment-curve slope from Paragraph C of Section 4.2.2.1, evaluated at the appropriate Mach number. The other parameters are defined in Paragraph A of this section.

D. HYPERSONIC

The body contribution to the derivative $C_{m\dot{\alpha}}$ in the hypersonic speed range is shown in Reference 1 to be zero when determined by the Newtonian impact theory.

REFERENCE

1. Tobak, M., and Wehrend, W. R.: Stability Derivatives of a Cone at Supersonic Speeds. NACA TN 3788, 1956. (U)

7.3 WING-BODY DYNAMIC DERIVATIVES

7.3.1 WING-BODY PITCHING DERIVATIVES

7.3.1.1 WING-BODY PITCHING DERIVATIVE C_{Lq}

The information contained in this section is for estimating the pitching derivative C_{Lq} of wing-body configurations at low angles of attack. In general, it consists of a synthesis of material presented in other sections; however, the method of application is new.

The Datcom methods are based on the assumption that the mutual interferences that occur between components for angle-of-attack variations, determined in references 1 and 2 and presented in Section 4.3.1.2, may be employed with reasonable accuracy to the case of steady pitching. This approach to the calculation of wing-body pitching derivatives has been used with reasonable success by Walker and Wolowicz in reference 3.

A. SUBSONIC

Two methods are presented for determining the pitching derivative C_{Lq} of a wing-body configuration, differing only in their treatment of the mutual interference effects.

DATCOM METHODS

Method 1

For wing-body configurations similar to sketch (d) of Section 4.3.1.2, the pitching derivative C_{Lq} , based on the area and mean aerodynamic chord of the total panel and referred to a moment center at the assumed center of gravity or center of rotation, is given by

$$(C_{Lq})_{WB} = [K_{W(B)} + K_{B(W)}] \left(\frac{S_e}{S} \right) \left(\frac{\bar{c}_e}{\bar{c}} \right) (C_{Lq})_e + (C_{Lq})_B \left(\frac{S_b}{S} \right) \left(\frac{\bar{c}_B}{\bar{c}} \right) \quad 7.3.1.1-a$$

where

$K_{W(B)}$ and $K_{B(W)}$ are the appropriate wing-body interference factors obtained from Section 4.3.1.2.

$(C_{Lq})_e$ is the contribution of the exposed panel to the pitching derivative C_{Lq} , obtained from Section 7.1.1.1. (See Section 4.3.1.2 for the definition of exposed surfaces.)

$(C_{Lq})_B$ is the contribution of the body to the pitching derivative C_{Lq} , obtained from Section 7.2.1.1.

$\frac{S_e}{S}$ is the ratio of the exposed to the total panel area.

$\frac{S_b}{S}$ is the ratio of the body base area to the total panel area.

$\frac{\bar{c}_e}{\bar{c}}$ is the ratio of the mean aerodynamic chord of the exposed panel to the mean aerodynamic chord of the total panel.

$\frac{\ell_B}{\bar{c}}$ is the ratio of the body length to the mean aerodynamic chord of the total panel.

Moment transfer calculations are included as an integral part of the wing and body derivative estimation methods of Sections 7.1.1.1 and 7.2.1.1, respectively.

Method 2

For wing-body configurations similar to sketch (c) of Section 4.3.1.2, the pitching derivative C_{Lq} , based on the area and mean aerodynamic chord of the total panel and referred to a moment center at the assumed center of gravity or center of rotation, is given by

$$(C_{Lq})_{WB} = K_{(WB)} (C_{Lq})_W + (C_{Lq})_B \left(\frac{S_b}{S} \right) \left(\frac{\ell_B}{\bar{c}} \right) \quad 7.3.1.1-b$$

where

$K_{(WB)}$ is the wing-body interference factor, obtained from figure 4.3.1.2-12c of Section 4.3.1.2.

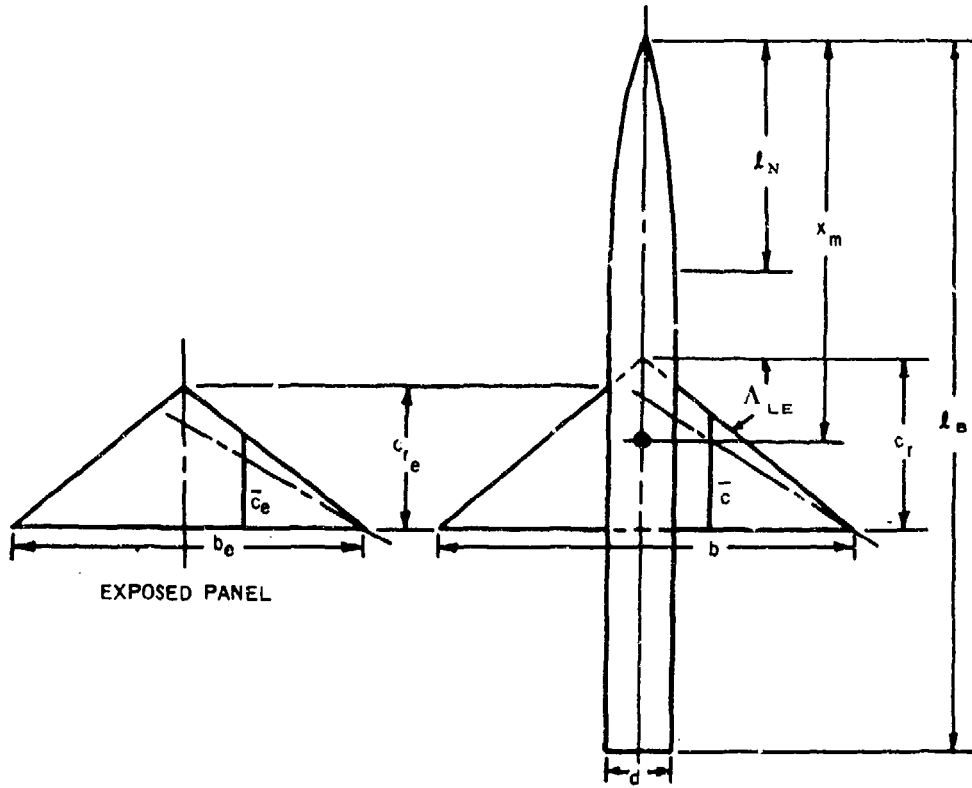
$(C_{Lq})_W$ is the contribution of the total panel to the pitching derivative C_{Lq} , obtained from Section 7.1.1.1.

The remaining terms are defined in method 1 above. Moment transfer calculations are included as an integral part of the wing and body derivative estimation methods of Sections 7.1.1.1 and 7.2.1.1, respectively.

Sample Problem

Method 1

Given: An ogive-cylinder-body-triangular-wing configuration



Wing Characteristics:

Total Panel		Exposed Panel	
$A = 5.0$	$\lambda = 0$	$A_e = 5.0$	$\lambda_e = 0$
$\Lambda_{LE} = 38.67^\circ$	$S = 414.0 \text{ sq ft}$	$b_e = 38.37 \text{ ft}$	$S_e = 294.50 \text{ sq ft}$
$i_w = 0$	$c_r = 18.20 \text{ ft}$	$\Lambda_{c/2} = 21.8^\circ$	$c_{r_e} = 15.375 \text{ ft}$
$b = 45.50 \text{ ft}$	$\bar{c} = 12,133 \text{ ft}$		$\bar{c}_e = 10.25 \text{ ft}$

NACA 66-206 airfoil section

Body Characteristics:

$$l_N = 25.0 \text{ ft} \quad l_B = 77.20 \text{ ft} \quad d = 7.127 \text{ ft}$$

The following ratios based on total panel dimensions:

$$\frac{S_e}{S} = 0.7113 \quad \frac{\bar{c}_e}{\bar{c}} = 0.845 \quad \frac{S_b}{S} = 0.0963 \quad \frac{l_B}{\bar{c}} = 6.363$$

Additional Characteristics:

$$M = 0.60 \quad x_m = 43.70 \text{ ft (moment center at } \bar{c}/4 \text{ of total panel)}$$

$$\beta = 0.80 \quad \frac{d}{b} = 0.157$$

Compute:

Step 1. Pitching derivative C_{L_q} for exposed panel (Section 7.1.1.1)

$$c_{L\alpha} = 6.19 \text{ per rad (table 4.1.1-B)}$$

$$\kappa = \frac{c_{L\alpha}}{2\pi} = 0.985$$

$$\frac{A_e}{\kappa} \left[\beta^2 + \tan^2 \Lambda_{c/2} \right]^{1/2} = \frac{5.0}{0.985} [0.64 + 0.16]^{1/2} = 4.54$$

$$\frac{(C_{L\alpha})_e}{A_e} = 0.90 \text{ per rad (figure 4.1.3.2-49)}$$

$$(C_{L\alpha})_e = 4.50 \text{ per rad}$$

$$\frac{\tan \Lambda_{LE}}{\beta} = 1.0$$

$$A_e \tan \Lambda_{LE} = 4.0$$

$$\left(\frac{x_{a.c.}}{c_r} \right)_e = 0.560 \text{ (figure 4.1.4.2-26a)}$$

$$\left(\frac{x_{c.g.}}{c_r} \right)_e = 0.408 \text{ (from planform geometry of exposed panel with c.g. at } \bar{c}/4 \text{ of total panel)}$$

$$\left(\frac{\bar{x}}{\bar{c}} \right)_e = \left(\frac{x_{a.c.}}{\bar{c}} - \frac{x_{c.g.}}{\bar{c}} \right)_e \text{ (equation 7.1.1.1-b)}$$

$$= \left(\frac{x_{a.c.}}{c_r} - \frac{x_{c.g.}}{c_r} \right)_e \left(\frac{c_r}{\bar{c}} \right)_e = (0.560 - 0.408) 1.50 = 0.228$$

$$(C_{L_q})_e = \left(\frac{1}{2} + 2 \frac{\bar{x}}{\bar{c}} \right)_e (C_{L_\alpha})_e \quad (\text{equation 7.1.1.1-a})$$

$$= (0.956) (4.50)$$

$$= 4.30 \text{ per rad (based on } S_e \bar{c}_e)$$

Step 2. Wing-body interference factors (Section 4.3.1.2)

$$\begin{aligned} K_{W(B)} &= 1.125 \\ K_{B(W)} &= 0.215 \end{aligned} \quad \left. \right\} \quad (\text{figure 4.3.1.2-10})$$

Step 3. Pitching derivative C_{L_q} for body (Section 7.2.1.1)

$$\frac{\ell}{d} = \frac{77.20}{7.127} = 10.83$$

$$(k_2 - k_1) = 0.947 \quad (\text{figure 4.2.1.1-20a})$$

$$x_1 = \ell_N = 25.0 \text{ ft}$$

$$\frac{x_1}{\ell_B} = \frac{25.0}{77.2} = 0.324$$

$$\frac{x_o}{\ell_B} = 0.55 \quad (\text{extrapolated using figure 4.2.1.1-20b})$$

$$x_o = 42.46 \text{ ft}$$

$$S_o = S_1 = 39.88 \text{ sq ft}$$

$$\frac{\ell_N}{d} = \frac{25.0}{7.127} = 3.508$$

$$\frac{V_N}{S_o \ell_N} = 0.535 \quad (\text{figure 2.3-5, ogive})$$

$$V_N = (0.535) (39.88) (25.0) = 533.4 \text{ cu ft}$$

$$\begin{aligned}
 V_B &= (\ell_B - \ell_N) S_1 + V_N \\
 &= (77.2 - 25.0)(39.88) + 533.4 \\
 &= 2615.1 \text{ cu ft}
 \end{aligned}$$

$$V_B^{2/3} = 189.8 \text{ sq ft}$$

$$\begin{aligned}
 (C_{L\alpha})_B &= \frac{2(k_2 - k_1) S_o}{V_B^{2/3}} \quad (\text{equation 4.2.1.1-a}) \\
 &= \frac{2(0.947)(39.88)}{189.8} \\
 &= 0.398 \text{ per rad (based on } V_B^{2/3})
 \end{aligned}$$

$$(C_{L\alpha})_B = 0.398 \frac{V_B^{2/3}}{S_b} = 0.398 \left(\frac{189.8}{39.88} \right) = 1.894 \text{ per rad (based on } S_b)$$

$$\left(1 - \frac{x_m}{\ell_B} \right) = \left(1 - \frac{43.70}{77.20} \right) = 0.434$$

$$\begin{aligned}
 (C_{Lq})_B &= 2(C_{L\alpha})_B \left(1 - \frac{x_m}{\ell_B} \right) \quad (\text{equation 7.2.1.1-a}) \\
 &= 2(1.894)(0.434) \\
 &= 1.644 \text{ per rad (based on } S_b \ell_B)
 \end{aligned}$$

Solution:

$$\begin{aligned}
 (C_{Lq})_{WB} &= [K_{W(B)} + K_{B(W)}] \left(\frac{S_e}{S} \right) \left(\frac{\bar{c}_e}{\bar{c}} \right) (C_{Lq})_e + (C_{Lq})_B \left(\frac{S_b}{S} \right) \left(\frac{\ell_B}{\bar{c}} \right) \quad (\text{equation 7.3.1.1-a}) \\
 &= (1.173 + 0.215)(0.7113)(0.845)(4.30) + (1.644)(0.0963)(6.363) \\
 &= 3.46 + 1.007 \\
 &= 4.467 \text{ per rad (based on the area and mean aerodynamic chord of the total panel and referred to a moment center at } \bar{c}/4 \text{ of the total panel!)}
 \end{aligned}$$

B. TRANSONIC

The aerodynamic interference effects for slender wing-body configurations are relatively insensitive to Mach number; consequently, the slender-body interference factors of Section 4.3.1.2 should give reasonable results. For nonslender configurations, transonic interference effects can become quite large and sensitive to minor changes in local contour.

DATCOM METHODS

It is recommended that the methods presented in paragraph A for estimating the pitching derivative C_{Lq} of a wing-body configuration be applied to the transonic speed regime. Care should be taken to estimate the contributions of the lifting panel and body at the appropriate Mach number. The interference factors should be obtained from paragraph C, Section 4.3.1.2.

C. SUPERSONIC

The information included in the Datcom accounts for most of the mutual interferences that occur between components of a wing-body configuration at supersonic speeds. These interference effects have been accounted for by the slender-body interference factors of Section 4.3.1.2.

DATCOM METHODS

The methods presented in paragraph A for estimating the pitching derivative C_{Lq} of a wing-body configuration are also applicable to the supersonic speed range. Care should be taken to estimate the contributions of the lifting panel and body at the appropriate Mach number.

Sample Problem

Method 1

Given: Same configuration as sample problem of paragraph A

$$M = 1.4 \quad \beta = 0.98$$

Compute:

Step 1. Pitching derivative C_{Lq} for exposed panel (Section 7.1.1.1)

$$\frac{\tan \Lambda_{LE}}{\beta} = 0.816$$

$$A_e \tan \Lambda_{LE} = 4.0$$

$$\beta (C_{N\alpha})_e = 4.0 \text{ per rad} \quad (\text{figure 4.1.3.2-56a})$$

$$(C_{N\alpha})_e = 4.08 \text{ per rad}$$

$$\left(\frac{x_{a.c.}}{c_r}\right)_e = 0.67 \quad (\text{figure 4.1.4.2-26a})$$

$$\left(\frac{x_{c.g.}}{c_r}\right)_e = 0.408 \quad (\text{from planform geometry of exposed panel with c.g. at } \bar{c}/4 \text{ of total panel})$$

$$\left(\frac{\bar{x}}{\bar{c}}\right)_e = \left(\frac{x_{a.c.}}{\bar{c}} - \frac{x_{c.g.}}{\bar{c}}\right)_e \quad (\text{equation 7.1.1.1-b})$$

$$= \left(\frac{x_{a.c.}}{c_r} - \frac{x_{c.g.}}{c_r}\right)_e \left(\frac{c_r}{\bar{c}}\right)_e = (0.67 - 0.408) 1.50 = 0.393$$

$$\beta \cot \Lambda_{LE} = 1.225 \quad (\text{supersonic leading edge})$$

$$\beta A_e = 4.90$$

$$\cot^{-1}(\beta \cot \Lambda_{LE}) = 39.23^\circ$$

$$(C_{Lq}')_e = 0 \quad (\text{figure 7.1.1.1-11a})$$

$$\begin{aligned} (C_{Lq})_e &= (C_{Lq}')_e + 2\left(\frac{\bar{x}}{\bar{c}}\right)_e (C_{N\alpha})_e \quad (\text{equation 7.1.1.1-c}) \\ &= 0 + 2(0.393)(4.08) \\ &= 3.21 \text{ per rad (based on } S_e \bar{c}_e) \end{aligned}$$

Step 2. Wing-body interference factors (Section 4.3.1.2)

$$K_{W(B)} = 1.125 \quad (\text{figure 4.3.1.2-10})$$

$$\frac{\beta d}{c_{r_e}} = \frac{(0.98)(7.127)}{15.375} = 0.455$$

$$K_{B(W)} \left[\beta (C_{N\alpha})_e (\lambda_e + 1) \left(\frac{b}{d} - 1 \right) \right] = 3.90 \quad (\text{figure 4.3.1.2-11a})$$

$$\left[\beta \left(C_{N\alpha} \right)_e (\lambda_e + 1) \left(\frac{b}{d} - 1 \right) \right] = (0.98) (4.08) (1) (6.38 - 1) = 21.51$$

$$K_{B(W)} = \frac{3.90}{21.51} = 0.181$$

Step 3. Pitching derivative C_{Lq} for body (Section 7.2.1.1)

$$f_A = \frac{\ell_A}{d} = \frac{77.2 - 25.0}{7.127} = 7.32$$

$$f_N = \frac{\ell_N}{d} = \frac{25.0}{7.127} = 3.51$$

$$f_A/f_N = 2.09$$

$$\frac{\beta}{f_N} = \frac{0.98}{3.51} = 0.279$$

$$(C_{N\alpha})_B = 2.74 \text{ per rad} \quad (\text{figure 4.2.1.1-21a, extrapolated})$$

$$\left(1 - \frac{x_m}{\ell_B} \right) = 0.434 \quad (\text{sample problem, paragraph A})$$

$$(C_{Lq})_B = 2 (C_{N\alpha})_B \left(1 - \frac{x_m}{\ell_B} \right) \quad (\text{equation 7.2.1.1-a})$$

$$= 2(2.74)(0.434)$$

$$= 2.378 \text{ per rad (based on } S_b \ell_B)$$

Solution:

$$(C_{Lq})_{WB} = [K_{W(B)} + K_{B(W)}] \left(\frac{S_e}{S} \right) \left(\frac{\bar{c}_e}{\bar{c}} \right) (C_{Lq})_e + (C_{Lq})_B \left(\frac{S_b}{S} \right) \left(\frac{\ell_B}{\bar{c}} \right) \quad (\text{equation 7.3.1.1-a})$$

$$= (1.125 + 0.181) (0.7113) (0.845) (3.21) + (2.378) (0.0963) (6.363)$$

$$= 2.520 + 1.457$$

$$= 3.977 \text{ per rad} \quad (\text{based on the area and mean aerodynamic chord of the total panel and referred to a moment center at } \bar{c}/4 \text{ of the total panel})$$

REFERENCES

1. Pitts, W., Neilsen, J., and Kaattari, G.: Lift and Center of Pressure of Wing-Body-Tail Combinations at Subsonic, Transonic, and Supersonic Speeds. NACA TR 1307, 1959. (U)
2. Spreiter, J.: The Aerodynamic Forces on Slender Plane and Cruciform-Wing and Body Combinations. NACA TR 962, 1950. (U)
3. Walker, H., and Wolowicz, C.: Theoretical Stability Derivatives for the X-15 Research Airplane at Supersonic and Hypersonic Speeds Including a Comparison with Wind-Tunnel Results. NASA TM X-287, 1960. (U)

7.3.1.2 WING-BODY PITCHING DERIVATIVE C_{m_q}

The information contained in this section is for estimating the pitching derivative C_{m_q} of wing-body configurations at low angles of attack. The derivative C_{m_q} is a measure of the pitching moment produced by rotational motion about a spanwise axis and is commonly referred to as the pitch-damping derivative.

The Datcom methods are based on the same assumption that was made in regard to the pitching derivative C_{L_q} of a wing-body configuration, and the general discussion of Section 7.3.1.1 is directly applicable here.

A. SUBSONIC

Two methods are presented for determining the pitching derivative C_{m_q} of a wing-body configuration, differing only in their treatment of the mutual interference effects.

DATCOM METHODS

Method 1

For wing-body configurations similar to sketch (d) of Section 4.3.1.2, the pitching derivative C_{m_q} , based on the area and the square of the mean aerodynamic chord of the total panel and referred to a moment center at the assumed center of gravity or center of rotation, is given by

$$(C_{m_q})_{WB} = [K_{W(B)} + K_{B(W)}] \left(\frac{S_e}{S} \right) \left(\frac{\bar{c}_e}{\bar{c}} \right)^2 (C_{m_q})_e + (C_{m_q})_B \left(\frac{S_b}{S} \right) \left(\frac{\bar{c}_B}{\bar{c}} \right)^2 \quad 7.3.1.2-a$$

where

$(C_{m_q})_e$ is the contribution of the exposed panel to the pitching derivative C_{m_q} , obtained from Section 7.1.1.2. (See Section 4.3.1.2 for the definition of exposed surfaces.)

$(C_{m_q})_B$ is the contribution of the body to the pitching derivative C_{m_q} , obtained from Section 7.2.1.2.

The remaining terms are defined in paragraph A of Section 7.3.1.1. Moment transfer calculations are included as an integral part of the wing- and body-derivative estimation methods of Sections 7.1.1.2 and 7.2.1.2, respectively.

Method 2

For wing-body configurations similar to sketch (c) of Section 4.3.1.2, the pitching derivative C_{m_q} , based on the area and the square of the mean aerodynamic chord of the total panel and referred to a moment center at the assumed center of gravity or center of rotation, is given by

$$(C_m)_W_B = K_{WB} (C_m)_W + (C_m)_B \left(\frac{S_b}{S} \right) \left(\frac{\ell_B}{c} \right)^2 \quad 7.3.1.2-b$$

where

$(C_m)_W$ is the contribution of the total panel to the pitching derivative C_m , obtained from Section 7.1.1.2.

The remaining terms are defined in method 1 above and paragraph A of Section 7.3.1.1. Moment transfer calculations are included as an integral part of the wing- and body-derivative estimation methods of Sections 7.1.1.2 and 7.2.1.2, respectively.

Sample Problem

Method 1

Given: Same configuration as sample problem of paragraph A, Section 7.3.1.1. The characteristics are repeated below.

Wing Characteristics:

Total Panel		Exposed Panel	
$A = 5.0$	$\lambda = 0$	$A_e = 5.0$	$\lambda_e = 0$
$\Lambda_{LE} \approx 38.67^\circ$	$S = 414.0 \text{ sq ft}$	$b_e = 38.37 \text{ ft}$	$S_e = 294.50 \text{ sq ft}$
$i_w = 0$	$c_t = 18.20 \text{ ft}$	$\Lambda_{c/4} = 30.96^\circ$	$c_{t_e} = 15.375 \text{ ft}$
$b = 45.50 \text{ ft}$	$\bar{c} = 12.133 \text{ ft}$		$\bar{c}_e = 10.25 \text{ ft}$

NACA 66-206 airfoil section

Body Characteristics:

$$\ell_N = 25.0 \text{ ft} \quad \ell_B = 77.20 \text{ ft} \quad d = 7.127 \text{ ft}$$

The following ratios based on total panel dimensions:

$$\frac{S_e}{S} = 0.7113 \quad \left(\frac{\bar{c}_e}{\bar{c}} \right)^2 = 0.7140$$

$$\frac{S_b}{S} = 0.0963 \quad \left(\frac{\ell_B}{\bar{c}} \right)^2 = 40.49$$

Additional Characteristics:

$$M = 0.60$$

$x_m = 43.70$ ft (moment center at $\bar{c}/4$ of total panel)

$$-\beta = 0.80$$

$$\frac{d}{b} = 0.157$$

Compute:

Step 1. Pitching derivative C_{m_q} for exposed panel (Section 7.1.1.2)

$$\left. \begin{aligned} c_{q\alpha} &= 6.19 \text{ per rad} \\ \left(\frac{\bar{x}}{c} \right)_e &= 0.228 \end{aligned} \right\}$$

(sample problem, paragraph A, Section 7.3.1.1)

$$\cos \Lambda_{c/4} = 0.8576$$

$$\tan \Lambda_{c/4} = 0.600$$

$$B = \sqrt{1 - M^2 \cos^2 \Lambda_{c/4}} = 0.8575$$

$$\left[(C_{m_q})_{M \approx 0.2} \right]_e = -0.7 c_{q\alpha} \cos \Lambda_{c/4} \left\{ \frac{A_e \left[\frac{1}{2} \frac{\bar{x}}{c} + 2 \left(\frac{\bar{x}}{c} \right)^2 \right]}{A_e + 2 \cos \Lambda_{c/4}} \right. \\ \left. + \frac{1}{24} \left(\frac{A_e^3 \tan^2 \Lambda_{c/4}}{A_e + 6 \cos \Lambda_{c/4}} \right) + \frac{1}{8} \right\} \quad (\text{equation 7.1.1.2-a})$$

$$= -0.7(6.19)(0.8576) \left\{ \frac{5 \left[\frac{1}{2} (0.228) + 2(0.228)^2 \right]}{5 + 2(0.8576)} \right. \\ \left. + \frac{1}{24} \left[\frac{(5)^3 (0.6)^2}{5 + 6(0.8576)} \right] + \frac{1}{8} \right\}$$

$$= -3.72 \left[\frac{1.090}{6.715} + \frac{1}{24} \left(\frac{45}{10.146} \right) + \frac{1}{8} \right]$$

$$= -3.72(0.4721)$$

$$= -1.76 \text{ per rad (based on } S_e \bar{c}_e^2)$$

$$(C_m q)_e = \left[\frac{\frac{A_e^3 \tan^2 \Lambda_{c/4}}{A_e B + 6 \cos \Lambda_{c/4}} + \frac{3}{B}}{\frac{A_e^3 \tan^2 \Lambda_{c/4}}{A_e + 6 \cos \Lambda_{c/4}} + 3} \right] \left[(C_m q)_M \approx 0.2 \right]_e \quad (\text{equation 7.1.1.2-b})$$

$$= \left[\frac{\frac{(5)^3 (0.6)^2}{(5)(0.8575) + 6(0.8576)} + \frac{3}{0.8575}}{\frac{(5)^3 (0.6)^2}{5 + 6(0.8576)} + 3} \right] (-1.76)$$

$$= \left(\frac{4.77 + 3.499}{4.435 + 3} \right) (-1.76)$$

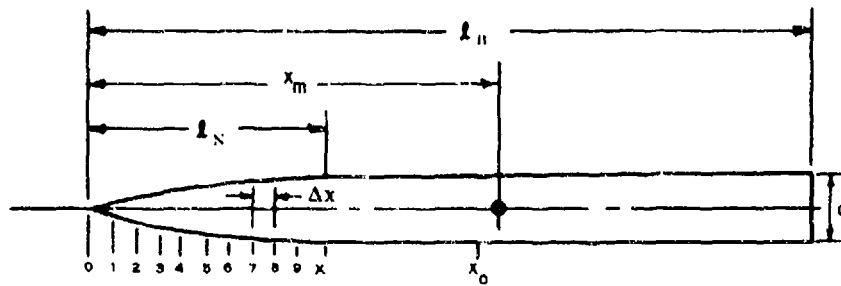
$$= \left(\frac{8.269}{7.435} \right) (-1.76)$$

$$= -1.96 \text{ per rad (based on } S_e \bar{c}_e^2)$$

Step 2. Wing-body interference factors (Section 4.3.1.2)

$$\left. \begin{array}{l} K_{W(B)} = 1.125 \\ K_{B(W)} = 0.215 \end{array} \right\} \text{ (sample problem, paragraph A, Section 7.3.1.1)}$$

Step 3. Pitching derivative $C_m q$ for body (Section 7.2.1.2)



$$\Delta x = 2.5 \text{ ft}$$

From sample problem, paragraph A, Section 7.3.1.1:

$$(k_2 - k_1) = 0.947 \quad V_B = 2615.1 \text{ cu ft} \quad S_b = 39.88 \text{ sq ft}$$

$$x_1 = 25.0 \text{ ft} \quad x_0 = 42.46 \text{ ft}$$

Determine $(C_m)_B$

Station	d ft	S_x sq ft	$\Delta S_x \approx \frac{dS_x}{dx} \Delta x$	$(x_m - x)^*$	$\frac{dS_x}{dx} (x_m - x) \Delta x$
1	1.137	1,016	1,016	42,033	42.71
2	2,600	5,309	4,293	39,787	170.81
3	3.725	10,898	5,589	37,376	208.89
4	4.650	16,982	6,084	34,904	212.36
5	5,450	23,328	6,346	32,417	205.72
6	6,150	29,706	6,378	29,926	190.86
7	6,625	34,472	4,766	27,425	130.71
8	6,950	37,937	3,405	24,940	86.42
9	7,100	39,592	1,655	22,446	37.15
x_1	7,127	39,800	0.288	19,949	5.74
x_0	7,127	39,880	0	9,970	0

$$\sum_{x=0}^{x_0} \frac{dS_x}{dx} (x_m - x) \Delta x = 1291$$

$$(C_m)_B = \frac{2(k_2 - k_1)}{V_B} \sum_{x=0}^{x_0} \frac{dS_x}{dx} (x_m - x) \Delta x \quad (\text{equation 4.2.2.1-a})$$

$$= \frac{2(0.947)(1291)}{2615.1} = 0.935 \text{ per rad (based on } V_B)$$

$$(C_m)_B = (0.935) \frac{V_B}{S_b l_B} = 0.935 \frac{(2615.1)}{(39.88)(77.2)} = 0.794 \text{ per rad (based on } S_b l_B)$$

*x is taken to be at the center of volume of each body segment.

Determine x_c

Station	d ft	S(x) sq ft	x^*	$S(x) \times \Delta x$
1	1.137	1.016	1.667	4.23
2	2.600	5.309	3.913	51.94
3	3.725	10.898	6.324	172.30
4	4.650	16.982	8.796	373.43
5	5.450	23.328	11.283	658.02
6	6.150	29.706	13.775	1023.00
7	6.625	34.472	16.275	1402.58
8	6.950	37.937	18.760	1779.24
9	7.100	39.592	21.254	2103.72
10	7.127	39.880	23.751	2367.97
ℓ_B	7.127	39.880	51.100	106,377.

$$\sum_{x=0}^{\ell_B} S(x) \times \Delta x = 116,313$$

$$x_c = \frac{\int_0^{\ell_B} S(x) x \, dx}{V_B} = \frac{116,313}{2615.1} = 44.48 \text{ ft} \quad (\text{equation 7.2.1.2-b})$$

$$\frac{V_B}{S_b \ell_B} = \frac{2615.1}{(39.88)(77.2)} = 0.849$$

$$\left(1 - \frac{x_m}{\ell_B}\right) = 0.434 \quad (\text{sample problem, paragraph A, Section 7.3.1.1})$$

$$(C_{m_q})_B = 2(C_{m_\alpha})_B \left[\frac{\left(1 - \frac{x_m}{\ell_B}\right)^2 - \frac{V_B}{S_b \ell_B} \left(\frac{x_c}{\ell_B} - \frac{x_m}{\ell_B}\right)}{\left(1 - \frac{x_m}{\ell_B}\right) - \frac{V_B}{S_b \ell_B}} \right] \quad (\text{equation 7.2.1.2-a})$$

$$= 2(0.794) \left[\frac{(0.434)^2 - 0.849 \left(\frac{44.48 - 43.70}{77.20}\right)}{0.434 - 0.849} \right]$$

* x is taken to be at the center of volume of each body segment.

$$= 1.59 \left[\frac{0.1884 - 0.849 (0.0101)}{-0.415} \right]$$

$$= 1.59 \left(\frac{0.1798}{-0.415} \right)$$

$$= -0.689 \text{ per rad (based on } S_b \ell_B^2)$$

Solution:

$$(C_m)_W_B = [K_{W(B)} + K_{B(W)}] \left(\frac{S_e}{S} \right) \left(\frac{\bar{c}_e}{\bar{c}} \right)^2 (C_m)_e + (C_m)_B \left(\frac{S_b}{S} \right) \left(\frac{\ell_B}{\bar{c}} \right)^2$$

(equation 7.3.1.2-a)

$$= (1.125 + 0.215) (0.7113) (0.7140) (-1.96) + (-0.689) (0.0963) (40.49)$$

$$= -1.334 - 2.687$$

$$= -4.021 \text{ per rad (based on the area and the square of the mean aerodynamic chord of the total panel and referred to a moment center at } \bar{c}/4 \text{ of the total panel)}$$

B. TRANSONIC

The comments of paragraph B of Section 7.3.1.1 are directly applicable here.

DATCOM METHODS

It is recommended that the methods presented in paragraph A for estimating the pitching derivative C_{m_q} of a wing-body configuration be applied to the transonic speed regime. Care should be taken to estimate the contributions of the lifting panel and body at the appropriate Mach number. The interference factors should be obtained from paragraph C, Section 4.3.1.2.

C. SUPERSONIC

The comments of paragraph C of Section 7.3.1.1 are directly applicable here.

DATCOM METHODS

The methods presented in paragraph A for estimating the pitching derivative C_{m_q} of a wing-body configuration are also applicable to the supersonic speed range. Care should be taken to estimate the contributions of the lifting panel and body at the appropriate Mach number.

Sample Problem

Method 1

Given: Same configuration as sample problem of paragraph C, Section 7.3.1.1 and paragraph A of this section.

$$M = 1.4 \quad \beta = 0.98$$

Compute:

Step 1. Pitching derivative C_{m_q} for exposed panel (Section 7.1.1.2)

$$\left(\frac{\bar{x}}{c}\right)_e = 0.393$$

$$\beta \cot \Lambda_{LE} = 1.225 \text{ (supersonic leading edge)}$$

$$A_e \beta = 4.90$$

$$\cot^{-1} (\beta \cot \Lambda_{LE}) = 39.23^\circ$$

$$(C_{Lq})_e = 3.21 \text{ per rad}$$

$$-\beta (C_{m_q}')_e = 1.018 \text{ per rad (figure 7.1.1.2-10a)}$$

$$(C_{m_q}')_e = -1.039 \text{ per rad}$$

$$(C_{m_q})_e = (C_{m_q}')_e - \left(\frac{\bar{x}}{c}\right)_e (C_{Lq})_e \quad (\text{equation 7.1.1.2-d})$$

$$= -1.039 - (0.393) (3.21)$$

$$= -2.301 \text{ per rad (based on } S_e \bar{c}_e^2 \text{)}$$

} (sample problem paragraph C, Section 7.3.1.1)

Step 2. Wing-body interference factors (Section 4.3.1.2)

$$\left. \begin{array}{l} K_{W(B)} = 1.125 \\ K_{B(W)} = 0.181 \end{array} \right\} \text{(sample problem, paragraph C, Section 7.3.1.1)}$$

Step 3. Pitching derivative C_{m_q} for body (Section 7.2.1.2)

$$\left. \begin{array}{l} f_N = 3.51 \\ f_A/f_N = 2.09 \\ \frac{\beta}{f_N} = 0.279 \\ (C_{N\alpha})_B = 2.74 \text{ per rad} \end{array} \right\} \quad (\text{sample problem, paragraph C, Section 7.3.1.1})$$

$$\left. \begin{array}{l} x_c = 44.48 \text{ ft} \\ \frac{V_B}{S_b l_B} = 0.849 \\ \left(1 - \frac{x_m}{l_B}\right) = 0.434 \end{array} \right\} \quad (\text{sample problem, paragraph A})$$

$$\frac{x_{c,p.}}{l_B} = 0.195 \quad (\text{figure 4.2.2.1-18a, extrapolated})$$

$$\frac{x_m}{l_B} = \frac{43.70}{77.20} = 0.566$$

$$(C_{m\alpha})_B = \left(\frac{x_m}{l_B} - \frac{x_{c,p.}}{l_B} \right) (C_{N\alpha})_B \quad (\text{equation 4.2.2.1-c})$$

$$= (0.566 - 0.195) 2.74$$

$$= 1.017 \text{ per rad (based on } S_b l_B)$$

$$(C_{m_q})_B = 2 (C_{m\alpha})_B \left[\frac{\left(1 - \frac{x_m}{l_B}\right)^2 - \frac{V_B}{S_b l_B} \left(\frac{x_c}{l_B} - \frac{x_m}{l_B}\right)}{\left(1 - \frac{x_m}{l_B}\right) - \frac{V_B}{S_b l_B}} \right] \quad (\text{equation 7.2.1.2-a})$$

$$= 2(1.017) \left[\frac{(0.434)^2 - (0.849) \left(\frac{44.48 - 43.70}{77.20} \right)}{0.434 - 0.849} \right]$$

$$= 2.034 \begin{pmatrix} 0.1798 \\ -0.415 \end{pmatrix}$$

$$= -0.881 \text{ per rad (based on } S_b l_b^2)$$

Solution:

$$(C_m q)_{WB} = [K_{W(B)} + K_{B(W)}] \left(\frac{S_e}{S} \right) \left(\frac{\bar{c}_e}{\bar{c}} \right)^2 (C_m q)_e + (C_m q)_B \left(\frac{S_b}{S} \right) \left(\frac{l_B}{\bar{c}} \right)^2$$

(equation 7.3.1.2-a)

$$= (1.125 + 0.181) (0.7113) (0.7140) (-2.301) + (-0.881) (0.0963) (40.49)$$

$$= -1.526 - 3.435$$

= -4.961 per rad (based on the area and the square of the mean aerodynamic chord of the total panel and referred to a moment center at $\bar{c}/4$ of the total panel)

7.3.2.1 WING-BODY ROLLING DERIVATIVE C_{Y_p}

This section presents methods for estimating the wing-body contribution to the rolling derivative C_{Y_p} at subsonic and supersonic speeds. This derivative is the change in side-force coefficient with change in the wing-tip helix angle.

A. SUBSONIC

Experimental evidence indicates that the effect of the fuselage on the side force due to rolling is negligible throughout the angle-of-attack range up to the stall. Therefore, the method of Section 7.1.2.1 for estimating the wing-alone derivative at subsonic speeds is also applicable to wing-body configurations. Available test data are limited to wing-body configurations with body diameters less than about 30 percent of the wing span. Therefore, the application of the wing-alone method is limited to values of $d/b \leq 0.3$.

The method consists of determining the value of C_{Y_p} at zero lift and extrapolating this result to high lift coefficients by using experimental values of lift and drag at high lift coefficients. The method also includes the effect of geometric dihedral.

DATCOM METHOD

The variation of the wing-body rolling derivative C_{Y_p} with lift coefficient at subsonic speeds is obtained by using the method of paragraph A of Section 7.1.2.1. In using this method experimental values of wing-body lift and drag are used in evaluating the dimensionless correction factor K. This method is limited to configurations with body diameters less than about 30 percent of the wing span, i.e., $d/b \leq 0.3$.

If experimental wing-body lift and drag data are not available, wing-alone test data may be used. If experimental lift and drag data are not available, no attempt should be made to extrapolate the zero-lift value to higher lift coefficients. The negligible importance of the derivative does not warrant the complexities involved in estimating the lift and drag characteristics. Furthermore, no known general method for estimating the variation of the drag coefficient will give results reliable enough to use in determining the correction factor for extrapolating the potential-flow values to higher lift coefficients.

The sample problem presented at the conclusion of paragraph A of Section 7.1.2.1 illustrates the use of this method.

B. TRANSONIC

No generalized method is available in the literature for estimating transonic values of the rolling derivative C_{Y_p} . Furthermore, no known experimental results are available for this derivative at transonic speeds.

C. SUPERSONIC

No generalized method is available in the literature for estimating the effect of the fuselage on the rolling derivative C_{Y_p} .

For the purposes of the Datcom the fuselage effect is considered to be negligible for wing-body

configurations with body diameters less than about 30 percent of the wing span. Therefore, for configurations with $d/b \leq 0.3$ the wing-body rolling derivative C_{Y_p} is estimated by the wing-alone method of paragraph C of Section 7.1.2.1.

No known experimental data are available for this derivative at supersonic speeds. Therefore, the validity of the Datcom application cannot be determined.

DATCOM METHOD

The wing-body rolling derivative C_{Y_p} at supersonic speeds and at low values of the lift coefficient is obtained by using the method of paragraph C of Section 7.1.2.1.

This method is limited to configurations with body diameters less than about 30 percent of the wing span, i.e., $d/b \leq 0.3$.

The sample problem at the conclusion of paragraph C of Section 7.1.2.1 illustrates the use of this method.

7.3.2.2 WING-BODY ROLLING DERIVATIVE C_{l_p}

This section presents methods for estimating the wing-body contribution to the rolling derivative C_{l_p} at subsonic and supersonic speeds. This derivative is the change in rolling-moment coefficient with change in the wing-tip helix angle and is commonly referred to as the roll-damping derivative.

A. SUBSONIC

Experimental evidence indicates that in general for configurations with the ratio of maximum body diameter to wing span less than about 30 percent, i.e., $d/b < 0.3$, the effect of the fuselage on the roll damping is negligible over the angle-of-attack range up to the stall. Therefore, the method of Section 7.1.2.2 for estimating the wing-alone derivative at subsonic speeds is applied in this section to estimate the wing-body roll damping at subsonic speeds.

The method consists of first determining the value of C_{l_p} at zero lift based on simplified lifting-surface theory, then assuming that variations in the lift-curve slope will affect C_{l_p} in the same proportion as $C_{L\alpha}$, and finally accounting for the drag associated with the additional lift on the outer portion of the wing resulting from flow separation and the attendant formation of a stable leading-edge vortex. The method also accounts for geometric dihedral.

The Datcom method accounts for the variations in wing-body lift-curve slope, drag due to lift, profile drag, and the effect of dihedral. The method requires knowledge of the variation of lift and drag over the angle-of-attack range to the stall. Therefore, the method is quite readily applied if experimental lift and drag data are available.

This method is restricted to configurations with values of $d/b \leq 0.3$.

Although all the bodies of the wing-body configurations analyzed were bodies of circular cross section, the method should give reasonable values for configurations with noncircular cross-section bodies, provided reliable values of the wing-body lift-curve-slope variation are available.

DATCOM METHOD

The variation of the wing-body rolling derivative C_{l_p} with lift coefficient at subsonic speeds is obtained by using the method of Paragraph A of Section 7.1.2.2. In using this method experimental values of wing-body lift and drag are used in evaluating the variations of lift-curve slope and profile drag.

The limitations of the method as applied to wing-alone configurations are equally applicable to the method when applied to a wing-body configuration.

A comparison of the roll-damping derivative calculated by using this method with test results is presented as Table 7.3.2.2-A. Experimental values of wing-body lift and drag have been used in evaluating the roll-damping derivative of all the configurations listed in the table.

If test data for wing-body lift and drag are not available, the wing-alone result should be used for the wing-body roll damping of configurations with $d/b \leq 0.3$. In this case wing-alone test data are preferred, but if they are not available, the wing-alone lift and drag should be estimated as outlined in Section 7.1.2.2. The Datcom methods for estimating the wing-body lift and drag variations with angle of attack have not been substantiated and, therefore, should not be used in evaluating the wing-body roll damping.

The sample problem presented at the conclusion of Paragraph A of Section 7.1.2.2 illustrates the use of this method.

B. TRANSONIC

There are no reliable methods for estimating the derivative C_{l_p} in the transonic region. Although this derivative might be expected to vary with Mach number in the same manner as lift-curve slope, this trend is not exhibited by experimental data. A considerable quantity of wing-body test data is available, however, and reference should be made to Table 7-A.

C. SUPERSONIC

Reference 1 presents a linear-theory method for estimating the roll damping of thin supersonic-leading-edge triangular and rectangular wings mounted on cylindrical bodies. The roll damping of thin subsonic-leading-edge triangular wings mounted on cylindrical bodies is presented in Reference 2 based on slender-wing theory. These theoretical results show that for most of the range of variables the net effect of the body is to decrease the roll damping. The body effect is small for body diameters less than about 30 percent of the wing span ($d/b \leq 0.3$) for both triangular and rectangular wing configurations. However, the body effect increases rapidly as the ratio of body diameter to wing span increases beyond this value. Unfortunately, at the higher values of d/b the theory does not show the same trend with Mach number for the body effects of configurations with triangular and rectangular wings. At these higher values of d/b the body effect increases with increasing Mach number for configurations with rectangular wings; whereas, the body effect decreases with increasing Mach number for configurations with triangular wings. Therefore, at higher values of d/b the theoretical results for triangular and rectangular wings cannot be applied to indicate the general trend of the body effect for configurations with other planforms.

The Datcom uses a design chart, based on the theoretical results of References 1 and 2 and a limited amount of experimental data, to account for the effect of a circular body on the roll damping of a wing-body configuration at zero lift. This chart is applicable to all straight-tapered wing configurations at values of $d/b \leq 0.3$, but is restricted to triangular wing configurations at higher values of d/b .

DATCOM METHOD

The wing-body roll-damping derivative at supersonic speeds, based on the product of the wing area and the square of the wing span $S_w b_w^2$, is given by

$$(C_{l_p})_{WB} = (C_{l_p})_w \frac{C_{l_p}}{(C_{l_p})_{d/b=0}} \quad (\text{per radian}) \quad 7.3.2.2-a$$

where $(C_{l_p})_w$ is the wing contribution to the roll-damping derivative at supersonic speeds, obtained by using the method of Paragraph C of Section 7.1.2.2, including the effects of wing thickness, and

$\frac{C_{l_p}}{(C_{l_p})_{d/b=0}}$ is the semiempirical body-correction factor obtained from Figure 7.3.2.2-13 as a function of the ratio of maximum body diameter to wing span and the Mach number normal to the leading edge.

Figure 7.3.2.2-13 is applicable to all straight-tapered wing configurations with circular bodies over the range $0 \leq d/b \leq 0.3$. For values of $d/b \geq 0.3$ this chart is applicable only to configurations consisting of triangular wings mounted on cylindrical bodies.

Experimental results reported in Reference 15 for triangular wing-body configurations with $d/b = 0.4$ and 0.6 , and for subsonic, sonic, and supersonic leading edges, show good agreement with the values given by Figure 7.3.2.2-13.

No experimental data are presently available to substantiate the theoretical results of Reference 1 for rectangular wing-body configurations with values of $d/b > 0.3$.

As noted above, the triangular- and rectangular-wing results of References 1 and 2 at values of $d/b > 0.3$ cannot be used to indicate the general trend of the body effects for other planforms.

The supersonic roll-damping derivative in the linear-lift range calculated by this method is compared with test results in Table 7.3.2.2-B. Although all configurations listed in Table 7.3.2.2-B have cylindrical bodies, the method may be applied to configurations having bodies which are not true cylinders, but which are almost cylindrical.

Sample Problem

A triangular wing-body configuration of Reference 14.

$$\Lambda_{LE} = 44.9^\circ \quad \Lambda_{c/2} = 26.7^\circ \quad A = 4.05 \quad \lambda = 0$$

$$d/b = 0.20 \quad M = 1.92; \beta = 1.639$$

$$\text{Airfoil: Hexagon, } \delta_L = 4.9^\circ$$

Compute:

$$\beta A = (1.639)(4.05) = 6.64$$

$$A \tan \Lambda_{c/2} = (4.05) (\tan 26.7^\circ) = 2.04$$

$$\frac{(C_{l_p})_{\text{theory}}}{A} = -0.0505 \text{ per rad} \quad (\text{Figure 7.1.2.2-25a})$$

$$\beta \cot \Lambda_{LE} = (1.639) (\cot 44.9^\circ) = 1.642 \quad (\text{supersonic leading edge})$$

$$\frac{\tan \Lambda_{LE}}{\beta} = \frac{\tan 44.9^\circ}{1.639} = 0.608$$

$$\frac{C_{l_p}}{(C_{l_p})_{\text{theory}}} = 0.970 \quad (\text{Figure 7.1.2.2-27})$$

$$\frac{C_{I_p}}{(C_{I_p})_{d/b=0}} = 0.970 \quad (\text{Figure 7.3.2.2-13})$$

Solution:

$$(C_{I_p})_w = \left[\frac{(C_{I_p})_{\text{theory}}}{A} \right] A \frac{C_{I_p}}{(C_{I_p})_{\text{theory}}} \quad (\text{Equation 7.1.2.2-d})$$

$$= [-0.0505] (4.05) (0.970)$$

$$= -0.198 \text{ per rad}$$

$$(C_{I_p})_{WB} = (C_{I_p})_w \frac{C_{I_p}}{(C_{I_p})_{d/b=0}} \quad (\text{Equation 7.3.2.2-a})$$

$$= (-0.198) 0.970$$

$$= -0.192 \text{ per rad} \quad (\text{based on } S_w b_w^2)$$

This compares with a test value of -0.182 per radian from Reference 14.

REFERENCES

1. Tucker, W. A., and Piland, R. O.: Estimation of the Damping in Roll of Supersonic-Leading-Edge Wing-Body Combinations. NACA TN 2151, 1950. (U)
2. Lomax, H., and Heaslet, M. A.: Damping in Roll Calculations for Slender Swept-Back Wings and Slender Wing-Body Combinations. NACA TN 1950, 1949. (U)
3. Queljo, M. J., and Wells, E. G.: Wind-Tunnel Investigation of the Low-Speed Static and Rotary Stability Derivatives of a 0.13-Scale Model of the Douglas D-558-II Airplane in the Landing Configuration. NACA RM L52G07, 1952. (U)
4. Kuhn, R. E., and Wiggins, J. W.: Wind-Tunnel Investigation to Determine the Aerodynamic Characteristics in Steady Roll of a Model at High Subsonic Speeds. NACA RM L52K24, 1953. (U)
5. Wiggins, J. W.: Wind-Tunnel Investigation at High Subsonic Speeds to Determine the Rolling Derivatives of Two Wing-Fuselage Combinations Having Triangular Wings, Including a Semiempirical Method of Estimating the Rolling Derivatives. NACA RM L53L18a, 1954. (U)
6. Myers, B. C., II, and Kuhn, R. E.: High-Subsonic Damping-in-Roll Characteristics of a Wing With the Quarter-Chord Line Swept Back 35° and With Aspect Ratio 3 and Taper Ratio 0.6. NACA RM L9C23, 1949. (U)
7. Fisher, L. R., and Michael, W. H., Jr.: An Investigation of the Effect of Vertical-Fin Location and Area on Low-Speed Lateral Stability Derivatives of a Semitailless Airplane Model. NACA RM L51A10, 1951. (U)

8. Bird, J. D., Lichtenstein, J. H., and Jaquet, B. M.: Investigation of the Influence of Fuselage and Tail Surfaces on Low-Speed Static Stability and Rolling Characteristics of a Swept-Wing Model. NACA TN 2741, 1952. (U)
9. Goodman, A., and Thomas, D. F., Jr.: Effects of Wing Position and Fuselage Size on the Low-Speed Static and Rolling Stability Characteristics of a Delta-Wing Model. NACA TR 1224, 1955. (U)
10. Letko, W., and Riley, D. R.: Effect of an Unswept Wing on the Contribution of Unswept-Tail Configurations to the Low-Speed Static- and Rolling-Stability Derivatives of a Midwing Airplane Model. NACA TN 2175, 1950. (U)
11. Williams, J. L.: Measured and Estimated Lateral Static and Rotary Derivatives of a 1/12-Scale Model of a High-Speed Fighter Airplane With Unswept Wings. NACA RM L53K09, 1954. (U)
12. Lockwood, V. E.: Effects of Sweep on the Damping-in-Roll Characteristics of Three Sweptback Wings Having an Aspect Ratio of 4 at Transonic Speeds. NACA RM L50J19, 1950. (U)
13. Jaquet, B. M., and Brewer, J. D.: Effects of Various Outboard and Central Fins on Low-Speed Static-Stability and Rolling Characteristics of a Triangular-Wing Model. NACA RM L9E18, 1949. (U)
14. Brown, C. E., and Heinke, H. S., Jr.: Preliminary Wind-Tunnel Tests of Triangular and Rectangular Wings in Steady Roll at Mach Numbers of 1.62 and 1.92. NACA TN 3740, 1958. (U)
15. Bland, W. M., Jr., and Dietz, A. E.: Some Effects of Fuselage Interference, Wing Interference, and Sweepback on the Damping in Roll of Untapered Wings as Determined by Techniques Employing Rocket-Propelled Vehicles. NACA RM L51D26, 1951. (U)
16. Bland, W. M., Jr.: Effect of Fuselage Interference on the Damping in Roll of Delta Wings of Aspect Ratio 4 in the Mach Number Range Between 0.6 and 1.6 as Determined With Rocket-Propelled Vehicles. NACA RM L52E13, 1952. (U)
17. Bland, W. M., Jr., and Sandahl, C. A.: A Technique Utilizing Rocket-Propelled Test Vehicles for the Measurement of the Damping in Roll of String-Mounted Models and Some Initial Results for Delta and Unswept Tapered Wings. NACA RM L50D24, 1950. (U)

TABLE 7.3.2.2-A
SUBSONIC WING-BODY ROLLING DERIVATIVE C_{I_p}
DATA SUMMARY

Ref.	A	λ	$\Lambda_{c/4}$ (deg)	Airfoil Section	Γ (deg)	$\frac{d}{b}$	M	$R_f \times 10^{-6}$	C_L	C_L Test (per deg)	C_{D_0} Test	C_{I_p} Calc. (per rad)	C_{I_p} Test (per rad)	ϵ Percent Error
4	4.0	0.60	45.0	65A006	0	0.139	0.85	3.44	0	0.116	0.011	-0.317	-0.304	4.3
									0.1			-0.317	-0.310	2.3
									0.2	↓		-0.316	-0.320	-1.3
									0.3	0.121		-0.328	-0.341	-4.1
									0.4	0.127		-0.342	-0.358	-4.5
									0.5	0.120		-0.319	-0.316	0.9
									0.6	0.102		-0.266	-0.232	14.7
									0.7	0.0255		-0.053	-0.175	-69.7
									0.75	0.020	↓	-0.035	-0.175	-80.0
							0.70	3.10	0	0.062	0.011	-0.314	-0.315	-0.2
									0.1			-0.314	-0.325	-3.4
									0.2			-0.313	-0.340	-7.9
									0.3	↓		-0.312	-0.356	-12.4
									0.4	0.065		-0.324	-0.383	-10.7
									0.5	0.065		-0.320	-0.340	-4.4
									0.75	0.032	↑	-0.142	-0.175	-18.9
5	2.31	0	52.4	65A003	0	0.183	0.50	3.60	0	0.0463	0.008	-0.176	-0.180	-2.2
									0.1	0.0463		-0.175	-0.195	-10.3
									0.2	0.056		-0.209	-0.200	4.5
									0.3	0.0615		-0.225	-0.200	12.5
									0.4	0.056		-0.197	-0.195	1.0
									0.5	0.051	↓	-0.170	-0.184	-7.6

TABLE 7.3.2.2-A (CONT'D)

Ref.	A	λ	$\Delta c/4$ (deg)	Airfoil Section	Γ (deg)	$\frac{d}{b}$	M	$R_f \times 10^{-6}$	C_L	C_L Test (per deg)	$C_D 0$ Test	C_{I_p} Calc. (per rad)	C_{I_p} Test (per rad)	* Percent Error
5	2.31	0	52.4	65A003	0	0.183	0.80	3.00	0.6	0.045	0.008	-0.137	-0.152	- 9.9
									0.7	0.051		-0.147	--	--
	4.0	0	36.9		0	0.138	0.80	2.80	0	0.061		-0.132	--	--
									0.1			-0.257	-0.260	- 1.2
									0.2			-0.257	-0.256	0.8
									0.3			-0.256	-0.247	3.6
									0.4	0.053		-0.220	-0.192	14.6
									0.5	0.046		-0.188	-0.150	25.3
									0.6	0.039		-0.155	-0.110	40.9
									0.7	0.035		-0.134	--	--
									0.8	0.014		-0.044	--	--
6	3.0	0.60	36.0	me ref.	0	0.121	0.70	4.25	0	0.085	0.007	-0.270	-0.282	- 4.3
									0.1			-0.270	-0.272	- 0.7
									0.2			-0.269	-0.280	- 3.9
									0.3			-0.267	-0.282	- 5.3
									0.4			-0.265	-0.305	-13.1
									0.5			-0.262	--	--
									0.6			-0.259	--	--
7	3.60	0.455	38.16	0010-64	0	0.067	0.16	1.138	0	0.055	0.018	-0.271	-0.287	1.5
									0.1			-0.271	-0.253	7.1
									0.2			-0.270	-0.295	- 8.5
									0.3	0.062		-0.294	-0.300	- 2.0
									0.4	0.059		-0.286	-0.305	- 6.2
									0.5	0.059		-0.284	-0.302	- 6.0
									0.6	0.0525		-0.249	-0.257	- 3.1

TABLE 7.3.2.2-A (CONTD)

Ref.	A	λ	$\Delta c/4$ (deg)	Airfoil Section	Γ (deg)	d/b	M	$R_f \times 10^{-6}$	C_L	C_L Test (per deg)	C_{D_0} Test	C_I/p Calc. (per rad)	C_I/p Test (per rad)	ϵ Percent Error
8	2.61	1.00	45.0	0012(LLE)	0	0.178	0.17	1.40	0	0.049	0.029	-0.218	-0.215	1.4
									0.1			-0.218	-0.210	3.8
									0.2			-0.216	-0.212	1.9
									0.3			-0.213	-0.215	-0.9
									0.4			-0.209	-0.223	-6.3
									0.5			-0.204	-0.233	-12.4
									0.6			-0.198	-0.248	-20.2
									0.7	0.061		-0.241	-0.275	-12.4
									0.8	0.077		-0.305	-0.330	-7.6
9	2.31	0	52.4	65A003	0	0.123	0.17	2.06	0	0.044	0.011	-0.170	-0.155	8.8
									0.1			-0.171	-0.156	9.6
									0.2			-0.166	-0.165	0.6
									0.3	0.0465		-0.171	-0.165	3.6
									0.4	0.048		-0.170	-0.167	1.8
									0.5	0.050		-0.169	-0.163	3.7
									0.6			-0.158	-0.161	-1.9
									0.7			-0.145	-0.155	-6.5
									0.8	0.044		-0.124	-0.156	-20.5
									0	0.044	0.020	-0.171	-0.130	31.5
									0.1			-0.170	-0.136	25.0
									0.2			-0.167	-0.140	19.3
									0.3			-0.162	-0.139	16.5
									0.4			-0.156	-0.134	16.4
									0.5	0.046		-0.154	-0.131	17.6
									0.6	0.046		-0.144	-0.136	5.9

TABLE 7.3.2.2-A (CONTD)

Ref.	A	λ	$\Delta c/4$ (deg)	Airfoil Section	Γ (deg)	d/b	M	$R_f \times 10^{-6}$	C_L	C_L Test (per deg)	C_{D_0} Test	C_p Calc. (per rad)	C_p Test (per rad)	e Percent Error
9	2.31	0	52.4	65A003	0	0.247	0.17	2.06	0.7	0.046	0.020	-0.127	-0.143	-11.2
10	4.0	0.6	0	65A008	0	0.167	0.166	0.88	0	0.066	0.031	-0.318	-0.330	-3.6
									0.1			-0.318	-0.338	-5.9
									0.2			-0.318	-0.368	-10.7
									0.3			-0.317	-0.371	-14.6
									0.4	0.069		-0.326	-0.371	-12.1
									0.5	0.063		-0.315	-0.380	-12.5
									0.6	0.0405		-0.236	-0.322	-26.7
									0.7	0.024		-0.094	-0.150	-37.3
11	5.90	0.473	-3.47	63-210	3.0	0.127	0.17	0.73	0	0.077	0.078	-0.396	-0.370	7.0
									0.1			-0.396	-0.372	6.5
									0.2			-0.385	-0.380	3.9
									0.3	0.072		-0.370	-0.375	-1.3
									0.4			-0.370	-0.370	0
									0.5			-0.389	-0.378	-2.4
									0.6	0.0673		-0.345	-0.385	-10.4
									0.7			-0.344	-0.386	-10.9
									0.8			-0.343	-0.375	-8.5
12	4.0	0.6	32.6	65A006	0	0.139	0.6	0.62	0	0.066	0.011	-0.313	-0.345	-9.3
									0.1	0.066		-0.313	-0.360	-10.6
									0.2	0.070		-0.332	-0.363	-8.5
									0.3	0.0725		-0.342	-0.395	-13.4
									0.4	0.075		-0.352	-0.380	-7.4
									0.5	0.061		-0.284	-0.290	-2.1

TABLE 7.3.2.2-A (CONT'D)

Ref.	A	λ	$\Delta c/4$ (deg)	Airfoil Section	Γ (deg)	$\frac{d}{b}$	M	$R_f \times 10^{-6}$	C_L	C_L Test (per deg)	C_{D_0} Test	C_I/p Calc. (per rad)	C_I/p Test (per rad)	e Percent Error
13	2.31	0	52.2	65(06)-006.5	0	0.172	0.13	1.624	0	0.042	0.020	-0.172	-0.171	0.6
									0.1	0.042		-0.171	-0.169	1.2
									0.2	0.045		-0.180	-0.173	4.0
									0.3			-0.175	-0.184	-4.9
									0.4			-0.168	-0.184	-8.7
									0.5			-0.160	-0.177	-9.6
									0.6	0.040		-0.129	-0.174	-25.9
									0.7			-0.117	-0.177	-33.9
									0.8			-0.102	--	--
									1.0	0.033		-0.039	--	--

TABLE 7.3.2.2-8

SUPersonic WING-BODY ROLLING DERIVATIVE C_{l_p}

DATA SUMMARY

Ref.	A	λ	Λ_{LE} (deg)	$\frac{d}{b}$	M	$\beta \cot \Lambda_{LE}$	Airfoil Section	δ_1 (deg)	$(C_{l_p})_{d/b=0}$ Calc. (per rad)	$\frac{C_{l_p}}{(C_{l_p})_{d/b=0}}$	C_{l_p} Calc. (per rad)	C_{l_p} Test (per rad)	ϵ Percent Error
14	1.47	0	39.8	0.23	1.62	0.469	Hexagon	4.9	-0.137	1.000	-0.137	-0.128	7.0
	1.86	0	65.0	0.19	1.62	0.577			-0.131	1.000	-0.131	-0.119	10.1
	2.13	0	61.5	0.19	1.62	0.692			-0.168	1.000	-0.168	-0.163	3.1
	2.38	0	59.5	0.19	1.62	0.751			-0.151	1.000	-0.151	-0.145	4.1
	2.60	0	56.9	0.19	1.62	0.830			-0.184	1.000	-0.184	-0.179	2.8
	2.85	0	54.6	0.18	1.62	0.905			-0.164	1.000	-0.164	-0.158	3.8
	3.06	0	52.4	0.19	1.62	0.980			-0.193	1.000	-0.193	-0.178	8.4
	3.38	0	49.7	0.18	1.62	1.080			-0.180	1.000	-0.180	-0.150	20.0
	3.97	0	45.4	0.20	1.92	1.390			-0.204	1.000	-0.204	-0.198	3.0
	4.06	0	44.9	0.20	1.62	1.280			-0.184	1.000	-0.184	-0.175	5.1
	2.00	1.00	0	0.26	1.62	∞	Circular Arc	6.8	-0.219	1.000	-0.219	-0.194	12.9
	2.73	1.00	0	0.26	1.62				-0.185	0.980	-0.181	-0.169	7.1
				0.19	1.92				-0.229	1.000	-0.229	-0.211	8.5
				0.19	1.92				-0.236	1.000	-0.236	-0.221	6.8
				0.19	1.92				-0.189	0.980	-0.184	-0.182	1.1
				0.19	1.92				-0.199	0.970	-0.193	-0.181	6.6
				0.19	1.92				-0.248	0.970	-0.241	-0.234	3.0
				0.19	1.92				-0.198	0.970	-0.192	-0.182	5.5
				0.19	1.92				-0.259	0.945	-0.244	-0.260	-6.2
				0.19	1.92				-0.235	0.975	-0.229	-0.242	-5.4
				0.19	1.92				-0.328	0.945	-0.310	-0.313	-0.9
				0.19	1.92				-0.280	0.975	-0.273	-0.273	0

TABLE 7.3.2.2-B (CONT'D)

Ref.	A	λ	Λ_{LE} (deg)	$\frac{d}{b}$	M	$\beta \cot \Lambda_{LE}$	Airfoil Section	δ_1 (deg)	$(C_{I_p})_{d/b=0}$ Calc. (per radi)	$\frac{C_{I_p}}{(C_{I_p})_{d/b=0}}$	C_{I_p} Calc. (per radi)	C_{I_p} Test (per rad)	Percent Error
15	3.70	1.00	0	0.191	1.60	∞	65A009	16.6	-0.374	0.975	-0.364	-0.346	5.2
					1.50				-0.398	0.975	-0.387	-0.355	9.0
					1.414				-0.423	0.975	-0.412	-0.360	14.4
					1.30				-0.457	0.975	-0.450	-0.370	19.0
	3.70	1.00	45.0	0.191	1.60	1.25	65A009	16.6	-0.304	0.975	-0.286	-0.300	-1.3
					1.50	1.12			-0.308	0.975	-0.300	-0.300	0
					1.414	1.00			-0.302	1.000	-0.302	-0.265	14.0
					1.30	0.83			-0.312	1.000	-0.312	-0.311	0.3
16	4.0	0	45.0	0.40	1.485	1.087	Symmetrical Double Wedge	3.24	-0.280	0.815	-0.228	-0.220	3.6
					0.60					0.530	-0.148	-0.155	-4.5
					0.40	1.414	1.00		-0.309	0.845	-0.261	-0.233	12.0
					0.60					0.550	-0.170	-0.210	19.0
					0.40	1.05	0.319		-0.380	0.970	-0.378	-0.278	36.0
					0.60					0.675	-0.256	-0.212	20.8
17	4.0	0	45.0	0.20	1.60	1.25	Hexagon	4.9	-0.246	0.970	-0.238	-0.241	-1.2
					1.50	1.12			-0.271	0.970	-0.263	-0.251	4.8
					1.40	0.98			-0.302	1.000	-0.302	-0.264	14.4
					1.30	0.83			-0.315	1.000	-0.315	-0.279	12.9
					1.20	0.663			-0.344	1.000	-0.344	-0.296	16.2

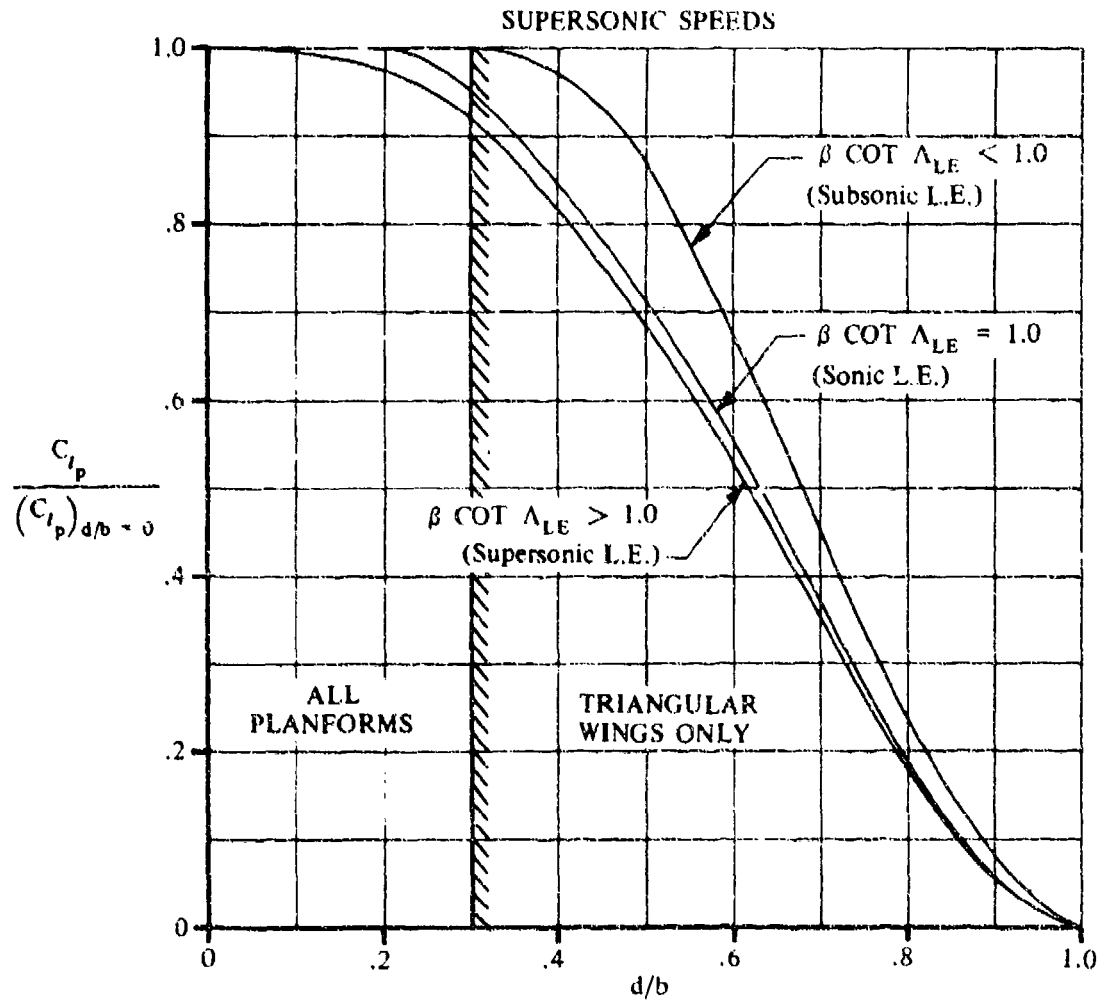


FIGURE 7.3.2.2-13 EFFECT OF THE FUSELAGE ON ROLL DAMPING

7.3.2.3 WING-BODY ROLLING DERIVATIVE C_{n_p}

This section presents methods for estimating the wing-body contribution to the rolling derivative C_{n_p} at subsonic and supersonic speeds. This derivative is the change in yawing-moment coefficient with change in wing-tip helix angle.

A. SUBSONIC

Experimental evidence indicates that the effect of the fuselage on the yawing moment due to rolling is negligible throughout the angle-of-attack range up to the stall. Therefore, the method of Section 7.1.2.3 for estimating the wing-alone derivative at subsonic speeds is also applicable to wing-body configurations. Available test data are limited to wing-body configurations with body diameters less than about 30 percent of the wing span. Therefore, the application of the wing-alone method is limited to values of $d/b \leq 0.3$.

The method consists of determining the value of C_{n_p} at zero lift and extrapolating the result to high lift coefficients by using experimental values of lift and drag at high lift coefficients. The method also includes the effects of wing twist and symmetric flap deflection.

DATCOM METHOD

The variation of the wing-body rolling derivative C_{n_p} with lift coefficient at subsonic speeds is obtained by using the method of Paragraph A of Section 7.1.2.3. In using this method experimental values of wing-body lift and drag are used in evaluating the dimensionless correction factor K. This method is limited to configurations with body diameters less than about 30 percent of the wing span, i.e., $d/b \leq 0.3$.

If experimental wing-body lift and drag data are not available, wing-alone test data may be used to determine the wing-body rolling derivative C_{n_p} . No attempt should be made to extrapolate the zero-lift value to higher lift coefficients using estimated lift and drag results. No known general method for estimating the variation of drag coefficient will give results reliable enough to use in determining the correction factor for extrapolating the potential-flow values to higher lift coefficients.

The sample problem at the conclusion of Paragraph A of Section 7.1.2.3 illustrates the use of this method.

B. TRANSONIC

No generalized method is available in the literature for estimating transonic values of the rolling derivative C_{n_p} . Furthermore, no known experimental results are available for this derivative at transonic speeds.

C. SUPERSONIC

- No generalized method is available in the literature for estimating the effect of the fuselage on the rolling derivative C_{n_p} at supersonic speeds.

For the purpose of the Datcom the fuselage effect is considered to be negligible for wing-body configurations with body diameters less than about 30 percent of the wing span. Therefore, for

configurations with $d/b \leq 0.3$ the wing-body rolling derivative C_{n_p} is estimated by the wing-alone method of Paragraph C of Section 7.1.2.3.

No known experimental data are available for this derivative at supersonic speeds. Therefore, the validity of the Datcom application cannot be determined.

DATCOM METHOD

The wing-body rolling derivative C_{n_p} at supersonic speeds in the range of lift coefficients for which C_{n_p} varies linearly with C_L is obtained by using the method of Paragraph C of Section 7.1.2.3.

This method is limited to configurations with body diameters less than about 30 percent of the wing span, i.e., $d/b \leq 0.3$.

7.3.3 WING-BODY YAWING DERIVATIVES

7.3.3.1 WING-BODY YAWING DERIVATIVE C_{Y_r}

This section recommends methods for estimating the wing-body contribution to the yawing derivative C_{Y_r} at subsonic speeds. However, at subsonic, transonic, and supersonic speeds no generalized methods are available for estimating the wing-body contribution to the yawing derivative C_{Y_r} . This derivative is the change in side-force coefficient with variation in yawing velocity.

A. SUBSONIC

Experimental evidence indicates that the effect of the fuselage on the side force due to yawing is negligible throughout the angle-of-attack range up to the stall. Therefore, the recommendations of Section 7.1.3.1 for estimating the wing-alone derivative at subsonic speeds are also applicable to wing-body configurations.

The recommendations of Section 7.1.3.1 consist of using available experimental data, when applicable, or the method of reference 1 to estimate C_{Y_r} .

B. TRANSONIC

No generalized method is available in the literature for estimating transonic values of the wing-body contribution to the yawing derivative C_{Y_r} . Furthermore, there is a scarcity of experimental data for this derivative at transonic speeds.

C. SUPERSONIC

No generalized method is available in the literature for estimating supersonic values of the wing-body contribution to the yawing derivative C_{Y_r} . Furthermore, there is a scarcity of experimental data for this derivative at supersonic speeds.

REFERENCE

1. Toll, T. A., and Queijo, M. J.: Approximate Relations and Charts for Low-Speed Stability Derivatives of Swept Wings. NACA TN 1581, 1948. (U)

7.3.3.2 WING-BODY YAWING DERIVATIVE C_{l_r}

This section presents a method for estimating the wing-body contribution to the yawing derivative C_{l_r} at subsonic speeds. However, at transonic and supersonic speeds no generalized methods are available for estimating the wing-body contribution to the yawing derivative C_{l_r} . This derivative is the change in rolling-moment coefficient with change in the yawing velocity.

A. SUBSONIC

Experimental evidence indicates that the effect of the fuselage on the rolling moment due to yawing is negligible. Therefore, the method of Section 7.1.3.2 for estimating the wing-alone derivative at subsonic speeds is also applicable to wing-body configurations. Available test data are limited to wing-body configurations with body diameters less than about 30 percent of the wing span. Consequently, the application of the wing-alone method to estimate the wing-body contribution to C_{l_r} is limited to values of $d/b \leq 0.3$.

DATCOM METHOD

The variation of the wing-body yawing derivative C_{l_r} is obtained by using the method of Section 7.1.3.2. The method consists of determining the value of C_{l_r} at zero lift and extending this value to high lift coefficients by using a semiempirical correction factor and test data for C_{l_β} . The method also includes the effect of geometric dihedral, wing twist, and flap deflection. The method is limited to configurations with body diameters less than about 30 percent of the wing span; i.e., $d/b \leq 0.3$.

The sample problem presented at the conclusion of paragraph A of Section 7.1.3.2 illustrates the use of this method.

B. TRANSONIC

No generalized method is available in the literature for estimating transonic values of the wing-body contribution to the yawing derivative C_{l_r} . Furthermore, there is a scarcity of experimental data for this derivative at transonic speeds.

C. SUPERSONIC

No generalized method is available in the literature for estimating supersonic values of the wing-body contribution to the yawing derivative C_{l_r} . Furthermore, there is a scarcity of experimental data for this derivative at supersonic speeds.

7.3.3.3 WING-BODY YAWING DERIVATIVE C_{n_r}

This section presents a method for estimating the wing-body contribution to the yawing derivative C_{n_r} at subsonic speeds. However, at transonic and supersonic speeds no generalized methods are available for estimating the wing-body contribution to the yawing derivative C_{n_r} . This derivative is the change in yawing-moment coefficient with change in the yawing-velocity parameter and is commonly referred to as the yaw damping.

A. SUBSONIC

In general, the wing-fuselage contribution to damping in yaw is small in comparison to the vertical-tail contribution. The contribution from the fuselage depends upon the relative size of the fuselage in comparison to the wing. For configurations in which the fuselage is large relative to the wing, the fuselage contribution is important. Fuselages having flat sides or having a flattened cross section with the major axis vertical can also make a significant contribution (reference 1). Experimental data have also shown that a flattened cross-section fuselage with the major axis horizontal can have negative damping in yaw at moderate and high angles of attack.

No generalized method exists in the literature for predicting the fuselage contribution to yaw damping. Therefore, for the purposes of the Datcom, fuselage effects are considered to be negligible. Consequently, the Datcom method of Section 7.1.3.3 for estimating the wing-alone derivative at subsonic speeds is also applicable to wing-body configurations.

DATCOM METHOD

The estimated value of the wing-body yawing derivative C_{n_r} is obtained by using the method of Section 7.1.3.3. In using this method experimental values of wing profile drag coefficient, evaluated at the appropriate Mach number, are used in conjunction with the lift coefficient. These coefficients are used to evaluate the two major contributions to C_{n_r} ; namely, that resulting from the drag due to lift and that resulting from the profile drag. The method does not account for the effects of wing flaps, wing twist, or wing dihedral.

The sample problem presented at the conclusion of paragraph A of Section 7.1.3.3 illustrates the use of this method.

B. TRANSONIC

No generalized method is available in the literature for estimating transonic values of the wing-body contribution to the yawing derivative C_{n_r} . Furthermore, there is a scarcity of experimental data for this derivative at transonic speeds.

C. SUPERSONIC

No generalized method is available in the literature for estimating supersonic values of the wing-body contribution to the yawing derivative C_{n_r} . Furthermore, there is a scarcity of experimental data for this derivative at supersonic speeds.

REFERENCE

1. Campbell, J. P., and McKinney, M. O.: Summary of Methods for Calculating Dynamic Lateral Stability and Response and for Estimating Lateral Stability Derivatives. NACA TR 1098, 1962. (U)

7.3.4 WING-BODY ACCELERATION DERIVATIVES

7.3.4.1 WING-BODY ACCELERATION DERIVATIVE $C_{L\dot{\alpha}}$

The information contained in this section is for estimating the acceleration derivative $C_{L\dot{\alpha}}$ of wing-body configurations at low angles of attack. In general, it consists of a synthesis of material presented in other sections; however, the method of application is new.

Datcom methods are based on the relatively simple results derived from slender-body theory in a manner similar to that used to predict the wing-body pitching derivatives. It is assumed that the mutual interferences that occur between components for angle-of-attack variations, determined in references 1 and 2 and presented in Section 4.3.1.2, may be applied with reasonable accuracy to the case of normal acceleration. This approach to the calculation of wing-body acceleration derivatives has been applied with reasonable success by Walker and Wolowicz in reference 3.

A. SUBSONIC

Two methods are presented for determining the acceleration derivative $C_{L\dot{\alpha}}$ of a wing-body configuration, differing only in their treatment of the mutual interference effects.

DATCOM METHODS

Method 1

For wing-body configurations similar to sketch (d) of Section 4.3.1.2, the acceleration derivative $C_{L\dot{\alpha}}$, based on the area and mean aerodynamic chord of the total panel, is given by

$$(C_{L\dot{\alpha}})_{WB} = [K_{W(B)} + K_{B(W)}] \left(\frac{S_e}{S} \right) \left(\frac{\bar{c}_e}{\bar{c}} \right) (C_{L\dot{\alpha}})_e + (C_{L\dot{\alpha}})_B \left(\frac{S_b}{S} \right) \left(\frac{\bar{c}_b}{\bar{c}} \right) \quad 7.3.4.1-a$$

where

$(C_{L\dot{\alpha}})_e$ is the contribution of the exposed panel to the acceleration derivative $C_{L\dot{\alpha}}$, obtained from Section 7.1.4.1. (See Section 4.3.1.2 for the definition of exposed surfaces.)

$(C_{L\dot{\alpha}})_B$ is the contribution of the body to the acceleration derivative $C_{L\dot{\alpha}}$, obtained from Section 7.2.2.1.

The remaining terms are defined in paragraph A of Section 7.3.1.1.

Method 2

For wing-body configurations similar to sketch (c) of Section 4.3.1.2, the acceleration derivative $C_{L\dot{\alpha}}$, based on the area and mean aerodynamic chord of the total panel, is given by

$$(C_{L\dot{\alpha}})_{WB} = K_{WB} (C_{L\dot{\alpha}})_W + (C_{L\dot{\alpha}})_B \left(\frac{S_b}{S} \right) \left(\frac{\ell_B}{c} \right) \quad 7.3.4.1-b$$

where $(C_{L\dot{\alpha}})_W$ is the contribution of the total panel to the acceleration derivative $C_{L\dot{\alpha}}$, obtained from Section 7.1.4.1, and the remaining terms are defined in paragraph A of Section 7.3.1.1 and method 1 above.

Sample Problem

Method 1

Given: Same configuration as sample problems of paragraph A, Sections 7.3.1.1 and 7.3.1.2. Some of the characteristics are repeated below.

The following ratios based on total panel dimensions:

$$\frac{S_e}{S} = 0.7113 \quad \frac{\bar{c}_e}{c} = 0.845 \quad \frac{S_b}{S} = 0.0963 \quad \frac{\ell_B}{c} = 6.363$$

Additional Characteristics:

$$M = 0.60 \quad \beta = 0.80 \quad A_e = 5.0 \quad \frac{d}{b} = 0.157 \quad \ell_B = 77.2 \text{ ft}$$

Compute:

Step 1. Acceleration derivative $C_{L\dot{\alpha}}$ for exposed panel (Section 7.1.4.1)

$$\left. \begin{aligned} \left(\frac{x_{a.c.}}{c_r} \right)_e &= 0.560 \\ (C_{L\dot{\alpha}})_e &= 4.50 \text{ per rad} \end{aligned} \right\} \text{ (sample problem, paragraph A, Section 7.3.1.1)}$$

$$\beta A_e = 4.0$$

$$\frac{-\beta^2 C_L(z)}{\pi A/2} = 0.140 \text{ per rad} \quad (\text{figure 7.1.4.1-6})$$

$$C_L(g) = -1.718 \text{ per rad}$$

$$\begin{aligned}
 (C_L \dot{\alpha})_e &= 1.5 \left(\frac{x_{a.c.}}{c_r} \right)_e (C_L \alpha)_e + 3 C_L(g) \quad (\text{equation 7.1.4.1-a}) \\
 &= (1.5)(0.560)(4.50) + 3(-1.718) \\
 &= 3.780 - 5.154 \\
 &= -1.374 \text{ per rad (based on } S_e \bar{c}_e)
 \end{aligned}$$

Step 2. Wing-body interference factors (Section 4.3.1.2)

$$\left. \begin{array}{l} K_{W(B)} = 1.125 \\ K_{B(W)} = 0.215 \end{array} \right\} \text{(sample problem, paragraph A, Section 7.3.1.1)}$$

Step 3. Acceleration derivative $C_{L \dot{\alpha}}$ for body (Section 7.2.2.1)

$$\left. \begin{array}{l} V_B = 2615.1 \text{ cu ft} \\ S_b = 39.88 \text{ sq ft} \\ (C_L \alpha)_B = 1.894 \text{ per rad (based on } S_b) \end{array} \right\} \text{(sample problem, paragraph A, Section 7.3.1.1)}$$

$$\left(\frac{V_B}{S_b l_B} \right) = \frac{2615.1}{(39.88)(77.20)} = 0.849$$

$$\begin{aligned}
 (C_L \dot{\alpha})_B &= 2(C_L \alpha)_B \left(\frac{V_B}{S_b l_B} \right) \quad (\text{equation 7.2.2.1-a}) \\
 &= 2(1.894)(0.849) \\
 &= 3.216 \text{ per rad (based on } S_b l_B)
 \end{aligned}$$

Solution:

$$\begin{aligned}
 (C_L \dot{\alpha})_{WB} &= [K_{W(B)} + K_{B(W)}] \left(\frac{S_e}{S} \right) \left(\frac{\bar{c}_e}{\bar{c}} \right) (C_L \dot{\alpha})_e + (C_L \dot{\alpha})_B \left(\frac{S_b}{S} \right) \left(\frac{l_B}{\bar{c}} \right) \\
 &\quad (\text{equation 7.3.4.1-a}) \\
 &= (1.125 + 0.215)(0.7113)(0.845)(-1.374) + (3.216)(0.0963)(6.363)
 \end{aligned}$$

$$= -1.107 + 1.971$$

= 0.864 per rad (based on the area and mean aerodynamic chord of the total panel)

B. TRANSONIC

The aerodynamic interference effects for slender wing-body configurations are relatively insensitive to Mach number; consequently, the slender-body interference factors of Section 4.3.1.2 should give reasonable results. For nonslender configurations transonic interference effects can become quite large and sensitive to minor changes in local contour.

DATCOM METHODS

It is recommended that the methods presented in paragraph A for estimating the acceleration derivative $C_{L\dot{\alpha}}$ of a wing-body configuration be applied to the transonic speed range. Care should be taken to estimate the contributions of the lifting panel and body at the appropriate Mach number. The interference factors should be obtained from paragraph C, Section 4.3.1.2.

C. SUPERSONIC

The information included in the Datcom accounts for most of the mutual interferences that occur between components of a wing-body configuration at supersonic speeds. These interference effects are accounted for by the slender-body interference factors of Section 4.3.1.2.

DATCOM METHODS

The methods presented in paragraph A for estimating the acceleration derivative $C_{L\dot{\alpha}}$ of a wing-body configuration are also applicable to the supersonic speed range. Care should be taken to estimate the contributions to the lifting panel and body at the appropriate Mach number.

Sample Problem

Method 1

Given: Same configuration as sample problems of paragraph C, Sections 7.3.1.1 and 7.3.1.2, and paragraph A of this section.

$$M = 1.4 \quad \beta = 0.98 \quad \frac{d}{b} = 0.157$$

Compute:

Step 1. Acceleration derivative $C_{N\dot{\alpha}}$ for exposed panel (Section 7.1.4.1)

$$\left. \begin{array}{l} \beta \cot \Lambda_{LE} = 1.225 \text{ (supersonic leading edge)} \\ \beta A_e = 4.90 \\ \cot^{-1} (\beta \cot \Lambda_{LE}) = 39.23^\circ \end{array} \right\} \text{(sample problem, paragraph C, Section 7.3.1.1)}$$

$$\beta [(C_N \dot{\alpha})_1]_e = 0 \text{ (figure 7.1.4.1-11a)}$$

$$[(C_N \dot{\alpha})_1]_e = 0$$

$$\beta [(C_N \dot{\alpha})_2]_e = 4.00 \text{ (figure 7.1.4.1-11c)}$$

$$[(C_N \dot{\alpha})_2]_e = 4.08 \text{ per rad}$$

$$(C_N \dot{\alpha})_e = \left(\frac{M^2}{\beta^2} \right) [(C_N \dot{\alpha})_1]_e - \left(\frac{1}{\beta^2} \right) [(C_N \dot{\alpha})_2]_e \text{ (equation 7.1.4.1-c)}$$

$$= \left(\frac{1.4}{0.98} \right)^2 (0) - \left[\frac{1}{(0.98)^2} \right] (4.08)$$

$$= -4.25 \text{ per rad (based on } S_e \bar{c}_e)$$

Step 2. Wing-body interference factors (Section 4.3.1.2)

$$\left. \begin{array}{l} K_{W(B)} = 1.125 \\ K_{B(W)} = 0.181 \end{array} \right\} \text{(sample problem, paragraph C, Section 7.3.1.1)}$$

Step 3. Acceleration derivative $C_{N \dot{\alpha}}$ for body (Section 7.2.2.1)

$$\frac{V_B}{S_b l_B} = 0.849 \text{ (sample problem, paragraph A)}$$

$$(C_{N \dot{\alpha}})_B = 2.74 \text{ per rad (sample problem, paragraph C, Section 7.3.1.1)}$$

$$(C_{N\dot{\alpha}})_B = 2(C_{N\alpha})_B \left(\frac{V_B}{S_b \ell_B} \right) \quad (\text{equation 7.2.2.1-a})$$

$$= 2(2.74)(0.849)$$

$$= 4.653 \text{ per rad (based on } S_b \ell_B \text{)}$$

Solution:

$$(C_{N\dot{\alpha}})_{WB} = [K_{W(B)} + K_{B(W)}] \left(\frac{S_e}{S} \right) \left(\frac{\bar{c}_e}{\bar{c}} \right) (C_{N\dot{\alpha}})_e + (C_{N\dot{\alpha}})_B \left(\frac{S_b}{S} \right) \left(\frac{\ell_B}{\bar{c}} \right) \quad (\text{equation 7.3.4.1-a})$$

$$= (1.125 + 0.181)(0.7113)(0.845)(-4.25) + (4.653)(0.0963)(6.363)$$

$$= -3.336 + 2.851$$

$$= -0.485 \text{ per rad (based on the area and mean aerodynamic chord of the total panel)}$$

REFERENCES

1. Pitts, W., Nielsen, J., and Kaattari, G.: Lift and Center of Pressure of Wing-Body-Tail Combinations at Subsonic, Transonic, and Supersonic Speeds. NACA TR 1307, 1959. (U)
2. Spreiter, J.: The Aerodynamic Forces on Slender Plane- and Cruciform-Wing and Body Combinations. NACA TR 962, 1950. (U)
3. Walker, H., and Wolowicz, C.: Theoretical Stability Derivatives for the X-15 Research Airplane at Supersonic and Hypersonic Speeds Including a Comparison with Wind-Tunnel Results. NASA TM X-287, 1960. (U)

7.3.4.2 WING-BODY ACCELERATION DERIVATIVE $C_{m\dot{\alpha}}$

The information contained in this section is for estimating the acceleration derivative $C_{m\dot{\alpha}}$ of wing-body configurations at low angles of attack.

The Datcom methods are based on the same assumption that was made in regard to the acceleration derivative $C_{L\dot{\alpha}}$ of a wing-body configuration, and the general discussion of Section 7.3.4.1 is directly applicable here.

A. SUBSONIC

Two methods are presented for determining the acceleration derivative $C_{m\dot{\alpha}}$ of a wing-body configuration, differing only in their treatment of the mutual interference effects.

DATCOM METHODS

Method 1

For wing-body configurations similar to sketch (d) of Section 4.3.1.2, the acceleration derivative $C_{m\dot{\alpha}}$, based on the area and the square of the mean aerodynamic chord of the total panel and referred to a moment center at the assumed center of gravity, is given by

$$(C_{m\dot{\alpha}})_{WB} = [K_{W(B)} + K_{B(W)}] \left(\frac{S_e}{S} \right) \left(\frac{\bar{c}_e}{\bar{c}} \right)^2 (C_{m\dot{\alpha}})_e + (C_{m\dot{\alpha}})_B \left(\frac{S_b}{S} \right) \left(\frac{\bar{c}_b}{\bar{c}} \right)^2 \quad 7.3.4.2-a$$

where

$(C_{m\dot{\alpha}})_e$ is the contribution of the exposed panel to the acceleration derivative $C_{m\dot{\alpha}}$, obtained from Section 7.1.4.2. (See Section 4.3.1.2 for the definition of exposed surfaces.)

$(C_{m\dot{\alpha}})_B$ is the contribution of the body to the acceleration derivative $C_{m\dot{\alpha}}$, obtained from Section 7.2.2.2.

The remaining terms are defined in paragraph A of Section 7.3.1.1. Moment transfer calculations are included as an integral part of the wing- and body-derivative estimation methods of Sections 7.1.4.2 and 7.2.2.2, respectively.

Method 2

For wing-body configurations similar to sketch (c) of Section 4.3.1.2, the acceleration derivative $C_{m\dot{\alpha}}$, based on the area and the square of the mean aerodynamic chord of the total panel and referred to a moment center at the assumed center of gravity, is given by

$$(C_{m\dot{\alpha}})_{WB} = K_{(WB)} (C_{m\dot{\alpha}})_W + (C_{m\dot{\alpha}})_B \left(\frac{S_b}{S} \right) \left(\frac{\bar{c}_b}{\bar{c}} \right)^2 \quad 7.3.4.2-b$$

where $(C_{m\dot{\alpha}})_W$ is the contribution of the total panel to the acceleration derivative $C_{m\dot{\alpha}}$, and the remaining terms are defined in paragraph A of Section 7.3.1.1 and method 1 above. Moment transfer calculations are included as an integral part of the wing- and body-derivative estimation methods of Sections 7.1.4.2 and 7.2.2.2, respectively.

Sample Problem

Method 1

Given: Same configuration as sample problems of paragraph A, Sections 7.3.1.1, 7.3.1.2, and 7.3.4.1. Some of the characteristics are repeated below.

The following ratios based on total panel dimensions:

$$\frac{S_e}{S} = 0.7113 \quad \left(\frac{\bar{c}_e}{\bar{c}} \right)^2 = 0.7140 \quad \frac{c_{r_e}}{\bar{c}_e} = 1.50$$

$$\frac{S_b}{S} = 0.0963 \quad \left(\frac{l_B}{\bar{c}} \right)^2 = 40.49$$

Additional Characteristics:

$$M = 0.60 \quad A_e = 5.0 \quad \frac{d}{b} = 0.157 \quad l_B = 77.20 \text{ ft}$$

$$\beta = 0.80 \quad x_m = 43.70 \text{ ft (moment center at } \bar{c}/4 \text{ of total panel)}$$

Compute:

Step 1. Acceleration derivative $C_{m\dot{\alpha}}$ for exposed panel (Section 7.1.4.2)

$$\left. \begin{aligned} \left(\frac{x_{s.c.}}{c_r} \right)_e &= 0.560 \\ \left(\frac{x_{c.g.}}{c_r} \right)_e &= 0.408 \\ \left(C_{L\dot{\alpha}} \right)_e &= 4.50 \text{ per rad} \end{aligned} \right\} \text{(sample problem, paragraph A, Section 7.3.1.1)}$$

$$\left(\frac{x_{c.g.}}{\bar{c}} \right)_e = \left(\frac{x_{c.g.}}{c_r} \right)_e \left(\frac{c_r}{\bar{c}_e} \right) = (0.408)(1.50) = 0.612$$

$$\left(C_{m \dot{\alpha}}'' \right)_e = -1.374 \text{ per rad} \quad (\text{sample problem, paragraph A, Section 7.3.4.1})$$

$$\beta A_e = 4.0$$

$$\frac{\beta^2 C_{m_0}(g)}{\pi A/2} = 0.0767 \text{ per rad} \quad (\text{figure 7.1.4.2-8})$$

$$C_{m_0}(g) = 0.941 \text{ per rad}$$

$$\begin{aligned} \left(C_{m \dot{\alpha}}'' \right)_e &= -\frac{27}{16} \left(\frac{x_{a.c.}}{c_r} \right)_e^2 \left(C_{L \dot{\alpha}} \right)_e + 3C_{m_0}(g) \quad (\text{equation 7.1.4.2-b}) \\ &= -\frac{27}{16} (0.560)^2 (4.50) + 3(0.941) \\ &= -2.381 + 2.823 \\ &= 0.442 \text{ per rad} \end{aligned}$$

$$\begin{aligned} \left(C_{m \dot{\alpha}} \right)_e &= \left(C_{m \dot{\alpha}}'' \right)_e + \left(\frac{x_{c.g.}}{\bar{c}} \right)_e \left(C_{L \dot{\alpha}} \right)_e \quad (\text{equation 7.1.4.2-a}) \\ &= 0.442 + (0.612)(-1.374) \\ &= -0.399 \text{ per rad} \quad (\text{based on } S_e \bar{c}_e^2) \end{aligned}$$

Step 2. Wing-body interference factors (Section 4.3.1.2)

$$\left. \begin{array}{l} K_{W(B)} = 1.125 \\ K_{B(W)} = 0.215 \end{array} \right\} \quad (\text{sample problem, paragraph A, Section 7.3.1.1})$$

Step 3. Acceleration derivative $C_{m\dot{\alpha}}$ for body (Section 7.2.2.2)

$$\frac{V_B}{S_b \ell_B} = 0.849$$

$$\left(1 - \frac{x_m}{\ell_B}\right) = 0.434$$

$$x_c = 44.48 \text{ ft}$$

$$(C_{m\dot{\alpha}})_B = 0.794 \text{ per rad}$$

} (sample problem, paragraph A, Section 7.3.1.2)

$$(C_{m\dot{\alpha}})_B = 2(C_{m\dot{\alpha}})_B \left[\frac{\frac{V_B}{S_b \ell_B} \left(\frac{x_c}{\ell_B} - \frac{x_m}{\ell_B} \right)}{\left(1 - \frac{x_m}{\ell_B}\right) - \frac{V_B}{S_b \ell_B}} \right] \quad (\text{equation 7.2.2.2-a})$$

$$= 2(0.794) \left[\frac{0.849 \left(\frac{44.48 - 43.70}{77.20} \right)}{0.434 - 0.849} \right]$$

$$= 1.59 \left[\frac{(0.849)(0.0101)}{-0.415} \right]$$

$$= -0.0328 \text{ per rad (based on } S_b \ell_B^2)$$

Solution:

$$(C_{m\dot{\alpha}})_{WB} = [K_{W(B)} + K_{B(W)}] \left(\frac{S_e}{S} \right) \left(\frac{\bar{c}_e}{\bar{c}} \right)^2 (C_{m\dot{\alpha}})_e + (C_{m\dot{\alpha}})_B \left(\frac{S_b}{S} \right) \left(\frac{\ell_B}{\bar{c}} \right)^2$$

(equation 7.3.4.2-a)

$$= (1.125 + 0.215)(0.7113)(0.7140)(-0.399) + (-0.0328)(0.0963)(40.49)$$

$$= -0.272 - 0.128$$

= -0.400 per rad (based on the area and the square of the mean aerodynamic chord of the total panel and referred to a moment center at $\bar{c}/4$ of the total panel)

B. TRANSONIC

The comments of paragraph B of Section 7.3.4.1 are directly applicable here.

DATCOM METHODS

It is recommended that the methods presented in paragraph A for estimating the acceleration derivative $C_{m\dot{\alpha}}$ of a wing-body configuration be applied to the transonic speed regime. Care should be taken to estimate the contributions of the lifting panel and body at the appropriate Mach number. The interference factors should be obtained from paragraph C, Section 4.3.1.2.

C. SUPERSONIC

The comments of paragraph C of Section 7.3.4.1 are directly applicable here.

DATCOM METHODS

The methods presented in paragraph A for estimating the acceleration derivative $C_{m\dot{\alpha}}$ of a wing-body configuration are also applicable to the supersonic speed range. Care should be taken to estimate the contributions of the lifting panel and body at the appropriate Mach number.

Sample Problem

Method 1

Given: Same configuration as sample problems of paragraph C, Sections 7.3.1.1, 7.3.1.2, and 7.3.4.1, and paragraph A of this section

$$M = 1.4$$

$$\beta = 0.98$$

$$\frac{d}{b} = 0.157$$

Compute:

Step 1. Acceleration derivative $C_{m\dot{\alpha}}$ for exposed panel (Section 7.1.4.2)

$$\beta \cot \Lambda_{LE} = 1.225 \text{ (supersonic leading edge)}$$

$$\cot^{-1} (\beta \cot \Lambda_{LE}) = 39.23^\circ$$

$$\beta A_e = 4.90$$

} (sample problem, paragraph C, Section 7.3.1.1)

$$\left(\frac{x_{c.g.}}{\bar{c}} \right)_e = 0.612 \text{ (sample problem, paragraph A)}$$

$$\left(C_{N\dot{\alpha}} \right)_e = -4.25 \text{ per rad (sample problem, paragraph C, Section 7.3.4.1)}$$

$$\beta \left[\left(C_{m\dot{\alpha}} \right)_1 \right]_e = 9.05 \text{ (figure 7.1.4.2-13a)}$$

$$\left[\left(C_{m\dot{\alpha}} \right)_1 \right]_e = 9.235 \text{ per rad}$$

$$\beta \left[\left(C_{m\dot{\alpha}} \right)_2 \right]_e = -4.52 \text{ (figure 7.1.4.2-13c)}$$

$$\left[\left(C_{m\dot{\alpha}} \right)_2 \right]_e = -4.612 \text{ per rad}$$

$$\left(C_{m\ddot{\alpha}} \right)_e = \left(\frac{M^2}{\beta^2} \right) \left[\left(C_{m\dot{\alpha}} \right)_1 \right]_e + \left(\frac{M^2}{\beta^2} + 1 \right) \left[\left(C_{m\dot{\alpha}} \right)_2 \right]_e \text{ (equation 7.1.4.2-e)}$$

$$= \left(\frac{1.4}{0.98} \right)^2 (9.235) + \left(\frac{1.4^2}{0.98^2} + 1 \right) (-4.612)$$

$$= 18.85 - 14.03$$

$$= 4.82 \text{ per rad}$$

$$\left(C_{m\dot{\alpha}} \right)_e = \left(C_{m\ddot{\alpha}} \right)_e + \left(\frac{x_{c.g.}}{\bar{c}} \right)_e \left(C_{L\dot{\alpha}} \right)_e \text{ (equation 7.1.4.2-a)}$$

$$= 4.82 + (0.612) (-4.25) \quad \left(C_{N\dot{\alpha}} \text{ is assumed to be equal to } C_{L\dot{\alpha}} \right)$$

$$= 2.219 \text{ per rad (based on } S_e \bar{c}_e^2 \text{)}$$

Step 2. Wing-body interference factors (Section 4.3.1.2)

$$\left. \begin{array}{l} K_{W(B)} = 1.125 \\ K_{B(W)} = 0.181 \end{array} \right\} \text{ (sample problem, paragraph C, Section 7.3.1.1)}$$

Step 3. Acceleration derivative $C_{m\dot{\alpha}}$ for body (Section 7.2.2.2)

$$\left. \begin{aligned} \frac{V_B}{S_b l_B} &= 0.849 \\ \left(1 - \frac{x_m}{l_B}\right) &= 0.434 \\ x_c &= 44.48 \text{ ft} \end{aligned} \right\} \quad (\text{sample problem, paragraph A, Section 7.3.1.2})$$

$$(C_{m\dot{\alpha}})_B = 1.017 \text{ per rad} \quad (\text{sample problem, paragraph C, Section 7.3.1.2})$$

$$(C_{m\dot{\alpha}})_B = 2(C_{m\dot{\alpha}})_B \left[\frac{\frac{V_B}{S_b l_B} \left(\frac{x_c}{l_B} - \frac{x_m}{l_B} \right)}{\left(1 - \frac{x_m}{l_B}\right) - \frac{V_B}{S_b l_B}} \right] \quad (\text{equation 7.2.2.2-a})$$

$$= 2(1.017) \left[\frac{(0.849) \left(\frac{44.48 - 43.70}{77.20} \right)}{0.434 - 0.849} \right]$$

$$= 2.034 \left[\frac{(0.849)(0.0101)}{-0.415} \right]$$

$$= -0.0420 \text{ per rad (based on } S_b l_B^2)$$

Solution:

$$(C_{m\dot{\alpha}})_{WB} = [K_{W(B)} + K_{B(W)}] \left(\frac{S_e}{S} \right) \left(\frac{\bar{c}_e}{\bar{c}} \right)^2 (C_{m\dot{\alpha}})_e + (C_{m\dot{\alpha}})_B \left(\frac{S_b}{S} \right) \left(\frac{l_B}{\bar{c}} \right)^2 \quad (\text{equation 7.3.4.2-a})$$

$$= (1.125 + 0.181)(0.7113)(0.7140)(2.219) + (-0.0420)(0.0963)(40.49)$$

$$= 1.472 - 0.164$$

$$= 1.308 \text{ per rad (based on the area and the square of the mean aerodynamic chord of the total panel and referred to a moment center at } \bar{c}/4 \text{ of the total panel)}$$

7.4 WING-BODY-TAIL DYNAMIC DERIVATIVES

7.4.1 WING-BODY-TAIL PITCHING DERIVATIVES

7.4.1.1 WING-BODY-TAIL PITCHING DERIVATIVE C_{Lq}

The information contained in this section is for estimating the nondimensional pitching derivative C_{Lq} of wing-body-tail combinations at low angles of attack. This derivative represents the lift due to pitching velocity at a constant angle of attack and is defined as

$$C_{Lq} = \frac{\partial C_L}{\partial \left(\frac{qc}{2V_\infty} \right)}$$

In general, the methods presented consist of a synthesis of material presented in other sections, although some new information is presented.

The derivative is presented in a manner similar to that used in reference 1 to calculate the lift of a wing-body-tail combination. The complete derivative is the sum of contributions of individual components, treated as isolated surfaces or bodies, and mutual interference effects. The mutual interference effects are assumed to correspond to those due to angle-of-attack variations, established in references 1 and 2 and presented in Section 4.3.1.2.

The horizontal-tail contribution to the derivative C_{Lq} is based on the assumption that instantaneous forces on the tail correspond to the instantaneous angle of attack. This assumption is also the basis used in estimating the horizontal-tail contribution to the derivative C_{m_q} in Section 7.4.1.2. The effect of this assumption is presented in numerous aerodynamic texts, for example, reference 3. The effects of C_{Lq} are generally small and frequently neglected in dynamic analyses.

A. SUBSONIC

Two methods are presented for determining the pitching derivative C_{Lq} of wing-body-tail combinations, differing only in their treatment of the effect of the flow field of the forward surface on the aft surface.

DATCOM METHODS

Method 1. ($b'/b'' > 1.5$)

For configurations in which the span of the forward surface is large compared to that of the aft surface, the following approach can be used. This method is to be used when the ratio of the forward-panel span to the aft-panel span is 1.5 or greater. The equation of the nondimensional pitching derivative C_{Lq} of a wing-body-tail configuration, based on the area and mean

aerodynamic chord of the total forward panel and referred to a moment center at the assumed center of gravity or center of rotation, is given by

$$C_{L_q} = (C_{L_q})_{WB} + 2 [K_{W(B)} + K_{B(W)}]'' \left(\frac{S_e''}{S'} \right) \left(\frac{x_{c.g.} - x''}{c'} \right) \left(\frac{q''}{q_\infty} \right) (C_{L\alpha})_e'' \quad 7.4.1.1-a$$

where the primed quantities refer to the forward panel, the double-primed quantities refer to the aft panel, and the subscript e refers to the exposed panel. (See Section 4.3.1.2 for the definition of exposed surfaces.)

$(C_{L_q})_{WB}$ is the contribution of the wing-body configuration to the pitching derivative C_{L_q} , obtained from Section 7.3.1.1.

$[K_{W(B)} + K_{B(W)}]''$ is the appropriate wing-body interference factor obtained from Section 4.3.1.2 for the aft panel.

$(C_{L\alpha})_e''$ is the lift-curve slope of the exposed aft panel, obtained from Section 4.1.3.2.

$\frac{S_e''}{S'}$ is the ratio of the exposed aft panel planform area to the total planform area of the forward panel.

$x_{c.g.} - x''$ is the distance parallel to the longitudinal axis between the moment reference center (usually the vehicle center of gravity) and the quarter-chord point of the mean aerodynamic chord of the total aft horizontal panel.

This parameter is approximated in Section 4.5.2.1 as $x_{c.g.} - x'' = \ell'' + x_{c.g.}$ (equation 4.5.2.1-e) where $x_{c.g.}$ and ℓ'' are defined in figures 4.5.2.1-7a and -7b.

$\frac{q''}{q_\infty}$ is the average dynamic-pressure ratio acting on the aft surface, obtained from Section 4.4.1.

Method 2. ($b'/b'' < 1.5$)

For configurations in which the span of the forward surface is approximately equal to or less than that of the aft surface, the vortex shed from the forward surface interacts directly with the aft surface and the resulting interference effects must be accounted for in the tail terms. This method is to be used when the ratio of the forward-panel span to the aft-panel span is less than 1.5. The equation for the nondimensional pitching derivative C_{L_q} of a wing-body-tail configuration, based on the area and mean aerodynamic chord of the total forward panel and referred to a moment center at the assumed center of gravity or center of rotation, is given by

$$C_{Lq} = (C_{Lq})_{WB} + 2 \cdot \frac{x_{c.g.} - x''}{\bar{c}} \left\{ [K_{W(B)} + K_{B(W)}]'' \left(\frac{S_e''}{S'} \right) \left(\frac{q''}{q_\infty} \right) (C_{L\alpha})_e'' + (C_{L\alpha})_{W''(v)} \right\}$$

7.4.1.1-b

The parameters in the first two terms on the right-hand side are the same as those in equation 7.4.1.1-a. The last term represents the effect of the forward-panel vortices on the aft panel and is given by

$$(C_{L\alpha})_{W''(v)} = \frac{(C_{L\alpha})'_e \left(\frac{S_e'}{S'} \right) (C_{L\alpha})_e'' \left(\frac{q''}{q_\infty} \right) K_{W(B)}' I_{vW'(W'')} \left(\frac{b''}{2} - \frac{d''}{2} \right)}{2\pi A_e'' \left(\frac{b_v'}{2} - \frac{d'}{2} \right)} \quad 7.4.1.1-c$$

where

d' and d'' are the body diameters at the midchord points of the MAC of the forward and aft surfaces, respectively.

b'' is the span of the total aft panel.

$\left(\frac{b_v'}{2} - \frac{d'}{2} \right)$ is obtained from figure 4.4.1-71 as a function of forward-panel geometry.

$I_{vW'(W'')}$ is the vortex interference factor, obtained from Section 4.4.1.

A_e'' is the aspect ratio of the exposed aft panel.

$(C_{L\alpha})'_e$ is the lift-curve slope of the exposed forward panel, obtained from Section 4.1.3.2 (per radian).

$(C_{L\alpha})_e''$ is the lift-curve slope of the exposed aft panel, obtained from Section 4.1.3.2 (per radian).

The remaining terms are defined in method 1 above.

The quantities $(C_{L\alpha})'_e$ and $(C_{L\alpha})_e''$ in the last term of equation 7.4.1.1-b must be expressed in radians. If the result of this term is desired per degree, the conversion must be applied after the term is evaluated.

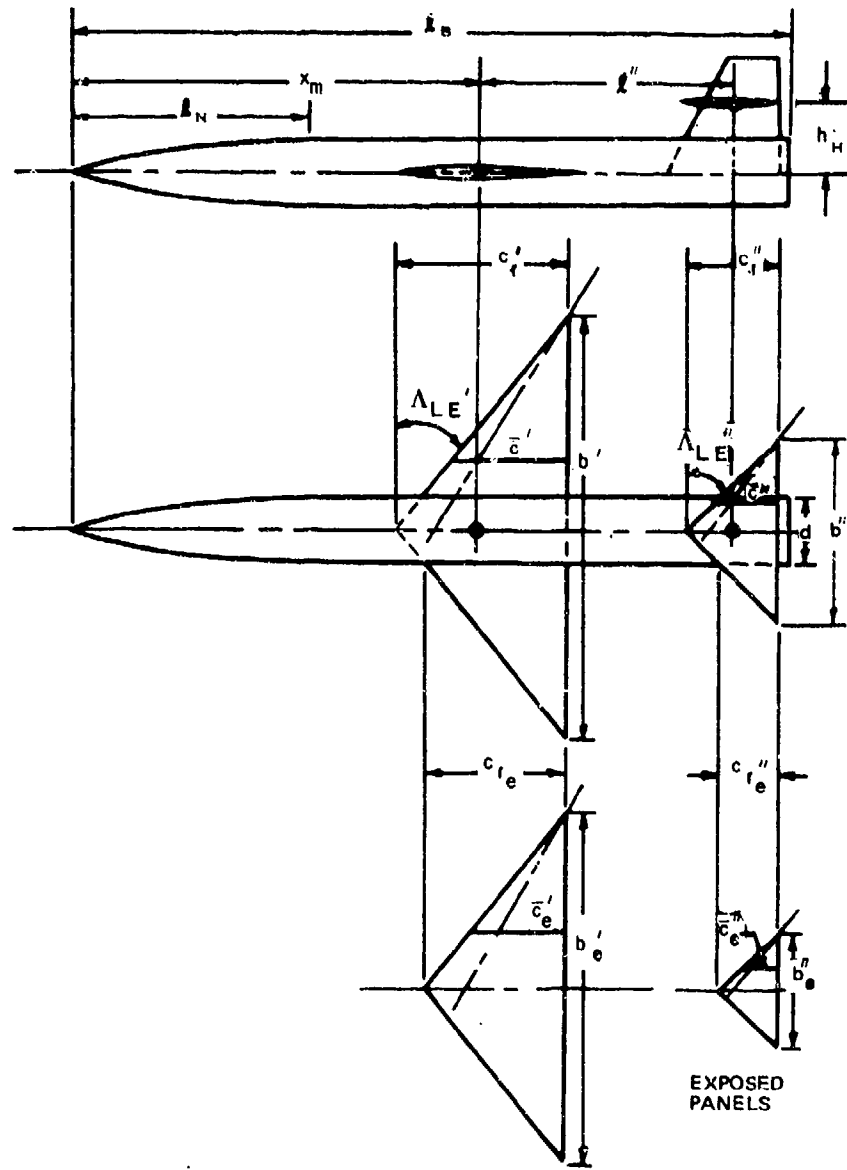
Because of the similarity of the two methods a sample problem of method 2 is not included. However, evaluation of the term $(C_{L\alpha})_{W''(v)}$ for a wing-body-tail configuration is presented in Section 4.5.1.1.

7.4.1.1-3

Sample Problem

Method 1

Given: An ogive-cylinder-body—triangular-wing and triangular-tail configuration. The wing-body configuration is the same as that of the sample problem of Sections 7.3.1 and 7.3.4. Many of the characteristics are repeated below.



Although a tail has been added to the wing-body configuration of Sections 7.3.1 and 7.3.4, for the sake of simplicity the vehicle center of gravity is taken at $\bar{c}'/4$. Therefore, $x_{c,g.} - x'' = l''$, the longitudinal distance from the quarter-chord point of the MAC of the forward surface to the quarter-chord point of the MAC of the aft surface.

Wing Characteristics:

Total Panel	Exposed Panel
$A' = 5.0$	$\lambda' = 0$
$\Lambda'_{LE} = 38.67^\circ$	$\Gamma' = 0$
$i' = 0$	$c_r' = 18.20 \text{ ft}$
$b' = 45.50 \text{ ft}$	$\bar{c}' = 12.133 \text{ ft}$
$S' = 414.0 \text{ sq ft}$	

NACA 66-206 airfoil section

Horizontal-Tail Characteristics:

Total Panel	Exposed Panel
$A'' = 4.0$	$\lambda'' = 0$
$\Lambda''_{LE} = 45^\circ$	$\Gamma'' = 0$
$i'' = 0$	$c_r'' = 9.958 \text{ ft}$
$b'' = 19.915 \text{ ft}$	$\bar{c}'' = 6.638 \text{ ft}$
$S'' = 99.16 \text{ sq ft}$	

NACA 66-206 airfoil section

Body Characteristics:

$$l_N = 25.0 \text{ ft} \quad l_B = 77.20 \text{ ft} \quad d = 7.127 \text{ ft}$$

The following ratios based on total forward-panel dimensions:

$$\frac{l''}{\bar{c}'} = 2.26 \quad \frac{S_e''}{S'} = 0.0988$$

Additional Characteristics:

$$\begin{array}{lll}
 h_H = 7.18 \text{ ft} & \frac{b''}{d''} = 2.794 & R_\rho = 5.16 \times 10^7 \text{ (based on } \bar{c}') \\
 l'' = 27.425 \text{ ft} & M = 0.60 & \text{Sea level} \\
 x = 18.32 \text{ ft*} & \beta = 0.80 & \text{Smooth surfaces} \\
 & \alpha' = 4^\circ & \frac{S_{\text{wet}}}{S_{\text{ref}}} = 2
 \end{array}$$

Compute:

Step 1. Wing-body C_{Lq} (Section 7.3.1.1)

$$\left(C_{Lq} \right)_{WB} = [K_{W(B)} + K_{B(W)}] \left(\frac{S_e'}{S'} \right) \left(\frac{\bar{c}_e'}{\bar{c}'} \right) \left(C_{Lq} \right)_e + \left(C_{Lq} \right)_B \left(\frac{S_b}{S'} \right) \left(\frac{l_B}{\bar{c}'} \right)$$

(equation 7.3.1.1-a)

$$\left(C_{Lq} \right)_{WB} = 4.467 \text{ per rad} \text{ (sample problem, paragraph A, Section 7.3.1.1)}$$

Step 2. Lift-curve slope for the exposed horizontal tail panel (Section 4.1.3.2)

$$c_{\rho_\alpha} = 6.19 \text{ per rad} \text{ (table 4.1.1-B)}$$

$$\kappa = \frac{c_{\rho_\alpha}}{2\pi} = 0.985$$

$$\frac{A_e''}{\kappa} \left[\beta^2 + \tan^2 \Lambda_{c/2}'' \right]^{1/2} = \frac{4.0}{0.985} [0.64 + 0.25]^{1/2} = 3.83$$

$$\frac{\left(C_{L\alpha} \right)_e''}{A_e''} = 1.00 \quad (\text{figure 4.1.3.2-49})$$

$$\left(C_{L\alpha} \right)_e'' = 4.00 \text{ per rad}$$

*x is the longitudinal distance measured from the wing root trailing edge aft. For this problem it is taken equal to ℓ_2 defined in Section 4.4.1.

Step 3. Tail-body interference factors (Section 4.3.1.2)

$$\frac{d''}{b''} = \frac{7.127}{19.915} = 0.358$$

$$\left. \begin{array}{l} K_{W(B)}'' = 1.315 \\ K_{B(W)}'' = 0.550 \end{array} \right\} \text{(figure 4.3.1.2-10)}$$

Step 4. Dynamic pressure ratio (Section 4.4.1)

Obtain value at $\alpha' = 4^\circ$

$$C_L' = 0.391 \text{ (sample problem, paragraph A, Section 7.4.4.1)}$$

$$\epsilon = \frac{1.62 C_L}{\pi A'} \quad \text{(equation 4.4.1-k)}$$

$$= \frac{1.62 (0.391)}{5\pi} 57.3$$

$$= 2.3^\circ$$

$$\gamma = \tan^{-1} \frac{h_H}{x} = \tan^{-1} \left(\frac{7.18}{18.32} \right) = 21.4^\circ \text{ (see sketch (d), Section 4.4.1)}$$

$$\gamma + \epsilon - \alpha' = 21.4 + 2.3 - 4 = 19.7^\circ$$

$$z = x \tan(\gamma + \epsilon - \alpha') \quad \text{(equation 4.4.1-l)}$$

$$= 18.32 (0.3581) = 6.56$$

$$C_f = 0.00236 \text{ (figure 4.1.5.1-26)}$$

$$C_{D_0} = C_f \left[1 + L \left(\frac{t}{c} \right) + 100 \left(\frac{t}{c} \right)^4 \right] R_{L.S.} \frac{S_{ref}}{S_{net}} \quad \text{(equation 4.1.5.1-a)}$$

$$\left[1 + L \left(\frac{t}{c} \right) + 100 \left(\frac{t}{c} \right)^4 \right] = 1.072 \quad \text{(figure 4.1.5.1-28a)}$$

$$\cos \Lambda_{(u/c)}_{max} = \cos \Lambda_{.45c} = \cos 23.76^\circ = 0.915$$

$$R_{L.S.} = 1.14 \quad \text{(figure 4.1.5.1-28b)}$$

$$C_{D_0} = (0.00236)(1.072)(1.14)(2) = 0.00577$$

$$\left(\frac{\Delta q}{q}\right)_o = \frac{2.42 (C_{D_0})^{1/2}}{\frac{x}{\bar{c}} + 0.30} \quad (\text{equation 4.4.1-m})$$

$$= \frac{2.42 (0.00577)^{1/2}}{1.51 + 0.30} = 0.102$$

$$\frac{z_w}{\bar{c}} = 0.68 \sqrt{C_{D_0} \left(\frac{x}{\bar{c}} + 0.15 \right)} \quad (\text{equation 4.4.1-j})$$

$$= 0.68 \sqrt{0.00577 (1.51 + 0.15)} = 0.0666$$

$$\frac{z}{z_w} = \frac{z/\bar{c}}{z_w/\bar{c}} = \frac{6.56/12.133}{0.0666} = 8.12$$

$$\frac{\Delta q}{q} = \left(\frac{\Delta q}{q}\right)_o \cos^2 \left(\frac{\pi}{2} - \frac{z}{z_w} \right) \quad (\text{equation 4.4.1-n})$$

$$= (0.102) \cos^2 \left[\left(\frac{3.14}{2} \right) (8.12) (57.3) \right]$$

$$= (0.102) (0.9834)^2$$

$$= 0.099$$

$$\frac{q''}{q_\infty} = 1 - \frac{\Delta q}{q} \quad (\text{equation 4.4.1-o})$$

$$= 1 - 0.099 = 0.901$$

Solution:

$$C_{L_q} = (C_{L_q})_{WB} + 2[K_{W(B)} + K_{B(W)}]'' \left(\frac{S_e''}{S'} \right) \left(\frac{x_{c.s.} - x''}{\bar{c}'} \right) \left(\frac{q''}{q_\infty} \right) (C_{L_\alpha})''_e \quad (\text{equation 7.4.1.1-a})$$

$$= 4.467 + 2(1.315 + 0.550)(0.0988)(2.26)(0.901)(4.00)$$

$$= 4.467 + 3.002$$

= 7.47 per rad (based on the area and mean aerodynamic chord of the total panel and referred to a moment center at $\bar{c}'/4$)

B. TRANSONIC

No accurate methods are available for estimating the characteristics of isolated panels or the dynamic-pressure ratio in the transonic speed regime. The aerodynamic interference "K" factors for slender configurations are relatively insensitive to Mach number; however, for nonslender configurations transonic interference effects can become quite large and sensitive to minor changes in local contour.

DATCOM METHODS

It is recommended that the methods presented in paragraph A above be applied directly to the transonic speed regime. Care should be taken to estimate the various parameters of equations 7.4.1.1-a and -b at the appropriate Mach number. The interference "K" factors should be obtained from paragraph C, Section 4.3.1.2.

C. SUPERSONIC

The information included in the Datcom accounts for most of the mutual interferences that occur between components of wing-body-tail configurations at supersonic speeds.

DATCOM METHODS

The methods presented in paragraph A above are also applicable to the supersonic speed range. Care should be taken to estimate the various parameters of equations 7.4.1.1-a and -b at the appropriate Mach number. Method 3 of paragraph C of Section 4.4.1 should be used to evaluate the last term of equation 7.4.1.1-b.

Sample Problem

Method 1

Given: Same configuration as sample problem of paragraph A. Some of the characteristics are repeated below.

The following ratios based on total forward-panel dimensions:

$$\frac{\ell''}{\bar{c}'} = 2.26 \quad \frac{S_e''}{S'} = 0.0988$$

Additional Characteristics:

$$\begin{aligned}
 M &= 1.40 & \alpha' &= 4^\circ & \text{Sea level} \\
 \beta &= 0.98 & \Lambda''_{LE} &= 45^\circ & R_\infty = 1.2 \times 10^8 \text{ (based on } \bar{c}') \\
 A' &= 5.0 & K &= \frac{16}{3} \text{ (page 4.1.5.1-16)} & \text{Smooth surfaces} \\
 && \text{cg at } \bar{c}'/4
 \end{aligned}$$

Compute:

Step 1. Wing-body C_{Lq} (Section 7.3.1.1)

$$\left(C_{Lq}\right)_{WB} = [K_{W(B)} + K_{B(W)}] \left(\frac{S_e'}{S'} \right) \left(\frac{\bar{c}_e'}{\bar{c}'} \right) \left(C_{Lq} \right)_e + \left(C_{Lq} \right)_B \left(\frac{S_b}{S'} \right) \left(\frac{\bar{c}_B}{\bar{c}'} \right)$$

(equation 7.3.1.1-a)

$$\left(C_{Lq}\right)_{WB} = 3.977 \text{ per rad (sample problem, paragraph C, Section 7.3.1.1)}$$

Step 2. Lift-curve slope for the exposed horizontal-tail panel (Section 4.1.3.2)

$$\frac{\beta}{\tan \Lambda''_{LE}} = 0.98$$

$$A_e'' \tan \Lambda''_{LE} = 4.0$$

$$\tan \Lambda''_{LE} \left(C_{N\alpha}\right)_e'' = 4.025 \text{ (figure 4.1.3.2-56a)}$$

$$\left(C_{N\alpha}\right)_e'' = 4.025 \text{ per rad}$$

Step 3. Tail-body interference factors (Section 4.3.1.2)

$$\frac{d''}{b''} = 0.358 \text{ (sample problem, paragraph A)}$$

$$K_{W(B)}'' = 1.315 \text{ (figure 4.3.1.2-10)}$$

$$\frac{\beta d''}{c_{re}''} = \frac{0.98 (7.127)}{6.394} = 1.092$$

$$\beta \cot \Lambda_{LE}'' = 0.98$$

$$K_{B(W)}'' \left[\beta (C_{N_\alpha})'' (\lambda_e'' + 1) \left(\frac{b''}{d''} - 1 \right) \right] = 2.85 \quad (\text{figure 4.3.1.2-11a})$$

$$\beta (C_{N_\alpha})'' (\lambda_e'' + 1) \left(\frac{b''}{d''} - 1 \right) = 0.98(4.025)(1)(1.794) = 7.076$$

$$K_{B(W)}'' = \frac{2.85}{7.076} = 0.4028$$

Step 4. Dynamic pressure ratio (Section 4.4.1)

Obtain at $\alpha' = 4^\circ$ Viscous flow field

$$\alpha_0' = -1.6^\circ \quad (\text{table 4.1.1-B})$$

$$C_{N_\alpha}' = 0.0712 \text{ per deg} \quad (\text{sample problem, paragraph C, Section 7.3.1.1})$$

$$C_N' = C_{N_\alpha}' (\alpha' - \alpha_0') = 0.0712[4 - (-1.6)] = 0.399$$

$$C_f = 0.0018 \quad (\text{figure 4.1.5.1-26})$$

$$C_{D_f} = C_f \frac{S_{\text{wet}}}{S_{\text{ref}}} \quad (\text{equation 4.1.5.1-i})$$

$$= (0.0018)(2) = 0.0036$$

$$\beta \cot \Lambda_{LE_{bw}} = (0.98)(1.25) = 1.225 \quad (\text{supersonic leading edge})$$

$$C_{D_w} = \frac{K}{\beta} \left(\frac{t}{c} \right)_{\text{eff}}^2 \left(\frac{S_{bw}}{S_{ref}} \right) \quad (\text{equation 4.1.5.1-k})$$

$$= \frac{16}{3(0.98)} (0.06)^2 (1)$$

$$= 0.0196$$

$$C_{D_0} = C_{D_f} + C_{D_w} \quad (\text{equation 4.1.5.1-h})$$

$$= 0.0036 + 0.0196 = 0.0232$$

$$\left(\frac{\Delta q}{q}\right)_o = \frac{2.42 (C_{D_0})^{1/2}}{\frac{x}{c} + 0.30} \quad (\text{equation 4.4.1-m})$$

$$= \frac{2.42(0.0232)^{1/2}}{1.51 + 0.30} = 0.204$$

$$\frac{z_w}{c} = 0.68 \sqrt{C_{D_0} \left(\frac{x}{c} + 0.15 \right)} \quad (\text{equation 4.4.1-j})$$

$$= 0.68 \sqrt{(0.0232)(1.51 + 0.15)}$$

$$= 0.1334$$

$$\epsilon = \frac{1.62 C_N}{\pi A'} \quad (\text{equation 4.4.1-k})$$

$$= \frac{(1.62)(0.399)}{5\pi} \quad (57.3)$$

$$= 2.36^\circ$$

$$\gamma = 21.4^\circ \quad (\text{sample problem, paragraph A})$$

$$\gamma + \epsilon - \alpha' = 21.4 + 2.36 - 4 = 19.76^\circ$$

$$z = x \tan(\gamma + \epsilon - \alpha') \quad (\text{equation 4.4.1-l})$$

$$= 18.32(0.3592) = 6.581$$

$$\frac{z}{z_w} = \frac{z/c}{z_w/c} = \frac{6.581/12.133}{0.1334} = 4.07$$

$$\frac{\Delta q}{q} = \left(\frac{\Delta q}{q}\right)_o \cos^2 \left(\frac{\pi}{2} \frac{z}{z_w} \right) \quad (\text{equation 4.4.1-n})$$

$$= (0.204) \cos^2 \left[\left(\frac{3.14}{2} \right) (4.07) (57.3) \right]$$

$$= (0.204) (0.9943)^2 = 0.20$$

$$\frac{q}{q_{\infty}} = 1 - \frac{\Delta q}{q} \quad (\text{equation 4.4.1-o})$$

$$= 1.0 - 0.20 = 0.80$$

Solution:

$$C_{L_q} = (C_{L_q})_{WB} + 2[K_{W(B)} + K_{B(W)}]'' \left(\frac{S_e''}{S'} \right) \left(\frac{x_{c.g.} - x''}{\bar{c}'} \right) \left(\frac{q''}{q_{\infty}} \right) (C_{N_c})_e''$$

(equation 7.4.1.1-a)

$$= 3.977 + 2(1.315 + 0.4028)(0.0988)(2.26)(0.80)(4.025)$$

$$= 3.977 + 2.47$$

= 6.447 per rad (based on the area and mean aerodynamic chord of the total panel and referred to a moment center at $\bar{c}'/4$)

REFERENCES

1. Pitts, W., Neilsen, J., and Keatner, G.: Lift and Center of Pressure of Wing-Body-Tail Combinations at Subsonic, Transonic, and Supersonic Speeds. NACA TR 1307, 1959. (U)
2. Sprriter, J.: The Aerodynamic Forces on Slender Plane- and Cruciform-Wing and Body Combinations. NACA TR 962, 1955. (U)
3. Etkin, B.: Dynamics of Flight. John Wiley and Sons, Inc., New York, 1959. (U)

7.4.1.2 WING-BODY-TAIL PITCHING DERIVATIVE C_{m_q}

The information contained in this section is for estimating the nondimensional pitching derivative C_{m_q} of wing-body-tail combinations at low angles of attack. The derivative C_{m_q} is the change in pitching-moment coefficient with varying pitch velocity and is commonly referred to as the pitch-damping derivative. It is expressed as

$$C_{m_q} = \frac{\partial C_m}{\partial \left(\frac{q \bar{c}}{2V_\infty} \right)}$$

This derivative is very important in longitudinal dynamics, since it represents a major portion of the damping of the short-period mode for conventional aircraft.

The Datcom methods are based on the same assumptions that were made for the total pitching derivative C_{L_q} of wing-body-tail combinations, and the general discussion of Section 7.4.1.1 is directly applicable here.

A. SUBSONIC

Two methods are presented for determining the pitching derivative C_{m_q} of wing-body-tail combinations, differing only in their treatment of the effect of the flow field of the forward surface on the aft surface.

DATCOM METHODS

Method 1. ($b'/b'' > 1.5$)

For configurations in which the spar of the forward surface is large compared to that of the aft surface, the following approach can be used. This method is to be used when the ratio of the forward-panel span to the aft-panel span is 1.5 or greater. The equation for the nondimensional pitching derivative C_{m_q} of a wing-body-tail configuration, based on the area and the square of the mean aerodynamic chord of the total forward panel and referred to a moment center at the assumed center of gravity or center of rotation, is given by

$$C_{m_q} = (C_{m_q})_{WB} - 2[K_{W(B)} + K_{(B)W}]'' \left(\frac{S_e''}{S'} \right) \left(\frac{x_{c.g.} - x''}{\bar{c}'} \right)^2 \left(\frac{q''}{q_\infty} \right) (C_{L\alpha})_e'' \quad 7.4.1.2-a$$

where the primed quantities refer to the forward panel, the double-primed quantities refer to the aft panel, and the subscript e refers to the exposed panel. (See Section 4.3.1.2 for the definition of exposed surfaces.)

$(C_{m_q})_{WB}$ is the contribution of the wing-body configuration to the pitching derivative C_{m_q} , obtained from Section 7.3.1.2.

The remaining terms are defined in paragraph A of Section 7.4.1.1.

Method 2. ($b'/b'' < 1.5$)

For configurations in which the span of the forward surface is approximately equal to or less than that of the aft surface, the vortex shed from the forward surface interacts directly with the aft surface, and the resulting interference effects must be accounted for in the tail terms. This method is to be used when the ratio of the forward-panel span to the aft-panel span is less than 1.5. The equation for the nondimensional pitching derivative C_{m_q} of a wing-body-tail configuration, based on the area and the square of the mean aerodynamic chord of the total forward panel and referred to a moment center at the assumed center of gravity or center of rotation, is given by

$$C_{m_q} = (C_{m_q})_{WB} - 2 \left(\frac{x_{c.g.} - x''}{\bar{c}'} \right)^2 \left\{ [K_{W(B)} + K_{B(W)}]'' \left(\frac{S_e''}{S'} \right) \left(\frac{q''}{q_\infty} \right) (C_{L\alpha})_e'' + (C_{L\alpha})_{W''(v)} \right\}$$

7.4.1.2-b

All the above terms are defined in paragraph A of Section 7.4.1.1 and method 1 above.

Because of the similarity of the two methods, a sample problem for method 2 is not included. However, evaluation of the term $(C_{L\alpha})_{W''(v)}$ for a wing-body-tail configuration is presented in Section 4.5.1.1.

Sample Problem

Method 1

Given: Same configuration as sample problem of paragraph A, Section 7.4.1.1. Some of the characteristics are repeated below.

The following ratios based on total forward panel dimensions:

$$\frac{\ell''}{\bar{c}'} = 2.26 \quad \frac{S_e''}{S'} = 0.0988$$

Additional Characteristics:

$$M = 0.60 \quad \beta = 0.80 \quad \alpha' = 4^\circ \quad cg \text{ at } \bar{c}'/4$$

7.4.1.2-2

Compute:

Step 1. Wing-body C_{m_q} (Section 7.3.1.2)

$$(C_{m_q})_{WB} = -4.021 \text{ per rad} \quad (\text{sample problem, paragraph A, Section 7.3.1.2})$$

Step 2. Lift-curve slope for the exposed horizontal tail (Section 4.1.3.2)

$$(C_{L\alpha})_e'' = 4.0 \text{ per rad} \quad (\text{sample problem, paragraph A, Section 7.4.1.1})$$

Step 3. Tail-body interference factors (Section 4.3.1.2)

$$\left. \begin{array}{l} K_{W(B)}'' = 1.315 \\ K_{B(W)}'' = 0.550 \end{array} \right\} \quad (\text{sample problem, paragraph A, Section 7.4.1.1})$$

Step 4. Dynamic pressure ratio (Section 4.4.1)

$$\frac{q''}{q_\infty} = 0.901 \quad (\text{sample problem, paragraph A, Section 7.4.1.1})$$

Solution:

$$\begin{aligned} C_{m_q} &= (C_{m_q})_{WB} - 2[K_{W(B)} + K_{B(W)}]'' \left(\frac{S_e''}{S'} \right) \left(\frac{x_{c.g.} - x''}{\bar{c}'} \right)^2 \left(\frac{q''}{q_\infty} \right) (C_{L\alpha})_e'' \\ &= -4.021 - 2(1.315 + 0.550)(0.0988)(2.26)^2(0.901)(4.0) \\ &= -4.021 - 6.78 \\ &= -10.80 \text{ per rad} \quad (\text{based on the area and the square of the mean aerodynamic chord of the total forward panel and referred to a moment center at } \bar{c}'/4) \end{aligned} \quad (\text{equation 7.4.1.2-a})$$

B. TRANSONIC

The comments of paragraph B of Section 7.4.1.1 are directly applicable here.

DATCOM METHODS

It is recommended that the methods presented in paragraph A above be applied to the transonic speed regime. Care should be taken to estimate the parameters of equations 7.4.1.2-a and -b at the appropriate Mach number. The interference "K" factors should be obtained from paragraph C, Section 4.3.1.2.

C. SUPERSONIC

The comments of paragraph C of Section 7.4.1.1 are directly applicable here.

DATCOM METHODS

The methods presented in paragraph A above are also applicable to the supersonic speed range. Care should be taken to estimate the parameters of equations 7.4.1.2-a and -b at the appropriate Mach number. Method 3 of paragraph C of Section 4.4.1 should be used to evaluate the last term of equation 7.4.1.2-b.

Sample Problem

Method 1

Given: Same configuration as sample problem of paragraph C Section 7.4.1.1 and paragraph A of this section. Some of the characteristics are repeated below.

The following ratios based on total forward panel dimensions:

$$\frac{S_e''}{S'} = 0.0988 \quad \frac{l''}{c'} = 2.26$$

Additional Characteristics:

$$M = 1.40 \quad \beta = 0.98 \quad \alpha' = 4^\circ \quad cg \text{ at } c'/4$$

Compute:

Step 1. Wing-body C_{m_q} (Section 7.3.1.2)

$$(C_{m_q})_{WB}'' = -4.961 \text{ per rad} \quad (\text{sample problem, paragraph C, Section 7.3.1.2})$$

Step 2. Lift-curve slope for the exposed horizontal tail (Section 4.1.3.2)

$$(C_N \alpha)''_e = 4.025 \text{ per rad} \quad (\text{sample problem, paragraph C, Section 7.4.1.1})$$

Step 3. Tail-body interference factors (Section 4.3.1.2)

$$\left. \begin{array}{l} K_{W(B)}'' = 1.315 \\ K_{B(W)}'' = 0.4028 \end{array} \right\} \text{(sample problem, paragraph C, Section 7.4.1.1)}$$

Step 4. Dynamic pressure ratio (Section 4.4.1)

$$\frac{q''}{q_\infty} = 0.80 \text{ (sample problem, paragraph C, Section 7.4.1.1)}$$

Solution:

$$\begin{aligned} C_{m_q} &= (C_{m_q})_{WB} - 2[K_{W(B)} + K_{B(W)}]'' \left(\frac{S_e''}{S'} \right) \left(\frac{x_{c.g.} - x''}{\bar{c}'} \right)^2 \left(\frac{q''}{q_\infty} \right) (C_{N\alpha})_e'' \\ &= -4.961 - 2(1.315 + 0.4028)(0.0988)(2.26)^2(0.80)(4.025) \\ &= -4.961 - 5.583 \\ &= -10.54 \text{ per rad (based on the area and the square of the mean aerodynamic chord of the total forward panel and referred to a moment center at } \bar{c}'/4) \end{aligned}$$

7.4.1.3 WING-BODY-TAIL PITCHING DERIVATIVE C_{D_q}

This section presents a method for estimating the wing-body-tail derivative C_{D_q} at subsonic speeds. This derivative is the change in the drag coefficient due to a change in pitching velocity at a constant angle of attack and is defined as

$$C_{D_q} = \frac{\partial C_D}{\partial \left(\frac{q \bar{c}}{2V} \right)}, \text{ where } C_D \text{ is based on } S_w.$$

In general, this derivative is small and has a negligible effect on longitudinal stability; hence, it is usually neglected.

A. SUBSONIC

The wing-body-tail derivative is obtained by adding the horizontal-tail contribution to the wing-alone contribution developed in Section 7.1.1.3. The body contribution is negligible and has been neglected. The horizontal-tail contribution to C_{D_q} was computed from the tail-damping angle of attack and also from wing-induced downwash at the tail due to pitch rate. The horizontal-tail lift was taken to act normal to the local flow direction at the tail to produce a force component in the direction of the free-stream flow.

DATCOM METHOD

The wing-body-tail derivative C_{D_q} is given by

$$C_{D_q} = C_{D_{q_W}} + \left(C_{D_{q_0}} \right)_H + \left(\frac{\partial C_{D_{q_H}}}{\partial \alpha_F} \right) \alpha_F \quad 7.4.1.3-a$$

where

$C_{D_{q_W}}$ is the wing contribution from Section 7.1.1.3-a

$\left(C_{D_{q_0}} \right)_H$ is the horizontal-tail contribution due to zero-angle-of-attack loading given by

$$\begin{aligned} \left(C_{D_{q_0}} \right)_H &= C_{L_{\alpha_H}} \frac{i_H}{57.3} \left(\frac{S_H}{S_w} \right) \left[\epsilon_q - \frac{2(\ell_H \cos \alpha_F + z_H \sin \alpha_F)}{\bar{c}} - \frac{2 \epsilon_q \epsilon}{i_H} \right. \\ &\quad \left. + \left(\frac{4\epsilon}{i_H} \right) \left(\frac{\ell_H \cos \alpha_F + z_H \sin \alpha_F}{\bar{c}} \right) \right] \text{ (per degree)} \end{aligned} \quad 7.4.1.3-b$$

where

$C_{L_{\alpha_H}}$ is the horizontal-tail lift-curve slope (based on S_H) obtained from test data or Section 4.1.3.2 (per degree).

i_H is the incidence of the horizontal tail with respect to the fuselage reference line in degrees.

S_H is the horizontal-tail reference area.

S_W is the wing reference area.

ϵ_q is the variation in downwash with respect to pitch rate, $\epsilon_q = \frac{\partial \epsilon}{\partial \left(\frac{q \bar{c}}{2V} \right)}$

(at $\bar{c}/4$ of the horizontal tail). Design charts are presented in Figures 7.4.1.3-4a through -4x for Mach numbers of 0.2 and 0.8. These charts are presented as a function of wing geometry and the spanwise location of the horizontal-tail MAC relative to the wing span.

l_H is the distance from the moment reference center to the center-of-pressure location of the horizontal stabilizer, measured parallel to the body center line. For Datcom purposes, the horizontal-tail center-of-pressure location is assumed to be at $\bar{c}_H/4$.

z_H is the distance from the moment reference center to the center-of-pressure location of the vertical stabilizer, measured normal to the body center line, positive for the stabilizer above the body.

α_F is the fuselage angle of attack.

\bar{c} is the wing MAC.

ϵ is the downwash of the wing at $\bar{c}/4$ of the horizontal tail, excluding the contribution due to pitch rate. This may be obtained from test data or from Section 4.4.1.

$\frac{\partial C_{D_{q_H}}}{\partial \alpha_F}$ is the change in horizontal-tail contribution with angle of attack, obtained by

$$\frac{\partial C_{D_q}}{\partial \alpha_F} = C_{L_{\alpha_H}} \frac{S_H}{S_W} \frac{1}{57.3} \left[\epsilon_q - \frac{2(l_H \cos \alpha_F + z_H \sin \alpha_F)}{\bar{c}} \right] \quad 7.4.1.3-c$$

where all the terms are defined above.

Sample Problem

Given: Same configuration as sample problem of Paragraph A of Section 7.1.1.3.

Tail Characteristics:

$$C_{L_{\alpha_H}} = 0.08 \text{ per deg} \quad i_H = 1 \text{ deg} \quad \frac{S_H}{S_W} = 0.37$$

$$l_H = 60.0 \text{ ft} \quad z_H = 8.0 \text{ ft} \quad \epsilon = 1.6 \text{ deg}$$

$$\frac{y_{\bar{c}_H}}{b/2} = 0.19$$

Compute:

$$\epsilon_q = -0.02 \quad (\text{interpolated using Figures 7.4.1.3-4p, -4q, and -4r})$$

$$\left(C_{D_{q_0}} \right)_H = C_{L_{\alpha_H}} \frac{i_H}{57.3} \frac{S_H}{S_W} \left[\epsilon_q - \frac{2(l_H \cos \alpha_F + z_H \sin \alpha_F)}{\bar{c}} - \frac{2\epsilon_q \epsilon}{i_H} + \frac{4\epsilon}{i_H} \frac{(l_H \cos \alpha_F + z_H \sin \alpha_F)}{\bar{c}} \right] \quad (\text{Equation 7.4.1.3-b})$$

$$= (0.08) \frac{1}{57.3} (0.37) \left\{ -0.02 - \frac{2[(60.0)(0.99985) + (8.0)(0.01745)]}{25.0} - \frac{2(-0.02)(1.6)}{1.0} + \frac{4(1.6)[(60.0)(0.99985) + (8.0)(0.01745)]}{1.0 \cdot 25.0} \right\}$$

$$= 0.00549 \text{ per deg}$$

$$\begin{aligned} \frac{\partial C_{D_{q_H}}}{\partial \alpha_F} &= C_{L_{\alpha_H}} \frac{S_H}{S_W} \frac{1}{57.3} \left[\epsilon_q - \frac{2(l_H \cos \alpha_F + z_H \sin \alpha_F)}{\bar{c}} \right] \quad (\text{Equation 7.4.1.3-c}) \\ &= (0.08)(0.37) \frac{1}{57.3} \left[-0.02 - \frac{2[(60.0)(0.99985) + (8.0)(0.01745)]}{25.0} \right] \\ &= -0.00249 \text{ per deg}^2 \end{aligned}$$

Solution:

$$C_{D_{q_W}} = 0.00272 \text{ per deg} \quad (\text{Sample Problem, Paragraph A Section 7.1.1.3})$$

$$C_{D_q} = C_{D_{q_W}} + \left(C_{D_{q_0}} \right)_H + \left(\frac{\partial C_{D_q}}{\partial \alpha_F} \right) \alpha_F$$

(Equation 7.4.1.3-a)

$$= 0.00272 + 0.00549 - (0.00249)(1.0)$$

$$= 0.00572 \text{ per deg}$$

B. TRANSONIC

No method is presented.

C. SUPERSONIC

No method is presented.

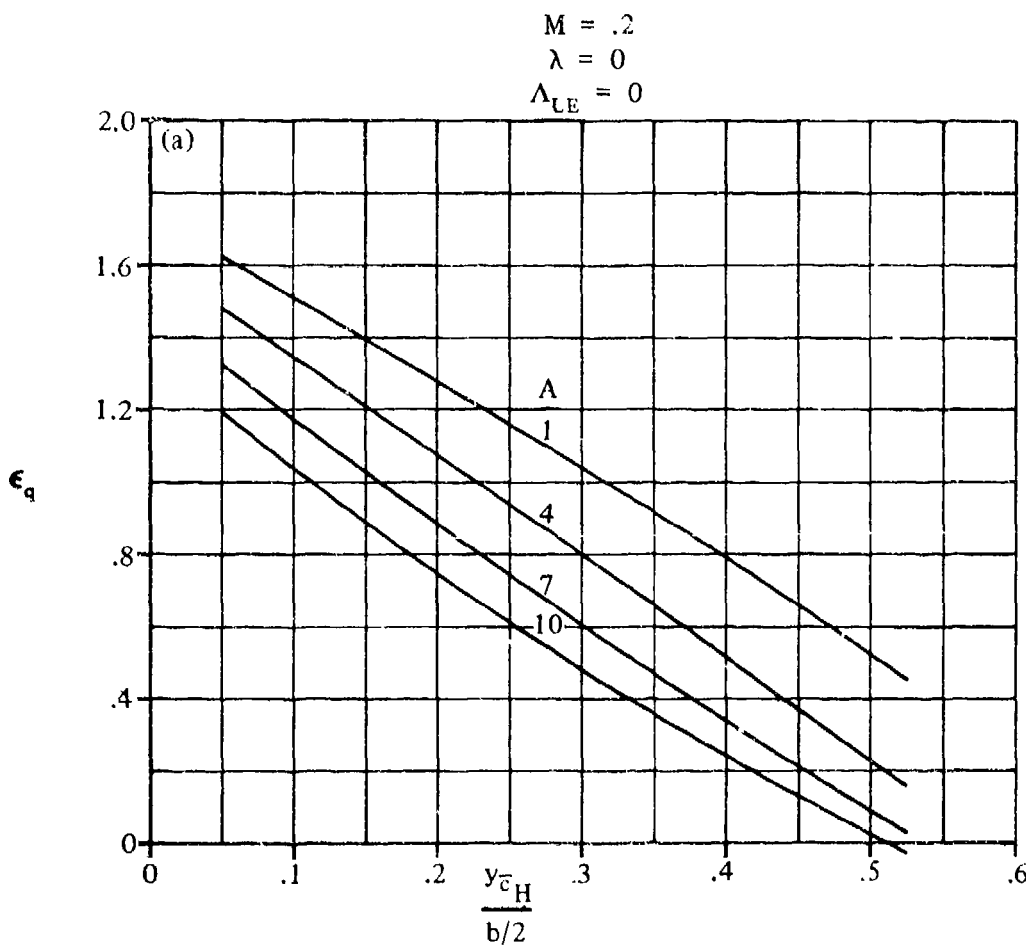


FIGURE 7.4.1.3-4 VARIATION IN DOWNWASH WITH PITCH RATE

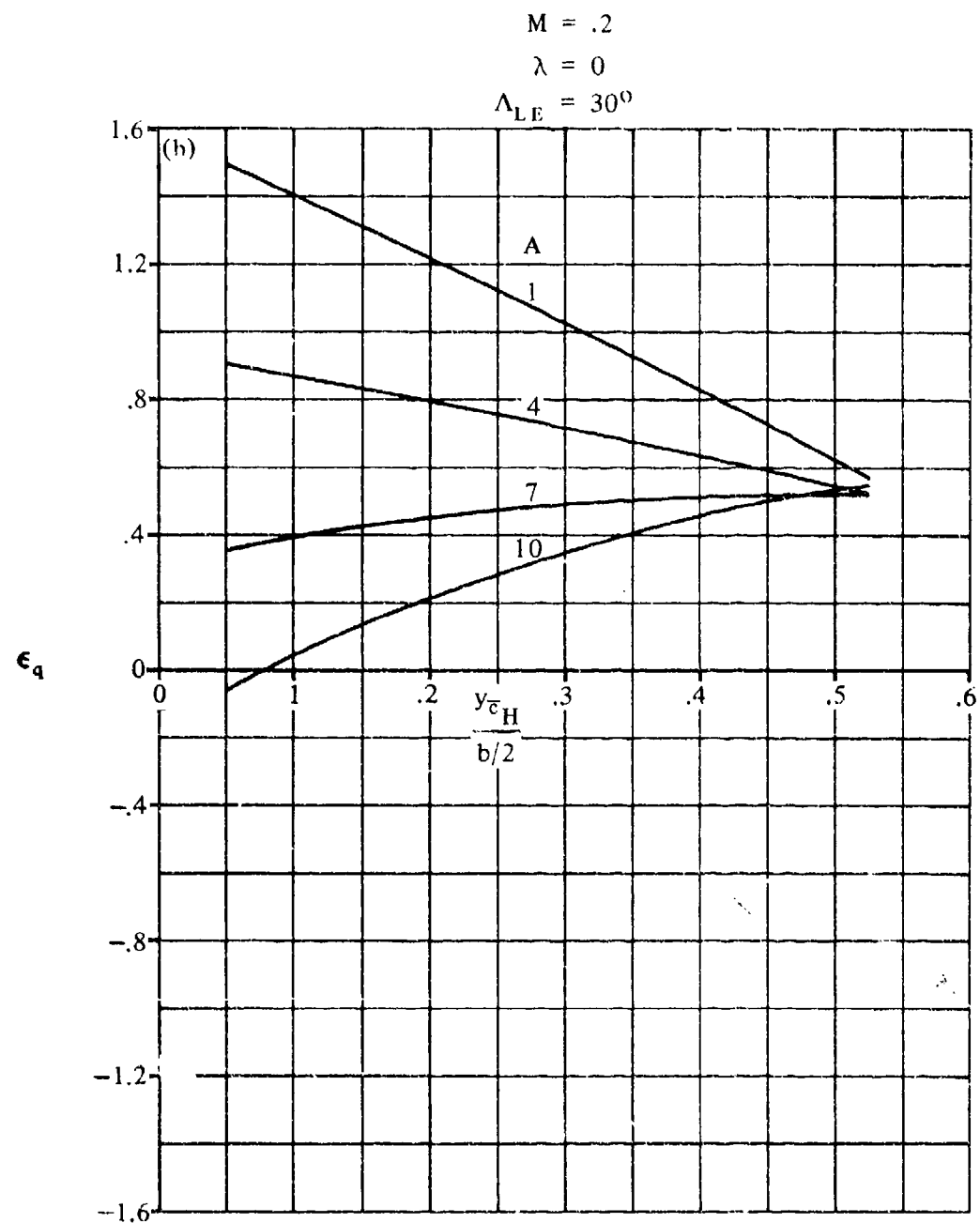


FIGURE 7.4.1.3-4 (CONTD)

7.4.1.3-5

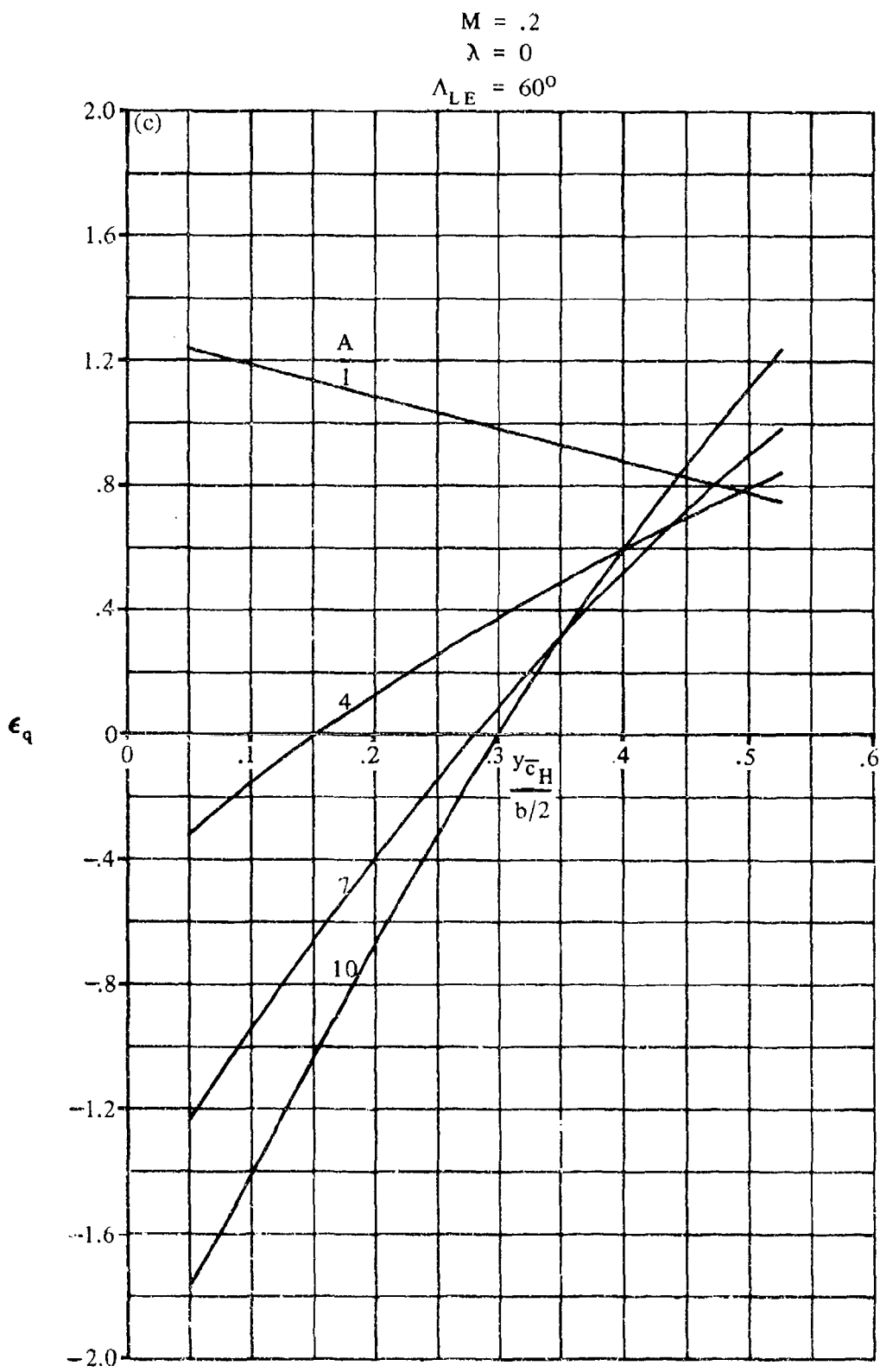


FIGURE 7.4.1.3-4 (CONTD)

7.4.1.3-6

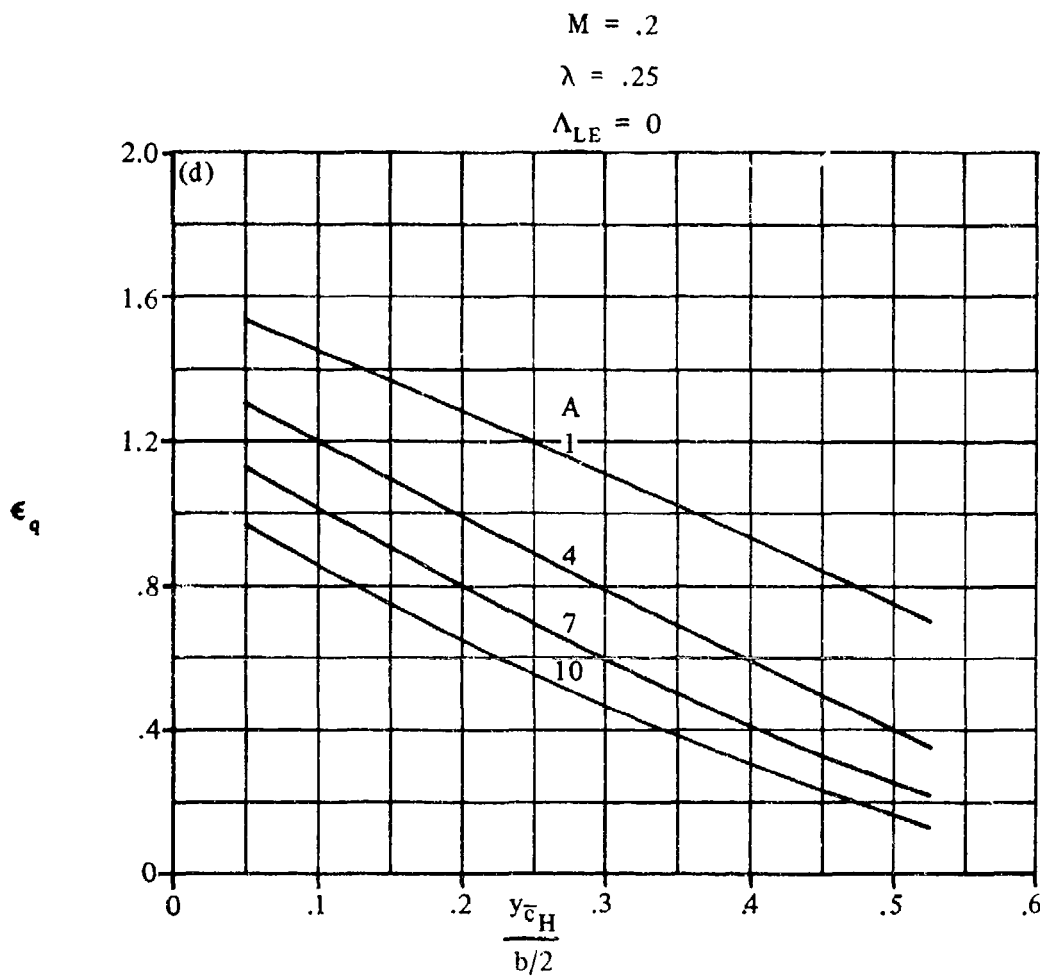


FIGURE 7.4.1.3-4 (CONTD)

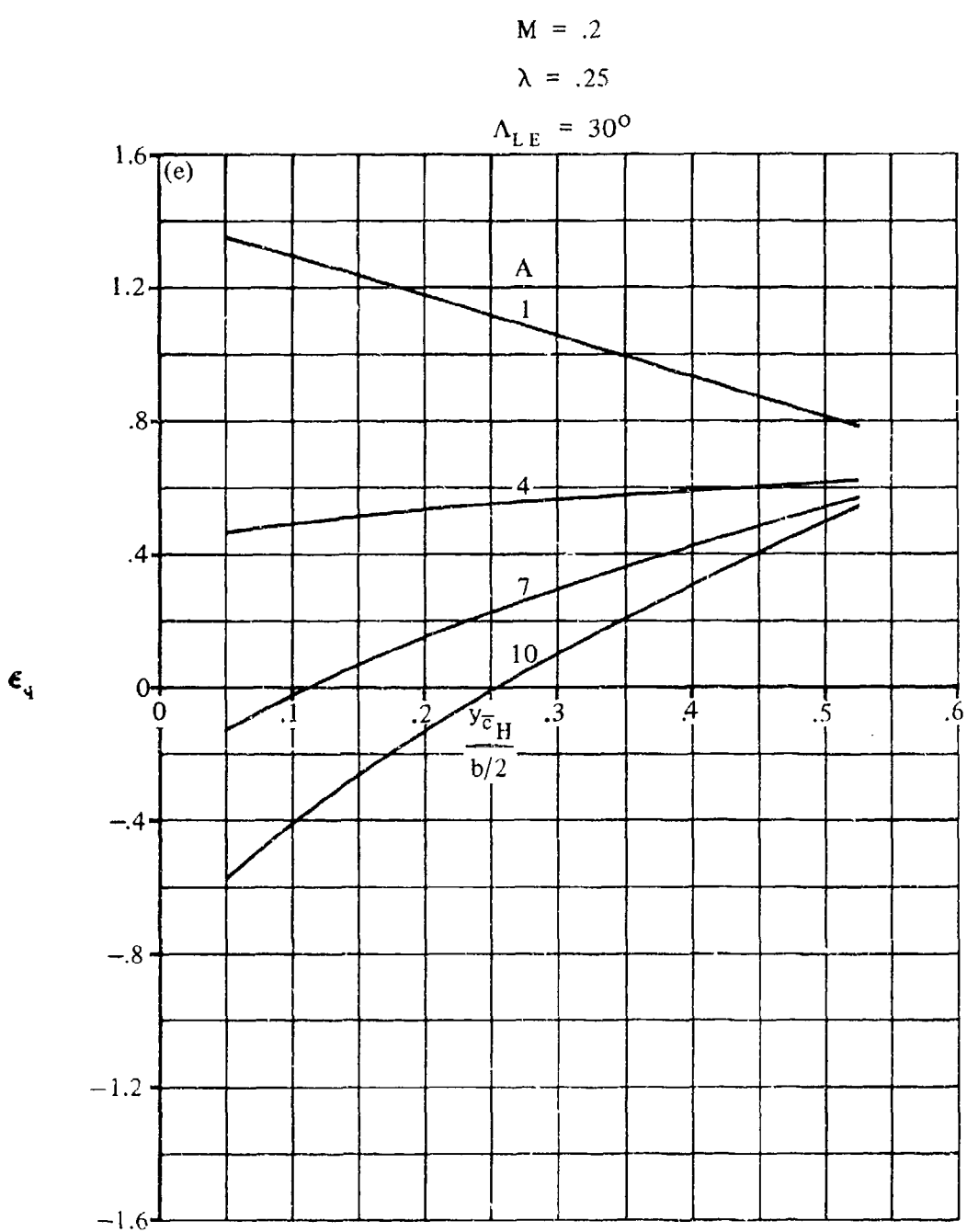


FIGURE 7.4.1.3-4 (CONTD)

7.4.1.3-8

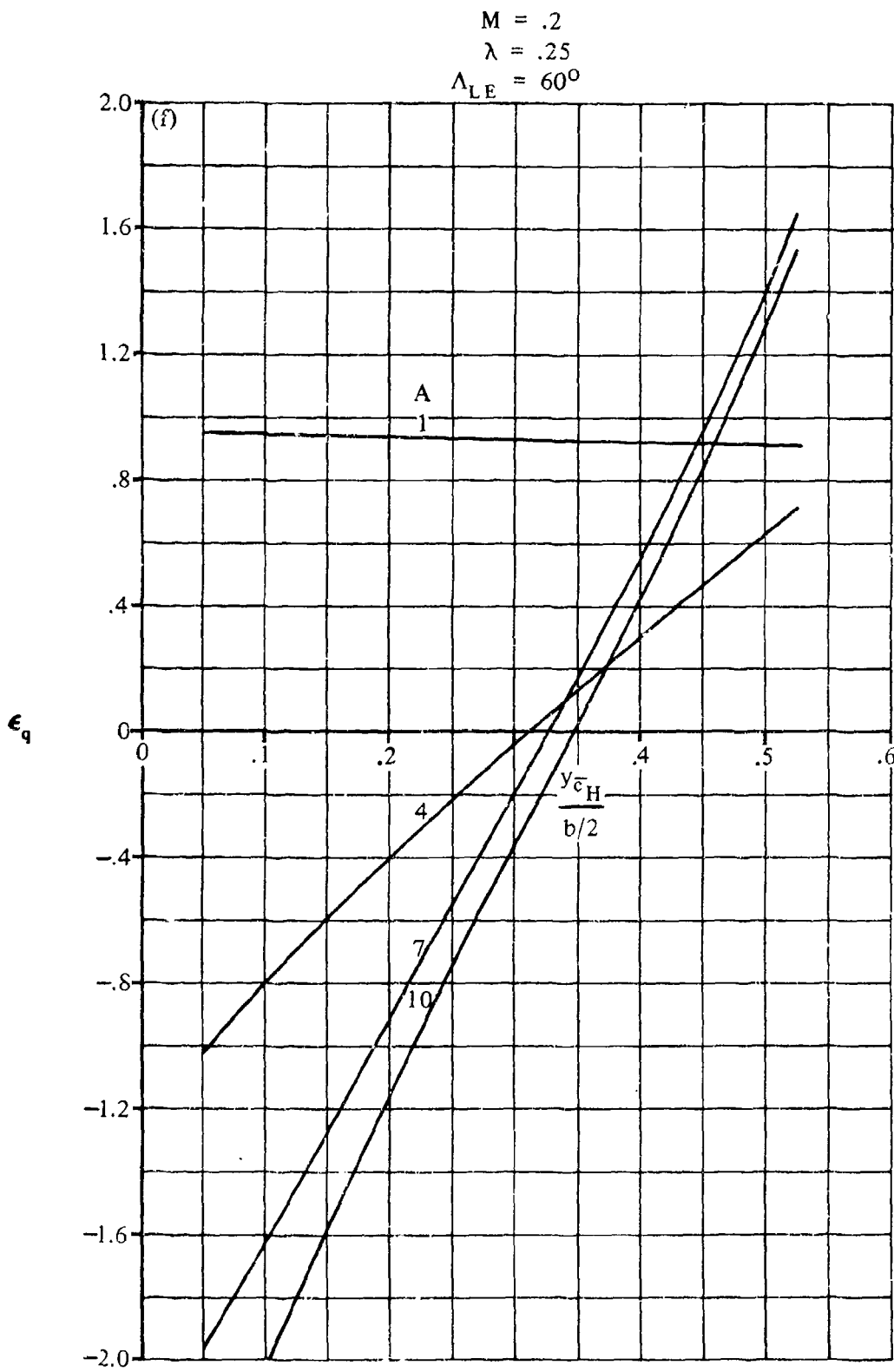


FIGURE 7.4.1.3-4 (CONTD)

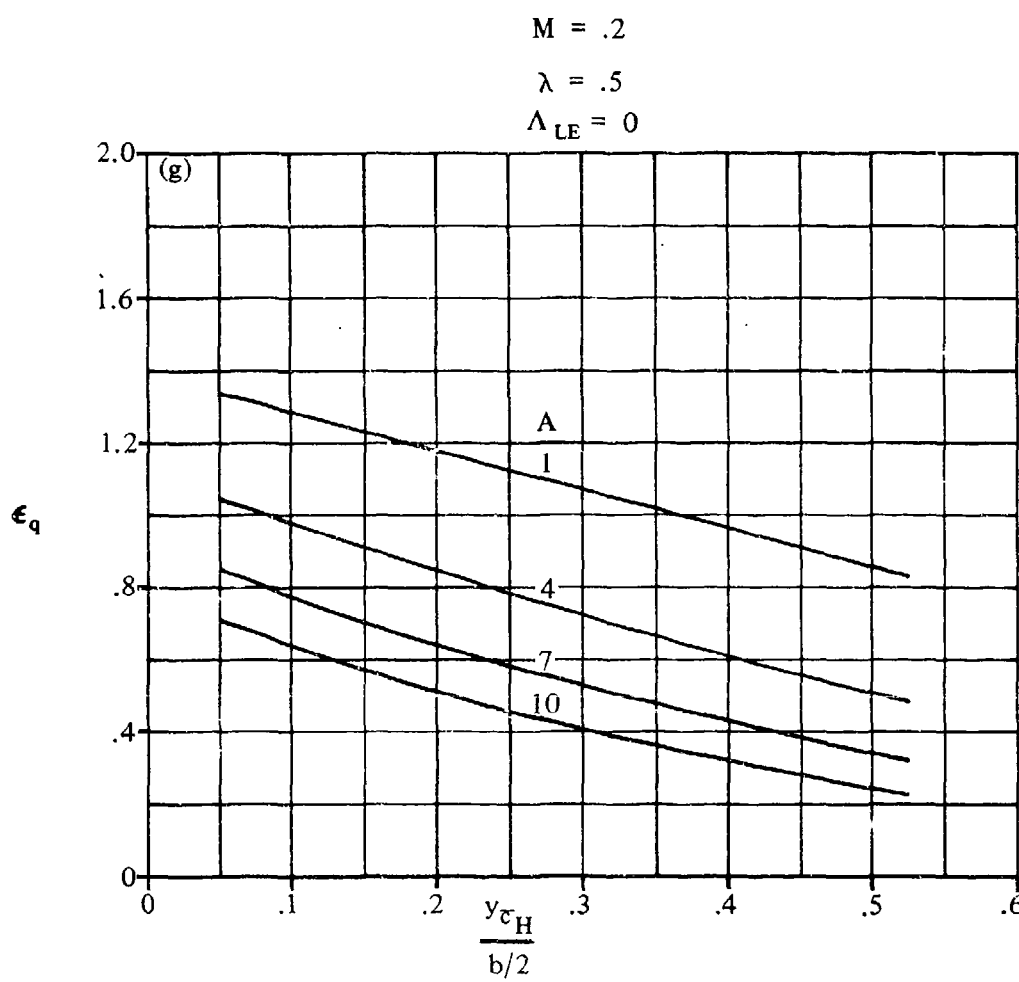


FIGURE 7.4.1.3-4 (CONTD)

7.4.1.3-10

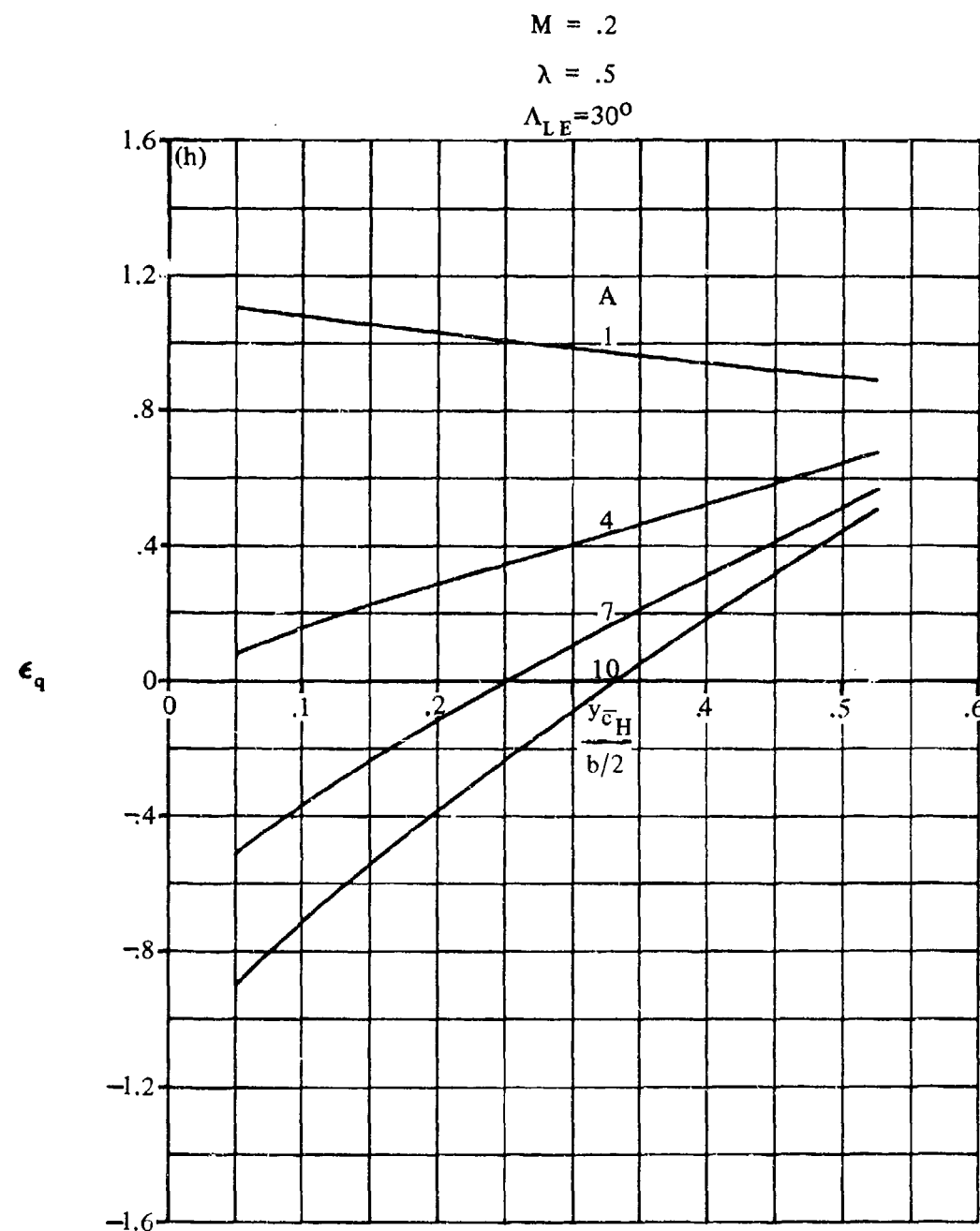


FIGURE 7.4.1.3-4 (CONTD)

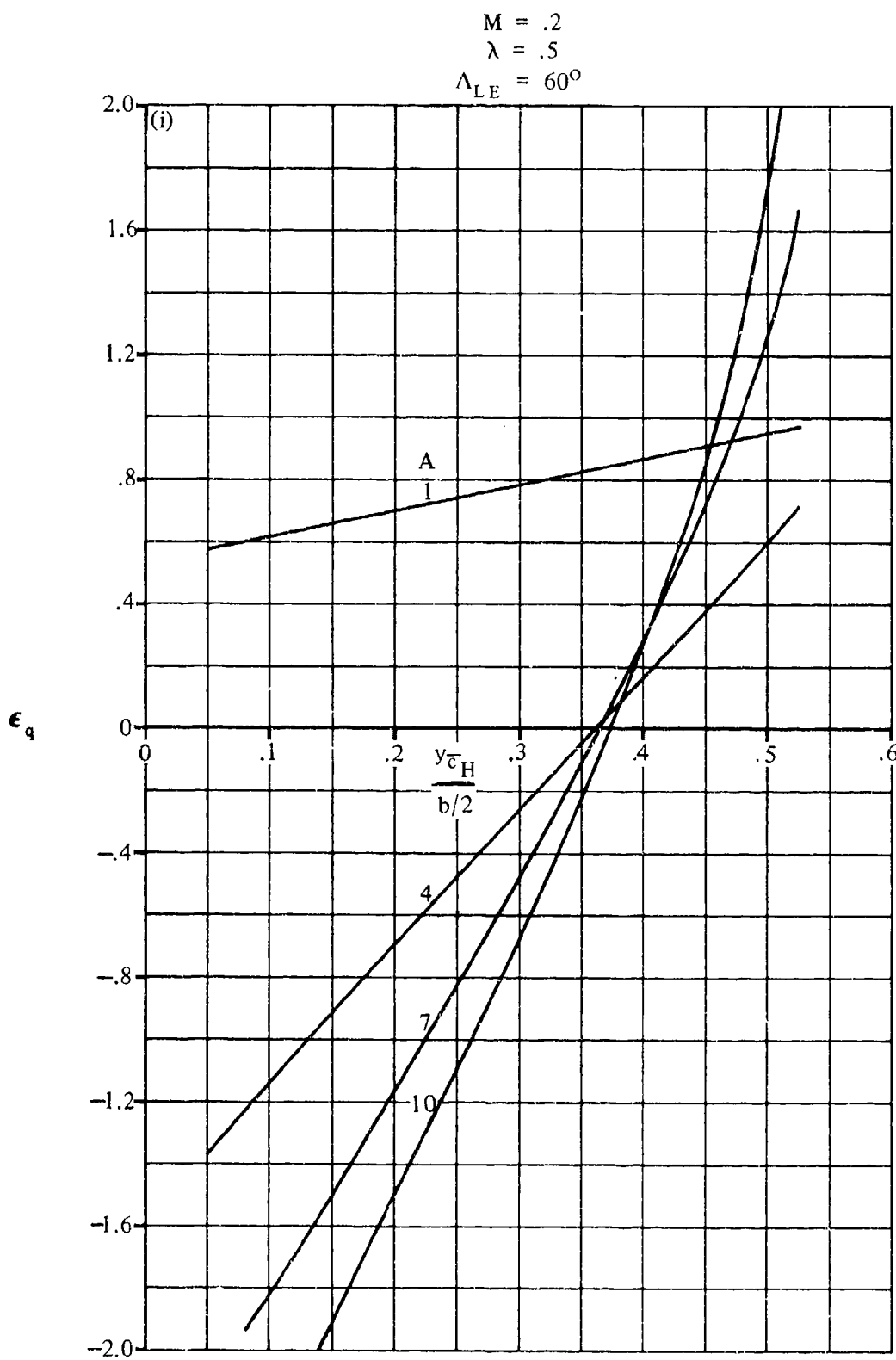


FIGURE 7.4.1.3-4 (CONTD)

7.4.1.3-12

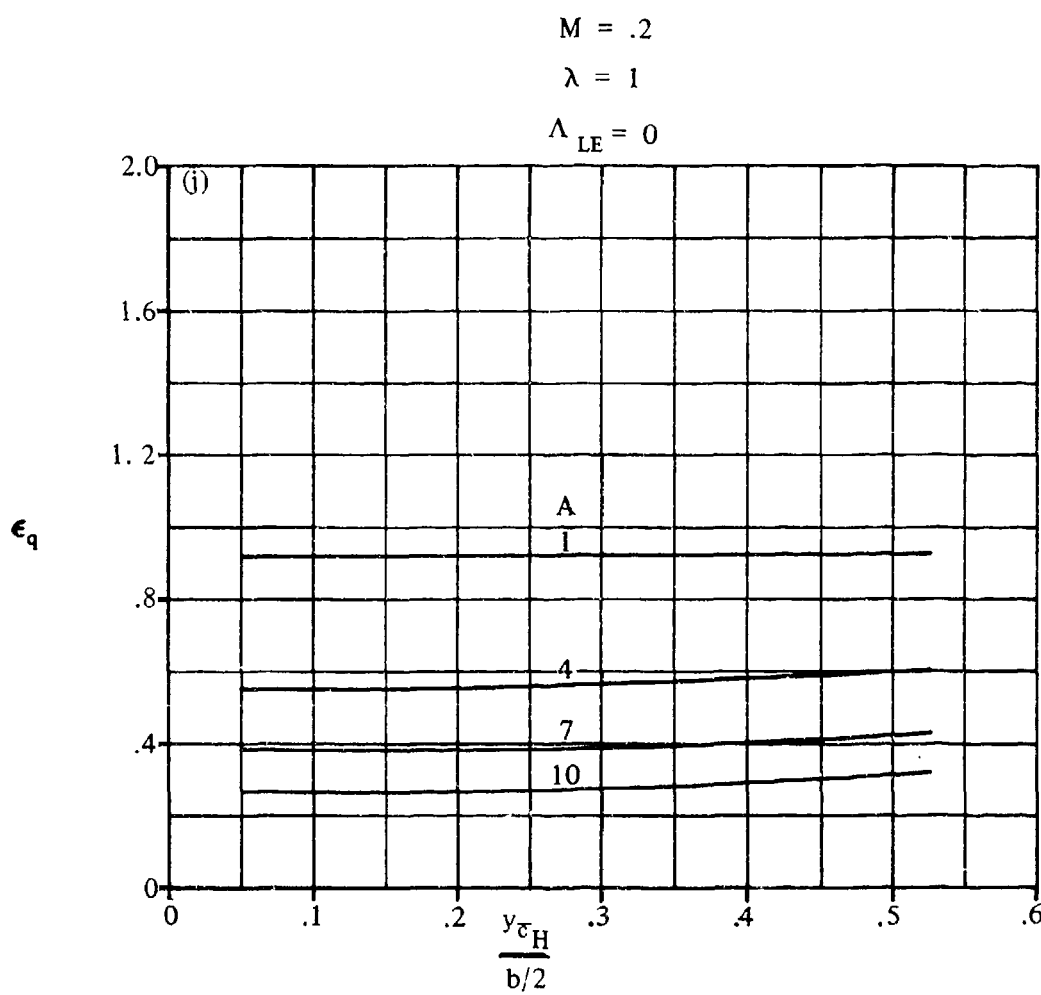


FIGURE 7.4.1.3-4 (CONTD)

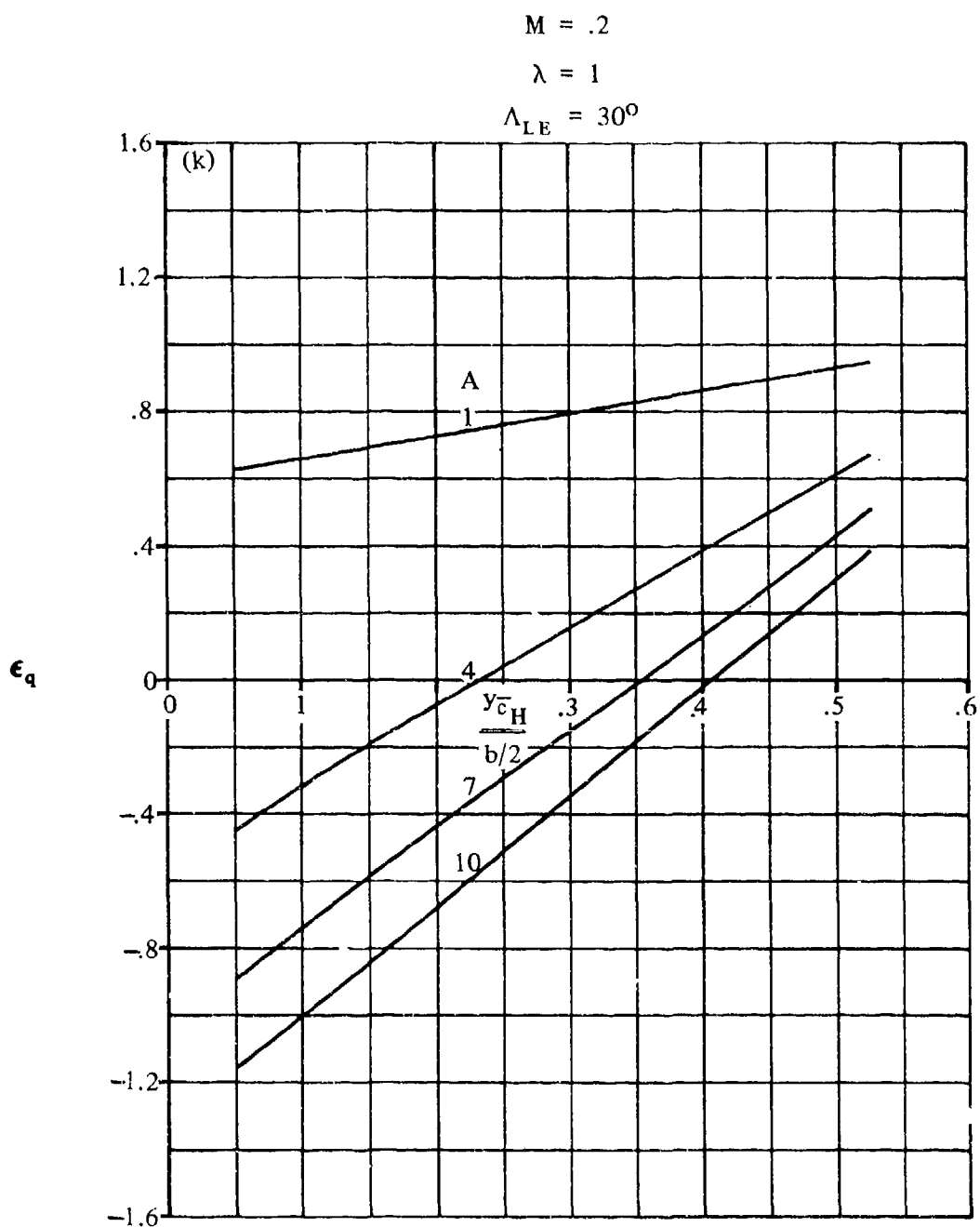


FIGURE 7.4.1.3-4 (CONTD)

7.4.1.3-14

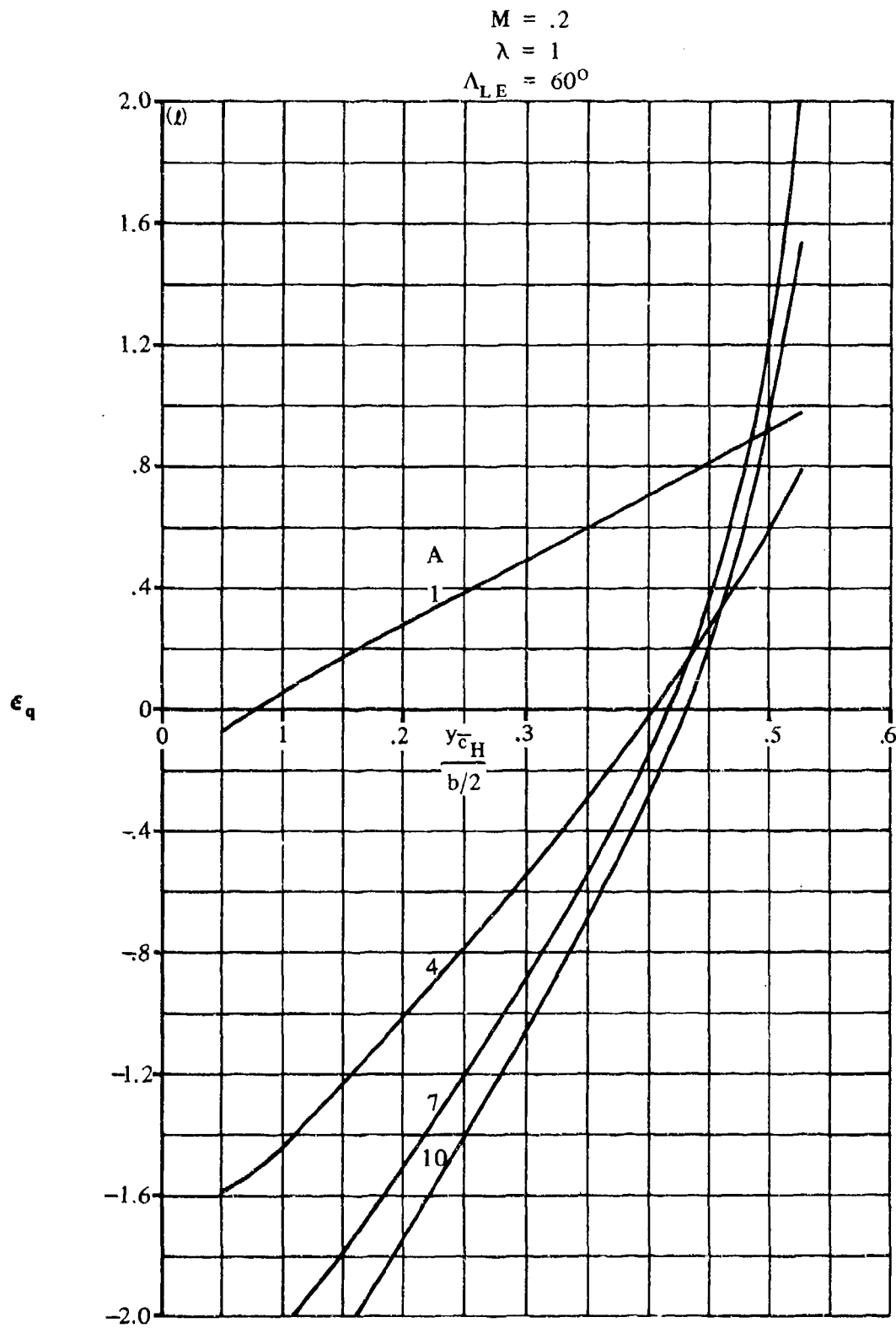


FIGURE 7.4.1.3-4 (CONTD)

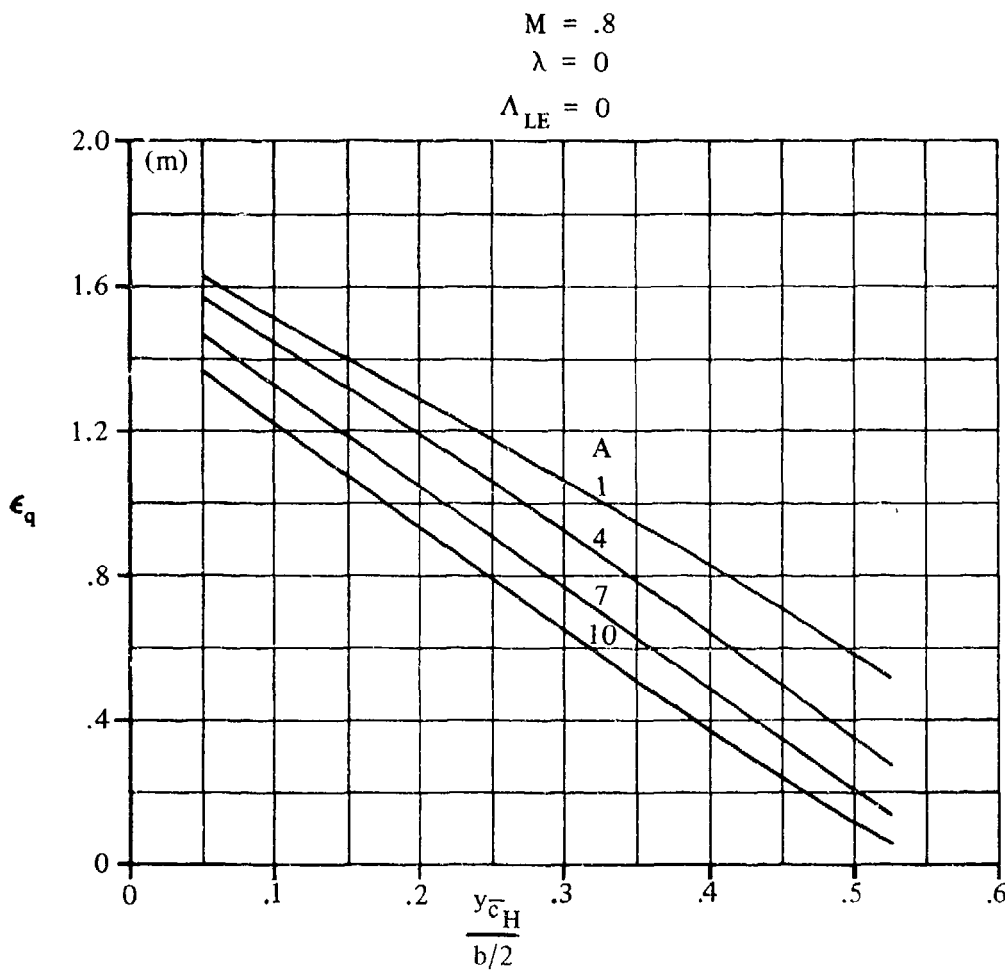


FIGURE 7.4.1.3-4 (CONTD)

7.4 1.3-16

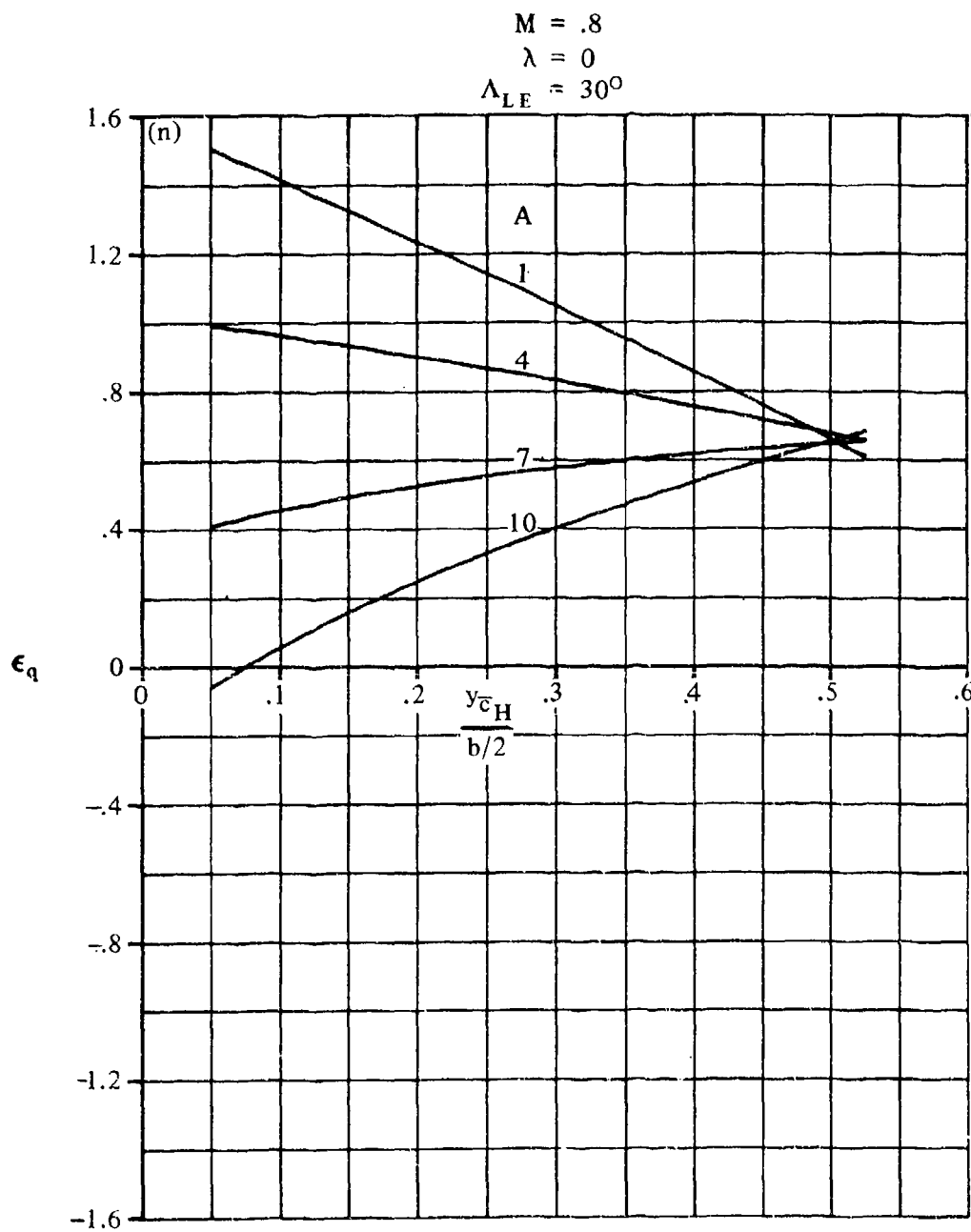


FIGURE 7.4.1.3-4 (CONTD)

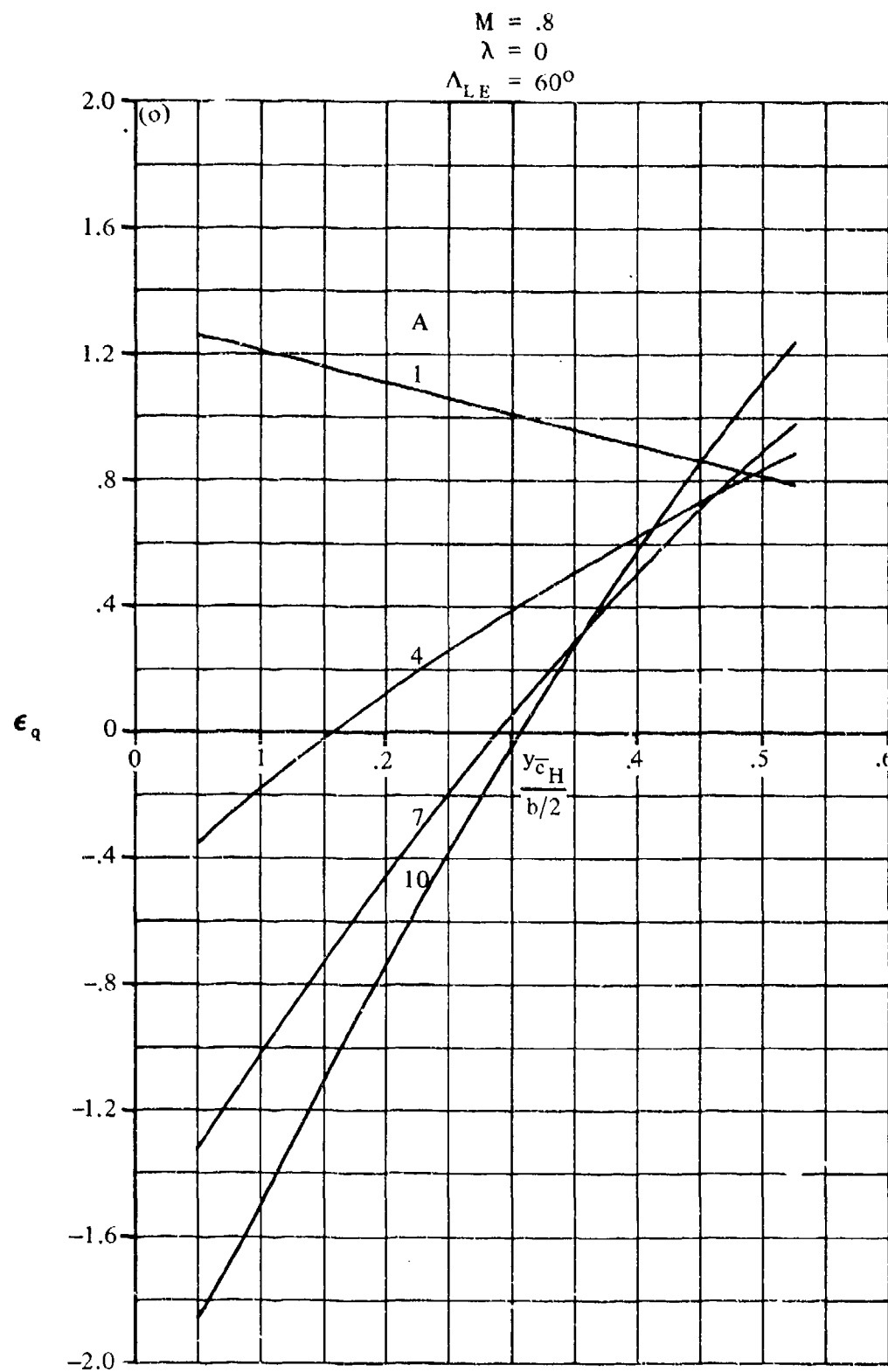


FIGURE 7.4.1.3-4 (CONTD)

7.4.1.3-18

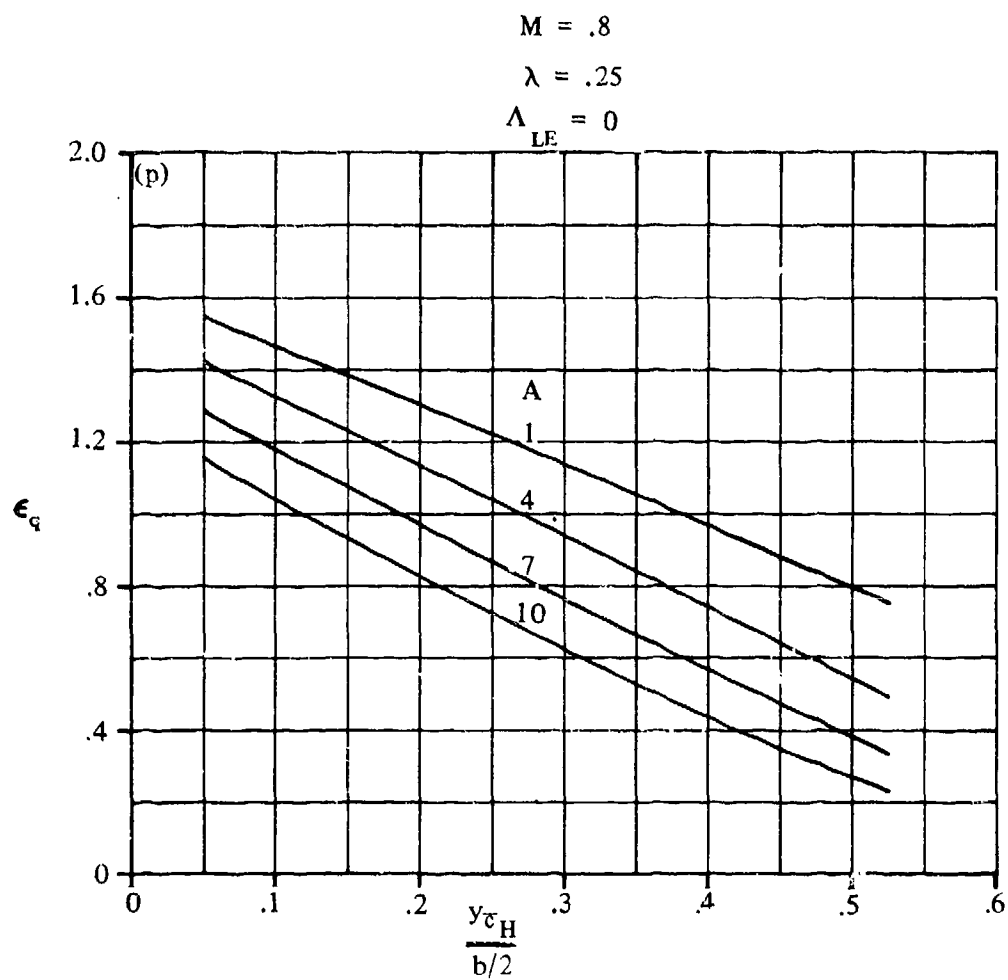


FIGURE 7.4.1.3-4 (CONTD)

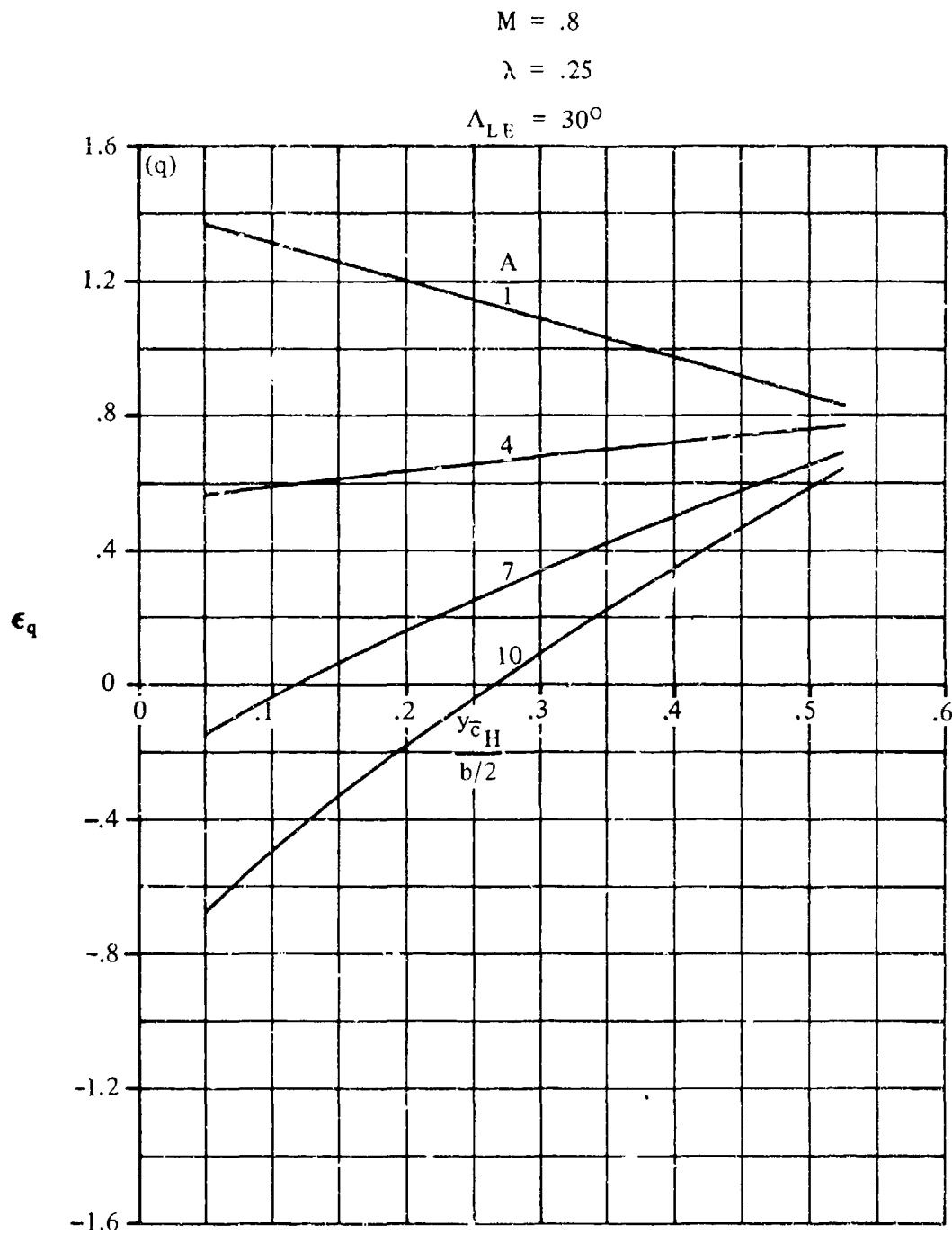


FIGURE 7.4.1.3-4 (CONTD)

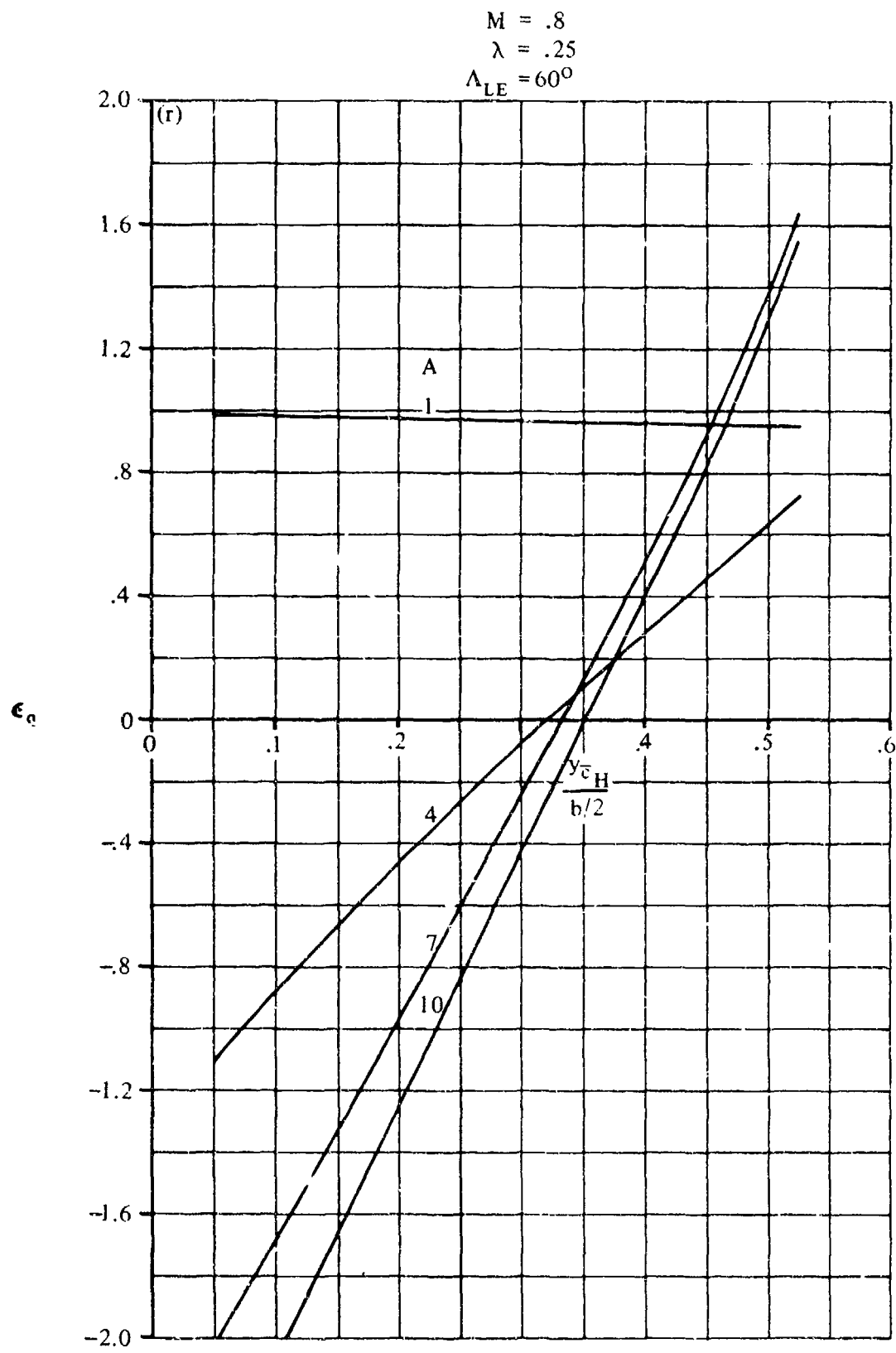


FIGURE 7.4.1.3-4 (CONTD)

$M = .8$

$\lambda = .5$

$\Lambda_{LE} = 0$

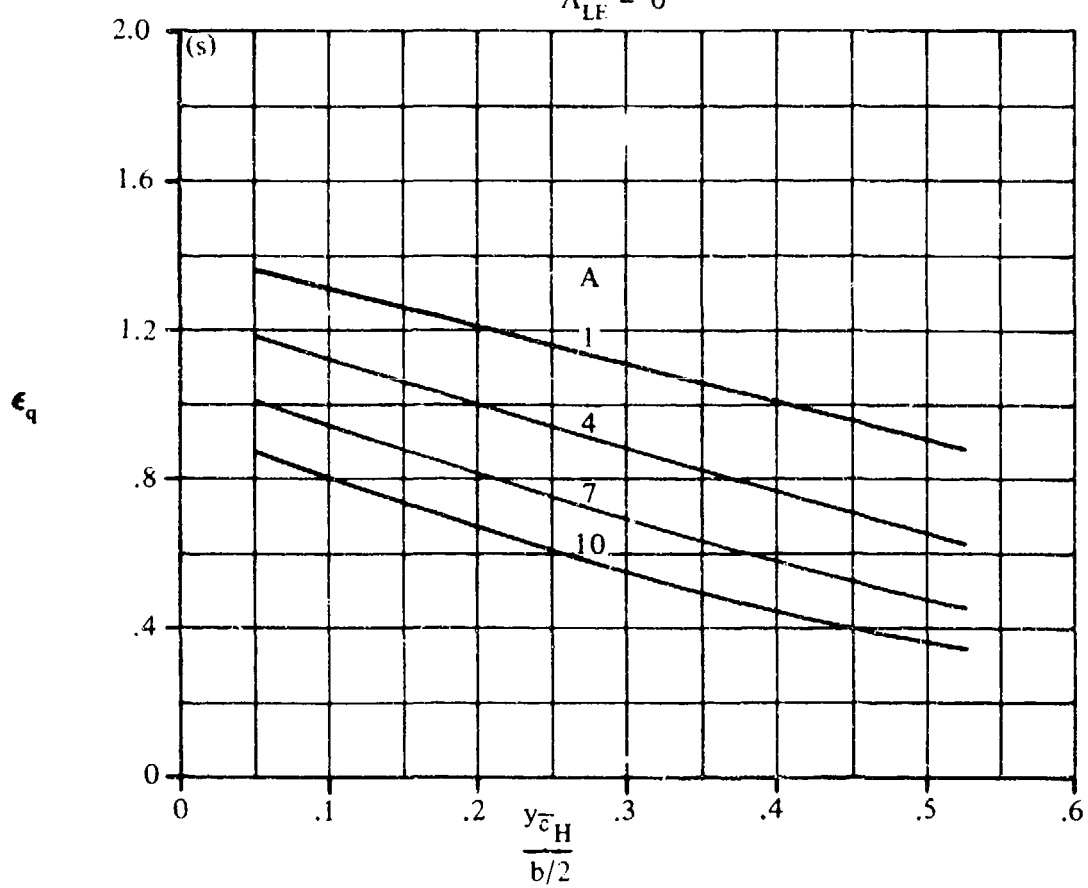


FIGURE 7.4.1.3-4 (CONTD)

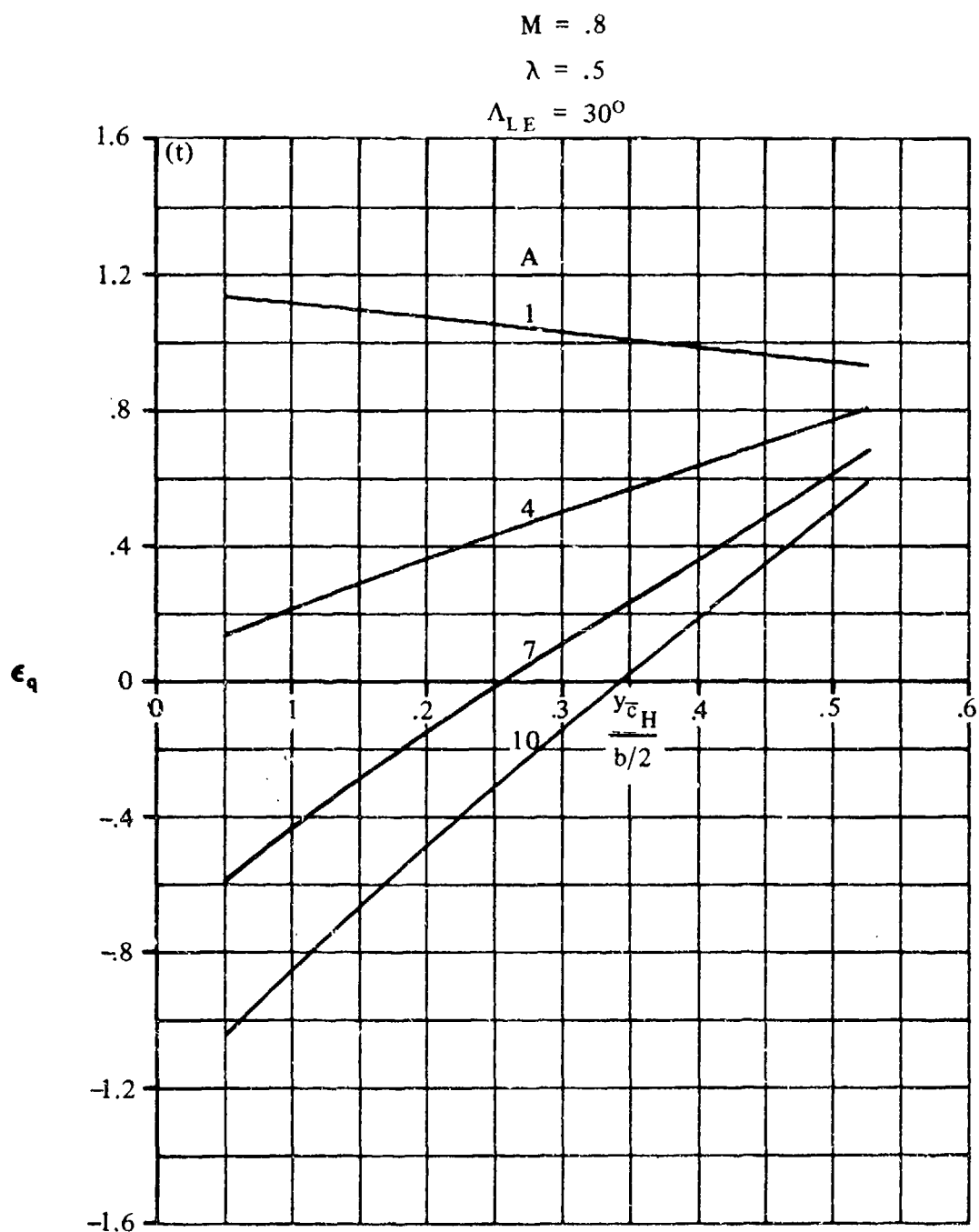


FIGURE 7.4.1.3-4 (CONTD)

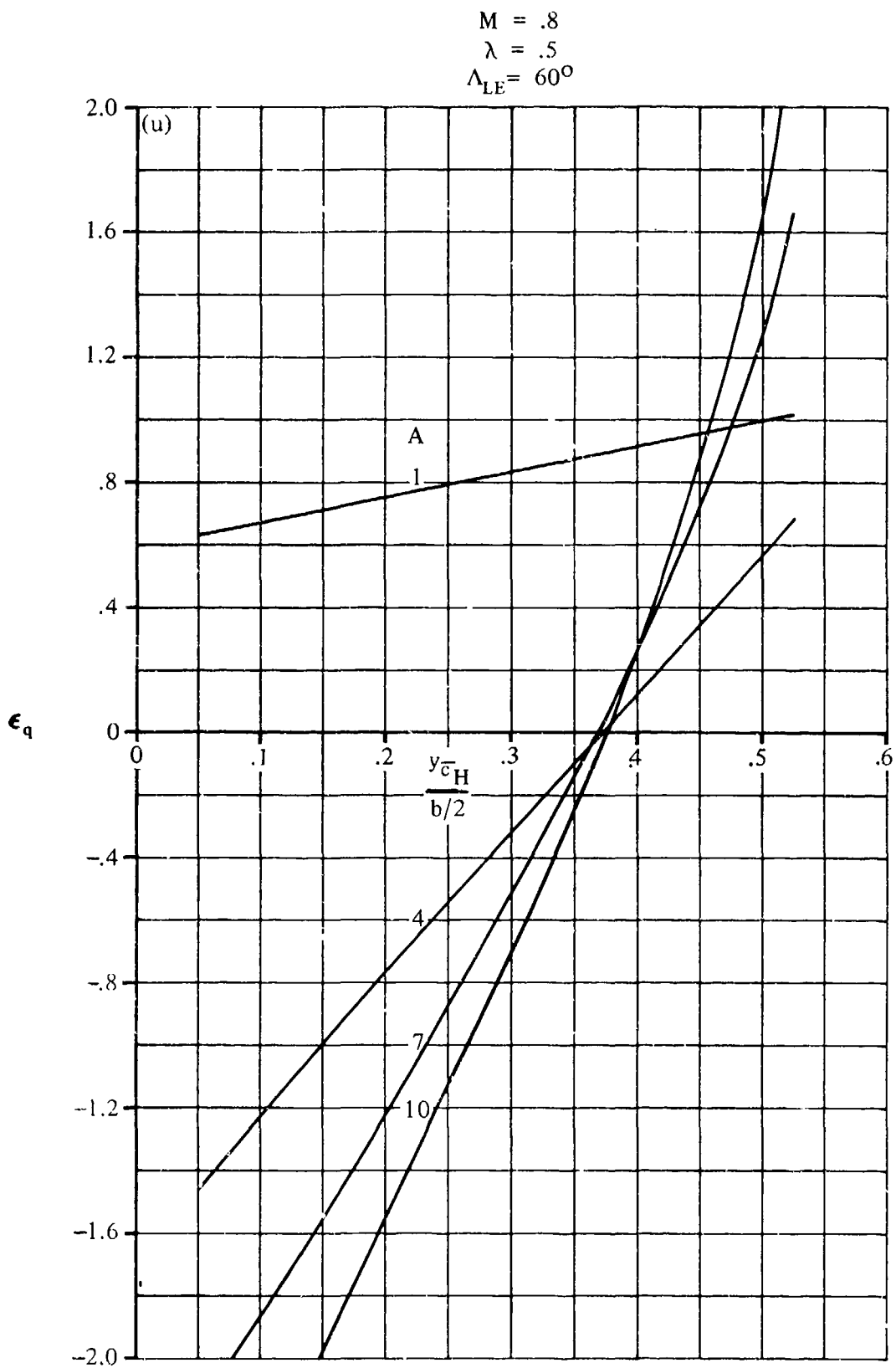


FIGURE 7.4.1.3-4 (CONTD)

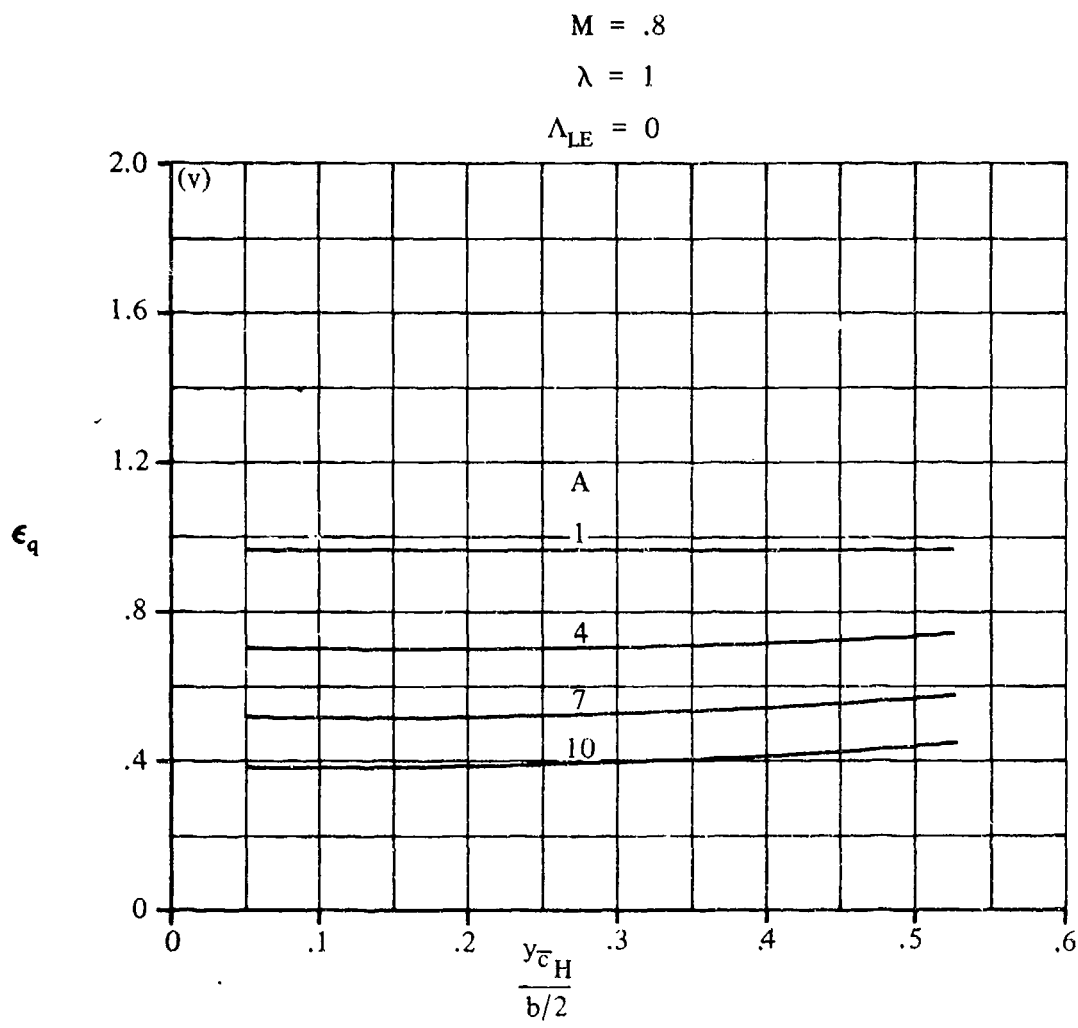


FIGURE 7.4.1.3-4 (CONTD)

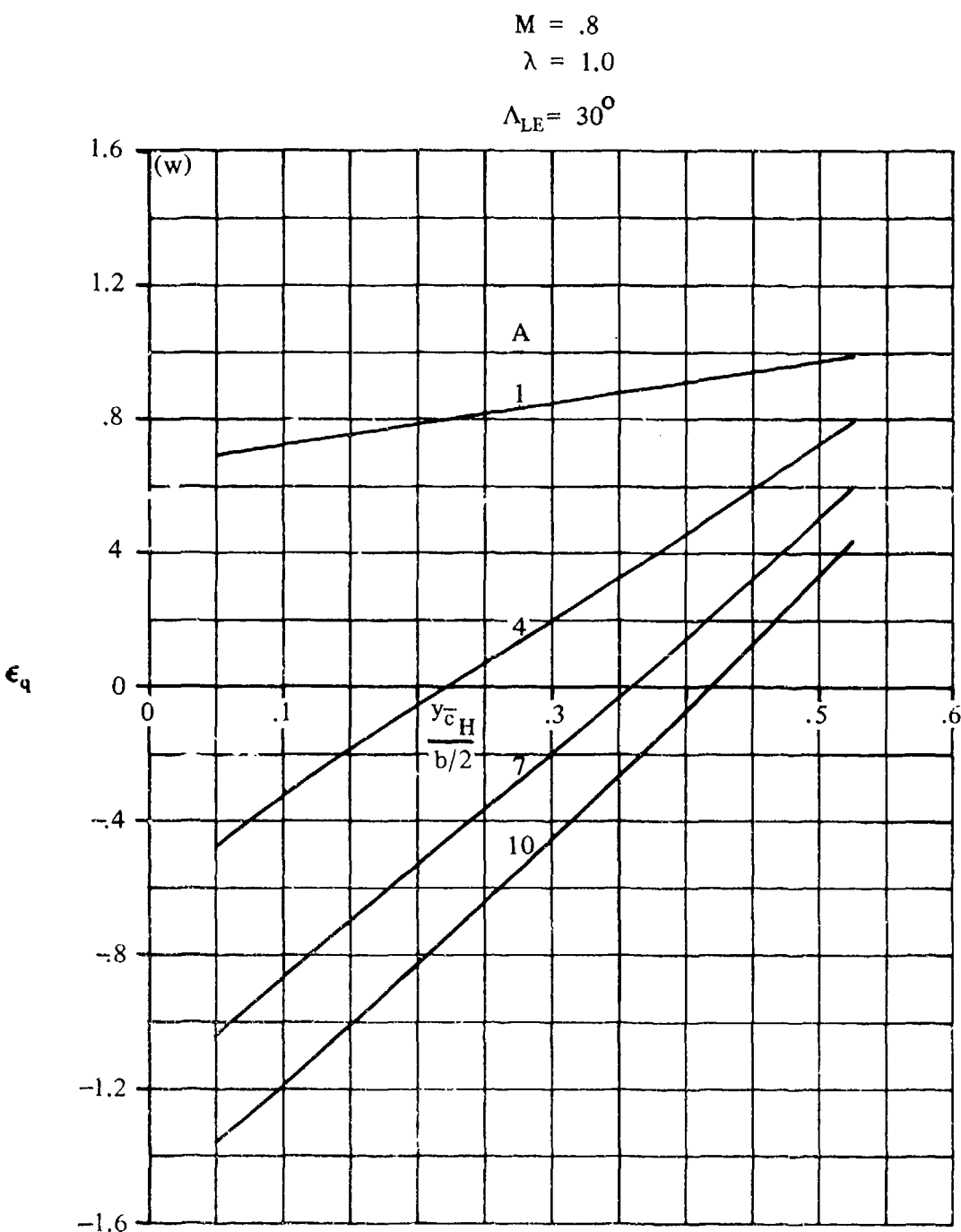


FIGURE 7.4.1.3-4 (CONTD)

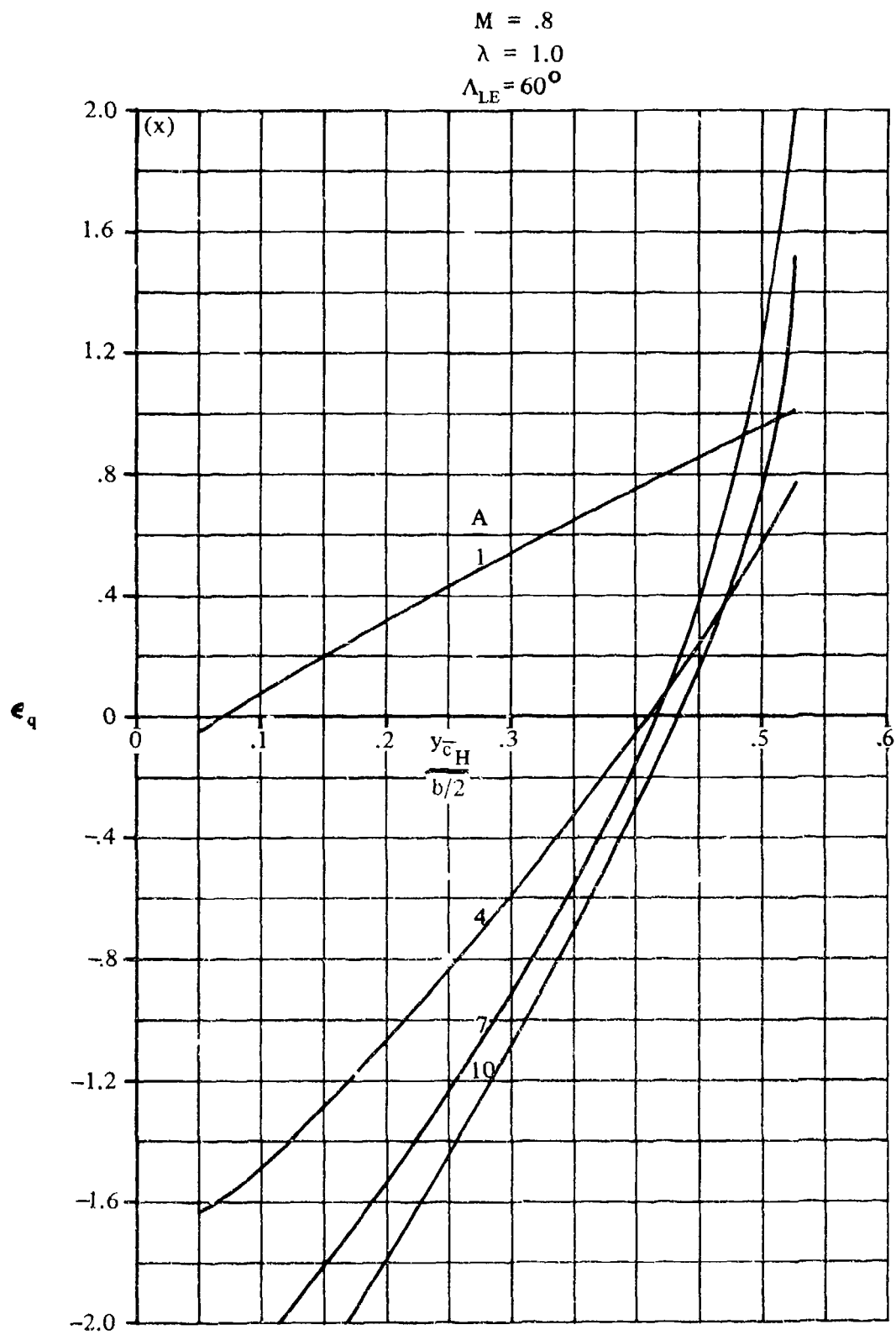


FIGURE 7.4.1.3-4 (CONTD)

7.4.2 WING-BODY-TAIL ROLLING DERIVATIVES

7.4.2.1 WING-BODY-TAIL ROLLING DERIVATIVE C_{Y_p}

This section presents methods for estimating the nondimensional rolling derivative C_{Y_p} of wing-body-tail combinations at subsonic speeds. However, at transonic and supersonic speeds no generalized methods are available for estimating the wing-body-tail rolling derivative C_{Y_p} . The derivative C_{Y_p} is the change in side-force coefficient with change in wing-tip helix angle and is expressed as

$$C_{Y_p} = \frac{\partial C_Y}{\partial \left(\frac{pb}{2V_\infty} \right)}$$

In general, the Datcom methods consist of a synthesis of material presented in Sections 7.1.2.1 and 7.3.2.1, and the vertical-tail contribution based on the methods of reference 1.

The derivative C_{Y_p} arises mainly from the wing and vertical tail. At high angles of attack the vertical-tail contribution predominates. The resultant side force on the vertical tail is generated when the aircraft has a rolling velocity p about its longitudinal body axis and the vertical tail is located either above or below the longitudinal axis. Generally C_{Y_p} is of little importance in lateral dynamics, hence is frequently neglected.

The side force at the vertical tail is created by the effective angle of attack due to the rolling velocity p and the sidewash generated from the wing and fuselage. The sidewash at the vertical tail can significantly alter the tail contribution. This effect is discussed more fully in reference 2. Studies have indicated that the effect of the sidewash varies considerably with tail size, location, and to some extent with wing planform.

A. SUBSONIC

Two methods are presented for determining the rolling derivative C_{Y_p} of the wing-body-tail combination, differing only in their treatment of wing sidewash on the vertical tail. The first method is applicable to conventionally located vertical tails, and the second method applies to tails located directly above, or above and slightly behind the wing. Both methods are based on the assumption that the vertical-tail contribution to C_{Y_p} is zero at $\alpha = 0$ and varies with angle of attack.

For an isolated-tail configuration the vertical-tail value of C_{Y_p} is approximated by

$$(C_{Y_p})_V = 2 \left(\frac{z}{b_w} \right) (\Delta C_{Y_s})_{V(WBH)}$$

For a conventionally located vertical tail the effect of wing sidewash on the vertical tail has been approximately accounted for by

$$(C_{Y_p})_V = 2 \left(\frac{z - z_p}{b_w} \right) (\Delta C_{Y_\beta})_{V(WBH)}$$

For configurations with tails located directly above or slightly behind the wing, the effect of wing sidewash has been approximated by using the average of the isolated-tail and conventional-tail values.

DATCOM METHODS

Method 1

For conventionally located vertical tails, the equation for the nondimensional rolling derivative C_{Y_p} of a wing-body configuration, based on the product of wing area and span $S_w b_w$, is given by

$$C_{Y_p} = (C_{Y_p})_{WB} + 2 \left[\frac{z - z_p}{b_w} \right] (\Delta C_{Y_\beta})_{V(WBH)} \text{ (per radian)} \quad 7.4.2.1-a$$

where

$(C_{Y_p})_{WB}$ is the wing-body contribution to C_{Y_p} obtained from test data or Section 7.3.2.1 and based on the product of wing area and span (per radian).

b_w is the wing span.

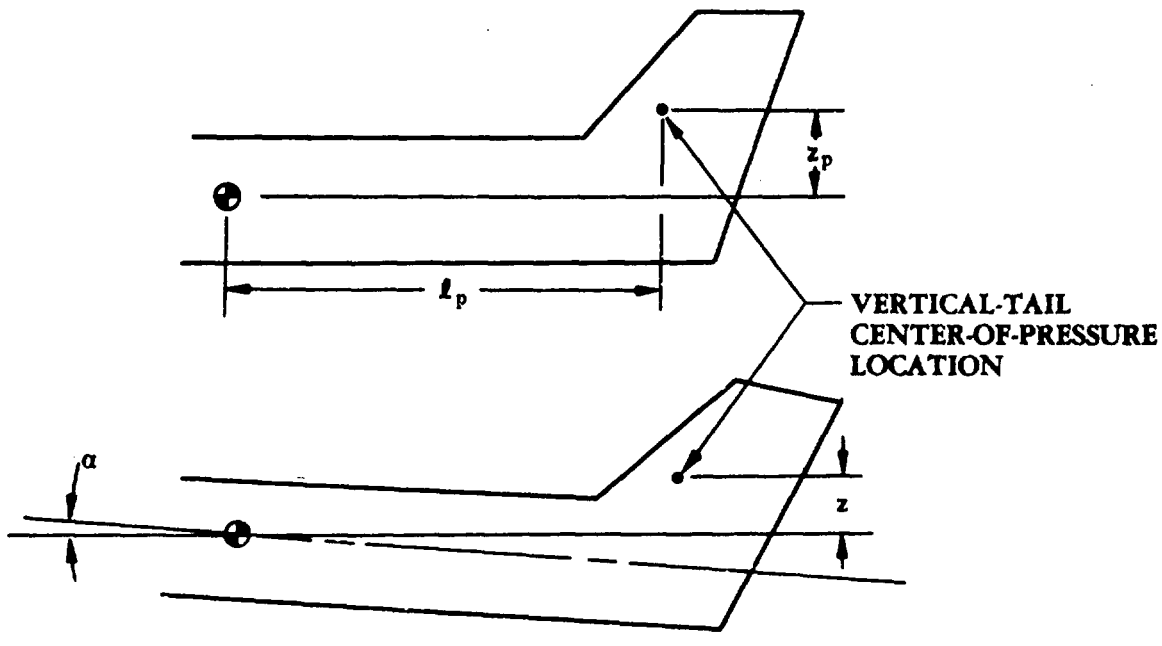
z_p is the distance from the moment reference center to the center-of-pressure location of the vertical stabilizer, measured normal to the body center line, positive for the stabilizer above the body. For Datcom purposes, the vertical-tail center-of-pressure location is assumed to be the quarter-chord point of the MAC of the total added panel.

ℓ_p is the distance from the moment reference center to the center-of-pressure location of the vertical stabilizer, measured parallel to the body center line. For Datcom purposes, the vertical-tail center-of-pressure location is assumed to be the quarter-chord point of the MAC of the total added panel.

z is the vertical distance of the vertical-tail center-of-pressure location above or below the moment-reference-center location. This value must be calculated for each angle of attack (see sketch (a)). From sketch (a), z may be expressed as

$$z = z_p \cos \alpha - \ell_p \sin \alpha \quad 7.4.2.1-b$$

$(\Delta C_{Y_\beta})_{V(WBH)}$ is the tail-body sideslip derivative from test data or Section 5.3.1.1, based on the wing area (per radian). This derivative should include the end-plate effects of the horizontal tail.



SKETCH (a)

Method 2

For vertical tails located either directly above, or above and slightly behind the wing, the equation for the nondimensional rolling derivative C_{Y_p} of a wing-body-tail configuration, based on the product of wing area and span $S_w b_w$, is given by

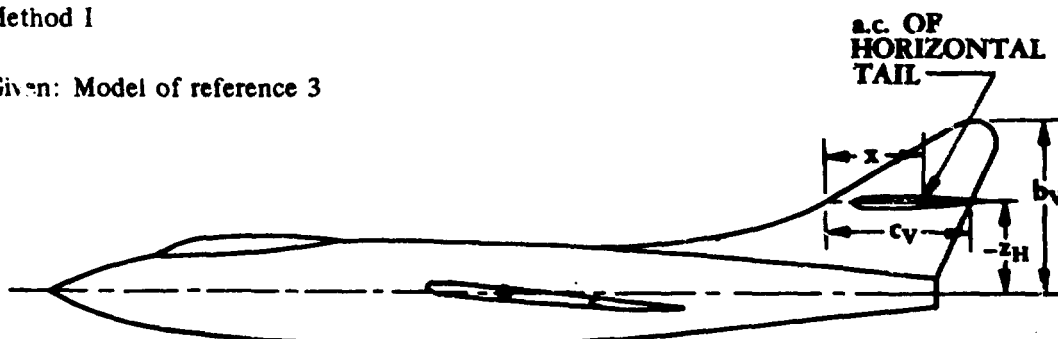
$$C_{Y_p} = (C_{Y_p})_{WB} + \left[\frac{2z - z_p}{b_w} \right] (\Delta C_{Y_\beta})_{V(WBH)} \text{ (per radian)} \quad 7.4.2.1-c$$

where the components are described in method 1 above.

Sample Problem

Method 1

Given: Model of reference 3



Wing Parameters:

$$S_w = 428.0 \text{ sq in.} \quad b_w = 38.84 \text{ in.} \quad A_w = 3.57$$

$$\lambda = 0.565 \quad \Lambda_{c/4} = 36.2^\circ \quad z_w = 0$$

Horizontal-Tail Parameters:

$$S_H = 97.10 \text{ sq in.} \quad b_H = 18.66 \text{ in.} \quad A_H = 3.59$$

$$\lambda = 0.50 \quad -z_H = 6.60 \text{ in.}$$

Vertical-Tail Parameters:

$$S_V = 140.5 \text{ sq in.} \quad b_V = 12.68 \text{ in.} \quad A_V = 1.15$$

$$\lambda = 0.176 \quad c_V = 11.0 \text{ in.} \quad \Lambda_{c/2} = 45^\circ$$

$$z_p = 5.0 \text{ in.} \quad \ell_p = 24.3 \text{ in.} \quad x = 7.25 \text{ in.}$$

Additional Parameters:

$$\alpha = 8.0^\circ \quad M = 0.17 \quad (C_{Y_p})_{WB} = 0.52 \text{ per rad (test data)}$$

$$2r_1 = 4.0 \text{ in.} \quad d = 7.5 \text{ in.}$$

Compute:

Calculate the tail-body sideslip derivative $(\Delta C_{Y_p})_{V(WBH)}$ from Section 5.3.1.1

$$\frac{b_V}{2r_1} = \frac{12.68}{4} = 3.17$$

$$\frac{A_{V(B)}}{A_V} = 1.29 \quad (\text{figure 5.3.1.1-22a})$$

$$\frac{z_H}{b_V} = \frac{-6.60}{12.68} = -0.52$$

$$\frac{x}{c_V} = \frac{7.25}{11.0} = 0.659$$

$$\frac{A_{V(HB)}}{A_{V(B)}} = 0.90 \quad (\text{figure 5.3.1.1-22b})$$

$$\frac{S_H}{S_V} = \frac{97.1}{140.5} = 0.691$$

$$K_H = 0.76 \quad (\text{figure 5.3.1.1-22 c})$$

$$\begin{aligned} A_{\text{eff}} &= \frac{A_{V(B)}}{A_V} A_V \left\{ 1 + K_H \left[\frac{A_{V(HB)}}{A_{V(B)}} - 1 \right] \right\} \quad (\text{equation 5.3.1.1-a}) \\ &= (1.29)(1.15) \{ 1 + 0.76 [0.90 - 1.0] \} \\ &= (1.29)(1.15)(0.924) \\ &= 1.37 \end{aligned}$$

$\kappa = 1$ (assumed)

$$\begin{aligned} \frac{A_{\text{eff}}}{\kappa} \left[\beta^2 + \tan^2 \Lambda_{c/2} \right]^{1/2} &= (1.37) [0.971 + 1]^{1/2} \\ &= (1.37)(1.404) \\ &= 1.923 \end{aligned}$$

$$\frac{C_{L_\alpha}}{A_{\text{eff}}} = 1.315 \quad (\text{figure 4.1.3.2-49})$$

$$\begin{aligned} C_{L_\alpha} &= (1.315)(1.37) \\ &= 1.80 \text{ per rad (based on } S_V) \end{aligned}$$

$$\begin{aligned} \left(1 + \frac{\partial \sigma}{\partial \beta} \right) \frac{q_V}{q_\infty} &= 0.724 + 3.06 \frac{S_V/S_W}{1 + \cos \Lambda_{c/4}} + \frac{0.4 z_W}{d} + 0.009A \quad (\text{equation 5.4.1-a}) \\ &= 0.724 + 3.06 \frac{(140.5)/(428.0)}{1.807} + \frac{(0.4) 0}{7.5} + (0.009)(3.57) \\ &= 0.724 + 0.556 + 0.0321 \\ &= 1.312 \end{aligned}$$

$k = 0.94$ (figure 5.3.1.1-22d)

$$\begin{aligned} (\Delta C_{Y_\beta})_{V(WBH)} &= -k (C_{L_\alpha})_V \left(1 + \frac{\partial \sigma}{\partial \beta} \right) \frac{q_V}{q_\infty} \frac{S_V}{S_W} \quad (\text{equation 5.3.1.1-b}) \\ &= -(0.94) (1.80) (1.312) \frac{140.5}{428.0} \\ &= -0.729 \text{ per rad (based on } S_W) \end{aligned}$$

Calculate the vertical distance z of the vertical-tail center-of-pressure location above or below the moment-reference-center location

$$\begin{aligned} z &= z_p \cos \alpha - l_p \sin \alpha \quad (\text{equation 7.4.2.1-b}) \\ &= (5.0) (0.9903) - (24.3) (0.1392) \\ &= 4.95 - 3.38 \\ &= 1.57 \text{ in.} \end{aligned}$$

Calculate the rolling derivative C_{Y_p} for the wing-body-tail configuration

$$\begin{aligned} C_{Y_p} &= (C_{Y_p})_{WB} + 2 \left[\frac{z - z_p}{b_W} \right] (\Delta C_{Y_\beta})_{V(WBH)} \quad (\text{equation 7.4.2.1-a}) \\ &= 0.52 + 2 \left[\frac{1.57 - 5.00}{38.84} \right] (-0.729) \\ &= 0.52 + (2)(-0.0883)(-0.729) \\ &\approx 0.52 + 0.129 \\ &= 0.649 \text{ per rad (based on } S_W b_W) \end{aligned}$$

This compares with a test value of 0.62 per radian from reference 3.

B. TRANSONIC

No generalized method is available in the literature for estimating transonic values of the rolling derivative C_{Y_p} . Furthermore, only limited experimental data are available for this derivative at transonic speeds (see table 7-A).

C. SUPERSONIC

No generalized method is available in the literature for estimating supersonic values of the rolling derivative C_{Y_p} . Furthermore, there is a scarcity of experimental data for this derivative at supersonic speeds.

For the purposes of the Datcom the fuselage effect is considered to be negligible for wing-body configurations with body diameters less than about 30 percent of the wing span. Therefore, for configurations with $d/b \leq 0.3$, the wing-body rolling derivative C_{Y_p} is estimated by the wing-alone method of paragraph C of Section 7.1.2.1.

Methods are presented in reference 4 for evaluating the vertical-tail contribution to C_{Y_p} . The stability derivatives presented therein are derived by using supersonic linearized theory for families of thin, isolated vertical tails performing steady rolling motions. Vertical-tail families (half-delta and rectangular planforms) are considered over a broad Mach number range. Also considered are vertical tails with arbitrary sweepback and taper ratio at Mach numbers for which both the leading edge and trailing edge of the tail are supersonic, and triangular vertical tails with a subsonic leading edge and a supersonic trailing edge.

REFERENCES

1. Campbell, J. P., and McKinney, M. O.: Summary of Methods for Calculating Dynamic Lateral Stability and Response and for Estimating Lateral Stability Derivatives. NACA TR 1098, 1952. (U)
2. Michael, W. H. Jr.: Analysis of the Effects of Wing Interference on the Tail Contributions to the Rolling Derivatives. NACA TR 1096, 1952. (U)
3. Queijo, M. J., and Wells, E. G.: Wind-Tunnel Investigation of the Low-Speed Static and Rotary Stability Derivatives of a 0.13-Scale Model of the Douglas D-558-II Airplane in the Landing Configuration. NACA RM L52G07, 1952. (U)
4. Margolis, K., and Bobbitt, P. J.: Theoretical Calculations of the Pressures, Forces, and Moments at Supersonic Speeds due to Various Lateral Motions Acting on Thin Isolated Vertical Tails. NACA TR 1268, 1956. (U)

7.4.2.2 WING-BODY-TAIL ROLLING DERIVATIVE C_{l_p}

This section presents methods for estimating the nondimensional rolling derivative C_{l_p} of wing-body-tail combinations at subsonic speeds. However, at transonic and supersonic speeds no generalized methods are available for estimating the wing-body-tail rolling derivative C_{l_p} . The derivative C_{l_p} is the change in rolling-moment coefficient with change in wing-tip helix angle and is commonly referred to as the roll-damping derivative. It is expressed as

$$C_{l_p} = \frac{\partial C_l}{\partial \left(\frac{pb}{2V_\infty} \right)}$$

In general, the Datcom methods consist of a synthesis of material presented in Sections 7.1.2.2 and 7.3.2.2, and the vertical-tail contribution based on the methods of reference 1.

The derivative C_{l_p} is important in lateral dynamics, since it determines the damping-in-roll characteristics of the vehicle. The derivative is composed of contributions, negative in sign, from the wing, the horizontal tail, and the vertical tail, with the main contribution coming from the wing. The contribution from the vertical tail is usually negligible at low and moderate angles of attack. However, the vertical-tail contribution can become significant at high angles of attack, when the effective moment arm of the tail (z/b_w) becomes a large negative value.

The rolling wing produces a sidewash at the vertical tail, which can significantly alter the vertical-tail contribution. This effect is discussed more fully in reference 2. Studies have indicated that the effect of the sidewash varies considerably with tail size, tail location, and to some extent with wing planform.

Conventional horizontal-tail effects on C_{l_p} are usually small and often neglected, although unusually large horizontal tails can contribute significantly (see references 1 and 3). The horizontal-tail contribution is obtained by using the horizontal-tail geometry and the method of Section 7.1.2.2. The value from Section 7.1.2.2 is then multiplied by a constant, which accounts for the flow rotation produced by the wing, and by the appropriate geometrical parameters to refer the result to the proper reference base.

A. SUBSONIC

Two methods are presented for determining the rolling derivative C_{l_p} of the wing-body-tail combination, differing only in their treatment of wing sidewash on the vertical tail. The first method is applicable to conventionally located vertical tails, and the second method applies to tails located directly above, or above and slightly behind the wing. Both methods are based on the assumption that the vertical-tail contribution to C_{l_p} is zero at $\alpha = 0$ and varies with angle of attack.

For an isolated-tail configuration the vertical-tail value of C_{l_p} is approximated by

$$(C_{l_p})_v = 2 \left(\frac{z}{b_w} \right)^2 (\Delta C_{Y_\beta})_{V(WBH)}$$

For a conventionally located vertical tail the effect of wing sidewash on the vertical tail has been approximately accounted for by

$$(C_{l_p})_v = 2 \frac{z(z - z_p)}{b_w^2} (\Delta C_{Y_\beta})_{V(WBH)}$$

For configurations with tails located directly above or slightly behind the wing, the effect of wing sidewash has been approximated by using the average of the isolated-tail and conventional-tail values.

DATCOM METHODS

Method 1

For conventionally located vertical tails, the equation for the nondimensional rolling derivative C_{l_p} of a wing-body-tail configuration, based on the product of wing area and the square of wing span $S_w b_w^2$, is given by

$$C_{l_p} = (C_{l_p})_{WB} + 0.5 (C_{l_p})_H \left(\frac{S_H}{S_w} \right) \left(\frac{b_H}{b_w} \right)^2 + \left| 2 \left(\frac{z}{b_w} \right) \left[\frac{z - z_p}{b_w} \right] \right| (\Delta C_{Y_\beta})_{V(WBH)}$$

(per radian) 7.4.2.2-a

where

$(C_{l_p})_{WB}$ is the wing-body contribution to C_{l_p} , obtained from test data or Section 7.1.2.2 and based on the product of wing area and the square of wing span (per radian).

$(C_{l_p})_H$ is the horizontal-tail contribution obtained from test data or Section 7.1.2.2, based on the horizontal-tail geometry (per radian).

$\frac{S_H}{S_w} \left(\frac{b_H}{b_w} \right)^2$ is the ratio of the horizontal-tail area to the wing area times the square of the ratio of the horizontal-tail span to the wing span.

z is the vertical distance of the vertical-tail center-of-pressure location above or below the moment-reference-center location. This value must be calculated for each angle of attack. (See sketch (a) in Section 7.4.2.1.) From equation 7.4.2.1-b, z is expressed as

$$z = z_p \cos \alpha - l_p \sin \alpha$$

x_p

is the distance from the moment reference center to the center-of-pressure location of the vertical stabilizer, measured parallel to the body center line (see sketch (a) in Section 7.4.2.1). For Datcom purposes, the vertical-tail center-of-pressure location is assumed to be the quarter-chord point of the MAC of the total added panel.

z_p

is the distance from the moment reference center to the center of pressure of the vertical stabilizer, measured normal to the body center line, positive for the stabilizer above the body. For Datcom purposes, the vertical-tail center-of-pressure location is assumed to be the quarter-chord point of the MAC of the total added panel.

$(\Delta C_{Y_\beta})_{V(WBH)}$

is the tail-body sideslip derivative obtained from test data or Section 5.3.1.1. It includes the end-plate effects of the horizontal tail and is based on the wing area (per radian).

Method 2

For vertical tails located either directly above, or above and slightly behind the wing, the equation of the nondimensional rolling derivative C_{l_p} of a wing-body-tail configuration, based on the product of wing area and the square of wing span $S_w b_w^2$, is given by

$$C_{l_p} = (C_{l_p})_{WB} + 0.5 (C_{l_p})_H \left(\frac{S_H}{S_w} \right) \left(\frac{b_H}{b_w} \right)^2 + \left| \frac{z}{b_w} - \left[\frac{2z - z_p}{b_w} \right] \right| (\Delta C_{Y_\beta})_{V(WBH)}$$

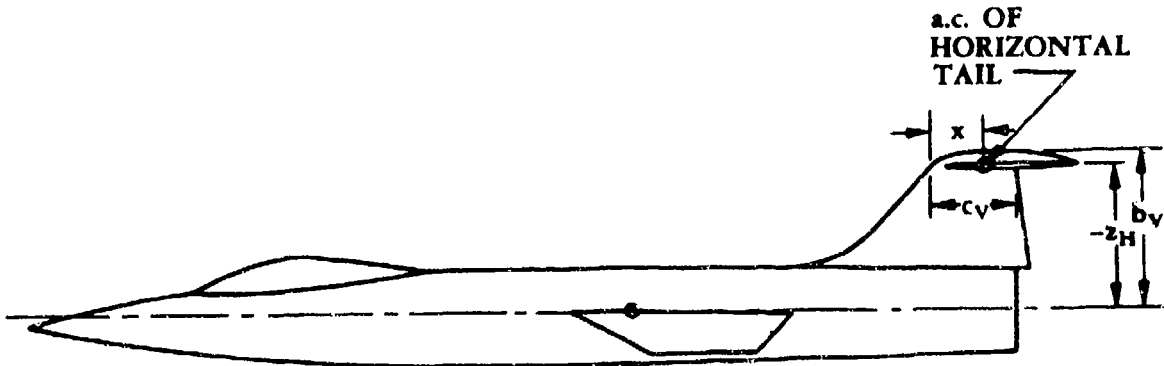
(per radian) 7.4.2.2-b

where the components are described in method 1 above.

Sample Problem

Method 1

Given: Model of reference 4



7.4.2.2-3

Wing Parameters:

$$S_W = 1.90 \text{ sq ft} \quad b_W = 2.16 \text{ ft} \quad A_W = 2.44 \quad \lambda = 0.38$$

$$\Gamma = -10^\circ \quad \bar{c} = 0.94 \text{ ft} \quad \Lambda_{c/4} = 18.0^\circ \quad z_W = 0$$

Horizontal-Tail Parameters:

$$S_H = 0.48 \text{ sq ft} \quad b_H = 1.20 \text{ ft} \quad A_H = 2.97 \quad \lambda = 0.31$$

$$\Lambda_{c/4} = 10.5^\circ \quad \Gamma = 0 \quad \frac{t}{c} = 0.05 \quad \bar{c} = 0.44 \text{ ft} \quad -z_H = 8.30 \text{ in.}$$

Vertical-Tail Parameters:

$$S_V = 0.56 \text{ sq ft} \quad b_V = 9.0 \text{ in.} \quad A_V = 0.86 \quad \lambda_V = 0.37$$

$$c_V = 0.42 \text{ ft} \quad \bar{c} = 0.87 \text{ ft} \quad \Lambda_{c/2} = 23.25^\circ \quad z_p = 0.308 \text{ ft}$$

$$l_p = 1.25 \text{ ft} \quad x = 0.25 \text{ ft}$$

Additional Parameters:

$$\alpha = 4.0^\circ \quad M = 0.25 \quad (C_{l_p})_{WB} = -0.30 \text{ per rad (test data)}$$

$$C_L = 0.3 \quad R_\ell = 1.5 \times 10^6 \quad 2r_1 = 4.88 \text{ in.}$$

Compute:

Calculate $(C_{l_p})_H$ for the horizontal tail from Section 7.1.2.2

$$(C_{l_p})_H = \left(\frac{\beta C_{l_p}}{\kappa} \right)_{C_L=0} \left(\frac{\kappa}{\beta} \right) \frac{(C_{L\alpha})_{C_L}}{(C_{L\alpha})_{C_L=0}} \frac{(C_{l_p})_R}{(C_{l_p})_{R=0}} + (\Delta C_{l_p})_{drag}$$

(equation 7.1.2.2-a)

$$\Lambda_\beta = \tan^{-1} \left(\frac{\tan \Lambda_{c/4}}{\beta} \right)$$

$$\beta = \sqrt{1 - M^2} = \sqrt{1 - (.25)^2} = 0.968$$

$$\Lambda_\beta = \tan^{-1} \left(\frac{0.1853}{0.968} \right)$$

$$= \tan^{-1} (0.1914) = 10.8^\circ$$

$\kappa = 1$ (assumed)

$$\frac{\beta A_H}{\kappa} = \frac{(0.968)(2.97)}{1.0} = 2.87$$

$$\left(\frac{\beta C_{I_p}}{\kappa} \right)_{C_L=0} = -0.245 \quad (\text{figure 7.1.2.2-20b})$$

$$\frac{(C_{L_a})_{C_L}}{(C_{L_a})_{C_L=0}} = 1.0 \text{ (assumed)}$$

$$\frac{(C_{I_p})_r}{(C_{I_p})_{r=0}} = 1 \text{ (no dihedral)}$$

$$(\Delta C_{I_p})_{\text{drag}} = \frac{(C_{I_p})_{C_{D_L}}}{C_L^2} C_L^2 - \frac{1}{8} C_{D_0} \quad (\text{equation 7.1.2.2-c})$$

$$\frac{(C_{I_p})_{C_{D_L}}}{C_L^2} = 0.015 \text{ per rad} \quad (\text{figure 7.1.2.2-24})$$

$$C_{D_0} = C_f \left[1 + L \left(\frac{t}{c} \right) + 100 \left(\frac{t}{c} \right)^4 \right] R_{L.S.} \frac{S_{\text{wet}}}{S_{\text{ref}}} \quad (\text{equation 4.1.5.1-a})$$

$$\lambda = \bar{c}_H = 0.44 \text{ ft}$$

$k = 0.05 \times 10^{-3}$ in (table 4.1.5.1-A, assume polished wood surface)

$$\frac{\lambda}{k} = \frac{(0.44)(12)}{5 \times 10^{-5}} = 1.056 \times 10^6$$

Cutoff Reynolds number, $R_\lambda = 7 \times 10^6$ (figure 4.1.5.1-27)

Test Reynolds number, $R_L = 1.5 \times 10^6$

$C_f = 0.00410$ (figure 4.1.5.1-26)

$L = 1.2$ (assume $(t/c)_{max}$ is located at $x = .50c$)

$$\left[1 + L \left(\frac{t}{c} \right) + 100 \left(\frac{t}{c} \right)^4 \right] = 1.06 \quad (\text{figure 4.1.5.1-28a})$$

$$\cos \Lambda_{(t/c)_{max}} = \cos 0^\circ = 1.0$$

$R_{L.S.} = 1.067$ (figure 4.1.5.1-28b)

$$\frac{S_{wet}}{S_{ref}} = 2.0 \text{ (assumed)} \quad S_{ref} = S_{\text{horizontal tail}}$$

$$C_{D_0} = C_f \left[1 + L \left(\frac{t}{c} \right) + 100 \left(\frac{t}{c} \right)^4 \right] R_{L.S.} \frac{S_{wet}}{S_{ref}} \quad (\text{equation 4.1.5.1-a})$$

$$= (0.00410) (1.06) (1.067) (2.0)$$

$$= 0.00927$$

$$(\Delta C_{I_p})_{\text{drag}} = \frac{(C_{I_p})_{C_D L}}{C_L^2} C_L^2 - \frac{1}{8} C_{D_0} \text{ (per radian)} \quad (\text{equation 7.1.2.2-c})$$

$$= (0.015) (0.3)^2 - \frac{0.00927}{8}$$

$$= 0.001350 - 0.001159$$

$$= 0.000191 \text{ per rad}$$

$$(C_{I_p})_H = \left(\frac{\beta C_{I_p}}{\kappa} \right)_{C_L=0} \left(\frac{\kappa}{\beta} \right) \frac{(C_{L\alpha})_{C_L}}{(C_{L\alpha})_{C_L=0}} \frac{(C_{I_p})_r}{(C_{I_p})_{r=0}} + (\Delta C_{I_p})_{\text{drag}} \text{ (per radian)}$$

(equation 7.1.2.2-a)

$$\begin{aligned}
 (C_{l_p})_H &= (-0.245) \left(\frac{1.0}{0.068} \right) (1)(1) + 0.000191 \\
 &= -0.253 + 0.000191 \\
 &\approx -0.253 \text{ per rad (based on product of horizontal tail area and the square} \\
 &\quad \text{of tail span } S_H b_H^2)
 \end{aligned}$$

Calculate the vertical distance z of the vertical-tail center-of-pressure location above or below the moment-reference-center location

$$\begin{aligned}
 z &= z_p \cos \alpha - l_p \sin \alpha \quad (\text{equation 7.4.2.1-b}) \\
 &= (0.308)(0.9976) - (1.25)(0.06976) \\
 &= 0.220 \text{ ft}
 \end{aligned}$$

Calculate the tail-body sideslip derivative $(\Delta C_{Y_\beta})_{V(WBH)}$ from Section 5.3.1.1

$$\frac{b_V}{2r_1} = \frac{9.0}{4.88} = 1.84$$

$$\frac{A_{V(B)}}{A_V} = 1.63 \quad (\text{figure 5.3.1.1-22a})$$

$$\frac{z_H}{b_V} = \frac{-8.30}{9.0} = -0.922$$

$$\frac{x}{c_V} = \frac{0.25}{0.42} = 0.595$$

$$\frac{A_{V(HB)}}{A_{V(B)}} = 1.39 \quad (\text{figure 5.3.1.1-22b})$$

$$\frac{S_H}{S_V} = \frac{0.48}{0.56} = 0.857$$

$$K_H = 0.85 \quad (\text{figure 5.3.1.1-22c})$$

$$A_{\text{eff}} = \frac{A_V(B)}{A_V} A_V \left\{ 1 + K_H \left[\frac{A_{V(\text{HB})}}{A_{V(B)}} - 1 \right] \right\} \quad (\text{equation 5.3.1.1-a})$$

$$= (1.63) (0.86) \{ 1 + 0.85 [1.39 - 1] \}$$

$$= (1.63) (0.86) (1.33)$$

$$= 1.86$$

$\kappa = 1$ (assumed)

$$\frac{A_{\text{eff}}}{\kappa} \left[\beta^2 + \tan^2 \Lambda_{c/2} \right]^{1/2} = 1.86 [0.9375 + (0.4296)^2]^{1/2} = 1.86 (1.06) = 1.97$$

$$\frac{C_{L_\alpha}}{A_{\text{eff}}} = 1.30 \quad (\text{figure 4.1.3.2-49})$$

$$C_{L_\alpha} = (1.30) (1.86)$$

= 2.42 per rad (based on S_V)

$$\left(1 + \frac{\partial \sigma}{\partial \beta} \right) \frac{q_V}{q_\infty} = 0.724 + 3.06 \frac{S_V/S_W}{1 + \cos \Lambda_{c/4}} + 0.4 \frac{z_W}{d} + 0.009A \quad (\text{equation 5.4.1-a})$$

$$= 0.724 + 3.06 \frac{0.56/1.90}{1.9511} + 0 + (0.009) (2.44)$$

$$= 0.724 + 0.462 + 0.022$$

$$= 1.208$$

$k = 0.75$ (figure 5.3.1.1-22d)

$$(\Delta C_{Y_\beta})_{V(\text{WBH})} = -k (C_{L_\alpha})_V \left(1 + \frac{\partial \sigma}{\partial \beta} \right) \frac{q_V}{q_\infty} \frac{S_V}{S_W} \quad (\text{equation 5.3.1.1-b})$$

$$= (0.75) (2.42) (1.208) \frac{0.56}{1.90}$$

= -0.646 per rad (based on S_W)

$$C_{l_p} = (C_{l_p})_{WB} + 0.5 (C_{l_p})_H \left(\frac{S_H}{S_W} \right) \left(\frac{b_H}{b_W} \right)^2 + \left| 2 \left(\frac{z}{b_W} \right) \left[\frac{z - z_p}{b_W} \right] \right| (\Delta C_{Y_p})_{V(WBH)}$$

(equation 7.4.2.2-a)

$$\begin{aligned}
 &= -0.30 + (0.5) (-0.253) \left(\frac{0.48}{1.90} \right) \left(\frac{1.20}{2.16} \right)^2 \\
 &\quad + \left| 2 \left(\frac{0.22}{2.16} \right) \left[\frac{0.22 - 0.308}{2.16} \right] \right| (-0.646) \\
 &= -0.30 - 0.00986 - 0.00536 \\
 &= -0.315 \text{ per rad} \quad (\text{based on the product of wing area and the square of wing span } S_W b_W^2)
 \end{aligned}$$

This compares with a test value of -0.33 per radian from reference 4.

B. TRANSONIC

No generalized reliable method is available in the literature for estimating transonic values of the roll-damping derivative C_{l_p} . However, a considerable quantity of test data is available and reference should be made to table 7-A.

C. SUPERSONIC

No generalized method is available in the literature for estimating supersonic values of the roll-damping derivative C_{l_p} .

The wing-body roll-damping derivative at supersonic speeds is estimated by the wing-body method of paragraph C of Section 7.3.2.2.

Methods are presented in reference 5 for evaluating the vertical-tail contribution to C_{l_p} . The stability derivatives presented therein are derived by using supersonic linearized theory for families of thin isolated vertical tails performing steady rolling motions. Vertical-tail families (half-delta and rectangular planforms) are considered over a broad Mach number range. Also considered are vertical tails with arbitrary sweepback and taper ratio at Mach numbers for which both the leading edge and trailing edge of the tail are supersonic, and triangular vertical tails with a subsonic leading edge and a supersonic trailing edge.

REFERENCES

1. Campbell, J. P., and McKinney, M. O.: Summary of Methods for Calculating Dynamic Lateral Stability and Response and for Estimating Lateral Stability Derivatives. NACA TR 1098, 1952. (U)
2. Michael, W. H. Jr.: Analysis of the Effects of Wing Interference on the Tail Contributions to the Rolling Derivatives. NACA TR 1086, 1952. (U)
3. Booth, K. W.: Effect of Horizontal-Tail Chord on the Calculated Subsonic Span Loads and Stability Derivatives of Isolated Unswept Tail Assemblies in Sideslip and Steady Roll. NASA Memo 4-1-59L, 1959. (U)
4. Buell, D. A., Reed, V. D., and Lopez, A. E.: The Static and Dynamic-Rotary Stability Derivatives at Subsonic Speeds of an Airplane Model with an Unswept Wing and a High Horizontal Tail. NACA RM A56(04), 1956. (U)
5. Margolis, K., and Bobbitt, P. J.: Theoretical Calculations of the Pressures, Forces, and Moments at Supersonic Speeds due to Various Lateral Motions Acting on Thin Isolated Vertical Tails. NACA TR 1268, 1956. (U)

7.4.2.3 WING-BODY-TAIL ROLLING DERIVATIVE C_{n_p}

This section presents methods for estimating the nondimensional rolling derivative C_{n_p} of wing-body-tail combinations at subsonic speeds. However, at transonic and supersonic speeds no generalized methods are available for estimating the wing-body-tail rolling derivative C_{n_p} . This derivative is the change in yawing-moment coefficient with change in wing-tip helix angle and is expressed as

$$C_{n_p} = \frac{\partial C_n}{\partial \left(\frac{pb}{2V_\infty} \right)}$$

In general, the Datcom methods consist of a synthesis of material presented in Sections 7.1.2.3 and 7.3.2.3, and the vertical-tail contribution based on the methods of reference 1.

Contributions to this derivative arise from two sources, the wing and the vertical tail. The wing contribution is usually negative; whereas the tail contribution may be positive or negative depending on vertical-tail geometry, sidewash, and equilibrium angle of attack.

The rolling wing produces a sidewash at the vertical tail, which can significantly alter the vertical-tail contribution. This effect is discussed more fully in reference 2. Studies have indicated that the effect of the sidewash varies considerably with tail size, tail location, and to some extent with wing planform.

The derivative C_{n_p} is important in lateral dynamics because of its influence on Dutch-roll damping. Although for most configurations C_{n_p} is negative, positive values of C_{n_p} are desired to increase the Dutch-roll damping characteristics.

A. SUBSONIC

Two methods are presented for determining the rolling derivative C_{n_p} of the wing-body-tail combination, differing only in their treatment of wing sidewash on the vertical tail. The first method is applicable to conventionally located vertical tails, and the second method applies to tails located directly above, or above and slightly behind the wing.

Both methods are based on the assumption that the vertical-tail contribution to C_{n_p} is zero at $\alpha = 0$ and varies with angle of attack.

For an isolated-tail configuration the vertical-tail value of C_{n_p} is approximated by

$$(C_{n_p})_V = 2 \left(\frac{z}{b_w} \right) (\Delta C_{n_p})_p$$

For a conventionally located vertical tail the effect of wing sidewash on the vertical tail has been approximately accounted for by $(C_{n_p})_V = 2 \left[\frac{z - z_p}{b_w} \right] (\Delta C_{n_p})_p$. For configurations with tails located directly above or slightly behind the wing, the effect of wing sidewash has been approximated by using the average of the isolated-tail and conventional-tail values.

DATCOM METHODS

Method 1

For conventionally located vertical tails, the equation for the nondimensional rolling derivative C_{n_p} of a wing-body-tail configuration, based on the product of wing area and the square of wing span $S_w b_w^2$, is given by

$$C_{n_p} = (C_{n_p})_{WB} - \frac{2}{b_w} (\ell_p \cos \alpha + z_p \sin \alpha) \left[\frac{z - z_p}{b_w} \right] (\Delta C_{n_p})_V (WBH) \text{ (per radian)}$$

7.4.2.3-a

However, if test data for $(\Delta C_{n_p})_p$ of the empennage are available, the above equation can be rewritten to include the effective tail length, i.e.,

$$C_{n_p} = (C_{n_p})_{WB} + 2 \left[\frac{z - z_p}{b_w} \right] (\Delta C_{n_p})_p \text{ (per radian)} \quad 7.4.2.3-b$$

where

$(C_{n_p})_{WB}$ is the wing-body contribution to C_{n_p} , obtained from test data or Section 7.3.2.3 and based on the product of wing area and the square of wing span (per radian).

ℓ_p is the distance from the moment reference center to the center-of-pressure location of the vertical stabilizer, measured parallel to the body center line (see sketch (a) in Section 7.4.2.1). For Datcom purposes, the vertical-tail center-of-pressure location is assumed to be the quarter-chord point of the MAC of the total added panel.

b_w is the wing span.

z is the vertical distance of the vertical-tail center-of-pressure location above or below the moment-reference-center location. This value must be calculated for each angle of attack. (See sketch (a) in Section 7.4.2.1.) From equation 7.4.2.1-b, z can be expressed as

$$z = z_p \cos \alpha - \ell_p \sin \alpha$$

7.4.2.3-2

z_p

is the distance from the moment reference center to the center of pressure of the vertical stabilizer, measured normal to the body center line, positive for the stabilizer above the body. For Datcom purposes, the vertical-tail center-of-pressure location is assumed to be the quarter-chord point of the MAC of the total added panel.

$(\Delta C_{Y_\beta})_{V(WBH)}$

is the tail-body sideslip derivative from test data or Section 5.3.1.1. It includes the end-plate effects of the horizontal tail and is based on the wing area (per radian).

$(\Delta C_{n_\beta})_p$

is the tail-body sideslip derivative from force-test data, where p refers to panels present in the empennage. It is based on the product of wing area and span (per radian).

Method 2

For vertical tails located either directly above, or above and slightly behind the wing, the equation for the nondimensional rolling derivative C_{n_p} of a wing-body-tail configuration, based on the product of wing area and the square of wing span $S_w b_w^2$, is given by

$$C_{n_p} = (C_{n_p})_{WB} - \left[\frac{\ell_p \cos \alpha + z_p \sin \alpha}{b_w} \right] \left[\frac{2z - z_p}{b_w} \right] (\Delta C_{Y_\beta})_{V(WBH)} \text{ (per radian)}$$

7.4.2.3-c

However, if test data for $(\Delta C_{n_\beta})_p$ of the empennage are available, the equation can be rewritten to include the effective tail length, i.e.,

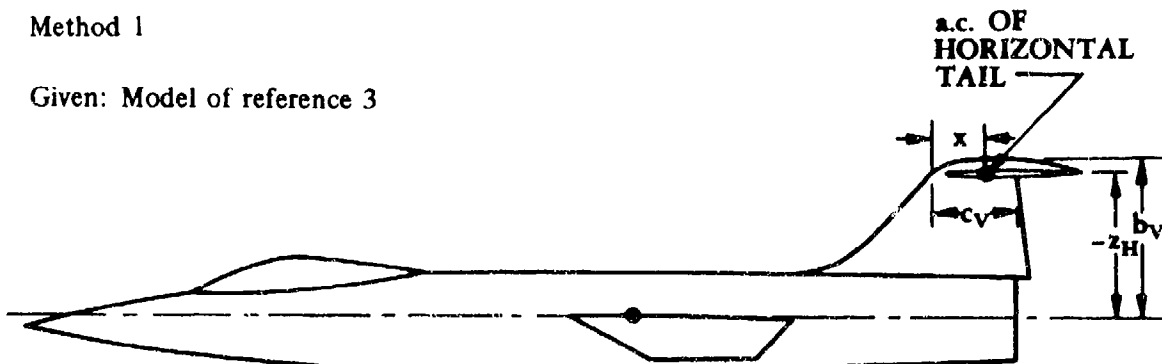
$$C_{n_p} = (C_{n_p})_{WB} + \left[\frac{2z - z_p}{b_w} \right] (\Delta C_{n_\beta})_p \text{ (per radian)} \quad 7.4.2.3-d$$

where the components are described in method 1 above.

Sample Problem

Method 1

Given: Model of reference 3



7.4.2.3-3

Wing Parameters:

$$S_w = 1.90 \text{ sq ft}$$

$$b_w = 2.16 \text{ ft}$$

$$A_w = 2.44$$

$$\gamma = 0.38$$

$$\Lambda_{c/4} = 18.0^\circ$$

Horizontal-Tail Parameters:

$$S_h = 0.48 \text{ sq ft}$$

$$b_h = 1.20 \text{ ft}$$

$$A_h = 2.97$$

$$\gamma = 0.31$$

$$-z_h = 8.30 \text{ in.}$$

Vertical-Tail Parameters:

$$S_v = 0.56 \text{ sq ft}$$

$$b_v = 9.0 \text{ in.}$$

$$A_v = 0.86$$

$$\lambda_v = 0.37$$

$$c_v = 0.42 \text{ ft}$$

$$\Lambda_{c/2} = 23.25^\circ$$

$$z_p = 0.308 \text{ ft}$$

$$l_p = 1.25 \text{ ft}$$

$$x = 0.25 \text{ ft}$$

Additional Parameters:

$$\alpha = 6.0^\circ$$

$$M = 0.25$$

$$(C_{n_p})_{WB} = 0.02 \text{ per rad (test data)}$$

$$2r_1 = 4.88 \text{ in.}$$

Compute:

Calculate the tail-body sideslip derivative $(\Delta C_{Y_\beta})_{V(WBH)}$ from Section 5.3.1.1

$$\frac{b_v}{2r_1} = \frac{9.0}{4.88} = 1.84$$

$$\frac{A_{V(B)}}{A_v} = 1.63 \quad (\text{figure 5.3.1.1-22a})$$

$$\frac{z_h}{b_v} = \frac{8.30}{9.0} = -0.922$$

$$\frac{x}{c_v} = \frac{0.25}{0.42} = 0.595$$

$$\frac{A_{V(HB)}}{A_{V(B)}} = 1.39 \quad (\text{figure 5.3.1.1-22b})$$

$$\frac{S_H}{S_V} = \frac{0.48}{0.56} = 0.857$$

$$K_H = 0.85 \quad (\text{figure 5.3.1.1-22c})$$

$$\begin{aligned} A_{\text{eff}} &= \frac{A_{V(B)}}{A_V} A_V \left\{ 1 + K_H \left[\frac{A_{V(HB)}}{A_{V(B)}} - 1 \right] \right\} \quad (\text{equation 5.3.1.1-a}) \\ &= (1.63)(0.85) \{ 1 + 0.85 [1.39 - 1] \} \\ &= (1.63)(0.86)(1.33) \\ &= 1.86 \end{aligned}$$

$$\kappa = 1 \text{ (assumed)}$$

$$\frac{A_{\text{eff}}}{\kappa} \left[\beta^2 + \tan^2 \Lambda_{c/2} \right]^{1/2} = 1.86 [0.9375 + (0.4296)^2]^{1/2} = 1.86(1.06) = 1.97$$

$$\frac{C_{L\alpha}}{A_{\text{eff}}} = 1.30 \quad (\text{figure 4.1.3.2-49})$$

$$C_{L\alpha} = (1.30)(1.86)$$

$$= 2.42 \text{ per rad (based on } S_V)$$

$$\left(1 + \frac{\partial \sigma}{\partial \beta} \right) \frac{q_V}{q_\infty} = 0.724 + 3.06 \frac{S_V/S_W}{1 + \cos \Lambda_{c/4}} 0.4 \frac{z_W}{d} + 0.009A \quad (\text{equation 5.4.1-a})$$

$$= 0.724 + 3.06 \left(\frac{0.56/1.90}{1.9511} \right) + 0 + (0.009)(2.44)$$

$$= 0.724 + 0.462 + 0.022$$

$$= 1.208$$

$$k = 0.75 \quad (\text{figure 5.3.1.1-22d})$$

$$\begin{aligned}
 (\Delta C_{Y_\beta})_{V(WBH)} &= -k (C_{L_\alpha})_V \left(1 + \frac{\partial \sigma}{\partial \beta} \right) \frac{q_V}{q_\infty} \frac{S_V}{S_W} \quad (\text{equation 5.3.1.1-b}) \\
 &= -(0.75) (2.42) (1.208) \left(\frac{0.56}{1.90} \right) \\
 &= -0.646 \text{ per rad (based on } S_W)
 \end{aligned}$$

Calculate the vertical distance z of the vertical-tail center-of-pressure location above or below the moment-reference-center location

$$\begin{aligned}
 z &= z_p \cos \alpha - l_p \sin \alpha \quad (\text{equation 7.4.2.1-b}) \\
 &= (0.308) (0.9945) - (1.25) (0.1045) \\
 &= 0.176 \text{ ft}
 \end{aligned}$$

$$\begin{aligned}
 C_{n_p} &= (C_{n_p})_{WB} - \frac{2}{b_W} (l_p \cos \alpha + z_p \sin \alpha) \left[\frac{z - z_p}{b_W} \right] (\Delta C_{Y_\beta})_{V(WBH)} \\
 &\quad (\text{equation 7.4.2.3-a}) \\
 &= (0.02) - \frac{2}{2.16} [(1.25) (0.9945) + (0.308) (0.1045)] \left[\frac{0.176 - 0.308}{2.16} \right] (-0.646) \\
 &= 0.02 - \frac{2}{2.16} (1.275) \left(\frac{-0.132}{2.16} \right) (-0.646) \\
 &= 0.02 - 0.0466 \\
 &= -0.0266 \text{ per rad (based on } S_W b_W^2)
 \end{aligned}$$

This compares with a test value of -0.048 per radian from reference 3.

B. TRANSONIC

No generalized method is available in the literature for estimating transonic values of the rolling derivative C_{n_p} .

C. SUPERSONIC

No generalized method is available in the literature for estimating supersonic values of the rolling derivative C_{n_p} .

For the purpose of the Datcom the fuselage effect is considered to be negligible for wing-body configurations with body diameters less than about 30 percent of the wing span. Therefore, for configurations with $d/b \leq 0.3$, the wing-body rolling derivative C_{n_p} is estimated by the wing-alone method of paragraph C of Section 7.1.2.3.

Methods are presented in reference 4 for evaluating the vertical-tail contribution to C_{n_p} . The stability derivatives presented therein are derived by using supersonic linearized theory for families of thin isolated vertical tails performing steady rolling motions. Vertical-tail families (half-delta and rectangular planforms) are considered over a broad Mach number range. Also considered are vertical tails with arbitrary sweepback and taper ratio at Mach numbers for which both the leading edge and trailing edge of the tail are supersonic, and triangular vertical tails with a subsonic leading edge and a supersonic trailing edge.

REFERENCES

1. Campbell, J. P., and McKinney, M. O.: Summary of Methods for Calculating Dynamic Lateral Stability and Response and for Estimating Lateral Stability Derivatives. NACA TR 1098, 1952. (U)
2. Michael, W. H. Jr.: Analysis of the Effects of Wing Interference on the Tail Contributions to the Rolling Derivatives. NACA TR 1086, 1952. (U)
3. Buell, D. A., Reed, V. D., and Lopez, A. E.: The Static and Dynamic-Rotary Stability Derivatives at Subsonic Speeds of an Airplane Model with an Unswept Wing and a High Horizontal Tail. NACA RM A56(04), 1956. (U)
4. Margolis, K., and Bobbitt, P. J.: Theoretical Calculations of the Pressures, Forces, and Moments at Supersonic Speeds due to Various Lateral Motions Acting on Thin Isolated Vertical Tails. NACA TR 1268, 1956. (U)

7.4.3 WING-BODY-TAIL YAWING DERIVATIVES

7.4.3.1 WING-BODY-TAIL YAWING DERIVATIVE C_{Y_r}

This section presents a method for estimating the nondimensional yawing derivative C_{Y_r} of wing-body-tail combinations at subsonic speeds. However, at transonic and supersonic speeds no generalized methods are available for estimating the wing-body-tail yawing derivative C_{Y_r} . This derivative is the change in side-force coefficient with variation in yawing velocity and is expressed as

$$C_{Y_r} = \frac{\partial C_Y}{\partial \left(\frac{rb}{2V_\infty} \right)}$$

In general, the Datcom method consists of a synthesis of material presented in Sections 7.1.3.1 and 7.3.3.1, and the vertical-tail contribution based on the methods of reference 1.

Contributions to the derivative C_{Y_r} arise from two sources, the wing and the vertical tail. The vertical-tail contribution, which constitutes the major portion, is small and positive in sign. Generally C_{Y_r} is of little importance in lateral dynamics, hence it is frequently neglected.

A. SUBSONIC

For the oscillatory mode, the effects due to lag of sidewash in free oscillation are important and hence should be considered. However, no generalized method is available in the literature to account for oscillating sidewash effects on C_{Y_r} ; therefore, only the aperiodic mode of C_{Y_r} is presented here.

In the equation for estimating the yawing derivative C_{Y_r} , the sideslip-derivative contribution of the vertical tail should include the end-plate effects of the horizontal tail.

DATCOM METHOD

The equation for the nondimensional yawing derivative C_{Y_r} of a wing-body-tail configuration, based on the product of wing area and wing span $S_W b_W$, is given by

$$C_{Y_r} = (C_{Y_r})_{WB} - \frac{2}{b_W} (\ell_p \cos \alpha + z_p \sin \alpha) (\Delta C_{Y_\beta})_{V(WBH)} \text{ (per radian)} \quad 7.4.3.1-a$$

However, if test data for $(\Delta C_{n_\beta})_p$ of the empennage are available, the above equation can be rewritten to include the effective tail length, i.e.,

$$C_{Y_r} = (C_{Y_r})_{WB} + 2 (\Delta C_{n_\beta})_p \text{ (per radian)} \quad 7.4.3.1-b$$

where

$$(C_{Y_r})_{WB}$$

is the wing-body contribution to C_{Y_r} , obtained from test data or by using the recommendations of Section 7.1.3.1, based on the product of wing area and wing span (per radian).

$$b_w$$

is the wing span.

$$x_p$$

is the distance from the moment reference center to the center-of-pressure location of the vertical stabilizer, measured parallel to the body center line. (See sketch (a) in Section 7.4.2.1.) For Datcom purposes, the vertical-tail center-of-pressure location is assumed to be the quarter-chord point of the MAC of the total added panel.

$$z_p$$

is the distance from the moment reference center to the center of pressure of the vertical stabilizer, measured normal to the body center line, positive for the stabilizer above the body. For Datcom purposes, the vertical-tail center-of-pressure location is assumed to be the quarter-chord point of the MAC of the total added panel.

$$(\Delta C_{Y_\beta})_{V(WBH)}$$

is the tail-body sideslip derivative obtained from test data or Section 5.3.1.1. It includes the end-plate effects of the horizontal tail and is based on the wing area (per radian).

$$(\Delta C_{n_\beta})_p$$

is the tail-body sideslip derivative from test data where p refers to panels in the empennage. It is based on the product of wing area and span (per radian).

Sample Problem

Given: Model of reference 2



$$\alpha = 8.0^\circ \quad (C_{Y_r})_{WB} = -0.10 \text{ per rad (test data)} \quad (\Delta C_{n_\beta})_p = 0.42 \text{ per rad (test data)}$$

Compute:

Calculate the yawing derivative C_{Y_r} for the wing-body-tail configuration

$$\begin{aligned} C_{Y_r} &= \left(C_{Y_r}\right)_{WB} + 2 \left(\Delta C_{n\beta}\right)_p \quad (\text{equation 7.4.3.1-b}) \\ &= -0.10 + 2(0.42) \\ &= 0.74 \text{ per rad (based on } S_w b_w) \end{aligned}$$

This compares with a test value of 0.50 per radian from reference 2.

B. TRANSONIC

No generalized method is available in the literature for estimating transonic values of the yawing derivative C_{Y_r} . Furthermore, there is a scarcity of experimental data for this derivative at transonic speeds.

C. SUPERSONIC

No generalized method is available in the literature for estimating supersonic values of the yawing derivative C_{Y_r} . Furthermore, there is a scarcity of experimental data for this derivative at supersonic speeds.

REFERENCES

1. Campbell, J. P., and McKinney, M. O.: Summary of Methods for Calculating Dynamic Lateral Stability and Response and for Estimating Lateral Stability Derivatives. NACA TR 1098, 1952. (U)
2. Queijo, M. J., and Wells, E. G.: Wind-Tunnel Investigation of the Low-Speed Static and Rotary Stability Derivatives of a 0.13-Scale Model of the Douglas D-558-II Airplane in the Landing Configuration. NACA RM L52G07, 1952. (U)

7.4.3.2 WING-BODY-TAIL YAWING DERIVATIVE C_{I_r}

This section presents a method for estimating the nondimensional yawing derivative C_{I_r} of wing-body-tail combinations at subsonic speeds. However, at transonic and supersonic speeds no generalized methods are available for estimating the yawing derivative C_{I_r} . This derivative is the change in rolling-moment coefficient with change in the yawing velocity and is expressed as

$$C_{I_r} = \frac{\partial C_I}{\partial \left(\frac{rb}{2V_\infty} \right)}$$

In general, the Datcom method consists of a synthesis of material presented in Sections 7.1.3.2 and 7.3.3.2, and the vertical-tail contribution based on the methods of reference 1.

Contributions to this derivative arise from two sources, the wing and the vertical tail. The wing contribution constitutes the major portion and is positive in sign. The lesser contribution of the vertical tail can be positive or negative, depending upon tail equilibrium angle of attack. This derivative is not of primary importance; however, it is not neglected in lateral dynamic calculations.

A. SUBSONIC

The method presented here is based on the assumption that the wing and fuselage interference effects on tail effectiveness can be determined from geometric dimensions and the sideslip derivatives. This is particularly true if experimental test data are available for $(\Delta C_{Y_\beta})_{V(WBH)}$ or $(\Delta C_{I_\beta})_p$ in the equations given below.

DATCOM METHOD

The equation for the nondimensional yawing derivative C_{I_r} of a wing-body-tail configuration, based on the product of the wing area and the square of wing span $S_w b_w^2$, is given by

$$C_{I_r} = (C_{I_r})_{WB} - \frac{2}{b_w^2} (\ell_p \cos \alpha + z_p \sin \alpha) (z_p \cos \alpha - \ell_p \sin \alpha) (\Delta C_{Y_\beta})_{V(WBH)} \quad 7.4.3.2-a$$

However, if test data for $(\Delta C_{I_\beta})_p$ are available, the above equation can be rewritten to approximate the effective vertical-tail center-of-pressure location (the height of the body center line).

$$C_{I_r} = (C_{I_r})_{WB} - \frac{2}{b_w^2} (\ell_p \cos \alpha + z_p \sin \alpha) (\Delta C_{I_\beta})_p \quad 7.4.3.2-b$$

If test data for $(\Delta C_{n_\beta})_p$ and $(\Delta C_{Y_\beta})_{V(WBH)}$ are available, the above equation can be rewritten to include the total effective vertical-tail center-of-pressure location.

$$C_{l_r} = (C_{l_r})_{WB} + 2 \frac{(\Delta C_{n_\beta})_p}{(\Delta C_{Y_\beta})_{V(WBH)}} (\Delta C_{l_\beta})_p \text{ (per radian)} \quad 7.4.3.2-c$$

where

$(C_{l_r})_{WB}$ is the wing-body contribution to C_{l_r} obtained from test data or Section 7.3.3.2, based on the product of wing area and the square of wing span (per radian).

b_w is the wing span.

ℓ_p is the distance from the moment reference center to the center-of-pressure location of the vertical stabilizer, measured parallel to the body center line. (See sketch (a) in Section 7.4.2.1.) For Datcom purposes, the vertical-tail center-of-pressure location is assumed to be the quarter-chord point of the MAC of the total added panel.

z_p is the distance from the moment reference center to the center of pressure of the vertical stabilizer, measured normal to the body center line, positive for the stabilizer above the body. For Datcom purposes, the vertical-tail center-of-pressure location is assumed to be the quarter-chord point of the MAC of the total added panel.

$(\Delta C_{Y_\beta})_{V(WBH)}$ is the tail-body sideslip derivative obtained from test data or Section 5.3.1.1. It includes the end-plate effects of the horizontal tail and is based on the wing area (per radian).

$(\Delta C_{l_\beta})_p$ is the tail-body sideslip derivative from test data, where p refers to the panels in the empennage. It is based on the product of wing area and span (per radian).

$(\Delta C_{n_\beta})_p$ is the tail-body sideslip derivative from test data, where p refers to the panels in the empennage. It is based on the product of wing area and span (per radian).

Sample Problem

Given: Model of reference 2



$$\alpha = 6.0^\circ \quad b_w = 38.84 \text{ in.} \quad l_p = 24.3 \text{ in.} \quad z_p = 5.0 \text{ in.}$$

$$(C_{I_r})_{WB} = 0.10 \text{ per rad (test data)} \quad (C_{Y_\beta})_{V(WBH)} = -0.64 \text{ per rad (test data)}$$

Compute:

Calculate the yawing derivative C_{I_r} for the wing-body-tail configuration

$$C_{I_r} = (C_{I_r})_{WB} - \frac{2}{b_w^2} (l_p \cos \alpha + z_p \sin \alpha) (z_p \cos \alpha - l_p \sin \alpha) (\Delta C_{Y_\beta})_{V(WBH)}$$

(equation 7.4.3.2-a)

$$= 0.10 - \frac{2}{(38.84)^2} [(24.3)(0.0045) + (5.0)(0.1045)]$$

$$[(5.0)(0.0045) - (24.3)(0.1045)] (-0.64)$$

$$= 0.10 + 0.051$$

$$= 0.151 \text{ per rad (based on } S_w b_w^2)$$

This compares with a test value of 0.15 per radian from reference 2.

B. TRANSONIC

No generalized method is available in the literature for estimating transonic values of the yawing derivative C_{I_r} . Furthermore, there is a scarcity of experimental data for this derivative at transonic speeds.

C. SUPERSONIC

No generalized method is available in the literature for estimating supersonic values of the yawing derivative C_{I_r} . Furthermore, there is a scarcity of experimental data for this derivative at supersonic speeds.

REFERENCES

1. Campbell, J. P., and Goodman, A.: A Semiempirical Method for Estimating the Rolling Moment Due to Yawing of Airplanes. NACA TN 1984, 1949. (U)
2. Queijo, M. J., and Wells, E. G.: Wind-Tunnel Investigation of the Low-Speed Static and Rotary Stability Derivatives of a 0.13-Scale Model of the Douglas D-558-II Airplane in the Landing Configuration. NACA RM L52G07, 1952. (U)

7.4.3.3 WING-BODY-TAIL YAWING DERIVATIVE C_{n_r}

This section presents a method for estimating the nondimensional yawing derivative C_{n_r} of wing-body-tail combinations at subsonic speeds. However, at transonic and supersonic speeds no generalized methods are available for estimating the wing-body-tail yawing derivative C_{n_r} . This derivative is the change in yawing-moment coefficient with change in the yawing-velocity parameter. It is commonly referred to as the yaw damping and is expressed as

$$C_{n_r} = \frac{\partial C_n}{\partial \left(\frac{rb}{2V_\infty} \right)}$$

In general, the Datcom method consists of a synthesis of material presented in Sections 7.1.3.3 and 7.3.3.3, and the vertical-tail contribution based on the methods of reference 1.

Contributions to this derivative arise from the wing, the fuselage, and the vertical tail. The vertical-tail contribution usually constitutes the major portion and is negative in sign (positive damping).

The derivative C_{n_r} is very important in lateral dynamics because of the important contribution it makes to the damping of the Dutch-roll oscillatory mode. Its contribution to the spiral-mode damping is also important. It is desirable to have a large negative value of C_{n_r} for each mode.

A. SUBSONIC

For the oscillatory mode, the effects due to lag of sidewash in free oscillation are important and hence should be considered. However, no generalized method is available in the literature to account for oscillating sidewash effects on C_{n_r} ; therefore, only the aperiodic mode of C_{n_r} is presented here.

In the equation for determining the yawing derivative C_{n_r} , the sideslip-derivative contribution of the vertical tail should include the end-plate effects of the horizontal tail.

DATCOM METHOD

The equation for the nondimensional yawing derivative C_{n_r} of a wing-body-tail configuration, based on the product of wing area and the square of wing span $S_w b_w^2$, is given by

$$C_{n_r} = (C_{n_r})_{WB} + \frac{2}{b_w^2} (\ell_p \cos \alpha + z_p \sin \alpha)^2 (\Delta C_{Y_\beta})_{V(WBH)} \quad (\text{per radian}) \quad 7.4.3.3-a$$

However, if test data for ΔC_{n_β} are available, the above equation can be expressed as

$$C_{n_r} = (C_{n_r})_{WB} + 2 \frac{(\Delta C_{n_\beta})_p^2}{(\Delta C_{Y_\beta})_{V(WBH)}} \quad (\text{per radian}) \quad 7.4.3.3-b$$

where

$$(C_{n_r})_{WB}$$

is the wing-body contribution to C_{n_r} obtained from test data or Section 7.3.3.3, based on the product of wing area and the square of wing span (per radian).

$$b_w$$

is the wing span.

$$l_p$$

is the distance from the moment reference center to the center-of-pressure location of the vertical stabilizer, measured parallel to the body center line. (See sketch (a) in Section 7.4.2.1.) For Datcom purposes, the vertical-tail center-of-pressure location is assumed to be the quarter-chord point of the MAC of the total added panel.

$$z_p$$

is the distance from the moment reference center to the center of pressure of the vertical stabilizer, measured normal to the body center line, positive for the stabilizer above the body. For Datcom purposes, the vertical-tail center-of-pressure location is assumed to be the quarter-chord point of the MAC of the total added panel.

$$(\Delta C_{Y_\beta})_{V(WBH)}$$

is the tail-body sideslip derivative from test data or Section 5.3.1.1 and is based on the wing area (per radian).

$$(\Delta C_{n_\beta})_p$$

is the tail-body sideslip derivative from test data, where p refers to the panels in the empennage. It is based on the product of wing area and span (per radian).

Sample Problem

Given: Model of reference 2



$$\alpha = 6^\circ$$

$$(C_{n_r})_{WB} = -0.15 \text{ per } 10^{-4} \quad (\text{test data})$$

$$(\Delta C_{n_\beta})_p = 0.43 \text{ per rad} \quad (\text{test data})$$

$$(\Delta C_{Y_\beta})_{V(WBH)} = -0.64 \text{ per } 10^{-4} \quad (\text{test data})$$

Compute:

Calculate the yawing derivative C_{n_z} for the wing-body-tail configuration

$$C_{n_z} = (C_{n_z})_{WB} + 2 \frac{(\Delta C_{n_\beta})_p^2}{(\Delta Y_\beta)_V (WBH)} \quad (\text{equation 7.4.3.3-b})$$
$$= -0.15 + (2) \frac{(0.43)^2}{(-0.64)}$$
$$= -0.15 - 0.578$$
$$= -0.728 \text{ per rad (based on } S_w b_w^2)$$

This compares with a test value of -0.60 per radian from reference 2.

B. TRANSONIC

No generalized method is available in the literature for estimating transonic values of the yawing derivative C_{n_z} . Furthermore, there is a scarcity of experimental data for this derivative at transonic speeds.

C. SUPERSONIC

No generalized method is available in the literature for estimating supersonic values of the yawing derivative C_{n_z} . Furthermore, there is a scarcity of experimental data for this derivative at supersonic speeds.

REFERENCES

1. Campbell, J. P., and McKinney, M. O.: Summary of Methods for Calculating Dynamic Lateral Stability and Response and for Estimating Lateral Stability Derivatives. NACA TR 1098, 1952. (U)
2. Queijo, M. J., and Wells, E. G.: Wind-Tunnel Investigation of the Low-Speed Static and Rotary Stability Derivatives of a 0.13-Scale Model of the Douglas D-558-II Airplane in the Landing Configuration. NACA RM L52G07, 1952. (U)

7.4.4 WING-BODY-TAIL ACCELERATION DERIVATIVES

7.4.4.1 WING-BODY-TAIL ACCELERATION DERIVATIVE $C_{L\dot{\alpha}}$

The information contained in this section is for estimating the nondimensional acceleration derivative $C_{L\dot{\alpha}}$ of wing-body-tail combinations at low angles of attack. This derivative is the change in lift coefficient with rate of change of angle of attack and is expressed as

$$C_{L\dot{\alpha}} = \frac{\partial C_L}{\partial \left(\frac{\dot{\alpha} \bar{c}}{2V_\infty} \right)}$$

In general, the methods presented consist of a synthesis of material presented in other sections, although some new information is presented.

This derivative is presented in a manner similar to that used in reference 1 to calculate the lift of a wing-body-tail combination. The complete derivative is the sum of contributions of individual components, treated as isolated surfaces or bodies, and mutual interference effects. The mutual interference effects are assumed to correspond to those due to angle-of-attack variations, established in references 1 and 2 and presented in Section 4.3.1.2.

The horizontal-tail contribution to the derivative $C_{L\dot{\alpha}}$ is based on the concept of the lag of the downwash. The nonstationary character of the lift response of the tail to changes in tail angle of attack is neglected, and the result is attributed entirely to the fact that the downwash at the tail does not respond instantaneously to changes in wing angle of attack. This concept is also the basis used in estimating the horizontal-tail contribution to the derivative $C_{m\dot{\alpha}}$ in Section 7.4.4.2. The result of this concept is presented in numerous aerodynamic texts, for example, reference 3. The effect of $C_{L\dot{\alpha}}$ on longitudinal stability is usually unimportant and is therefore frequently neglected in dynamic analyses.

A. SUBSONIC

Two methods are presented for determining the acceleration derivative $C_{L\dot{\alpha}}$ of wing-body-tail combinations, differing only in their treatment of the effect of the flow field of the forward surface on the aft surface.

DATCOM METHODS

Method 1. ($b'/b'' \geq 1.5$)

For configurations in which the span of the forward surface is large compared to that of the aft surface, the following approach can be used. This method is to be used when the ratio of the forward-panel span to the aft-panel span is 1.5 or greater. The equation of the nondimensional acceleration derivative $C_{L\dot{\alpha}}$ of a wing-body-tail configuration, based on the area and mean

aerodynamic chord of the total forward panel and referred to a moment center at the assumed center of gravity or center of rotation, is given by

$$C_{L\dot{\alpha}} = (C_{L\dot{\alpha}})_{WB} + 2[K_{W(B)} + K_{B(W)}]'' \left(\frac{S_e''}{S'} \right) \left(\frac{x_{c.g.} - x''}{\bar{c}'} \right) \left(\frac{q''}{q_\infty} \right) \left(\frac{\partial \bar{e}}{\partial \alpha} \right) (C_{L\dot{\alpha}})_e''$$

7.4.4.1-a

where the primed quantities refer to the forward panel, the double-primed quantities refer to the aft panel, and the subscript e refers to the exposed panel. (See Section 4.3.1.2 for the definition of exposed surfaces.)

$(C_{L\dot{\alpha}})_{WB}$ is the contribution of the wing-body configuration to the acceleration derivative $C_{L\dot{\alpha}}$, obtained from Section 7.3.4.1.

$\frac{\partial \bar{e}}{\partial \alpha}$ is the downwash gradient averaged over the aft surface, obtained from Section 4.4.1.

The remaining terms are defined in paragraph A of Section 7.4.1.1.

Method 2. ($b'/b'' < 1.5$)

For configurations in which the span of the forward surface is approximately equal to or less than that of the aft surface, the vortex shed from the forward surface interacts directly with the aft surface and the resulting interference effects must be accounted for in the tail terms. This method is to be used when the ratio of the forward-panel span to the aft-panel span is less than 1.5. The equation for the nondimensional acceleration derivative $C_{L\dot{\alpha}}$ of a wing-body-tail configuration, based on the area and mean aerodynamic chord of the total forward panel and referred to a moment center at the assumed center of gravity or center of rotation, is given by

$$C_{L\dot{\alpha}} = (C_{L\dot{\alpha}})_{WB} - 2 \left(\frac{x_{c.g.} - x''}{\bar{c}'} \right) (C_{L\dot{\alpha}})_{W''(v)}$$

7.4.4.1-b

All the terms are defined in paragraph A of Section 7.4.1.1 and method 1 above.

Because of the similarity of the two methods a sample problem for method 2 is not included. However, evaluation of the term $(C_{L\dot{\alpha}})_{W''(v)}$ for a wing-body-tail configuration is presented in Section 4.5.1.1.

7.4.4.1-2

Sample Problem

Method 1

Given: Same configuration as sample problems of paragraph A, Sections 7.4.1.1 and 7.4.1.2. Some of the characteristics are repeated below. Note that for the sake of simplicity the vehicle center of gravity has been taken at $\bar{c}'/4$ and $x_{c.g.} - x'' = \ell''$.

The following ratios based on total forward panel dimensions:

$$\frac{b''}{b'} = 0.4377 \quad \frac{2\ell_2}{b'} = 0.8053 \quad \frac{\ell_{\text{eff}}}{b} = 0.4026 \quad \frac{h_H}{b'} = 0.1578$$

$$\frac{\ell''}{\bar{c}'} = 2.26 \quad \frac{\ell_3}{b'} = 0.2667 \quad \frac{S_e''}{S'} = 0.0988$$

Additional Characteristics:

$$h_H = 7.18 \text{ feet} \quad M = 0.60 \quad R_\ell = 5.16 \times 10^7 \text{ (based on } \bar{c}')$$

$$\ell_{\text{eff}} = \ell_2 = 18.32 \text{ feet} \quad \beta = 0.80 \quad \text{Sea level}$$

$$\ell_3 = \bar{c}' = 12.133 \text{ feet} \quad \alpha' = 4^\circ \quad \text{Smooth surfaces}$$

$$\ell'' = 27.425 \text{ feet} \quad \Gamma = 0 \quad \text{NACA 66-206 airfoil sections}$$

$$\Lambda'_{c/4} = 30.97^\circ$$

Compute:

Step 1. Wing-body $C_{L\dot{\alpha}}$ (Section 7.3.4.1)

$$(C_{L\dot{\alpha}})_{WB} = 0.864 \text{ per rad} \quad (\text{sample problem, paragraph A, Section 7.3.4.1})$$

Step 2. Lift-curve slope for the exposed horizontal-tail panel (Section 4.1.3.2)

$$(C_{L\dot{\alpha}})_e'' = 4.0 \text{ per rad} \quad (\text{sample problem, paragraph A, Section 7.4.1.1})$$

Step 3. Tail-body interference factors (Section 4.3.1.2)

$$\left. \begin{array}{l} K_{W(B)}'' = 1.315 \\ K_{B(W)}'' = 0.550 \end{array} \right\} \quad (\text{sample problem, paragraph A, Section 7.4.1.1})$$

Step 4. Dynamic pressure ratio (Section 4.4.1)

$$\frac{q''}{q_\infty} = 0.901 \quad (\text{sample problem, paragraph A, Section 7.4.1.1})$$

Step 5. Downwash parameter (Section 4.4.1)

Obtain value for $\alpha' = 4^\circ$ at $M = 0.2$ and correct for Mach number effects by equation 4.4.1-g

$$\alpha'_0 = -1.6^\circ \quad (\text{table 4.1.1-B})$$

$$\tan \Lambda_{c/2} = 0.4003$$

$$\frac{A'}{\kappa} \left(\beta^2 + \tan^2 \Lambda_{c/2} \right)^{1/2} = \frac{5}{0.985} [0.98 + (0.4003)^2]^{1/2} = 5.43$$

$$\frac{C_{L\alpha}}{A} = 0.80 \quad (\text{figure 4.1.3.2-49})$$

$$C_{L\alpha}' = 4.00 \text{ per rad} = 0.0698 \text{ per deg}$$

$$(C_{L\alpha})_{\alpha'=4^\circ} = C_{L\alpha'} (\alpha' - \alpha'_0) = 0.0698 [4 - (-1.6)] = 0.391$$

$$\alpha'_{C_{L\max}} = 21.0^\circ \quad (\text{Section 4.1.3.4})$$

$$\frac{\alpha' - \alpha_0}{\alpha'_{C_{L\max}} - \alpha'_0} = \frac{4 - (-1.6)}{21.0 - (-1.6)} = 0.248$$

$$\left. \begin{aligned} \frac{A'_{\text{eff}}}{A'} &= 1.0 \\ \frac{b'_{\text{eff}}}{b'} &= 1.0 \end{aligned} \right\} \quad (\text{figure 4.4.1-66})$$

$$A'_{\text{eff}} = 5.0$$

$$b'_{\text{eff}} = 45.50 \text{ ft}$$

$$\left. \begin{aligned} \left(\frac{\partial \epsilon}{\partial \alpha} \right)_{\infty} &= 0.40 \\ \left(\frac{\partial \epsilon}{\partial \alpha} \right)_v &= 0.49 \end{aligned} \right\} \quad (\text{figure 4.4.1-67})$$

$$\Delta y = 1.10 \quad (\text{figure 2.2.1-8})$$

Type of flow separation: Leading-edge separation is predominant (figure 4.4.1-68a)

$$\begin{aligned} a &= h_H - (\ell_2 + \ell_3) \left(\alpha - \frac{0.41 C_L}{\pi A_{\text{eff}}} \right) - \frac{b_{\text{eff}}}{2} \tan \Gamma \quad (\text{equation 4.4.1-d}) \\ &= 7.18 - (18.32 + 12.133) \left(\frac{4}{57.3} - \frac{(0.41)(0.391)}{(3.14)(5.0)} \right) - \frac{45.50}{2} (0) \\ &= 7.18 - (30.453)(0.0596) = 5.37 \end{aligned}$$

$$\xi_{ru} = \frac{0.56 A'}{C_L'} = \frac{0.56(5.0)}{0.391} = 7.16 \quad (\text{See page 4.4.1-6})$$

$$\begin{aligned} b_{v_{ru}} &= [0.78 + 0.10(\lambda' - 0.4) + 0.003 \Lambda'_{c/4}] b'_{\text{eff}} \quad (\Lambda_{c/4} \text{ in deg}) \quad (\text{equation 4.4.1-f}) \\ &= (0.833)(45.50) \\ &= 37.90 \text{ ft} \end{aligned}$$

$$\begin{aligned} b_v &= b'_{\text{eff}} - \left(b'_{\text{eff}} - b_{v_{ru}} \right) \left[\frac{2\ell_{\text{eff}}}{b' \xi_{ru}} \right]^{1/2} \quad (\text{equation 4.4.1-e}) \\ &= 45.5 - (45.5 - 37.9) \left[\frac{36.64}{(45.5)(7.16)} \right]^{1/2} \\ &= 45.5 - 2.5 = 43.0 \end{aligned}$$

$$\frac{b_H}{b_v} = \frac{b''}{b_v} = \frac{19.915}{43.0} = 0.463$$

$$\frac{2a}{b_v} = \frac{2(5.37)}{43.0} = 0.25$$

$$\frac{\left(\frac{\partial \bar{\epsilon}}{\partial \alpha}\right)}{\left(\frac{\partial \epsilon}{\partial \alpha}\right)_v} = 0.93 \quad (\text{figure 4.4.1-68b})$$

$$\left(\frac{\partial \bar{\epsilon}}{\partial \alpha}\right)_{\substack{\text{low} \\ \text{speed}}} = \frac{\left(\frac{\partial \bar{\epsilon}}{\partial \alpha}\right)}{\left(\frac{\partial \epsilon}{\partial \alpha}\right)_v} \left(\frac{\partial \epsilon}{\partial \alpha}\right)_v = (0.93)(0.49) = 0.4557$$

$$\left(C_{L\alpha}'\right)_{M=0.6} = 4.50 \quad (\text{sample problem, paragraph A, Section 7.3.1.1})$$

$$\left(\frac{\partial \bar{\epsilon}}{\partial \alpha}\right)_{M=0.6} = \left(\frac{\partial \bar{\epsilon}}{\partial \alpha}\right)_{\substack{\text{low} \\ \text{speed}}} \frac{\left(C_{L\alpha}'\right)_{M=0.6}}{\left(C_{L\alpha}'\right)_{\substack{\text{low} \\ \text{speed}}}} \quad (\text{equation 4.4.1-g})$$

$$= (0.4557) \left(\frac{4.50}{4.00}\right)$$

$$= (0.513)$$

Solution:

$$C_{L\dot{\alpha}} = \left(C_{L\dot{\alpha}}\right)_{WB} + 2[K_{W(B)} + K_{B(W)}]'' \left(\frac{S_e''}{S'}\right) \left(\frac{x_{c.g.} - x''}{\bar{c}'}\right) \left(\frac{\partial \bar{\epsilon}}{\partial \alpha}\right) \left(\frac{q''}{q_\infty}\right) \left(C_{L\alpha}\right)_e''$$

(equation 7.4.4.1-a)

$$= 0.864 + 2(1.315 + 0.550)(0.0988)(2.26)(0.513)(0.901)(4.0)$$

$$= 0.864 + 1.540$$

$$= 2.404 \text{ per rad} \quad (\text{based on the area and mean aerodynamic chord of the total forward panel and referred to a moment center at } \bar{c}/4)$$

B. TRANSONIC

No accurate methods are available for estimating the characteristics of isolated panels, the dynamic-pressure ratio, or the downwash gradient in the transonic speed regime. The aerodynamic interference "K" factors for slender configurations are relatively insensitive to Mach number; however, for nonslender configurations transonic interference effects can become quite large and sensitive to minor changes in local contour.

DATCOM METHODS

It is recommended that the methods presented in paragraph A above be applied directly to the transonic speed regime. Care should be taken to estimate the various parameters of equations 7.4.4.1-a and -b at the appropriate Mach number. The interference "K" factors should be obtained from paragraph C, Section 4.3.1.2.

C. SUPERSONIC

The information included in the Datcom accounts for most of the mutual interferences that occur between components of wing-body-tail configurations at supersonic speeds.

DATCOM METHODS

The methods presented in paragraph A above are also applicable to the supersonic speed range. Care should be taken to estimate the various parameters of equations 7.4.4.1-a and -b at the appropriate Mach number. Method 3 of paragraph C of Section 4.4.1 should be used to evaluate the last term of equation 7.4.4.1-b.

Sample Problem

Method 1

Given: Same configuration as sample problems of paragraph C, Sections 7.4.1.1 and 7.4.1.2, and paragraph A of this section. Some of the characteristics are repeated below.

The following ratios based on total forward panel dimensions:

$$\frac{q''}{c'} = 2.26 \quad \frac{S_e''}{S'} = 0.0988$$

Additional Characteristics:

$$h_H = 7.18 \text{ ft}$$

$$M = 1.40$$

$$\alpha' = 4^\circ$$

$$A' = 5.0$$

$$\beta = 0.98$$

$$\text{cg at } \bar{c}'/4$$

Compute:

Step 1. Wing-body $C_{N\dot{\alpha}}$ (Section 7.3.4.1)

$$(C_{N\dot{\alpha}})_{WB} = [K_{W(B)} + K_{B(W)}] \left(\frac{S_e'}{S'} \right) \left(\frac{\bar{c}_e'}{\bar{c}'} \right) (C_{L\dot{\alpha}})_e + (C_{L\dot{\alpha}})_B \left(\frac{S_b}{S'} \right) \left(\frac{\bar{c}_b}{\bar{c}'} \right)$$

(equation 7.3.4.1-a)

$$(C_{N\dot{\alpha}})_{WB} = -0.485 \text{ per rad (sample problem, paragraph C, Section 7.3.4.1)}$$

Step 2. Lift-curve slope for the exposed horizontal-tail panel (Section 4.1.3.2)

$$(C_{N\dot{\alpha}})' = 4.025 \text{ per rad (sample problem, paragraph C, Section 7.4.1.1)}$$

Step 3. Tail-body interference factors (Section 4.3.1.2)

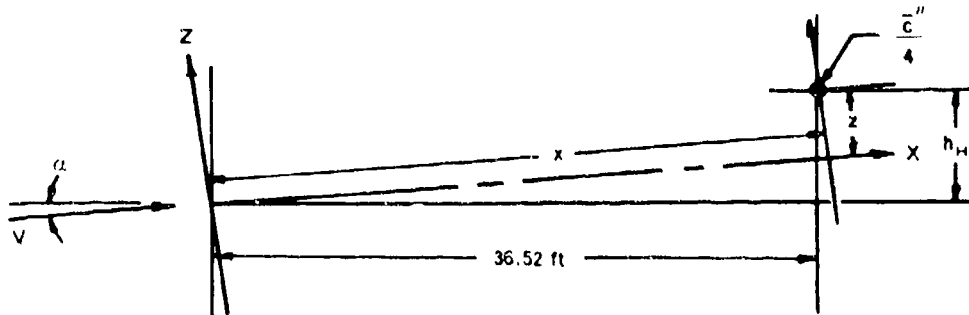
$$\left. \begin{array}{l} K_{W(B)}'' = 1.315 \\ K_{B(W)}'' = 0.4028 \end{array} \right\} \text{(sample problem, paragraph C, Section 7.4.1.1)}$$

Step 4. Dynamic pressure ratio (Section 4.4.1)

$$\frac{q''}{q_\infty} = 0.80 \text{ (sample problem, paragraph C, Section 7.4.1.1)}$$

Step 5. Downwash parameter (Section 4.4.1)

Obtain value in the plane of symmetry at $\frac{\bar{c}''}{4}$



x, y, and z referred to wind axes:

$$x = h_H \sin \alpha + (36.52) \cos \alpha = 36.93$$

$y = 0$ (plane of symmetry)

$$z = h_H \cos \alpha - (36.52) \sin \alpha = 4615$$

$$\frac{2x}{\beta b'} = 1.656$$

$$\frac{2z}{b'} = 0.2029$$

$$\frac{2y}{b'} = 0$$

$$\beta A' = 4.90$$

$$\frac{2h}{\alpha' \beta b'} = 1.0^* \quad (\text{figure 4.4.1-74a})$$

$$\left(\frac{2z}{b'} \right)_{\text{eff}} = \frac{2z}{b'} + \frac{2h}{\alpha' \beta b'} \alpha' \beta \quad (\alpha' \text{ in rad})$$

$$= 0.2029 + (1.0) (0.0684)$$

$$= 0.2713$$

$$\frac{\partial \bar{e}}{\partial \alpha} = 0.29^* \quad (\text{figure 4.4.1-76a})$$

Solution:

$$C_{L\dot{\alpha}} = (C_{L\dot{\alpha}})_{WB} + 2[K_{W(B)} + K_{B(W)}]''' \left(\frac{S_e''}{S'} \right) \left(\frac{x_{c.g.} - x''}{\bar{c}'} \right) \left(\frac{q''}{q_\infty} \right) \left(\frac{\partial \bar{e}}{\partial \alpha} \right) (C_{N\alpha})_e''$$

(equation 7.4.4.1-a)

$$= -0.485 + 2(1.315 + 0.4028) (0.0988) (2.26) (0.80) (0.29) (4.025)$$

$$= -0.485 + 0.716$$

= 0.231 per rad (based on the area and mean aerodynamic chord of the total forward panel and referred to a moment center at $\bar{c}'/4$)

REFERENCES

1. Pitts, W., Nielsen, J., and Kaettner, G.: Lift and Center of Pressure of Wing-Body-Tail Combinations at Subsonic, Transonic, and Supersonic Speeds. NACA TR 1307, 1959. (U)
2. Spreiter, J.: The Aerodynamic Forces on Slender Plane- and Cruciform-Wing and Body Combinations. NACA TR 962, 1950. (U)
3. Etkin, B.: Dynamics of Flight. John Wiley and Sons, Inc., New York, 1959. (U)

*The data obtained from figures 4.4.1-74a and 4.4.1-76a for triangular planforms have been extrapolated to $\beta A' = 4.90$. (See reference 14, Section 4.4.1.)

7.4.4.2 WING-BODY-TAIL ACCELERATION DERIVATIVE $C_{m\dot{\alpha}}$

The information contained in this section is for estimating the nondimensional acceleration derivative $C_{m\dot{\alpha}}$ of wing-body-tail combinations at low angles of attack. This derivative is the change in pitching-moment coefficient with rate of change of angle of attack and is expressed by

$$C_{m\dot{\alpha}} = \frac{\partial C_m}{\partial \left(\frac{\dot{\alpha} \bar{c}}{2V_\infty} \right)}$$

This derivative is important in longitudinal dynamics, since it is involved in the damping of the short-period mode.

The Datcom methods are based on the same assumptions that were made for the total pitching derivative $C_{L\dot{\alpha}}$ of the wing-body-tail combinations, and the general discussion of Section 7.4.4.1 is directly applicable here.

A. SUBSONIC

Two methods are presented for determining the acceleration derivative $C_{m\dot{\alpha}}$ of wing-body-tail combinations, differing only in their treatment of the effect of the flow field of the forward surface on the aft surface.

DATCOM METHODS

Method 1. ($b'/b'' \geq 1.5$)

For configurations in which the span of the forward surface is large compared to that of the aft surface, the following approach can be used. This method is to be used when the ratio of the forward-panel span to the aft-panel span is 1.5 or greater. The equation for the nondimensional acceleration derivative $C_{m\dot{\alpha}}$ of a wing-body-tail configuration, based on the area and the square of the mean aerodynamic chord of the total forward panel and referred to a moment center at the assumed center of gravity or center of rotation, is given by

$$C_{m\dot{\alpha}} = (C_{m\dot{\alpha}})_{WB} - 2[K_{W(B)} + K_{B(W)}]'' \left(\frac{S_e''}{S'} \right) \left(\frac{x_{cg} - x''}{\bar{c}} \right)^2 \left(\frac{q''}{q_\infty} \right) \left(\frac{\partial \bar{e}}{\partial \alpha} \right) (C_{L\alpha})_e''$$

7.4.4.2-a

where the primed quantities refer to the forward panel, the double-primed quantities refer to the aft panel, and the subscript e refers to the exposed panel. (See Section 4.3.1.2 for the definition of exposed surfaces.)

7.4.4.2-1

$(C_{m\dot{\alpha}})_{WB}$ is the contribution of the wing-body configuration to the acceleration derivative $C_{m\dot{\alpha}}$, obtained from Section 7.3.4.2.

$\frac{\partial \bar{e}}{\partial \alpha}$ is the downwash gradient averaged over the aft panel, obtained from Section 4.4.1.

The remaining terms are defined in paragraph A of Section 7.4.1.1.

Method 2. ($b'/b'' < 1.5$)

For configurations in which the span of the forward surface is approximately equal to or less than that of the aft surface, the vortex shed from the forward surface interacts directly with the aft surface, and the resulting interference effects must be accounted for in the tail- or aft-surface-contribution terms. This method is to be used when the ratio of the forward-panel span to the aft-panel span is less than 1.5. The equation for the nondimensional acceleration derivative $C_{m\dot{\alpha}}$ of a wing-body-tail configuration, based on the area and the square of the mean aerodynamic chord of the total forward panel and referred to a moment center at the assumed center of gravity or center of rotation, is given by

$$C_{m\dot{\alpha}} = (C_{m\dot{\alpha}})_{WB} + 2 \left(\frac{x_{cg.} - x''}{\bar{c}'} \right)^2 (C_{L\dot{\alpha}})_{W''(v)} \quad 7.4.4.2-b$$

All the above terms are defined in paragraph A of Section 7.4.1.1 and method 1 above.

Because of the similarity of the two methods a sample problem for method 2 is not included. However, evaluation of the term $(C_{L\dot{\alpha}})_{W''(v)}$ for a wing-body-tail configuration is presented in Section 4.5.1.1.

Sample Problem

Method 1

Given: Same configuration as sample problems of paragraph A, Sections 7.4.1.1, 7.4.1.2, and 7.4.4.1. Some of the characteristics are repeated below.

The following ratios based on total forward-panel dimensions:

$$\frac{\bar{c}''}{\bar{c}'} = 2.26 \quad \frac{S_e''}{S'} = 0.0988$$

Additional Characteristics:

$$M = 0.60 \quad \beta = 0.80 \quad \alpha' = 4^\circ \quad cg \text{ at } \bar{c}'/4$$

Compute:

Step 1 Wing-body $C_{m\dot{\alpha}}$ (Section 7.3.4.2)

$$(C_{m\dot{\alpha}})_{WB} = [K_{W(B)} + K_{B(W)}]'' \left(\frac{S_e}{S'} \right) \left(\frac{\bar{c}_e}{\bar{c}'} \right)^2 (C_{m\dot{\alpha}})_e' + (C_{m\dot{\alpha}})_B \left(\frac{S_b}{S'} \right) \left(\frac{\bar{c}_b}{\bar{c}'} \right)^2$$

(equation 7.3.4.2-a)

$$(C_{m\dot{\alpha}})_{WB} = -0.400 \text{ per rad} \text{ (sample problem, paragraph A, Section 7.3.4.2)}$$

Step 2. Lift-curve slope for the exposed horizontal-tail panel (Section 4.1.3.2)

$$(C_L\dot{\alpha})_e'' = 4.0 \text{ per rad} \text{ (sample problem, paragraph A, Section 7.4.1.1)}$$

Step 3. Tail-body interference factors (Section 4.3.1.2)

$$\left. \begin{array}{l} K_{W(B)}'' = 1.315 \\ K_{B(W)}'' = 0.550 \end{array} \right\} \text{ (sample problem, paragraph A, Section 7.4.1.1)}$$

Step 4. Dynamic pressure ratio (Section 4.4.1)

$$\frac{q''}{q_\infty} = 0.901 \text{ (sample problem, paragraph A, Section 7.4.1.1)}$$

Step 5. Downwash parameter (Section 4.4.1)

$$\frac{\partial \bar{\epsilon}}{\partial \alpha} = 0.513 \text{ (sample problem, paragraph A, Section 7.4.4.1)}$$

Solution:

$$C_{m\dot{\alpha}} = (C_{m\dot{\alpha}})_{WB} - 2[K_{W(B)} + K_{B(W)}]'' \left(\frac{S_e''}{S'} \right) \left(\frac{x_{c.g.} - x''}{\bar{c}'} \right)^2 \left(\frac{q''}{q_\infty} \right) \left(\frac{\partial \bar{\epsilon}}{\partial \alpha} \right) (C_L\dot{\alpha})_e''$$

(equation 7.4.4.2-a)

$$= -0.400 - 2(1.315 + 0.550)(0.0988)(2.26)^2(0.901)(0.513)(4.0)$$

$$= -0.400 - 3.48$$

$$= -3.88 \text{ per rad} \text{ (based on the area and the square of the mean aerodynamic chord of the total forward panel and referred to a moment center at } \bar{c}'/4)$$

B. TRANSONIC

The comments of paragraph B of Section 7.4.4.1 are directly applicable here.

DATCOM METHODS

It is recommended that the methods presented in paragraph A above be applied to the transonic speed regime. Care should be taken to estimate the parameters of equations 7.4.4.2-a and -b at the appropriate Mach number. The interference "K" factors should be obtained from paragraph C, Section 4.3.1.2.

C. SUPERSONIC

The comments of paragraph C of Section 7.4.4.1 are directly applicable here.

DATCOM METHODS

The methods presented in paragraph A above are also applicable to the supersonic speed range. Care should be taken to estimate the parameters of equations 7.4.4.2-a and -b at the appropriate Mach number. Method 3 of paragraph C of Section 4.4.1 should be used to evaluate the last term of equation 7.4.4.2-b.

Sample Problem

Method 1

Given: Same configuration as sample problems of paragraph C, Sections 7.4.1.1, 7.4.1.2, and 7.4.4.1, and paragraph A of this section. Some of the characteristics are repeated below.

The following ratios based on total forward-panel dimensions:

$$\frac{\ell''}{\bar{c}'} = 2.26 \quad \frac{S_e''}{S'} = 0.0988$$

Additional Characteristics:

$$M = 1.4 \quad \beta = 0.98 \quad \alpha' = 4^\circ \quad cg \text{ at } \bar{c}'/4$$

Compute:

Step 1. Wing-body $C_{m\dot{\alpha}}$ (Section 7.3.4.2)

$$(C_{m\dot{\alpha}})_{WB} = [K_{W(B)} + K_{B(W)}] \left(\frac{S_e}{S'} \right) \left(\frac{\bar{c}_e'}{\bar{c}'} \right)^2 (C_{m\dot{\alpha}})_e + (C_{m\dot{\alpha}})_B \left(\frac{S_b}{S'} \right) \left(\frac{\ell_b}{\bar{c}'} \right)^2$$

(equation 7.3.4.2-a)

$$(C_m \dot{\alpha})_{WB} = 1.308 \text{ per rad (sample problem, paragraph C, Section 7.3.4.2)}$$

Step 2. Lift-curve slope for the exposed horizontal-tail panel (Section 4.1.3.2)

$$(C_N \alpha)_e'' = 4.025 \text{ per rad (sample problem, paragraph C, Section 7.4.1.1)}$$

Step 3. Tail-body interference factors (Section 4.3.1.2)

$$\left. \begin{array}{l} K_{W(B)}'' = 1.315 \\ K_{B(W)}'' = 0.4028 \end{array} \right\} \text{(sample problem, paragraph C, Section 7.4.1.1)}$$

Step 4. Dynamic pressure ratio (Section 4.4.1)

$$\frac{q''}{q_\infty} = 0.80 \text{ (sample problem, paragraph C, Section 7.4.1.1)}$$

Step 5. Downwash parameter (Section 4.4.1)

$$\frac{\partial \bar{\epsilon}}{\partial \alpha} = 0.29 \text{ (sample problem, paragraph C, Section 7.4.4.1)}$$

Solution:

$$C_m \dot{\alpha} = (C_m \dot{\alpha})_{WB} - 2[K_{W(B)} + K_{B(W)}]'' \left(\frac{S_e''}{S'} \right) \left(\frac{x_{c.g.} - x''}{\bar{c}'} \right)^2 \left(\frac{q''}{q_\infty} \right) \left(\frac{\partial \bar{\epsilon}}{\partial \alpha} \right) (C_N \alpha)_e''$$

(equation 7.4.4.2-a)

$$= 1.308 - 2(1.315 + 0.4028)(0.0988)(2.26)^2(0.80)(0.29)(4.025)$$

$$= 1.308 - 1.619$$

= -0.31 per rad (based on the area and the square of the mean aerodynamic chord of the total forward panel and referred to a moment center at $\bar{c}'/4$)

7.4.4.3 WING-BODY-TAIL DERIVATIVE $C_{D\dot{\alpha}}$

This section presents a method for estimating the wing-body-tail derivative $C_{D\dot{\alpha}}$ at subsonic speeds. This derivative is the change in the drag coefficient due to a change in $\dot{\alpha}$ at a constant pitch rate and is defined as

$$C_{D\dot{\alpha}} = \frac{\partial C_D}{\partial \left(\frac{\dot{\alpha}c}{2V} \right)}, \text{ where } C_D \text{ is based on } S_W.$$

In general, this derivative is small and has a negligible effect on longitudinal stability; hence, it is usually neglected.

A. SUBSONIC

The wing contribution to $C_{D\dot{\alpha}}$ can be estimated using unsteady-flow theory. The body contribution is small and has been neglected. The tail contribution is computed from conventional downwash-lag theory. The horizontal-tail lift due to $\dot{\alpha}$ was taken to act normal to the local flow direction at the tail, to produce a force component in the direction of the free-stream.

DATCOM METHOD

The wing-body-tail derivative is given by

$$C_{D\dot{\alpha}} = \left(C_{D\dot{\alpha}} \right)_W + \left(C_{D\dot{\alpha}_0} \right)_H + \left(\frac{\partial C_D}{\partial \alpha_F} \right)_H \alpha_F \quad 7.4.4.3-a$$

where

$\left(C_{D\dot{\alpha}} \right)_W$ is the wing contribution to $C_{D\dot{\alpha}}$ obtained from Section 7.1.4.3.

$\left(C_{D\dot{\alpha}_0} \right)_H$ is the horizontal-tail contribution independent of angle of attack, obtained by

$$\left(C_{D\dot{\alpha}_0} \right)_H = \frac{1}{57.3} C_{L\alpha_H} \frac{S_H}{S_W} \frac{(\ell_H \cos \alpha_F + z_H \sin \alpha_F)}{\bar{c}/2} \frac{\partial \epsilon}{\partial \alpha} (2\epsilon_0 - i_H) \quad 7.4.4.3-b$$

where

$C_{L\alpha_H}$ is the horizontal-tail lift-curve slope (based on S_H) obtained from test data or from Section 4.1.3.2 (per degree).

S_H is the horizontal-tail reference area.

S_W is the wing reference area.

ℓ_H is the distance from the moment reference center to the center-of-pressure location of the horizontal stabilizer, measured parallel to the body center line. For Datcom purposes, the horizontal-tail center-of-pressure location is assumed to be at the quarter-chord point of the MAC of the total added panel.

z_H is the distance from the moment reference center to the center-of-pressure location of the horizontal stabilizer, measured normal to the body center line, positive for the stabilizer above the body. For Datcom purposes, the horizontal-tail center-of-pressure location is assumed to be at the quarter-chord point of the MAC of the total added panel.

α_F is the fuselage angle of attack.

$\frac{\partial \epsilon}{\partial \alpha}$ is the downwash gradient at $\bar{c}/4$ of the horizontal tail, obtained from test data or from Section 4.4.1.

\bar{c} is the wing MAC.

ϵ_0 is the downwash angle at $\bar{c}/4$ of the horizontal tail at $\alpha_F = 0$.

i_H is the horizontal-tail incidence with respect to the fuselage reference line.

$\left(\frac{\partial C_{D_\alpha}}{\partial \alpha} \right)_H$ is the change in horizontal-tail contribution with angle of attack, obtained by

$$\left(\frac{\partial C_{D_\alpha}}{\partial \alpha} \right)_H = \frac{1}{57.3} C_{L_{\alpha_H}} \frac{S_H}{S_W} \frac{(\ell_H \cos \alpha_F + z_H \sin \alpha_F)}{\bar{c}/2} \frac{\partial \epsilon}{\partial \alpha} \left(2 \frac{\partial \epsilon}{\partial \alpha} - 1 \right) \quad 7.4.4.3-c$$

where all of the terms are defined above.

Sample Problem

Given: Same configuration as sample problem of Paragraph A of Section 7.1.4.3.

Tail Characteristics:

$$C_{L_{\alpha_H}} = 0.05 \text{ per deg} \quad S_H = 16 \text{ ft}^2$$

$$\ell_H = 8 \text{ ft} \quad z_H = 0 \quad \frac{\partial \epsilon}{\partial \alpha} = 0.32$$

$$\epsilon_0 = 1^\circ \quad i_H = 0$$

Compute:

$$\left(C_{D_{\alpha_0}} \right)_H = \frac{1}{57.3} C_{L_{\alpha_H}} \frac{S_H}{S_W} \frac{(\ell_H \cos \alpha_F + z_H \sin \alpha_F)}{\bar{c}/2} \frac{\partial \epsilon}{\partial \alpha} (2 \epsilon_0 - i_H) \quad (\text{Equation 7.4.4.3-b})$$

$$= \left(\frac{1}{57.3} \right) (0.05) \left(\frac{16.0}{64.0} \right) \frac{[(8.0)(0.9998) + 0]}{4/2} (0.32)[2(1.0) - 0] \\ = 0.000558$$

$$\left(\frac{\partial C_{D\dot{\alpha}}}{\partial \alpha_F} \right)_H = \frac{1}{57.3} C_{L_{\alpha_H}} \frac{S_H}{S_W} \frac{(\ell_H \cos \alpha_F + z_H \sin \alpha_F)}{c/2} \frac{\partial \epsilon}{\partial \alpha} \left(2 \frac{\partial \epsilon}{\partial \alpha} - 1 \right) \quad (\text{Equation 7.4.4.3-c}) \\ = \left(\frac{1}{57.3} \right) (0.05) \left(\frac{16.0}{64.0} \right) \frac{[(8.0)(0.9998) + 0]}{4/2} (0.32)[2(0.32) - 1] \\ = -0.000100$$

Solution:

$$C_{D\dot{\alpha}} = \left(C_{D\dot{\alpha}} \right)_W + \left(C_{D\dot{\alpha}_0} \right)_H + \left(\frac{\partial C_{D\dot{\alpha}}}{\partial \alpha_F} \right)_H \alpha_F \quad (\text{Equation 7.4.4.3-a}) \\ \left(C_{D\dot{\alpha}} \right)_W = 0.0085 \text{ per deg} \quad (\text{Sample Problem, Paragraph A, Section 7.1.4.3}) \\ C_{D\dot{\alpha}} = 0.0085 + 0.000558 + (-0.000100) 1.0 \\ = 0.00896 \text{ per degree}$$

B. TRANSONIC

No method is presented.

C. SUPERSONIC

No method is presented.

7.4.4.4 WING-BODY-TAIL DERIVATIVE $C_{Y\dot{\beta}}$

This section presents a method for estimating the contribution of the vertical tail, in the presence of the wing and body, to the derivative $C_{Y\dot{\beta}}$ at subsonic speeds. This derivative is the change in side-force coefficient with variations in the rate of change of sideslip angle at a constant yaw rate and is defined as

$$C_{Y\dot{\beta}} = \frac{\partial C_Y}{\partial \left(\frac{\dot{\beta} b}{2V} \right)}, \text{ where } C_Y \text{ is based on } S_W.$$

In general, at low to moderate angles of attack, this derivative is small and has a negligible effect on lateral stability; hence, it is usually neglected.

A. SUBSONIC

A wing contribution to $C_{Y\dot{\beta}}$ can be evaluated by using unsteady-flow theory, but at low to moderate angles of attack it is generally considered small and is neglected. At low angles of attack and for attached-flow conditions, the largest contributor to $C_{Y\dot{\beta}}$ is the vertical tail. The method herein applies a sidewash-lag theory in an analogous manner to the downwash-lag theory that is used in finding the horizontal-tail contribution to $C_{L\dot{\alpha}}$. The body contribution is small and has been neglected.

For a brief discussion of the physical flow phenomena at high angles of attack, i.e., leading-edge vortex sheets and flow separation, and a comprehensive bibliography on related subject matter, the reader is referred to Reference 1.

DATCOM METHOD

Design charts for predicting the change of wing sidewash angle with the change of sideslip angle are presented as a function of wing geometry, i.e., aspect ratio, sweep, and taper ratio, at Mach numbers 0.2 and 0.8. These design charts were generated from wing loadings in sideslip by using the theory presented in References 2 and 3.

The vertical-tail contribution to the derivative $C_{Y\dot{\beta}}$ at low to moderate angles of attack is given by

$$C_{Y\dot{\beta}} = 2 C_{L_{\alpha_V}} \sigma_\beta \frac{S_V}{S_W} \frac{(l_p \cos \alpha_F + z_p \sin \alpha_F)}{b_W} \quad 7.4.4.4-a$$

where

$C_{L_{\alpha_V}}$ is the lift-curve slope of the vertical tail obtained from test data or Section 4.1.3.2.

σ_β is the change of sidewash angle (due only to the wing, i.e., no sidewash due to fuselage cross flow) with respect to the change in the sideslip angle. This factor can be estimated by

$$\sigma_{\beta} = \sigma_{\beta_{\alpha}} \alpha_F + \frac{\sigma_{\beta_{\Gamma}}}{57.3} \Gamma - \sigma_{\beta_{\theta}} \theta + \sigma_{\beta_{WB}} \quad 7.4.4.4-b^*$$

where

$\sigma_{\beta_{\alpha}}$ is the sidewash contribution due to angle of attack, obtained from Figures 7.4.4.4-6a through -6p as a function of $\frac{z_V}{b/2}$ and wing geometry. z_V is the distance between the wing $\bar{c}/4$ point and the vertical-stabilizer center-of-pressure location, measured normal to the free-stream direction. For Datcom purposes the vertical-tail center-of-pressure location is assumed to be at the quarter-chord point of the MAC of the total added panel.

$$z_V = z_p \cos \alpha_F - l_p \sin \alpha_F \quad 7.4.4.4-c$$

where z_p and l_p are defined below.

α_F is the fuselage angle of attack in degrees.

$\sigma_{\beta_{\Gamma}}$ is the sidewash contribution due to wing dihedral, obtained from Figures 7.4.4.4-22a through -22d as a function of $\frac{z_V}{b/2}$ and wing geometry.

Γ is the wing dihedral in degrees.

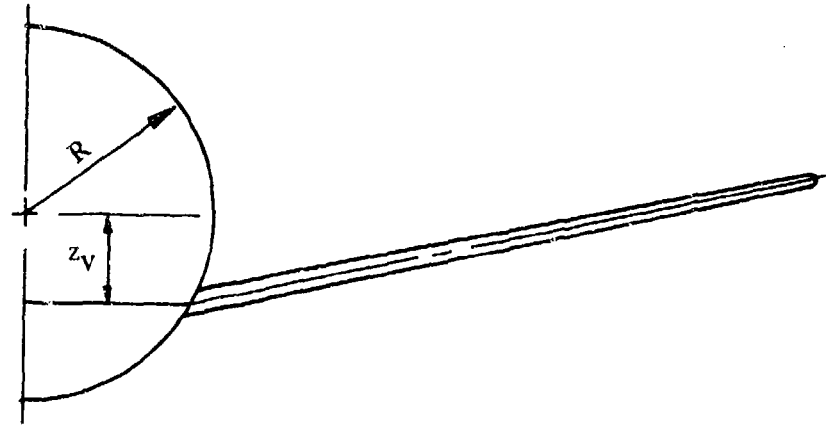
$\sigma_{\beta_{\theta}}$ is the sidewash contribution due to wing twist, obtained from Figures 7.4.4.4-26a through -26p as a function of $\frac{z_V}{b/2}$ and wing geometry.

θ is the wing twist in degrees between the root and tip sections, negative for washout (see Figure 5.1.2.1-30b).

$\sigma_{\beta_{WB}}$ is the sidewash contribution due to the body effect on the wing loading. It is presented as a function of $\frac{z_V}{b/2}$ and wing geometry, at three different body-radius-to-wing-span ratios of 0.06, 0.12, and 0.24. In addition, the wing position on the body has an effect on this term. However, for Datcom considerations a low-wing position was assumed as shown in Sketch (a). For a high-wing position as shown in Sketch (b), the sign of $\sigma_{\beta_{WB}}$ in Figures 7.4.4.4-42a through -42p becomes negative.

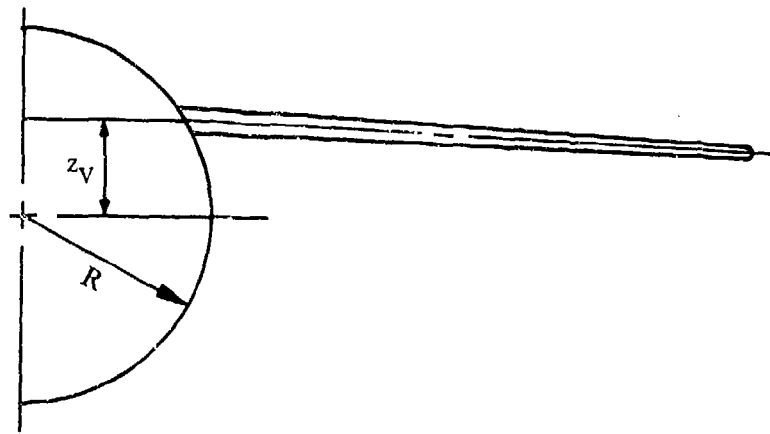
*A more accurate result can be obtained from the equation

$$\sigma_{\beta} = \frac{1}{S_V} \int_0^{b_V} \sigma_{\beta_{local}} c_V dz$$



SKETCH (a)

high-wing position as shown in sketch (b), the sign of $\sigma_{\beta WB}$ in Figures 7.4.4.4-42a through -42p becomes negative.



SKETCH (b)

- S_V is the vertical-tail area, consistent with the vertical-tail area used to define $C_{L_{\alpha_V}}$.
- S_W is the wing reference area.
- ℓ_p is the distance from the wing quarter-chord point to the center-of-pressure location of the vertical stabilizer, measured parallel to the body center line. For Datcom purposes, the vertical-tail center-of-pressure location is assumed to be at the quarter-chord point of the MAC of the total added panel. (See Sketch (a) of Section 7.4.2.1.)
- z_p is the distance from the wing quarter-chord point to the center-of-pressure location of the vertical stabilizer, measured normal to the body center line, positive for the stabilizer above the body. For Datcom purposes, the vertical-tail center-of-pressure location is assumed to be at the quarter-chord point of the MAC of the total added panel.
- b_W is the wing span.

Sample Problem

Given: The following wing-body-tail configuration

Wing Characteristics:

$$\begin{array}{lll} A = 7 & \lambda = 0.25 & \Lambda_{LE} = 35^\circ \quad \text{Low wing} \\ S_W = 3500 \text{ ft}^2 & b_W = 156.52 \text{ ft} & \theta = -5^\circ \quad \Gamma = 3^\circ \end{array}$$

Vertical-Tail Characteristics:

$$C_{L_{\alpha_V}} = 0.055 \text{ per deg} \quad S_V = 600 \text{ ft}^2$$

$$\frac{z_V}{b/2} = 0.242$$

Additional Characteristics:

$$\begin{array}{lll} \ell_p = 60.0 \text{ ft} & z_p = 20.0 \text{ ft} & \alpha_F = 1^\circ \\ M = 0.8 & \frac{\text{Body Radius}}{b/2} = 0.12 & \end{array}$$

Compute:

Determine σ_β

$$\sigma_\beta = \sigma_{\beta_\alpha} \alpha_F + \frac{\sigma_{\beta_\Gamma}}{57.3} \Gamma - \sigma_{\beta_\theta} \theta + \sigma_{\beta_{WB}} \quad (\text{Equation 7.4.4.4-b})$$

$$\sigma_{\beta_\alpha} = -0.013 \quad (\text{Figure 7.4.4.4-6l})$$

$$\sigma_{\beta_\Gamma} = -0.56 \quad (\text{Figure 4.4.4.4-22d})$$

$$\sigma_{\beta_\theta} = -0.0113 \quad (\text{Figure 7.4.4.4-26l})$$

$$\sigma_{\beta_{WB}} = 0.07 \quad (\text{Figure 7.4.4.4-42l})$$

$$\begin{aligned}\sigma_\beta &= (-0.013)(1) + \left(\frac{-0.56}{57.3}\right) 3 - (-0.0113)(-5) + (0.07) \\ &= -0.013 - 0.0293 - 0.0565 + 0.07 \\ &= -0.0288\end{aligned}$$

Solution:

$$\begin{aligned}C_{Y\dot{\beta}} &= 2 C_{L_{qV}} \sigma_\beta \frac{S_V}{S_W} \frac{(l_p \cos \alpha_F + z_p \sin \alpha_F)}{b_W} \quad (\text{Equation 7.4.4.4-a}) \\ &= 2(0.055)(-0.0288) \frac{600}{3500} \left[\frac{(60)(0.9998) + (20)(0.01745)}{156.52} \right] \\ &= -0.000209 \text{ per deg}\end{aligned}$$

B. TRANSONIC

No method is presented.

C. SUPERSONIC

No method is presented.

REFERENCES

1. Coe, P. L., Jr., Graham, A. B., and Chambers, J. R.: Summary of Information on Low-Speed Lateral-Directional Derivatives Due to Rate of Change of Sideslip $\dot{\beta}$. NASA TN D-7972, 1975. (U)
2. De Young, J., and Harper, C. W.: Theoretical Symmetric Span Loading at Subsonic Speeds for Wings Having Arbitrary Planform. NACA TR 921, 1948. (U)
3. Queijo, M. J.: Theoretical Span Loading Distribution and Rolling Moments for Sideslipping Wings of Arbitrary Planform in Incompressible Flow. NACA TR 1269, 1956. (U)

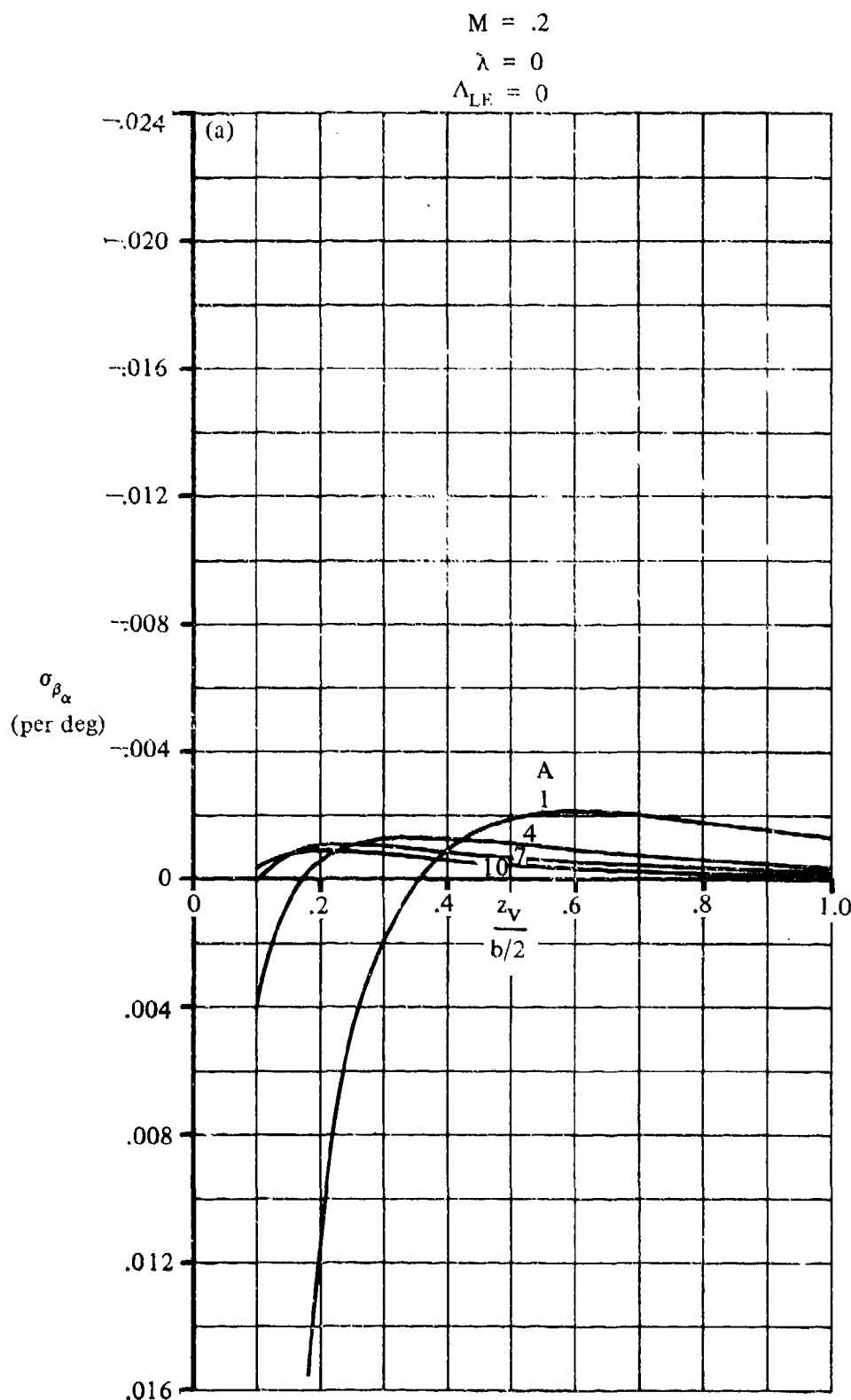


FIGURE 7.4.4.4-6 SIDEWASH CONTRIBUTION DUE TO ANGLE OF ATTACK

7.4.4.4-6

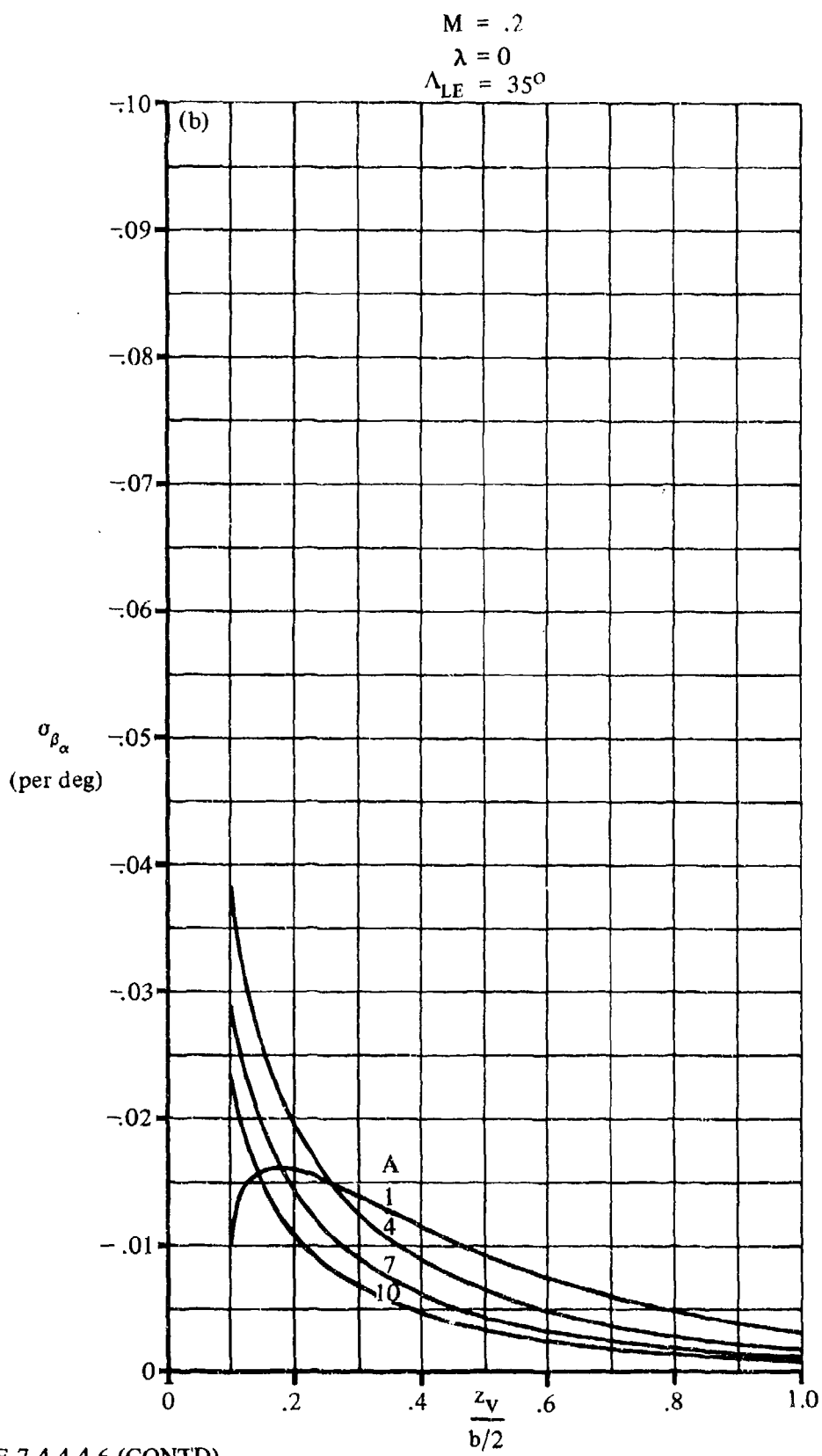


FIGURE 7.4.4.4-6 (CONTD)

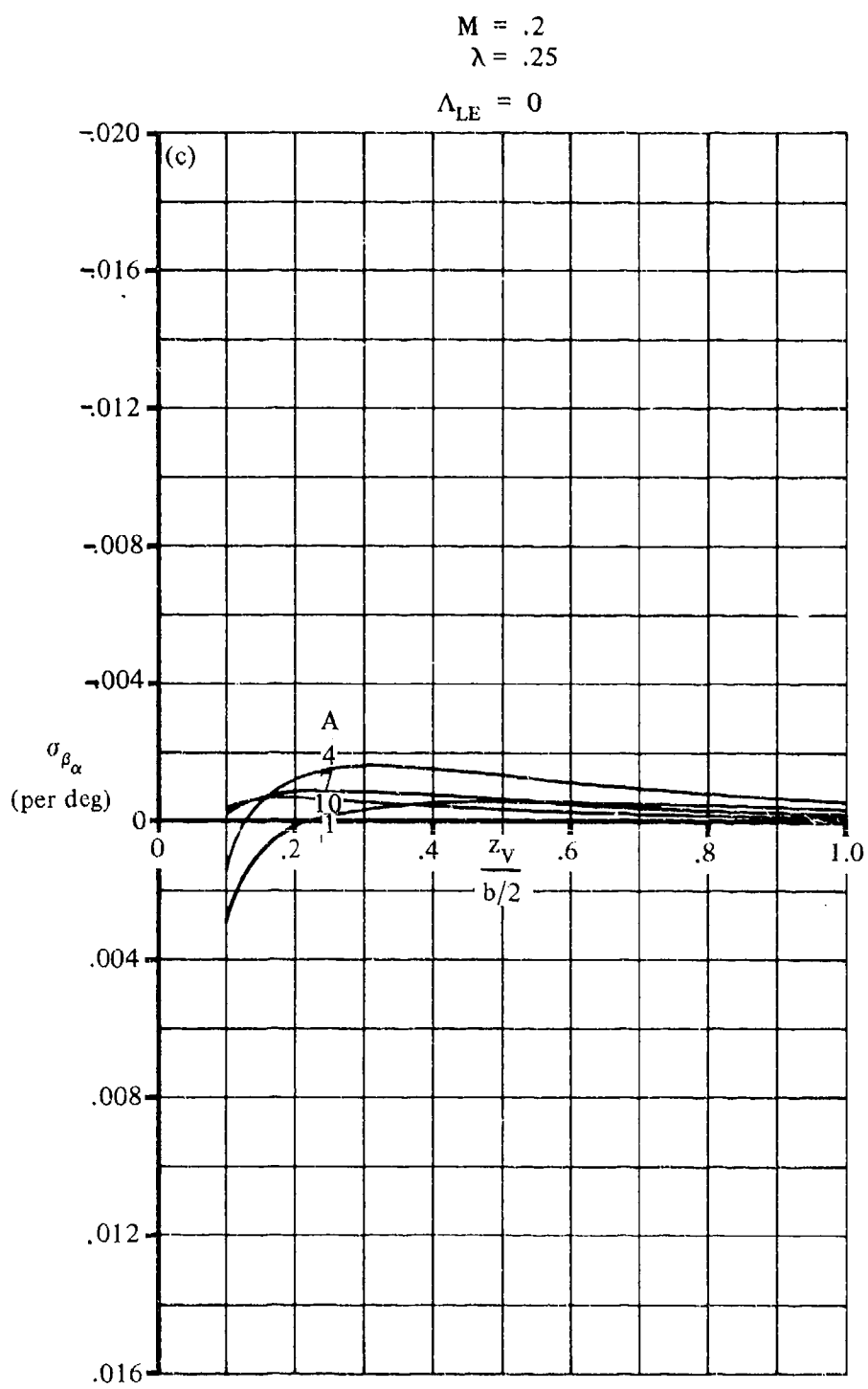


FIGURE 7.4.4.4-6 (CONTD)

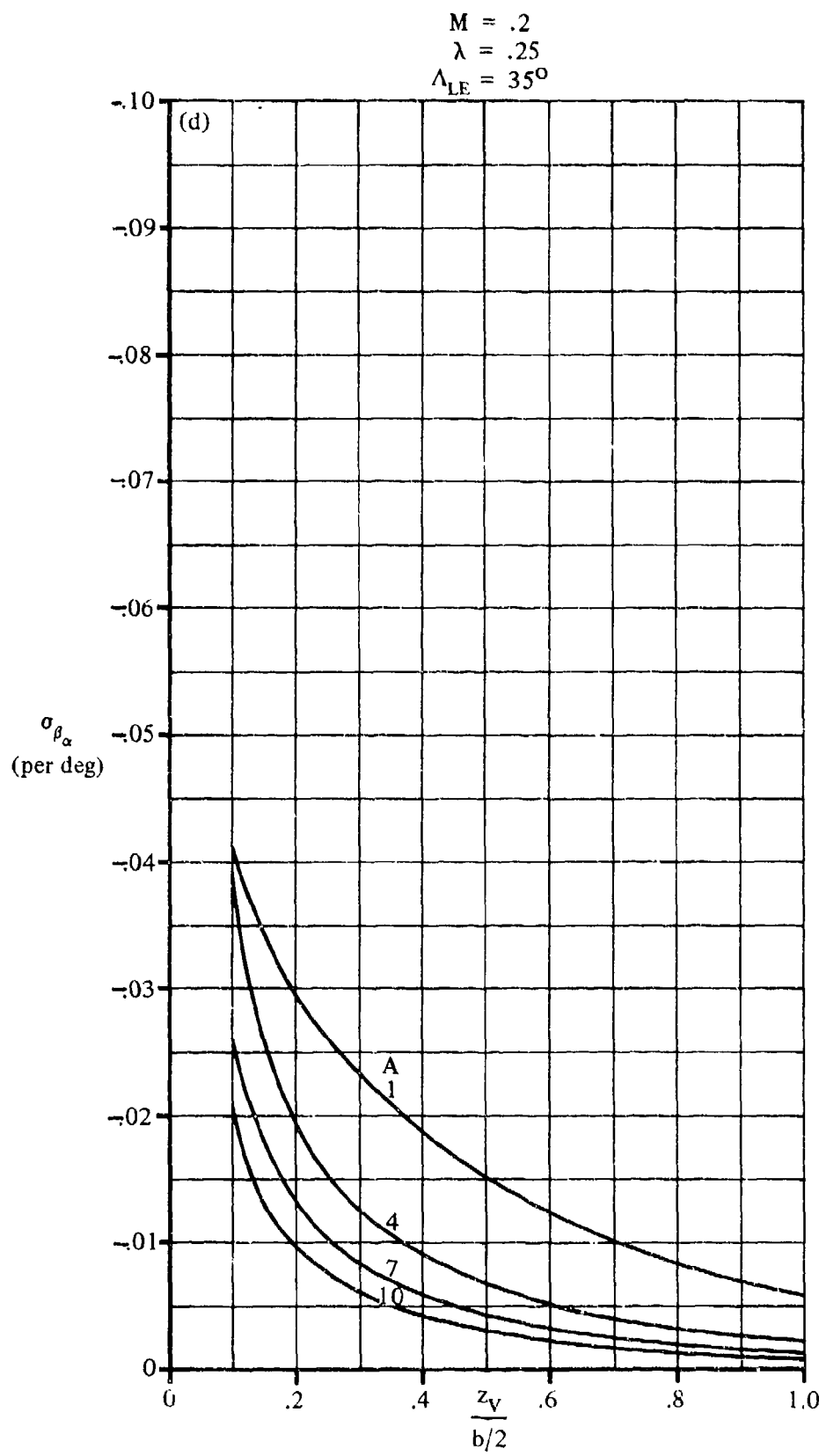


FIGURE 7.4.4.4-6 (CONTD)

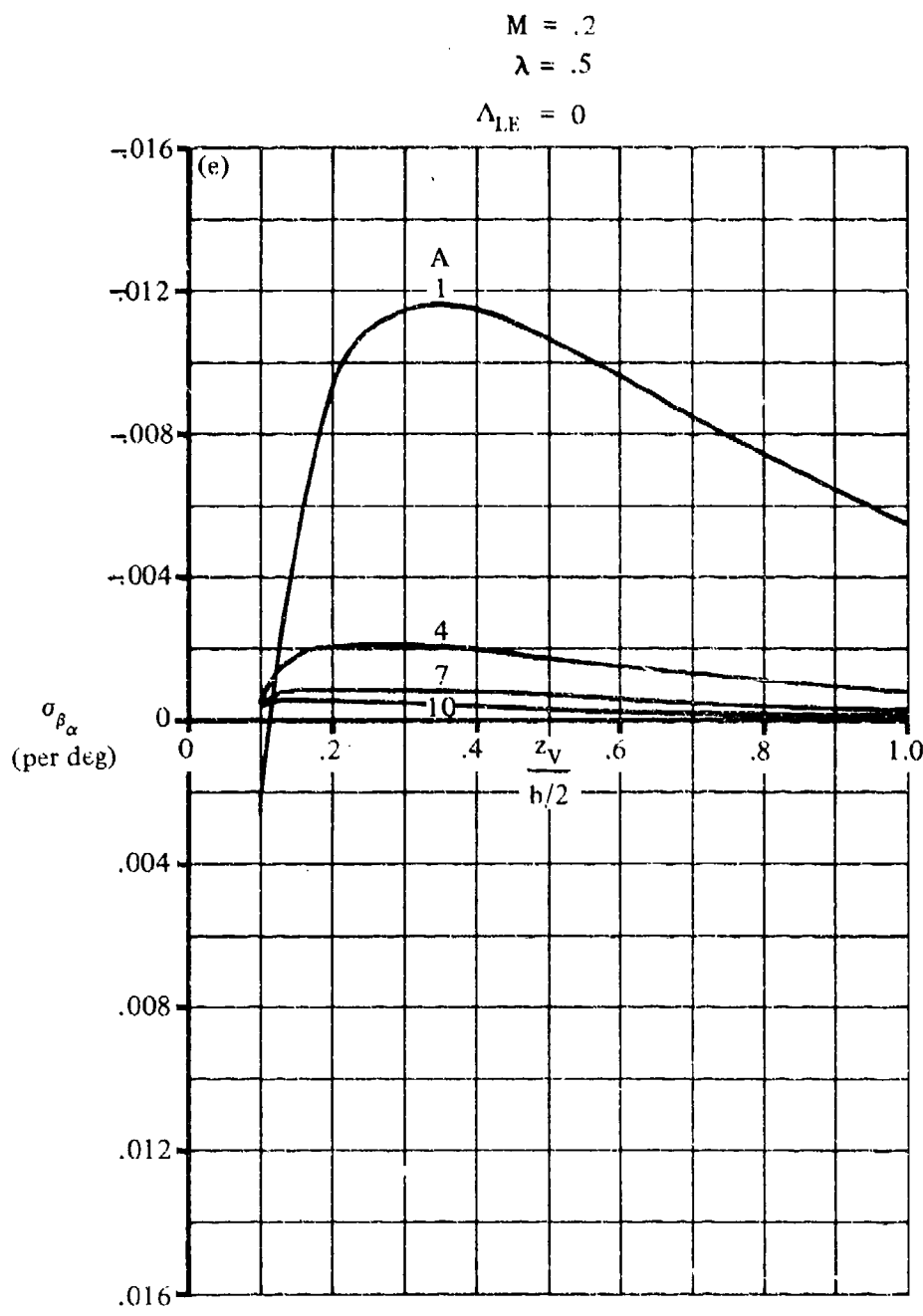


FIGURE 7.4.4.4-6 (CONT'D)

7.4.4.4-10

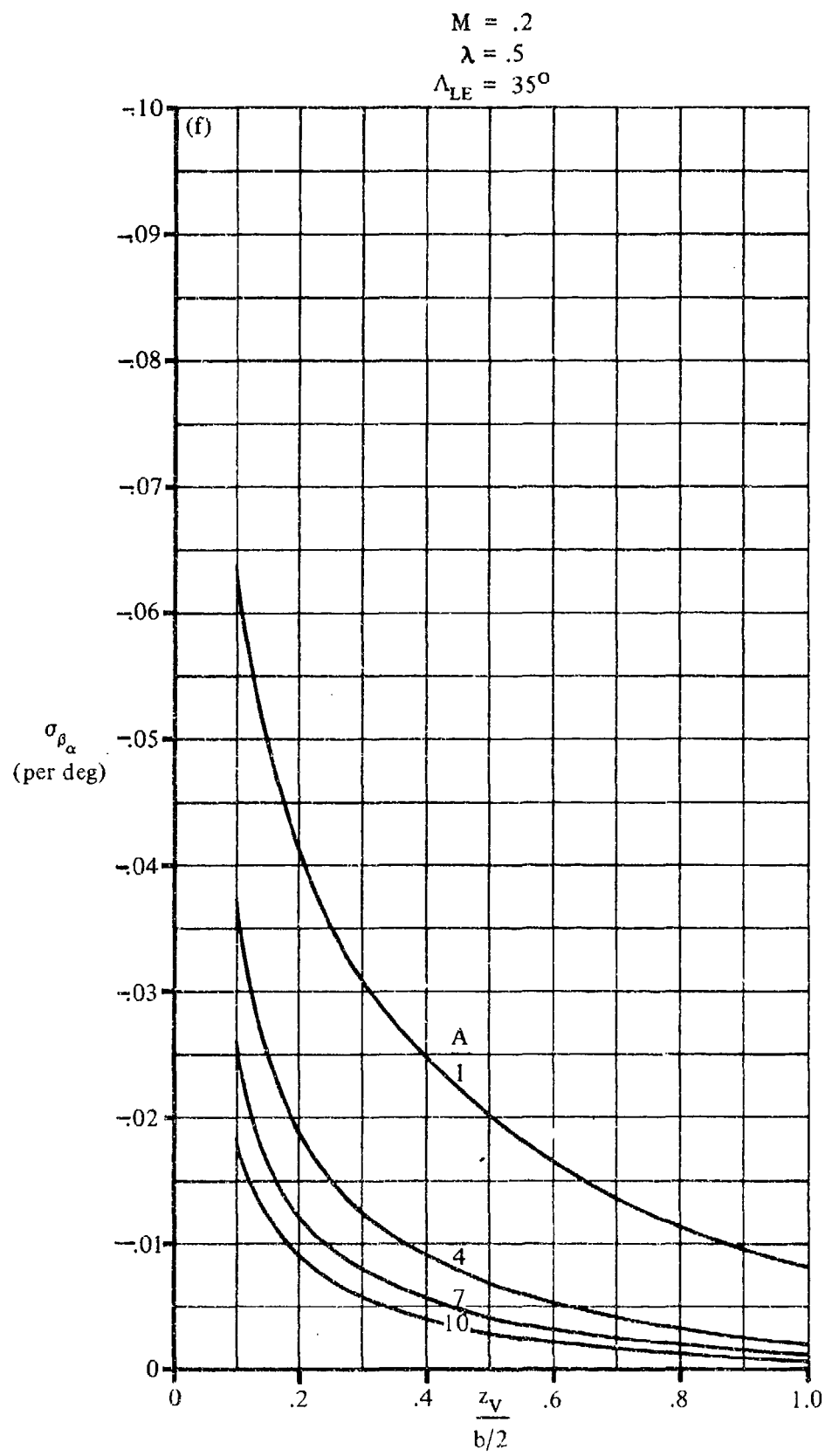


FIGURE 7.4.4.4-6 (CONTD)

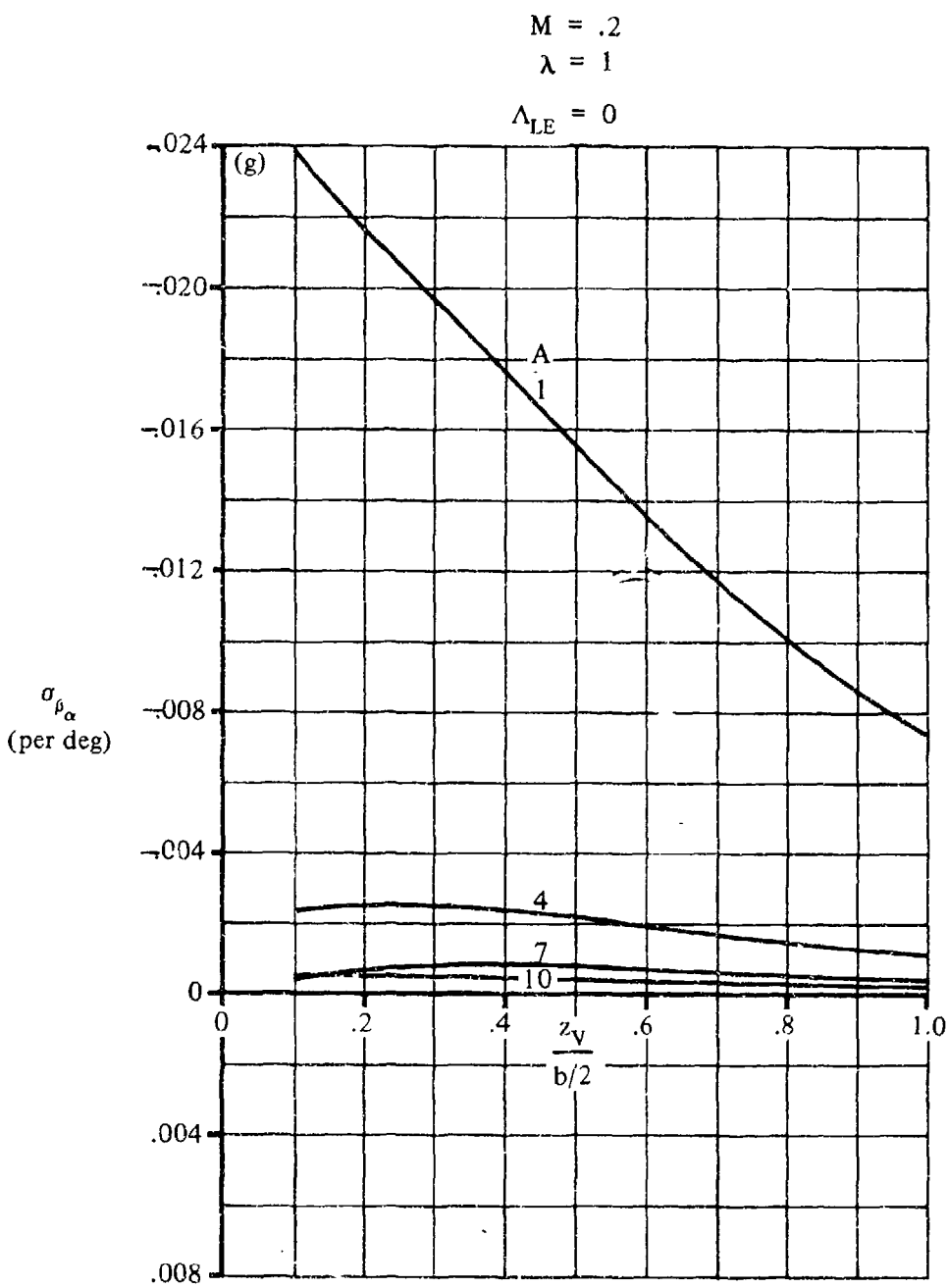


FIGURE 7.4.4.4-6 (CONTD)

7.4.4.4-12

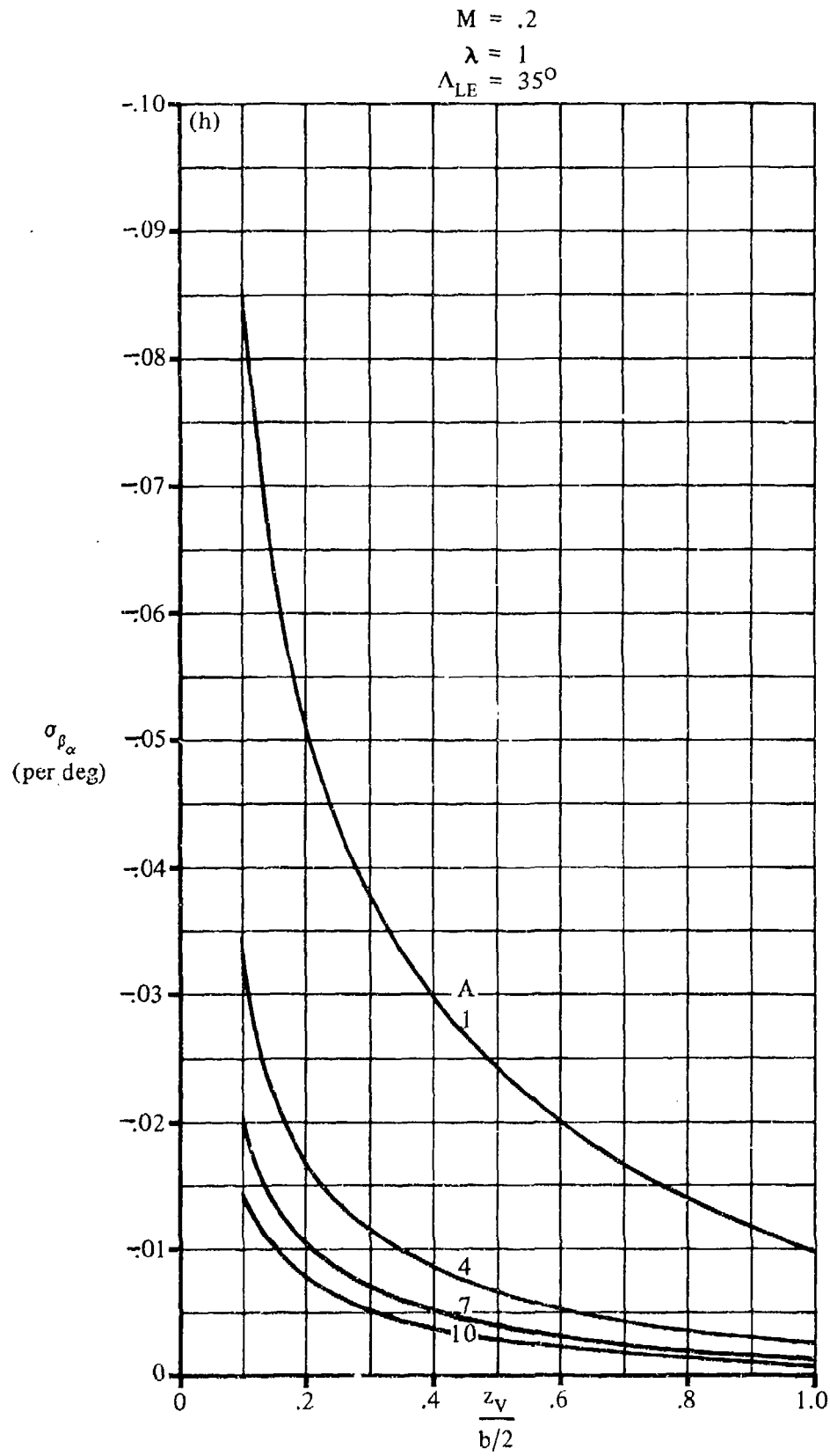


FIGURE 7.4.4.4-6 (CONTD)

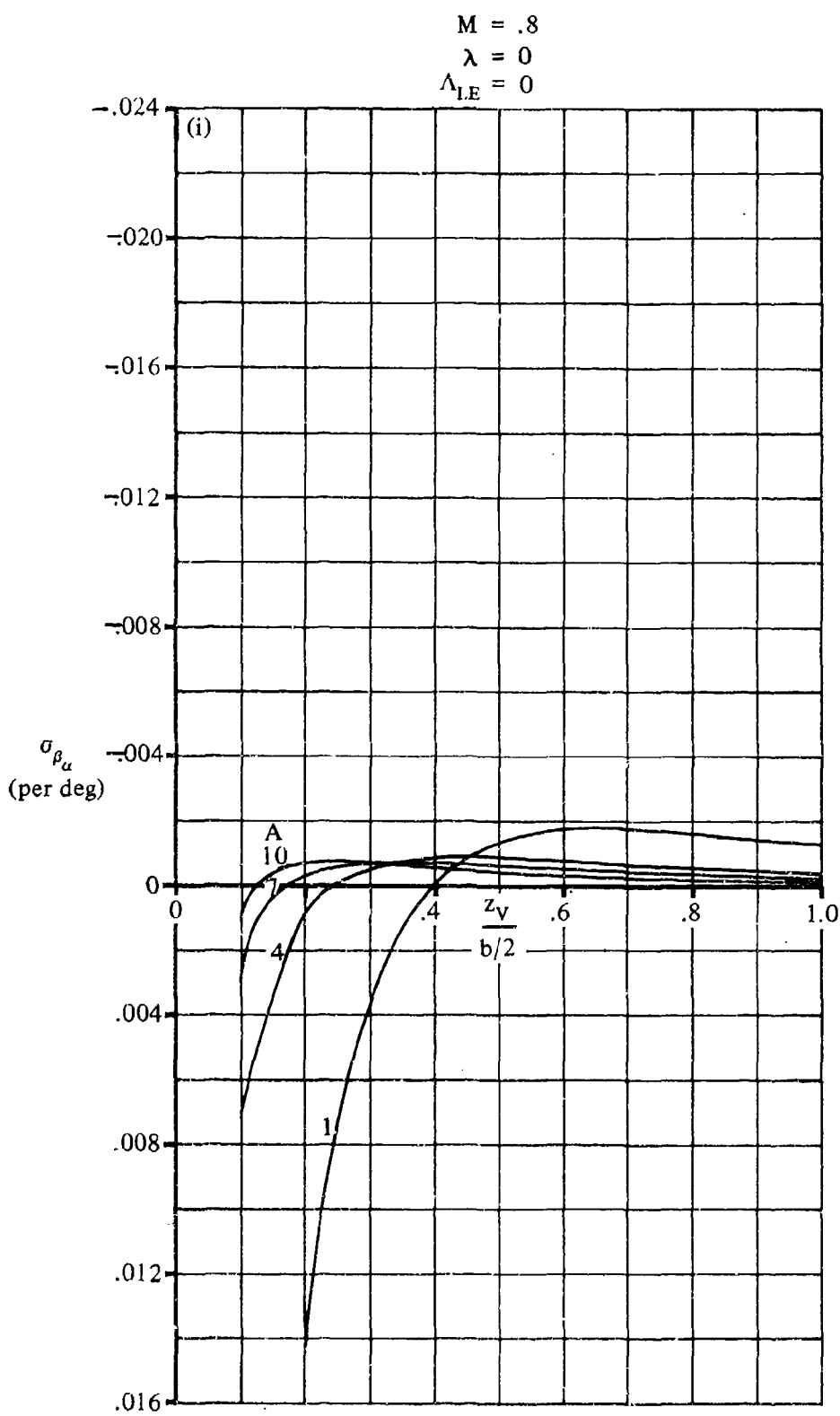


FIGURE 7.4.4.6 (CONT'D)

7.4.4.4-14

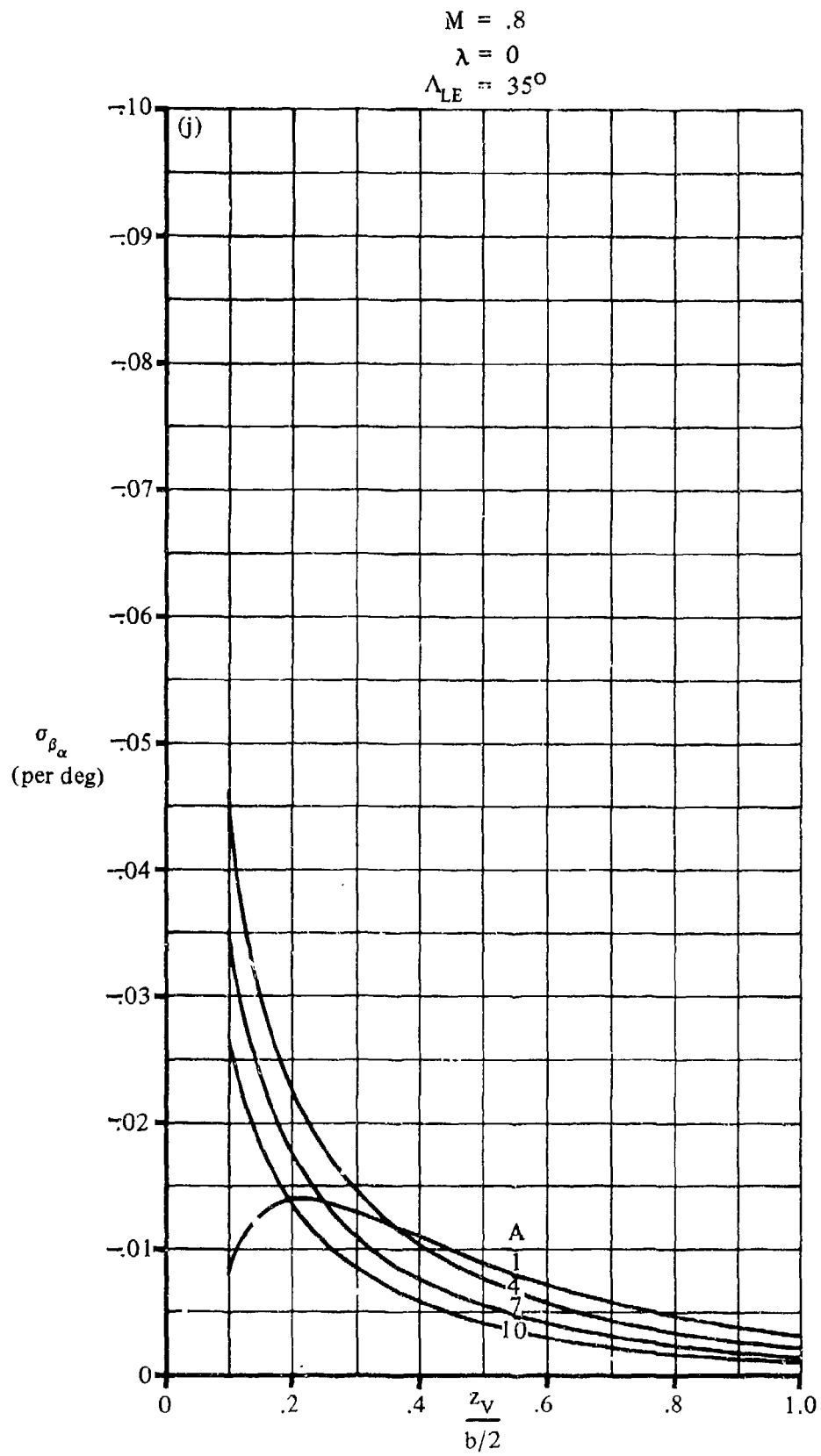


FIGURE 7.4.4.4-6 (CONTD)

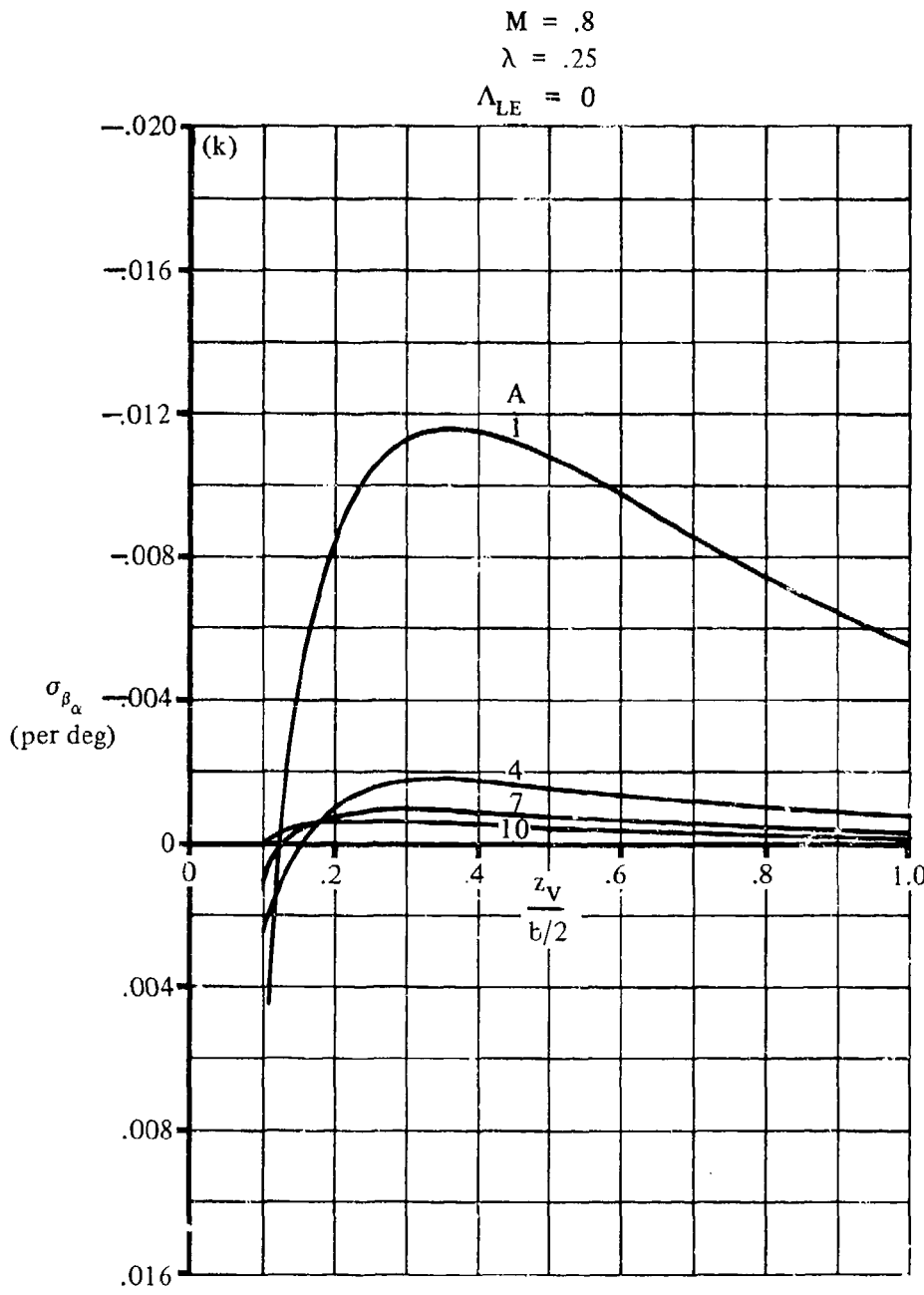


FIGURE 7.4.4.4-6 (CONTD)

7.4.4.4-16

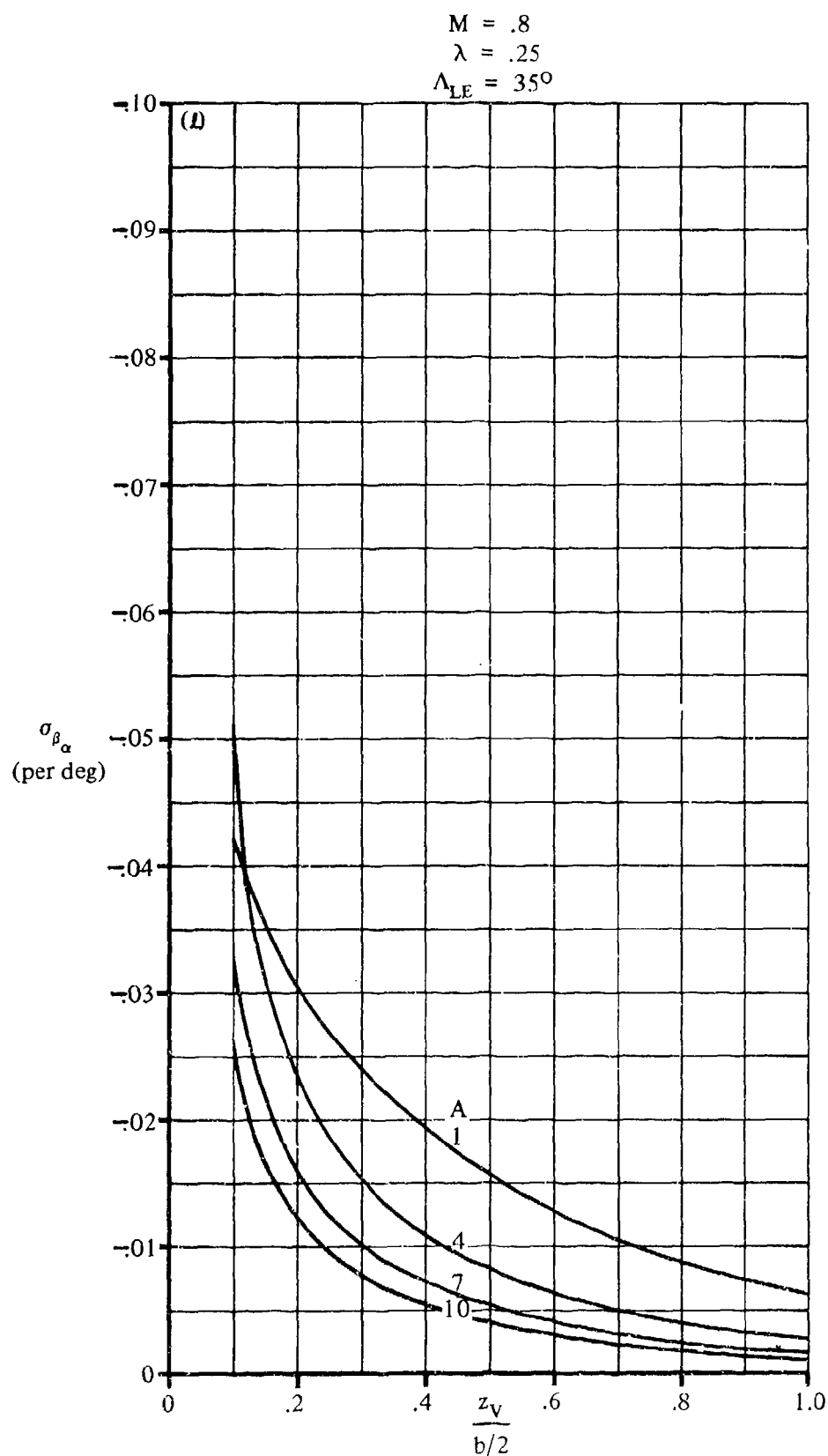


FIGURE 7.4.4.4-6 (CONT'D)

7.4.4.4-17

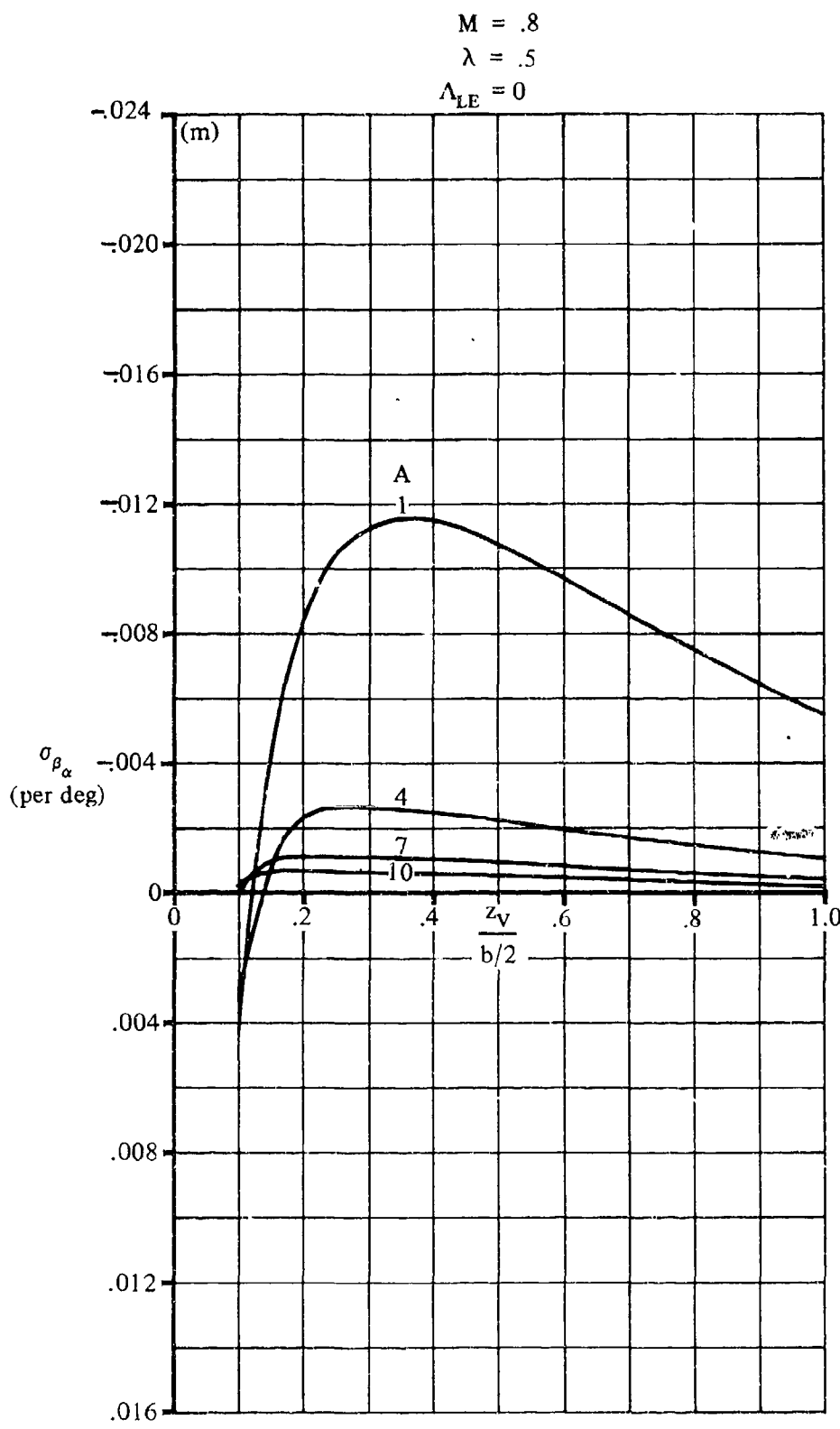


FIGURE 7.4.4.4-6 (CONTD)

7.4.4.4-18

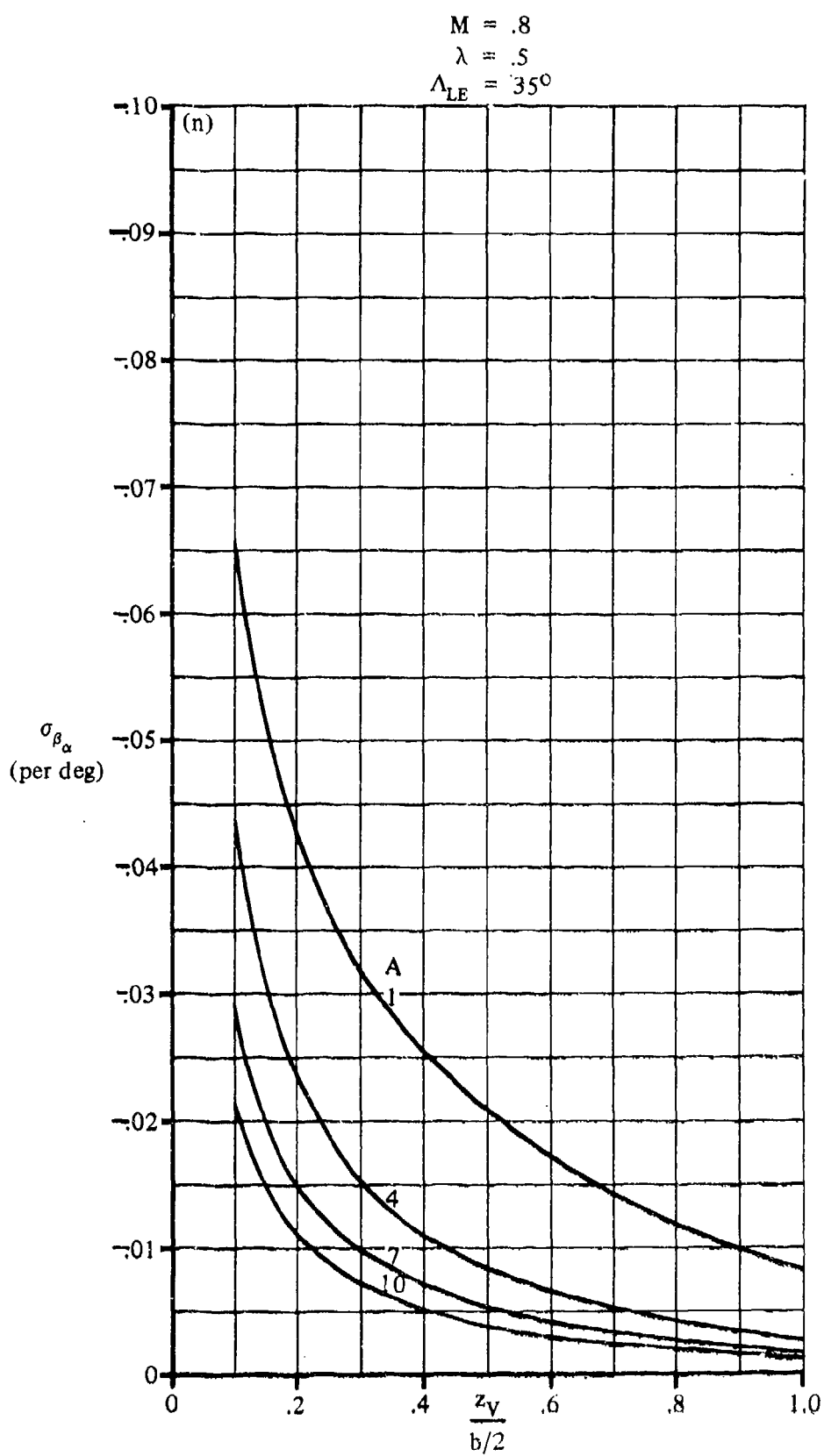


FIGURE 7.4.4.4-6 (CONTD)

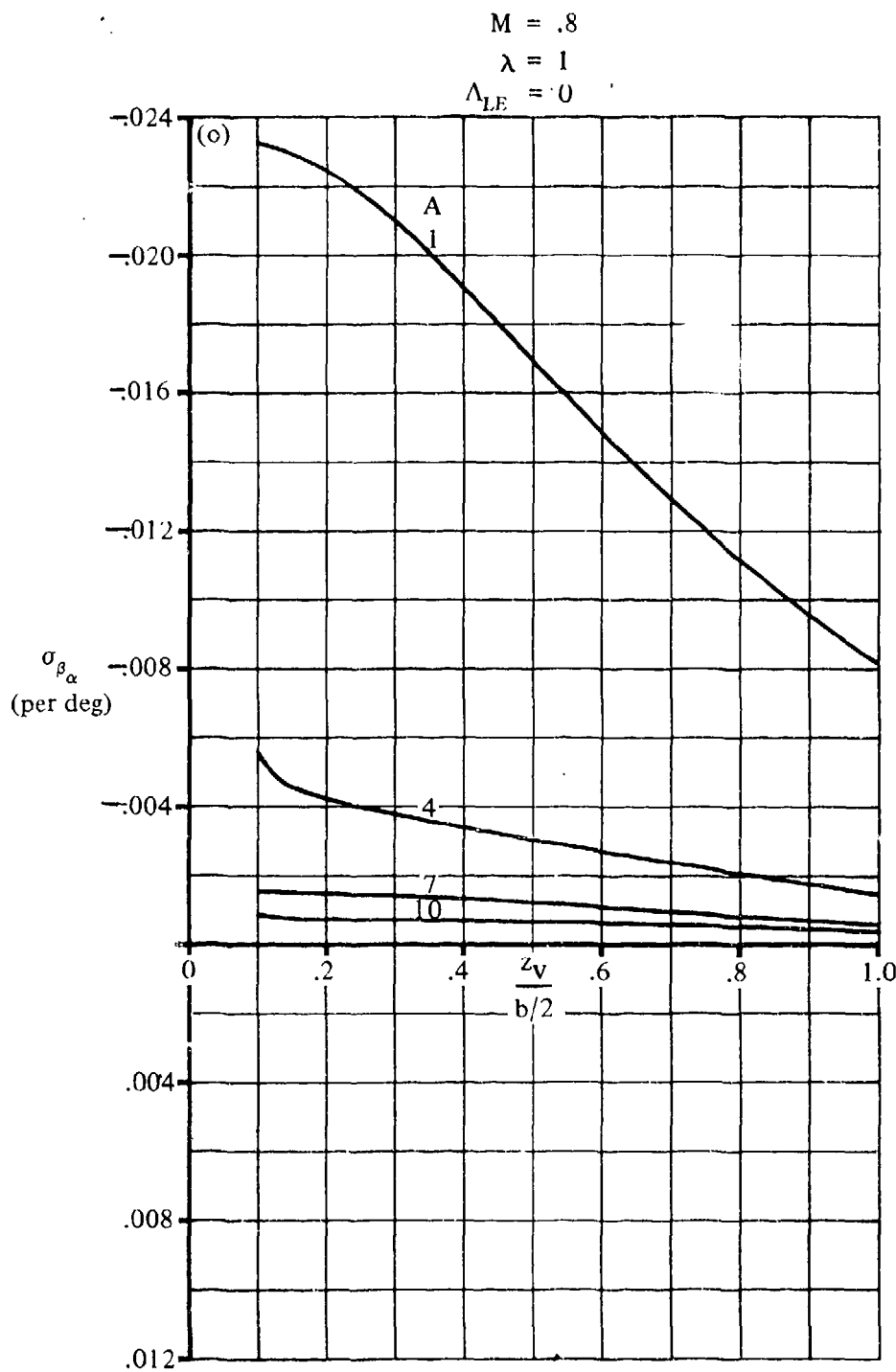


FIGURE 7.4.4.4-6' (CONT'D)

7.4.4.4-20

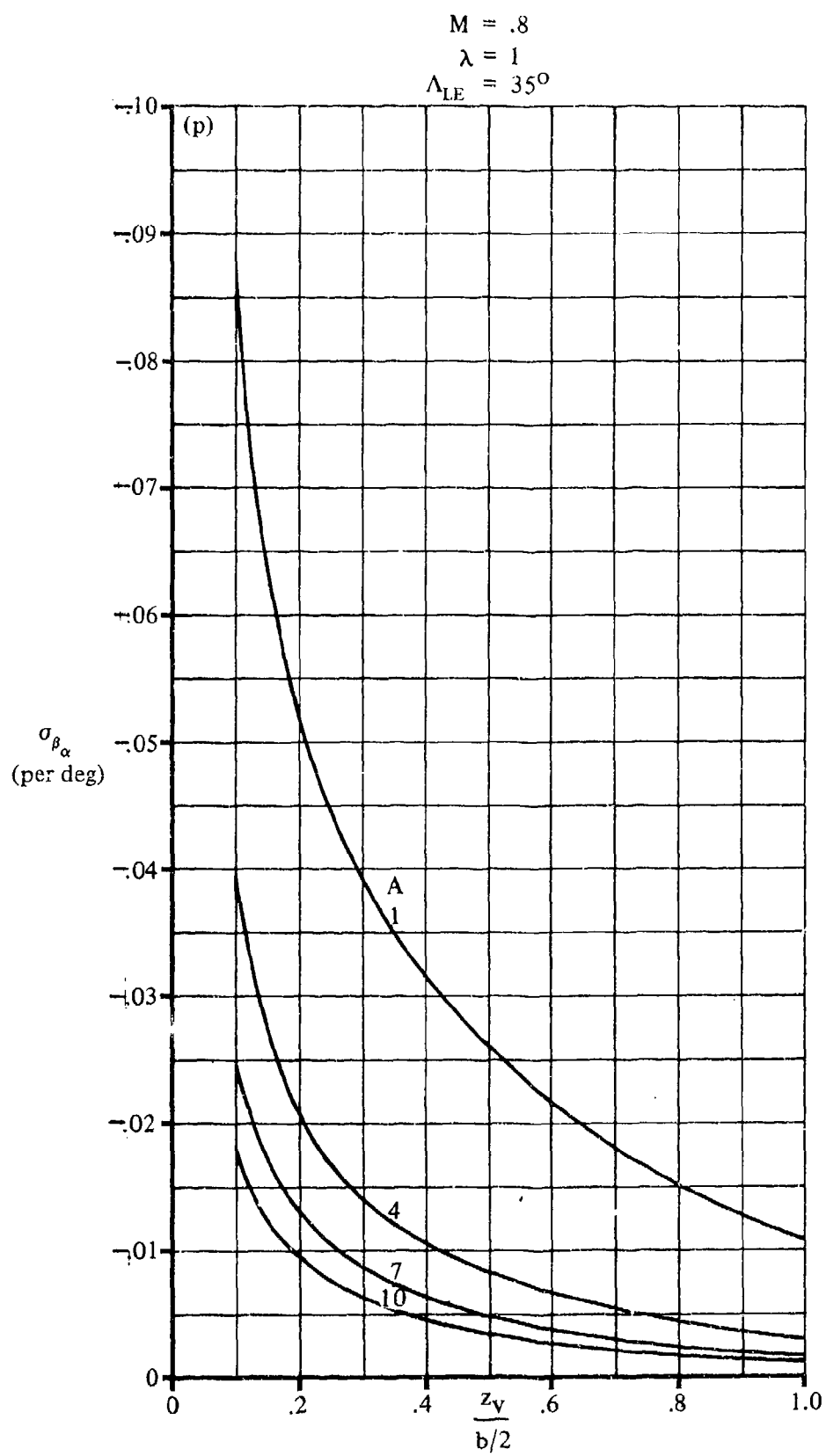


FIGURE 7.4.4.4-6 (CONTD)

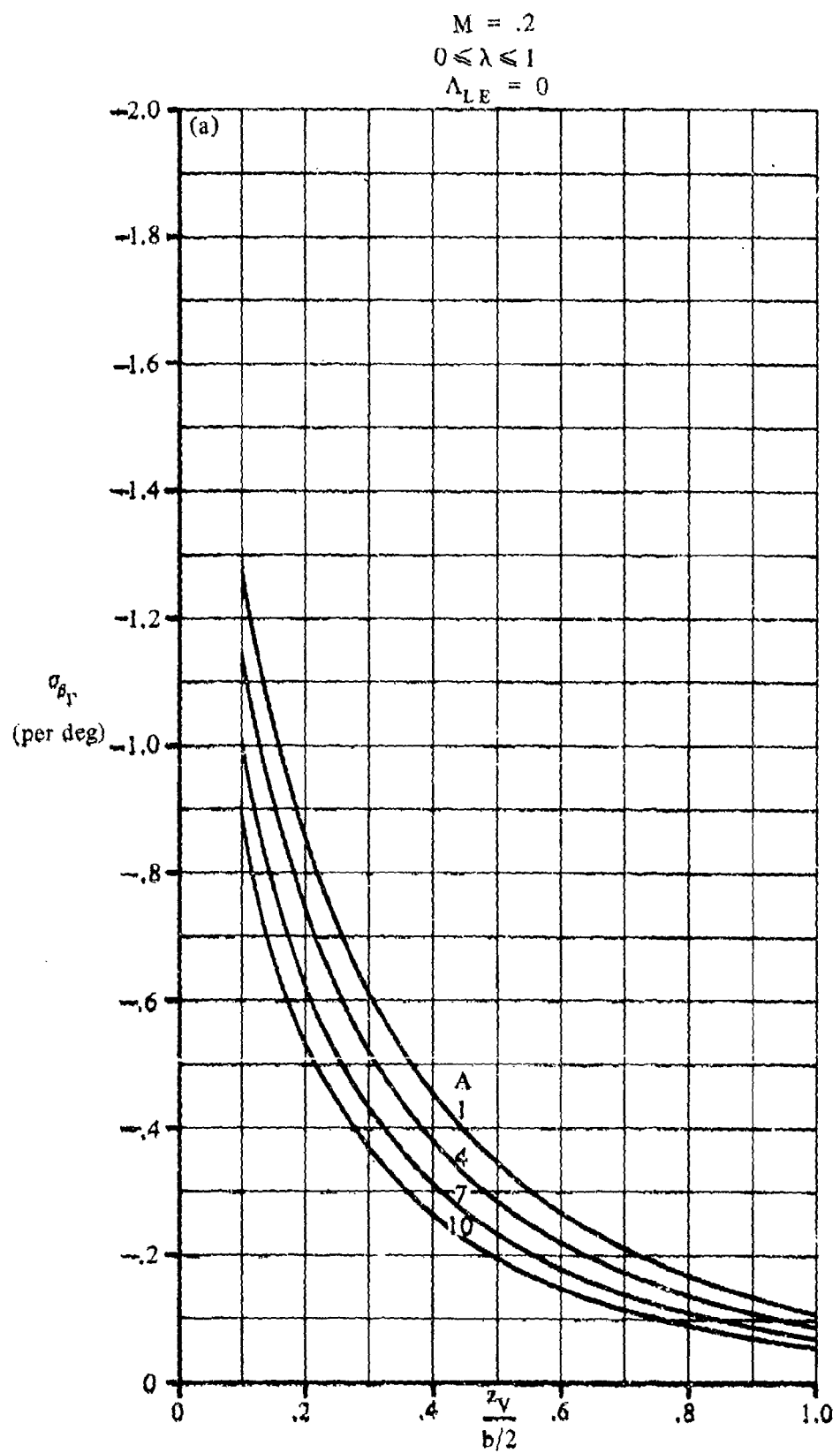


FIGURE 7.4.4.4-22 SIDEWASH CONTRIBUTION DUE TO DIHEDRAL

7.4.4.4-22

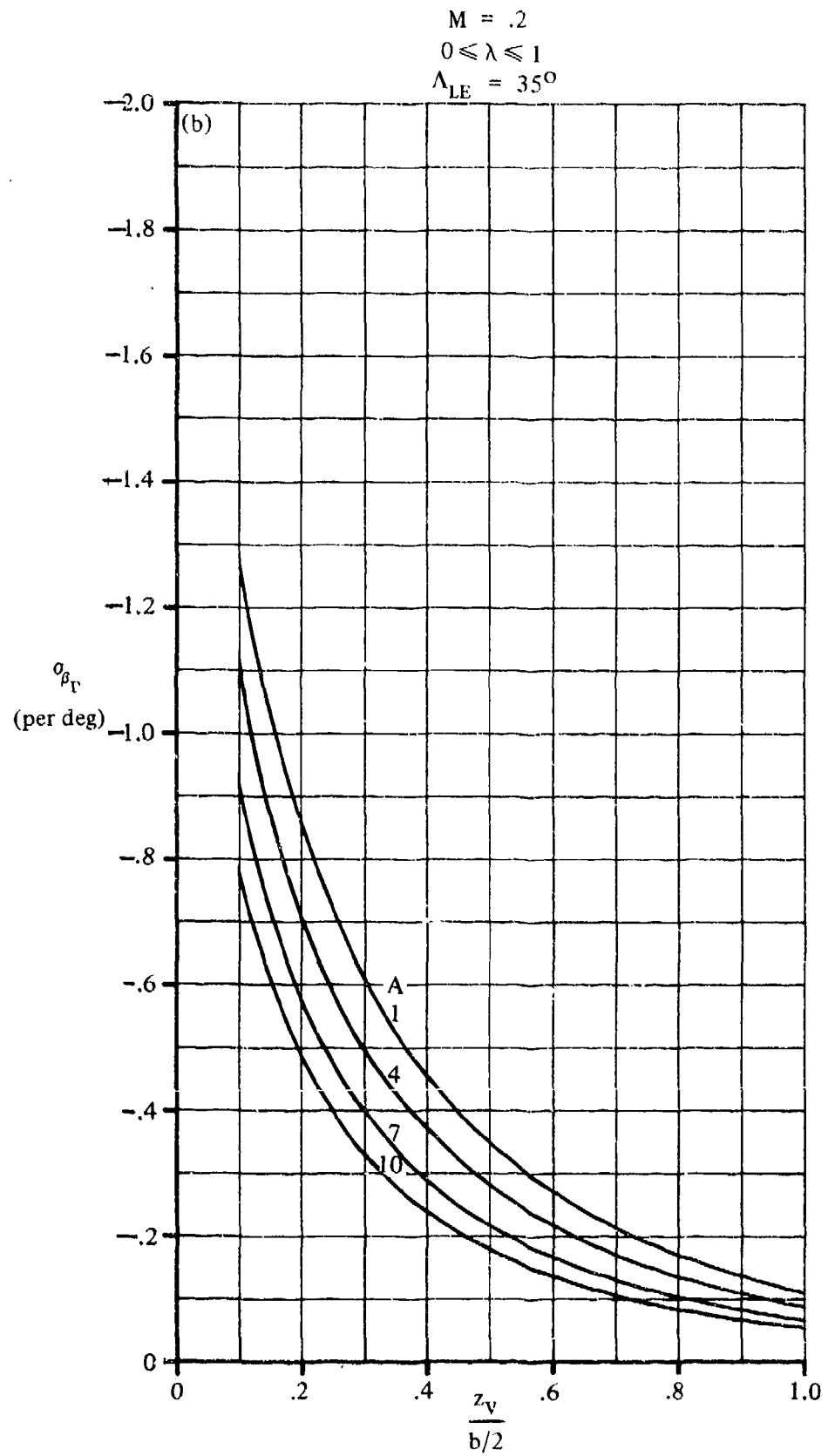


FIGURE 7.4.4.4-22 (CONTD)

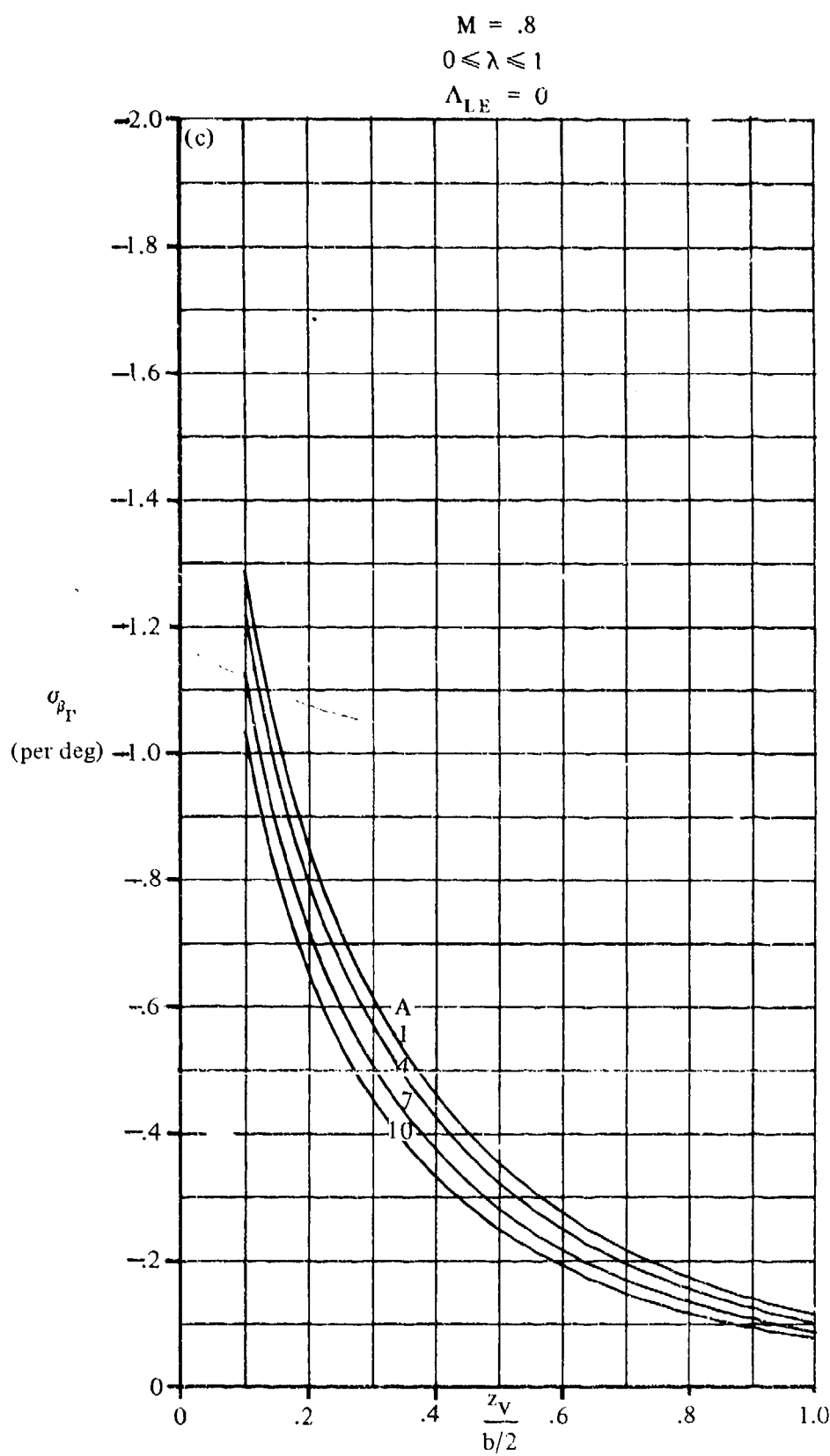


FIGURE 7.4.4.4-22 (CONTD)

7.4.4.4-24

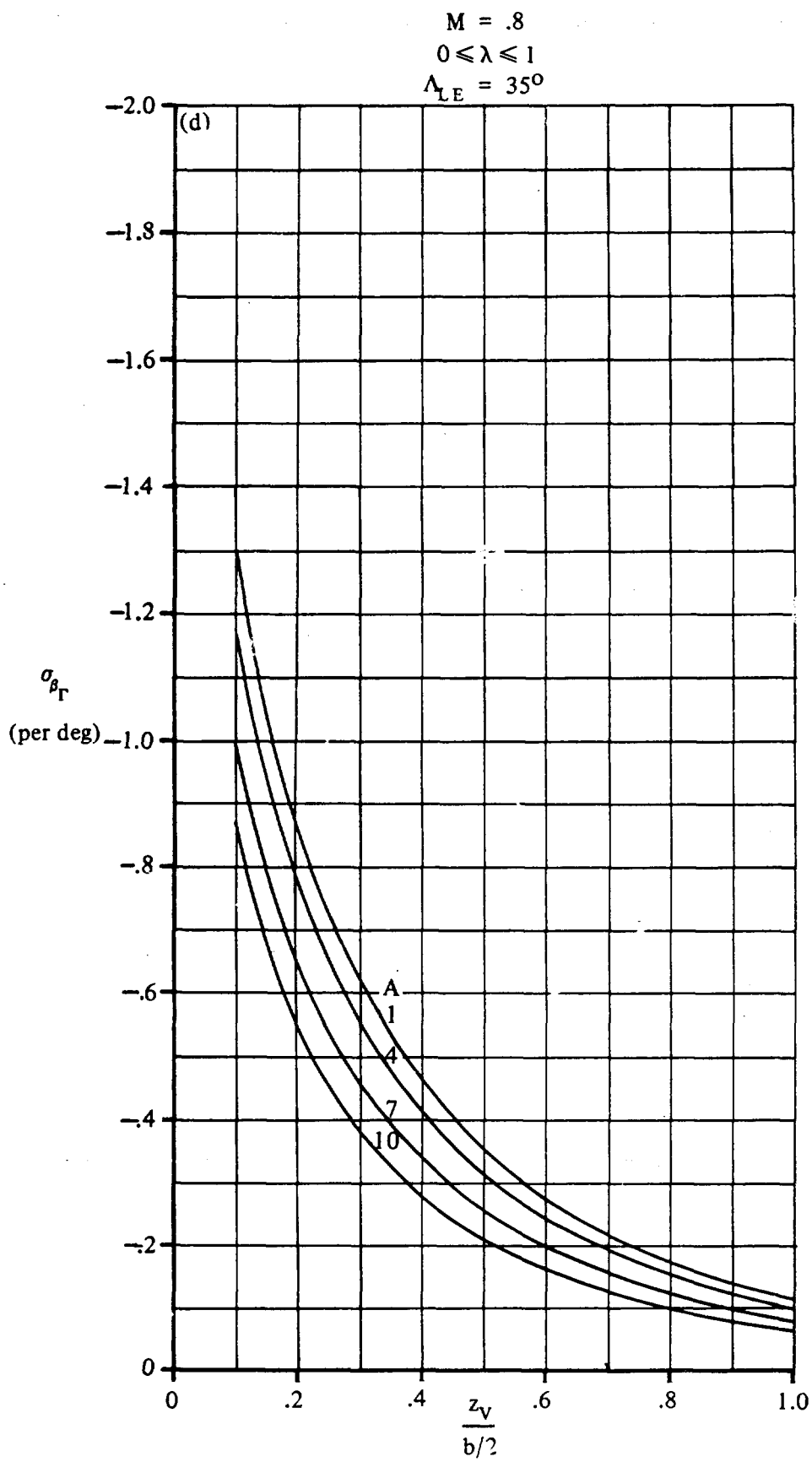


FIGURE 7.4.4.4-22 (CONTD)

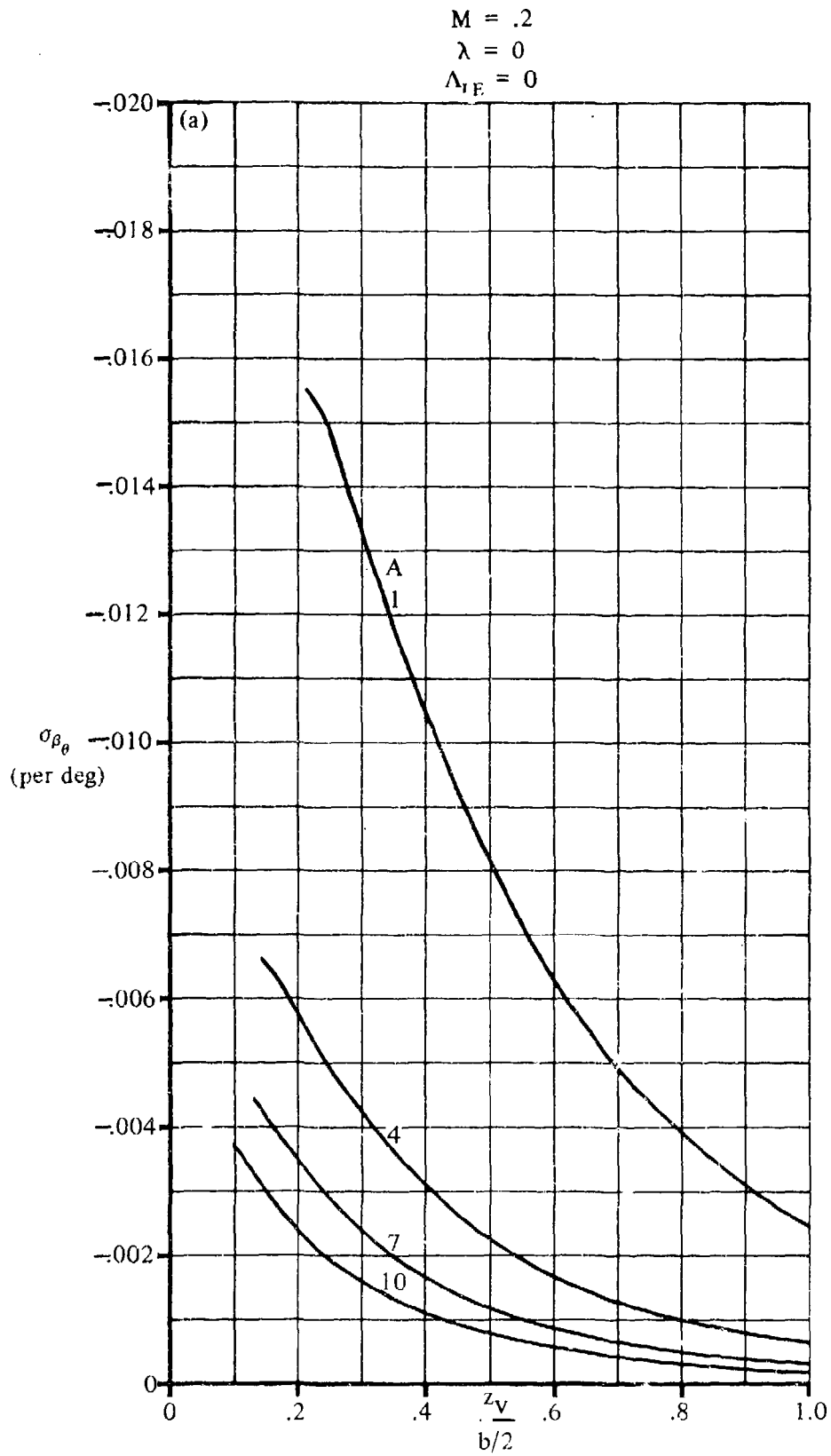


FIGURE 7.4.4.4-26 SIDEWASH CONTRIBUTION DUE TO WING TWIST
7.4.4.4-26

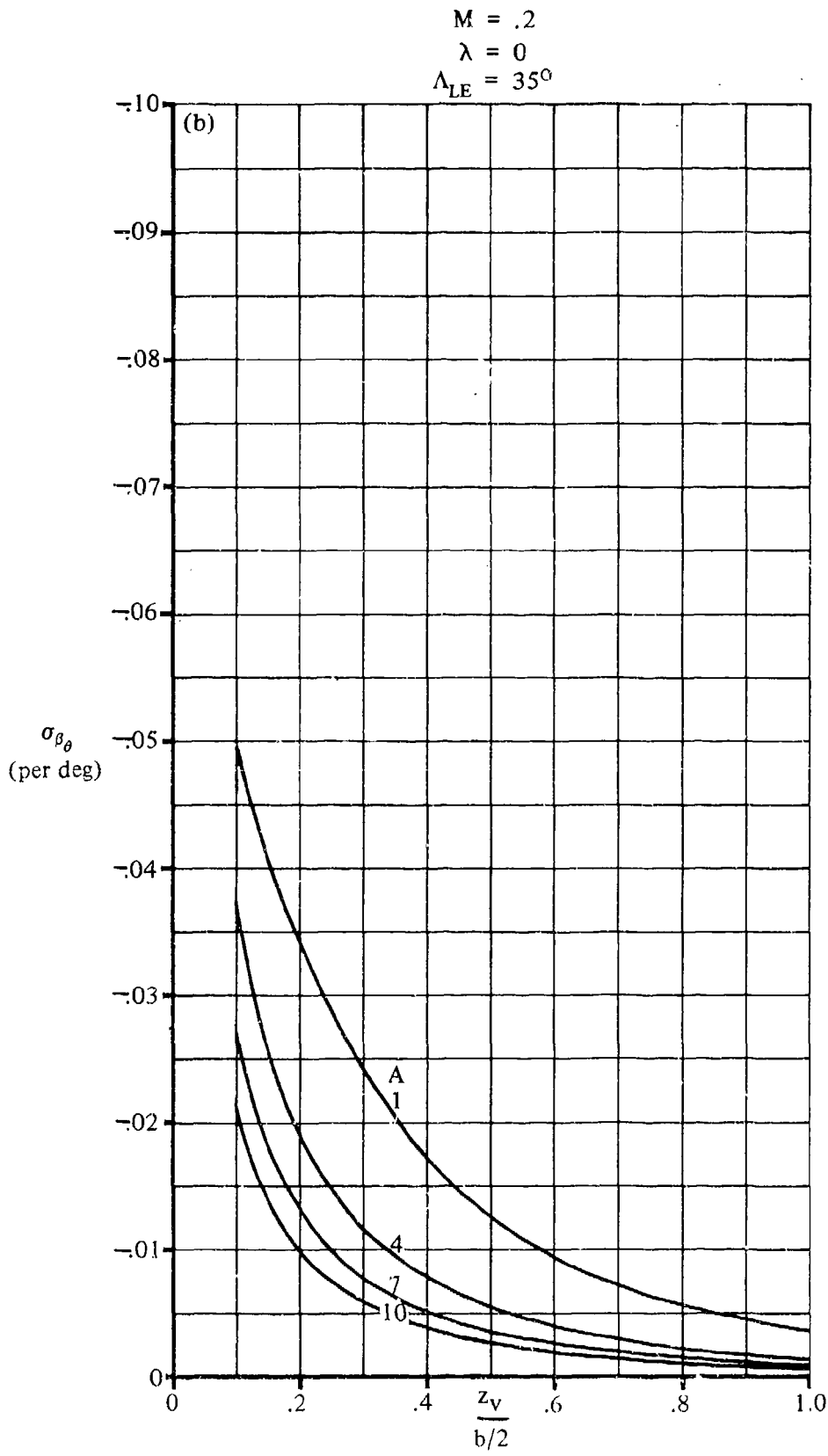


FIGURE 7.4.4-26 (CONTD)

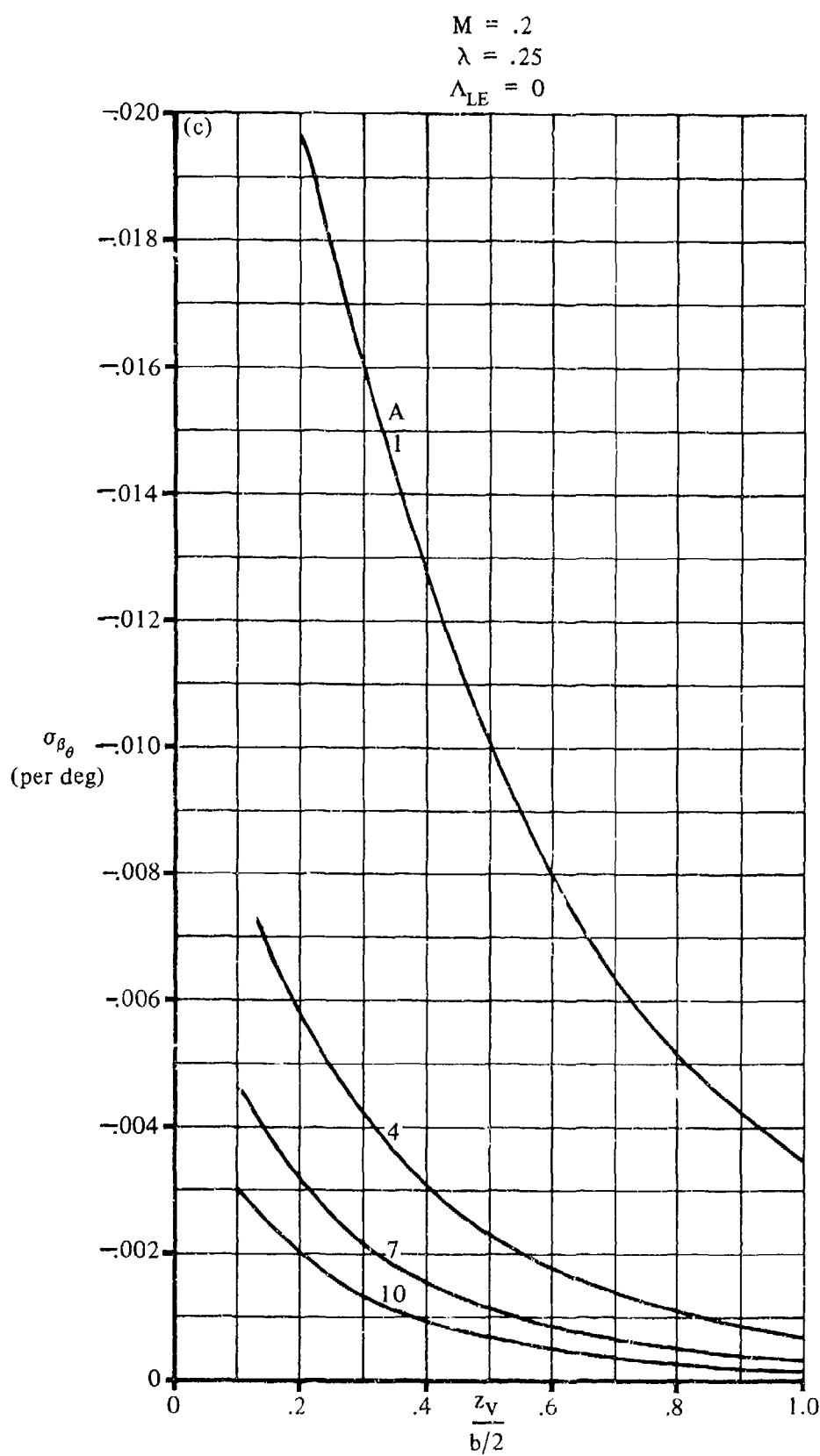


FIGURE 7.4.4-26 (CONT'D)

7.4.4-28

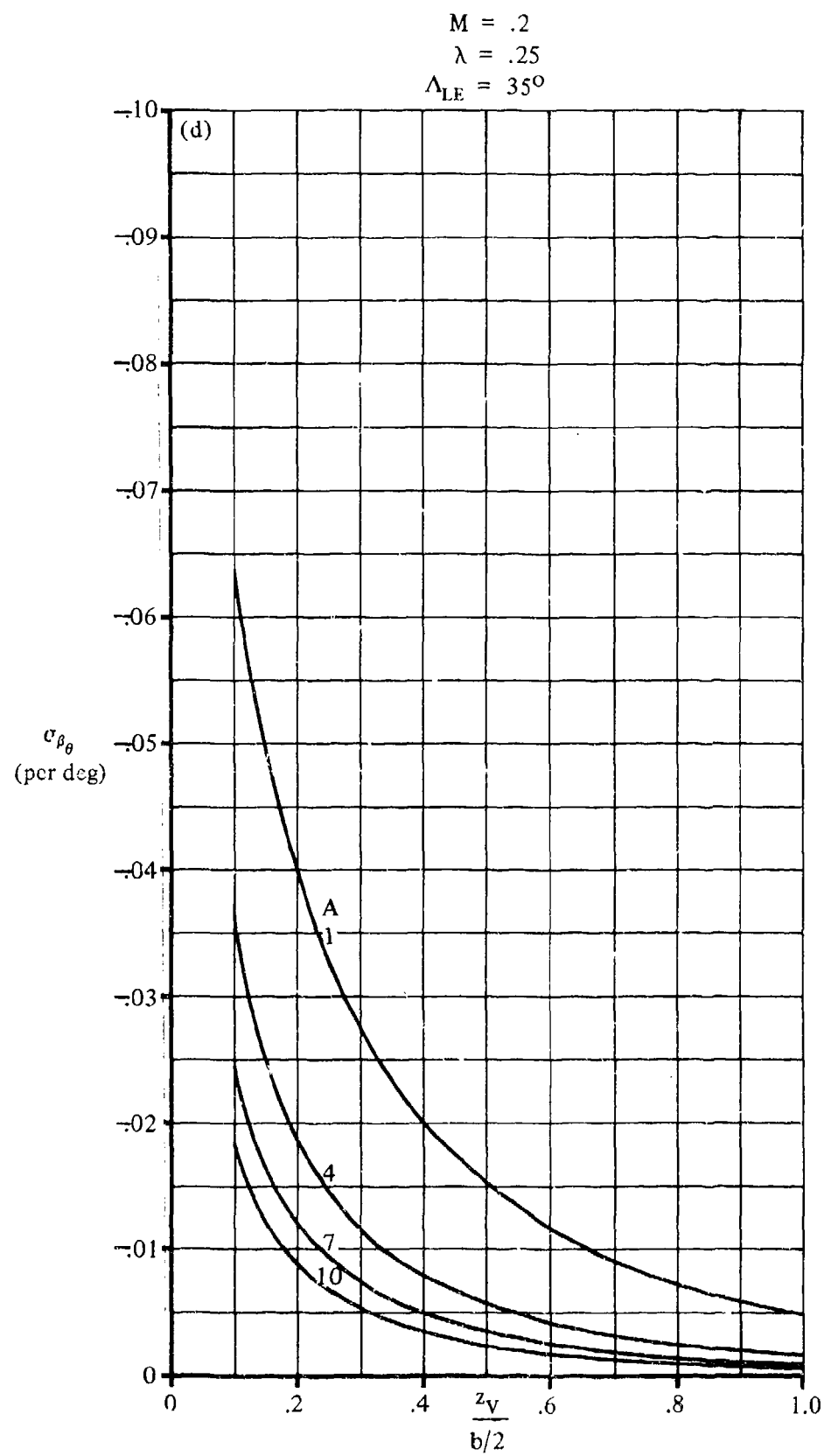


FIGURE 7.4.4.4-26 (CONTD)

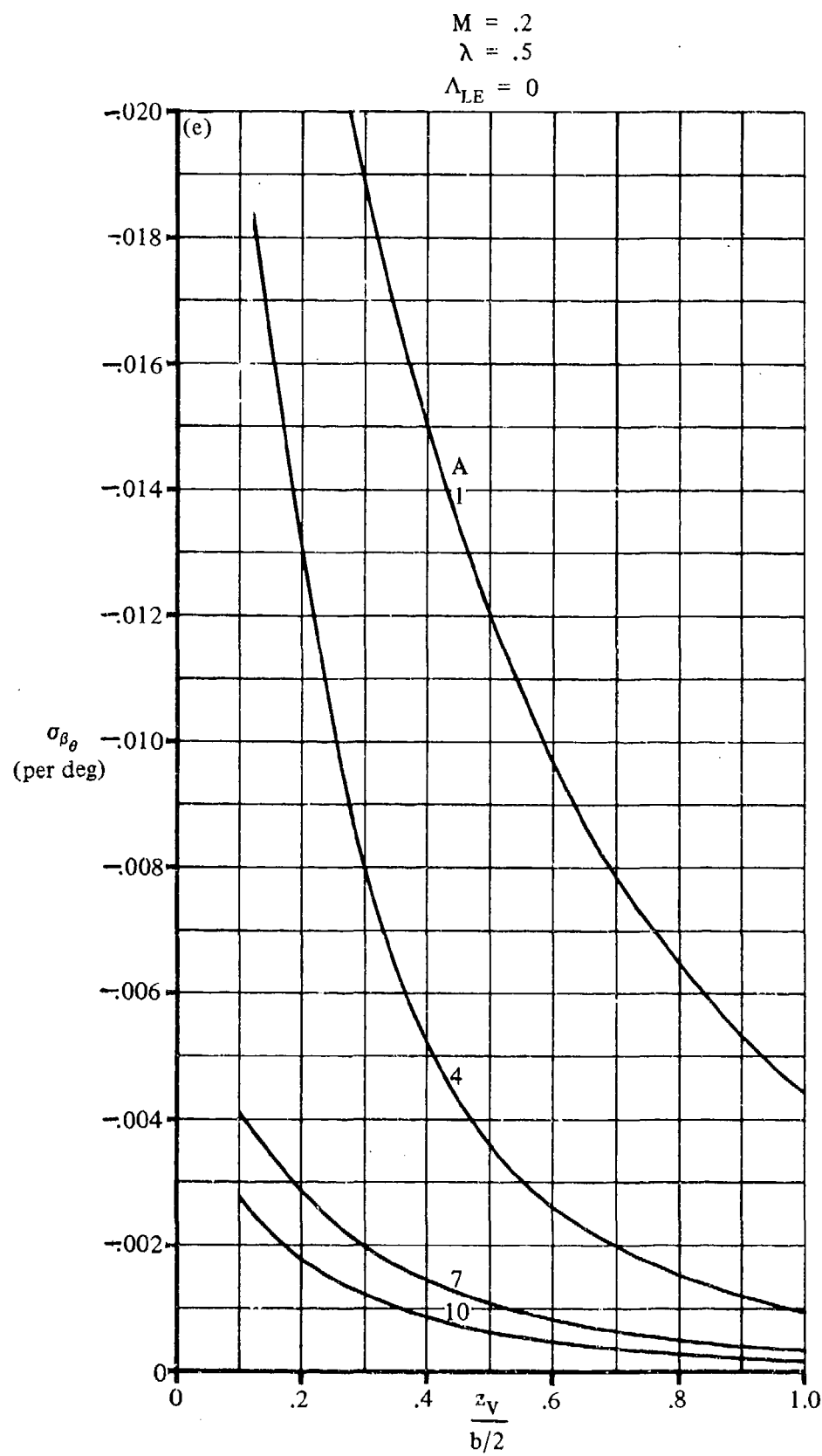


FIGURE 7.4.4.4-26 (CONTD)

7.4.4.4-30

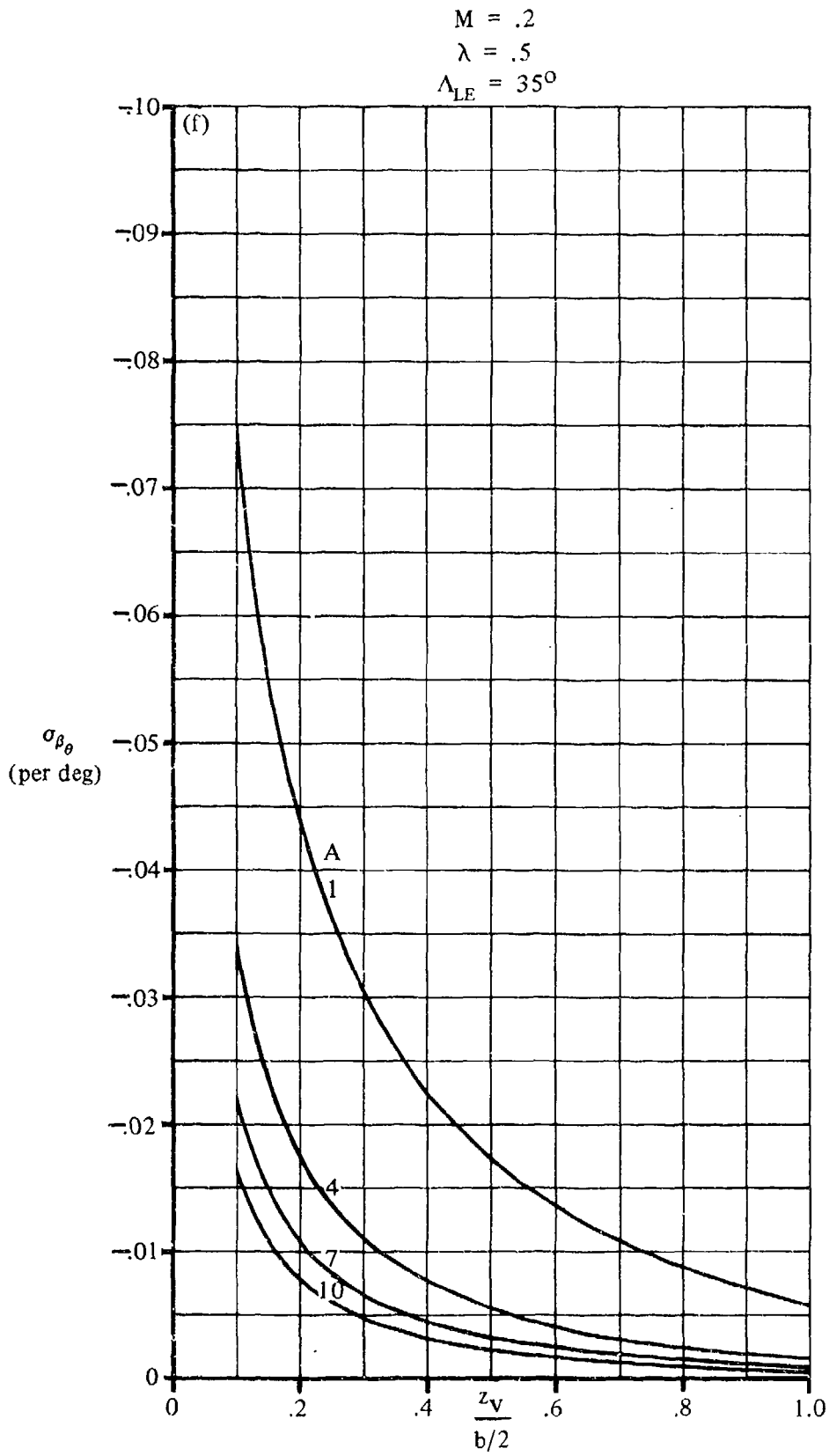


FIGURE 7.4.4.4-26 (CONTD)

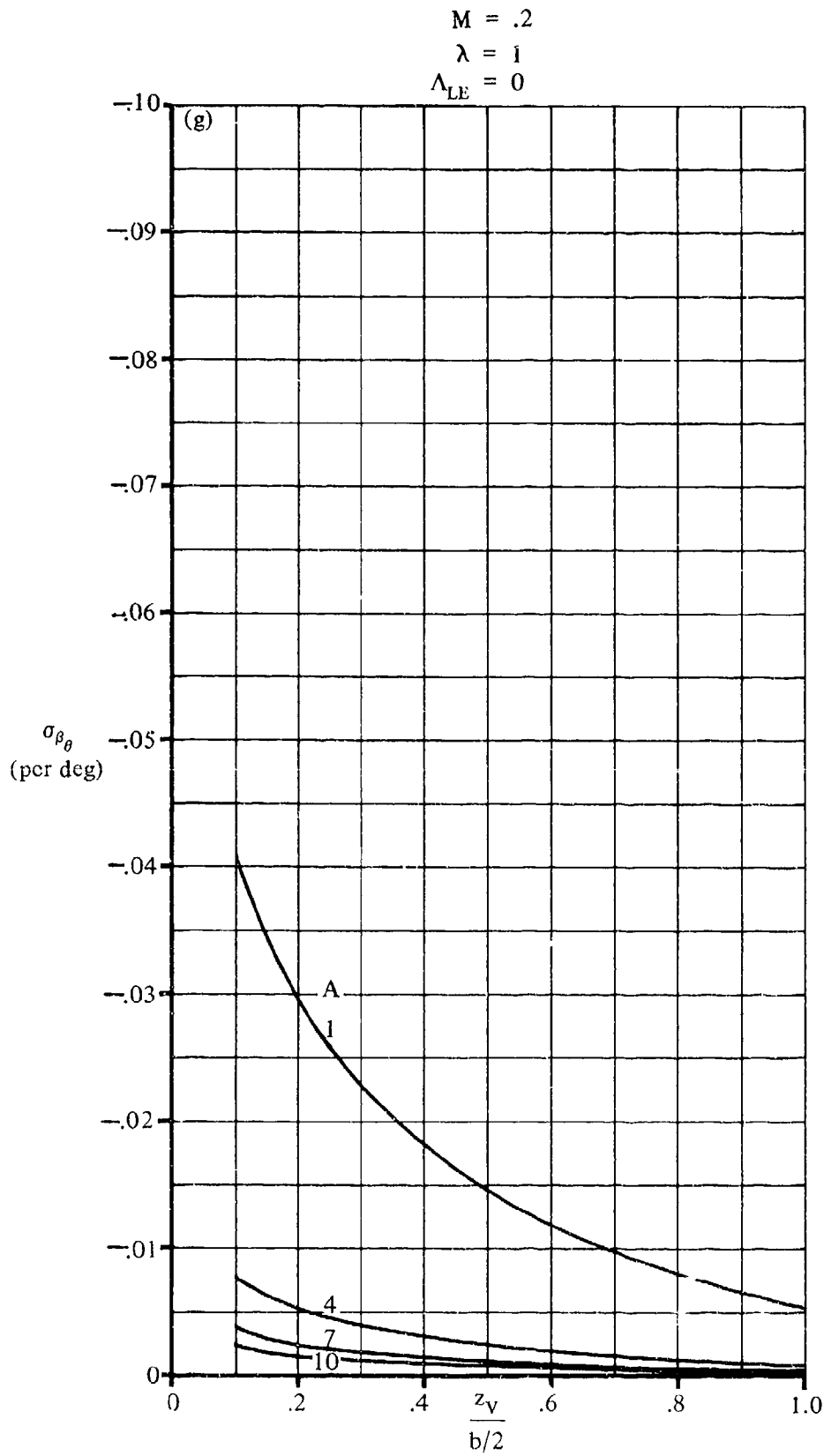


FIGURE 7.4.4.4-26 (CONTD)

7.4.4.4-32

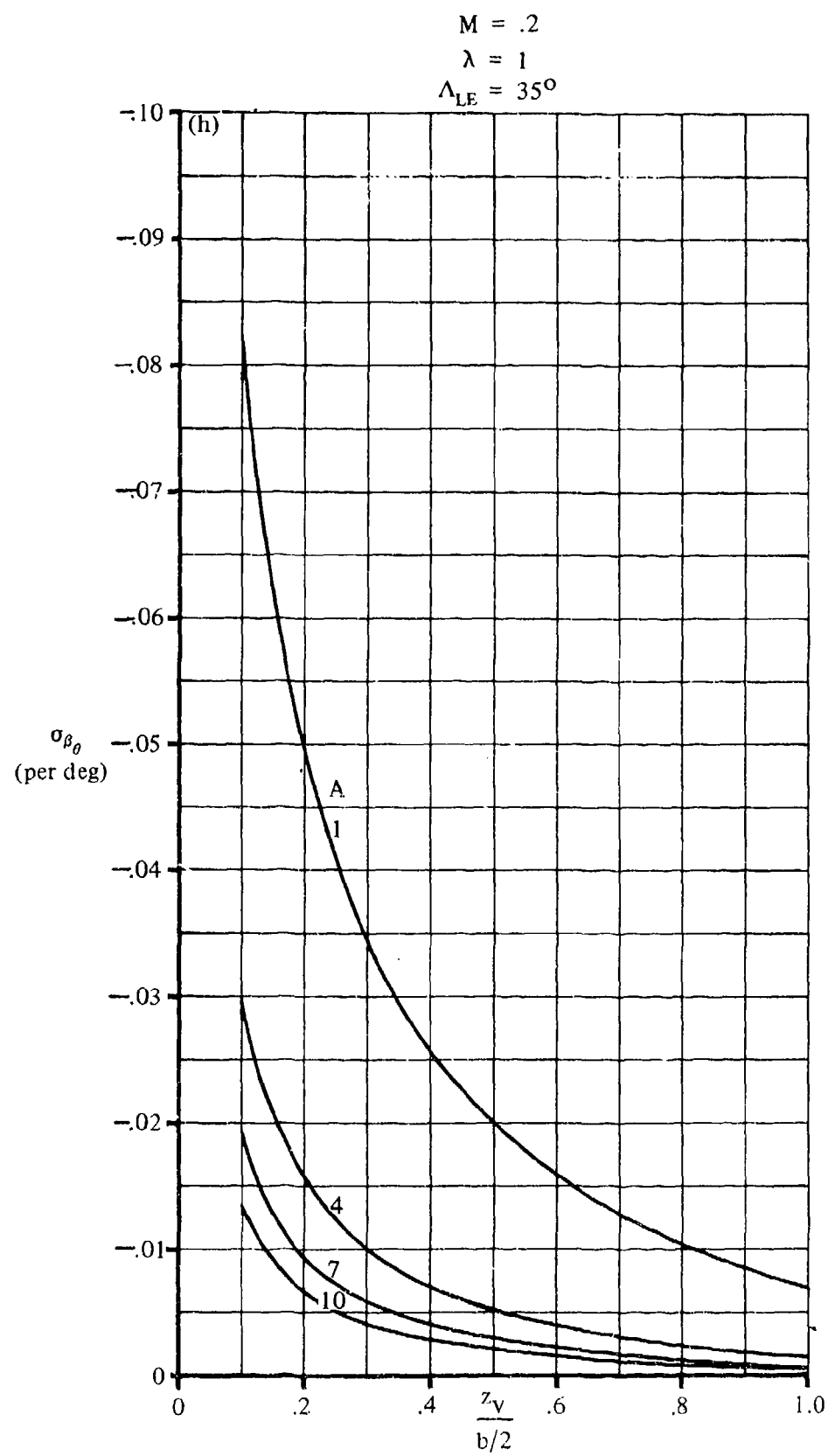


FIGURE 7.4.4.4-26 (CONTD)

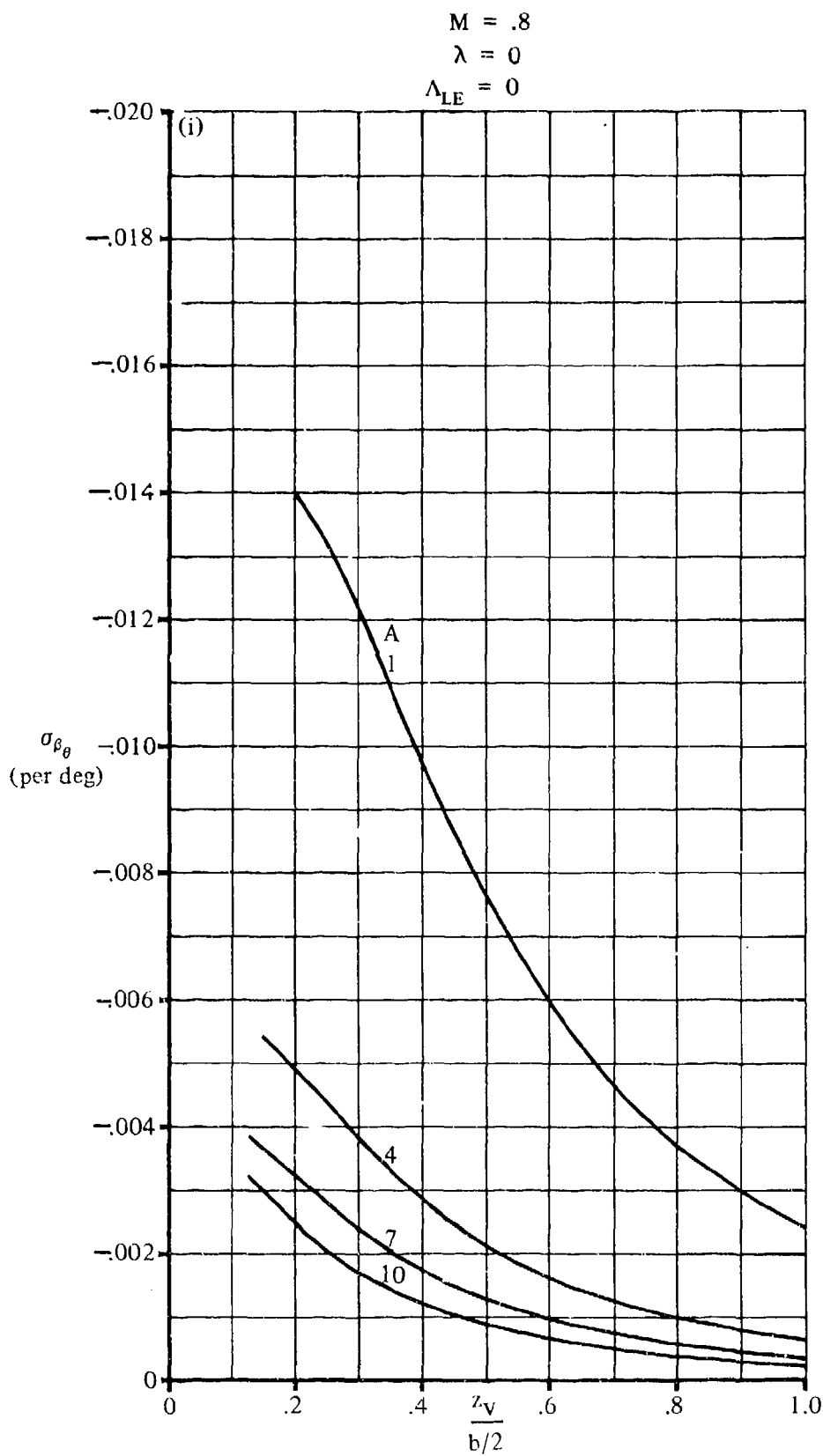


FIGURE 7.4.4.4-26 (CONT'D)

7.4.4.4-34

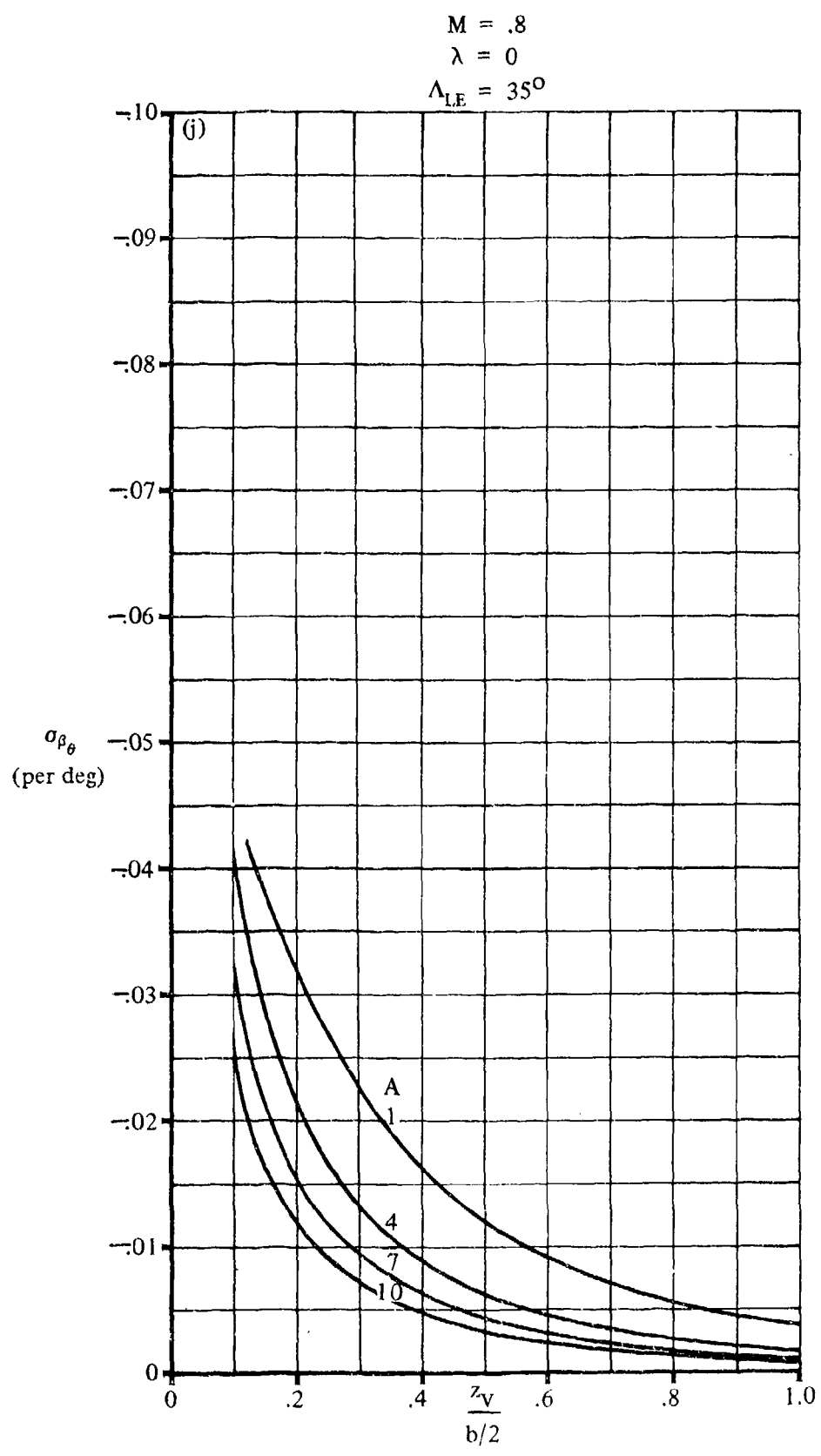


FIGURE 7.4.4.4-26 (CONTD)

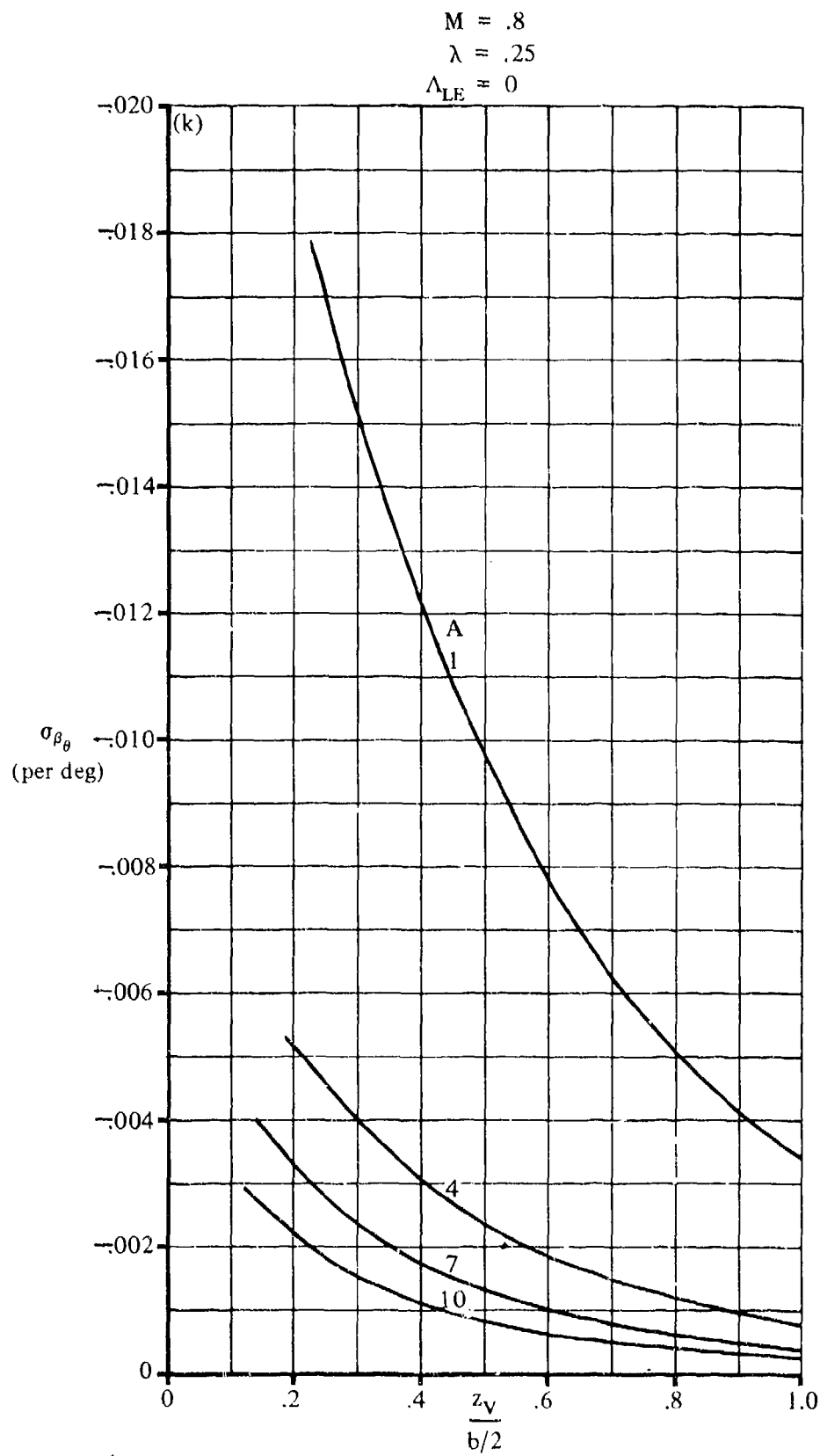


FIGURE 7.4.4-26 (CONTD)

7.4.4-36

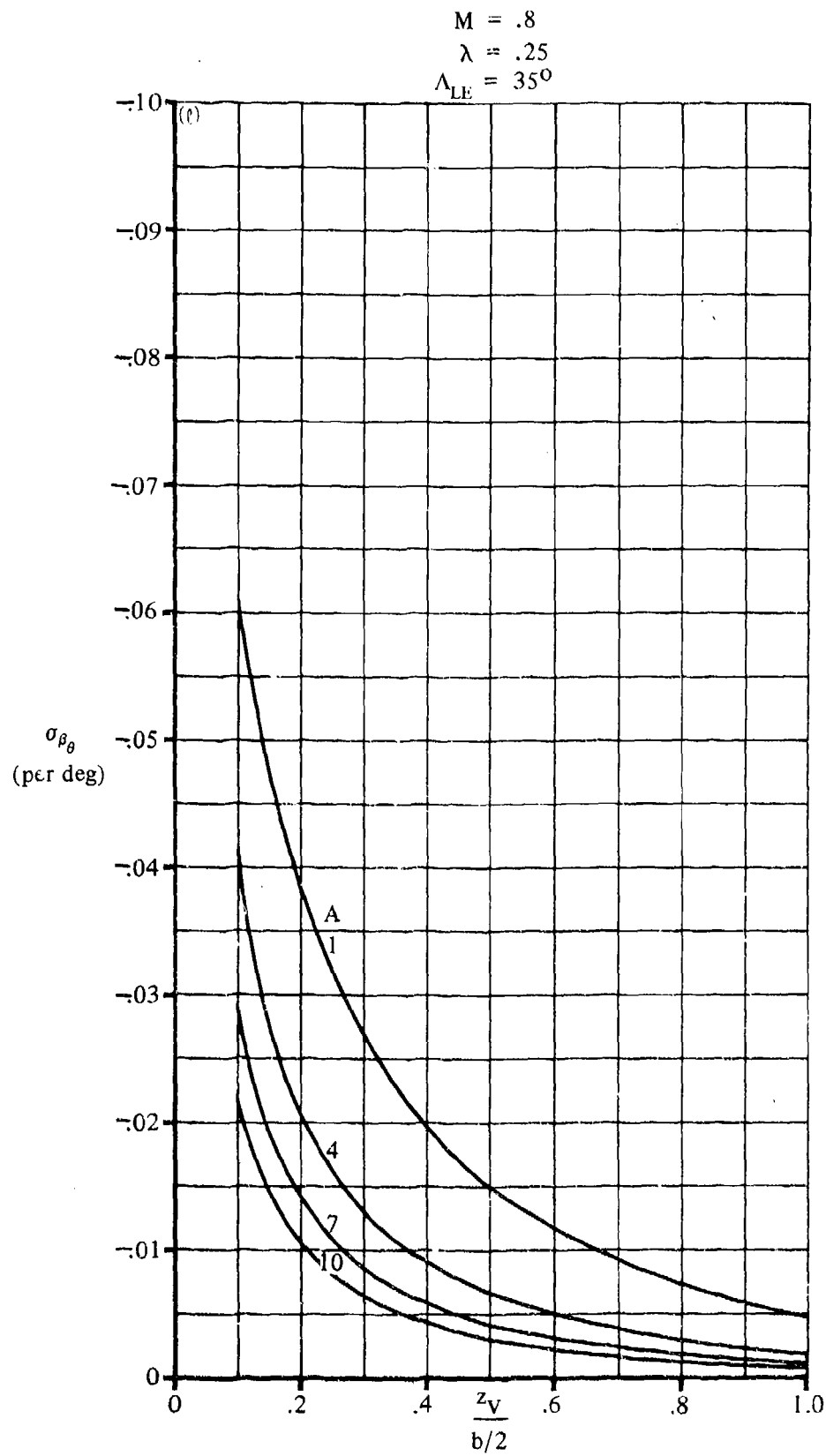


FIGURE 7.4.4.4-26 (CONTD)

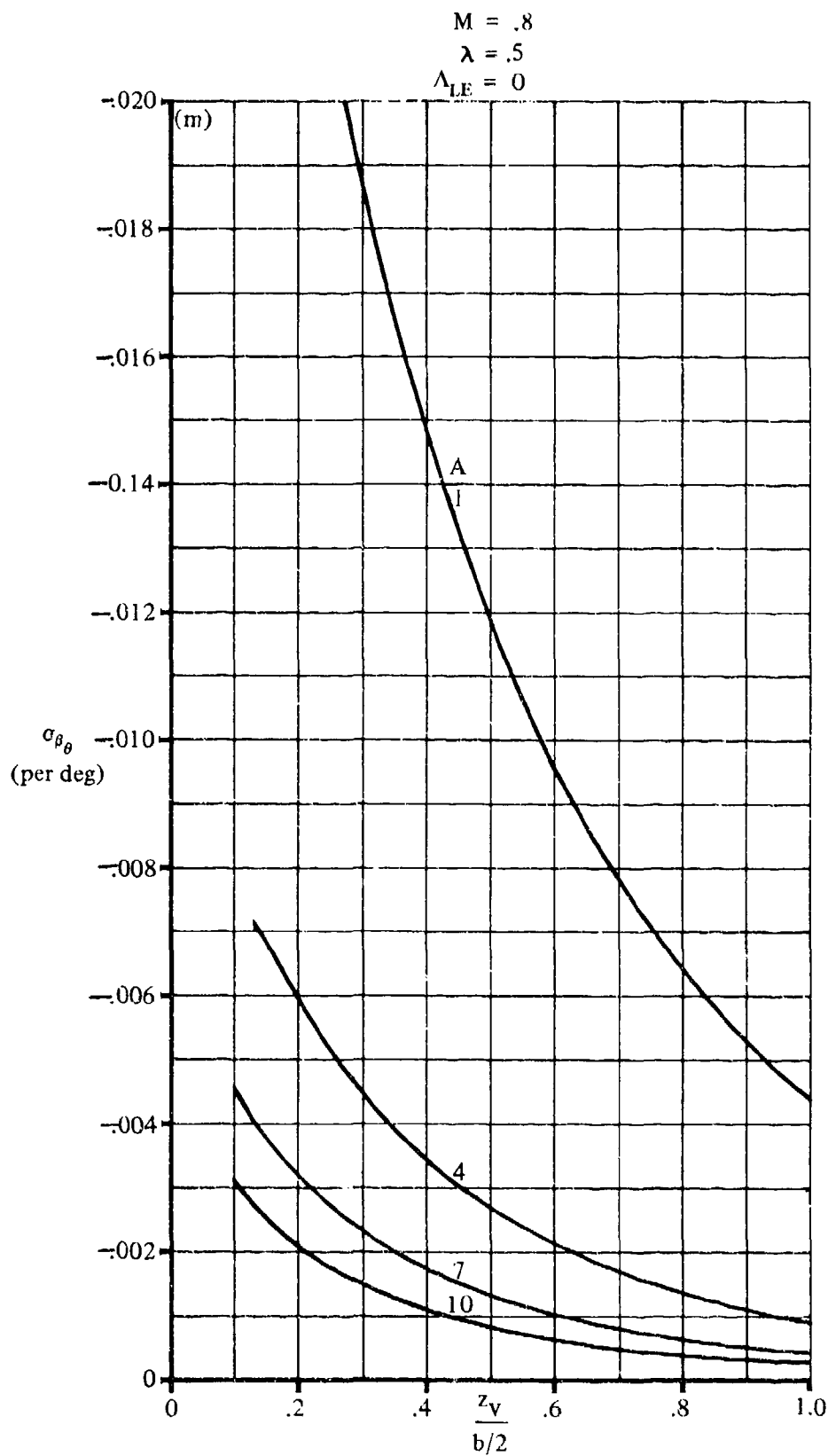


FIGURE 7.4.4.4-26 (CONT'D)

7.4.4.4-38

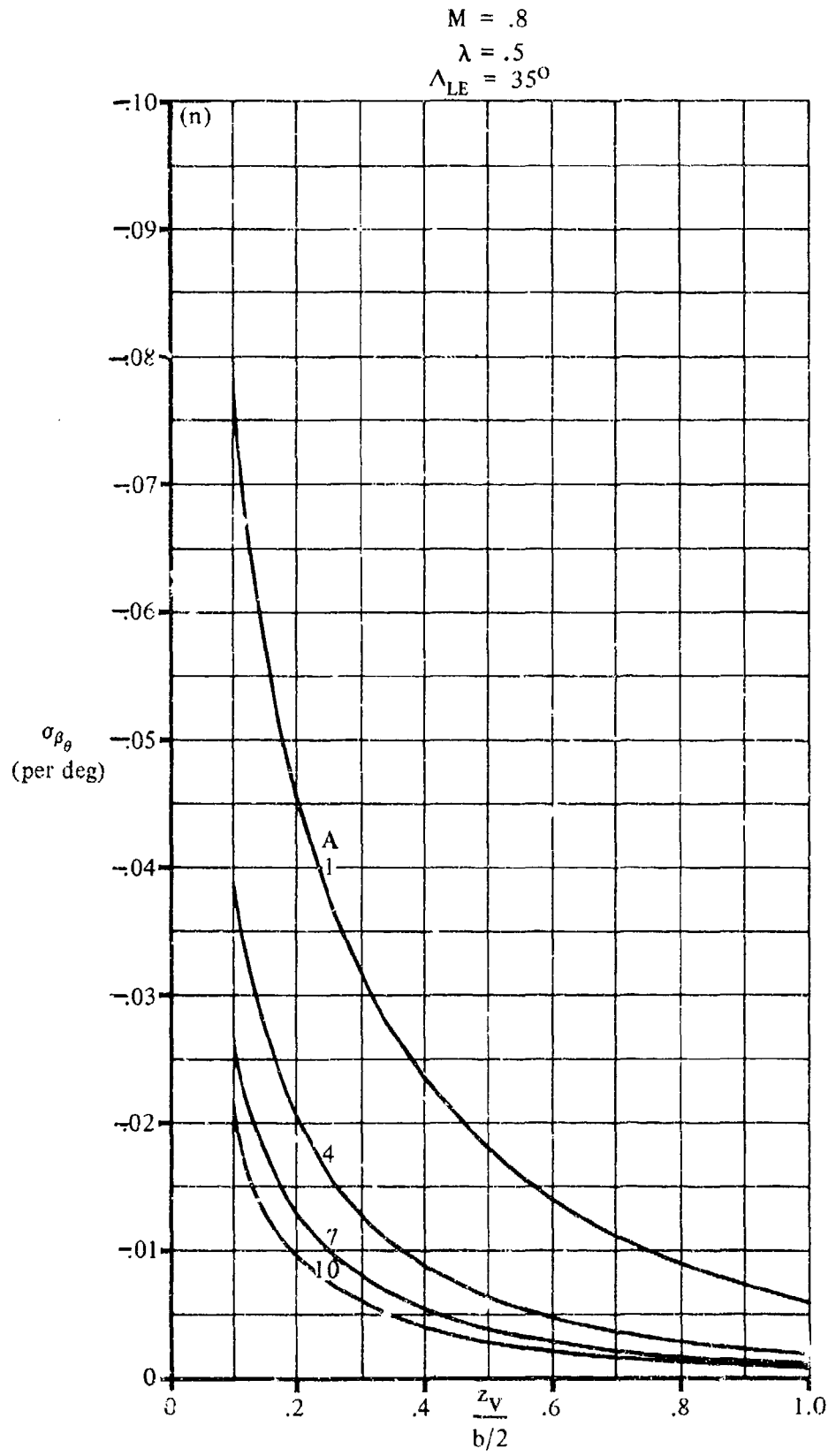


FIGURE 7.4.4.4-26 (CONT'D)

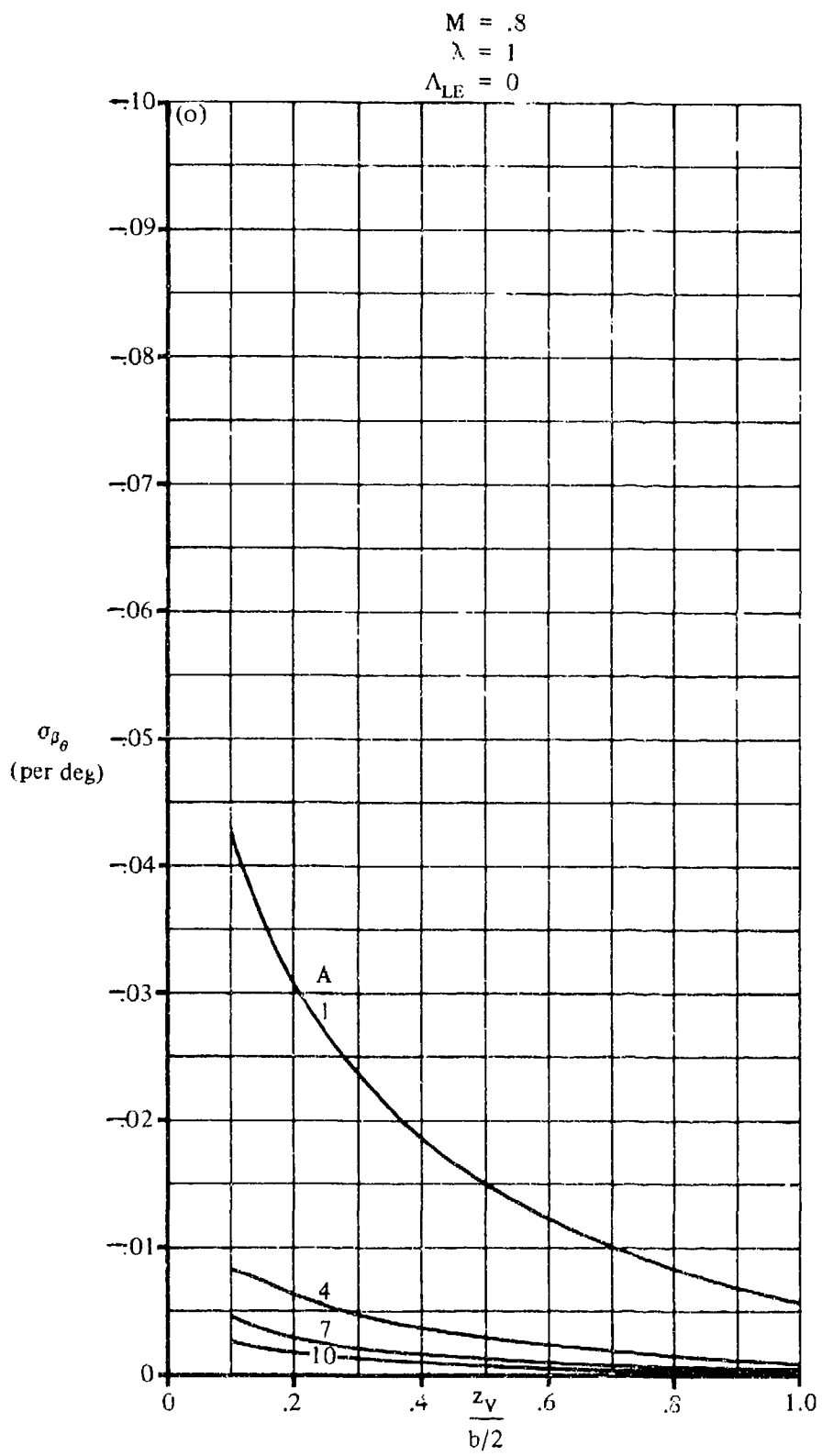


FIGURE 7.4.4-26 (CONTD)

7.4.4-40

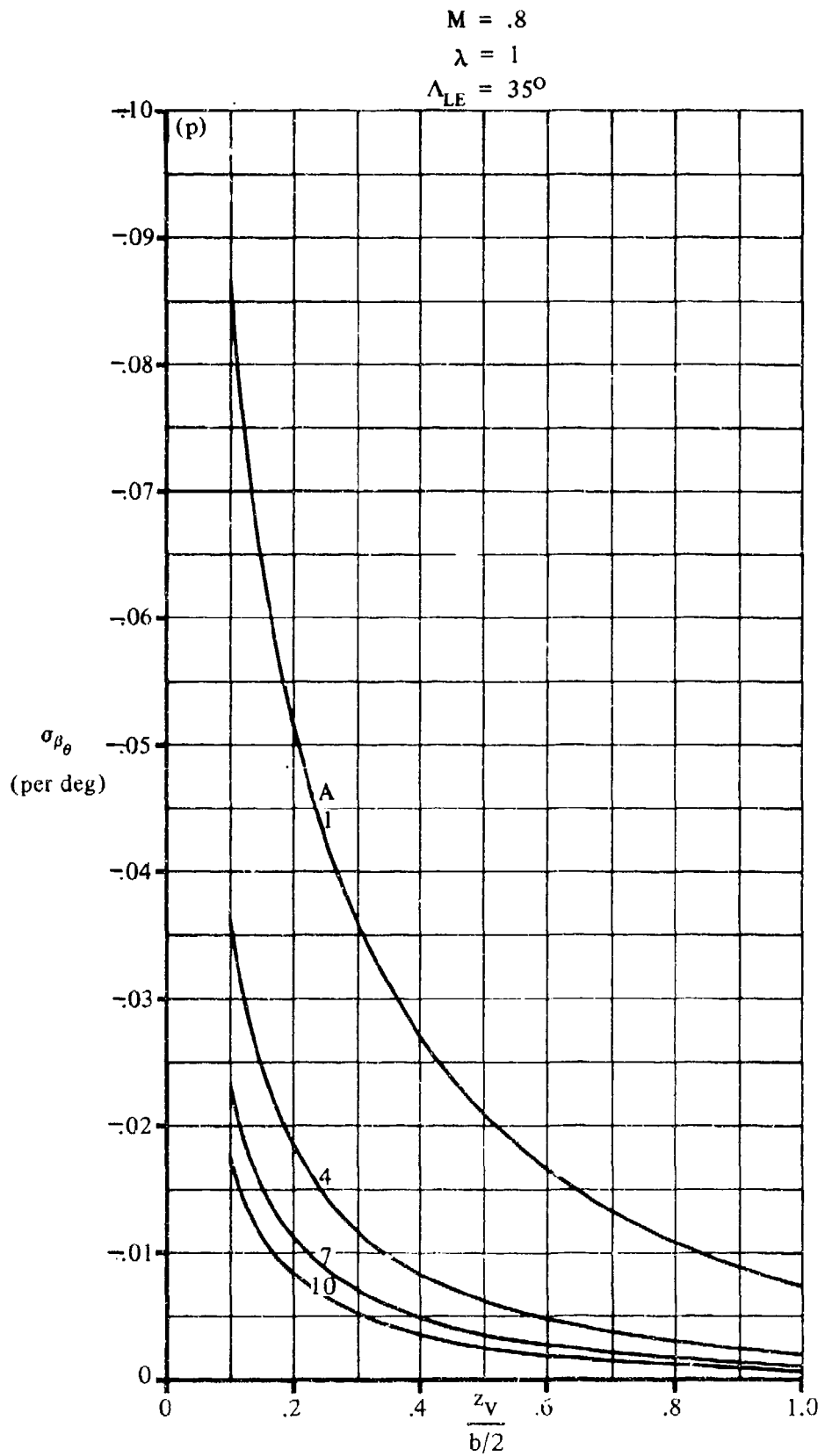


FIGURE 7.4.4-26 (CONTD)

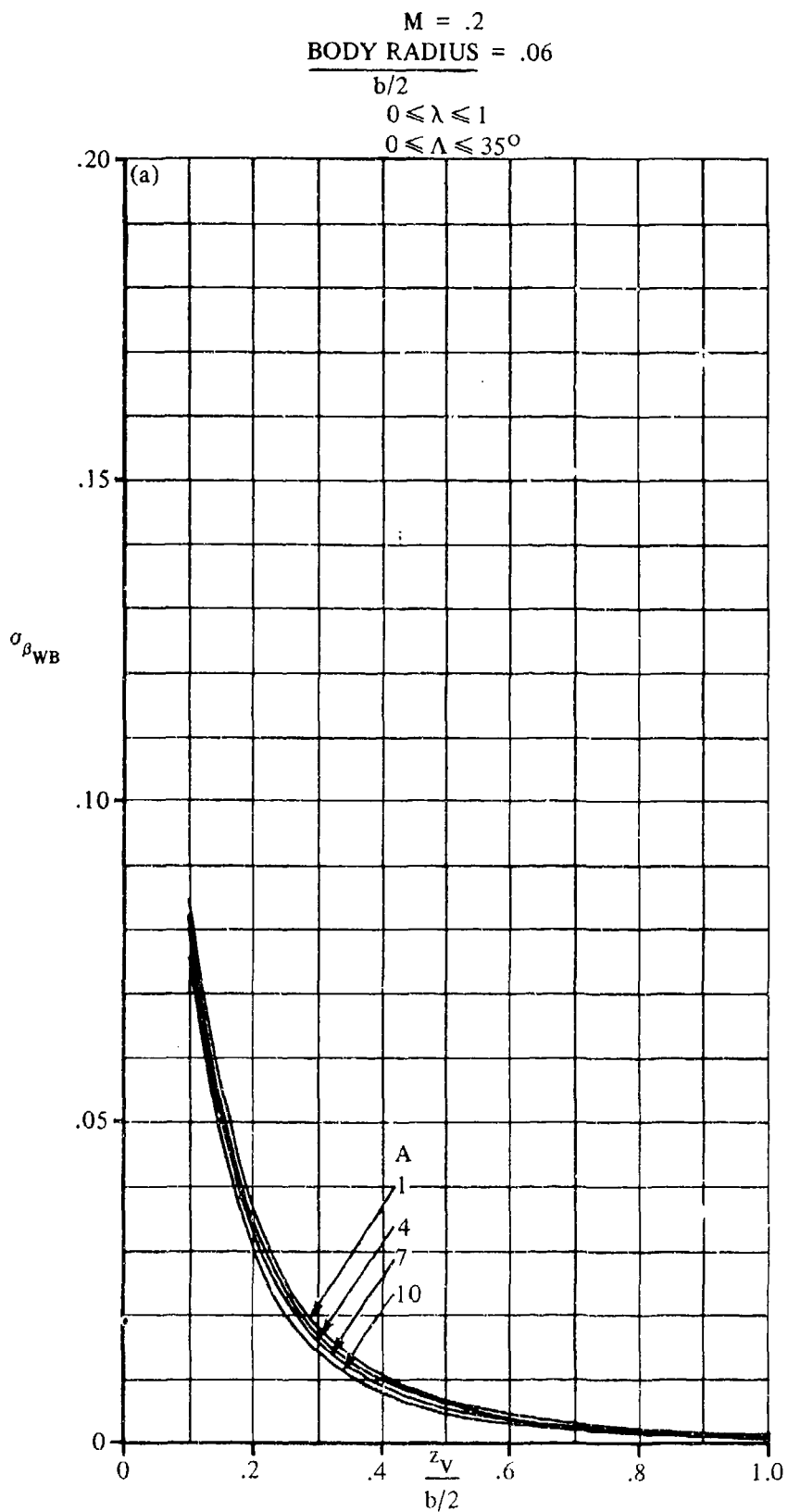


FIGURE 7.4.4.4-42 SIDEWASH CONTRIBUTION DUE TO BODY EFFECT

7.4.4.4-42

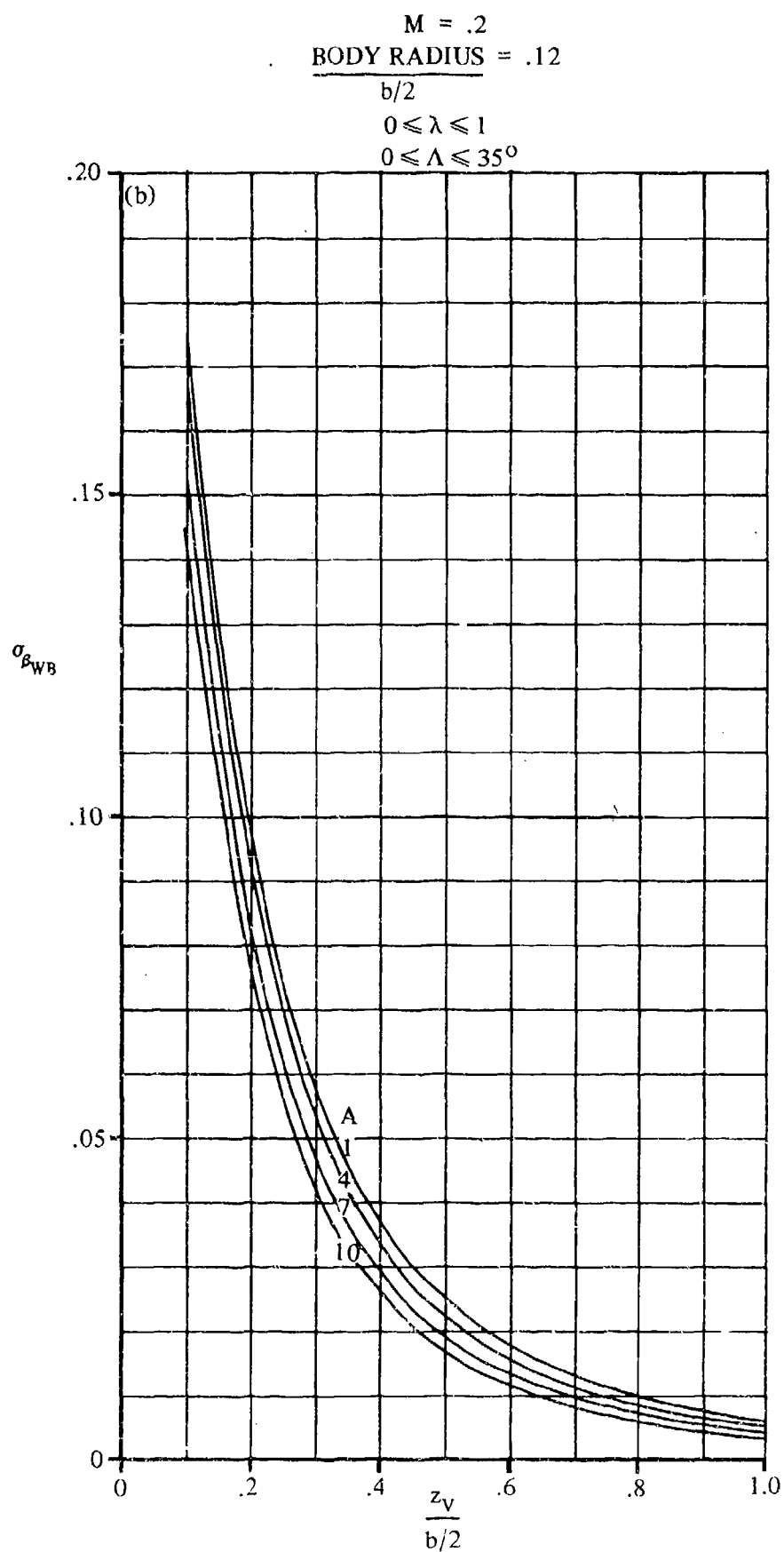


FIGURE 7.4.4.4-42 (CONTD)

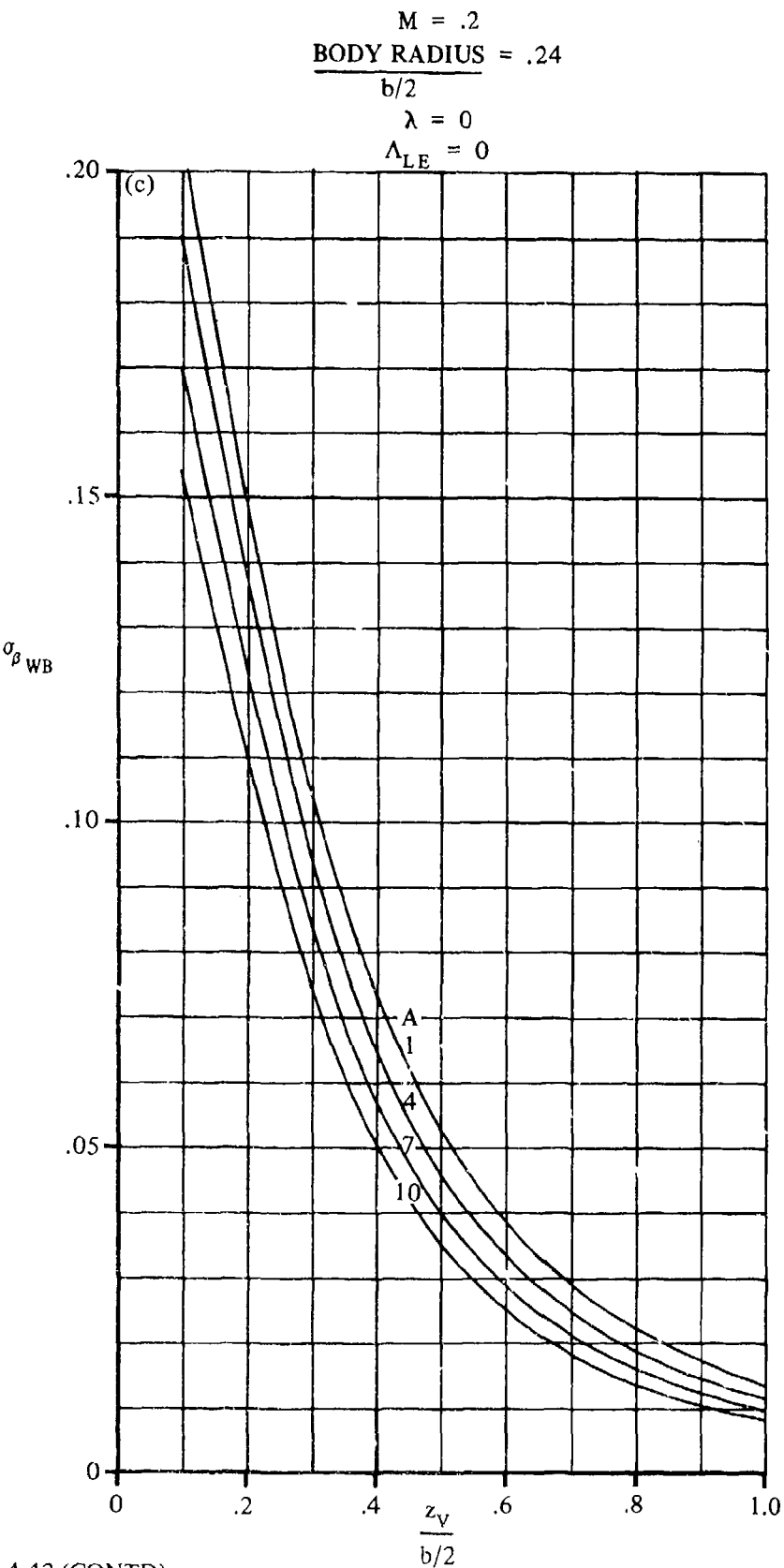


FIGURE 7.4.4.4-42 (CONTD)

7.4.4.4-44

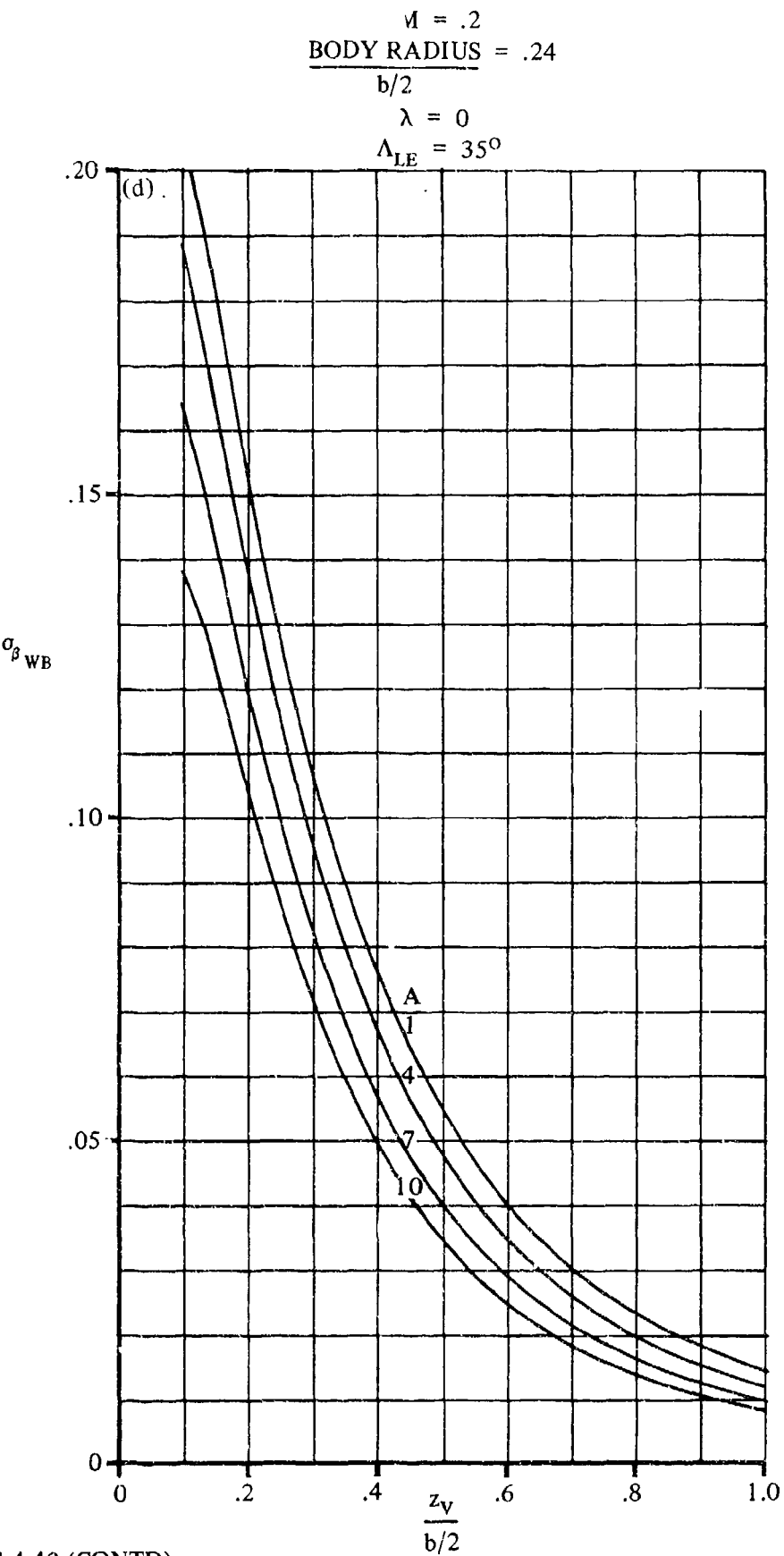


FIGURE 7.4.4.4-42 (CONTD)

$M = .2$
BODY RADIUS = .24
 $b/2$
 $\lambda = .25$
 $\Lambda_{LE} = 0$

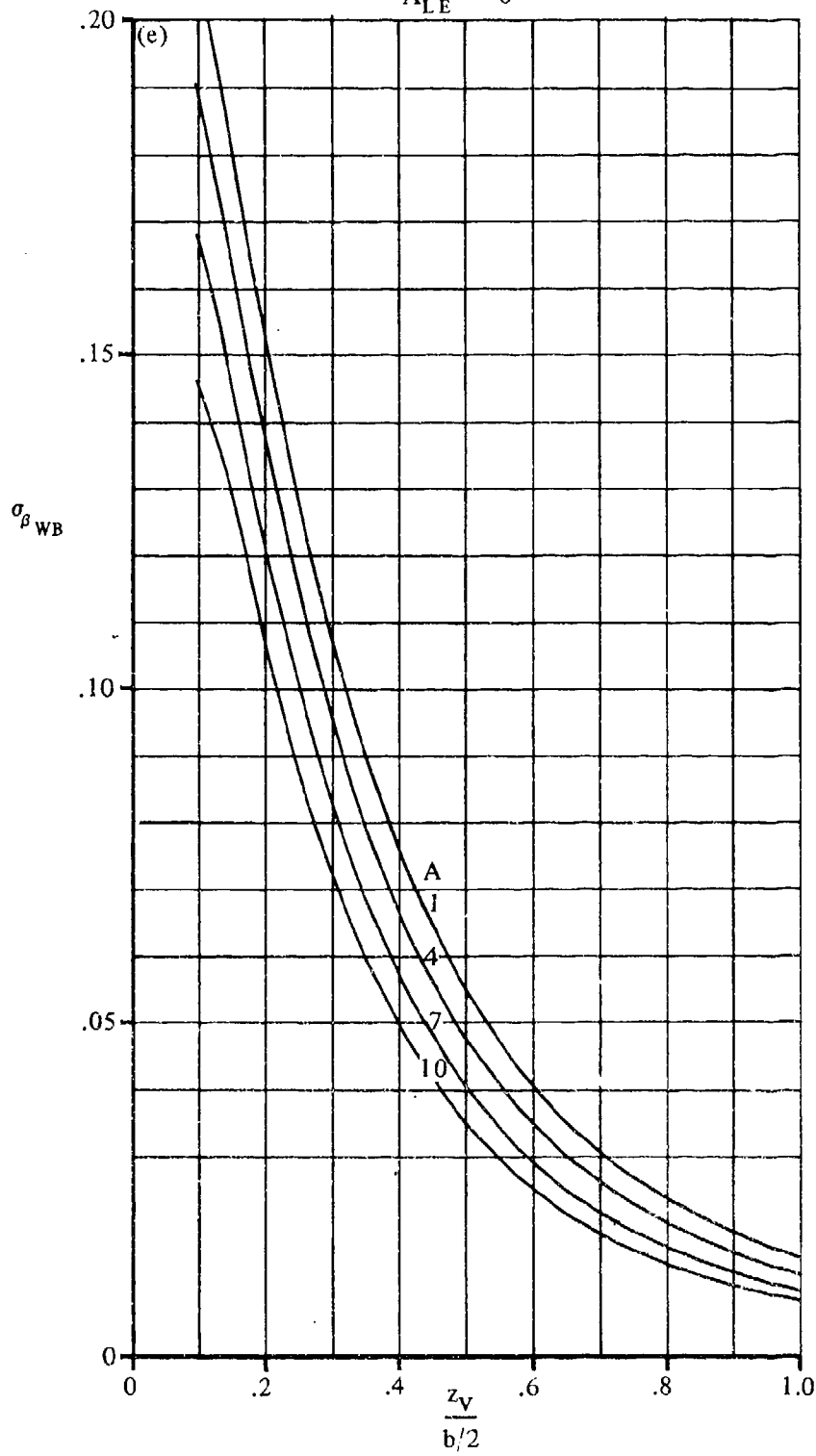


FIGURE 7.4.4.4-42 (CONTD)

7.4.4.4-46

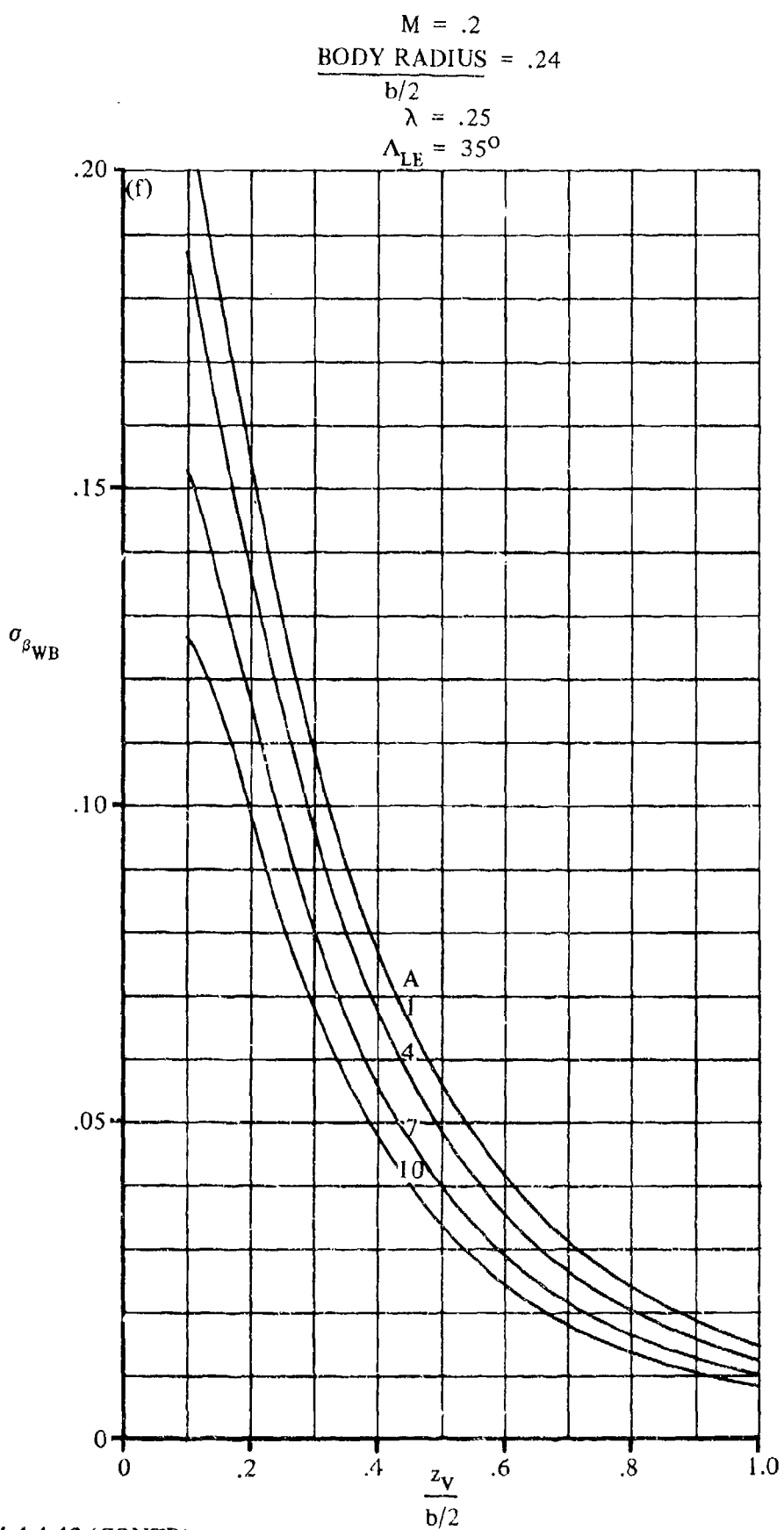


FIGURE 7.4.4-42 (CONTD)

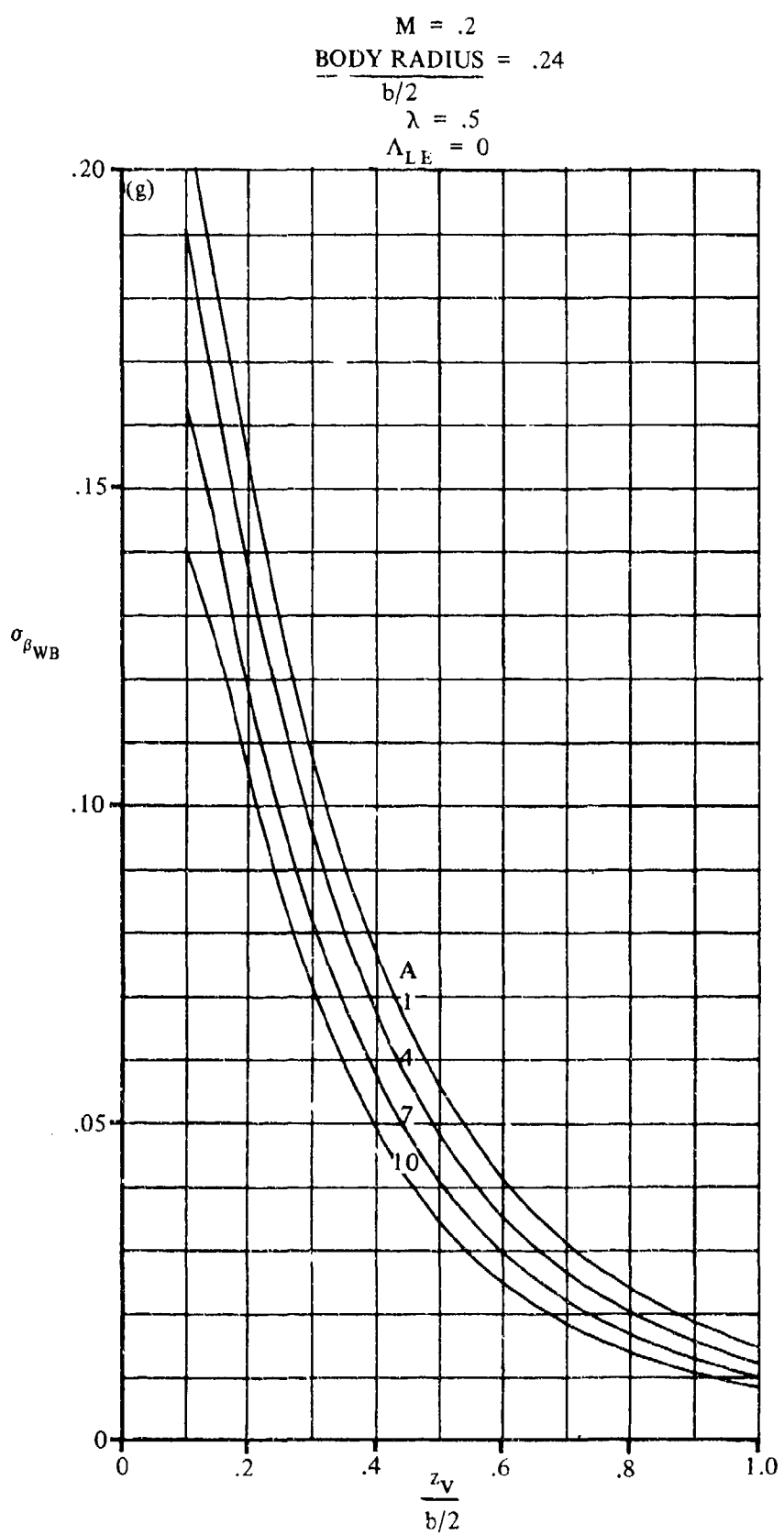


FIGURE 7.4.4.4-42 (CONTD)

7.4.4.4-48

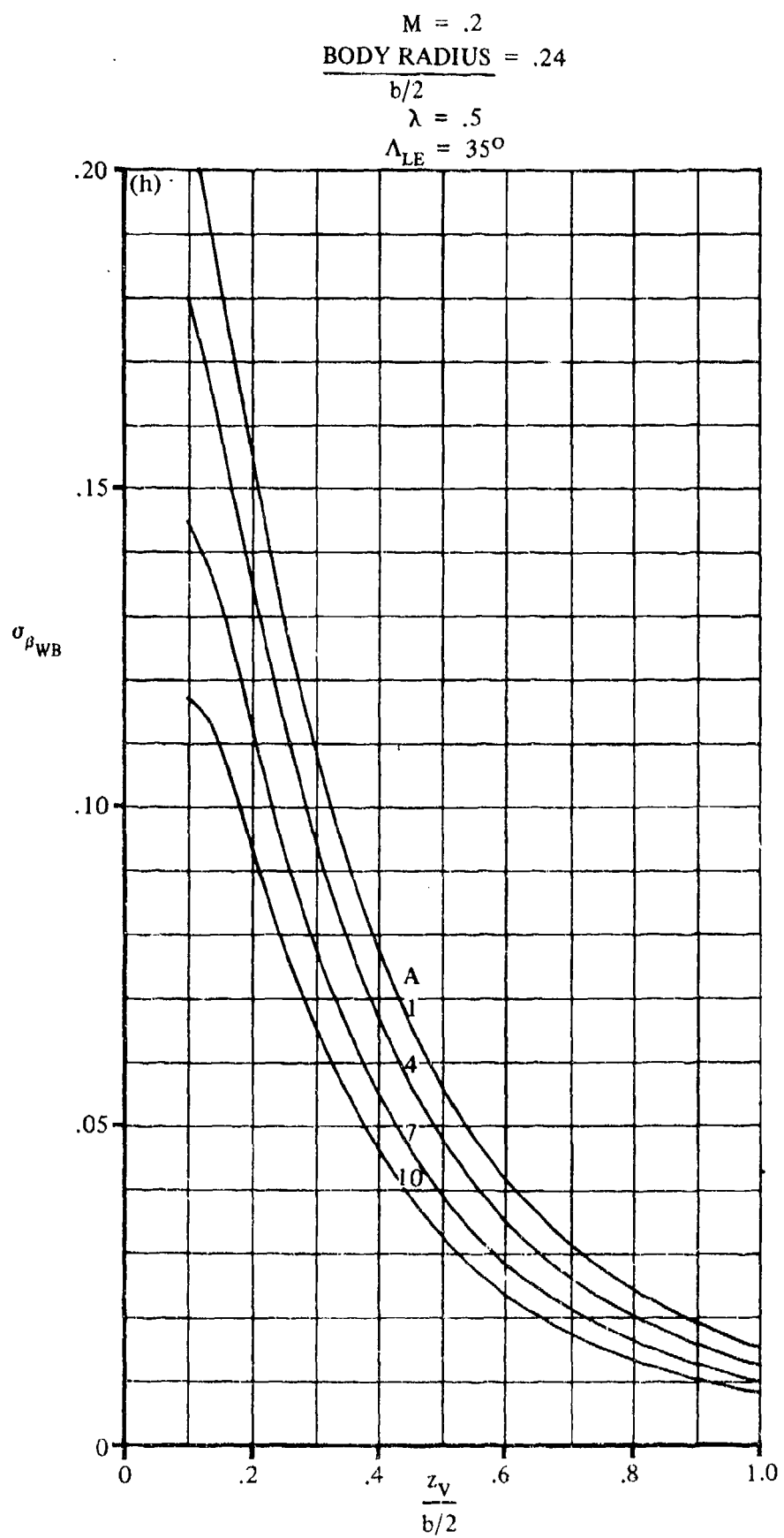


FIGURE 7.4.4.4-42 (CON1D)

7.4.4.4-49

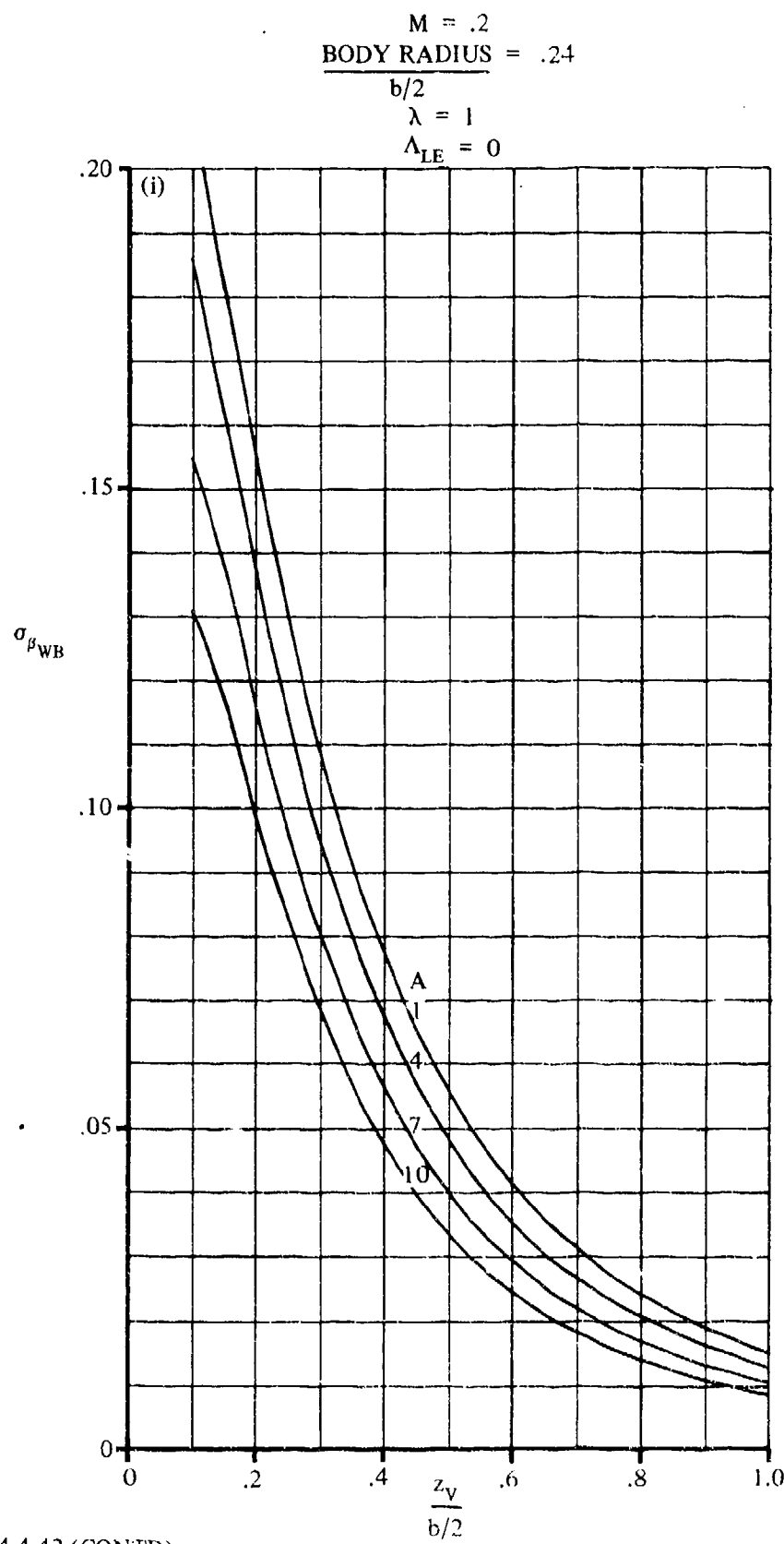


FIGURE 7.4.4.4-42 (CONTD)

7.4.4.4-50

$M = .2$
BODY RADIUS = .24
 $b/2$
 $\lambda = 1$
 $\Delta_{LE} = 35^\circ$

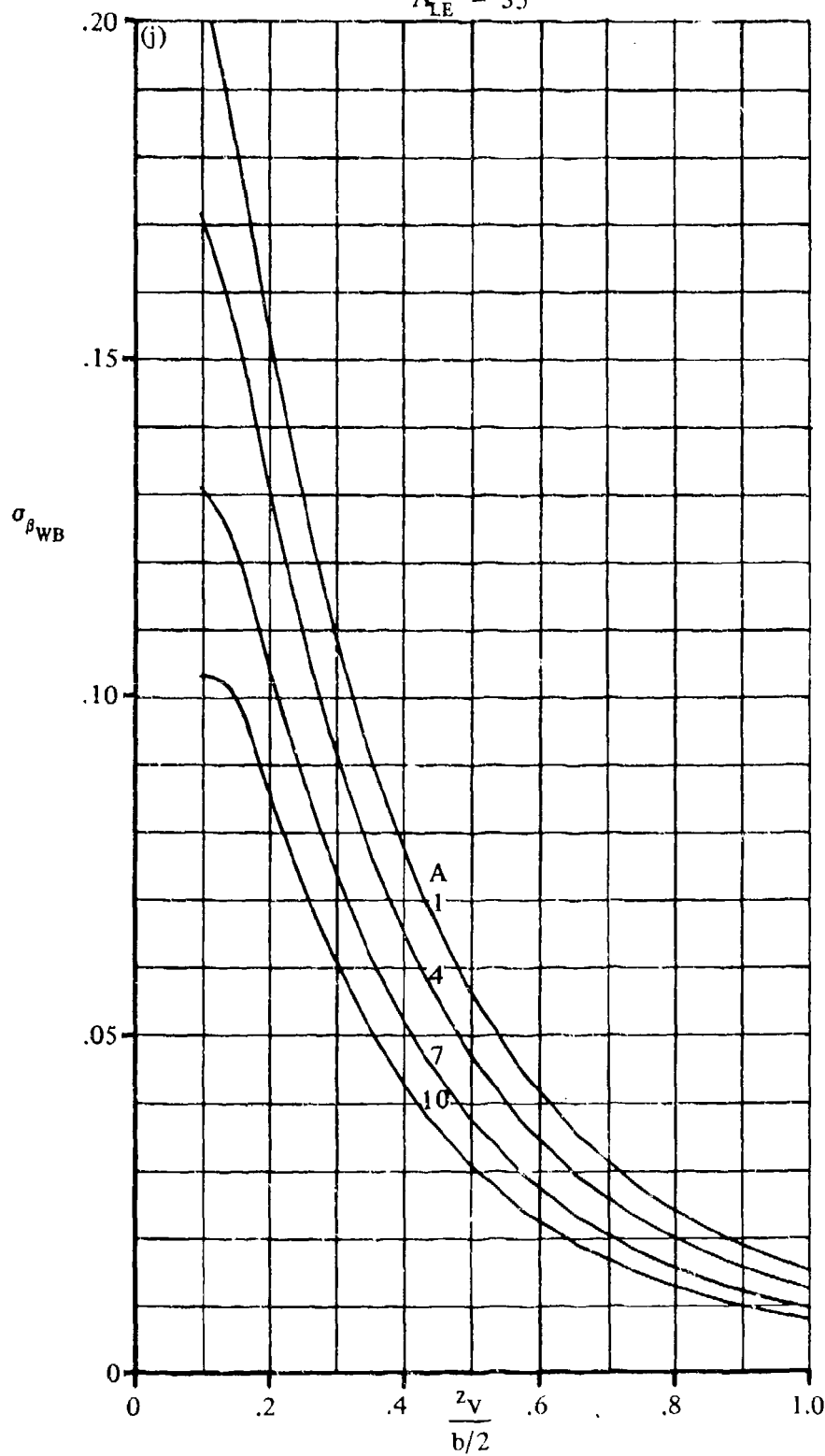


FIGURE 7.4.4.4-42 (CONTD)

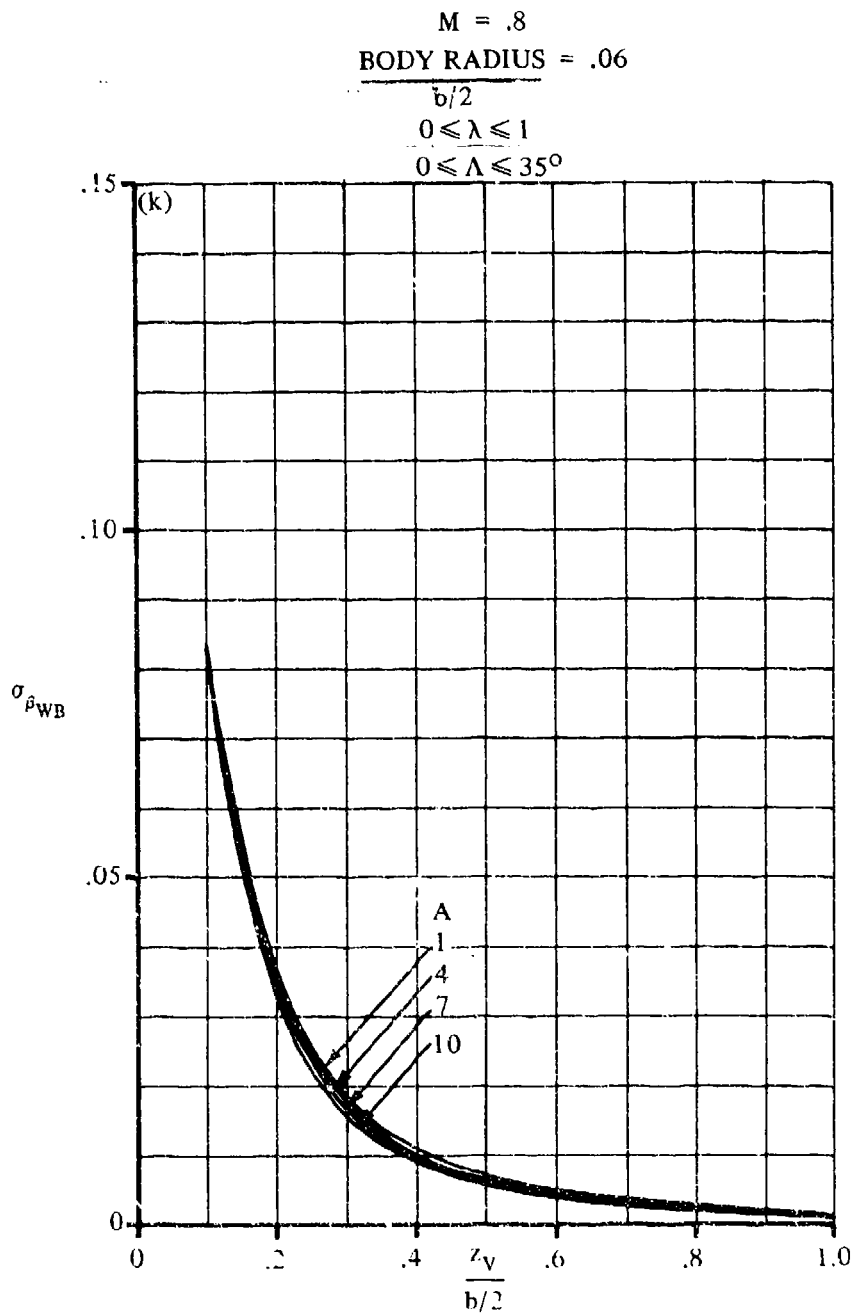


FIGURE 7.4.4.4-42 (CONTD)

$M = .8$
BODY RADIUS = .12

$b/2$

$0 \leq \lambda \leq 1$

$0 \leq \Lambda \leq 35^\circ$

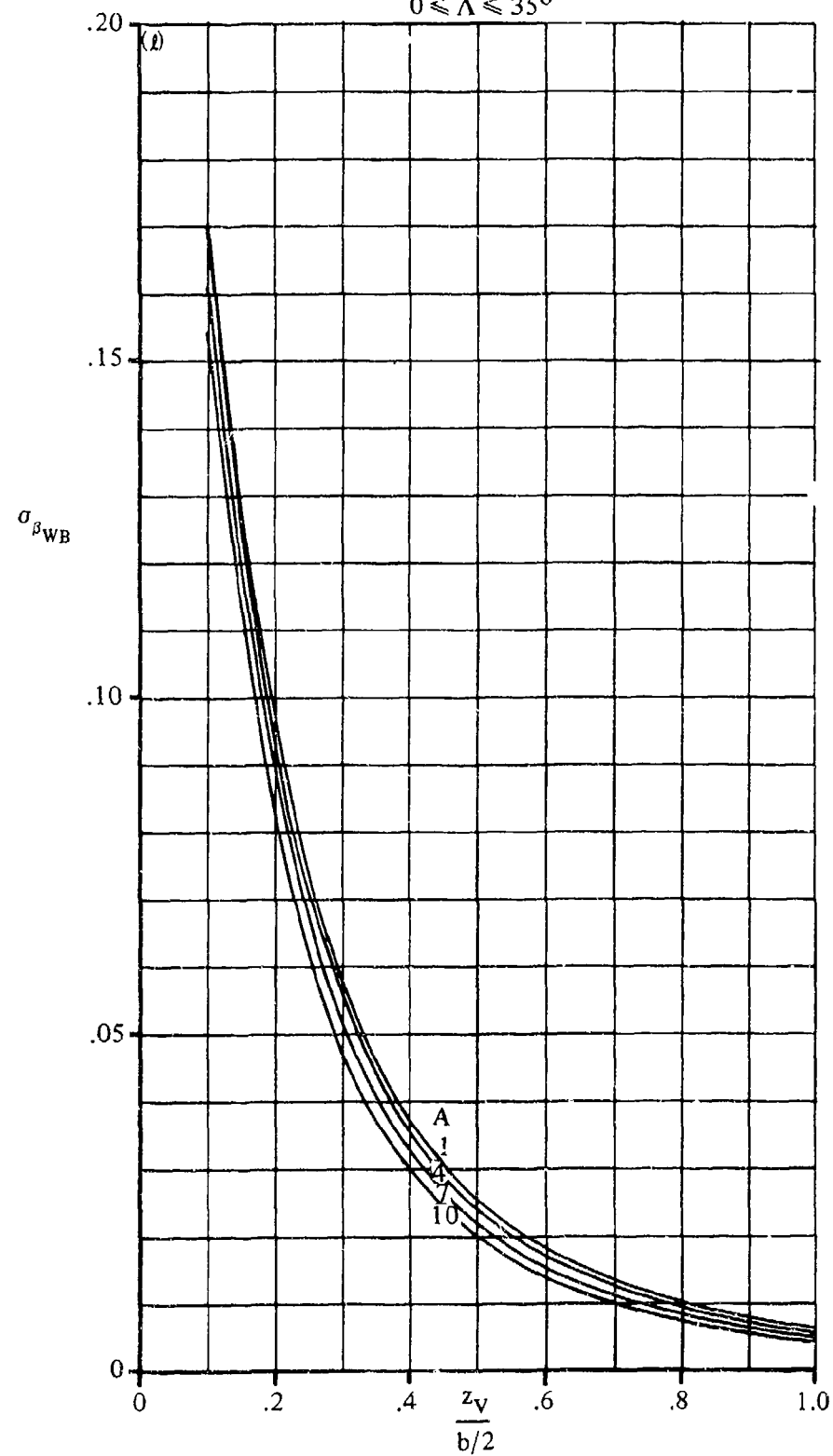


FIGURE 7.4.4.4-42 (CONTD)

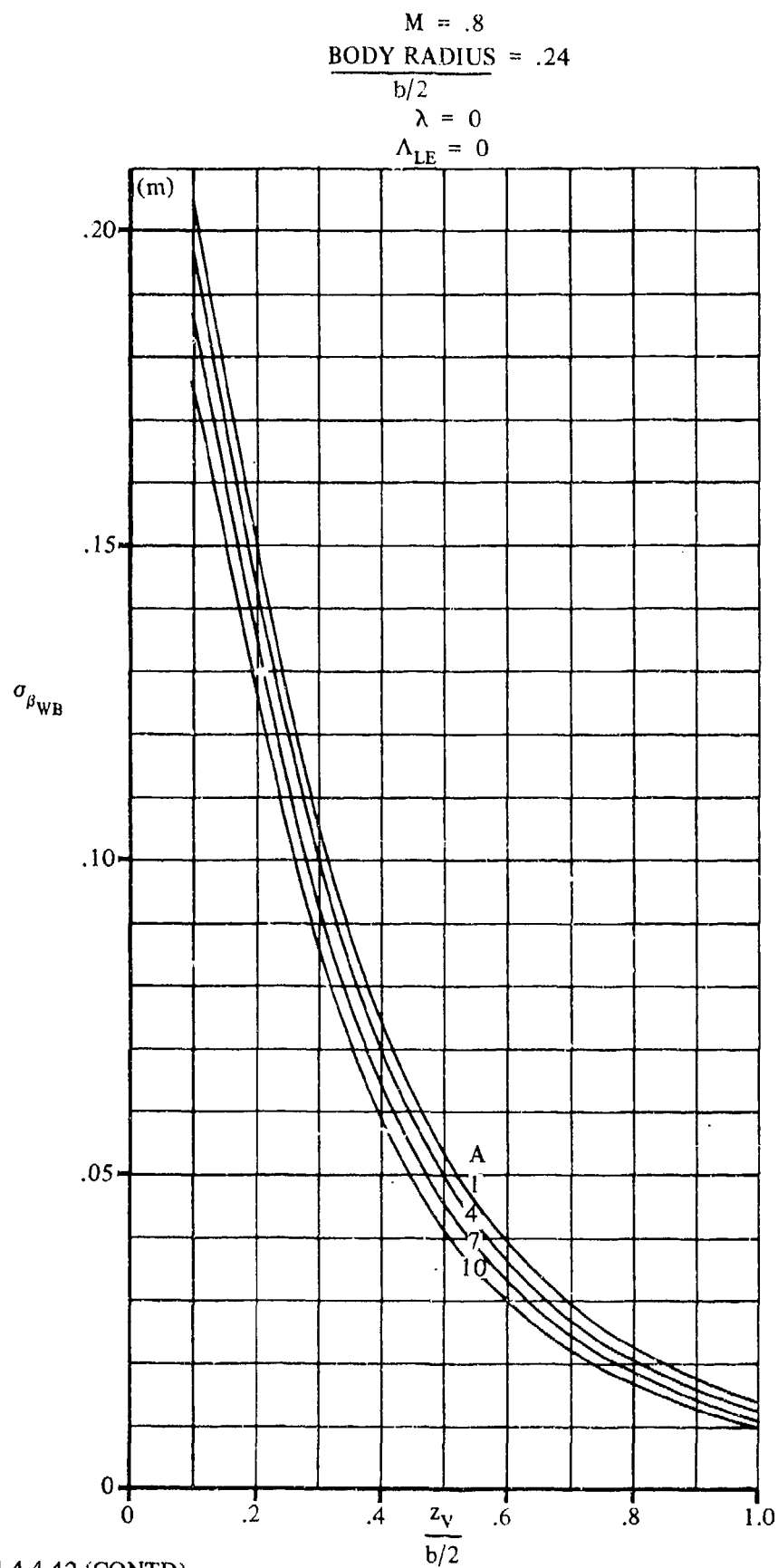


FIGURE 7.4.4.4-42 (CONTD)

7.4.4.4-54

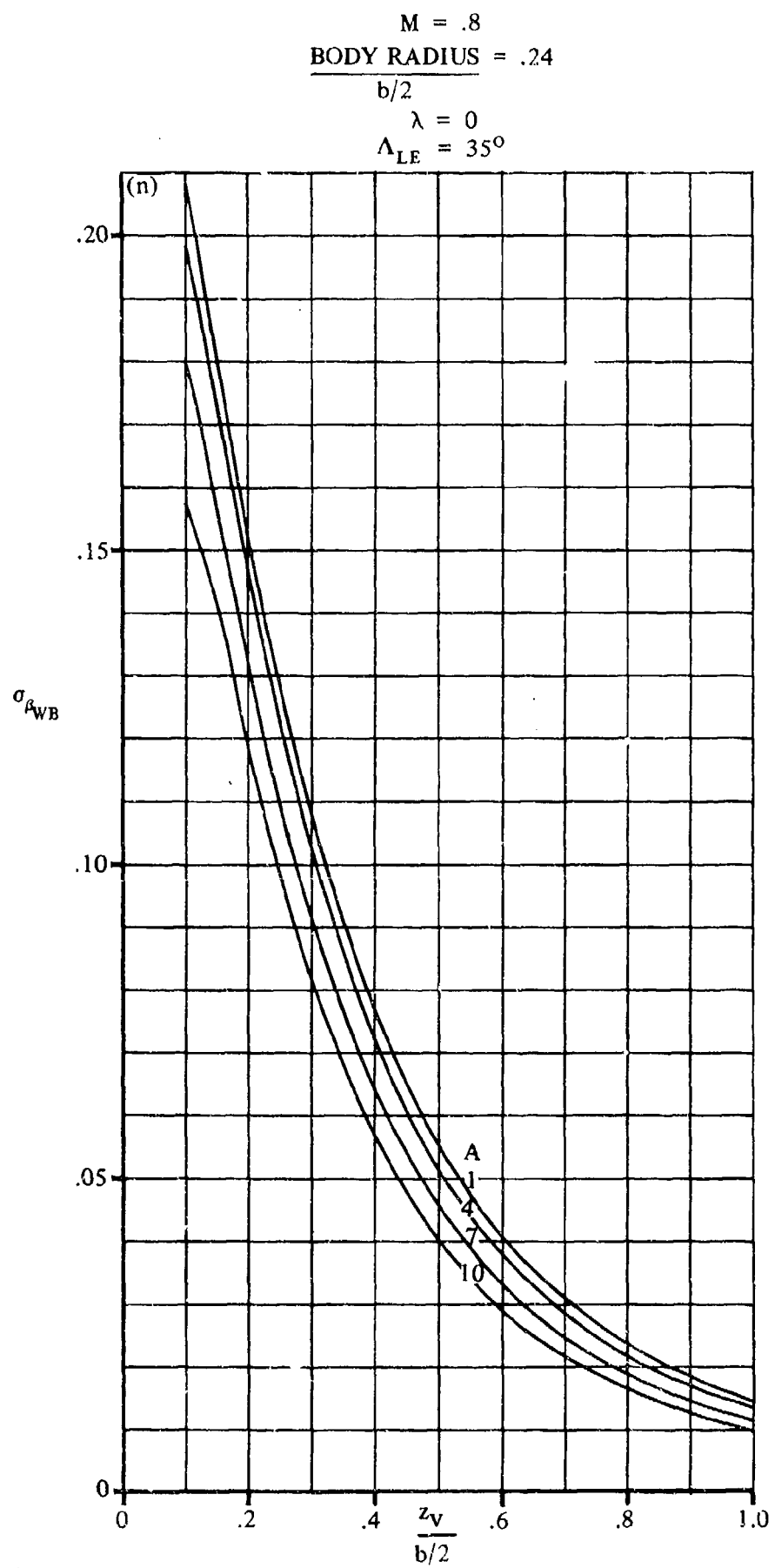


FIGURE 7.4.4.4-42 (CONTD)

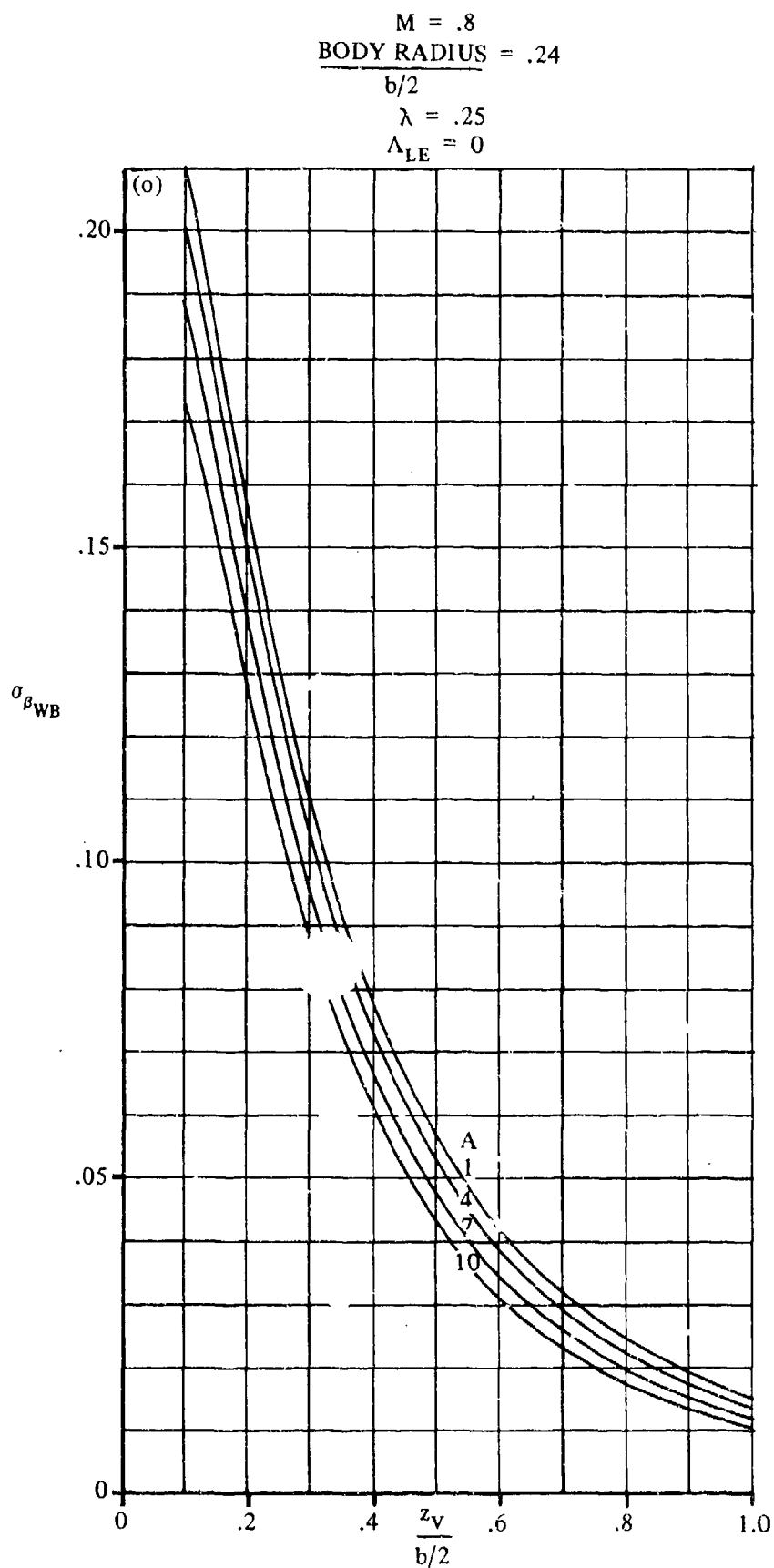


FIGURE 7.4.4.4-42 (CONTD)

7.4.4.4-56

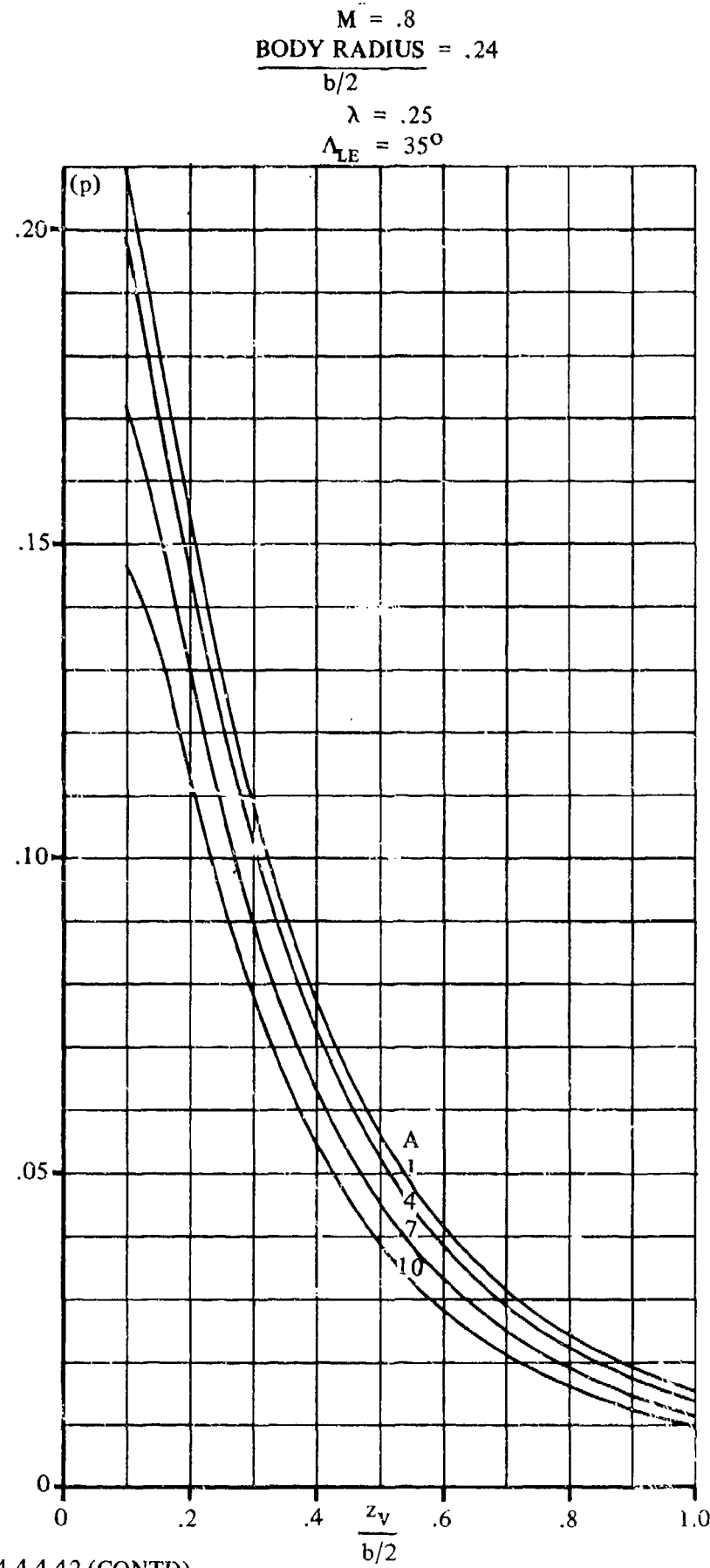


FIGURE 7.4.4.4-42 (CONTD)

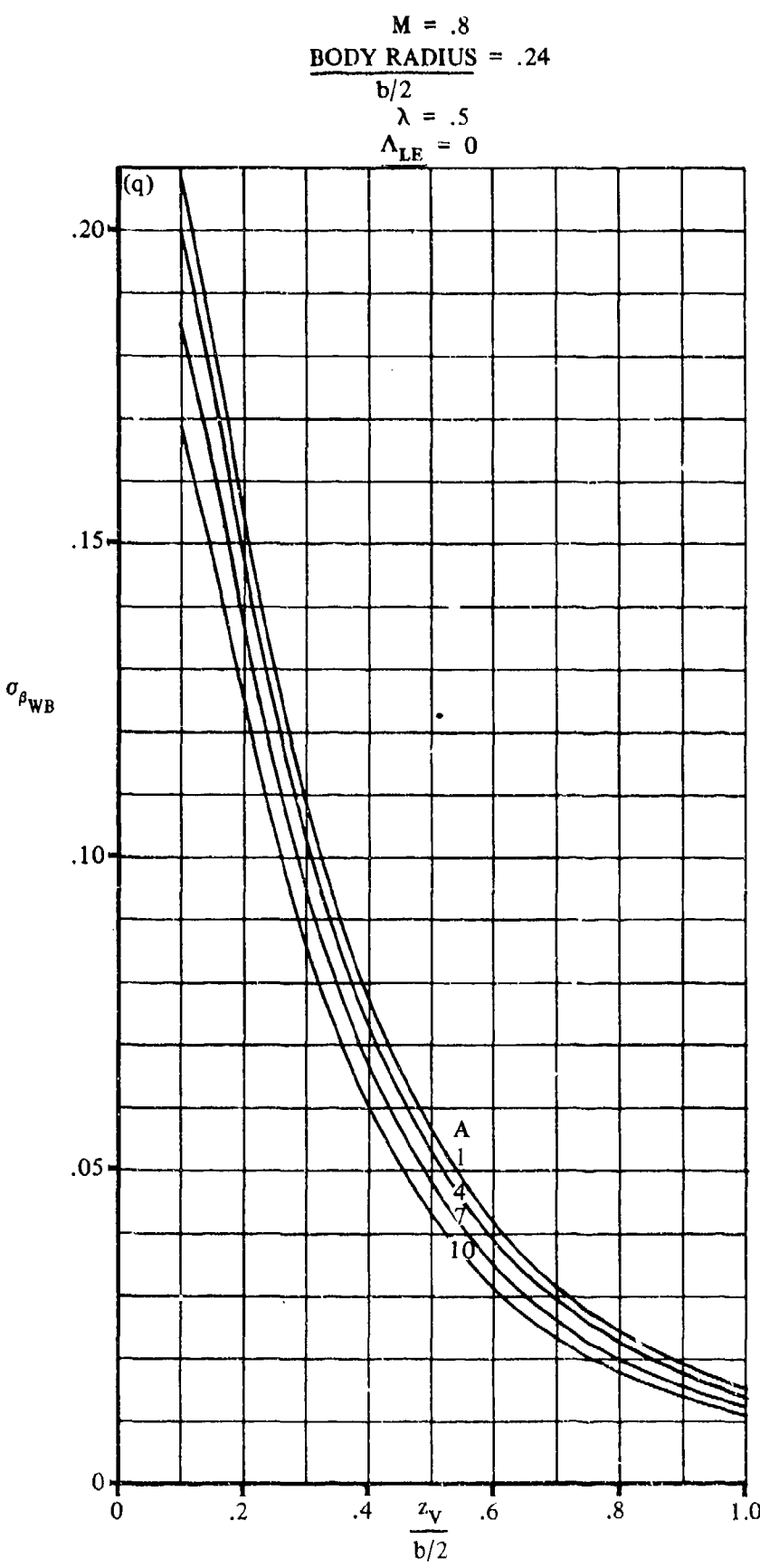


FIGURE 7.4.4.4-42 (CONTD)

7.4.4.4-58

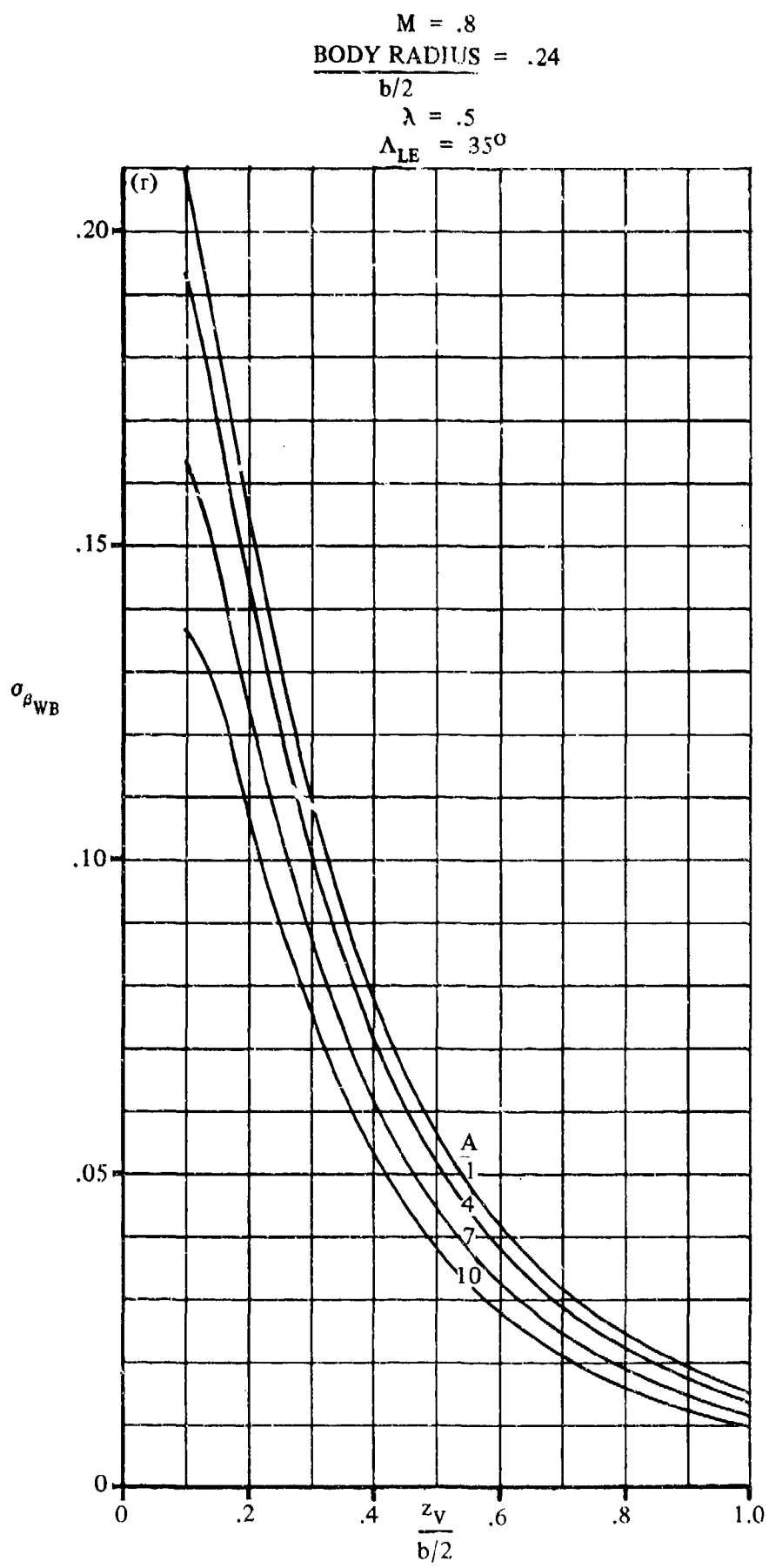


FIGURE 7.4.4-42 (CONT'D)

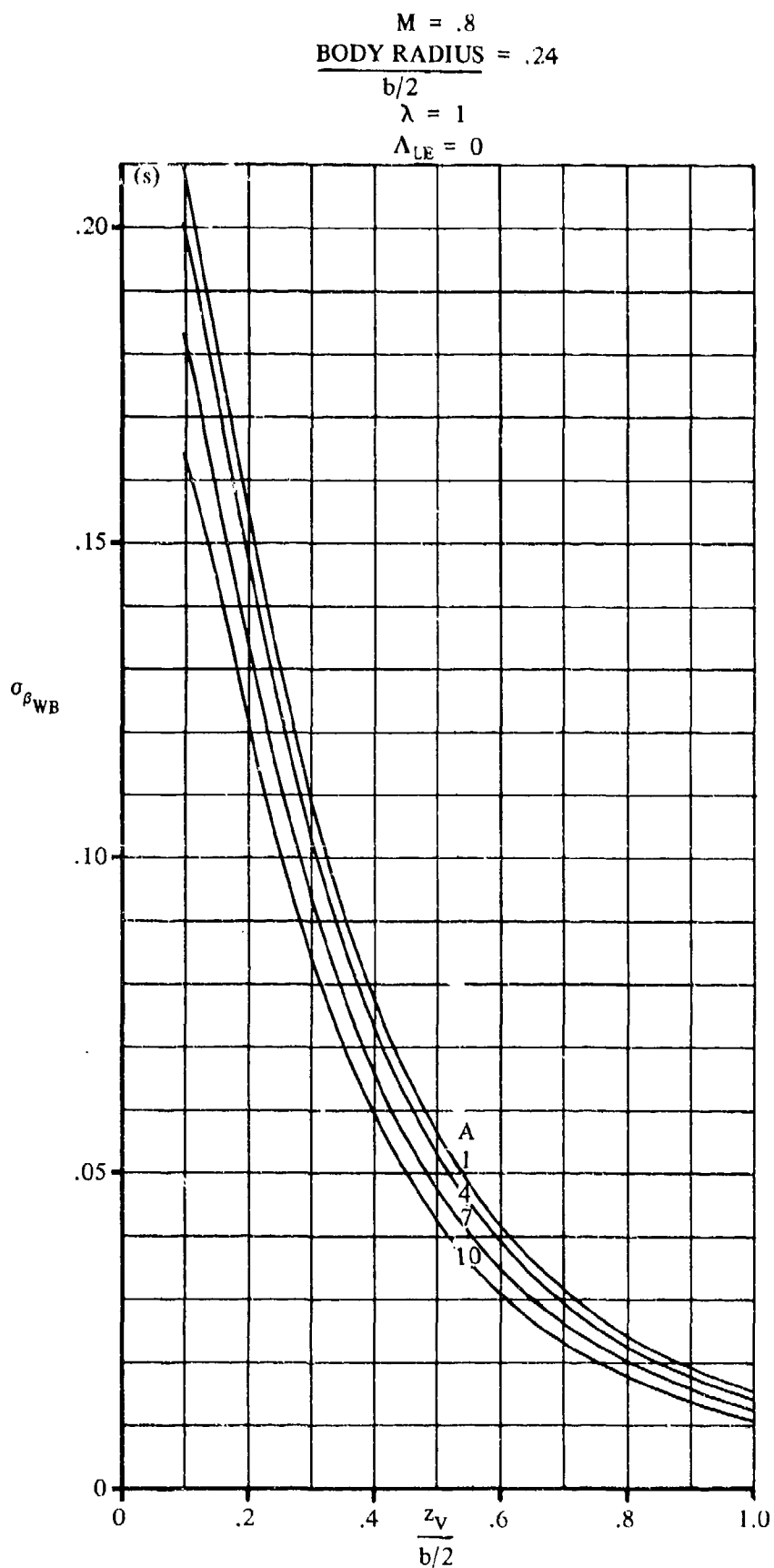


FIGURE 7.4.4.4-42 (CONTD)

7.4.4.4-60

$M = .8$
BODY RADIUS = .24
 $b/2$
 $\lambda = 1.0$
 $\Lambda_{LE} = 35^\circ$

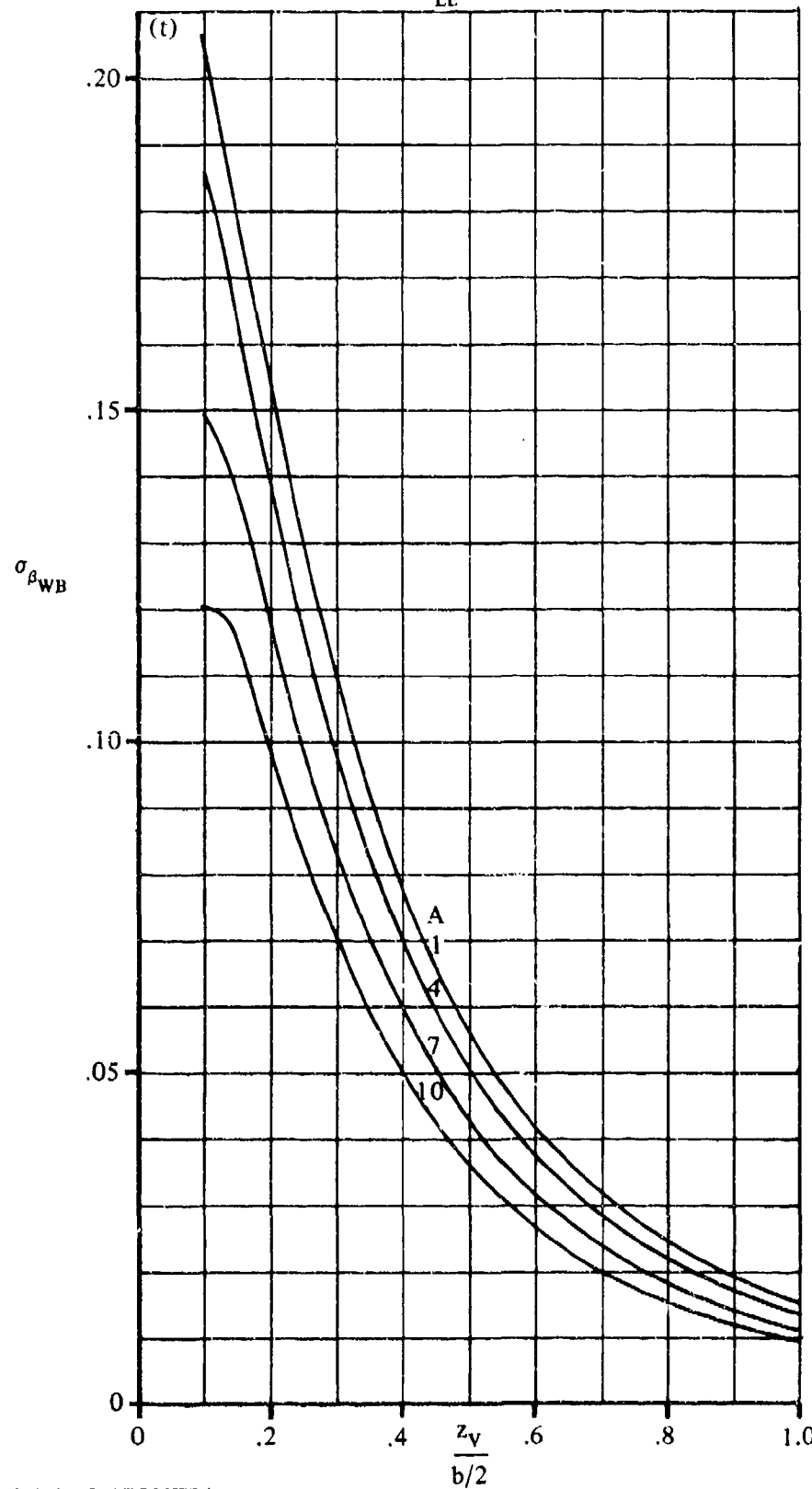


FIGURE 7.4.4.4-42 (CONTD)

7.4.4.5 WING-BODY-TAIL DERIVATIVE $C_{I\beta}$

This section presents a method for estimating the contribution of the vertical tail, in the presence of the wing and body, to the derivative $C_{I\beta}$ at subsonic speeds. This derivative is the change in rolling-moment coefficient with variation in the rate of change of sideslip angle at a constant yaw rate and is defined as

$$C_{I\beta} = \frac{\partial C_l}{\partial \left(\frac{\beta b}{2V} \right)}, \text{ where } C_l \text{ is based on } S_w b_w.$$

In general, at low to moderate angles of attack, this derivative is small and has a negligible effect on lateral stability; hence, it is usually neglected.

A. SUBSONIC

The wing contribution to $C_{I\beta}$ can be evaluated by using unsteady-flow theory, but at low to moderate angles of attack it is generally considered small and is neglected. At low angles of attack and for attached-flow conditions, the largest contributor to $C_{I\beta}$ is the vertical tail. The rolling moment produced on the airframe by the vertical tail is due to the sidewash: time-lag effects from the wing. The body contribution is small and has been neglected.

For a brief discussion of the physical flow phenomena at high angles of attack, i.e., leading-edge vortex sheets and flow separation, and a comprehensive bibliography on related subject matter, the reader is referred to Reference 1. Reference 1 also discusses the inadequacy of oscillating-airfoil theory and sidewash-lag theory for predicting the vertical-tail contribution to $C_{I\beta}$ at high angles of attack. However, a modified flow-field-lag theory is discussed in Reference 1 that appears to give qualitative agreement with experimental data for a current twin-jet fighter configuration.

DATCOM METHOD

The vertical-tail contribution to the derivative $C_{I\beta}$ at low to moderate angles of attack is given by

$$C_{I\beta} = C_{Y\beta} \left(\frac{z_p \cos \alpha_F - l_p \sin \alpha_F}{b_w} \right) \quad 7.4.4.5-a$$

where

$C_{Y\beta}$ is the vertical-tail contribution to the derivative $C_{Y\beta}$ obtained from Section 7.4.4.4.

z_p is the distance from the wing quarter-chord point to the center-of-pressure location of the vertical stabilizer, measured normal to the body center line, positive for the stabilizer above the body. For Datcom purposes, the vertical-tail center-of-pressure location is assumed to be the quarter-chord point of the MAC of the total added panel.

ℓ_p is the distance from the wing quarter-chord point to the center-of-pressure location of the vertical stabilizer, measured parallel to the body center line. For Datcom purposes, the vertical-tail center-of-pressure location is assumed to be at the quarter-chord point of the MAC of the total added panel. (See Sketch (a) of Section 7.4.2.1.)

α_F is the fuselage angle of attack.

b_w is the wing span.

Sample Problem

Given: Same configuration as sample problem of Paragraph A of Section 7.4.4.4.

Compute:

$$C_{Y\dot{\beta}} = -0.000209 \quad (\text{Sample Problem, Paragraph A, Section 7.4.4.4})$$

$$C_{I\dot{\beta}} = C_{Y\dot{\beta}} \left(\frac{z_p \cos \alpha_F - \ell_p \sin \alpha_F}{b_w} \right) \quad (\text{Equation 7.4.4.5-a})$$

$$\begin{aligned} C_{I\dot{\beta}} &= (-0.000209) \left[\frac{(20)(0.9998) - (60)(0.0175)}{156.52} \right] \\ &= -0.0000253 \text{ per deg} \end{aligned}$$

B. TRANSONIC

No method is presented.

C. SUPERSONIC

No method is presented.

REFERENCE

1. Coe, P. L., Jr., Graham, A. B., and Chambers, J. R.: Summary of Information on Low-Speed Lateral-Directional Derivatives Due to Rate of Change of Sideslip $\dot{\beta}$. NASA TN D-7972, 1975. (U)

7.4.4.6 WING-BODY-TAIL DERIVATIVE $C_{n\dot{\beta}}$

This section presents a method for estimating the contribution of the vertical tail, in the presence of the wing and body, to the derivative $C_{n\dot{\beta}}$ at subsonic speeds. This derivative is the change in yawing-moment coefficient with variation in the rate of change of sideslip angle at a constant yaw rate and is defined as

$$C_{n\dot{\beta}} = \frac{\partial C_n}{\partial \left(\frac{\dot{\beta} b}{2V} \right)}, \text{ where } C_n \text{ is based on } S_w b_w.$$

For most configurations at low to moderate angles of attack, $C_{n\dot{\beta}}$ is rather small and can be neglected in lateral dynamic calculations. However, at high angles of attack for swept- and delta-wing configurations, $C_{n\dot{\beta}}$ can approach the magnitude of C_{n_r} and consequently have large effects on the calculated dynamic stability of these configurations.

A. SUBSONIC

The wing contribution to $C_{n\dot{\beta}}$ can be evaluated by using unsteady-flow theory, but at low to moderate angles of attack it is generally considered small and is neglected. At low angles of attack and for attached-flow conditions, the largest contributor to $C_{n\dot{\beta}}$ is the vertical tail. The yawing moment produced on the airframe by the vertical tail is due to the sidewash time-lag effects from the wing. The body contribution is small and has been neglected.

For a brief discussion of the physical flow phenomena at high angles of attack, i.e., leading-edge vortex sheets and flow separation, and a comprehensive bibliography on related subject matter, the reader is referred to Reference 1. Reference 1 also discusses the inadequacy of oscillating-airfoil theory and sidewash-lag theory for predicting the vertical-tail contribution to $C_{n\dot{\beta}}$ at high angles of attack. However, a modified flow-field-lag theory is discussed in Reference 1 that appears to give qualitative agreement with experimental data for a current twin-jet fighter configuration.

DATCOM METHOD

The vertical-tail contribution to the derivative $C_{n\dot{\beta}}$ at low to moderate angles of attack is given by

$$C_{n\dot{\beta}} = -C_{Y\dot{\beta}} \left(\frac{l_p \cos \alpha_F + z_p \sin \alpha_F}{b_w} \right) \quad 7.4.4.6-a$$

where

$C_{Y\dot{\beta}}$ is the vertical-tail contribution to the derivative $C_{Y\dot{\beta}}$, obtained from Section 7.4.4.4.

l_p is the distance from the moment reference center to the center-of-pressure location of the vertical stabilizer, measured parallel to the body center line. (See Sketch (a) in Section 7.4.2.1.) For Datcom purposes the vertical-tail center-of-pressure location is assumed to be at the quarter-chord point of the MAC of the total added panel.

z_p

is the distance from the moment reference center to the center of pressure of the vertical stabilizer, measured normal to the body center line, positive for the stabilizer above the body. For Datcom purposes, the vertical-tail center-of-pressure location is assumed to be at the quarter-chord point of the MAC of the total added panel.

b_w

is the wing span.

α_F

is the fuselage angle of attack.

Sample Problem

Given: Same configuration as sample problem of Paragraph A of Section 7.4.4.4.

Compute:

$$C_{Y\dot{\beta}} = -0.000209 \quad (\text{Sample Problem, Paragraph A, Section 7.4.4.4})$$

$$C_{n\dot{\beta}} = -C_{Y\dot{\beta}} \left(\frac{l_p \cos \alpha_F + z_p \sin \alpha_F}{b_w} \right) \quad (\text{Equation 7.4.4.6-a})$$

$$= -(-0.000209) \left[\frac{(60)(0.9998) + (20)(0.01745)}{156.52} \right]$$

$$= +0.0000805 \text{ per deg}$$

B. TRANSONIC

No method is presented.

C. SUPERSONIC

No method is presented.

REFERENCE

1. Coe, P. L., Jr., Graham, A. B., and Chambers, J. R.: Summary of Information on Low-Speed Lateral-Directional Derivatives Due to Rate of Change of Sideslip $\dot{\beta}$. NASA TN D-7972, 1975. (U)